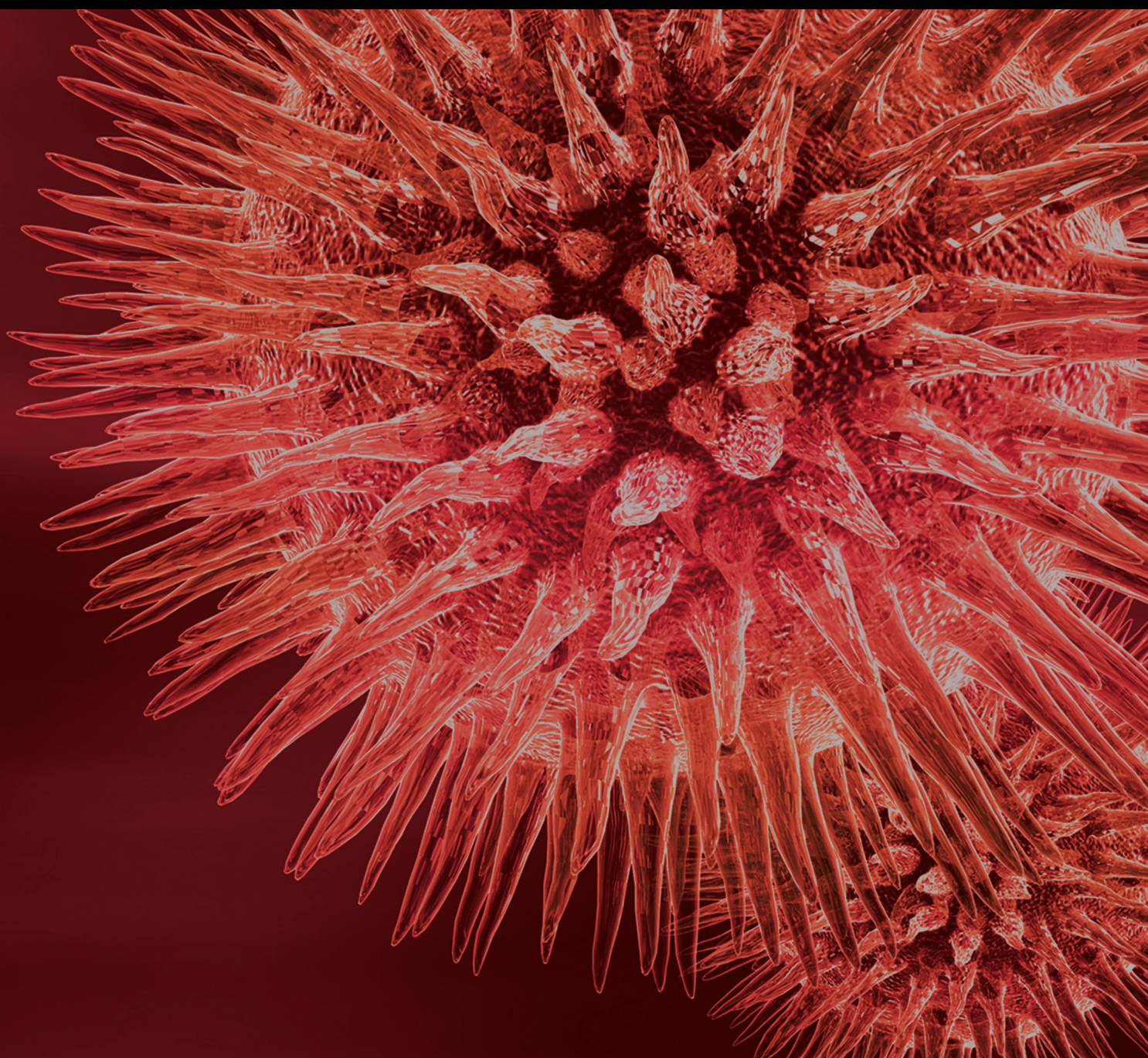


# Natural Compounds against Cancer, Inflammation, and Oxidative Stress

Lead Guest Editor: Claudio Tabolacci

Guest Editors: Francesco Facchiano, Cinzia Forni, and Ravirajsinh N. Jadeja





---

# **Natural Compounds against Cancer, Inflammation, and Oxidative Stress**



## **Natural Compounds against Cancer, Inflammation, and Oxidative Stress**

Lead Guest Editor: Claudio Tabolacci

Guest Editors: Francesco Facchiano, Cinzia Forni,  
and Ravirajsinh N. Jadeja







Copyright © 2019 Hindawi. All rights reserved.

This is a special issue published in “BioMed Research International.” All articles are open access articles distributed under the Creative Commons Attribution License, which permits unrestricted use, distribution, and reproduction in any medium, provided the original work is properly cited.




## Contents








### **Natural Compounds against Cancer, Inflammation, and Oxidative Stress**

Claudio Tabolacci , Cinzia Forni , Ravirajsinh N. Jadeja , and Francesco Facchiano   
Editorial (2 pages), Article ID 9495628, Volume 2019 (2019)

### **Effect of Immunomodulatory Supplements Based on Echinacea Angustifolia and Echinacea Purpurea on the Posttreatment Relapse Incidence of Genital Condylomatosis: A Prospective Randomized Study**

Nicoletta De Rosa , Pierluigi Giampaolino, Giada Lavitola, Ilaria Morra, Carmen Formisano, Carmine Nappi, and Giuseppe Bifulco  
Research Article (7 pages), Article ID 3548396, Volume 2019 (2019)


### **Beneficial Role of Phytochemicals on Oxidative Stress and Age-Related Diseases**

Cinzia Forni, Francesco Facchiano , Manuela Bartoli, Stefano Pieretti, Antonio Facchiano , Daniela D'Arcangelo , Sandro Norelli, Giorgia Valle, Roberto Nisini , Simone Beninati , Claudio Tabolacci , and Ravirajsinh N. Jadeja   
Review Article (16 pages), Article ID 8748253, Volume 2019 (2019)


### **Diosgenin and Its Fenugreek Based Biological Matrix Affect Insulin Resistance and Anabolic Hormones in a Rat Based Insulin Resistance Model**

Rita Kiss , Georgina Pesti-Asbóth, Mária Magdolna Szarvas, László Stündl, Zoltán Cziáky, Csaba Hegedűs, Diána Kovács, Andrea Badale, Endre Máthé, Zoltán Szilvássy, and Judit Remenyik   
Research Article (13 pages), Article ID 7213913, Volume 2019 (2019)

### **Selectivity of Dietary Phenolics for Inhibition of Human Monoamine Oxidases A and B**

Zhenxian Zhang, Hiroki Hamada, and Phillip M. Gerck   
Research Article (12 pages), Article ID 8361858, Volume 2019 (2019)

### **Effect of Chemotherapeutics and Tocopherols on MCF-7 Breast Adenocarcinoma and KGN Ovarian Carcinoma Cell Lines *In Vitro***

Daniela Figueroa , Mohammad Asaduzzaman, and Fiona Young  
Research Article (13 pages), Article ID 6146972, Volume 2019 (2019)


### **The Effects of Korea Red Ginseng on Inflammatory Cytokines and Apoptosis in Rat Model with Chronic Nonbacterial Prostatitis**

Sang Wook Kang , Je-Hoon Park, Hosik Seok, Hae Jeong Park, Joo-Ho Chung , Chang-Ju Kim, Young Ock Kim, Young Rok Han, DongWhan Hong, Young Sik Kim, and Su Kang Kim   
Research Article (8 pages), Article ID 2462561, Volume 2019 (2019)



### **Effects of a New Combination of Medical Food on Endothelial Function and Lipid Profile in Dyslipidemic Subjects: A Pilot Randomized Trial**

Francesco Landi , Anna Maria Martone, Sara Salini, Beatrice Zazzara, Riccardo Calvani , Emanuele Marzetti , Antonio Nesci, Angela Di Giorgio, Bianca Giupponi, Luca Santoro , and Angelo Santoliquido  
Clinical Study (7 pages), Article ID 1970878, Volume 2019 (2019)



**Natural Compound Oridonin Inhibits Endotoxin-Induced Inflammatory Response of Activated Hepatic Stellate Cells**

Claire B. Cummins, Xiaofu Wang, Christian Sommerhalder, Frederick J. Bohanon, Omar Nunez Lopez, Hong-Yan Tie, Victoria G. Rontoyanni, Jia Zhou, and Ravi S. Radhakrishnan   
Research Article (10 pages), Article ID 6137420, Volume 2018 (2019)

**Degalactotigonin, a Steroidal Glycoside from *Solanum nigrum*, Induces Apoptosis and Cell Cycle Arrest via Inhibiting the EGFR Signaling Pathways in Pancreatic Cancer Cells**

Hoang Le Tuan Anh, Phuong Thao Tran , Do Thi Thao, Duong Thu Trang, Nguyen Hai Dang , Pham Van Cuong, Phan Van Kiem, Chau Van Minh, and Jeong-Hyung Lee   
Research Article (9 pages), Article ID 3120972, Volume 2018 (2019)

***Cannabis sativa* L. and Nonpsychoactive Cannabinoids: Their Chemistry and Role against Oxidative Stress, Inflammation, and Cancer**

Federica Pellati , Vittoria Borgonetti, Virginia Brighenti, Marco Biagi, Stefania Benvenuti, and Lorenzo Corsi   
Review Article (15 pages), Article ID 1691428, Volume 2018 (2019)


**Gallic Acid Attenuates Dimethylnitrosamine-Induced Liver Fibrosis by Alteration of Smad Phosphoisoform Signaling in Rats**

Yuxin Chen , Ziping Zhou, Qigui Mo, Gao Zhou, and Youwei Wang   
Research Article (14 pages), Article ID 1682743, Volume 2018 (2019)




**Natural Compounds for the Management of Parkinson's Disease and Attention-Deficit/Hyperactivity Disorder**

Juan Carlos Corona   
Review Article (12 pages), Article ID 4067597, Volume 2018 (2019)


**Plumbagin-Loaded Nanoemulsion Drug Delivery Formulation and Evaluation of Antiproliferative Effect on Prostate Cancer Cells**

Adrian Chrastina , Veronique T. Baron, Parisa Abedinpour, Gaelle Rondeau, John Welsh, and Per Borgström  
Research Article (7 pages), Article ID 9035452, Volume 2018 (2019)

**Analysis of *In Vitro* Cyto- and Genotoxicity of Barbatimão Extract on Human Keratinocytes and Fibroblasts**

Neida L. Pellenz, Fernanda Barbisan , Veronica F. Azzolin, Thiago Duarte, Aline Bolignon, Moisés H. Mastella, Cibele F. Teixeira , Euler E. Ribeiro, Ivana B. Mânica da Cruz , and Marta M. M. F. Duarte  
Research Article (11 pages), Article ID 1942451, Volume 2018 (2019)

**Protective Effects of Silymarin and Silibinin against DNA Damage in Human Blood Cells**

Flávio Fernandes Veloso Borges, Carolina Ribeiro e Silva, Wanessa Moreira Goes, Fernanda Ribeiro Godoy, Fernanda Craveiro Franco, Jefferson Hollanda Vêras, Elisa Flávia Luiz Cardoso Bailão, Daniela de Melo e Silva, Clever Gomes Cardoso, Aparecido Divino da Cruz, and Lee Chen-Chen   
Research Article (8 pages), Article ID 6056948, Volume 2018 (2019)




**$\alpha$ -Hederin Arrests Cell Cycle at G2/M Checkpoint and Promotes Mitochondrial Apoptosis by Blocking Nuclear Factor- $\kappa$ B Signaling in Colon Cancer Cells**

Dongdong Sun, Weixing Shen, Feng Zhang, Huisen Fan, Jiani Tan, Liu Li, Changliang Xu, Haibin Zhang, Ye Yang , and Haibo Cheng 

Research Article (11 pages), Article ID 2548378, Volume 2018 (2019)

**Pharmacokinetics and Bioavailability Study of Monocrotaline in Mouse Blood by Ultra-Performance Liquid Chromatography-Tandem Mass Spectrometry**

Lianguo Chen, Bin Zhang, Jinlai Liu, Zhehua Fan, Ziwei Weng, Peiwu Geng, Xianqin Wang , and Guanyang Lin 





Research Article (10 pages), Article ID 1578643, Volume 2018 (2019)

**Antioxidant, Anti-Inflammatory, and Antitumoral Effects of Aqueous Ethanolic Extract from *Phoenix dactylifera* L. Parthenocarpic Dates**

Hanen El Abed , Mouna Chakroun, Zaineb Abdelkafi-Koubaa, Nouredine Drira, Naziha Marrakchi, Hafedh Mejdoub, and Bassem Khemakhem 

Research Article (7 pages), Article ID 1542602, Volume 2018 (2019)

***Angelica gigas* Nakai Has Synergetic Effects on Doxorubicin-Induced Apoptosis**

Yong-Joon Jeon , Jong-Il Shin , Sol Lee, Yoon Gyeong Lee, Ji Beom Kim, Hak Cheol Kwon, Sung Hun Kim, Inki Kim, Kyungho Lee , and Ye Sun Han 


Research Article (11 pages), Article ID 6716547, Volume 2018 (2019)

**Volatile Oil of *Amomum villosum* Inhibits Nonalcoholic Fatty Liver Disease via the Gut-Liver Axis**

Shanhong Lu, Ting Zhang, Wen Gu , Xingxin Yang, Jianmei Lu, Ronghua Zhao , and Jie Yu 

Research Article (16 pages), Article ID 3589874, Volume 2018 (2019)





**Effects of *Juniperus phoenicea* Hydroalcoholic Extract on Inflammatory Mediators and Oxidative Stress Markers in Carrageenan-Induced Paw Oedema in Mice**

Karama Zouari Bouassida , Samar Makni, Amina Tounsi, Lobna Jlaiel, Mohamed Trigui , and Slim Tounsi 

Research Article (11 pages), Article ID 3785487, Volume 2018 (2019)

## Editorial

# Natural Compounds against Cancer, Inflammation, and Oxidative Stress

**Claudio Tabolacci** <sup>1,2</sup>, **Cinzia Forni** <sup>3</sup>,  
**Ravirajsinh N. Jadeja** <sup>4</sup>, and **Francesco Facchiano** <sup>2</sup>

<sup>1</sup>Department of Medicine, University Campus Bio-Medico, Rome, Italy

<sup>2</sup>Department of Oncology and Molecular Medicine, Istituto Superiore di Sanità, Rome, Italy

<sup>3</sup>Department of Biology, University of Rome “Tor Vergata”, Rome, Italy

<sup>4</sup>Department of Biochemistry and Molecular Biology, Medical College of Georgia at Augusta University, Augusta, GA, USA

Correspondence should be addressed to Claudio Tabolacci; [claudiotabolacci@tiscali.it](mailto:claudiotabolacci@tiscali.it)

Received 24 April 2019; Accepted 24 April 2019; Published 9 May 2019

Copyright © 2019 Claudio Tabolacci et al. This is an open access article distributed under the Creative Commons Attribution License, which permits unrestricted use, distribution, and reproduction in any medium, provided the original work is properly cited.

Natural products, compounds derived from animals, micro-organisms and, especially, from plants, have been used in prevention and treatment of various human diseases for thousands of years. Some of these bioactive compounds, which have beneficial effects on human health, are also present in foods and beverages. In recent years, the interest towards the use of natural compounds and their derivatives has been renewed, even for the discovery and development of new drugs [1].

Phytochemicals show positive effects on human health by a large variety of mechanisms, including epigenetic modifications, modulation of signal transduction and metabolic pathways, and regulation of antioxidant enzymes activity [2, 3]. This is the reason why they have been extensively studied for their anticancer activities, through the potential modulation of cancer initiation and growth, cellular differentiation, apoptosis and autophagy, angiogenesis, and metastatic dissemination. Moreover, several active herbal compounds are tested in human clinical trials, used as adjuvants with conventional anticancer therapies in order to reduce side effects like nausea and fatigue [4].

Further, phytochemicals are considered today potent and effective weapons against several human diseases, due to their mechanism of action that in many cases is against oxidative stress. In fact, a considerable number of studies reported the use of natural compounds for their anti-inflammatory

activity, since inflammation is considered the basis of various disease conditions, including cancer. The use of herbal preparation in combination with suitable diet represents also one of the most promising strategies to treat metabolic disorders like diabetes, obesity, and metabolic syndrome [5]. Moreover, due to their several biological activities, natural compounds represent good candidates for preventing and even curing the effects of neurodegenerative diseases.

The aim of this Special Issue was to provide a contribution in collecting new findings in the use of natural products against cancer, inflammation, and oxidative stress. After a careful peer review process, twenty-one papers were accepted for publication in this Special Issue, including three review articles and one clinical study.

## Conflicts of Interest

The Guest Editors report no conflicts of interest.

## Acknowledgments

We are grateful to all authors for their important contribution to this Special Issue. We sincerely thank all reviewers for their fundamental efforts. We are also grateful to the Editorial Board of BioMed Research International for giving us the opportunity to take care of a Special Issue focused on a



so important research field. Claudio Tabolacci was partially supported by Fondazione Umberto Veronesi.

Claudio Tabolacci  
Cinzia Forni  
Ravirajsinh N. Jadeja  
Francesco Facchiano

## References

- [1] N. Thomford, D. Senthebane, A. Rowe et al., “Natural products for drug discovery in the 21st century: innovations for novel drug discovery,” *International Journal of Molecular Sciences*, vol. 19, no. 6, p. 1578, 2018.
- [2] E. Ratovitski, “Anticancer natural compounds as epigenetic modulators of gene expression,” *Current Genomics*, vol. 18, no. 2, pp. 175–205, 2017.
- [3] P. Pratheeshkumar, C. Sreekala, Z. Zhang et al., “Cancer prevention with promising natural products: mechanisms of action and molecular targets,” *Anti-Cancer Agents in Medicinal Chemistry*, vol. 12, no. 10, pp. 1159–1184, 2012.
- [4] T. Costea, A. Hudiță, O. Ciolac et al., “Chemoprevention of colorectal cancer by dietary compounds,” *International Journal of Molecular Sciences*, vol. 19, no. 12, p. 3787, 2018.
- [5] L. Carrera-Quintanar, R. I. López Roa, S. Quintero-Fabián et al., “Phytochemicals that influence gut microbiota as prophylactics and for the treatment of obesity and inflammatory diseases,” *Mediators of Inflammation*, vol. 2018, Article ID 9734845, 18 pages, 2018.

## Research Article

# Effect of Immunomodulatory Supplements Based on *Echinacea Angustifolia* and *Echinacea Purpurea* on the Posttreatment Relapse Incidence of Genital Condylomatosis: A Prospective Randomized Study

Nicoletta De Rosa , Pierluigi Giampaolino, Giada Lavitola, Ilaria Morra, Carmen Formisano, Carmine Nappi, and Giuseppe Bifulco

Department of Obstetrics, Gynecology, and Urology, University of Naples "Federico II", Naples, Italy

Correspondence should be addressed to Nicoletta De Rosa; [derosa.nicoletta@gmail.com](mailto:derosa.nicoletta@gmail.com)

Received 11 July 2018; Accepted 6 February 2019; Published 11 April 2019

Guest Editor: Francesco Facchiano

Copyright © 2019 Nicoletta De Rosa et al. This is an open access article distributed under the Creative Commons Attribution License, which permits unrestricted use, distribution, and reproduction in any medium, provided the original work is properly cited.

**Introduction.** HPV infection is a highly infectious disease; about 65% of partners of individuals with genital warts will develop genital condylomatosis. Only in 20-30% it regresses spontaneously and relapse rates range deeply (9-80%). *Echinacea* extracts possess antiviral and immunomodulator activities. The aim of this study was to evaluate the efficacy of the therapy, using a formulation based on HPVADL18® (on dry extracts of 200 mg *Echinacea Purpurea* (EP) roots plus *E. Angustifolia* (EA)), on the posttreatment relapse incidence of genital condylomatosis. **Materials and Methods.** It is a prospective single-arm study. Patients with a satisfactory and positive vulvoscopy, colposcopy, or peniscopy for genital condylomatosis were divided into two random groups and subjected to destructive therapy with Co2 Laser. Group A (N=64) immediately after the laser therapy started a 4-month treatment with oral HPVADL18®; Group B (N=61) did not undergo any additional therapy. Patients were subjected to a follow-up after 1, 6, and 12 months. Differences in relapse incidence between the two groups during follow-up controls were evaluated by  $\chi^2$ -test; the groups were stratified by age, gender, and condylomatosis extension degree. **Results and Discussion.** Gender, age, and condyloma lesions' extension degree showed no statistically significant differences between the two trial groups. The relapse incidence differs statistically between the two studied groups and progressively decreases during the 12 months after treatment in both groups. Statistically significant reduction of relapse rates has been shown in Group A in patients over 25 years old. This difference is significant for both men and women. The relapse incidence is superior in case of extended condylomatosis. **Conclusions.** In conclusion, the presence of a latent infection causes condylomatosis relapse; in order to reduce the relapse risk an induction of a protective immune response seems to be essential to allow rapid viral clearance from genital areas surrounding lesion and treatment zones. *Echinacea* promotes this process. EP and EA dry root extracts seem to be a valid adjuvant therapy in reducing relapse incidence of lesions in patients treated for genital condylomatosis.

## 1. Introduction

HPV infection is one of the most common sexually transmitted infections in the world. More than 50% of sexually active adults contract the infection during their life. In the two years after a sexual debut the sexual risk of infection varies from 40 to 80% depending on the studied population and the HPV type [1]. There is a similar incidence of genital

condylomatosis in males and females (0-2% and 0-7%) [2-4]. In men, compared to women, infections with multiple genotypes and low-oncogenic risk genotypes are more frequent [5]. Only 20-30% of the genital condylomatosis regresses spontaneously. This is a highly infectious disease; about 65% of partners of individuals with genital warts will develop genital condylomatosis. The risk of infection and the risk of progression of HPV-associated lesions are related to several



factors including number of sexual partners experienced during the life and early age of the first intercourse; tobacco smoking; and eating habits [6–8].

It has long since known that the above-ground portion and the roots of *Echinacea Angustifolia* (EA) and of *E. Purpurea* (EP) possess anti-inflammatory and immunostimulatory properties. Numerous *in vitro* and *in vivo* studies have been recently conducted in an effort to validate some of the traditional uses of *Echinacea* extracts [9]. Early studies have shown that only a few *Echinacea* extracts possess significant antiviral activity. In particular, above-ground portions and roots of EP show a strong antiviral activity, as they have a virucidal effect against influenza virus, herpes simplex virus, and coronaviruses [10, 11]. The EP appeared much less effective against intracellular viruses [12, 13], which could be resistant to the EP inhibitory effect; on the contrary, viral particles located in the extracellular fluids appeared to be vulnerable. Therefore, EP can act during an initial contact with virus, that is, at the beginning of infection and also during the transmission of the virus from the infected cells.

Numerous viral and bacterial infections cause an increase of expression of proinflammatory cytokines, in particular, of IL-6 and IL-8, which are therefore considered as markers of an inflammatory state [14, 15]. Any compound or herbal extract that inhibits or inverts the increase of IL-6/8 can be considered a potential anti-inflammatory agent. All the portions of the roots, leaves, stems, and flowers of EP show this effect [16].

These studies make it evident that *Echinacea* not exactly acts as an “immunostimulant” or “immune system booster,” but more likely has an immunomodulatory action, rather than a generalized immunostimulatory effect [17–20].

The aim of the present study was to evaluate the efficacy of the therapy, using a formulation based on 200 mg of HPVADL18® (equal to 4 mg polyphenols plus 0.6 mg of echinacosides), on the post-treatment relapse incidence of genital condylomatosis.

## 2. Materials and Methods

Between July 2014 and July 2017, all patients with a genital condylomatosis diagnosis received in the Colposcopy and Cervical-Vaginal Pathology Unit of University Federico II, Naples, were invited to participate in a prospective randomized trial.

Patients were properly informed and provided their written consent to participate in the trial and to undergo ambulatory diagnostic examinations; afterwards, colposcopy or peniscopy was conducted and, if appropriate, biopsy examinations. All procedures performed in the study were in accordance with the ethical standards of the institutional and/or national research committee and with the 1964 Helsinki Declaration and its later amendments or comparable ethical standards.

The criteria for participation in the trial were as follows: satisfactory and positive colposcopy / peniscopy for genital condylomatosis (cervix, vagina, perianal vulva, or perineum for females and penis, scrotum, or anal region for males) and /

or histological examination for koilocytosis or condylomatosis in case of positive cervical biopsy.

Patients with H-SIL cytological diagnosis, CIN 1-3 histologic diagnosis, or invasive cervical carcinoma, pregnant women, immunosuppressed patients, and individuals infected with Human Immunodeficiency Virus (HIV-positive) were not enrolled in the trial.

Colposcopy and peniscopy were conducted after an application of 3% acetic acid. Visible acetowhite lesions have been classified in accordance with the criteria of the International Federation of Cervical Pathology and Colposcopy [21].

In case of genital condylomatosis, to standardize extension of the lesions, genitals were divided into 10 genital areas for women, that is, cervix, left/right vaginal wall, left/right major labia, left/right minor labia, clitoris, pubis, perineum, and perianus and into 5 genital areas for men, that is, pubis, scrotum, glans, preputial balanus grooves, and penis. Patients were classified into 3 lesion degrees, according to the number of genital areas affected by condylomas and the number of the condylomas:

- (1) From 1 to 5 condylomas on 1-2 genital areas (mild and localized condylomatosis)
- (2) > 5 condylomas on 2-3 genital areas (mild and diffuse condylomatosis)
- (3) > 5 condylomas on > 3 genital areas (extended condylomatosis).

Patients with low grade (ZTAG1) or high grade (ZTAG2) cervical lesions were subjected to a targeted biopsy using a biopsy forceps (CFS CHIMO Schumacher Pliers) with 5-6 mm jaw in order to obtain 4-5 mm tissue specimens.

Two serial 4 micron sections of the formalin-fixed and paraffin-embedded sample were stained with hematoxylin and eosin. The specimens were examined by optical microscope and classified as normal, CIN 1, CIN 2, and CIN 3 carcinoma *in situ* or microinvasive carcinoma according to the criteria of the World Health Organization.

Patients with low grade (CIN 1) or high grade (CIN2-3) preneoplastic lesions were excluded from the trial and carried on all the therapeutic and diagnostic procedures as recommended by national and international guidelines.

Patients with genital condylomatosis, diagnosed through colposcopy, vulvoscopy, peniscopy, and/or biopsy examinations, were included in the study. All enrolled individuals were divided into two random groups and subjected to destructive therapy with Co2 Laser.

Group A immediately after the laser therapy started a 4-month treatment with oral immunomodulatory supplements based on HPVADL18®; Group B did not undergo any additional therapy (control group). The medical device administered to Group A was composed of 200 mg of HPVADL18® (equal to 4 mg polyphenols plus 0.6 mg of echinacosides), 40 mg vitamin C, 5 mg of zinc, and 0.5 mg of copper.

Patients were subjected to a follow-up colposcopy after 1, 6, and 12 months. In case the infection persisted and relapse condyloma lesions occurred, patients were again subjected to destructive therapy until the full lesion elimination.

TABLE 1: Clinical characteristics of the study groups.

	Group A N = 64 N (%)	Group B N = 61 N (%)	P value <sup>1</sup>
<i>Age (years)</i>			
≤ 25	9 (14.1)	7 (11.5)	NS
> 25	55 (85.9)	54 (88.5)	
<i>Gender</i>			
Females	48 (75.0)	41 (68.9)	NS
Males	16 (25.0)	19 (31.1)	
<i>Grade<sup>2</sup></i>			
1	37 (57.8)	33 (54.1)	NS
2	22 (34.4)	22 (36.1)	
3	5 (7.8)	6 (9.8)	

<sup>1</sup>χ<sub>2</sub> test.

<sup>2</sup>Patients were classified into 3 lesion degrees, according to the number of genital areas affected by condylomas and the number of the condylomas: (1) from 1 to 5 condylomas on 1-2 genital areas (mild and localized condylomatosis); (2) > 5 condylomas on 2-3 genital areas (mild and diffuse condylomatosis); and (3) > 5 condylomas on > 3 genital areas (extended condylomatosis).

All colposcopy, peniscopy and biopsy examinations and therapies were performed by our team.

**2.1. Statistical Analysis.** Statistical analysis of the data was executed by SPSS software 20.0 (SPSS Inc., Chicago, IL, USA). Data with p-values <0.05 were considered statistically significant.

Demographic and clinical data of the two groups were compared by Student's t-test for the data with parametric distribution (age) and by χ<sub>2</sub>-test for ordinal variables (gender and condylomatosis extension degree). Differences in relapse incidence between two groups during follow-up controls were evaluated by χ<sub>2</sub>-test; the groups were stratified by age, gender, and condylomatosis extension degree.

### 3. Results

One hundred and forty women appeared to be suitable for destructive therapy with Co2 Laser and were divided into Group A (n = 70) and Group B (n = 70) at random. Of these, 6 patients did not undergo a required operation and 9 patients did not undergo a programmed follow-up or interrupted the therapy before the 4-month period expired.

One hundred and twenty-five patients, 90 (72%) women and 35 (28%) men, completed the diagnostic-therapeutic procedure as scheduled by the protocol and were therefore included in the analysis. Of the studied population, 64 women (51.2%) underwent Echinacea therapy after the treatment (Group A) and 61 (48.8%) did not undergo any additional therapy (Group B, control group). The mean age of female patients in Group A is 33.0±8.4 years, in Group B 32.1±7.3 years (p = N.S.); the mean age of male patients in Group A is 31.4±7.2 years, in Group B 34.4±7.1 years (p = NS). Table 1 shows epidemiological data and condyloma lesions' extension degree for Groups A and B. There were no statistically significant differences in these data in the two trial

groups. No severe side effects were recorded in Group A. Only 5 (7.8%) patients reported some digestive difficulties.

The relapse incidence differs statistically between the two studied groups (Table 2, Figure 1) and progressively decreases during the 12 months after treatment in both groups. Therapy does not seem to modify the relapse incidence in very young female patients under the age of 25. Instead, statistically significant reduction of relapse rates has been shown in patients over 25 years old. This difference is significant for both men and women. The relapse incidence is superior in case of extended condylomatosis (extension degree n.3) (Table 2, Figure 1).

### 4. Discussion and Conclusions

Clinical trials conducted on patients with genital condylomatosis show quite different relapse rates, depending on the studies and on the treatment and range from 9% to 80% [22–25]. Our data show a global relapse rate of about 30%.

Therapy with HPVADL18 is effective in reducing relapse incidence of lesions in patients treated for genital condylomatosis. Our data prove, indeed, that the relapse incidence of lesion is greater in the control group compared to the treatment group at the first, second, and third follow-up controls.

Spontaneous remission of genital condylomatosis is possible, but not frequent; the percentage of spontaneously recovered patients varies considerably and ranges from 0% to 50% [24, 25].

Most commonly used therapy is cryotherapy or diathermocoagulation (65% and 28%); drug therapy is much less frequent (6%). Approximately 50% of patients undergo a single treatment procedure; the number of patients that undergo more than one treatment procedures progressively decreases; 3% of patients undergo 5 or more treatments [26].

TABLE 2: Posttreatment relapse incidence of genital condylomatosis stratified for age, gender, and grade.

		Group A N = 64 N (%)	Group B N = 61 N (%)	P value <sup>1</sup>
<i>1-month follow-up</i>				
Total group	Negative	54 (84.4)	36 (59.0)	<.01
	Positive	10 (15.6)	25 (41.0)	
<i>Age (years)</i>				
≤ 25	Negative	6 (66.7)	3 (42.9)	NS
	Positive	3 (33.3)	4 (57.1)	
> 25	Negative	48 (87.3)	33 (61.1)	<.01
	Positive	7 (12.7)	21 (38.9)	
<i>Gender</i>				
Females	Negative	42 (87.5)	29 (69.0)	<.05
	Positive	6 (12.5)	13 (31.0)	
Males	Negative	12 (75.0)	7 (36.8)	<.05
	Positive	4 (25.0)	12 (63.2)	
<i>Grade<sup>2</sup></i>				
1	Negative	34 (91.9)	25 (75.8)	NS
	Positive	3 (8.1)	8 (24.2)	
2	Negative	17 (77.3)	11 (50.0)	NS
	Positive	5 (22.7)	11 (50.0)	
3	Negative	3 (60.0)	0 (0)	<.05
	Positive	2 (40.0)	6 (100)	
<i>6-month follow-up</i>				
Total	Negative	56 (87.5)	37 (60.7)	<.001
	Positive	8 (12.5)	24 (39.3)	
<i>Age (years)</i>				
≤ 25	Negative	7 (77.8)	4 (57.1)	NS
	Positive	2 (22.2)	3 (42.9)	
> 25	Negative	49 (89.1)	33 (61.1)	<.001
	Positive	6 (10.9)	21 (38.9)	
<i>Gender</i>				
Females	Negative	43 (89.6)	30 (71.4)	<.05
	Positive	5 (10.4)	12 (28.6)	
Males	Negative	13 (81.2)	7 (36.8)	<.05
	Positive	3 (18.8)	12 (63.2)	
<i>Grade<sup>2</sup></i>				
1	Negative	35 (94.6)	25 (75.8)	<.05
	Positive	2 (5.4)	8 (24.2)	
2	Negative	17 (77.3)	11 (50.0)	NS
	Positive	5 (22.7)	11 (50.0)	
3	Negative	4 (80.0)	1 (16.7)	<.05
	Positive	1 (20.0)	5 (83.3)	
<i>12-month follow-up</i>				
Total	Negative	61 (95.3)	44 (72.1)	<.0001
	Positive	3 (4.7)	17 (27.9)	
<i>Age (years)</i>				
≤ 25	Negative	9 (100.0)	5 (71.4)	NS

TABLE 2: Continued.

		Group A N = 64 N (%)	Group B N = 61 N(%)	P value <sup>1</sup>
> 25	Positive	0 (0)	2 (28.6)	<.005
	Negative	52 (94.5)	39 (72.2)	
	Positive	3 (5.5)	15 (27.8)	
Gender				
Females	Negative	45 (93.8)	32 (76.2)	<.05
	Positive	3 (6.2)	10 (23.8)	<.05
Males	Negative	16 (100)	12 (63.2)	
	Positive	0 (0)	7 (36.8)	
Grade <sup>2</sup>				
1	Negative	37 (100)	29 (87.9)	<.05
	Positive	0 (0)	4 (12.1)	
2	Negative	19 (86.4)	14 (63.6)	NS
	Positive	3 (13.6)	8 (36.4)	
3	Negative	5 (100)	1 (16.7)	<.05
	Positive	0 (0)	5 (83.3)	

<sup>1</sup>X<sub>2</sub> test.  
<sup>2</sup>Patients were classified into 3 lesion degrees, according to the number of genital areas affected by condylomas and the number of the condylomas: (1) from 1 to 5 condylomas on 1-2 genital areas (mild and localized condylomatosis); (2) > 5 condylomas on 2-3 genital areas (mild and diffuse condylomatosis); and (3) > 5 condylomas on > 3 genital areas (extended condylomatosis).

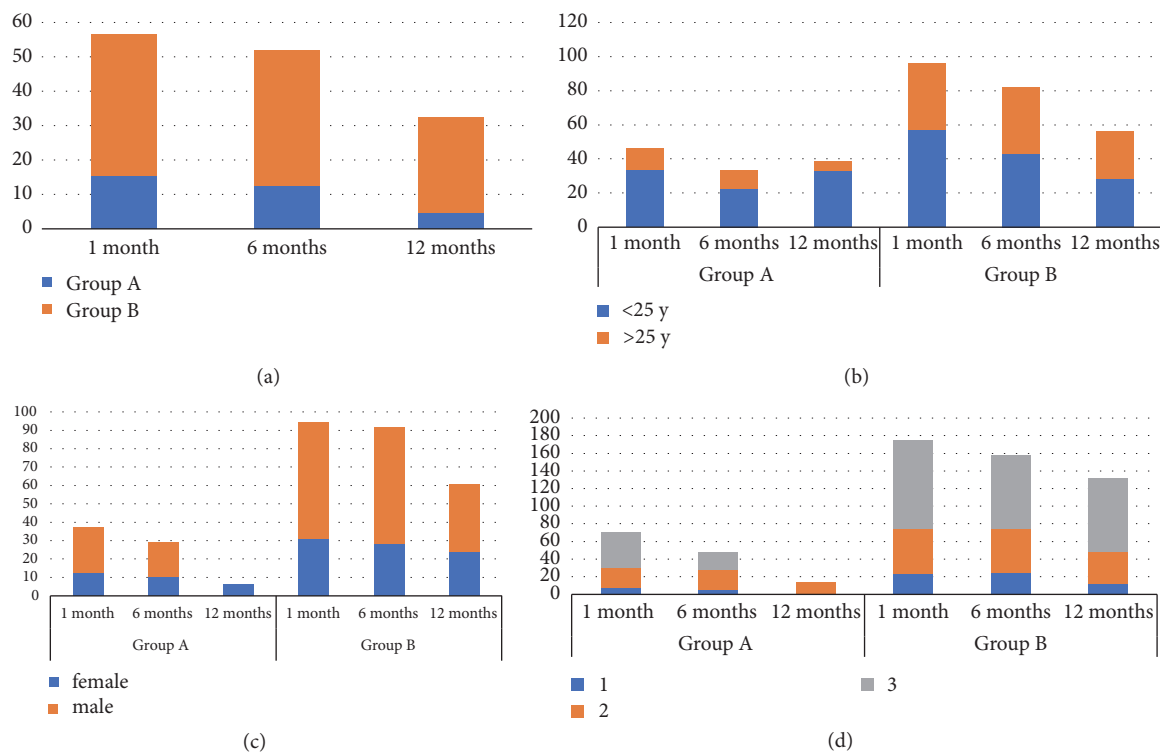


FIGURE 1: (a) Posttreatment relapses incidence in both study groups; (b) posttreatment relapses incidence stratified by age; (c) posttreatment relapses incidence stratified by sex; and (d) posttreatment relapses incidence stratified by lesion extension degree.

This pattern is similar for both sexes and is according to the anatomical site [26].

In compliance with these data, the difference in relapse incidence between the two trial groups is statistically significant even when these are stratified by gender and extension degree of the lesion.

On the other hand, age appears to be a determinant factor; in fact, in individuals under the age of 25, the therapy does not seem to influence significantly the relapse incidence of lesion. The small numbers of younger age groups, however, cannot induce us to generalize this data.

Based on these data, it follows that in very young individuals additional therapy with HPVADL18 could be superfluous. Moreover, individuals under the age of 25 show greater relapse incidence at the first follow-up.

The relapse incidence decreases progressively in both groups as the time passes and is related to the extension degree; in fact, the extension degree 3 of condylomatous lesions corresponds to a higher relapse incidence than degrees 1 and 2.

The presence of a latent infection causes lesion relapse; in order to reduce the relapse risk after the treatment of condyloma lesions, an induction of a protective immune response seems to be essential to allow rapid viral clearance from genital areas surrounding lesion and treatment zones. Introduction of an immunostimulatory substance such as Echinacea seems to promote this process.

The HPV-induced immune response is both humoral and cell mediated.

A humoral immune response to HPV capsid protein L1 is weak during natural infection.

The humoral immune response to the viral capsid can be detected averagely starting from 6 months after the infection, though 30-50% of patients with persistent infection will never present a seroconversion [27]. The seropositivity to the infectious genotype persists only in 50% of the cases, even when the initial lesion transformed to a cervical cancer [28]. When viral DNA has been eliminated, specific antibodies can be detected only in half of cases after 5 years [29].

HPV infection promotes a cellular immune response, especially in the active phase of the clearance of genital condylomatosis infection, when a cell infiltration of macrophages and T cells develops in correspondence to the lesion [30]. In the blood, an immune response of CD4+ T cells against E2, E6, and E7 proteins is associated with HPV 16 and HPV 18 infection and occurs in particular in early disease phases and in case of regressing lesions, less when a persistent disease takes place.

In individuals with a deficiency of cell-mediated immune response, HPV infection, genital condylomatosis, or precancerous lesions are destined to persist. Therefore, this type of response seems to be essential for the viral clearance.

The EP immunomodulatory effect has been widely demonstrated. EP extract was used for the preventive care and for the treatment of various viral infections [31].

In vitro studies have shown that EP acts directly on a number of cell types, including natural killer cells [32], polymorphonuclear leukocytes [33], and macrophages [34]. EP induces a proliferation of T cells. This has been conferred

to the activation of macrophages that stimulates a production of IFN- $\gamma$  and, consequently, a secondary activation of T lymphocytes [35]. IFN- $\gamma$  is one of the fundamental mediators for the latency prevention [36]; it has been proven that this mechanism is responsible for reducing the latency incidence of herpes virus simplex infection and, consequently, reducing the relapse risk of HSV lesions [36]. It is possible that an analogous mechanism induces a cell-mediated response to HPV infection, which allows the reduction of the persistence of infection and, therefore, the lesion relapse.

This study has some limitations: this is a single institution study with a small number of participants and it lacks placebo controls. On the other hand, the strengths of this study are as follows: the rigorous inclusions criteria, the evaluation of patients at colposcope (so not only grossly visible genital warts were evaluated and treated but also small lesions), and the treatment modality with laser CO2 for all patients.

In conclusion, HPVADL18® seems to be a valid adjuvant therapy in reducing relapse incidence of lesions in patients treated for genital condylomatosis.

## Data Availability

The data used to support the findings of this study are included within the article.

## Conflicts of Interest

The authors state that there are no conflicts of interest.

## References






- [1] P. L. Reiter, W. F. Pendergraft, and N. T. Brewer, "Meta-analysis of human papillomavirus infection concordance," *Cancer Epidemiology Biomarkers & Prevention*, vol. 19, no. 11, pp. 2916–2931, 2010.
- [2] Health Protection Agency, "Trends in genital warts and genital herpes diagnoses in the United Kingdom," *Health Protection Report*, vol. 1, no. 35, pp. 4–9, 2007.
- [3] J. Monsonégo, J.-G. Breugelmans, S. Bouée, A. Lafuma, S. Bénard, and V. Rémy, "Anogenital warts incidence, medical management and costs in women consulting gynaecologists in France," *Gynecologie Obstetrique et Fertilité*, vol. 35, no. 2, pp. 107–113, 2007.
- [4] X. Castellsagué, C. Cohet, L. M. Puig-Tintoré et al., "Epidemiology and cost of treatment of genital warts in Spain," *European Journal of Public Health*, vol. 19, no. 1, pp. 106–110, 2009.
- [5] A. G. Nyitray, L. Menezes, B. Lu et al., "Genital human papillomavirus (HPV) concordance in heterosexual couples," *The Journal of Infectious Diseases*, vol. 206, no. 2, pp. 202–211, 2012.
- [6] R. L. Winer, Q. Feng, J. P. Hughes, S. O'Reilly, N. B. Kiviat, and L. A. Koutsky, "Risk of female human papillomavirus acquisition associated with first male sex partner," *The Journal of Infectious Diseases*, vol. 197, no. 2, pp. 279–282, 2008.
- [7] S. K. Kjaer, B. Chackerian, A. J. C. van den Brule et al., "High-risk human papillomavirus is sexually transmitted: evidence from a follow-up study of virgins starting sexual activity (intercourse)," *Cancer Epidemiology, Biomarkers & Prevention*, vol. 10, no. 2, pp. 101–106, 2001.



- [8] P. C. Giraldo, J. Eleutério Jr., D. I. M. Cavalcante, A. K. S. Gonçalves, J. A. A. Romão, and R. M. N. Eleutério, "The role of high-risk HPV-DNA testing in the male sexual partners of women with HPV-induced lesions," *European Journal of Obstetrics & Gynecology and Reproductive Biology*, vol. 137, no. 1, pp. 88–91, 2008.
- [9] M. Sharifi-Rad, D. Mnayer, M. F. Morais-Braga et al., "Echinacea plants as antioxidant and antibacterial agents: From traditional medicine to biotechnological applications," *Phytotherapy Research*, vol. 32, no. 9, pp. 1653–1663, 2018.
- [10] J. Hudson, S. Vimalanathan, L. Kang, V. T. Amiguet, J. Livesey, and J. T. Arnason, "Characterization of antiviral activities in Echinacea root preparations," *Pharmaceutical Biology*, vol. 43, no. 9, pp. 790–796, 2005.
- [11] S. Vimalanathan, L. Kang, V. T. Amiguet, J. Livesey, J. T. Arnason, and J. Hudson, "Echinacea purpurea aerial parts contain multiple antiviral compounds," *Pharmaceutical Biology*, vol. 43, no. 9, pp. 740–745, 2005.
- [12] S. Pleschka, M. Stein, R. Schoop, and J. B. Hudson, "Antiviral properties and mode of action of standardized Echinacea purpurea extract against highly pathogenic avian Influenza virus (H5N1, H7N7) and swine-origin H1N1 (S-OIV)," *Virology Journal*, vol. 6, p. 197, 2009.
- [13] M. Sharma, S. A. Anderson, R. Schoop, and J. B. Hudson, "Induction of multiple pro-inflammatory cytokines by respiratory viruses and reversal by standardized Echinacea, a potent antiviral herbal extract," *Antiviral Research*, vol. 83, no. 2, pp. 165–170, 2009.
- [14] J. J. Burns, L. Zhao, E. W. Taylor, and K. Spelman, "The influence of traditional herbal formulas on cytokine activity," *Toxicology*, vol. 278, no. 1, pp. 140–159, 2010.
- [15] J. B. Calixto, M. M. Campos, M. F. Otuki, and A. R. S. Santos, "Anti-inflammatory compounds of plant origin. Part II. Modulation of pro-inflammatory cytokines, chemokines and adhesion molecules," *Planta Medica*, vol. 70, no. 2, pp. 93–103, 2004.
- [16] S. Vimalanathan, J. T. Arnason, and J. B. Hudson, "Anti-inflammatory activities of Echinacea extracts do not correlate with traditional marker components," *Pharmaceutical Biology*, vol. 47, no. 5, pp. 430–435, 2009.
- [17] M. Altamirano-Dimas, M. Sharma, and J. B. Hudson, "Echinacea and anti-inflammatory cytokine responses: Results of a gene and protein array analysis," *Pharmaceutical Biology*, vol. 47, no. 6, pp. 500–508, 2009.
- [18] A. Matthias, L. Banbury, L. M. Stevenson, K. M. Bone, D. N. Leach, and R. P. Lehmann, "Alkylamides from echinacea modulate induced immune responses in macrophages," *Immunological Investigations*, vol. 36, no. 2, pp. 117–130, 2007.
- [19] P. Guiotto, K. Woelkart, I. Grabnar et al., "Pharmacokinetics and immunomodulatory effects of phytotherapeutic lozenges (bonbons) with Echinacea purpurea extract," *Phytomedicine*, vol. 15, no. 8, pp. 547–554, 2008.
- [20] A. M. Sullivan, J. G. Laba, J. A. Moore, and T. D. G. Lee, "Echinacea-induced macrophage activation," *Immunopharmacology and Immunotoxicology*, vol. 30, no. 3, pp. 553–574, 2008.
- [21] J. Bornstein, J. Bentley, P. Bösze et al., "2011 colposcopic terminology of the international federation for cervical pathology and colposcopy," *Obstetrics & Gynecology*, vol. 120, no. 1, pp. 166–172, 2012.
- [22] L. A. Brodell, M. G. Mercurio, and R. T. Brodell, "The diagnosis and treatment of human papillomavirus-mediated genital lesions," *Cutis; Cutaneous Medicine for the Practitioner*, vol. 79, no. 4, pp. 5–10, 2007.
- [23] N. Scheinfeld and D. S. Lehman, "An evidence-based review of medical and surgical treatments of genital warts," *Dermatology Online Journal*, vol. 12, no. 5, 2006.
- [24] D. J. Wiley, J. Douglas, K. Beutner et al., "External genital warts: diagnosis, treatment, and prevention," *Clinical Infectious Diseases*, vol. 35, supplement 2, pp. S210–S224, 2002.
- [25] C. M. Kodner and S. Nasraty, "Management of genital warts," *American Family Physician*, vol. 70, no. 12, pp. 2335–2346, 2004.
- [26] M. M. Gianino, S. Delmonte, E. Lovato et al., "A retrospective analysis of the costs and management of genital warts in Italy," *BMC Infectious Diseases*, vol. 13, no. 1, p. 470, 2013.
- [27] J. J. Carter, L. A. Koutsy, J. P. Hughes et al., "Comparison of human papillomavirus types 16, 18, and 6 capsid antibody responses following incident infection," *The Journal of Infectious Diseases*, vol. 181, no. 6, pp. 1911–1919, 2000.
- [28] J. J. Carter, M. M. Madeleine, K. Shera et al., "Human papillomavirus 16 and 18 L1 serology compared across anogenital cancer sites," *Cancer Research*, vol. 61, no. 5, pp. 1934–1940, 2001.
- [29] S. S. Wang, M. Schiffman, R. Herrero et al., "Determinants of human papillomavirus 16 serological conversion and persistence in a population-based cohort of 10 000 women in Costa Rica," *British Journal of Cancer*, vol. 91, no. 7, pp. 1269–1274, 2004.
- [30] S. A. Jenison, X.-P. Yu, J. M. Valentine, and D. A. Galloway, "Characterization of human antibody-reactive epitopes encoded by human papillomavirus types 16 and 18," *Journal of Virology*, vol. 65, no. 3, pp. 1208–1218, 1991.
- [31] B. P. Barrett, R. L. Brown, K. Locken, R. Maberry, J. A. Bobula, and D. D'Alessio, "Treatment of the common cold with unrefined Echinacea: A randomized, double-blind, placebo-controlled trial," *Annals of Internal Medicine*, vol. 137, no. 12, pp. 939–946, 2002.
- [32] N. L. Currier and S. C. Miller, "Echinacea purpurea and melatonin augment natural-killer cells in leukemic mice and prolong life span," *The Journal of Alternative and Complementary Medicine*, vol. 7, no. 3, pp. 241–251, 2001.
- [33] D. R. Cundell, M. A. Matrone, P. Ratajczak, and J. D. Pierce Jr., "The effect of aerial parts of Echinacea on the circulating white cell levels and selected immune functions of the aging male Sprague-Dawley rat," *International Immunopharmacology*, vol. 3, no. 7, pp. 1041–1048, 2003.
- [34] V. Goel, C. Chang, J. V. Slama et al., "Echinacea stimulates macrophage function in the lung and spleen of normal rats," *The Journal of Nutritional Biochemistry*, vol. 13, no. 8, pp. 487–492, 2002.
- [35] L. Corey, "The current trend in genital herpes: progress in prevention," *Sexually Transmitted Diseases*, vol. 21, no. 2, pp. S38–S44, 1994.
- [36] R. L. Sparks-Thissen, D. C. Braaten, and K. Hildner, "CD4 T cell control of acute and latent murine gamma herpes virus infection requires IFN $\gamma$ ," *Virology*, vol. 338, no. 2, pp. 201–208, 2005.

## Review Article

# Beneficial Role of Phytochemicals on Oxidative Stress and Age-Related Diseases

**Cinzia Forni,<sup>1</sup> Francesco Facchiano ,<sup>2</sup> Manuela Bartoli,<sup>3</sup> Stefano Pieretti,<sup>4</sup> Antonio Facchiano ,<sup>5</sup> Daniela D'Arcangelo ,<sup>5</sup> Sandro Norelli,<sup>6</sup> Giorgia Valle,<sup>1</sup> Roberto Nisini ,<sup>6</sup> Simone Beninati ,<sup>1</sup> Claudio Tabolacci ,<sup>7</sup> and Ravirajsinh N. Jadeja ,<sup>8</sup>**

<sup>1</sup>Department of Biology, University of Rome "Tor Vergata", Rome, Italy

<sup>2</sup>Department of Oncology and Molecular Medicine, Istituto Superiore di Sanità, Rome, Italy

<sup>3</sup>Department of Ophthalmology, Medical College of Georgia at Augusta University, Augusta, GA, USA

<sup>4</sup>National Center for Drug Research and Evaluation, Istituto Superiore di Sanità, Rome, Italy

<sup>5</sup>Laboratory of Molecular Oncology, Istituto Dermopatico dell'Immacolata, IDI-IRCCS, Rome, Italy

<sup>6</sup>Department of Infectious Diseases, Istituto Superiore di Sanità, Rome, Italy

<sup>7</sup>Department of Medicine, University Campus Bio-Medico, Rome, Italy

<sup>8</sup>Department of Biochemistry and Molecular Biology, Medical College of Georgia at Augusta University, Augusta, GA, USA

Correspondence should be addressed to Claudio Tabolacci; [claudiotabolacci@tiscali.it](mailto:claudiotabolacci@tiscali.it)

Received 29 November 2018; Revised 11 February 2019; Accepted 20 March 2019; Published 7 April 2019

Academic Editor: Ji-Fu Wei

Copyright © 2019 Cinzia Forni et al. This is an open access article distributed under the Creative Commons Attribution License, which permits unrestricted use, distribution, and reproduction in any medium, provided the original work is properly cited.

Aging is related to a number of functional and morphological changes leading to progressive decline of the biological functions of an organism. Reactive Oxygen Species (ROS), released by several endogenous and exogenous processes, may cause important oxidative damage to DNA, proteins, and lipids, leading to important cellular dysfunctions. The imbalance between ROS production and antioxidant defenses brings to oxidative stress conditions and, related to accumulation of ROS, aging-associated diseases. The purpose of this review is to provide an overview of the most relevant data reported in literature on the natural compounds, mainly phytochemicals, with antioxidant activity and their potential protective effects on age-related diseases such as metabolic syndrome, diabetes, cardiovascular disease, cancer, neurodegenerative disease, and chronic inflammation, and possibly lower side effects, when compared to other drugs.

## 1. Introduction

Aging in multicellular organisms is a biological process characterized by the progressive decline of cellular functions and by diminished tissue renewal capability, leading to a reduced ability to counteract the environmental stressors. Aging is controlled by several heterogeneous mechanisms involving genetic, epigenetic, and environmental factors [1, 2]. As largely demonstrated by literature data, aging has a strong relationship with several pathological conditions, including metabolic syndrome, obesity, cardiovascular diseases (CVD), cancer, and neurodegenerative diseases [3, 4]. Interestingly,

the age-related pathologies are tightly associated with an increase in Reactive Oxygen Species (ROS) and subsequent oxidative stress [4]. In particular, a large number of studies emphasizes the antioxidant potential of natural compounds ("phytochemicals") (Figure 1). Since oxidative stress and inflammation are closely related to pathophysiological processes, here we focused our attention on phytochemicals with well-known anti-inflammatory effects. Starting from the large available literature, the most used compounds and with the strongest evidence-based efficacy were summarized in Figure 2.

TABLE 1: Some of the plant metabolites possessing antioxidant and antitumor activities.

Secondary metabolites	Common dietary sources	References
Polyphenols	Fruit, vegetables, coffee, tea, and cereals	[5, 6]
Anthocyanins	Strawberries, black rice, berries, cherry etc.	[7, 8]
Flavones	Blueberries, blood orange juice	[9]
Flavonols	Cherries, chokeberry, elderberries, Goji berry (wolfberry)	[9]
Resveratrol	Purple wine, peanuts	[10, 11]
Theaflavins	Black tea	[8, 12]
Carotenoids	Carrots, tomatoes, pumpkins, peppers, among others	[6, 13]
Lycopene	Tomatoes, watermelon, red peppers, papaya, apricot, pink grapefruit	[14, 15]

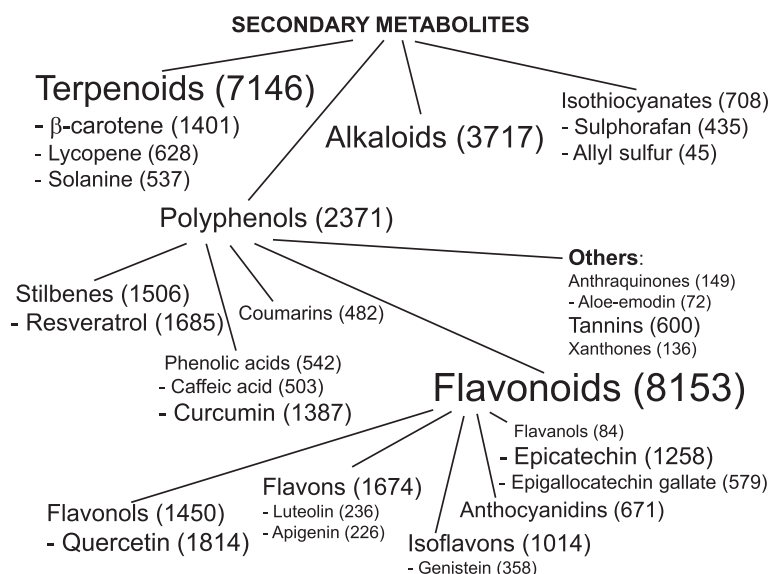


FIGURE 1: A word-tree-cloud showing the body of published evidence indexed on PubMed up today, regarding the most studied phytochemicals as related to oxidative stress. Between brackets, the number of published manuscripts containing the name of each phytochemical and “oxidative stress”, within Title or Abstract, is reported.

## 2. Plant Secondary Metabolites as Powerful Antioxidant Agents

Phytochemicals are a powerful group of compounds, belonging to secondary metabolites of plants and including a diverse range of chemical entities such as polyphenols, flavonoids, steroidal saponins, organosulphur compounds, and vitamins. They have important roles in plant development, being part of relevant physiological process, i.e., reproduction, symbiotic association, and interactions with other organisms and the environment. Even though most of these compounds occur constitutively, their synthesis can be enhanced under stress conditions, in a manner dependent on the growth conditions and on stressor [16–18]. In plants, following the exposure to stressful conditions, an oxidative burst may cause an imbalance between ROS production and scavenging, leading

to the activation of reactive antioxidant enzymatic and non-enzymatic responses [16]. The first one includes changes in the activity of antioxidant enzymes, such as superoxide dismutase, peroxidases, and catalase, while the non-enzymatic response is related to the synthesis of low molecular (ascorbic acid, glutathione, carotenoids, phenolic acids, flavonoids, and others) and high molecular weight antioxidants (tannins).

Many of these plant metabolites have been tested on animal and human cells, showing very interesting biological activities (Table 1). They have been shown to be useful in pharmaceutical applications and in cosmetics, nutrition, and dietary supplements [19]. Plants have been always considered as source of food and medical compounds [20]: actually, up to 200 species are considered as medicinal plants and about 25% of the medicines have plants origins [21]. Most of phytochemicals, components of food, beverages, and herbal

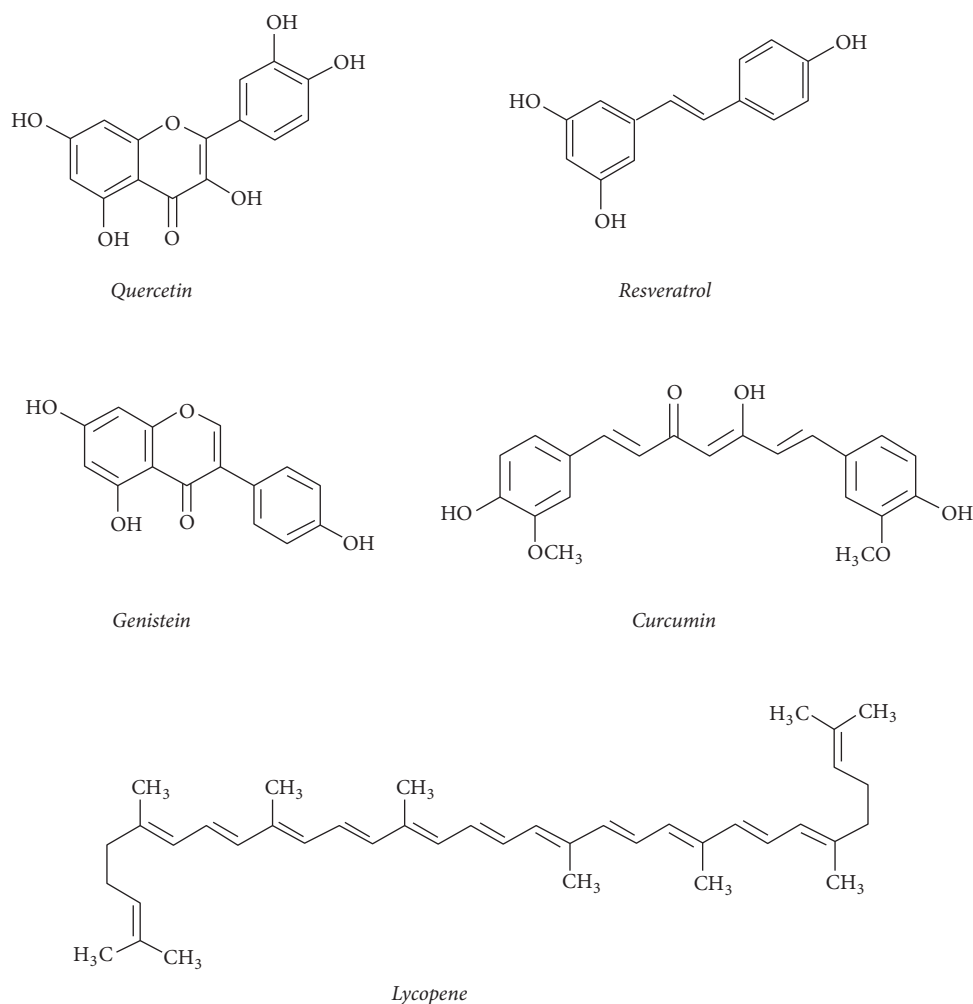


FIGURE 2: Structures of main secondary plant metabolites with demonstrated antioxidant and anti-inflammatory activity summarized in this review.

products are often reported in literature as “nutraceutical”, emphasizing their health promoting properties, including the prevention and treatment of pathologies like cancer, cardiovascular diseases, neural disorders, and Alzheimer’s disease [22], as reported in the following paragraphs. Thus a plethora of information on the effects of phytochemicals on *in vitro* and *in vivo* systems is available in the literature. It is worthy to underline that the antioxidant activity of plant metabolites, detected by *in vitro* assays, does not always correspond to an effective action *in vivo*. This may be due to different metabolic processes that can affect their antioxidant activity [23] (see also paragraph 3 of this paper); thus some *in vitro* data have to be considered with caution.

The first antioxidant molecule discovered is ascorbic acid, i.e., vitamin C, that is, produced during aerobic metabolism, and reacts rapidly with  $O_2^{\bullet-}$ , singlet oxygen and ozone (chemically), and  $H_2O_2$  (enzymatically) through ascorbate peroxidase to neutralize their toxic effects. Besides this, in plants, such acid is also involved in the regeneration of carotenoids and vitamin E (tocopherol). The latter can also act as antioxidant and important liposoluble redox

system, providing protection against lipid peroxidation [24]. Data from *in vitro* studies have shown that  $\beta$ -carotene can regenerate tocopherol from the tocopheroxyl radical; then the resulting carotenoid radical cation may be repaired by vitamin C [25]. The role of vitamins as potent antioxidants has been recently reviewed [26]; therefore, we decided to be more focused on other food-derived phytochemicals.

Carotenoids, responsible for many of the red, orange, and yellow hues of flowers, leaves, and fruits, are powerful antioxidants. Readily available due to their large occurrence in fruits and vegetables (Table 1), their antioxidant activity is based on the scavenging peroxyl radicals [27]. The number of conjugated double bonds of these molecules is related to the efficiency of quenching, i.e.,  $\alpha$ - and  $\beta$ -carotene, but also zeaxanthin, cryptoxanthin belong to the group of highly active quenchers of  $^1O_2$  [25]. For example, lycopene, an intermediate in biosynthetic pathway of carotenoids, acts as scavenger of ROS, lipid peroxyl radicals, and nitric oxide and may exert protective activity against cancer, atherosclerosis, diabetes, and diseases related to inflammatory processes [28]. Synergistic effects in scavenging reactive nitrogen species

have been reported for  $\beta$ -carotene and vitamins C and E [25]. While several data show the antioxidant activity of carotenoids, controversy exists about their antioxidant potential in biological systems, since a number of factors may affect their efficacy and, in some cases, prooxidant effects at high concentration and oxygen pressure have been reported [29].

The most promising molecules for further health promoting studies are phenolic compounds. These phytochemicals comprehend a vast range of molecules (about 8000 different structures), playing important roles in the life of plants [30], where they are widely distributed. These compounds can be divided into phenolic acids, lignans, lignins, stilbenes, tannins, and flavonoids, as schematically summarized in Figure 1. Even though they are constitutively present, stressful growth conditions and/or changes of growth medium components may further induce their synthesis and can be used to enhance their production by *in vitro* plant cultures [31, 32]. In plants, phenolics are involved in  $H_2O_2$  detoxification, providing protection against UV radiation, also acting as enzyme modulators and feeding deterrents for herbivores [33]. The broad spectrum of biological activities of phenolics, among which antioxidant (i.e., reducing agents, free radical scavenger, and quenchers of single oxygen formation) and antitumor properties, is widely acknowledged in several studies [23, 34]. The presence of at least one phenol ring is important for such activity, with hydroxyl, methyl, or acetyl groups replacing the hydrogen. An increased antioxidant activity has been related to the enhanced number of free hydroxyls and conjugation of side chains to aromatic rings [35].

Flavonoids contain the following subclasses: flavonols, flavones, flavanones, flavan-3-ols, isoflavones, and anthocyanidins. They have attracted the attention of the researchers because of their positive effects on a number of diseases as reported in this review. For instance, quercetin and anthocyanins have been reported to be effective in reducing the growth rate of malignant cells, influencing carcinogen metabolism, reducing parameters of tissue inflammation, and inhibiting angiogenesis [7, 36]. According to some authors, the antitumor activities of phenolic compounds may be related to apoptosis, scavenging of radicals, antioxidant, and prooxidant characteristics [37].

Terpenoids represent another very large family of plant secondary metabolites [38]. *In vitro* assays showed that monoterpenes, sesquiterpenes, and diterpenes extracted from aromatic plants have notable antioxidant activity [39]. The hypoglycemic and antioxidant activity of the alkaloid vindoline, vindolidine, vindolicine, and vindolinine, obtained from *Catharanthus roseus* leaves, have been reported [40]. Moreover, vindolicine shows the highest antioxidant effects, and also decreases  $H_2O_2$ -induced oxidative damage to pancreatic cells, suggesting it as a potential antidiabetic agent.

### 3. Natural Compounds and Inflammation

It is well known that ROS represent physiologic activators of transcription factors, such as Activator Protein-1 (AP-1) or Nuclear Factor  $\kappa$ B (NF- $\kappa$ B), which in turn are able to modulate the transcription of proinflammatory cytokines

such as Tumor Necrosis Factor  $\alpha$  (TNF- $\alpha$ ), Interleukin (IL)-6, IL-8, and IL-1 [41]. In fact, ROS, acting as an intracellular signaling component, are associated with inflammatory response and with autoimmune diseases [42]. Therefore, the use of natural products with antioxidant and anti-inflammatory activity represents an intriguing strategy for future clinical applications. These natural compounds have been shown to interfere with various proinflammatory mediators. Herbal medicines, nutraceuticals, which contain food or plant-derived constituents, or functional foods with anti-inflammatory features, can be used as complementary to anti-inflammatory drugs leading to the reduction in dose level of such drugs, thereby reducing their side effects. Phytochemicals with anti-inflammatory activities have been systematically reviewed [43].

A wide range of flavonoids with various chemical structures was associated with different anti-inflammatory mechanistic effects [44]. Glycosides of apigenin and luteolin are the most diffuse flavones. Important edible sources of flavones are parsley, rosemary, and celery [45]. Apigenin suppresses nitric oxide (NO) and prostaglandin production via inhibition of inducible nitric oxide synthase (iNOS) and COX-2, respectively [46]. Luteolin was also proved to inhibit chronic inflammation by *in vitro* co-culture of adipocytes and macrophages and the phosphorylation of JNK in macrophages [47]. One of the most studied flavonols is quercetin, which may be found in various vegetables and fruits, such as apples. Apple flavonoids have been associated with anti-inflammatory effects. In particular, quercetin and its glycosides were demonstrated to be potent anti-inflammatory agents on sarcoidosis patients and *in vivo* models of arthritis and allergic airway inflammation [48, 49].

Flavonoids and flavones from fruits of the *Citrus* spp. inhibit a range of pro-inflammatory mediators, including those derived from the arachidonic acid cascade [50]. In fact, *Citrus* flavanones (e.g., naringenin) mediate anti-inflammatory effects by modulating neuro-inflammation via interaction with p38 signaling cascades and STAT-1 [51] or suppressing the inflammatory response in an animal model of arthritis when administered orally [52].

Genistein, daidzein, and glycitein are isoflavones found almost exclusively in leguminous plants like soya (*Glycine max*). Genistein may inhibit inflammation inhibiting NF- $\kappa$ B activation, downregulating TNF- $\alpha$  and IL-6 expression and secretion, endothelin-1, and vascular cell adhesion molecule-1 (VCAM-1) expression [53]. In plants, flavanols can occur as monomers (e.g., catechin and epicatechin) and oligomers or polymers, described as proanthocyanidins or condensed tannins. Catechins interfere with the inflammatory processes that contribute to atherosclerosis progression [54], while, among the effects of flavan-3-ols, present in dietary plants, like tea (*Camellia sinensis*) and cocoa (*Theobroma cacao*), inhibition of eicosanoid production, reduction of platelet activation and modulation of NO-dependent mechanisms, and modulation of proinflammatory cytokine production can be included [55]. Anthocyanins exert their anti-inflammatory effects, particularly via the mitogen-activated protein kinase (MAPK) pathway [56]. Mechanistic studies report the glycosides of malvidin, delphinidin, cyanidin, petunidin, and



peonidin to dose-dependently reduce IL-1 $\beta$  -activation of NF- $\kappa$ B *in vitro* [57].

Diterpenes from *Stevia rebaudiana* leaves, used as a source of natural sweeteners in the food industry, have also been shown to attenuate proinflammatory cytokines (TNF- $\alpha$ , IL-1 $\beta$ , and IL-6) production via modulation of the I $\kappa$ -B $\alpha$ /NF- $\kappa$ B pathway [58]. Triterpenes from licorice root (*Glycyrrhiza glabra*) are glycyrrhizin and glycyrrhetic acid: they have several effects, including gastric protection and modulation of blood pressure through their mineralocorticoid activity [59], but also anti-inflammatory function acting *via* the PI3K/Akt/GSK3- $\beta$  pathway to reduce cytokine production, while 18  $\beta$ -glycyrrhetic acid also blocks inflammation by causing dissociation of the glucocorticoid receptor [60].

Curcumin was demonstrated to inhibit LPS-induced production of TNF- $\alpha$  and IL-1 $\beta$  in a human monocytic macrophage cell line and, at the same millimolar concentration, to inhibit LPS-induced activation of NF- $\kappa$ B and reduce the biological activity of TNF- $\alpha$  [61].

Stilbenes are found in only low quantities in the human diet. Resveratrol inhibits TNF- $\alpha$ , IL-1 $\beta$ , and IL-6 expression [62] and its ability to suppress NF- $\kappa$ B activation, possibly via SIRT-1 activation, is suggested to be important in counteracting microglial inflammation. Rosmarinic acid is a phenolic acid occurring in herbs such as rosemary and sage. Its anti-inflammatory effects were shown by testing its topical application improving symptoms in atopic dermatitis patients [63].

Chronic inflammation is the main pathogenetic factor of many autoimmune diseases whose treatment is based on long or life-long administration of anti-inflammatory drugs. The possibility to use safe and effective natural products to reduce the dosage and side effects of conventional drugs represents an interesting field of study. Monoclonal antibodies against TNF- $\alpha$  or TNF- $\alpha$  soluble receptors are among the most efficient biological DMARDs (disease-modifying antirheumatic drugs) available for the chronic treatment of rheumatoid arthritis (RA) and other chronic inflammatory diseases. In nature, many natural compounds have been found to reduce the levels of TNF- $\alpha$  by interfering with various pro-inflammatory mediators and upstream targets. Thus, these compounds may represent alternative or adjunctive means of treating inflammatory diseases by modulating production, rather than activity, of TNF- $\alpha$  (reviewed in [64]).

On the other hand, fatty acids and their derivatives were shown to exert profound suppressive effects on the expression of iNOS, COX-II, IL-6, and TNF- $\alpha$  via a blockade of the NF- $\kappa$ B and AP-1 pathways. The strong anti-inflammatory potential and improved clinical parameters of RA of marine n-3 long-chain PUFA were also reported by Barden et al. [65].

Among flavonoids, luteolin and quercetin were the most potent TNF- $\alpha$  inhibitors [66]. The anti-inflammatory power of quercetin was clinically tested in women with RA demonstrating a significant effect in controlling inflammation and clinical symptoms [67]. Irrespective of their activity on the synthesis of TNF- $\alpha$ , green tea extract has also been proven in recent clinical trials to have anti-inflammatory and immunomodulatory properties in autoimmune disease [68].

Therefore, although natural product probably cannot substitute anti-inflammatory drugs, including DMARDs, they could significantly contribute to the reduction of dosage, for a more economic and safer treatment of autoimmune, as well as many other inflammation-related diseases.

#### 4. Oxidative Stress, Metabolic Syndrome and Aging

Aging is a series of morphological and functional changes taking place over the time that can lead to deterioration of the biological functions of an organism [69]. ROS generated as byproducts of biological oxidations can induce severe oxidative damage to macromolecules eventually leading to cellular dysfunction [70]. Combination of aging, insulin resistance, and CVD can precipitate into metabolic syndrome [69, 71]. Although insulin resistance is considered as the main pathogenic mechanism underlying onset of metabolic syndrome, a low-level chronic inflammation and oxidative stress have received much attention recently [72]. Additionally, evidences from experimental and clinical studies have shown that oxidative stress is a pivotal factor for obesity-associated diabetes, metabolic syndrome, and non-alcoholic steatohepatitis (NASH) [73, 74]. On the other hand, metabolic syndrome is the major health challenge of the 21<sup>st</sup> century that can significantly affect ever-increasing life and health spans in the developed world. Although the exact mechanism responsible is largely unknown, it is considered that metabolic syndrome can significantly advance aging.

Since the ancient times, natural products have always been suggested to improve longevity of an organism [75]. Epidemiological and experimental data suggest natural products to be powerful antioxidants that can improve stress-related diseases. Scientific literature also suggests potential of natural products in improving metabolic syndrome and aging [76, 77]. Therefore, detailed preclinical evaluation on underlying mechanism of action and bioactivities of the natural compounds may provide solid scientific foundation for clinical applications.

Polyphenols and in particular flavonoids have been shown to protect from various age-related disease [78]. Several studies have indicated that supplementation with dietary polyphenols such as (-)-epigallocatechin-3-gallate (EGCG) and curcumin can improve age-associated cellular damage by reducing generation of ROS [79]. On the other hand, resveratrol and pterostilbene are considered excellent as anti-aging natural compounds that can modulate oxidative damage, inflammation, and cell senescence; components associated with aging [80] as well as flavonoids have been shown to improve aging mainly by controlling metabolic syndrome [81]. Some of the commonly reported flavonoids that can tackle one or more components associated with aging or metabolic syndrome are hesperidin, hesperetin, naringin, and naringenin [82].

It is noteworthy that the literature on preclinical use of phytochemicals to treat various conditions associated with aging is ever expanding. However, a large number of phytochemicals have been tested successfully in clinical trials

for age-related condition. It is noteworthy that some limitations of pre-clinical studies that can affect their translational significance are (1) choice of experimental models that is not clinically relevant, (2) poorly characterized mechanism of action, and (3) clinically irrelevant dosing/time points for data interpretation.

## 5. Natural Compounds and Vascular Diseases

Alteration of vascular function is a key pathogenic process common to many important and highly diffuse human pathologies [83]. The morpho-functional integrity of the vascular endothelium is a complex and highly homeostatic process involving maintenance of vasorelaxation ability as well as anti-inflammatory and barrier functions with important effects on atherogenesis and increased risk of cardiovascular diseases (CVD) [84, 85].

Aging and chronic inflammatory conditions, such as diabetes, alter vascular homeostasis disrupting the “protective” functions of the vascular endothelium, a mechanism known as vascular dysfunction [86]. Physiological aging progressively deteriorates vascular function; however, poor life style, hyperlipidemia, and hyperglycemia associated with oxidative stress can significantly accelerate these pathologic processes leading to CVD and macro- and microvascular complications of diabetes mellitus [87], including ocular pathologies such as ischemic retinopathies. Crucial to the development of vascular dysfunction in aging is the induction of oxidative/nitrative stress [88], which is also involved in the pathogenesis of other human diseases discussed in this review.

Vascular redox imbalance linked to aging and diabetes share important common features such as the induction of the so-called senescence-associated secretory phenotype (SASP) [89]. According to this emerging concept, aging and metabolic stress lead to redox imbalance and trigger enhanced expression of senescence markers and production/secretion of inflammatory cytokines [90, 91]. Suppression of sirtuins, class III NAD<sup>+</sup>-dependent protein histone deacetylases, is an important feature of SASP [92]. In particular, SIRT-1 plays a key role in maintenance of these cellular homeostasis and energy metabolism [93, 94]. The role of natural compounds as potent anti-oxidant players able to prevent, at least partially, pathologic processes associated with aging and metabolic diseases was recently reviewed [95]. Here we will focus on the therapeutic effects of omega 3 polyunsaturated fatty acids (PUFA) and the flavonoid resveratrol because of their predominant effects on vascular dysfunction, SASP and CVD.

Omega 3 polyunsaturated fatty acids (PUFAs) include alpha linoleic acid (18:3) (ALA), eicosapentaenoic acid (EPA) (20:5n-3), and docosahexaenoic acid (DHA) (22:6n-3). ALA is not synthesized in humans and is considered plant-derived omega 3, whereas EPA and DHA are found predominantly in fish. The effects of omega 3 PUFAs are primarily attributed to their lipid lowering effects and consequent reduction of risk of atherosclerosis [96]. Omega 3 PUFAs have shown to reduce vascular inflammation by downregulating adhesion molecules and limiting leukocytes adhesion to the vascular wall [97]. This latter directly influences production of

endothelial-derived nitric oxide due to stabilization of lipid rafts such as the endothelial cells caveolae, as demonstrated in retinal endothelial cells [98]. However, the experimental studies appear to be much more supportive of PUFA's positive effects than the clinical evidence. In fact, the omega 3 PUFA effects on increased endothelial regenerative capacity and maintenance of vascular endothelial cells homeostasis due to membrane stabilizing ability were demonstrated to have important effects on prevention of CVD [98]. An extensive review of the literature, recently appeared on Cochrane Database Systematic Review [99] and summarized the results of a large number of randomized clinical trials assessing the effects of different doses of PUFA on CVD outcomes. The results of this study showed that higher PUFA intake only slightly reduces risk of coronary heart disease and CVD acute events (i.e., stroke) and mortality, but overall has not significant effects on all-cause or cardiovascular disease mortality. Most of the positive effects were associated with modulation of lipid metabolism [99]. In any case, even a slight but significant reduction of 10% of morbidity and mortality for CVD associated with PUFA supplementation remains a significant clinical outcome [100].

The cardioprotective effects of resveratrol in human studies have been reported [101]. However, the *in vivo* evidence and the clinical studies are less conclusive, mostly because of the poor intestinal absorption of these flavonoids and the extensive degradation in various phenolic acids, which may retain some antioxidant activity [102]. It is noteworthy that one additional function of resveratrol was linked to enhanced SIRT-1 expression and activity and was extensively linked to longevity [103], while a prooxidant activity of resveratrol under certain conditions was reported [104].

Ultimately, the deleterious effects of aging and metabolic diseases (i.e., diabetes) in promoting oxidative stress and vascular dysfunction can negatively affect the cardiovascular system by promoting vascular dysfunction. There is no doubt that a correct life style including a balanced healthy nutrition, physical exercise, and the use of nutraceuticals can positively impact longevity by preventing CVD. However, when CVD pathologies have been established, nutraceuticals such as omega 3 and resveratrol can still find therapeutic application as effective adjuvant therapies because of their numerous positive effects on vascular homeostasis.

Finally, other phytochemicals with antioxidant effects have been reported to play a protective action on the risk or the development of CVD and therefore were proposed as important factors in diet, like, for instance,  $\beta$ -carotene, curcuma, and others [105, 106]. In particular, several studies underline the anti-atherogenic effect of lycopene in association with the inhibition of proinflammatory cytokines secretion [107].

## 6. Phytochemicals for Neurodegenerative Diseases Prevention

Neurodegenerative diseases (NDDs) are a heterogeneous group of chronic and untreatable conditions, characterized by progressive functional impairment of the nervous system,

induced by deterioration of neurons, myelin sheath, neurotransmission, and movement control. Among one of the most disabling of these, Alzheimer's disease (AD) is a NDD that destroys memory and other important mental functions. AD is characterized by the accumulation of amyloid-beta peptide ( $A\beta$ ) in the brain, the presence of neurofibrillary tangles (NFTs) containing hyperphosphorylated tau fragments, and the loss of cortical neurons and synapses [108]. Parkinson's disease (PD) affects predominately dopaminergic neurons in the substantia nigra, associated with accumulation of Lewy bodies containing  $\alpha$ -synuclein in neurons and increased neuroinflammatory cells. Huntington disease (HD) is a progressive brain disorder that causes uncontrolled movements, emotional problems, and loss of thinking ability and occurs in early middle life, even if it is recognized as a juvenile form. HD is an autosomal dominant NDD, characterized by the abnormal expansion of the CAG triplet repeats in the polyglutamine region of the huntingtin (HTT) gene [109]. Multiple sclerosis (MS) is a chronic, autoimmune, inflammatory disease that affects the brain and spinal cord, caused by autoimmune-mediated loss of myelin and axonal damage [110]. At present, there is no effective treatment for NDDs, and, in order to identify novel therapy or adjuvant strategy for NDDs, several natural medicinal plants have gained attention as potential neuroprotective agents, and a number of studies have suggested that a diet rich in vegetable products can prevent or delay the NDDs onset [111]. These properties might be due to the presence of polyphenols, an important group of phytochemicals that are abundantly present in fruits, vegetables, cereals, and beverages (Table 1) and already discussed in other sections of this review. In this chapter, we focused on the potential role of polyphenols for preventive and therapeutic purposes for NDDs treatment, based on related research evidence.

Resveratrol demonstrates significant neuroprotective activity both *in vitro* and *in vivo*. Several studies have demonstrated that resveratrol is cytoprotective in cells exposed to  $A\beta$  and/or to  $A\beta$ -metal complex via Sirt3-mediated mechanisms [112, 113]. *In vivo*, in a mouse model of cerebral amyloid deposition, orally administered resveratrol lowered microglial activation associated with cortical amyloid plaque formation [114]. Furthermore, long-term dietary resveratrol reduces cognitive impairment and has a neuroprotective role, decreasing the amyloid burden and reducing tau hyperphosphorylation in SAMP8 mice, a model of age-related AD [115]. Increasing evidence has also suggested that resveratrol shows enhanced benefits in cell and animal models of PD. In rat primary midbrain neuron-glia cultures, resveratrol protected dopaminergic neurons against lipopolysaccharide (LPS)-induced neurotoxicity in concentration- and time-dependent manners, through the inhibition of microglial activation and the subsequent reduction of proinflammatory factors release [116]. *In vivo*, resveratrol ameliorated both motor deficits and pathological changes in MPTP-treated mice *via* activation of SIRT-1 and subsequent LC3 deacetylation-mediated autophagic degradation of  $\alpha$ -synuclein [117]. All the above findings suggest that resveratrol may be a potential prophylactic

or therapeutic agent for NDDs, with the caution reported elsewhere in this review regarding intestinal absorption.

Curcuminoids consist of three components: curcumin (75%–80%), demethoxycurcumin (15%–20%), and bisdemethoxycurcumin (3%–5%). Curcumin also induces neuroprotective effects through the control of pathogenetic oxidative and inflammatory mechanisms both *in vitro* and *in vivo* models of AD and PD. In Neuro2a mouse neuroblastoma cells infected with Japanese encephalitis virus, curcumin enhances cell viability by decreasing ROS and inhibiting proapoptotic signals [118]. Furthermore, curcumin protects against  $\alpha$ -synuclein-induced cytotoxicity in SH-SY5Y neuroblastoma cells decreasing cytotoxicity of aggregated  $\alpha$ -synuclein, reducing intracellular ROS, and inhibiting caspase-3 activation [119]. *In vivo*, curcumin significantly alleviated spatial memory deficits in APP/PS1 mouse model of AD, promoting cholinergic neuronal function [120]. Curcumin also reduced the activation of microglia and astrocytes, as well as cytokine production and inhibited NF- $\kappa$ B signaling pathway, suggesting the beneficial effects of curcumin on AD mice are attributable to the suppression of neuroinflammation [120]. In the PD animal model induced by the neurotoxin MPTP, curcumin is neuroprotective and prevents glutathione depletion and lipid peroxidation induced by this toxin. More recently, curcumin restored motor deficits and enhanced the activities of antioxidant enzymes in rotenone induced Parkinson's in mice [121]. All these findings suggest a neuroprotective role of curcumin, and offer strong justification for the therapeutic prospective of this compound in the management of NDDs.

Pretreatment of primary hippocampal cultures with quercetin significantly attenuated  $A\beta$ (1-42)-induced cytotoxicity, protein oxidation, lipid peroxidation, and apoptosis by modulating oxidative stress [122]. More interestingly, quercetin decreases extracellular  $\beta$ -amyloidosis, tauopathy, astrogliosis, and microgliosis in the hippocampus and the amygdala and improves performance on learning and spatial memory tasks in aged triple transgenic Alzheimer's disease model mice [123].

Taken together, the above evidences suggest polyphenols as neuroprotective agents. The habitual consumption of dietary polyphenols is proven to inhibit various secondary sources of ROS and proinflammatory cytokines, thus reducing the risk of NDDs [124]. A beneficial clinical use of polyphenols to attenuate oxidative damage in aging and age-related disorders may be a viable and promising approach for the prevention and treatment of NDDs.

## 7. Natural Compounds as Anti-Cancer Agents

Although large progress was achieved, some tumors still present poor prognosis and research is currently geared towards the use of non-toxic doses of plant-extracted compounds. The road for a new therapeutic approach, based on natural molecules and drugs, was opened by the identification and use of natural chemotherapeutic agents like taxanes, vinca alkaloids, and anthracyclines [125]. Therefore, it is logical to hypothesize that compounds found in foods are likely to have some protective effects.



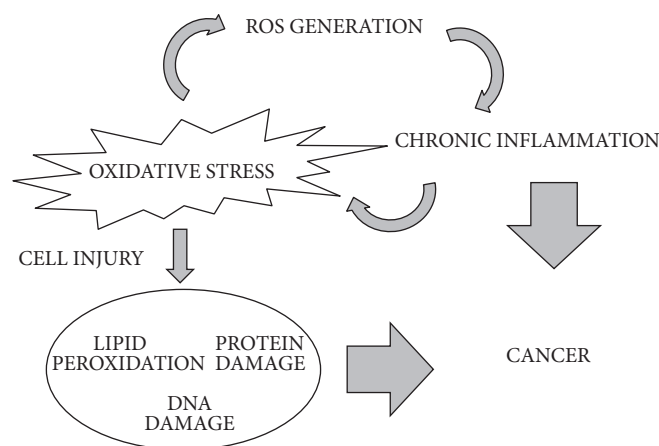


FIGURE 3: Schematic view of complex cross-talk between oxidative stress, chronic inflammation, and cancer.

Numerous studies suggest that chronic inflammation is able to promote all stages of cancer development, including initiation, progression, and metastatic potential [126]. Moreover, recent data [127] show a close relationship between age-related pathologies, including cancer, and inflammation (Figure 3). ROS are mainly responsible of inflammation and cancer promotion by oxidative stress [128]. In particular, there are increasing evidences on the role of  $\text{TNF-}\alpha$ , a well-known pro-inflammatory cytokine and a regulator of the generation of ROS, in the promotion of carcinogenesis through the activation of the transcription factor  $\text{NF-}\kappa\text{B}$  [129].

Interestingly, recent literature data indicate an emerging role of polyamines metabolism as a novel target against inflammatory diseases. Polyamines are naturally occurring aliphatic compounds, ubiquitous to all living organisms, which interact with DNA, RNA and proteins and are required for eukaryotic cell growth, survival, and differentiation. Notably, excessive polyamine catabolism can lead to ROS formation, increasing oxidative stress, with subsequent enhancement of inflammatory response [130]. For that reason, polyamines metabolism represents an interesting target for anticancer therapy using natural compounds [131]. Therefore, the use of different natural substances, mainly polyphenols, coming from plants and foods, may exert promising results in antitumor therapy due to their anti-oxidant activities [132]. In particular, diet with high polyphenol content has been shown positive effects against cancer-related anorexia/cachexia syndrome and oxidative stress [133].

The flavonol quercetin is a well-known antioxidant molecule with well-documented anticancer activity [134]. Mechanisms underlying its anticancer activity are not completely elucidated; however, it is known that quercetin affects negatively the synthesis of polyamines, well known growth factors, by the inhibition of ornithine decarboxylase (ODC) expression [135]. Interestingly, it has been demonstrated that high flavonols intake, especially quercetin and kaempferol, is able to induce a significative reduction of serum IL-6 concentration, a well-known inflammation-related cytokine [136].

Also curcumin shows anti-inflammatory and anti-oxidant properties and potential anti-cancer activity [137]. Indeed, this molecule has been tested in a wide range of cancer cell lines, like cervical cancer [138], colorectal cancer [139], and breast cancer [140]. Moreover, curcumin has been shown to have effects on many signalling and polyamine pathways [141]. Although several studies underline curcumin therapeutic efficacy, its clinical administration is difficult due to its poor oral bioavailability, low solubility, and degradation [142].

Resveratrol shows a potent cytotoxic effect on cancer cells [143]. For example, recently it was reported that this effect is abolished by Transglutaminase type 2 inhibition on cholangiocarcinoma and gallbladder cancer cell lines [144]. In the last decades, resveratrol has been one of the most studied natural compounds, often leading to contradictory results [145]. Although resveratrol is considered a good candidate as chemopreventive and synergistic agent, further studies are needed [146].

Genistein is a soybean isoflavone. The antitumor activity of genistein has been observed in various forms of cancer such as neuroblastoma and chronic lymphatic leukemia and in several organs such as breast, ovary, prostate, urinary bladder, colon, liver, and stomach [147]. Due to its structural similarity to mammalian estradiol, genistein is known as a phytoestrogen. A large number of studies suggest a beneficial role of this isoflavone in the inhibition of carcinogenesis in animal models. Although the effects of genistein as chemoprevention agent remain controversial [148], several human intervention studies have been undertaken. In fact, it has been demonstrated that dietary soy supplementation may reduce inflammatory processes related to prostate carcinogenesis [149].

One of the most well-known anticancer agents with anti-oxidant and anti-inflammatory properties is lycopene that exerts therapeutic effects on a large variety of cancers [150, 151]. In particular, it has been demonstrated that lycopene intake reduces prostate cancer risk [152].

During the last few decades, it has emerged how genomic instability, telomere attrition and epigenetic changes may

underlie aging and senescence phenomena [153]. Telomeres are short tandem repeated sequences (TTAGGG) that are localized on the 5' ends of chromosomes. The length of telomeres is guaranteed by the activity of telomerase enzyme, widely expressed in tumor cells. The G-rich telomeric sequence can assume G-quadruplex DNA secondary structures, able to inhibit telomerase activity. Therefore, inhibition of telomerase or the stabilization of G-quadruplex by natural compounds may represent an important anti-cancer strategy [154, 155].

The identification of natural compounds has contributed to the improvement of cancer therapies and indeed many of these molecules are currently used in clinical practice. It is important, however, to emphasize that rigorous studies and preclinical investigations are needed to clarify their potential chemopreventive and antitumor activities.

## 8. Phytochemicals in Skin Diseases

According to the European Medicines agency (<http://www.ema.europa.eu/ema/>), several studies analyze in depth the actual efficacy of herbal medicinal products and derived molecules. Herbal products can be sorted according to their clinical use in several diseases such as appetite disorders, sleep disorders, pain and inflammation control, eye disorders, gastrointestinal disorders, and others ([http://www.ema.europa.eu/ema/index.jsp?curl=pages/medicines/landing/herbal\\_search.jsp&mid=WC0b01ac058001fa1d](http://www.ema.europa.eu/ema/index.jsp?curl=pages/medicines/landing/herbal_search.jsp&mid=WC0b01ac058001fa1d) for a complete list). We focus here the attention on the beneficial use of herbal medicinal products in skin disorders, with a specific attention on pathologies often related to the skin-aging process [156]. Since in most cases they have been studied or proposed through topical applications, they are often referred to as oils or herbal preparations whose classification in terms of phytochemical content is rather complex.

Therapeutic applications to skin pathologies are proposed for Agrimoniae herba (*Agrimonia eupatoria*; in minor inflammation and superficial wounds), *Echinacea purpurea* (in small superficial wounds and mild acne), Soiae oleum (*Glycine max*; in mild recurrent eczema), Juglandis folium (*Juglans regia*; in minor skin inflammation), Matricariae aetheroleum (in anous and genitals irritation), Matricariae flos (*Matricaria recutita*; in mild skin inflammation and sunburns and superficial wounds), *Melaleuca* spp. (in insects bites, mild acne, itching, minor skin inflammation), Meliloti herba (*Melilotus officinalis*; in minor skin inflammation), Origan dictamni herba and Origan majoranae herba (*Origanum* spp.; in minor skin inflammation and irritation), Rosae flos (*Rosa* spp.; in skin and mouth inflammation), and Solani dulcamarae stipites (*Solanum dulcamara*; in itchy and rash from mild eczema) (see [http://www.ema.europa.eu/ema/index.jsp?currentCategory=Skin+disorders+%26+minor+wounds&curl=pages%2Fmedicines%2Flanding%2Fherbal\\_search.jsp&mid=WC0b01ac058001fa1d&searchType=Latin+name+of+herbal+substance&taxonomyPath=&keyword=Enter+keywords&alreadyLoaded=true&treeNumber=&searchkwByEnter=false&pageNo=2](http://www.ema.europa.eu/ema/index.jsp?currentCategory=Skin+disorders+%26+minor+wounds&curl=pages%2Fmedicines%2Flanding%2Fherbal_search.jsp&mid=WC0b01ac058001fa1d&searchType=Latin+name+of+herbal+substance&taxonomyPath=&keyword=Enter+keywords&alreadyLoaded=true&treeNumber=&searchkwByEnter=false&pageNo=2) for more details).

The European Medicines Agency official list of herbal substances, preparations, and combinations for use as

traditional herbal medicinal products contains 12 substances, according to the European Community decision reported at the EU site (<https://eur-lex.europa.eu/legal-content/EN/TXT/?uri=CELEX:02008D0911-20180126>).

The 12 herbal substances are as follows: *Calendula officinalis*, *Echinacea purpurea*, *Eleutherococcus senticosus*, *Foeniculum vulgare*, *Hamamelis virginiana*, *Melaleuca* spp., *Mentha* spp., *Pimpinella anisum*, *Sideritis scardica*, *Thymus vulgaris*, *Valeriana officinalis*, and *Vitis vinifera*.

Their introduction within such official list is sustained by scientific reports demonstrating their therapeutic effectiveness in different pathological settings. We collected the scientific literature reported in PubMed for each of these substances co-occurring in the ALL fields with any of the common skin diseases reported in the following list: acne, allergy, basal cell carcinoma, blister, carbuncle, cellulitis, chickenpox, dermatitis, eczema, hives, impetigo, lupus, measles, melanoma, psoriasis, pruritus, ringworm, rosacea, squamous cell carcinoma, vitiligo, and wart.

As reported in Figure 4, the investigated phytotherapeutic agents are mostly associated to allergy, dermatitis, and melanoma, related in most cases to either *Melaleuca*, or *Mentha* or *Thymus vulgaris* or *Vitis vinifera*.

More in detail, local application of *Melaleuca alternifolia* derived oils has been consistently reported to achieve a significant improvement of acne lesions, according to several independent studies [157]. The clinical efficacy of *Melaleuca* oil is likely related to its known antibacterial action [158] as well as anti-inflammatory activity [159]. The essential oil from *Melaleuca alternifolia* also shows antioxidant activities potentially useful in dermatitis and skin cancers [160]. Extracts from *Melaleuca quinquenervia* have been shown to inhibit melanin content in mouse melanoma cells, thus exerting potential cosmetic applications [161]. Minor side effects are associated with *Melaleuca* such as burning, scaling, itch, redness, dryness, pruritus, and stinging. Contact allergy to *Melaleuca* oil has been reported in some cases as well as dermatitis reactions indicating the essential oil from *Melaleuca* as a sensitizers and potentially irritant agent. *Mentha*-derived oil is used to relief skin inflammation and pruritus [162]; nevertheless, allergic reactions have been reported in some cases.

Finally, regarding *Vitis vinifera*, a meta-analysis recently published demonstrates *Vitis vinifera* as one of the effective components of medical devices useful in atopic dermatitis local treatment [163]. Interesting results have also been collected in oncological conditions; *Vitis vinifera* has shown some efficacy in reducing radiotherapy-induced dermatitis [164] and in inhibiting cell proliferation in melanoma [165, 166] and skin non-melanoma cancer [167], indicating grape seed proanthocyanidin as an apoptosis and autophagy inducer. Rare allergic reactions are reported for *Vitis vinifera* [168].

Hundreds of other phytochemicals are reported in literature with potential effects on skin, such as anti-age activity [169], photoprotection [170], wound healing [171], and anti-infection [172].



	<i>Calendula officinalis</i>	<i>Echinacea purpurea</i>	<i>Eleutherococcus senticosus</i>	<i>Foeniculum vulgare</i>	<i>Hamamelis virginiana</i>	<i>Melaleuca</i>	<i>Mentha</i>	<i>Pimpinella anisum</i>	<i>Sideritis scardica</i>	<i>Thymus vulgaris</i>	<i>Valeriana officinalis</i>	<i>Vitis vinifera</i>	Horiz sum
Acne (20)	1	1	0	0	1	6	0	0	0	<b>10</b>	0	5	24
Allergy (158)	<b>6</b>	<b>35</b>	<b>5</b>	4	5	<b>29</b>	<b>38</b>	7	0	<b>95</b>	5	<b>60</b>	289
Basal cell carcinoma (19)	1	0	0	0	0	0	0	0	0	3	0	0	4
Blister (4)	0	1	0	0	0	0	0	0	0	3	0	1	5
Carbuncle (1)	0	0	0	0	0	0	0	0	0	0	0	0	0
Cellulitis (4)	0	0	0	0	0	0	0	0	0	0	0	0	0
Chickenpox (12)	0	0	0	0	0	0	0	0	0	0	0	0	0
Dermatitis (114)	<b>30</b>	9	2	0	<b>13</b>	<b>27</b>	<b>26</b>	2	0	<b>48</b>	2	<b>17</b>	176
Eczema (57)	0	2	0	0	2	4	2	0	0	4	0	1	15
Hives (1)	0	4	1	0	0	0	3	1	0	1	1	4	15
Impetigo (1)	0	0	0	0	0	0	0	0	0	0	0	0	0
Lupus (115)	0	0	1	0	0	0	1	0	0	<b>18</b>	0	0	20
Measles (277)	0	1	0	0	0	0	0	1	0	2	0	1	5
Melanoma (166)	4	2	2	1	1	6	4	0	0	<b>12</b>	0	<b>20</b>	52
Psoriasis (76)	0	1	0	0	1	3	0	1	0	<b>17</b>	0	3	26
Ringworm (2)	0	0	0	1	0	5	1	0	0	1	0	0	8
Rosacea (3)	0	0	0	0	0	0	0	0	0	0	0	0	0
Squamous cell carcinoma (79)	1	2	0	0	0	0	4	0	0	4	0	<b>12</b>	23
Vitiligo (11)	0	0	0	0	1	0	0	0	0	2	0	1	4
Wart (1)	0	0	0	0	0	0	0	0	0	0	0	0	0
Oxidative stress (394)	<b>19</b>	<b>21</b>	<b>18</b>	<b>14</b>	2	<b>16</b>	<b>44</b>	7	2	<b>111</b>	<b>17</b>	<b>536</b>	807
<b>Vertical sum</b>	62	79	29	20	26	96	123	19	2	331	25	661	

FIGURE 4: Number of published studies regarding plant-derived nutraceuticals and age-related skin diseases. In the first column, within brackets, the number of PubMed abstracts containing in the Title field the diseases name and the word “age” is reported. In several diseases a strong relation with the age is evident (namely, in allergy, basal cell carcinoma, chickenpox, dermatitis, eczema, lupus, measles, melanoma, psoriasis, squamous cell carcinoma, and oxidative stress). In the other columns, the number of PubMed abstracts containing the diseases name and the phytochemical name in All field is reported. Co-occurrence > 10 is highlighted in bold and gray background. The raw named Oxidative stress reports the number of studies indexed on PubMed containing experimental data which correlate each plant-derived nutraceutical with an “oxidative stress” (as present in All field of database).

## 9. Conclusions

The body of evidence reported in this review demonstrates the large interest around phytochemicals and their potential use against oxidative stress-related human diseases, with a focus on those in which inflamed cells play a crucial and pivotal role on pathogenic mechanisms. Their potential use, in combination with drugs like for instance DMARDs, may be very useful to reduce side effects and be cost-effective. Further, socioeconomical issues are playing an even more important role on the rate of new drugs development. This is coupled to an increasing interest toward the repurposing and repositioning of old drugs or others largely used in traditional medicine. Therefore, it is expected that in the next future phytochemicals-based drugs will be object of a growing interest for inflammation and oxidative stress-related diseases.

## Disclosure

Giorgia Valle's present address is Via Giovanni Spadolini 2, 00046 Grottaferrata (Roma).

## Conflicts of Interest

The authors report no conflicts of interest in this work.

## Acknowledgments

The financial support from Italian Ministry of Health (Ricerca Corrente) is kindly acknowledged.

## References

- [1] M. Cardelli, "The epigenetic alterations of endogenous retroelements in aging," *Mechanisms of Ageing and Development*, vol. 174, pp. 30–46, 2018.
- [2] F. Ciccarone, S. Tagliatesta, P. Caiata, and M. Zampieri, "DNA methylation dynamics in aging: how far are we from understanding the mechanisms?" *Mechanisms of Ageing and Development*, vol. 174, pp. 3–17, 2018.
- [3] C. Franceschi, P. Garagnani, P. Parini, C. Giuliani, and A. Santoro, "Inflammaging: a new immune-metabolic viewpoint for age-related diseases," *Nature Reviews Endocrinology*, vol. 14, no. 10, pp. 576–590, 2018.
- [4] I. Liguori, G. Russo, F. Curcio et al., "Oxidative stress, aging, and diseases," *Clinical Interventions in Aging*, vol. 13, pp. 757–772, 2018.
- [5] C. C. Neto, "Cranberry and blueberry: evidence for protective effects against cancer and vascular diseases," *Molecular Nutrition & Food Research*, vol. 51, no. 6, pp. 652–664, 2007.
- [6] G. A. Manganaris, V. Goulas, I. Mellidou, and P. Drogoudi, "Antioxidant phytochemicals in fresh produce: exploitation of genotype variation and advancements in analytical protocols," *Frontiers in Chemistry*, vol. 5, article 95, 2016.
- [7] C. Forni, R. Braglia, N. Mulinacci et al., "Antineoplastic activity of Strawberry Crude Extracts on B16-F10 melanoma cells," *Molecular BioSystems*, vol. 10, no. 6, pp. 1255–1263, 2014.
- [8] C. Peng, X. Wang, J. Chen et al., "Biology of ageing and role of dietary antioxidants," *BioMed Research International*, vol. 2014, Article ID 831841, 13 pages, 2014.
- [9] S. Bhagwat, D. B. Haytowitz, and J. M. Holden, "U.S. Department of Agriculture Agricultural Research Service. USDA Database for the Flavonoid Content of Selected Foods. Release 3.1. pp. 1-173, 2014," <http://www.ars.usda.gov/nutrientdata>.
- [10] A. R. Santamaria, N. Mulinacci, A. Valletta, M. Innocenti, and G. Pasqua, "Effects of elicitors on the production of resveratrol and viniferins in cell cultures of *Vitis vinifera* L. cv Italia," *Journal of Agricultural and Food Chemistry*, vol. 59, no. 17, pp. 9094–9101, 2011.
- [11] S. Pervaiz and A. L. Holme, "Resverastrol: its biologic targets and functional activity," *Antioxidants & Redox Signaling*, vol. 11, no. 11, pp. 2851–2897, 2009.
- [12] M. Takemoto and H. Takemoto, "Synthesis of theaflavins and their functions," *Molecules*, vol. 23, no. 4, article 918, 2018.
- [13] K. M. Ranard, S. Jeon, E. S. Mohn, J. C. Griffiths, E. J. Johnson, and J. W. Erdman, "Dietary guidance for lutein: consideration for intake recommendations is scientifically supported," *European Journal of Nutrition*, vol. 56, no. S3, pp. 537–542, 2017.
- [14] L. G. Wood, M. L. Garg, J. M. Smart, H. A. Scott, D. Barker, and P. G. Gibson, "Manipulating antioxidant intake in asthma: a randomized controlled trial," *American Journal of Clinical Nutrition*, vol. 96, no. 3, pp. 534–543, 2012.
- [15] Z. Liu, Z. Ren, J. Zhang et al., "Role of ROS and nutritional antioxidants in human diseases," *Frontiers in Physiology*, vol. 9, article 477, 2018.
- [16] S. Mahajan and N. Tuteja, "Cold, salinity and drought stresses: an overview," *Archives of Biochemistry and Biophysics*, vol. 444, no. 2, pp. 139–158, 2005.
- [17] C. Forni, D. Duca, and B. R. Glick, "Mechanisms of plant response to salt and drought stress and their alteration by rhizobacteria," *Plant and Soil*, vol. 410, no. 1-2, pp. 335–356, 2017.
- [18] A. Ramakrishna and G. A. Ravishankar, "Influence of abiotic stress signals on secondary metabolites in plants," *Plant Signaling and Behavior*, vol. 6, no. 11, pp. 1720–1731, 2011.
- [19] D. Hidalgo, R. Sanchez, L. Lalaleo, M. Bonfill, P. Corchete, and J. Palazon, "Biotechnological production of pharmaceuticals and biopharmaceuticals in plant cell and organ cultures," *Current Medicinal Chemistry*, vol. 25, no. 30, pp. 3577–3596, 2018.
- [20] J. D. Phillipson, "Phytochemistry and medicinal plants," *Phytochemistry*, vol. 56, no. 3, pp. 237–243, 2001.
- [21] N. Gurnani, D. Mehta, M. Gupta, and B. K. Mehta, "Natural products: source of potential drugs," *African Journal of Basic & Applied Sciences*, vol. 6, no. 6, pp. 171–186, 2014.
- [22] A. N. Winter, M. C. Brenner, N. Punessen et al., "Comparison of the neuroprotective and anti-inflammatory effects of the anthocyanin metabolites, protocatechuic acid and 4-hydroxybenzoic acid," *Oxidative Medicine and Cellular Longevity*, vol. 2017, Article ID 6297080, 13 pages, 2017.
- [23] D. M. Kasote, S. S. Katyare, M. V. Hegde, and H. Bae, "Significance of antioxidant potential of plants and its relevance to therapeutic applications," *International Journal of Biological Sciences*, vol. 11, no. 8, pp. 982–991, 2015.
- [24] C. H. Foyer and G. Noctor, "Redox homeostasis and antioxidant signaling: a metabolic interface between stress perception and physiological responses," *The Plant Cell*, vol. 17, no. 7, pp. 1866–1875, 2005.
- [25] W. Stahl and H. Sies, "Antioxidant activity of carotenoids," *Molecular Aspects of Medicine*, vol. 24, no. 6, pp. 345–351, 2003.

- [26] B. N. Ames, "Prolonging healthy aging: longevity vitamins and proteins," *Proceedings of the National Academy of Sciences of the United States of America*, vol. 105, pp. 10836–10844, 2018.
- [27] K. Jomova and M. Valko, "Health protective effects of carotenoids and their interactions with other biological antioxidants," *European Journal of Medicinal Chemistry*, vol. 70, pp. 102–110, 2013.
- [28] I. M. Petyaev, "Lycopene deficiency in ageing and cardiovascular disease," *Oxidative Medicine and Cellular Longevity*, vol. 2016, Article ID 3218605, 6 pages, 2016.
- [29] A. J. Young and G. M. Lowe, "Antioxidant and prooxidant properties of carotenoids," *Archives of Biochemistry and Biophysics*, vol. 385, no. 1, pp. 20–27, 2001.
- [30] S. Hassan and U. Mathesius, "The role of flavonoids in root–rhizosphere signalling: opportunities and challenges for improving plant–microbe interactions," *Journal of Experimental Botany*, vol. 63, no. 9, pp. 3429–3444, 2012.
- [31] C. Forni, A. Frattarelli, A. Lentini, S. Beninati, S. Lucioi, and E. Caboni, "Assessment of the antiproliferative activity on murine melanoma cells of extracts from elicited cell suspensions of strawberry, strawberry tree, blackberry and red raspberry," *Plant Biosystems*, vol. 150, no. 5–6, pp. 1233–1239, 2016.
- [32] S. Lucioi, C. Di Bari, P. Nota, A. Frattarelli, C. Forni, and E. Caboni, "Methyl jasmonate promotes anthocyanins production in *Prunus salicina* × *Prunus persica* in vitro shoot cultures," *Plant Biosystems*, vol. 151, no. 5, pp. 788–791, 2017.
- [33] R. N. Bennett and R. M. Wallsgrove, "Secondary metabolites in plant defence mechanisms," *New Phytologist*, vol. 127, no. 4, pp. 617–633, 1994.
- [34] K. B. Pandey and S. I. Rizvi, "Plant polyphenols as dietary antioxidants in human health and disease," *Oxidative Medicine and Cellular Longevity*, vol. 2, no. 5, pp. 270–278, 2009.
- [35] J. F. Moran, R. V. Klucas, R. J. Grayer, J. Abian, and M. Becana, "Complexes of iron with phenolic compounds from soybean nodules and other legume tissues: prooxidant and antioxidant properties," *Free Radical Biology & Medicine*, vol. 22, no. 5, pp. 861–870, 1997.
- [36] A. Bunea, D. Ruginã, Z. Sconta et al., "Anthocyanin determination in blueberry extracts from various cultivars and their antiproliferative and apoptotic properties in B16-F10 metastatic murine melanoma cells," *Phytochemistry*, vol. 95, pp. 436–444, 2013.
- [37] S. Nandi, M. Vracko, and M. C. Bagchi, "Anticancer activity of selected phenolic compounds: QSAR studies using ridge regression and neural networks," *Chemical Biology & Drug Design*, vol. 70, no. 5, pp. 424–436, 2007.
- [38] A. Aharoni, M. A. Jongsma, and H. J. Bouwmeester, "Volatile science? Metabolic engineering of terpenoids in plants," *Trends in Plant Science*, vol. 10, no. 12, pp. 594–602, 2005.
- [39] M. T. Baratta, H. J. Damien, S. G. Deans, D. M. Biondi, and G. Ruberto, "Chemical composition, antimicrobial and antioxidative activity of laure, sage, rosemary, oregano essential oils," *Journal of Essential Oil Research*, vol. 10, no. 6, pp. 618–627, 1998.
- [40] S. H. Tiong, C. Y. Looi, H. Hazni et al., "Antidiabetic and antioxidant properties of alkaloids from *Catharanthus roseus* (L.) G. Don," *Molecules*, vol. 18, no. 8, pp. 9770–9784, 2013.
- [41] J. Nordberg and E. S. J. Arnér, "Reactive oxygen species, antioxidants, and the mammalian thioredoxin system," *Free Radical Biology & Medicine*, vol. 31, no. 11, pp. 1287–1312, 2001.
- [42] A.-R. Phull, B. Nasir, I. U. Haq, and S. J. Kim, "Oxidative stress, consequences and ROS mediated cellular signaling in rheumatoid arthritis," *Chemico-Biological Interactions*, vol. 281, pp. 121–136, 2018.
- [43] M. J. R. Howes, "Phytochemicals as anti-inflammatory nutraceuticals and phytopharmaceuticals," in *Immunity and Inflammation in Health and Disease: Emerging Roles of Nutraceuticals and Functional Foods in Immune Support*, S. Chatterjee, W. Jungraithmayr, and D. Bagchi, Eds., pp. 363–388, Academic Press, Elsevier, Cambridge, Mass, USA, 2017.
- [44] A. Gomes, E. Fernandes, J. L. F. C. Lima, L. Mira, and M. L. Corvo, "Molecular mechanisms of anti-inflammatory activity mediated by flavonoids," *Current Medicinal Chemistry*, vol. 15, no. 16, pp. 1586–1605, 2008.
- [45] H. G. C. King, "Phenolic compounds of commercial wheat germ," *Journal of Food Science*, vol. 27, no. 5, pp. 446–454, 1962.
- [46] G. M. Raso, R. Meli, G. di Carlo, M. Pacilio, and R. di Carlo, "Inhibition of inducible nitric oxide synthase and cyclooxygenase-2 expression by flavonoids in macrophage J774A.1," *Life Sciences*, vol. 68, no. 8, pp. 921–931, 2001.
- [47] S. Hirai, N. Takahashi, T. Goto et al., "Functional food targeting the regulation of obesity-induced inflammatory responses and pathologies," *Mediators of Inflammation*, vol. 2010, Article ID 367838, 8 pages, 2010.
- [48] A. W. Boots, M. Drent, V. C. J. de Boer, A. Bast, and G. R. M. M. Haenen, "Quercetin reduces markers of oxidative stress and inflammation in sarcoidosis," *Clinical Nutrition*, vol. 30, no. 4, pp. 506–512, 2011.
- [49] R. A. D. Oliveira and I. M. Fierro, "New strategies for patenting biological medicines used in rheumatoid arthritis treatment," *Expert Opinion on Therapeutic Patents*, vol. 28, no. 8, pp. 635–646, 2018.
- [50] K. Vafeiadou, D. Vauzour, H. Y. Lee, A. Rodriguez-Mateos, R. J. Williams, and J. P. E. Spencer, "The citrus flavanone naringenin inhibits inflammatory signalling in glial cells and protects against neuroinflammatory injury," *Archives of Biochemistry and Biophysics*, vol. 484, no. 1, pp. 100–109, 2009.
- [51] M. Hämäläinen, R. Nieminen, P. Vuorela, M. Heinonen, and E. Moilanen, "Anti-inflammatory effects of flavonoids: genistein, kaempferol, quercetin, and daidzein inhibit STAT-1 and NF-kappaB activations, whereas flavone, isorhamnetin, naringenin, and pelargonidin inhibit only NF-kappaB activation along with their inhibitory effect on iNOS expression and NO production in activated macrophages," *Mediators of Inflammation*, vol. 2007, Article ID 45673, 10 pages, 2007.
- [52] A. P. Rogerio, C. L. Dora, E. L. Andrade et al., "Anti-inflammatory effect of quercetin-loaded microemulsion in the airways allergic inflammatory model in mice," *Pharmacological Research*, vol. 61, no. 4, pp. 288–297, 2010.
- [53] J. Wang, R. Zhang, Y. Xu, H. Zhou, B. Wang, and S. Li, "Genistein inhibits the development of atherosclerosis via inhibiting NF-kappaB and VCAM-1 expression in LDLR knockout mice," *Canadian Journal of Physiology and Pharmacology*, vol. 86, no. 11, pp. 777–784, 2008.
- [54] C. Selmi, T. K. Mao, C. L. Keen, H. H. Schmitz, and M. Eric Gershwin, "The anti-inflammatory properties of cocoa flavanols," *Journal of Cardiovascular Pharmacology*, vol. 47, no. 2, pp. S163–S171, 2006.
- [55] H. E. Khoo, A. Azlan, S. T. Tang, and S. M. Lim, "Anthocyanidins and anthocyanins: colored pigments as food, pharmaceutical ingredients, and the potential health benefits," *Food & Nutrition Research*, vol. 61, Article ID 1361779, 2017.

- [56] P. Mena, R. Domínguez-Perles, A. Gironés-Vilaplana, N. Baenas, C. García-Viguera, and D. Villaño, "Flavan-3-ols, anthocyanins, and inflammation," *IUBMB Life*, vol. 66, no. 11, pp. 745–758, 2014.
- [57] A. Murakami and K. Ohnishi, "Target molecules of food phytochemicals: food science bound for the next dimension," *Food & Function*, vol. 3, no. 5, pp. 462–476, 2012.
- [58] A. A. Momtazi-Borojeni, S.-A. Esmaili, E. Abdollahi, and A. Sahebkar, "A review on the pharmacology and toxicology of steviol glycosides extracted from *stevia rebaudiana*," *Current Pharmaceutical Design*, vol. 23, no. 11, pp. 1616–1622, 2017.
- [59] T. C. Kao, M. H. Shyu, and G. C. Yen, "Glycyrrhizic acid and 18beta-glycyrrhetic acid inhibit inflammation via PI3K/Akt/GSK3beta signaling and glucocorticoid receptor activation," *Journal of Agricultural and Food Chemistry*, vol. 58, no. 15, pp. 8623–8629, 2010.
- [60] A. Salminen, M. Lehtonen, T. Suuronen, K. Kaarniranta, and J. Huuskonen, "Terpenoids: natural inhibitors of NF-kappaB signaling with anti-inflammatory and anticancer potential," *Cellular and Molecular Life Sciences*, vol. 65, no. 19, pp. 2979–2999, 2008.
- [61] G. Liang, H. Zhou, Y. Wang et al., "Inhibition of LPS-induced production of inflammatory factors in the macrophages by mono-carbonyl analogues of curcumin," *Journal of Cellular and Molecular Medicine*, vol. 13, no. 9 B, pp. 3370–3379, 2009.
- [62] F. Zhang, J. Liu, and J.-S. Shi, "Anti-inflammatory activities of resveratrol in the brain: role of resveratrol in microglial activation," *European Journal of Pharmacology*, vol. 636, no. 1–3, pp. 1–7, 2010.
- [63] J. Lee, E. Jung, J. Koh, Y. S. Kim, and D. Park, "Effect of rosmarinic acid on atopic dermatitis," *The Journal of Dermatology*, vol. 35, no. 12, pp. 768–771, 2008.
- [64] A. Murakami, T. Nishizawa, K. Egawa et al., "New class of linoleic acid metabolites biosynthesized by corn and rice lipoxygenases: suppression of proinflammatory mediator expression via attenuation of MAPK- and Akt-, but not PPARgamma-, dependent pathways in stimulated macrophages," *Biochemical Pharmacology*, vol. 70, no. 9, pp. 1330–1342, 2005.
- [65] M. Veselinovic, D. Vasiljevic, V. Vucic et al., "Clinical Benefits of n-3 PUFA and  $\gamma$ -Linolenic Acid in Patients with Rheumatoid Arthritis," *Nutrients*, vol. 9, no. 4, article E325, 2017.
- [66] A. Xagorari, A. Papapetropoulos, A. Mauromatis, M. Economou, T. Fotsis, and C. Roussos, "Luteolin inhibits an endotoxin-stimulated phosphorylation cascade and proinflammatory cytokine production in macrophages," *The Journal of Pharmacology and Experimental Therapeutics*, vol. 296, no. 1, pp. 181–187, 2001.
- [67] F. Javadi, A. Ahmadzadeh, S. Eghtesadi et al., "The effect of quercetin on inflammatory factors and clinical symptoms in women with rheumatoid arthritis: a double-blind, randomized controlled trial," *Journal of the American College of Nutrition*, vol. 36, no. 1, pp. 9–15, 2017.
- [68] Z. Shamekhi, R. Amani, Z. Habibagahi, F. Namjoyan, A. Ghadiri, and A. Saki Malehi, "A randomized, double-blind, placebo-controlled clinical trial examining the effects of green tea extract on systemic lupus erythematosus disease activity and quality of life," *Phytotherapy Research*, vol. 31, no. 7, pp. 1063–1071, 2017.
- [69] F. Bonomini, L. F. Rodella, and R. Rezzani, "Metabolic syndrome, aging and involvement of oxidative stress," *Aging and Disease (A&D)*, vol. 6, no. 2, pp. 109–120, 2015.
- [70] D. Harman, "Aging: a theory based on free radical and radiation chemistry," *Journal of Gerontology*, vol. 11, no. 3, pp. 298–300, 1956.
- [71] V. Guarner-Lans, M. E. Rubio-Ruiz, I. Pérez-Torres, and G. Baños de MacCarthy, "Relation of aging and sex hormones to metabolic syndrome and cardiovascular disease," *Experimental Gerontology*, vol. 46, no. 7, pp. 517–523, 2011.
- [72] K. E. Wellen and G. S. Hotamisligil, "Inflammation, stress, and diabetes," *The Journal of Clinical Investigation*, vol. 115, no. 5, pp. 1111–1119, 2005.
- [73] S. Furukawa, T. Fujita, M. Shimabukuro et al., "Increased oxidative stress in obesity and its impact on metabolic syndrome," *The Journal of Clinical Investigation*, vol. 114, no. 12, pp. 1752–1761, 2004.
- [74] P. Portincasa, I. Grattagliano, V. O. Palmieri, and G. Palasciano, "Nonalcoholic steatohepatitis: recent advances from experimental models to clinical management," *Clinical Biochemistry*, vol. 38, no. 3, pp. 203–217, 2005.
- [75] D. A. Dias, S. Urban, and U. Roessner, "A Historical Overview of Natural Products in Drug Discovery," *Metabolites*, vol. 2, no. 4, pp. 303–336, 2012.
- [76] A. M. Patti, K. Al-Rasadi, R. V. Giglio et al., "Natural approaches in metabolic syndrome management," *Archives of Medical Science*, vol. 14, no. 2, pp. 422–441, 2018.
- [77] O. Tabatabaei-Malazy, B. Larijani, and M. Abdollahi, "Targeting metabolic disorders by natural products," *Journal of Diabetes and Metabolic Disorders*, vol. 14, article 57, 2015.
- [78] V.-L. Truong, M. Jun, and W.-S. Jeong, "Role of resveratrol in regulation of cellular defense systems against oxidative stress," *BioFactors*, vol. 44, no. 1, pp. 36–49, 2018.
- [79] B. L. Queen and T. O. Tollefsbol, "Polyphenols and aging," *Current Aging Science*, vol. 3, no. 1, pp. 34–42, 2010.
- [80] Y.-R. Li, S. Li, and C.-C. Lin, "Effect of resveratrol and pterostilbene on aging and longevity," *BioFactors*, vol. 44, no. 1, pp. 69–82, 2018.
- [81] J. K. Prasain, S. H. Carlson, and J. M. Wyss, "Flavonoids and age-related disease: Risk, benefits and critical windows," *Maturitas*, vol. 66, no. 2, pp. 163–171, 2010.
- [82] M. A. Alam, N. Subhan, M. M. Rahman, S. J. Uddin, H. M. Reza, and S. D. Sarker, "Effect of citrus flavonoids, naringin and naringenin, on metabolic syndrome and their mechanisms of action," *Advances in Nutrition*, vol. 5, no. 4, pp. 404–417, 2014.
- [83] L. F. Van Gaal, I. L. Mertens, and C. E. De Block, "Mechanisms linking obesity with cardiovascular disease," *Nature*, vol. 444, no. 7121, pp. 875–880, 2006.
- [84] D. Grassi, G. Desideri, and C. Ferri, "Cardiovascular risk and endothelial dysfunction: the preferential route for atherosclerosis," *Current Pharmaceutical Biotechnology*, vol. 12, no. 9, pp. 1343–1353, 2011.
- [85] R. Bordy, P. Totson, C. Prati, C. Marie, D. Wendling, and C. Demougeot, "Microvascular endothelial dysfunction in rheumatoid arthritis," *Nature Reviews Rheumatology*, vol. 14, no. 7, pp. 404–420, 2018.
- [86] M. A. Gimbrone and G. García-Cardena, "Endothelial cell dysfunction and the pathobiology of atherosclerosis," *Circulation Research*, vol. 118, no. 4, pp. 620–636, 2016.
- [87] T. Head, S. Daunert, and P. J. Goldschmidt-Clermont, "The aging risk and atherosclerosis: A fresh look at arterial homeostasis," *Frontiers in Genetics*, vol. 8, article 216, 2017.
- [88] S. Lacroix, C. Des Rosiers, J.-C. Tardif, and A. Nigam, "The role of oxidative stress in postprandial endothelial dysfunction," *Nutrition Research Reviews*, vol. 25, no. 2, pp. 288–301, 2012.



- [89] M. Wang, R. E. Monticone, and E. G. Lakatta, "Arterial aging: a journey into subclinical arterial disease," *Current Opinion in Nephrology and Hypertension*, vol. 19, no. 2, pp. 201–207, 2010.
- [90] M. T. Ventura, M. Casciaro, S. Gangemi, and R. Buquicchio, "Immunosenescence in aging: between immune cells depletion and cytokines up-regulation," *Clinical and Molecular Allergy*, vol. 15, article 15, 2017.
- [91] W. Wei and S. Ji, "Cellular senescence: molecular mechanisms and pathogenicity," *Journal of Cellular Physiology*, vol. 233, no. 12, pp. 9121–9135, 2018.
- [92] T. Hayakawa, M. Iwai, S. Aoki et al., "SIRT1 suppresses the senescence-associated secretory phenotype through epigenetic gene regulation," *PLoS ONE*, vol. 10, no. 1, Article ID e0116480, 2015.
- [93] B. Sosnowska, M. Mazidi, P. Penson, A. Gluba-Brzózka, J. Rysz, and M. Banach, "The sirtuin family members SIRT1, SIRT3 and SIRT6: Their role in vascular biology and atherogenesis," *Atherosclerosis*, vol. 265, pp. 275–282, 2017.
- [94] M. Zhou, J. Luo, and H. Zhang, "Role of sirtuin 1 in the pathogenesis of ocular disease (review)," *International Journal of Molecular Medicine*, vol. 42, no. 1, pp. 13–20, 2018.
- [95] D. R. Seals, V. E. Brunt, and M. J. Rossman, "Keynote lecture: Strategies for optimal cardiovascular aging," *American Journal of Physiology-Heart and Circulatory Physiology*, vol. 315, no. 2, pp. H183–H188, 2018.
- [96] K. W. J. Wahle, D. Caruso, J. J. Ochoa, and J. L. Quiles, "Olive oil and modulation of cell signaling in disease prevention," *Lipids*, vol. 39, no. 12, Article ID L9617, pp. 1223–1231, 2004.
- [97] E. J. Baker, M. H. Yusof, P. Yaqoob, E. A. Miles, and P. C. Calder, "Omega-3 fatty acids and leukocyte-endothelium adhesion: novel anti-atherosclerotic actions," *Molecular Aspects of Medicine*, vol. 64, pp. 169–181, 2018.
- [98] G. Colussi, C. Catena, M. Novello, N. Bertin, and L. A. Sechi, "impact of omega-3 polyunsaturated fatty acids on vascular function and blood pressure: relevance for cardiovascular outcomes," *Nutrition, Metabolism & Cardiovascular Diseases*, vol. 27, no. 3, pp. 191–200, 2017.
- [99] A. S. Abdelhamid, N. Martin, C. Bridges et al., "Interventions for fatigue and weight loss in adults with advanced progressive illness," *Cochrane Database of Systematic Reviews*, vol. 7, Article ID CD012345, 2012.
- [100] R. Kones, S. Howell, and U. Rumana, "N-3 polyunsaturated fatty acids and cardiovascular disease: principles, practices, pitfalls, and promises - a contemporary review," *Medical Principles and Practice*, vol. 26, no. 6, pp. 497–508, 2017.
- [101] L.-M. Hung, J.-K. Chen, S.-S. Huang, R.-S. Lee, and M.-J. Su, "Cardioprotective effect of resveratrol, a natural antioxidant derived from grapes," *Cardiovascular Research*, vol. 47, no. 3, pp. 549–555, 2000.
- [102] P. Vitaglione, S. Sforza, G. Galaverna et al., "Bioavailability of trans-resveratrol from red wine in humans," *Molecular Nutrition & Food Research*, vol. 49, no. 5, pp. 495–504, 2005.
- [103] C.-L. Kao, L.-K. Chen, Y.-L. Chang et al., "Resveratrol protects human endothelium from H<sub>2</sub>O<sub>2</sub>-induced oxidative stress and senescence via Sirt1 activation," *Journal of Atherosclerosis and Thrombosis*, vol. 17, no. 9, pp. 970–979, 2010.
- [104] C. A. de La Lastra and I. Villegas, "Resveratrol as an antioxidant and pro-oxidant agent: mechanisms and clinical implications," *Biochemical Society Transactions*, vol. 35, no. 5, pp. 1156–1160, 2007.
- [105] M. A. Gammone, K. Efthymakis, F. R. Pluchinotta et al., "Impact of chocolate on the cardiovascular health," *Frontiers in Bioscience - Landmark*, vol. 23, no. 5, pp. 852–864, 2018.
- [106] H. Zhang, H. Liu, Y. Chen, and Y. Zhang, "The curcumin-induced vasorelaxation in rat superior mesenteric arteries," *Annals of Vascular Surgery*, vol. 48, pp. 233–240, 2018.
- [107] M. A. Gammone, F. R. Pluchinotta, S. Bergante, G. Tettamanti, and N. D'Orazio, "Prevention of cardiovascular diseases with carotenoids," *Frontiers in Bioscience - Scholar*, vol. 9, no. 1, pp. 165–171, 2017.
- [108] S. Jeong, "Molecular and cellular basis of neurodegeneration in alzheimer's disease," *Molecules and Cells*, vol. 40, no. 9, pp. 613–620, 2017.
- [109] S. Podvin, H. T. Reardon, K. Yin, C. Mosier, and V. Hook, "Multiple clinical features of Huntington's disease correlate with mutant HTT gene CAG repeat lengths and neurodegeneration," *Journal of Neurology*, vol. 266, no. 3, pp. 551–564, 2019.
- [110] A. P. Jones, A. G. Kermode, R. M. Lucas et al., "Circulating immune cells in multiple sclerosis," *Clinical & Experimental Immunology*, vol. 187, no. 2, pp. 193–203, 2017.
- [111] J. Joseph, G. Cole, E. Head, and D. Ingram, "Nutrition, brain aging, and neurodegeneration," *The Journal of Neuroscience*, vol. 29, no. 41, pp. 12795–12801, 2009.
- [112] A. Granzotto and P. Zatta, "Resveratrol acts not through Anti-Aggregative pathways but mainly via its scavenging properties against A $\beta$  and A $\beta$ -metal complexes toxicity," *PLoS ONE*, vol. 6, no. 6, Article ID e21565, 2011.
- [113] W. Yan, R. Liu, L. Wang et al., "Sirt3-mediated autophagy contributes to resveratrol-induced protection against ER stress in HT22 cells," *Frontiers in Neuroscience*, vol. 12, article 116, 2018.
- [114] H. Capiralla, V. Vingtdoux, H. Zhao et al., "Resveratrol mitigates lipopolysaccharide- and A $\beta$ -mediated microglial inflammation by inhibiting the TLR4/NF- $\kappa$ B/STAT signaling cascade," *Journal of Neurochemistry*, vol. 120, no. 3, pp. 461–472, 2012.
- [115] D. Porquet, G. Casadesús, S. Bayod et al., "Dietary resveratrol prevents alzheimer's markers and increases life span in SAMP8," *Age (Dordr)*, vol. 35, no. 5, pp. 1851–1865, 2013.
- [116] F. Zhang, J.-S. Shi, H. Zhou, B. Wilson, J.-S. Hong, and H.-M. Gao, "Resveratrol protects dopamine neurons against lipopolysaccharide-induced neurotoxicity through its anti-inflammatory actions," *Molecular Pharmacology*, vol. 78, no. 3, pp. 466–477, 2010.
- [117] Y.-J. Guo, S.-Y. Dong, X.-X. Cui et al., "Resveratrol alleviates MPTP-induced motor impairments and pathological changes by autophagic degradation of  $\alpha$ -synuclein via SIRT1-deacetylated LC3," *Molecular nutrition & food research*, vol. 60, no. 10, pp. 2161–2175, 2016.
- [118] K. Dutta, D. Ghosh, and A. Basu, "Curcumin protects neuronal cells from japanese encephalitis virus-mediated cell death and also inhibits infective viral particle formation by dysregulation of ubiquitin-proteasome system," *Journal of Neuroimmune Pharmacology*, vol. 4, no. 3, pp. 328–337, 2009.
- [119] M. S. Wang, S. Boddapati, S. Emadi, and M. R. Sierks, "Curcumin reduces alpha-synuclein induced cytotoxicity in Parkinson's disease cell model," *BMC Neuroscience*, vol. 11, article 57, pp. 1–10, 2010.
- [120] Z. Liu, Z. Li, L. Liu et al., "Curcumin attenuates beta-amyloid-induced neuroinflammation via activation of peroxisome proliferator-activated receptor-gamma function in a rat model of alzheimer's disease," *Frontiers in Pharmacology*, vol. 7, article 261, 2016.

- [121] D. K. Khatri and A. R. Juvekar, "Neuroprotective effect of curcumin as evinced by abrogation of rotenone-induced motor deficits, oxidative and mitochondrial dysfunctions in mouse model of Parkinson's disease," *Pharmacology Biochemistry & Behavior*, vol. 150-151, pp. 39-47, 2016.
- [122] M. A. Ansari, H. M. Abdul, G. Joshi, W. O. Opii, and D. A. Butterfield, "Protective effect of quercetin in primary neurons against Abeta(1-42): relevance to Alzheimer's disease," *The Journal of Nutritional Biochemistry*, vol. 20, no. 4, pp. 269-275, 2009.
- [123] A. M. Sabogal-Guáqueta, J. I. Muñoz-Manco, J. R. Ramírez-Pineda, M. Lamprea-Rodriguez, E. Osorio, and G. P. Cardona-Gómez, "The flavonoid quercetin ameliorates Alzheimer's disease pathology and protects cognitive and emotional function in aged triple transgenic Alzheimer's disease model mice," *Neuropharmacology*, vol. 93, pp. 134-145, 2015.
- [124] H. Gardener and M. R. Caunca, "Mediterranean diet in preventing neurodegenerative diseases," *Current Nutrition Reports*, vol. 7, no. 1, pp. 10-20, 2018.
- [125] S. Nobili, D. Lippi, E. Witort et al., "Natural compounds for cancer treatment and prevention," *Pharmacological Research*, vol. 59, no. 6, pp. 365-378, 2009.
- [126] T. Shrihari, "Dual role of inflammatory mediators in cancer," *ecancermedicallscience*, vol. 11, article 721, 2017.
- [127] G. C. Leonardi, G. Accardi, R. Monastero, F. Nicoletti, and M. Libra, "Ageing: from inflammation to cancer," *Immunity & Ageing*, vol. 15, article 1, 2018.
- [128] S. Lin, Y. Li, A. A. Zamyatnin, J. Werner, and A. V. Bazhin, "Reactive oxygen species and colorectal cancer," *Journal of Cellular Physiology*, vol. 233, no. 7, pp. 5119-5132, 2018.
- [129] H. Blaser, C. Dostert, T. W. Mak, and D. Brenner, "TNF and ROS crosstalk in inflammation," *Trends in Cell Biology*, vol. 26, no. 4, pp. 249-261, 2016.
- [130] T. Hussain, B. Tan, W. Ren et al., "Polyamines: therapeutic perspectives in oxidative stress and inflammatory diseases," *Amino Acids*, vol. 49, no. 9, pp. 1457-1468, 2017.
- [131] A. Lentini, C. Tabolacci, B. Provenzano, S. Rossi, and S. Beninati, "Phytochemicals and protein-polyamine conjugates by transglutaminase as chemopreventive and chemotherapeutic tools in cancer," *Plant Physiology and Biochemistry*, vol. 48, no. 7, pp. 627-633, 2010.
- [132] X. Y. Mao, M. Z. Jin, J. F. Chen, H. H. Zhou, and W. L. Jin, "Live or let die: Neuroprotective and anti-cancer effects of nutraceutical antioxidants," *Pharmacology & Therapeutics*, vol. 183, pp. 137-155, 2018.
- [133] G. Mantovani, C. Madeddu, A. Macciò et al., "Cancer-related anorexia/cachexia syndrome and oxidative stress: an innovative approach beyond current treatment," *Cancer Epidemiology, Biomarkers & Prevention*, vol. 13, no. 10, pp. 1651-1659, 2004.
- [134] A. Rauf, M. Imran, I. A. Khan et al., "Anticancer potential of quercetin: a comprehensive review," *Phytotherapy Research*, vol. 32, no. 11, pp. 2109-2130, 2018.
- [135] M. Linsalata, A. Orlando, C. Messa, M. G. Refolo, and F. Russo, "Quercetin inhibits human DLD-1 colon cancer cell growth and polyamine biosynthesis," *Anticancer Research*, vol. 30, no. 9, pp. 3501-3507, 2010.
- [136] G. Bobe, P. S. Albert, L. B. Sansbury et al., "Interleukin-6 as a potential indicator for prevention of high-risk adenoma recurrence by dietary flavonols in the polyp prevention trial," *Cancer Prevention Research*, vol. 3, no. 6, pp. 764-775, 2010.
- [137] P. Anand, A. B. Kunnumakkara, R. A. Newman, and B. B. Aggarwal, "Bioavailability of curcumin: problems and promises," *Molecular Pharmaceutics*, vol. 4, no. 6, pp. 807-818, 2007.
- [138] R. P. A. de Matos, M. F. Calmon, C. F. Amantino et al., "Effect of curcumin-nanoemulsion associated with photodynamic therapy in cervical carcinoma cell lines," *BioMed Research International*, vol. 2018, Article ID 4057959, 11 pages, 2018.
- [139] M. Jalili-Nik, A. Soltani, S. Moussavi et al., "Current status and future prospective of Curcumin as a potential therapeutic agent in the treatment of colorectal cancer," *Journal of Cellular Physiology*, vol. 233, no. 9, pp. 6337-6345, 2018.
- [140] H. Danafar, A. Sharafi, S. Kheiri, and H. K. Manjili, "Co-delivery of sulforaphane and curcumin with pegylated iron oxide-gold core shell nanoparticles for delivery to breast cancer cell line," *Iranian Journal of Pharmaceutical Research*, vol. 17, no. 2, pp. 480-494, 2018.
- [141] T. Murray-Stewart and R. A. Casero, "Regulation of by cancer prevention and therapy," *Medical Sciences (Basel)*, vol. 4, no. 4, article E38, 2017.
- [142] S. S. D. Kumar, N. N. Houreld, and H. Abrahamse, "Therapeutic potential and recent advances of curcumin in the treatment of aging-associated diseases," *Molecules*, vol. 23, no. 4, article E835, 2018.
- [143] L. G. Carter, J. A. D'Orazio, and K. J. Pearson, "Resveratrol and cancer: focus on in vivo evidence," *Endocrine-Related Cancer*, vol. 21, no. 3, pp. R209-R225, 2014.
- [144] L. Roncoroni, L. Elli, P. Braidotti et al., "Transglutaminase 2 mediates the cytotoxicity of resveratrol in a human cholangiocarcinoma and gallbladder cancer cell lines," *Nutrition and Cancer*, vol. 70, no. 5, pp. 761-769, 2018.
- [145] J. M. Pezzuto, "Resveratrol: twenty years of growth, development and controversy," *Biomolecules & Therapeutics (Seoul)*, vol. 27, pp. 1-14, 2019.
- [146] Q. Xiao, W. Zhu, W. Feng et al., "A review of resveratrol as a potent chemoprotective and synergistic agent in cancer chemotherapy," *Frontiers in Pharmacology*, vol. 9, article 1534, 2019.
- [147] V. Mukund, D. Mukund, V. Sharma, M. Mannarapu, and A. Alam, "Genistein: Its role in metabolic diseases and cancer," *Critical Review in Oncology/Hematology*, vol. 119, pp. 13-22, 2017.
- [148] S. H. Kim, C. W. Kim, S. Y. Jeon, R. E. Go, K. A. Hwang, and K. C. Choi, "Chemopreventive and chemotherapeutic effects of genistein, a soy isoflavone, upon cancer development and progression in preclinical animal models," *Laboratory Animal Research*, vol. 30, no. 4, pp. 143-150, 2014.
- [149] G. B. Lesinski, P. K. Reville, T. A. Mace et al., "Consumption of soy isoflavone enriched bread in men with prostate cancer is associated with reduced proinflammatory cytokines and immunosuppressive cells," *Cancer Prevention Research*, vol. 8, no. 11, pp. 1036-1044, 2015.
- [150] F. Carini, S. David, G. Tomasello et al., "Colorectal cancer: an update on the effects of lycopene on tumor progression and cell proliferation," *Journal of Biological Regulators & Homeostatic Agents*, vol. 31, pp. 769-774, 2017.
- [151] L. Jiang, Y. Liu, and B. Li, "Lycopene exerts anti-inflammatory effect to inhibit prostate cancer progression," *Asian Journal of Andrology*, vol. 21, no. 1, p. 80, 2019.
- [152] J. L. Rowles, K. M. Ranard, J. W. Smith, R. An, and J. W. Erdman, "Increased dietary and circulating lycopene are associated with reduced prostate cancer risk: a systematic review and meta-analysis," *Prostate Cancer and Prostatic Diseases*, vol. 20, no. 4, pp. 361-377, 2017.



- [153] G. Lidzbarsky, D. Gutman, H. A. Shekhidem, L. Sharvit, and G. Atzmon, "Genomic instabilities, cellular senescence, and aging: in vitro, in vivo and aging-like human syndromes," *Frontiers in Medicine*, vol. 5, article 104, 2018.
- [154] A. Artese, G. Costa, F. Ortuso, L. Parrotta, and S. Alcaro, "Identification of new natural DNA G-quadruplex binders selected by a structure-based virtual screening approach," *Molecules*, vol. 18, no. 10, pp. 12051–12070, 2013.
- [155] G. Ait-Ghezala, S. Hassan, M. Tweed et al., "Identification of telomerase-activating blends from naturally occurring compounds," *Alternative Therapies in Health and Medicine*, vol. 2, 2, pp. 6–14, 2016.
- [156] R. Ganceviciene, A. I. Liakou, A. Theodoridis, E. Makrantonaki, and C. C. Zouboulis, "Skin anti-aging strategies," *Dermato-Endocrinology*, vol. 4, no. 3, pp. 308–319, 2012.
- [157] K. A. Hammer, "Treatment of acne with tea tree oil (melaleuca) products: a review of efficacy, tolerability and potential modes of action," *International Journal of Antimicrobial Agents*, vol. 45, no. 2, pp. 106–110, 2015.
- [158] H. H. Kwon, J. Y. Yoon, S. Y. Park, S. Min, and D. H. Suh, "Comparison of clinical and histological effects between lactobacillus-fermented chamaecyparis obtusa and tea tree oil for the treatment of acne: an eight-week double-blind randomized controlled split-face study," *Dermatology*, vol. 229, no. 2, pp. 102–109, 2014.
- [159] G. Ramage, S. Milligan, D. F. Lappin et al., "Antifungal, cytotoxic, and immunomodulatory properties of tea tree oil and its derivative components: Potential role in management of oral candidosis in cancer patients," *Frontiers in Microbiology*, vol. 3, article 220, 2012.
- [160] N. Pazyar, R. Yaghoobi, N. Bagherani, and A. Kazerouni, "A review of applications of tea tree oil in dermatology," *International Journal of Dermatology*, vol. 52, no. 7, pp. 784–790, 2013.
- [161] W.-W. Chao, C.-C. Su, H.-Y. Peng, and S.-T. Chou, "Melaleuca quinquenervia essential oil inhibits  $\alpha$ -melanocyte-stimulating hormone-induced melanin production and oxidative stress in B16 melanoma cells," *Phytomedicine*, vol. 34, pp. 191–201, 2017.
- [162] E. Herro and S. E. Jacob, "Mentha piperita (peppermint)," *Dermatitis*, vol. 21, no. 6, pp. 327–329, 2010.
- [163] G. Micali, V. Paternò, R. Cannarella, F. Dinotta, and F. Lacarrubba, "Evidence-based treatment of atopic dermatitis with topical moisturizers," *Giornale Italiano di Dermatologia e Venereologia*, vol. 153, no. 3, pp. 396–402, 2018.
- [164] R. Di Franco, E. Sammarco, M. G. Calvanese et al., "Preventing the acute skin side effects in patients treated with radiotherapy for breast cancer: the use of corneometry in order to evaluate the protective effect of moisturizing creams," *Journal of Radiation Oncology*, vol. 8, article 57, 2013.
- [165] S. Turk, U. Y. Malkan, M. Ghasemi et al., "Growth inhibitory activity of Ankaferd hemostat on primary melanoma cells and cell lines," *SAGE Open Medicine*, vol. 5, p. 205031211668951, 2017.
- [166] L. Tartaglione, A. Gambuti, P. De Cicco et al., "NMR-based phytochemical analysis of vitis vinifera cv Falanghina leaves. characterization of a previously undescribed biflavonoid with antiproliferative activity," *Fitoterapia*, vol. 125, pp. 13–17, 2018.
- [167] Y.-S. Hah, J. G. Kim, H. Y. Cho, J. S. Park, E. P. Heo, and T.-J. Yoon, "Procyanidins from vitis vinifera seeds induce apoptotic and autophagic cell death via generation of reactive oxygen species in squamous cell carcinoma cells," *Oncology Letters*, vol. 14, no. 2, pp. 1925–1932, 2017.
- [168] F. F. Brito, P. M. Gimeno, B. Bartolomé et al., "Vine pollen allergy in areas with a high density of vineyards," *Annals of Allergy, Asthma & Immunology*, vol. 100, no. 6, pp. 596–600, 2008.
- [169] I. Kalyana Sundaram, D. D. Sarangi, V. Sundararajan, S. George, and S. Sheik Mohideen, "Poly herbal formulation with anti-elastase and anti-oxidant properties for skin anti-aging," *BMC Complementary and Alternative Medicine*, vol. 18, no. 1, article 33, 2018.
- [170] R. Prasad, T. Singh, and S. K. Katiyar, "Honokiol inhibits ultraviolet radiation-induced immunosuppression through inhibition of ultraviolet-induced inflammation and DNA hypermethylation in mouse skin," *Scientific Reports*, vol. 7, no. 1, article 1657, 2017.
- [171] M. M. Sarandy, R. D. Novaes, A. A. Xavier et al., "Hydroethanolic extract of strychnos pseudoquina accelerates skin wound healing by modulating the oxidative status and microstructural reorganization of scar tissue in experimental type I diabetes," *BioMed Research International*, vol. 2017, Article ID 9538351, 11 pages, 2017.
- [172] D. M. J. Houston, B. Robins, J. J. Bugert, S. P. Denyer, and C. M. Heard, "In vitro permeation and biological activity of punicalagin and zinc (II) across skin and mucous membranes prone to herpes simplex virus infection," *European Journal of Pharmaceutical Sciences*, vol. 96, pp. 99–106, 2017.

## Research Article

# Diosgenin and Its Fenugreek Based Biological Matrix Affect Insulin Resistance and Anabolic Hormones in a Rat Based Insulin Resistance Model

Rita Kiss<sup>1</sup> ,<sup>1</sup> Georgina Pesti-Asbóth,<sup>2</sup> Mária Magdolna Szarvas,<sup>2</sup> László Stündl,<sup>2</sup> Zoltán Cziáky,<sup>3</sup> Csaba Hegedűs,<sup>4</sup> Diána Kovács,<sup>1</sup> Andrea Badale,<sup>1</sup> Endre Máthé,<sup>2</sup> Zoltán Szilvássy,<sup>1</sup> and Judit Remenyik<sup>2</sup> 

<sup>1</sup>Department of Pharmacology and Pharmacotherapy, Faculty of Medicine, University of Debrecen, Nagyerdei krt. 98, 4032 Debrecen, Hungary

<sup>2</sup>Institute of Food Technology, Faculty of Agricultural and Food Sciences and Environmental Management, University of Debrecen, Böszörményi út 138, 4032 Debrecen, Hungary

<sup>3</sup>Agricultural and Molecular Research and Service Institute, University of Nyíregyháza, Sóstói út 31/B, 4400 Nyíregyháza, Hungary

<sup>4</sup>Cera-Med Ltd., Kútvölgyi u. 1, 4225 Debrecen, Hungary

Correspondence should be addressed to Rita Kiss; [kiss.rita@med.unideb.hu](mailto:kiss.rita@med.unideb.hu) and Judit Remenyik; [remenyik@agr.unideb.hu](mailto:remenyik@agr.unideb.hu)

Received 7 August 2018; Accepted 21 March 2019; Published 4 April 2019

Academic Editor: Ravirajsinh N. Jadeja

Copyright © 2019 Rita Kiss et al. This is an open access article distributed under the Creative Commons Attribution License, which permits unrestricted use, distribution, and reproduction in any medium, provided the original work is properly cited.

Fenugreek is known since ancient times as a traditional herbal medicine of its multiple beneficial effects. Fenugreek's most studied and employed effect is its hypoglycemic property, but it can also be useful for the treatment of certain thyroid disorders or for the treatment of anorexia. The regulation of glucose homeostasis is a complex mechanism, dependent on the interaction of different types of hormones and neurotransmitters or other compounds. For the study of how diosgenin and fenugreek seeds modify insulin sensitivity, we used a rat insulin resistance model induced by high-fat diet. Diosgenin in three different doses (1mg/bwkg, 10mg/bwkg, and 50 mg/bwkg, respectively) and fenugreek seed (0.2 g/bwkg) were administered orally for 6 weeks. Insulin sensitivity was determined by hyperinsulinemic euglycemic glucose clamp method. Our research group found that although glucose infusion rate was not significantly modified in either group, the increased insulin sensitivity index and high metabolic clearance rate of insulin found in the 1 mg/kg diosgenin and the fenugreek seed treated group suggested an improved peripheral insulin sensitivity. Results from the 10 mg/kg diosgenin group, however, suggest a marked insulin resistance. Fenugreek seed therapy results on the investigated anabolic hormones support the theory that, besides insulin and gastrointestinal peptides, the hypothalamic-hypopituitary axis regulated hormones synchronized action with IGF-1 also play an important role in the maintaining of normal glucose levels. Both diosgenin and fenugreek seeds are capable of interacting with substrates of the above-mentioned regulatory mechanisms, inducing serious hormonal disorders. Moreover, fenugreek seeds showed the ability to reduce the thyroid hormone levels at the periphery and to modify the T4/T3 ratio. It means that in healthy people this effect could be considered a severe side effect; however, in hypothyroidism this effect represents a possibility of alternative natural therapy.

## 1. Introduction

Fenugreek (*Trigonella foenum-graecum*) appears to be rich in phytonutrients with multiple pharmacological effects [1–4]. Extracts have been made using fenugreek vegetative organs and/or seeds, and multiple *in vivo* and *in vitro* studies revealed analgesic [5, 6], hepatoprotective [7, 8], and hypolipidemic

[9–14] effects. It was suggested that the hypolipidemic effects could be put on the expense of saponins that transformed into sapogenins in the gastrointestinal tract would trigger the reduction of serum cholesterol levels [15, 16]. Among saponins, the diosgenin was found to induce changes in the lipid profile of different tissues or organs, such as plasma, liver, heart, or brain in a diabetic rat model [17], indicating

that these modifications might be correlated with a hypoglycemic effect. In another study, it was demonstrated that both fenugreek and diosgenin treatment prevented high-fat, high-sugar diet-induced endothelial dysfunction, and redox changes [18]. Besides diosgenin, the 4-hydroxyisoleucine (4-HIL), a fairly rare amino acid found in fenugreek, was shown to increase insulin secretion upon glucose stimulation [19, 20]. Moreover, 4-HIL could reduce insulin resistance (IR) in muscle and/or liver by stimulating phosphoinositide 3 (PI3) kinase activity [21]. Interestingly, increased insulin receptor [22], adiponectin, and PPAR $\gamma$  [23] expression were also associated with the IR reducing effects of fenugreek. These results, together with the fenugreek seed administration induced improvement of hepatic steatosis, strongly plead for a cause-and-effect type of relationship between liver specific IR and steatosis [23]. It is also demonstrated that the health promoting effect of fenugreek is mostly due to its antioxidant capacity [24]. Among phytonutrients, the polyphenols from fenugreek seeds were shown to exert antioxidant properties by inhibiting lipid peroxidation [8]. A fenugreek seed and/or seed extracts were found to increase glucose uptake; reduced glycosylated haemoglobin levels together with proinflammatory cytokines and pancreatic enzymes; in dose-dependent manner restored the glycogen levels in muscle and liver; inhibited lipid peroxidation; and reinstated some antioxidant enzymes-glutathione (GSH) and superoxide dismutase (SOD) activities in the liver and pancreas [25]. It has also been suggested that, in the case of fenugreek, the antioxidant potential complements the hypolipidemic, hypoglycemic, and anti-inflammatory effects [26]. Accordingly, diabetic rats treated with fenugreek showed reduced serum glucose levels, and the activities of antioxidant defence enzymes increased due to the expression of the mentioned genes in the liver or/and brain [27]. Another study concluded that fenugreek seed extract could efficiently suppress testicular oxidative stress in combination with apoptosis and inflammation [28]. Interestingly, a comparative study showed substantial differences between the antioxidant activity of fenugreek leaf and seed extracts with respect to the DNA damage protective activities [29]. Another study was indicating a functional link between the antioxidant and anticancer effects of fenugreek [30]. Nevertheless, the anticancer effect of fenugreek has been thoroughly assessed [31–33], and selective cytotoxicity has been observed in case of various cancer cell lines. Thus, for example, in the case of breast cancer, T cell lymphoma, B cell lymphoma, and thyroid papillary carcinoma cell lines, significant cytotoxic effects were observed while no significant cytotoxicity was evident for normal human cells. [28]. Furthermore, Vigh et al. were able to correlate the chemical composition of fenugreek seed extracts with reduced viability of the T-47D and ZR-75-1 breast cancer cell lines [34]. Moreover, they could also show that an aqueous fenugreek seed extract could affect the viability of cancerous cells in a dose-dependent antagonistic fashion. However, only diosgenin from fenugreek was proven to efficiently reduce cancer cell viability, while inducing apoptosis [35]. More specifically, it was ascertained that diosgenin inhibited telomerase activity by downregulating the hTERT gene expression could reverse multidrug resistance in cancer cells by sensitizing them to

standard chemotherapy, activating p53 gene and the STAT3 signalling pathway [36–38]. In addition to fenugreek beneficial properties, some toxic effects were also reported related to embryonic development, spermatogenesis, allergic reactions, neurotoxicity, and altered levels of thyroid hormones or inhibition of hematopoietic regulatory elements [39].

Taken together, plethora of research has been conducted to analyze independently the fenugreek composition and the generated biological effects, yet studies to relate composition to function are available in limited numbers, mostly due to the limitation of research models and methodology. Among the constituents of fenugreek, diosgenin stands at the forefront of current research, and results are indicating multiple biological effects depending on the characteristics of assessed models. Our research reported in current paper describes a comparative dose-dependent study based on fenugreek and diosgenin in conjunction with an improved peripheral insulin sensitivity and the interference with hypothalamic-hypopituitary axis regulated hormones. To the best of our knowledge there is no published evidence suggesting the interdependence between the possible concentration-dependent toxic effects of fenugreek treatment and the most important anabolic hormones, such as the growth hormone, IGF-1, T3, and T4. Our results further demonstrate the importance of careful dose-dependent assessment of fenugreek specific pharmacological effects.

## 2. Materials and Methods

### 2.1. Analytical Examination of Fenugreek Seeds

**2.1.1. Preparation of Extract.** The seeds of fenugreek were obtained from an authorized local distributor. Powdered fenugreek seeds were extracted with water: ethanol mixture (1:1) for 72 h at 70°C using Soxhlet apparatus. This extract was then concentrated to dryness by removing the solvent in the rotary evaporator under reduced pressure.

**2.1.2. Preparation of Sample for Analysis.** One gram of thoroughly milled fenugreek seeds was accurately weighed. To the fine powder obtained, 80 mL of 3 M hydrochloric acid was added, and then it was kept on reflux for 1 h on water bath at 100°C. Mixture was allowed to cool at room temperature and was diluted further up to the mark with water. Diethyl ether was used for the extraction process of the mixture. After that the ether layer was separated and left to evaporate. The remained residue was dissolved in 25 mL of methanol. This resulting solution was used as test solution [40].

**2.1.3. Chromatographic Conditions for Ultra High Performance Liquid Chromatography.** The preparation of diosgenin was done with Chromaster Rs ultra high performance liquid chromatography system (with a 6430 diode array detector (DA), 6270 autosampler, 6170 binary pump, 6310 column oven, software Agilent Open LAB chromatography data system). Diosgenin was separated on a reverse-phase 10 mm  $\times$  4.6 mm  $\times$  2.5  $\mu$ m Kinetex XB-C18 column. The mobile phase was prepared from water (solvent A) and acetonitrile

(solvent B). The mobile phase was degassed and filtered through 0.45  $\mu\text{m}$  filter before use. The gradient program used was from A to B (10:90 v/v); 20-21 min, linear change from A-B (10:90 v/v) to A-B (2:98 v/v); 21-25 min, constant change from A-B (2:98 v/v); 25-26 min, linear changes from A-B (2:98 v/v) to A-B (10:90 v/v); and 26-30 min, constant change from A to B (10:90 v/v). The flow rate of the mobile phase was 0.7 mL/min. The temperature of the column was set to 25°C. The injection volume was 10  $\mu\text{L}$ . The DA was set at 254 nm to acquire the chromatogram. Diosgenin was identified by comparing the retention time and spectra obtained from sample and standard solutions (see Figure 1) [1]. We performed a total ion chromatogram of fenugreek (alcoholic extract) in negative ionization mode including fragmentation spectra of the parent ion (see Figure 2) [40, 41].

## 2.2. Animals and Protocols

**2.2.1. Ethics.** The study was approved by and was in accordance with the guidelines of and the Animal Ethics Committee of the University of Debrecen (25/2013 DE MÁB).

**2.2.2. Animals.** Male Wistar rats ( $n=42$ ) were used throughout the study. Rats were maintained in a controlled environment (22-24°C, 12-12 h light/dark cycle). For the animals a week of acclimation period was provided; thereafter the rats were randomly selected into six experimental groups: healthy control (C), high-fat diet control (HF), high-fat diet + 1 mg/kg diosgenin (1D), high-fat diet + 10 mg/kg diosgenin (10D), high-fat diet + 50 mg/kg diosgenin (50D), and high-fat diet + 0,2 mg/kg fenugreek seed (FG). The healthy control rats had access to a standard laboratory chow (S8106-S011 SM R/M-Z+H, ssniff Spezialdiäten GmbH, Germany) and fresh tap water ad libitum. Animals in the five other groups received ad libitum a diet with high proportion of crude fats and carbohydrates, defined as high-fat diet (HFD) and 5% sucrose in the drinking water. This special rodent chow ("824018-45%AFE FAT") was provided by "Special Diets Services", UK. For the treated groups, the previously mentioned diosgenin doses, or the thoroughly milled fenugreek seeds were incorporated into the food. As the endpoint of the experiment the seventh week of treatment period was determined.

**2.2.3. Hyperinsulinemic Euglycemic Glucose Clamp (HEGC).** The hyperinsulinemic euglycemic glucose clamp (HEGC) method is a well-known and the most acceptance investigation to determine the exact and precise insulin sensitivity of insulin dependent tissues described by DeFronzo et al. [42, 43]. According to our previously configured and validated method to measure whole body insulin sensitivity [44] we performed the HEGC method on each animal of our current investigation. The animals needed to be anaesthetized before the procedure. After an overnight starvation, general anaesthesia was induced and sustained by an intraperitoneal injection of 50 mg/kg sodium thiopental (Thiopental Sandoz®, Sandoz Pharmaceutical PLC, Switzerland). To allow the spontaneous breathing of the animals, a polyethylene tube was inserted into the trachea. The HEGC method presumes

two separate venous infusion lines for the administration of the insulin and glucose solution and an arterial cannula that serves for blood sampling for the subsequent determination of blood glucose levels and for monitoring the blood pressure during the whole period of the investigation. Two branches of the jugular vein and same side carotid artery were exposed and cannulated. After thirty-minute stabilization period continuous insulin (Humulin R®, Eli Lilly, Indianapolis, IN, USA) and 20% w/v glucose infusion were initiated simultaneously through the jugular vein. The rate of insulin infusion was set to 3 mU/kg/min while the glucose infusion rate was adjusted in accordance with maintaining the euglycemic ( $5.5 \pm 0.5$  mmol/l) blood glucose status. The blood glucose concentration was determined before the starting of the infusions (insulin and glucose respectively), during the first 80 minutes of the experiment in 5-minute intervals, and at every 10 minutes after the "steady state" condition developed, using a blood glucose testing device (Accu-Chek, Roche Diagnostics, Budaörs, Hungary). In addition, the fasting and steady state levels of insulin were determined from the plasma obtained from blood samples collected in EDTA tubes (0.5 ml, in 20  $\mu\text{L}$  EDTA, 10  $\mu\text{L}$  Trasylol; Bayer, Leverkusen, Germany) before the initiation of insulin infusion and during the steady state period of the experiment. The blood samples were centrifuged for two minutes, at 10.000 g and 4°C (Centrifuge 5415R, Eppendorf GmbH, Germany), and the plasma was frozen and stored at -70°C for further determinations.

## 2.3. Sample Preparation and Determination of Hormone Levels

**2.3.1. Description of the Blood Sample Preparation.** To determine the plasma concentration of insulin, IGF-1, T3, T4, and GH from each animal blood samples were collected into EDTA-coated blood collection tubes (BD, Franklin Lakes, NJ, USA). The samples were centrifuged at 3000 rpm for 10 min (Centrifuge 5418, nonrefrigerated, with rotor FA-45-18-11, 230V/50-60Hz, 36 ml, 5418 000.017). The plasma was then aliquoted and stored frozen at -20°C until analysis.

**2.3.2. Determination of Insulin.** The concentration of insulin was determined using a commercially available ELISA kit (Insulin ELISA, Immuno Diagnostics, Woodland Hills, California, USA, kit number: 1606-15). The absorbance was measured at 450 nm colorimetrically. The insulin concentrations were determined by comparing the absorbance values of the samples to the standard curve. The insulin concentrations were expressed as plasma insulin concentration (in  $\mu\text{IU/mL}$ ). The reagents were prepared according to the manufacturer's instructions. 50  $\mu\text{L}$  samples were added to sample wells. The standard curve was prepared as it was described in the protocol and 50  $\mu\text{L}$  of the diluted standard solution was added to the appropriate wells. 100  $\mu\text{L}$  of the Enzyme Reagent was added to each well; then the microplate was swirled gently for 20-30 seconds to mix and covered with a plastic wrap and was incubated for 120 minutes at room temperature (20-27°C). The liquid of the microplate was discarded by decantation and tap and blot the plate dry with absorbent paper. 350  $\mu\text{L}$  of



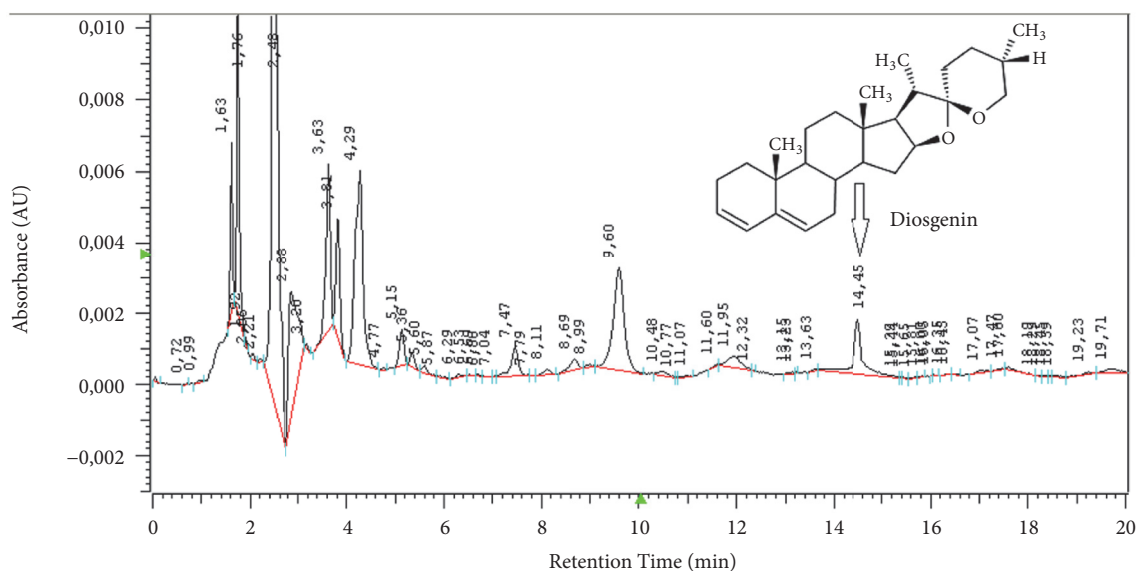


FIGURE 1: Chromatogram of fenugreek (*Trigonella foenum-graecum* L.).

wash buffer was added, decanted, and aspirated, and this step was repeated two additional times for a total of three washes. 100  $\mu$ L of working substrate was added to solution in all wells and the microplate was incubated at room temperature for 15 minutes. Then 50  $\mu$ L of stop solution was added to each well and mixed gently 15-25 seconds. Absorbance was measured at 450 nm. Sample insulin concentration was compared with the insulin standard curve and the concentration of insulin was expressed as plasma insulin concentration (in  $\mu$ IU/ml).

**2.3.3. Determination of Insulin-Like Growth Factor-1 (IGF-1).** The insulin-like growth factor-1 was determined using a commercially available ELISA kit (Eagle Biosciences, INC., Nashua, New Hampshire, kit number: IGF31-K01). The reagents were prepared according to the manufacturer's instructions. Standards and samples were prepared as described in the protocol book. 20  $\mu$ L of the samples and standard were added to the appropriate wells and 100  $\mu$ L of the biotinylated IGF was added to each well and the plate was incubated at room temperature for two hours. The solution was aspirated from the microplate and each well was rinsed with 300  $\mu$ L of 1x Wash solution and repeated 3 times. 150  $\mu$ L of the enzyme complex was added to each well after the wash process and the plate was incubated one hour at room temperature. Then the wash process was repeated three times. 100  $\mu$ L of substrate was added to each well and incubated for 15 minutes. 100  $\mu$ L of stopping solution was added to each well. Absorbance was measured at 450 nm. Sample IGF-1 concentration was compared with the IGF-1 standard curve and the concentration of IGF-1 was expressed as plasma IGF-1 concentration (in ng/mL).

**2.3.4. Determination of Growth Hormone (GH).** The concentration of growth hormone was assessed with a commercially available assay kit (Elisa Cloud Immunoassay, Huston, USA,

kit number: SEA044). In the first step, the wells were determined wells for diluted standards, blank, and samples. 100  $\mu$ L of each of dilutions standards, blank, and samples was added to the correct wells, then the plate was covered and incubated for 1 hour at 37°C. After incubation the liquid was removed from each well and 100  $\mu$ L of Detection Reagent A working solution was added to each well and incubated for 1 hour at 37°C. The plate was washed with 350  $\mu$ L of 1x wash solution and repeated 3 times. After the last wash any remaining wash buffer was removed by aspirating and 100  $\mu$ L of Detection Reagent B working solution was added to each well and incubated for 30 minutes at 37°C. The aspiration and wash process were repeated 5 times. After the washing process 90  $\mu$ L of Substrate Solution was added to each well; then the plate was covered and incubated for 10-20 minutes at 37°C. After incubation, 50  $\mu$ L of Stop Solution were added to each well. Absorbance was measured at 450 nm. Sample GH concentration was compared with the GH standard curve and the concentration of GH was expressed as plasma GH concentration (in pg/mL).

**2.3.5. Determination of Triiodothyronine (T3).** The concentration triiodothyronine was determined using a commercially available ELISA kit (Wuxi Donglin Sci & Tech Development Co., Ltd. Wuxi, Jiangsu, China, kit number: DL-T3-Ge). The color change was measured spectrophotometrically at a wavelength of 450 nm. The concentrations of T3 in the samples were determined by comparing the absorbance of the samples to the standard curve. The T3 concentrations of the samples were expressed as plasma T3 concentration (in ng/mL). The reagents were prepared according to the manufacturer's instructions. A standard curve was prepared; the diluted standard solutions, the blank, and the samples were added to the appropriate wells (50  $\mu$ L). 50  $\mu$ L of Detection A was also added to each well immediately and the



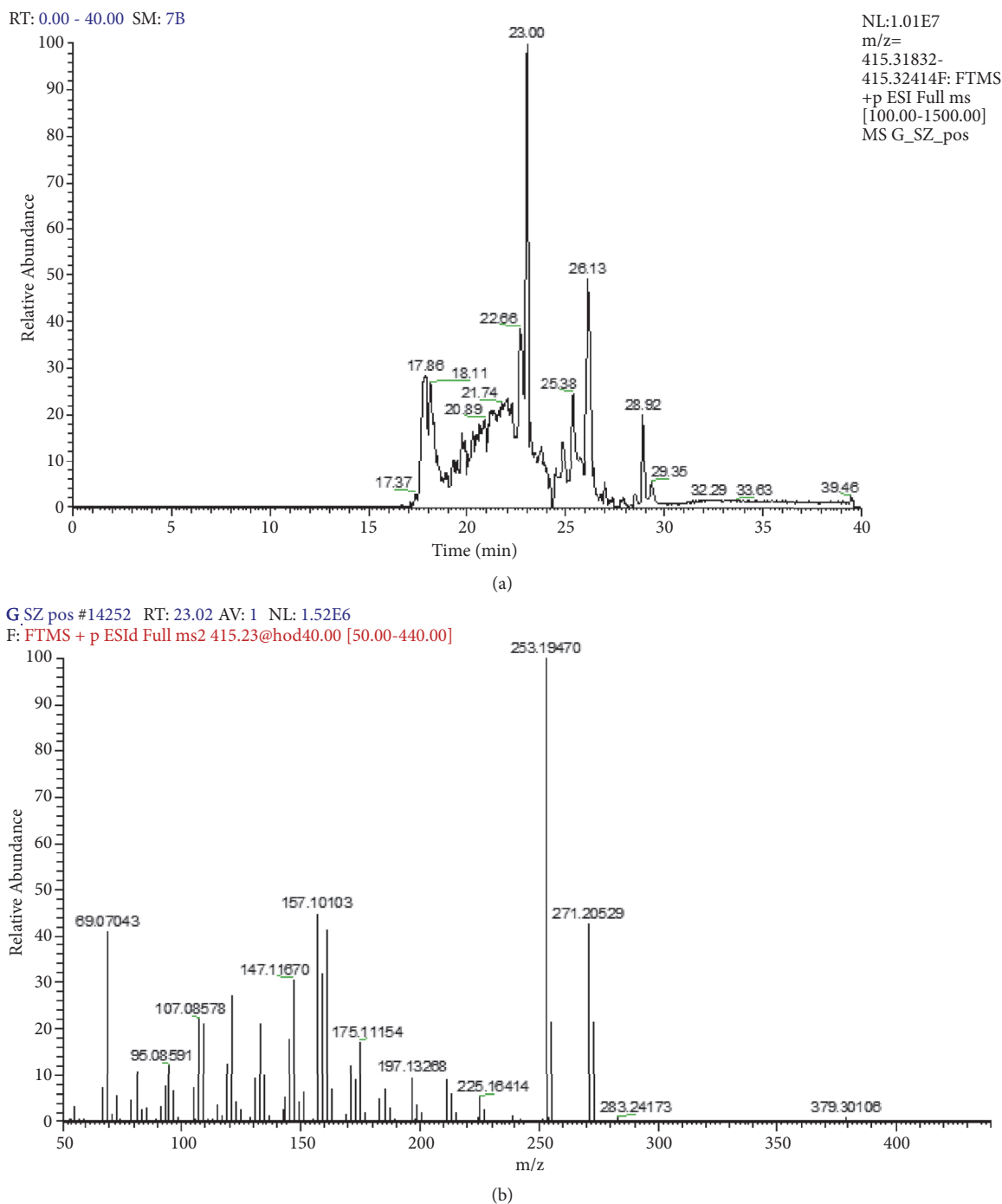


FIGURE 2: Total ion chromatogram of alcoholic extract of fenugreek (*Trigonella Foenum-graecum* L.) in negative ionization mode (a) including fragmentation spectra of the parent ion (b).

plate was shaking gently and covered with a plate sealer and incubated for 1 hour at 37°C. The solution was aspirated from the microplate and each well was washed with 350 µL of 1x Wash solution 3 times. To each well then 100 µL of Detection Reagent B was added; then the plate was incubated at 37°C for 1 hour. After the incubation, the aspiration/wash cycle was repeated 5 times; then 90 µL of Substrate Solution was added to each well after the end of the wash process. The plate was

incubated for 15-25°C minutes at 37°C; then 50 µL of Stop solution was added to each well. Absorbance was measured at 450 nm. Sample T3 concentration was compared with the T3 standard curve and the concentration of T3 was expressed as plasma T3 concentration (in ng/mL).

2.3.6. *Determination of Thyroxine (T4)*. The concentrations of thyroxine were determined using a commercially available

ELISA kit (Wuxi Donglin Sci & Tech Development Co., Ltd. Wuxi, Jiangsu, China, kit number: DL-T4-Ge). The reagents were prepared according to the manufacturer's instructions. A standard curve was prepared; the diluted standard solutions, the blank, and the samples were added to the appropriate wells (50  $\mu$ l). 50  $\mu$ L of Detection A was also added to each well immediately and the plate was shaking gently and covered with a plate sealer and incubated at 37°C for 1 hour. The solution was aspirated from microplate. Each well was washed with 350  $\mu$ L of 1x Wash solution 3 times. To each well then 100  $\mu$ L of Detection Reagent B was added and at 37°C the plate was incubated for 1 hour. After the incubation, the aspiration/wash cycle was repeated 5 times; then 90  $\mu$ L of Substrate Solution was added to each well after the end of the wash process. The plate was incubated for 15-25°C minutes at 37°C; then 50

$\mu$ L of Stop solution was added to each well. Absorbance was measured at 450 nm. Sample T4 concentration was compared with the T4 standard curve and the concentration of T4 was expressed as plasma T4 concentration (in ng/mL).

2.4. *Formulas for Calculations* [45–49]: Glucose infusion rate (GIR) is

$$GIR = \frac{\text{glucose infusion (mg/min)}}{\text{body weight (kg)}} \quad (1)$$

Metabolic clearance rate of insulin (MCRI), expressed in  $\text{mU/m}^2/\text{min}$ , is

$$MCRI = \frac{\text{insulin infusion rate}}{\text{steady state plasma insulin concentration} - \text{basal plasma insulin concentration}} \quad (2)$$

Insulin sensitivity index (ISI), expressed in  $\text{mg/kg/min/mU/mL}$ , is

$$ISI = \frac{\text{glucose infusion rate}}{\text{steady state plasma insulin concentration}} \quad (3)$$

Quantitative insulin sensitivity check index (QUICKI) is

$$QUICKI = \frac{1}{\log(\text{fasting plasma insulin } (\mu\text{IU/mL})) + \log(\text{fasting plasma glucose (mg/dL)})} \quad (4)$$

To estimate insulin resistance the universally accepted homeostatic model assessment (HOMA) was applied.

HOMA for insulin resistance (HOMA-IR) is

$$HOMA - IR = \frac{\text{fasting plasma insulin } (\mu\text{IU/mL}) \times \text{fasting plasma glucose (mmol/L)}}{22.5} \quad (5)$$

2.5. *Data Analysis*. Statistical analysis was carried out with GraphPad Prism 7.04. All data were analyzed with one-way analysis of variance (ANOVA) followed by Tukey posttesting. In the figures, data are presented as mean  $\pm$  SEM. \*, \*\*, and \*\*\* indicate significant difference in comparison to the healthy control group (\* for  $p < 0.05$ , \*\* for  $p < 0.01$ , and \*\*\* for  $p < 0.001$ ). #, ##, and ### indicate the statistically significant difference compared to the HFHSD (high-fat and high-sugar diet) control group ( $p < 0.05$ ,  $p < 0.01$ , and  $p < 0.001$ , respectively). \$, \$\$, and \$\$\$ indicate significant difference compared to the corresponding 0 min value ( $p < 0.05$ ,  $p < 0.01$ , and  $p < 0.001$ , respectively).

### 3. Results

Fasting glucose levels showed statistically significant difference only between the ID and HF group (see Figure 3). In the steady state, since in HEGC blood glucose is artificially kept in the euglycemic state, there was no significant difference between groups.

Fasting plasma insulin levels were not statistically significant between the groups (see Figure 4). In the steady state period of HEGC due to the insulin infusion, insulin levels elevated significantly in each group compared to their respective fasting values. Furthermore, ID animals showed a significant decrease to healthy controls and high-fat controls,

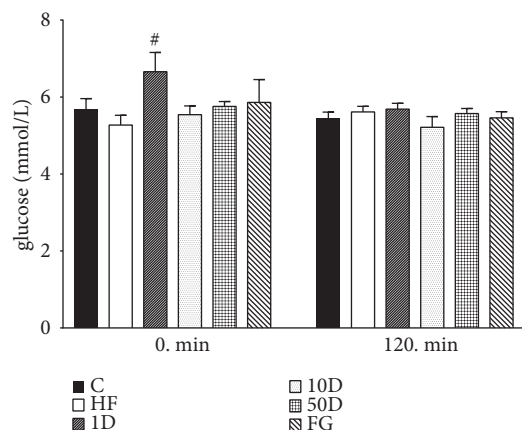


FIGURE 3: Blood glucose levels after 10 weeks of diosgenin or fenugreek treatment.

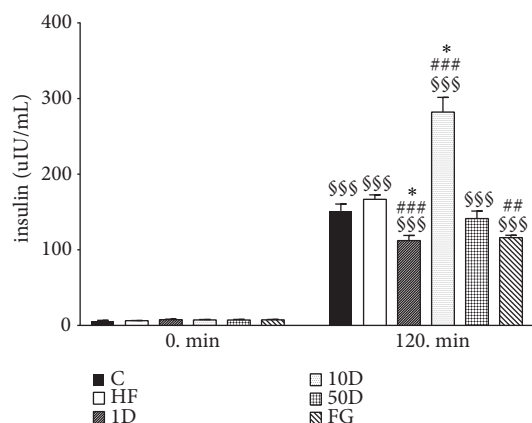


FIGURE 4: Plasma insulin levels after 10 weeks of diosgenin or fenugreek treatment.

while the FG group had a statistically significant decrease in insulin levels compared to the HF group only. 10D rats, however, showed a significant increase in insulin levels compared to both C and HF animals.

There was no statistically significant difference between the groups in glucose infusion rate (see Figure 5).

In the 10D animals, insulin sensitivity index significantly decreased compared to healthy controls (see Figure 6). The FG group showed a statistically significant elevation compared to the HF rats.

The metabolic clearance rate of insulin was significantly increased in 1D and fenugreek groups compared to both the healthy and high-fat controls (see Figure 7). 10D rats showed a statistically significant decrease in comparison to the C and HF groups.

In HOMA-IR, the groups showed no statistically significant difference between each other (see Figure 8).

QUICKI showed no statistically significant difference between the groups (see Figure 9).

In 0 min, IGF-1 levels showed no statistically significant difference between the groups (see Figure 10). In the steady state period of HEGC, however, IGF-1 levels significantly

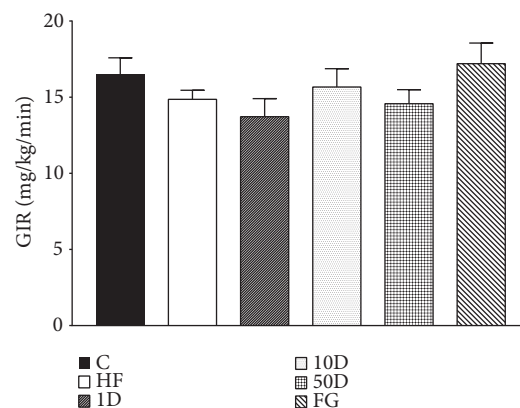


FIGURE 5: GIR after 10 weeks of diosgenin or fenugreek treatment.

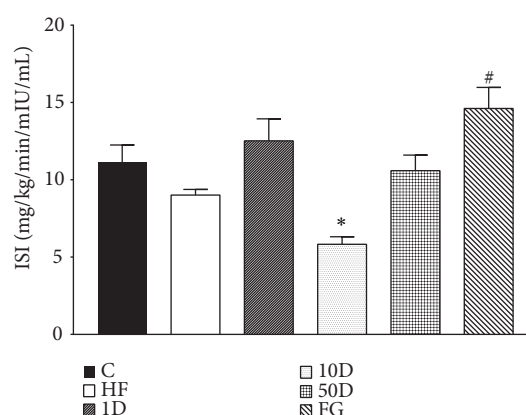


FIGURE 6: ISI after 10 weeks of diosgenin or fenugreek treatment.

increased in HF, 1D, 10D, and FG animals compared to their respective 0 min values.

In the fasting state, all diosgenin groups, but not the FG group, showed a significant increase compared to the HF animals (see Figure 11). In the steady state period of the HEGC, however, GH levels increased in the healthy controls and the HF group, although without reaching significance compared to the corresponding 0 min value, and the diosgenin groups showed an apparent dose-dependent decrease in GH levels. With the 10D and 50D rats the decrease was statistically significant compared to healthy controls, and the 50D group also showed a significant decrease to its 0 min value. Fenugreek treatment caused a significant decrease in GH levels by the steady state period compared to both the C and HF groups.

Fasting levels of T3 were significantly decreased in all groups compared to healthy control rats (see Figure 12). During steady state, however, T3 decreased in healthy controls, despite not reaching statistical significance. The rats treated with diosgenin showed significant increase compared to their corresponding 0 min values, and the 50D group also showed a significant elevation in T3 levels compared to the steady state value of HF animals.

The FG group showed a statistically significant increase in fasting T4 levels compared to healthy and high-fat controls

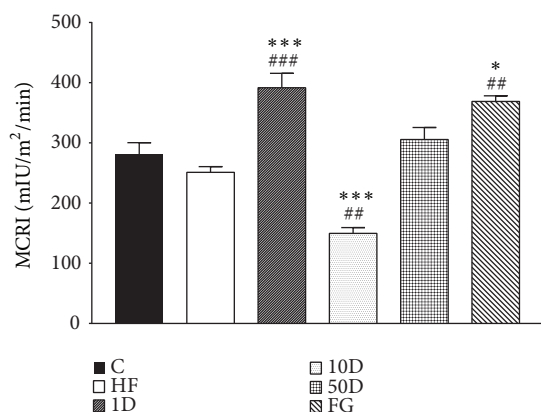


FIGURE 7: MCRI after 10 weeks of diosgenin or fenugreek treatment.

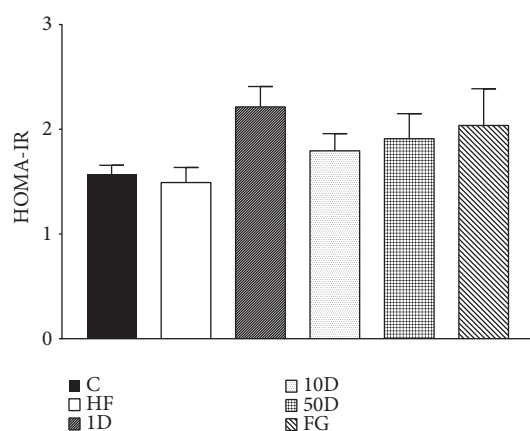


FIGURE 8: HOMA-IR after 10 weeks of diosgenin or fenugreek treatment.

(see Figure 13). In the steady state period of HEGC there was an apparent increase in T4 levels in the diosgenin treated animals, but only the 10D group reached statistical significance. The fenugreek seed treated rats, however, showed a significant decrease in T4 levels compared to their elevated fasting value.

#### 4. Discussion

Literature data confirms that fenugreek is a widely used plant since ancient times as a spice, herb, nutritional supplement, or a therapeutic agent in different types of disorders, including diabetes mellitus, metabolic syndrome or hyperlipidaemia [3, 50–53]. It is also very effective in reducing oxidative stress damage and stimulating apoptosis in hyperplasia of different types of cells [54–58]. Both the leaves and the seeds can be administered in therapeutic or nutritional regards [53]. Some researchers and pharmaceutical manufacturers use the aqueous or alcoholic extracts of the fenugreek to enhance its effect or to prepare the best formulation of the plant. We reported in our previous study that the aqueous and alcoholic fenugreek extracts are significantly different in the profile of bioactive compounds [1]. According to our results, 4-HIL, asparagine, and various nucleotides were present only

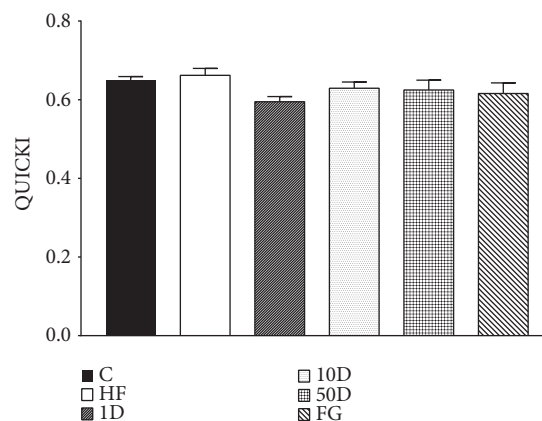


FIGURE 9: QUICKI after 10 weeks of diosgenin or fenugreek treatment.

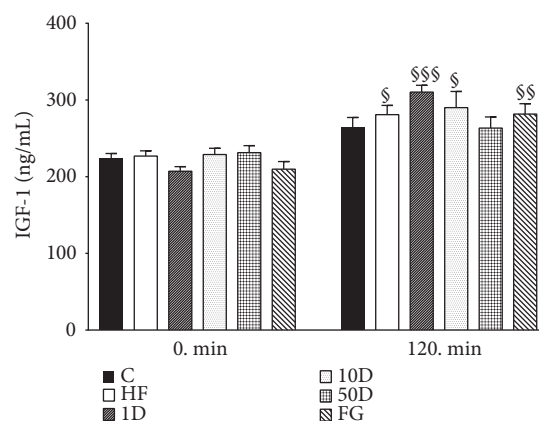


FIGURE 10: IGF-1 levels after 10 weeks of diosgenin or fenugreek treatment.

in the aqueous extract, and on the other hand the flavonoids, soyasaponins, steroidal saponins, and some vitamins such as vitamin C and B3 were detectable only in the alcoholic extract. Since the different types of extracts contain only a part of the active compounds of fenugreek; therefore, the whole plant is preferable to be administered to the healthy or diseased.

Several research data supports that besides insulin regulation fenugreek can also influence the synthesis and function of other metabolic hormones, like IGF-1, GH, T3, and T4 [59–62]. All these hormones play an important role in the regulation of glucose metabolism and the pathomechanism of diabetes mellitus. IGF-1 is by structure and function familiar to insulin, and in case of insulin deficiency it can activate the insulin receptor but the hypoglycemic effect develops at a slower rate [63]. Furthermore, IGF-1 is a very important antiapoptotic and hypertrophic agent, involved especially in the thyroid tissue hyperplasia [64–67]. Moreover, IGF-1 also stimulates the production and secretion of TSH. Both effects can contribute to the increase of thyroid hormone levels. The growth hormone is considered the most important anabolic hormone, with major role in lipolysis and the synthesis of proteins. GH plays an important role in the regulation

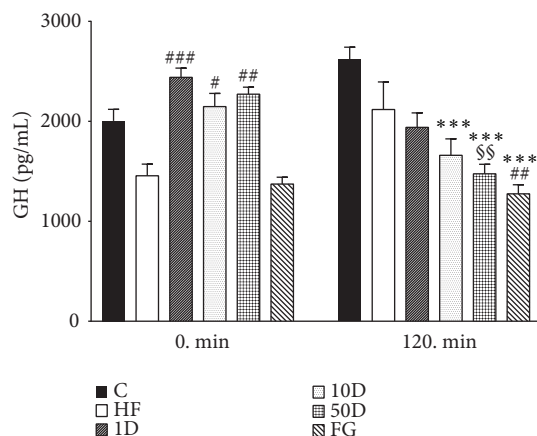


FIGURE 11: GH levels after 10 weeks of diosgenin or fenugreek treatment.

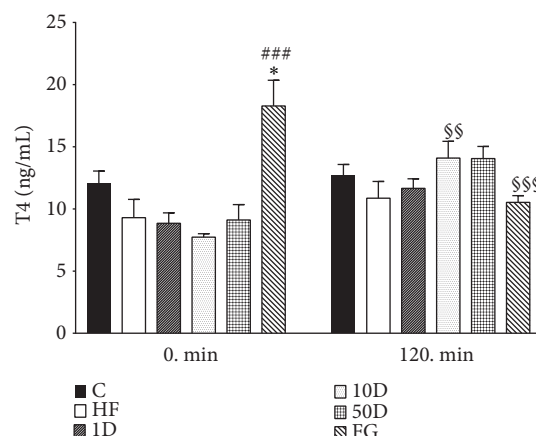


FIGURE 13: T4 levels after 10 weeks of diosgenin or fenugreek treatment.

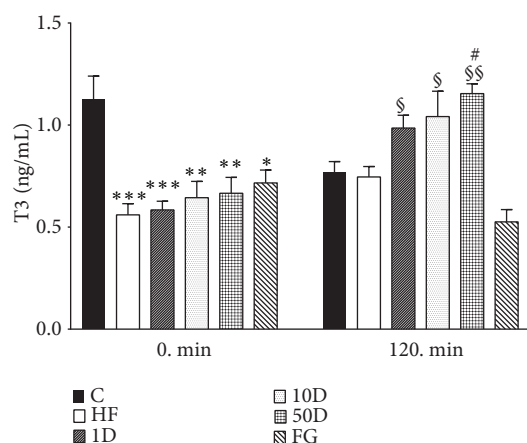


FIGURE 12: T3 levels after 10 weeks of diosgenin or fenugreek treatment.

of glucose metabolism, contributing to the development of hyperglycemia, hyperinsulinemia, and insulin resistance [68–75]. In addition, GH secretion can be modified by thyroidal hormones: in hypothyroidism GH levels and GH response is decreased [76]. Thyroidal hormones are able to influence metabolism in the whole body. They have an important role in metabolic regulation and growth, but in addition these endocrine compounds can modify cardiovascular functions, energy balance, and the central nervous system function. Thyroidal hormones greatly influence glucose metabolism either via altering IGF-1 and GH functions and increasing hepatic glucose production. Apart from being used in hypothyroidism they have indication in the treatment of depression, as well as in treatment of obesity due to the stimulation of lipolysis, but long-term usage is limited by their possible diabetes promoting and cardiovascular side effects.

During hyperinsulinemic euglycemic glucose clamp performed at the end of the six week long experimental period we found no significant differences between the groups regarding glucose infusion rate, suggesting that in response to the insulin infusion and consequent hyperinsulinemia

the rate of disappearance of glucose have not changed; therefore the insulin stimulated glucose uptake was the same. However, the parameters calculated from blood samples taken in fasted and steady state suggest that the lowest dose of diosgenin and the comparable dose fenugreek seed treatment significantly improved insulin resistance. In the fenugreek group insulin sensitivity index was increased, showing that less amount of insulin was needed to achieve the same rate of disappearance of glucose from blood circulation compared to other groups. This finding is also corroborated by the increased metabolic clearance rate of insulin, suggesting that the body had to compensate against hypoglycemia by eliminating excess insulin, an effect also shown by rats treated with 1 mg/kg diosgenin. Though the latter group failed to show an increased ISI, the elevated MCRI demonstrates the improved insulin sensitivity and glucose uptake. The explanation behind the difference in insulin sensitivity effect between the fenugreek seed and the comparable dose of diosgenin might be that fenugreek might be that apart from diosgenin; fenugreek seeds contain other active compounds that can influence glucose metabolism. One such compound is the newly identified 4-hydroxyisoleucine (4-HIL). Several studies demonstrated that 4-HIL is able to enhance insulin sensitivity via different molecular targets, such as AMP-activated protein kinase, suppressor of cytokine signalling-3, insulin receptor substrate-1, and in some reports showing an effect comparable to that of metformin [77–79]. The 50 mg/kg diosgenin treatment failed to alter insulin sensitivity, but rats treated with 10 mg/kg diosgenin showed a marked drop in ISI and MCRI, suggesting insulin resistance in peripheral tissues. This seemingly contradictory response compared to the lowest dose of diosgenin might be explained with the phenomena of hormesis, a relatively new, but not well understood theory in toxicology that states that certain compounds in low dose have a stimulating, but in high doses, an opposite, inhibitory effect. Hormesis might be explained if we assume that in low doses the toxic compound activates adaptive responses in the body, thus achieving a beneficial effect, but in higher doses these adaptive mechanisms cannot



counterbalance the stress and undesired effects manifest [80–82]. Based on our results we suggest that, in 1 mg/kg dose, diosgenin has an insulin sensitizing effect, but in 10 mg/kg dose it promotes insulin resistance.

Continuous insulin infusion effectively increased IGF-1 levels in the high-fat control, 1 and 10 mg/kg diosgenin, as well as in the fenugreek groups. IGF-1 elevation might have appeared as a result of hyperinsulinemia and the significantly increased GH levels. In response to elevated basal GH levels IGF-1 increased by the steady state period, activating growth hormone inhibiting hormone (GHIH), and, in turn, decreasing GH levels that can contribute to normalization of blood glucose levels [83]. Hyperinsulinemia also stimulates thyroid hormone production and secretion, and IGF-1 levels elevate in the thyroid gland, possibly as a result of elevated GH [84]. IGF-1 stimulates TSH and the proliferation of thyroid tissue that leads to increased secretion of thyroid hormones and consequent hypoglycemia. In the state of high plasma glucose levels less T4 prohormone is transformed into T3, T3/T4 ratio decreases, and obesity might develop [60]. Our results showed that in chronic diosgenin and fenugreek treatment the basal level of thyroid hormones, especially T3 significantly decreased, but the consequent IGF-1 elevation in response to hyperinsulinemia in the steady state effectively balances this reduction in the diosgenin groups. The FG rats showed a significant elevation of basal T4 levels, but in the steady state period the insulin infusion reduces T4, possibly through stimulating its transformation into T3 due to elevated GH that promotes hypothyroidism [85, 86]. Our results corroborate that there are complex feedback mechanisms and interplay between the studied anabolic hormones that play an important role in the regulation of glucose metabolism, development of insulin resistance, and modulating insulin sensitivity. Our additional find is that fenugreek seed may have different physiological effects than its active component diosgenin due to the fact that apart from compounds with potentially therapeutic value it might also contain molecules that cause undesired or even toxic side effects, especially in long-term treatment. However, it is important to note the significance of proper dosing, since low dose had beneficial effects, but elevation of doses impaired insulin sensitivity and the homeostasis of the examined hormones.

## 5. Conclusion

Our study shed light to that chronic consumption of fenugreek seed is able to influence the complex interplay of anabolic hormones. Our results also indicate that apart from its proven insulin sensitizing effect fenugreek might have a therapeutic potential in the adjuvant treatment of thyroid diseases. We plan to conclude further research to determine the effect of fenugreek and its saponin agents in different thyroid disease models.

## Data Availability

The authors confirm that all relevant data are presented in the results section of this publication. Nonetheless, the raw data

that support the findings of this work are available from the corresponding author upon reasonable request.

## Conflicts of Interest

The authors contributing to this study declare no conflicts of interest.

## Authors' Contributions

Rita Kiss and Georgina Pesti-Asbóth contribute to present work in equal measure.

## Acknowledgments

The Hungarian-European Research Infrastructure Network was supporting this study, by its Tender with [EFOP-3.6.2-16-2017-00009] code and reference no., titled "Establishing Thematic Scientific and Cooperation Network for Clinical Research".

## References

- [1] S. Vigh, Z. Cziaky, L. T. Sinka et al., "Analysis of phytoconstituent profile of fenugreek –*Trigonella Foenum-graecum* L. - seed extracts," *Studia Universitatis Babeş-Bolyai, Chemia*, vol. 62, no. 2, pp. 145–166, 2017.
- [2] U. C. S. Yadav and N. Z. Baquer, "Pharmacological effects of *Trigonella foenum-graecum* L. in health and disease," *Pharmaceutical Biology*, vol. 52, no. 2, pp. 243–254, 2014.
- [3] N. Moradi Kor and K. Moradi, "Physiological and pharmaceutical effects of fenugreek (*Trigonella foenum-graecum* L.) as a multipurpose and valuable medicinal plant," *Global Journal of Medicinal Plant Research*, vol. 1, pp. 199–206, 2013.
- [4] A. Mehrafarin, A. Qaderi, S. Rezazadeh, H. Naghdi Badi, G. Noormohammadi, and E. Zand, "Bioengineering of important secondary metabolites and metabolic pathways in fenugreek (*Trigonella foenum-graecum* L.)," *Journal of Medicinal Plants*, vol. 9, no. 35, pp. 1–18, 2010.
- [5] A. Parvizpur, A. Ahmadiani, and M. Kamalinejad, "Spinal serotonergic system is partially involved in antinociception induced by *Trigonella foenum-graecum* (TFG) leaf extract," *Journal of Ethnopharmacology*, vol. 95, no. 1, pp. 13–17, 2004.
- [6] A. Parvizpur, A. Ahmadiani, and M. Kamalinejad, "Probable role of spinal purinoceptors in the analgesic effect of *Trigonella foenum* (TFG) leaves extract," *Journal of Ethnopharmacology*, vol. 104, no. 1-2, pp. 108–112, 2006.
- [7] P. Kumar and U. Bhandari, "Protective effect of *Trigonella foenum-graecum* Linn. on monosodium glutamate-induced dyslipidemia and oxidative stress in rats," *Indian Journal of Pharmacology*, vol. 45, no. 2, pp. 136–140, 2013.
- [8] S. Kaviarasan, R. Sundarapandian, and C. V. Anuradha, "Protective action of fenugreek (*Trigonella foenum-graecum*) seed polyphenols against alcohol-induced protein and lipid damage in rat liver," *Cell Biology and Toxicology*, vol. 24, no. 5, pp. 391–400, 2008.
- [9] M. Al-Habori, A. M. Al-Aghbari, and M. Al-Mamary, "Effects of fenugreek seeds and its extracts on plasma lipid profile: a study on rabbits," *Phytotherapy Research*, vol. 12, no. 8, pp. 572–575, 1998.

- [10] M. Al-Habori and A. Raman, "Antidiabetic and hypocholesterolemic effects of fenugreek," *Phytotherapy Research*, vol. 12, no. 4, pp. 233–242, 1998.
- [11] P. R. Petit, Y. D. Sauvaire, D. M. Hillaire-Buys et al., "Steroid saponins from fenugreek seeds: extraction, purification, and pharmacological investigation on feeding behavior and plasma cholesterol," *Steroids*, vol. 60, no. 10, pp. 674–680, 1995.
- [12] P. Petit, Y. Sauvaire, G. Ponsin, M. Manteghetti, A. Fave, and G. Ribes, "Effects of a fenugreek seed extract on feeding behaviour in the rat: metabolic-endocrine correlates," *Pharmacology Biochemistry & Behavior*, vol. 45, no. 2, pp. 369–374, 1993.
- [13] A. Stark and Z. Madar, "The effect of an ethanol extract derived from fenugreek (*Trigonella foenum-graecum*) on bile acid absorption and cholesterol levels in rats," *British Journal of Nutrition*, vol. 69, no. 1, pp. 277–287, 1993.
- [14] G. Valette, Y. Sauvaire, J.-C. Baccou, and G. Ribes, "Hypocholesterolaemic effect of Fenugreek seeds in dogs," *Atherosclerosis*, vol. 50, no. 1, pp. 105–111, 1984.
- [15] Y. Sauvaire, G. Ribes, J.-C. Baccou, and M.-M. Loubatieres-Mariani, "Implication of steroid saponins and sapogenins in the hypocholesterolemic effect of fenugreek," *Lipids*, vol. 26, no. 3, pp. 191–197, 1991.
- [16] M. Yoshikawa, T. Murakami, H. Komatsu, N. Murakami, J. Yamahara, and H. Matsuda, "Medicinal foodstuffs. IV. fenugreek seed. (1): structures of trigoneosides Ia, Ib, IIa, IIb, IIIa, and IIIb, new furostanol saponins from the seeds of indian *Trigonella foenum-graecum* L," *Chemical & Pharmaceutical Bulletin*, vol. 45, no. 1, pp. 81–87, 1997.
- [17] P. B. Naidu, P. Ponmurugan, M. S. Begum et al., "Diosgenin reorganises hyperglycaemia and distorted tissue lipid profile in high-fat diet-streptozotocin-induced diabetic rats," *Journal of the Science of Food and Agriculture*, vol. 95, no. 15, pp. 3177–3182, 2015.
- [18] K. Szabó, R. Gesztelyi, N. Lampé et al., "Fenugreek (*Trigonella foenum-graecum*) seed flour and diosgenin preserve endothelium-dependent arterial relaxation in a rat model of early-stage metabolic syndrome," *International Journal of Molecular Sciences*, vol. 19, no. 3, p. 798, 2018.
- [19] C. Broca, V. Breil, C. Cruciani-Guglielmacci et al., "Insulinotropic agent ID-1101 (4-hydroxyisoleucine) activates insulin signaling in rat," *American Journal of Physiology Endocrinology and Metabolism*, vol. 287, no. 3, pp. E463–E471, 2004.
- [20] Y. Sauvaire, P. Petit, C. Broca et al., "4-hydroxyisoleucine: a novel amino acid potentiator of insulin secretion," *Diabetes*, vol. 47, no. 2, pp. 206–210, 1998.
- [21] L. Jette, L. Harvey, K. Eugeni, and N. Levens, "4-Hydroxyisoleucine: a plant-derived treatment for metabolic syndrome," *Current Opinion in Investigational Drugs*, vol. 10, no. 4, pp. 353–358, 2009.
- [22] T. C. Raghuram, R. D. Sharma, B. Sivakumar, and B. K. Sahay, "Effect of fenugreek seeds on intravenous glucose disposition in non-insulin dependent diabetic patients," *Phytotherapy Research*, vol. 8, no. 2, pp. 83–86, 1994.
- [23] J. Raju and R. P. Bird, "Alleviation of hepatic steatosis accompanied by modulation of plasma and liver TNF- $\alpha$  levels by *Trigonella foenum graecum* (fenugreek) seeds in Zucker obese (fa/fa) rats," *International Journal of Obesity*, vol. 30, no. 8, pp. 1298–1307, 2006.
- [24] K. Srinivasan, "Antioxidant potential of spices and their active constituents," *Critical Reviews in Food Science and Nutrition*, vol. 54, no. 3, pp. 352–372, 2014.
- [25] D. V. Joshi, R. R. Patil, and S. R. Naik, "Hydroalcohol extract of *Trigonella foenum-graecum* seed attenuates markers of inflammation and oxidative stress while improving exocrine function in diabetic rats," *Pharmaceutical Biology*, vol. 53, no. 2, pp. 201–211, 2015.
- [26] M. G. A. Hegazy and M. A. Emam, "Ethanol extract of *Trigonella foenum graecum* attenuates cisplatin-induced nephro- and hepatotoxicities in rats," *Cellular and Molecular Biology*, vol. 61, no. 7, pp. 81–87, 2015.
- [27] S. Sharma, V. Mishra, S. K. Jayant, and N. Srivastava, "Effect of *Trigonella foenum graecum* l on the activities of antioxidant enzyme and their expression in tissues of alloxan-induced diabetic rats," *Evidence-Based Complementary and Alternative Medicine*, vol. 20, no. 3, pp. 203–211, 2015.
- [28] A. Alsemari, F. Alkhodairy, A. Aldakan et al., "The selective cytotoxic anti-cancer properties and proteomic analysis of *Trigonella foenum-graecum*," *BMC Complementary and Alternative Medicine*, vol. 14, article 114, 2014.
- [29] P. Singh, S. P. Vishwakarma, and R. L. Singh, "Antioxidant, oxidative DNA damage protective and antimicrobial activities of the plant *Trigonella foenum-graecum*," *Journal of the Science of Food and Agriculture*, vol. 94, no. 12, pp. 2497–2504, 2014.
- [30] T. Devasena and V. P. Menon, "Enhancement of circulatory antioxidants by fenugreek during 1, 2-dimethylhydrazine-induced rat colon carcinogenesis," *The Journal of Biochemistry Molecular Biology and Biophysics*, vol. 6, no. 4, pp. 289–292, 2002.
- [31] M. Jesus, A. P. J. Martins, E. Gallardo, and S. Silvestre, "Diosgenin: recent highlights on pharmacology and analytical methodology," *Journal of Analytical Methods in Chemistry*, vol. 2016, Article ID 4156293, 16 pages, 2016.
- [32] B. Sung, S. Prasad, V. R. Yadav, and B. B. Aggarwal, "Cancer cell signaling pathways targeted by spice-derived nutraceuticals," *Nutrition and Cancer*, vol. 64, no. 2, pp. 173–197, 2012.
- [33] B. B. Aggarwal, A. B. Kunnumakkara, K. B. Harlkumar, S. T. Tharakan, B. Sung, and P. Anand, "Potential of spice-derived phytochemicals for cancer prevention," *Planta Medica*, vol. 74, no. 13, pp. 1560–1569, 2008.
- [34] S. Vigh, Z. Zsvér-Vadas, C. Pribac et al., "Fenugreek (*Trigonella foenum-graecum* L.) extracts are inducing dose-dependent hormetic response and cytotoxic effects in case of human breast cancer cell lines," *Studia Universitatis Vasile Goldis Arad, Seria Stiintele Vietii*, vol. 26, no. 4, pp. 435–448, 2016.
- [35] J. Raju, J. M. R. Patlolla, M. V. Swamy, and C. V. Rao, "Diosgenin, a steroid saponin of *Trigonella foenum graecum* (Fenugreek), inhibits azoxymethane-induced aberrant crypt foci formation in F344 rats and induces apoptosis in HT-29 human colon cancer cells," *Cancer Epidemiology, Biomarkers & Prevention*, vol. 13, no. 8, pp. 1392–1398, 2004.
- [36] N. Verma, K. Usman, N. Patel et al., "A multicenter clinical study to determine the efficacy of a novel fenugreek seed (*Trigonella foenum-graecum*) extract (Fenfurol™) in patients with type 2 diabetes," *Food & Nutrition Research*, vol. 60, no. 1, p. 32382, 2016.
- [37] A. Maheshwari, N. Verma, A. Swaroop et al., "Efficacy of furosap™, a novel *Trigonella foenum-graecum* seed extract, in enhancing testosterone level and improving sperm profile in male volunteers," *International Journal of Medical Sciences*, vol. 14, no. 1, pp. 58–66, 2017.
- [38] T. Assad and R. A. Khan, "Effect of methanol extract of *Trigonella foenum-graecum* L. seeds on anxiety, sedation and

- motor coordination," *Metabolic Brain Disease*, vol. 32, no. 2, pp. 343–349, 2017.
- [39] M. Ouzir, K. El Bairi, and S. Amzazi, "Toxicological properties of fenugreek (*Trigonella foenum graecum*)," *Food and Chemical Toxicology*, vol. 96, pp. 145–154, 2016.
- [40] P. K. Gupta, D. H. Nagore, V. V. Kuber, and S. Purohit, "A validated RP-HPLC method for the estimation of diosgenin from polyherbal formulation containing *Tribulus terrestris* Linn," *Asian Journal of Pharmaceutical and Clinical Research*, vol. 5, no. 4, pp. 91–94, 2012.
- [41] K. Szabó, R. Gesztelyi, N. Lampé et al., "Fenugreek (*Trigonella Foenum-Graecum*) seed flour and diosgenin preserve endothelium-dependent arterial relaxation in a rat model of early-stage metabolic syndrome," *International Journal of Molecular Sciences*, vol. 19, no. 3, 2018.
- [42] R. A. DeFronzo, J. D. Tobin, and R. Andres, "Glucose clamp technique: a method for quantifying insulin secretion and resistance," *American Journal of Physiology—Endocrinology Metabolism and Gastrointestinal Physiology*, vol. 6, no. 3, pp. E214–E223, 1979.
- [43] L. Kloock, "The correlation of liver fat content and insulin resistance with skeletal muscle energy metabolism," Scientific theses Dissertation, Heinrich Heine University Düsseldorf, <https://docserv.uni-duesseldorf.de/servlets/DocumentServlet?id=42618>, 2017.
- [44] C. Hegedus, D. Kovács, L. Drimba et al., "Investigation of the metabolic effects of chronic clozapine treatment on CCK-1 receptor deficient Otsuka Long Evans Tokushima Fatty (OLETF) rats," *European Journal of Pharmacology*, vol. 718, no. 1–3, pp. 188–196, 2013.
- [45] R. Muniyappa, S. Lee, H. Chen, and M. J. Quon, "Current approaches for assessing insulin sensitivity and resistance in vivo: advantages, limitations, and appropriate usage," *American Journal of Physiology-Renal Physiology*, vol. 294, no. 1, pp. E15–E26, 2008.
- [46] M. Gutch, S. Kumar, S. M. Razi, K. Gupta, and A. Gupta, "Assessment of insulin sensitivity/resistance," *Indian Journal of Endocrinology and Metabolism*, vol. 19, no. 1, pp. 160–164, 2015.
- [47] R. Bradley, E. B. Oberg, C. Calabrese, and L. J. Standish, "Algorithm for complementary and alternative medicine practice and research in type 2 diabetes," *The Journal of Alternative and Complementary Medicine*, vol. 13, no. 1, pp. 159–175, 2007.
- [48] Y. Song, J. E. Manson, L. Tinker et al., "Insulin sensitivity and insulin secretion determined by homeostasis model assessment and risk of diabetes in a multiethnic cohort of women: the women's health initiative observational study," *Diabetes Care*, vol. 30, no. 7, pp. 1747–1752, 2007.
- [49] T. M. Wallace, J. C. Levy, and D. R. Matthews, "Use and abuse of HOMA modeling," *Diabetes Care*, vol. 27, no. 6, pp. 1487–1495, 2004.
- [50] N. Neelakantan, M. Narayanan, R. J. De Souza, and R. M. Van Dam, "Effect of fenugreek (*Trigonella foenum-graecum* L.) intake on glycemia: a meta-analysis of clinical trials," *Nutrition Journal*, vol. 13, no. 1, article no. 7, 2014.
- [51] A. Pandey, P. Tripathi, R. Pandey, R. Srivatava, and S. Goswami, "Alternative therapies useful in the management of diabetes: a systematic review," *Journal of Pharmacy and Bioallied Sciences*, vol. 3, no. 4, pp. 504–512, 2011.
- [52] D. K. Patel, R. Kumar, D. Laloo, and S. Hemalatha, "Diabetes mellitus: an overview on its pharmacological aspects and reported medicinal plants having antidiabetic activity," *Asian Pacific Journal of Tropical Biomedicine*, vol. 2, no. 5, pp. 411–420, 2012.
- [53] E. Basch, C. Ulbricht, G. Kuo, P. Szapary, and M. Smith, "Therapeutic applications of fenugreek," *Alternative Medicine Review*, vol. 8, no. 1, pp. 20–27, 2003.
- [54] B. Liagre, P. Vergne-Salle, C. Corbiere, J. L. Charissoux, and J. L. Beneytout, "Diosgenin, a plant steroid, induces apoptosis in human rheumatoid arthritis synoviocytes with cyclooxygenase-2 overexpression," *Arthritis Research & Therapy*, vol. 6, no. 4, pp. R373–383, 2004.
- [55] C.-T. Chiang, T.-D. Way, S.-J. Tsai, and J.-K. Lin, "Diosgenin, a naturally occurring steroid, suppresses fatty acid synthase expression in HER2-overexpressing breast cancer cells through modulating Akt, mTOR and JNK phosphorylation," *FEBS Letters*, vol. 581, no. 30, pp. 5735–5742, 2007.
- [56] M.-J. Liu, Z. Wang, Y. Ju, R. N.-S. Wong, and Q.-Y. Wu, "Diosgenin induces cell cycle arrest and apoptosis in human leukemia K562 cells with the disruption of  $Ca^{2+}$  homeostasis," *Cancer Chemotherapy and Pharmacology*, vol. 55, no. 1, pp. 79–90, 2005.
- [57] M. Tharahaswari, N. Jayachandra Reddy, R. Kumar, K. C. Varshney, M. Kannan, and S. Sudha Rani, "Trigonelline and diosgenin attenuate ER stress, oxidative stress-mediated damage in pancreas and enhance adipose tissue PPAR $\gamma$  activity in type 2 diabetic rats," *Molecular and Cellular Biochemistry*, vol. 396, no. 1–2, pp. 161–174, 2014.
- [58] A. Pallag, E. Rosca, T. D. ti et al., "Monitoring the effects of treatment in colon cancer cells using immunohistochemical and histoenzymatic techniques," *Romanian Journal of Morphology and Embryology*, vol. 56, no. 3, pp. 1103–1109, 2015.
- [59] S. H. Shim, E. J. Lee, J. S. Kim et al., "Rat growth-hormone release stimulators from fenugreek seeds," *Chemistry Biodiversity*, vol. 5, no. 9, pp. 1753–1761, 2008.
- [60] S. Panda, P. Tahiliani, and A. Kar, "Inhibition of triiodothyronine production by fenugreek seed extract in mice and rats," *Pharmacological Research*, vol. 40, no. 5, pp. 405–409, 1999.
- [61] P. Tahiliani and A. Kar, "The combined effects of *Trigonella* and *Allium* extracts in the regulation of hyperthyroidism in rats," *Phytomedicine*, vol. 10, no. 8, pp. 665–668, 2003.
- [62] D. Bian, Z. Li, H. Ma et al., "Effects of diosgenin on cell proliferation induced by IGF-1 in primary human thyrocytes," *Archives of Pharmacol Research*, vol. 34, no. 6, pp. 997–1005, 2011.
- [63] J. Boucher, Y.-H. Tseng, and C. R. Kahn, "Insulin and insulin-like growth factor-1 receptors act as ligand-specific amplitude modulators of a common pathway regulating gene transcription," *The Journal of Biological Chemistry*, vol. 285, no. 22, pp. 17235–17245, 2010.
- [64] T. Kofidis, J. L. de Bruin, T. Yamane et al., "Insulin-like growth factor promotes engraftment, differentiation, and functional improvement after transfer of embryonic stem cells for myocardial restoration," *Stem Cells*, vol. 22, no. 7, pp. 1239–1245, 2004.
- [65] K. Radcliff, T.-B. Tang, J. Lim et al., "Insulin-like growth factor-I regulates proliferation and osteoblastic differentiation of calcifying vascular cells via extracellular signal-regulated protein kinase and phosphatidylinositol 3-kinase pathways," *Circulation Research*, vol. 96, no. 4, pp. 398–400, 2005.
- [66] T. Kimura, A. van Keymeulen, J. Golstein, A. Fusco, J. E. Dumont, and P. P. Roger, "Regulation of thyroid cell proliferation by tsh and other factors: a critical evaluation of in vitro models," *Endocrine Reviews*, vol. 22, no. 5, pp. 631–656, 2001.



- [67] J. Saito, A. D. Kohn, R. A. Roth et al., "Regulation of FRTL-5 thyroid cell growth by phosphatidylinositol (OH) 3 kinase-dependent Akt-mediated signaling," *Thyroid*, vol. 11, no. 4, pp. 339–351, 2001.
- [68] N. J. Hopwood, P. J. Forsman, F. M. Kenny, and A. L. Drash, "Hypoglycemia in hypopituitary children," *American Journal of Diseases of Children*, vol. 129, no. 8, pp. 918–926, 1975.
- [69] T. J. Merimee, D. Rabinowitz, D. L. Rimoin, and V. A. McKusick, "Isolated human growth hormone deficiency. III. Insulin secretion in sexual ateliotic dwarfism," *Metabolism*, vol. 17, no. 11, pp. 1005–1011, 1968.
- [70] G. Costin, M. D. Kogut, and S. D. Frasier, "Effect of low-dose human growth hormone on carbohydrate metabolism in children with hypopituitarism," *Journal of Pediatrics*, vol. 80, no. 5, pp. 788–795, 1972.
- [71] L. E. Underwood, J. L. Van den Brande, G. J. Antony, S. J. Voina, and J. J. Van Wyk, "Islet cell function and glucose homeostasis in hypopituitary dwarfism: synergism between growth hormone and cortisone," *Journal of Pediatrics*, vol. 82, no. 1, pp. 28–37, 1973.
- [72] M. Emmer, P. Gorden, and J. Roth, "Diabetes in association with other endocrine disorders," *Medical Clinics of North America*, vol. 55, no. 4, pp. 1057–1064, 1971.
- [73] S. E. Fineberg, T. J. Merimee, D. Rabinowitz, and P. J. Edgar, "Insulin secretion in acromegaly," *The Journal of Clinical Endocrinology & Metabolism*, vol. 30, no. 3, pp. 288–292, 1970.
- [74] P. Beck, D. S. Schalch, M. L. Parker, D. M. Kipnis, and W. H. Daughaday, "Correlative studies of growth hormone and insulin plasma concentrations with metabolic abnormalities in acromegaly," *The Journal of Laboratory and Clinical Medicine*, vol. 66, no. 3, pp. 366–379, 1965.
- [75] P. H. Sönksen, F. C. Greenwood, J. P. Ellis, C. Lowy, A. Rutherford, and J. D. Nabarro, "Changes of carbohydrate tolerance in acromegaly with progress of the disease and in response to treatment," *The Journal of Clinical Endocrinology & Metabolism*, vol. 27, no. 10, pp. 1418–1430, 1967.
- [76] R. Valcavi, C. Dieguez, M. Preece, A. Taylor, I. Portioli, and M. F. Scanlon, "Effect of thyroxine replacement therapy on plasma insulin-like growth factor 1 levels and growth hormone responses to growth hormone releasing factor in hypothyroid patients," *Clinical Endocrinology*, vol. 27, no. 1, pp. 85–90, 1987.
- [77] C. K. Maurya, R. Singh, N. Jaiswal, K. Venkateswarlu, T. Narender, and A. K. Tamrakar, "4-Hydroxyisoleucine ameliorates fatty acid-induced insulin resistance and inflammatory response in skeletal muscle cells," *Molecular and Cellular Endocrinology*, vol. 395, no. 1–2, pp. 51–60, 2014.
- [78] N. Naicker, S. Nagiah, A. Phulukdaree, and A. Chuturgoon, "Trigonella foenum-graecum seed extract, 4-Hydroxyisoleucine, and metformin stimulate proximal insulin signaling and increase expression of glycogenic enzymes and GLUT2 in HepG2 cells," *Metabolic Syndrome and Related Disorders*, vol. 14, no. 2, pp. 114–120, 2016.
- [79] S. Gautam, N. Ishrat, P. Yadav, R. Singh, T. Narender, and A. K. Srivastava, "4-Hydroxyisoleucine attenuates the inflammation-mediated insulin resistance by the activation of AMPK and suppression of SOCS-3 coimmunoprecipitation with both the IR- $\beta$  subunit as well as IRS-1," *Molecular and Cellular Biochemistry*, vol. 414, no. 1–2, pp. 95–104, 2016.
- [80] E. J. Calabrese, "Evidence that hormesis represents an 'overcompensation' response to a disruption in homeostasis," *Ecotoxicology and Environmental Safety*, vol. 42, no. 2, pp. 135–137, 1999.
- [81] E. J. Calabrese and L. A. Baldwin, "Chemical hormesis: its historical foundations as a biological hypothesis," *Human & Experimental Toxicology*, vol. 19, no. 1, pp. 2–31, 2000.
- [82] V. Calabrese, C. Cornelius, A. T. Dinkova-Kostova et al., "Cellular stress responses, hormetic phytochemicals and vitagenes in aging and longevity," *Biochimica et Biophysica Acta*, vol. 1822, no. 5, pp. 753–783, 2012.
- [83] S. Y. Nam, E. J. Lee, K. R. Kim et al., "Effect of obesity on total and free insulin-like growth factor (IGF)-1, and their relationship to IGF-binding protein (BP)-1, IGFBP-2, IGFBP-3, insulin, and growth hormone," *International Journal of Obesity*, vol. 21, no. 5, pp. 355–359, 1997.
- [84] A. Tsatsoulis, "The role of insulin resistance/hyperinsulinism on the rising trend of thyroid and adrenal nodular disease in the current environment," *Journal of Clinical Medicine*, vol. 7, no. 3, p. 37, 2018.
- [85] A. W. Root, D. Shulman, J. Root, and F. Diamond, "The interrelationships of thyroid and growth hormones: Effect of growth hormone releasing hormone in hypo and hyperthyroid male rats," *Acta Endocrinologica*, vol. 113, no. 279, pp. 367–375, 1986.
- [86] P. Tahiliani and A. Kar, "Mitigation of thyroxine-induced hyperglycaemia by two plant extracts," *Phytotherapy Research*, vol. 17, no. 3, pp. 294–296, 2003.

## Research Article

# Selectivity of Dietary Phenolics for Inhibition of Human Monoamine Oxidases A and B

Zhenxian Zhang,<sup>1</sup> Hiroki Hamada,<sup>2</sup> and Phillip M. Gerk<sup>1</sup> 

<sup>1</sup>Virginia Commonwealth University School of Pharmacy, Department of Pharmaceutics, 410 N. 12<sup>th</sup> Street, Richmond, VA 23298-0533, USA

<sup>2</sup>Department of Life Science, Okayama University of Science, 1-1 Ridai-cho Kita-ku Okayama, 700-0005, Japan

Correspondence should be addressed to Phillip M. Gerk; [pmgerk@vcu.edu](mailto:pmgerk@vcu.edu)

Received 3 October 2018; Revised 12 December 2018; Accepted 31 December 2018; Published 23 January 2019

Guest Editor: Claudio Tabolacci

Copyright © 2019 Zhenxian Zhang et al. This is an open access article distributed under the Creative Commons Attribution License, which permits unrestricted use, distribution, and reproduction in any medium, provided the original work is properly cited.

Monoamine oxidases (MAOs) regulate local levels of neurotransmitters such as dopamine, norepinephrine, and serotonin and thus have been targeted by drugs for the treatment of certain CNS disorders. However, recent studies have shown that these enzymes are upregulated with age in nervous and cardiac tissues and may be involved in degeneration of these tissues, since their metabolic mechanism releases hydrogen peroxide leading to oxidative stress. Thus, targeting these enzymes may be a potential anti-aging strategy. The purpose of this study was to compare the MAO inhibition and selectivity of selected dietary phenolic compounds, using a previously validated assay that would avoid interference from the compounds. Kynuramine metabolism by human recombinant MAO-A and MAO-B leads to formation of 4-hydroxyquinoline, with  $V_{max}$  values of  $10.2 \pm 0.2$  and  $7.35 \pm 0.69$  nmol/mg/min, respectively, and  $K_m$  values of  $23.1 \pm 0.8$   $\mu$ M and  $18.0 \pm 2.3$   $\mu$ M, respectively. For oral dosing and interactions with the gastrointestinal tract, curcumin, guaiacol, isoeugenol, pterostilbene, resveratrol, and zingerone were tested at their highest expected luminal concentrations from an oral dose. Each of these significantly inhibited both enzymes except for zingerone, which only inhibited MAO-A. The  $IC_{50}$  values were determined, and selectivity indices (MAO-A/MAO-B  $IC_{50}$  ratios) were calculated. Resveratrol and isoeugenol were selective for MAO-A, with  $IC_{50}$  values of  $0.313 \pm 0.008$  and  $3.72 \pm 0.20$   $\mu$ M and selectivity indices of 50.5 and 27.4, respectively. Pterostilbene was selective for MAO-B, with  $IC_{50}$  of  $0.138 \pm 0.013$   $\mu$ M and selectivity index of 0.0103. The inhibition of resveratrol (MAO-A) and pterostilbene (MAO-B) was consistent with competitive time-independent mechanisms. Resveratrol 4'-glucoside was the only compound which inhibited MAO-A, but itself, resveratrol 3-glucoside, and pterostilbene 4'-glucoside failed to inhibit MAO-B. Additional studies are needed to establish the effects of these compounds on MAO-A and/or MAO-B in humans.

## 1. Introduction

Monoamine oxidases (MAO) A and B are enzymes found in the mitochondria of the liver and other tissues, metabolizing neurotransmitters such as dopamine, serotonin, and norepinephrine [1]. Several approved therapeutic MAO inhibitors have long been used for the treatment of anxiety and depression and more recently for Parkinson's disease [2]. MAO reaction products include hydrogen peroxide, aldehydes, and ammonia; these may exhibit toxic effects in various tissues. Notably, expression of MAO increases with age by 6-fold for cardiac MAO-A and 4-fold for neuronal MAO-B [3]. As a result, both MAO-A and MAO-B have

been investigated for their roles in oxidative stress, aging, and degenerative disease in the heart and the brain [1, 3–6].

In addition to FDA-approved drugs, natural products have also been investigated for their potential MAO inhibition. Some phenolic dietary compounds such as curcumin, eugenol, piperine, quercetin, and resveratrol are not substrates for MAO, but they have inhibitory effects on MAO [7–12]. Curcumin inhibits both MAO-A and MAO-B in mouse brain after p.o. administration [7]. Piperine and paeonol are reversible inhibitors for both MAO-A and MAO-B in rat brain. The mode of inhibition with piperine on MAO-A and MAO-B is mixed and competitive inhibition giving  $K_i$  values of 35.8  $\mu$ M and 79.9  $\mu$ M, respectively [9]. Paeonol has  $K_i$



values of 51.1  $\mu\text{M}$  and 38.2  $\mu\text{M}$  on MAO-A and MAO-B with non-competitive and competitive inhibition, respectively [9]. Emodin shows mixed mode inhibition on MAO-B with  $K_i$  values of 15.1  $\mu\text{M}$  in rat brain [9]. Quercetin is a previously established inhibitor of MAO-A [3, 10, 11] and MAO-B [13]. Resveratrol is a potent inhibitor of MAO-A in rat brain with  $K_i$  of 2.5  $\mu\text{M}$  [12]. Eugenol can competitively inhibit both human recombinant MAO-A and MAO-B with  $K_i$  of 26  $\mu\text{M}$  and 211  $\mu\text{M}$  [8]. Kaempferol is a selective MAO-A inhibitor [14]; furthermore, certain flavonoid structures have been established as reversible and competitive inhibitors, while glycosidation of these structures decreases or abolishes their MAO inhibition [15]. These phenolic compounds all lack amine groups and therefore MAO inhibition is unexpected and not immediately explained.

The drug-drug interactions between many oral sympathomimetic amines and monoamine oxidase (MAO) inhibitors have been well studied in the literature. The most common adverse effect is high blood pressure. Other adverse effects include headache, chest pain, cardiac arrhythmias, and circulation insufficiency [16]. MAO inhibitors inhibit presynaptic and systemic metabolism of some sympathomimetic amines, which are substrates for MAO, resulting in the elevated level of these sympathomimetic amines in circulation [16]. Furthermore, the metabolism of exogenous and endogenous sympathomimetic amines in circulation and tissues could be inhibited by systemic exposure to MAO inhibitors.

Sympathomimetic amines can be divided into two types: direct and indirect acting amines. Indirect acting sympathomimetic amines stimulate the release of noradrenaline from the storage in the sympathetic nerve terminals to interact with postsynaptic adrenergic receptors. MAO inhibitors can increase the level of noradrenaline stored in the nerve terminals. These effects from sympathomimetic amines and MAO inhibitors cause the adverse interaction [16, 17]. Direct acting sympathomimetic amines bind directly to adrenergic receptors. Elimination of these direct acting sympathomimetics from interacting with adrenergic receptors occurs via metabolism by MAO, catechol-O-methyl transferase, and reuptake into presynaptic neurons. Therefore, MAO inhibitors can affect indirectly acting sympathomimetic amines more than directly acting sympathomimetic amines such as phenylephrine [17].

The purpose of this study was to compare the MAO inhibition potential and selectivity of selected phenolic compounds which may have utility in oral dietary supplement products. Since phenolic compounds can act as antioxidants and thus interfere with assay methods depending on the detection of peroxidase activity, a direct chromatographic method measuring the MAO product should yield more reliable results [18]. Therefore kynuramine, a typical substrate of both MAO-A and MAO-B, was used to test if these phenolic compounds can inhibit MAO-A or MAO-B followed by fluorescent HPLC analysis. The metabolite of kynuramine produced by MAO enzymes (3-(2-aminophenyl)-3-oxo-propionaldehyde) rapidly and spontaneously rearranges (by the Schiff base reaction) to the commercially available 4-hydroxyquinoline (shown in Figure 1), which has strong fluorescence for sensitive detection [13].

## 2. Materials and Methods

**2.1. Chemicals and Reagents.** Curcumin (mixture of curcumin, demethoxycurcumin, and bisdemethoxycurcumin) was purchased from Acros Organics (New Jersey, USA). Guaiacol and isoeugenol were purchased from TCI America (Portland, OR). 4-Hydroxyquinoline, zingerone, and trifluoroacetic acid were purchased from Alfa Aesar (Ward Hill, MA). Kynuramine dihydrobromide was purchased from Sigma-Aldrich (St. Louis, MO). Pterostilbene was purchased from ChromaDex (Irvine, CA). Resveratrol was purchased from Beta Pharma, Inc. (New Haven, CT). Piceid (resveratrol 3-glucoside) and vanillin were purchased from TCI America (Portland, OR);  $\alpha$ -mangostin was purchased from Indofine (Hillsborough Township, NJ); gnetin-C was donated by Hosoda Nutritional (Fukui City, Japan). Silybin was purchased from Cayman Chemicals (Ann Arbor, MI) and chrysin was purchased from Hawkins Pharmaceutical (Roseville, MN). Acetonitrile was purchased from Avantor Performance Materials, Inc. (Center Valley, PA). Dimethyl sulfoxide, perchloric acid (70%), sodium hydroxide, and triethylamine were purchased from Fisher Scientific (Fair Lawn, NJ). Potassium phosphate monobasic was purchased from Sigma (St. Louis, MO). Potassium phosphate dibasic was purchased from J.T. Baker (Phillipsburg, NJ). Recombinant human MAO-A and MAO-B were purchased from BD Biosciences (San Jose, CA) or Corning Discovery Labware (Woburn, MA). Resveratrol 4'-glucoside and pterostilbene 4'-glucoside were synthesized as previously described [19, 20]. All test compounds were dissolved in DMSO.

**2.2. Chromatographic Conditions and Detection.** The chromatographic experiments were conducted by HPLC systems including Waters 2695 separation module, Waters 2487 dual  $\lambda$  absorbance detector, and Waters 2475 multi  $\lambda$  fluorescence detector (Waters Corporation, Milford, MA). The HPLC method was developed to simultaneously detect and quantify kynuramine and 4-hydroxyquinoline to monitor the enzymatic reaction of recombinant MAO-A/B. The analytical method used was similar with some modifications to those already published and validated [21, 22]. A Microsorb MV C18 column (100  $\times$  4.6 mm, 3  $\mu\text{m}$ , Agilent Technologies) was used at 30°C to separate kynuramine and 4-hydroxyquinoline. The gradient elution was applied at a flow rate of 1 mL/min with 6.5 mM triethylamine and 13 mM trifluoroacetic acid in water as mobile phase A and acetonitrile as mobile phase B, starting at 10% B and increasing to 50%. Kynuramine was detected by UV at 364 nm, and 4-hydroxyquinoline was detected by fluorescence (excitation 316 nm, emission 357 nm). Further details on the HPLC method are in Supplemental Data (available here).

**2.3. MAO Enzyme Kinetic Assay and  $K_m$  Determination.** The optimized incubation time and human recombinant MAO concentration were selected in the linear range from the time-dependent and MAO concentration-dependent studies (Supplemental Data). Briefly, samples were prepared in potassium phosphate buffer (100 mM, pH 7.4) with a final concentration

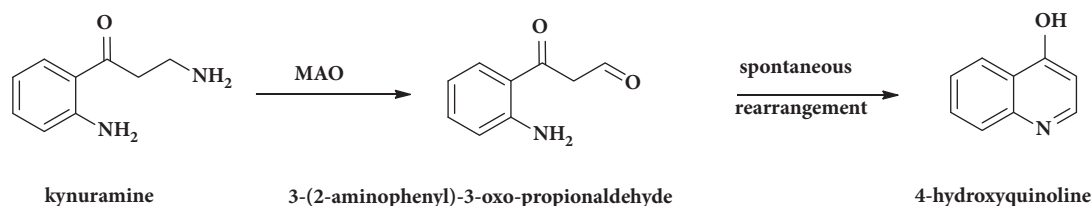


FIGURE 1: Kynuramine converted to 4-hydroxyquinoline via 3-(2-aminophenyl)-3-oxo-propionaldehyde.

of MAO in the reaction solution of 0.01 mg/mL, incubated at 37°C for 15 min. Saturation of kynuramine metabolism with MAO-A/B was carried out at concentrations of 2, 5, 10, 25, 50, 100, 250, 500  $\mu\text{M}$ . The enzymatic reactions (200  $\mu\text{L}$ ) were stopped by 2 N NaOH (75  $\mu\text{L}$ ) followed with 70% perchloric acid (25  $\mu\text{L}$ ). The samples were vortexed and centrifuged for 5 min at 10,000 $\times$ g. The supernatant was analyzed by HPLC as described above.

**2.4. Inhibition Screening and  $\text{IC}_{50}$  Determination.** According to the  $K_m$  value determined in the experiment described above, the final concentration of kynuramine was set at 10  $\mu\text{M}$  for the inhibition assay, which was less than the  $K_m$  values for MAO-A and MAO-B. The incubation time was 15 min and MAO concentration was 0.01 mg/mL. The concentration used to screen the inhibitors of MAO-A/B for curcumin, guaiacol, isoeugenol, pterostilbene, resveratrol, and zingerone was 140, 435, 110, 270, 94, and 51  $\mu\text{M}$ , respectively. If the compounds at these concentrations significantly decrease the formation of 4-hydroxyquinoline, further study would be accomplished to determine their  $\text{IC}_{50}$  for the inhibition of MAO-A/B. Additionally, clorgyline and selegiline were tested as positive controls for MAO-A and MAO-B inhibition [23, 24], while several other natural phenolic compounds were tested for MAO inhibition.

**2.5. Inhibition Mechanism Studies.** To describe the inhibition mechanism for resveratrol or pterostilbene, competition and time dependence were determined. For competition, MAO-A or MAO-B was incubated with varying concentrations of kynuramine (2–450  $\mu\text{M}$ ) for 30 minutes in the absence (control) or presence of resveratrol (1  $\mu\text{M}$ ; MAO-A) or pterostilbene (0.45  $\mu\text{M}$ ). To determine time dependence, the protocol by Obach et al. was followed [25]. Briefly, the enzymes were incubated directly with the inhibitor at 10-fold higher than a quarter of their  $\text{IC}_{50}$  values determined herein for resveratrol and pterostilbene for times from 0 to 60 minutes, before diluting 10-fold with kynuramine at a concentration (20  $\mu\text{M}$ ) approximating its  $K_m$  values. Tranylcypromine was used as a positive control for time-dependent inhibition [24], and DMSO (0.9% v/v) was used as a negative control [23]. After adding kynuramine, the enzymes were incubated for 30 minutes before processing as described above.

**2.6. Data Analysis.** GraphPad Prism 5 was applied to fit a Michaelis-Menten model to the data to obtain the  $K_m$  values in the saturation experiments. In the screening experiments, significant differences between control and treated group

were determined by a one-way ANOVA followed by Dunnett's posttest ( $p < 0.05$ ). The condition of the  $\text{IC}_{50}$  study was incubation of kynuramine (10  $\mu\text{M}$ ) and a broad concentration range of inhibitors with MAO-A/B (0.01 mg/mL) for 15 min. GraphPad Prism 5 was applied to fit the data to obtain  $\text{IC}_{50}$  values by using the concentration-response equation as follows:

$$\frac{v_i}{v_0} = \frac{1}{1 + 10^{((\log [I] - \log \text{IC}_{50}) \times \text{Hill Coefficient})}} \quad (1)$$

This equation included the Hill coefficient as the parameter and could help to characterize the inhibition. If the 95% confidence interval of the Hill coefficient did include 1, the concentration-response equation with the Hill coefficient fixed at 1 was fitted to the data again by the following equation:

$$\frac{v_i}{v_0} = \frac{1}{1 + 10^{(\log [I] - \log \text{IC}_{50})}} \quad (2)$$

The selectivity index was calculated as a ratio of MAO-B  $\text{IC}_{50}$ /MAO-A  $\text{IC}_{50}$  for each compound. The calculated solubility values for phenolic dietary compounds (all unionized at pH values ranging from 1 to 7) are from SciFinder [26]. The maximum single doses are from published sources [27–32]. The relevant GI concentration is the lesser of either solubility or the concentration after a single dose.

Time depended data were analyzed by fitting either straight line or one-phase exponential decay models to the data in GraphPad Prism v5.

### 3. Results

**3.1. Optimized Enzyme Kinetic Assay and  $K_m$  Determination.** The concentration dependence for oxidative deamination of kynuramine with MAO-A and MAO-B is shown in Figure 2. Kynuramine (2 to 500  $\mu\text{M}$ ) was incubated in 200  $\mu\text{L}$  potassium phosphate buffer (100 mM, pH 7.4) for 15 min with MAO-A or MAO-B (0.01 mg/mL). Michaelis-Menten model was used to fit the data by GraphPad Prism 5. The experiments were conducted 3 times in triplicate. Single representative experiments are shown. For MAO-A,  $K_m$  and  $V_{\max}$  were  $23.1 \pm 0.8 \mu\text{M}$  and  $10.2 \pm 0.2 \text{ nmol/min/mg}$  (mean  $\pm$  SEM), respectively. For MAO-B,  $K_m$  and  $V_{\max}$  were  $18.0 \pm 2.3 \mu\text{M}$  and  $7.35 \pm 0.69 \text{ nmol/min/mg}$  (mean  $\pm$  SEM), respectively. From these data, the concentration of kynuramine was set at 10  $\mu\text{M}$  for both MAO-A and MAO-B for the following studies so that the kynuramine concentration was  $< K_m$ .

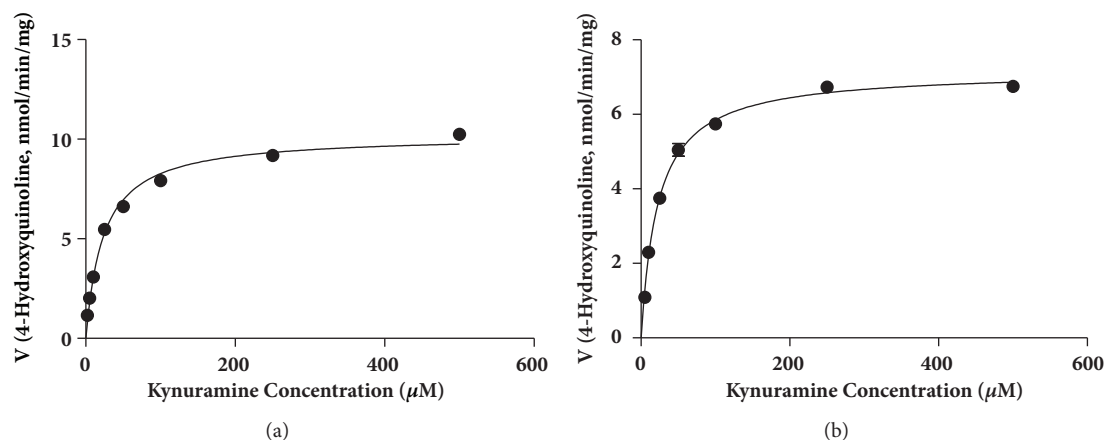


FIGURE 2: **Concentration dependence of oxidative deamination of kynuramine by MAO-A (a) or MAO-B (b).** Kynuramine was incubated with MAO-A (a) or MAO-B (b) (0.01mg/ml) for 15 minutes. The formation of 4-hydroxyquinoline (mean  $\pm$  SD) was determined in three experiments in triplicate; a representative experiment is shown. The Michaelis-Menten model was fitted to the data, represented by the curve.

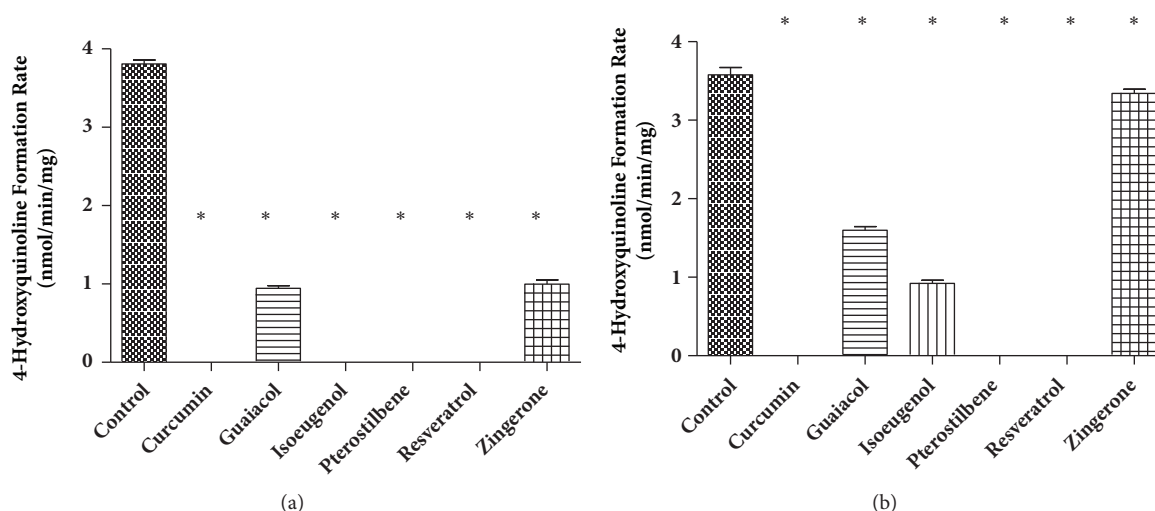


FIGURE 3: **The inhibition of MAO-A (a) or MAO-B (b) activity by phenolic dietary compounds.** The inhibition screening for oxidative deamination of kynuramine with MAO-A (a) or MAO-B (b) was conducted with kynuramine (10  $\mu$ M) incubated with either enzyme (0.01 mg/mL) and one of these phenolic dietary compounds. Concentrations tested: curcumin 140 $\mu$ M, guaiacol 435 $\mu$ M, isoeugenol 110 $\mu$ M, pterostilbene 270 $\mu$ M, resveratrol 94 $\mu$ M, and zingerone 51 $\mu$ M. The numbers are expressed as means  $\pm$  SD; \* indicates that the significant differences were analyzed between the control (no inhibitor) and phenolic compounds. Absent bars indicate that the formation of 4-hydroxyquinoline was below the quantification limit.

**3.2. Inhibition Screening and  $IC_{50}$  Determination.** The inhibition screening for oxidative deamination of kynuramine with MAO-A or MAO-B is shown in Figure 3. Kynuramine (10  $\mu$ M) was incubated in 200  $\mu$ L potassium phosphate buffer (100 mM, pH 7.4) for 15 min with MAO-A or MAO-B (0.01 mg/mL) and one of these phenolic dietary compounds. The control was the incubation with kynuramine but without any dietary compounds. The numbers are expressed as means  $\pm$  SD and the significant differences were analyzed between the control treatment (with no inhibitor) and treatments in presence of phenolic dietary compounds using one-way ANOVA analysis followed by Dunnett's *post hoc* test in GraphPad Prism 5. All the phenolic compounds tested in the experiments showed significant inhibition of MAO-A

activity with  $p < 0.05$ . All the phenolic compounds tested in the experiments showed significant inhibition of MAO-B activity with  $p < 0.05$ . However, zingerone showed less than 10% inhibition at its GI concentration (51  $\mu$ M) expected from maximum single dose. Therefore zingerone was not investigated further with MAO-B.

The  $IC_{50}$  curves for the inhibitors for kynuramine oxidative deamination with MAO-A are shown in Figures 4 and 5. MAO activities were measured by the formation of 4-hydroxyquinoline with inhibitors in a broad range of concentrations (at least  $10^4$ -fold) for 15 min incubation of kynuramine with MAO-A or MAO-B. The fractional activity is the value divided by the control (in absence of inhibitor). The formation of 4-hydroxyquinoline was under

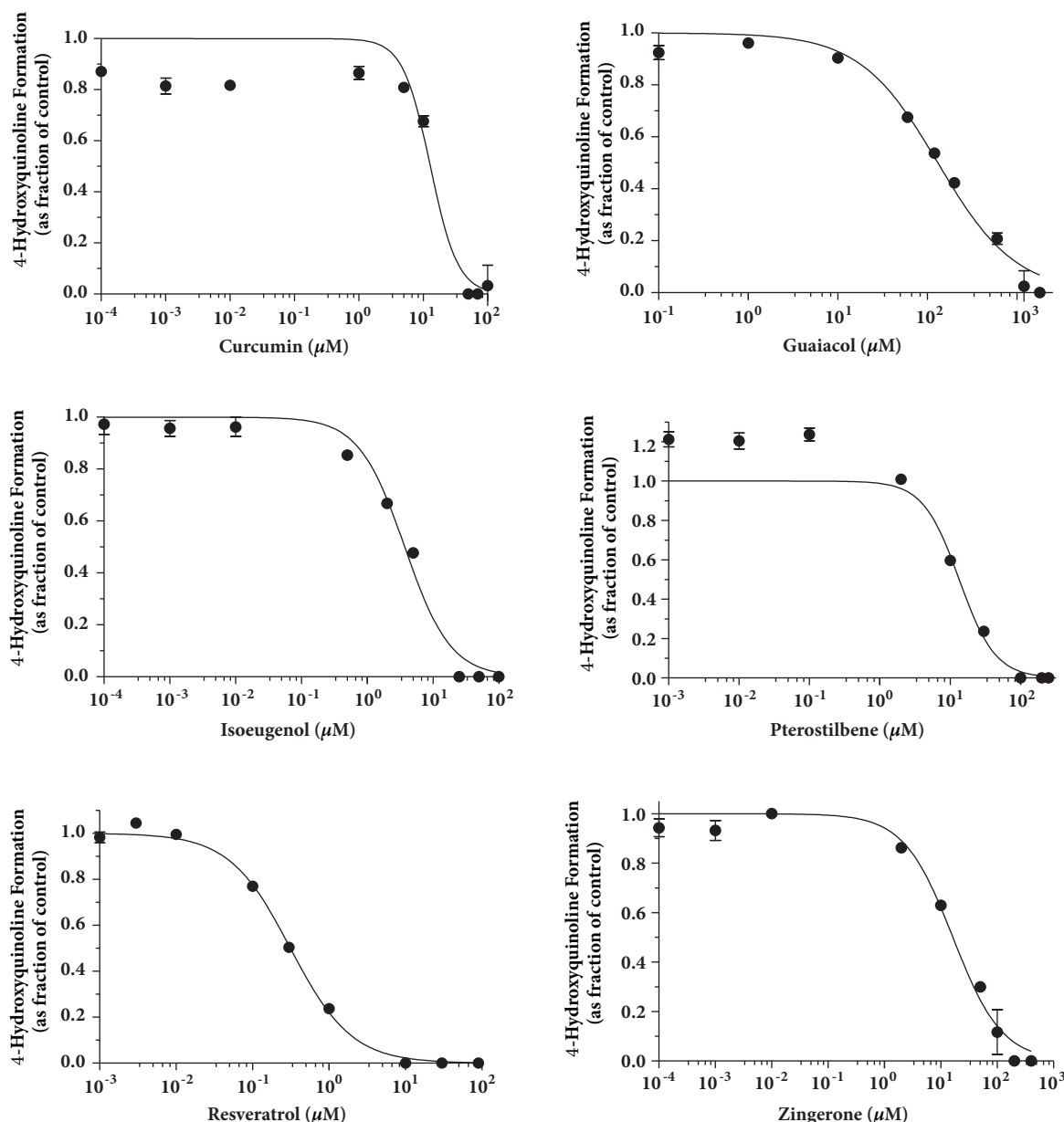


FIGURE 4: **Determination of  $\text{IC}_{50}$  for curcumin, guaiacol, isoeugenol, pterostilbene, resveratrol, and zingerone on MAO-A activity.** MAO-A activity was measured by the formation of 4-hydroxyquinoline with inhibitors in a broad range of concentrations (at least  $10^4$ -fold) for 15 min. The Y-axis is expressed as fraction of the control (in absence of inhibitor) and all points on the curves are expressed as means  $\pm$  SD.

the lower limit of detection when incubating kynuramine with the negative control for MAO activity.  $\text{IC}_{50}$  values, Hill coefficients, and selectivity indices are shown in Table 1.

In Figure 6, Clorgyline or selegiline selectively inhibited MAO-A or MAO-B as expected [24]. Among the glucosides, only resveratrol 4'-glucoside inhibited MAO-A while MAO-B was not inhibited. As previously reported [23], chrysin inhibited both enzymes.

**3.3. Inhibition Mechanism.** Figure 7 showed that in the absence or presence of resveratrol ( $1 \mu\text{M}$ ), the  $V_{\text{max}}$  and  $K_m$  values for MAO-A were  $17.4 \pm 0.7$  or  $15.8 \pm 0.4 \text{ nmol/min/mg}$

protein and  $8.46 \pm 1.56$  or  $16.1 \pm 1.8 \mu\text{M}$ , respectively. For MAO-B, in the absence or presence of pterostilbene ( $0.45 \mu\text{M}$ ), the  $V_{\text{max}}$  and  $K_m$  values were  $3.44 \pm 0.07$  or  $3.28 \pm 0.19 \text{ nmol/min/mg}$  protein and  $14.4 \pm 1.2$  or  $24.4 \pm 5.4 \mu\text{M}$ , respectively. MAO-A activity showed dependence upon preincubation time with tranylcypromine ( $1 \mu\text{M}$ ), with a preincubation half-life of 1.1 minutes, and a plateau showing 48% inhibition. However, resveratrol ( $1.6 \mu\text{M}$ ) preincubation revealed a time profile not significantly different from the control. MAO-B preincubation with tranylcypromine ( $0.5 \mu\text{M}$ ) also showed time dependence, with a half-life of 4.7 minutes, and a plateau at 85% inhibition, while preincubation with pterostilbene



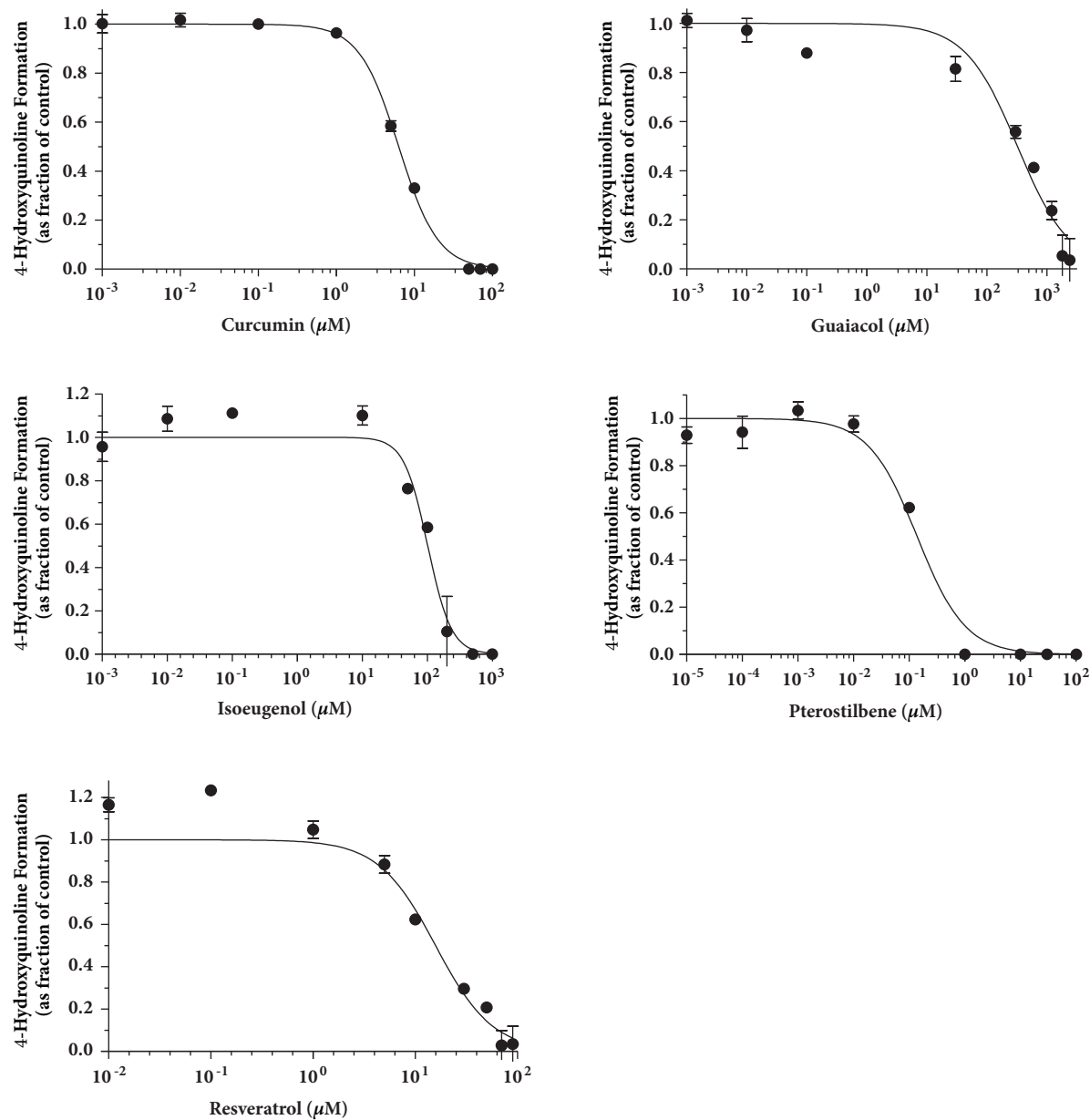


FIGURE 5: **Determination of  $\text{IC}_{50}$  for curcumin, guaiacol, isoeugenol, pterostilbene, and resveratrol on MAO-B activity.** MAO-B activity was measured by the formation of 4-hydroxyquinoline with inhibitors in a broad range of concentrations (at least  $10^4$ -fold) for 15 min. The Y axis is expressed as fraction of the control (in absence of inhibitor) and all points on the curves are expressed as means  $\pm$  SD.

	MAO-A		MAO-B		Selectivity Index
	$\text{IC}_{50}$ ( $\mu\text{M}$ )	Hill coefficient	$\text{IC}_{50}$ ( $\mu\text{M}$ )	Hill coefficient	
curcumin	$12.9 \pm 1.3$	$2.0 \pm 0.4$	$6.30 \pm 0.11$	$1.7 \pm 0.1$	0.488
guaiacol	$131 \pm 6$	1.0	$322 \pm 27$	1.0	2.46
isoeugenol	$3.72 \pm 0.20$	$1.2 \pm 0.1$	$102 \pm 5$	$2.4 \pm 0.3$	27.4
pterostilbene	$13.4 \pm 1.5$	$1.7 \pm 0.3$	$0.138 \pm 0.013$	1.0	0.0103
resveratrol	$0.313 \pm 0.008$	$1.1 \pm 0.0$	$15.8 \pm 1.3$	$1.6 \pm 0.2$	50.5
zingerone	$16.3 \pm 1.1$	1.0			

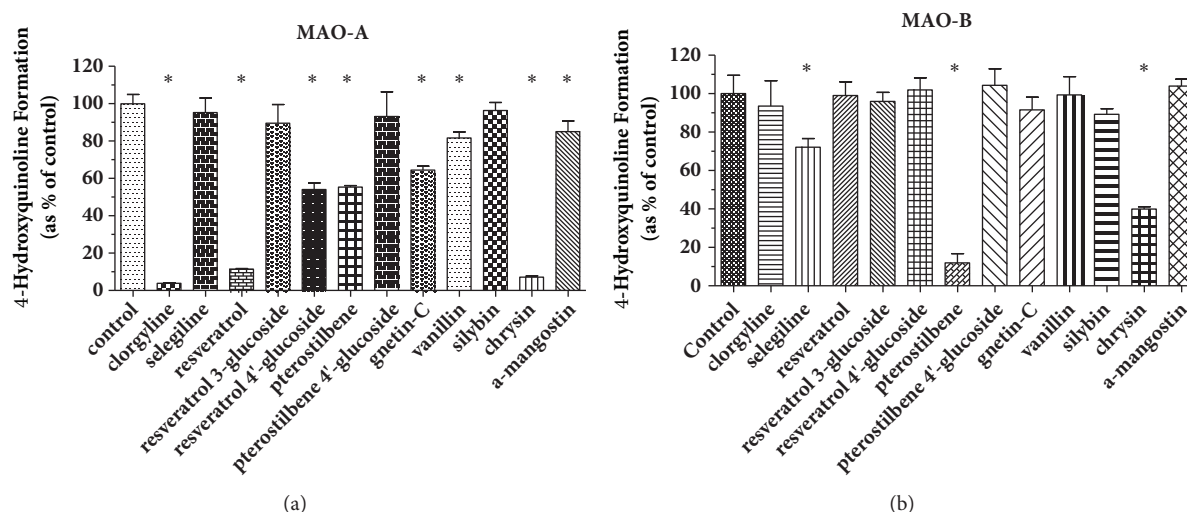


FIGURE 6: MAO inhibition by natural phenolic compounds. Recombinant human monoamine oxidases A (a) and B (b) (0.01mg/ml) were exposed to kynuramine dihydrobromide (10 $\mu$ M) for 15 minutes in the absence (control; n=6) or presence (n=3) of clorgyline (1 $\mu$ M), selegiline (0.5 $\mu$ M), or 15  $\mu$ M of resveratrol, resveratrol 3-glucoside, resveratrol 4'-glucoside, pterostilbene, pterostilbene 4'-glucoside, gnetin-C, vanillin, silybin, chrysin, or  $\alpha$ -mangostin. Comparisons were made by one-way ANOVA with Dunnett's posttest; \* indicates p<0.05. Control rates for MAO-A and MAO-B were 0.357  $\pm$  0.018 and 0.105  $\pm$  0.010 nmol/min/mg protein, respectively.

(0.7 $\mu$ M) revealed a time profile not significantly different from the control.

#### 4. Discussion

Previously validated HPLC methods [21, 23] were adapted to simultaneously quantitate kynuramine and the product of its metabolism by MAO 4-hydroxyquinoline. We applied this assay to facilitate the quantitation and comparison of several phenolic compounds on human MAO enzymes. Interestingly, some of these compounds showed considerable selectivity toward MAO-A or MAO-B. A previous study shows that resveratrol had similar potency for inhibiting MAO-A and MAO-B [33]; however, our study showed that resveratrol had higher potency and selectivity for MAO-A. The reason for the difference is unknown, but may be due to differences in assay methods, i.e., Amplex Red vs. kynuramine. The interference with peroxidase-based assays has been previously established [18].

From the optimization studies (Supplementary Materials), the formation of 4-hydroxyquinoline was linear over 60 min with the protein concentration range of 0.003 mg/mL–0.03 mg/mL, which was comparable with the results from the paper published by Herraiz et al. in 2006 [21]. The  $K_m$  values of kynuramine oxidative deamination by MAO-A and MAO-B were 23  $\mu$ M and 18  $\mu$ M, respectively, which indicated MAO-A has similar affinity toward kynuramine, compared to MAO-B. In the literature, the  $K_m$  values of kynuramine for human MAO-A and MAO-B were reported as 42  $\mu$ M and 26  $\mu$ M [34]. Another study obtained the  $K_m$  values of MAO-A and MAO-B with kynuramine as 44.1 and 90.0  $\mu$ M, respectively [35].  $K_m$  values reported here were similar to the values in literature, although differences in methods or recombinant enzyme sources may account for

differences in reported  $K_m$  or  $V_{max}$  values. The concentration of kynuramine for the inhibition study with phenolic compounds was set at 10  $\mu$ M, which was below the  $K_m$  value for both MAO-A and MAO-B.

Nonlinear regression revealed Hill coefficients of unity for guaiacol and zingerone showing 1-to-1 apparent binding to MAO-A, and guaiacol and pterostilbene followed 1-to-1 apparent binding to MAO-B. The Hill coefficient of resveratrol with MAO-A was 1.08, while curcumin, isoeugenol, and pterostilbene had Hill coefficients larger than 1, suggesting positive cooperativity, multiple active sites, or non-ideal inhibition behavior [36]. Positive cooperativity could be a possible reason. The binding of the inhibitor to one active site on the enzyme may increase the binding affinity of the inhibitor to other active sites [36]. Another possibility is that the complete inhibition of an enzyme can be achieved by binding of more than one molecule of inhibitor to the enzyme [36]. Further study is required to investigate the mechanism of inhibition which leads to the Hill coefficient larger than 1, including possible allosterism.

Among these tested phenolic dietary compounds, the inhibitory effects on MAO-A and MAO-B in animal models were reported in the literature previously [7, 12]. However, in this study, human recombinant MAO-A and MAO-B enzymes were used as models to test these phenolic compounds. Curcumin can inhibit MAO-A and MAO-B in mouse brain after p.o. administration [7]. We also found curcumin inhibited both MAO-A and MAO-B with  $IC_{50}$  values of 12.89  $\mu$ M and 6.30  $\mu$ M, respectively. In this study, resveratrol was the most potent inhibitor for MAO-A with  $IC_{50}$  as 0.31  $\mu$ M; its inhibition was consistent with a competitive mechanism, as previously demonstrated by Ryu et al. [12]. Resveratrol is a potent competitive inhibitor of MAO-A in rat brain with  $IC_{50}$  of 2  $\mu$ M and  $K_i$  of 2.5  $\mu$ M [12]. Resveratrol

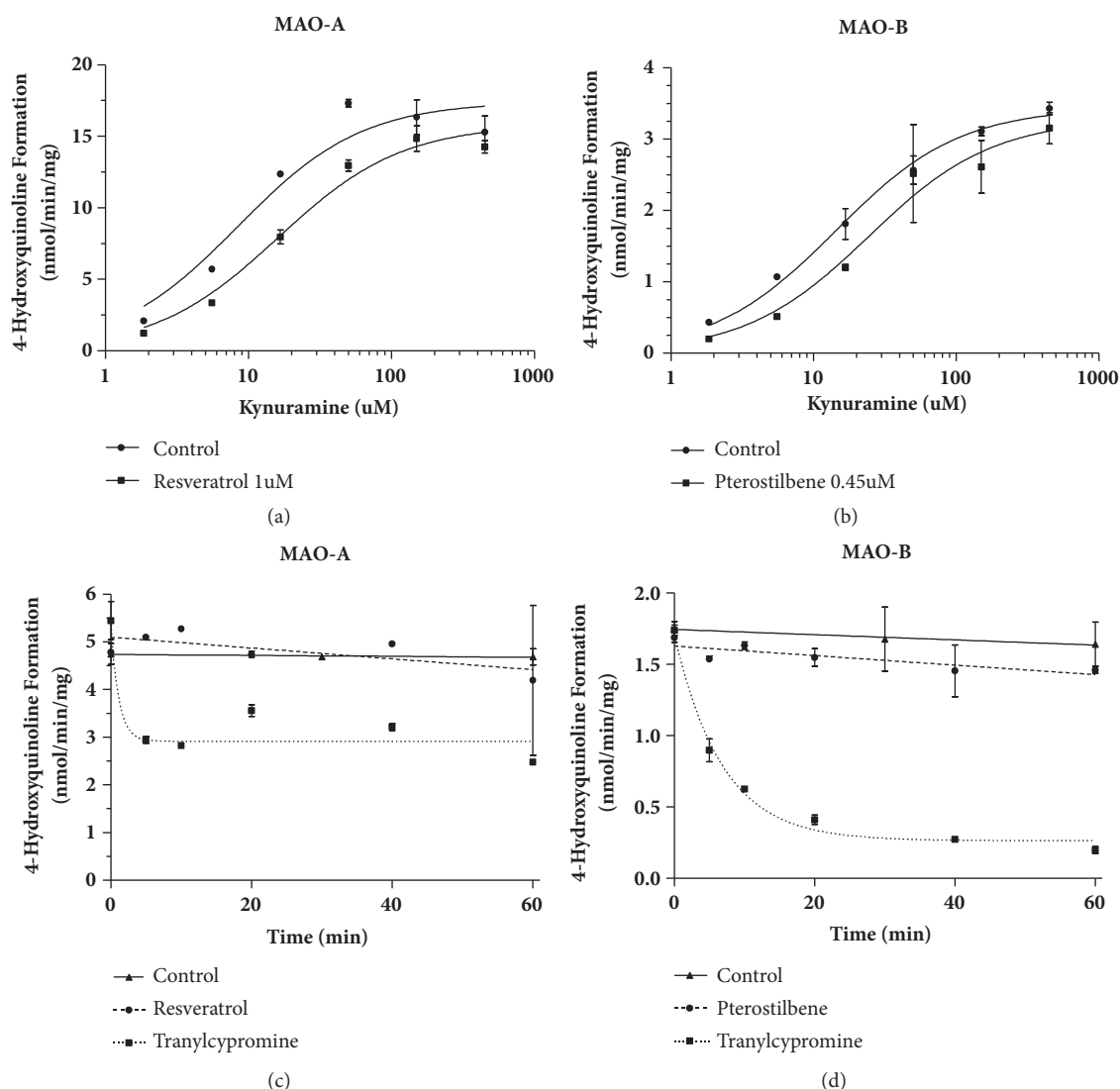


FIGURE 7: **Mechanism of resveratrol and pterostilbene inhibition of MAO enzymes.** Kynuramine (2-450 $\mu$ M) and MAO-A or MAO-B (0.01mg/ml) were incubated for 15 minutes in the absence or presence of resveratrol (1 $\mu$ M) (a) or pterostilbene (0.45 $\mu$ M) (b). The Michaelis-Menten equation was fit to the data by nonlinear regression to compare any changes in  $K_m$  or  $V_{max}$ . (c) MAO-A was preincubated with tranlycypromine (1 $\mu$ M), resveratrol (1.6 $\mu$ M), or DMSO (control) for 0-60 minutes before the addition of kynuramine (20 $\mu$ M). (d) MAO-A was preincubated with tranlycypromine (0.5 $\mu$ M), pterostilbene (0.7 $\mu$ M), or DMSO (control) for 0-60 minutes before the addition of kynuramine (20 $\mu$ M). All samples were incubated at 37°C for 30 minutes. One-phase decay or straight line equations were fit to the data.

was also previously reported to be an inhibitor of MAO-A but did not significantly inhibit MAO-B up to 10 $\mu$ M [18], which is consistent with our study in which resveratrol showed a relatively high  $IC_{50}$  value for MAO-B of 15.8 $\mu$ M (Table 1). Pterostilbene has never been reported as an MAO inhibitor, but it was the most potent MAO-B inhibitor in our study, with an  $IC_{50}$  of 0.138  $\mu$ M.

Compared to the GI concentration converted from the maximum single dose, the  $IC_{50}$  values of all phenolic inhibitors on MAO-A and MAO-B are smaller than the maximum concentration in GI tract. The most potent inhibitor for MAO-A was resveratrol followed by isoeugenol, curcumin, pterostilbene, zingerone, and guaiacol in descending order of potency. The most potent inhibitor for MAO-B was

pterostilbene followed by curcumin, resveratrol, isoeugenol, and guaiacol in descending order of potency.

Additionally, the selectivity indices expressed as the ratios of MAO-B/MAO-A  $IC_{50}$  values (Table 1) showed that resveratrol and isoeugenol are selective MAO-A inhibitors, while pterostilbene is a selective MAO-B inhibitor. These data are especially intriguing, considering that only two methyl groups differentiate resveratrol and pterostilbene. Besides resveratrol, isoeugenol showed the next highest level of potency and selectivity for MAO-A. Isoeugenol has a methylated catechol moiety (as do zingerone and guaiacol) and also a hydrophobic side chain, which may contribute to its MAO-A inhibition exceeding those of zingerone and guaiacol. Furthermore, among the glucosides of resveratrol

and pterostilbene tested herein, MAO-A was inhibited only by resveratrol 4'-glucoside, while MAO-B was not inhibited. This is consistent with the loss of inhibitory activity by glycosides of kaempferol [15].

Phenolic compounds are substrates for neither MAO-A or MAO-B and, unlike other MAO, substrates and inhibitors are devoid of any nitrogen atoms. The mechanism of the inhibition of phenolic compounds on MAO is not clear, but none of them was reported to have irreversible inhibition on MAO-A or MAO-B [8, 9]. The researchers found that they are reversible inhibitors with various mode of inhibition such as competitive inhibition, non-competitive, or mixed-type inhibition [8, 9]. Furthermore, several flavonoids have been established as reversible and competitive inhibitors [15].

Published studies show that these phenolic MAO-A inhibitors all have low oral bioavailability in animal models, although this has not been determined in humans. Curcumin has poor bioavailability after oral administration in humans even after a high dose of 12 g/day, which leads to low plasma concentrations [37]. At doses of 4 g, 6 g, and 8 g, the maximum concentration of curcumin in plasma is 0.51  $\mu$ M, 0.64  $\mu$ M, and 1.77  $\mu$ M, respectively [38]. After gavage administration, the absolute bioavailability of isoeugenol in female and male rats is 19% and 10%, respectively. The low bioavailability of isoeugenol was also observed in mice as 28% for male mice and 31% for female mice after gavage bolus [39]. The peak plasma concentration of resveratrol in humans is very low after oral dosing [40, 41]. At 25 mg, 50 mg, 100 mg, and 150 mg doses, the maximum plasma concentrations of resveratrol are 1.48 ng/mL, 6.59 ng/mL, 21.4 ng/mL, and 24.8 ng/mL, respectively [40]. At higher doses of 0.5 g, 1.0 g, 2.5 g, and 5.0 g, the corresponding peak plasma concentrations of resveratrol are 72.6 ng/mL, 117.0 ng/mL, 268.0 ng/mL, and 538.8 ng/mL [41]. The oral bioavailability in rats was determined as 12.5% after 10 mg/kg gavage administration by Lin et al. [42]. After giving rats 56 or 168 mg/kg/day for pterostilbene by gavage for 14 continuous days, the oral bioavailability is 80% [43]. The reason why these phenolic compounds have such low bioavailability is that they all undergo extensive presystemic metabolism and are converted to their metabolites before going to the systemic circulation [41, 43–51].

As described above, in the dose range of 25 mg to 5.0 g, and considering the plasma protein binding of 91% for resveratrol [52], the unbound maximal peak plasma concentrations range from 0.584 to 212 nM. With the  $IC_{50}$  values of 0.313 and 15.8  $\mu$ M for MAO-A and MAO-B and assuming competitive inhibition of resveratrol on human MAO-A and MAO-B, the values of  $K_i$  would be 0.218 and 10.2  $\mu$ M for MAO-A and MAO-B, respectively. The drug-drug interaction index (unbound  $C_{max}/K_i$  [53]) for MAO-A is in the range of  $2.7 \times 10^{-3}$  to 0.97. Thus at high resveratrol doses (5.0 g), inhibition of MAO-A may occur. However, the drug-drug interaction index for MAO-B is in the range of  $5.7 \times 10^{-5}$  to 0.021, making clinically relevant MAO-B interactions with resveratrol unlikely. As with many other natural phenolic compounds, human plasma concentration data and absolute oral bioavailability for oral

doses of pterostilbene are lacking [54], making predictions of gastrointestinal or systemic MAO-B interactions speculative. A human clinical study with pterostilbene shows that 125mg twice daily orally for 6-8 weeks reduces both systolic and diastolic blood pressure, although it slightly raised plasma low-density lipoproteins [55]. Another clinical study with pterostilbene 50mg in combination with nicotinamide riboside 250mg for two months also reduced diastolic blood pressure [56]. Acute, severe, systemic MAO inhibition is expected to increase blood pressure and result in serotonin syndrome [2]; however, such adverse reactions were not reported in these studies. As with many dietary compounds, the absolute oral bioavailability of pterostilbene has not been reported, but animal studies show that it is much greater than that of resveratrol [43]. Additional studies are required to determine the absolute oral bioavailability of pterostilbene and other potentially beneficial phenolic compounds and to establish their antiaging effects on human cardiac and neuronal tissues.

Since these phenolic compounds all have relatively low bioavailability, the inhibition occurring after first-pass metabolism is likely to be limited. Most inhibitory effects on MAO-A and MAO-B would be limited to GI tract and liver. Nishimura et al. established the mRNA levels of MAO-A and MAO-B in various human tissues [57]. From their data, the MAO-A mRNA/MAO-B mRNA ratio in the liver is 0.727, whereas the ratio in the small intestine is 4.41, suggesting that MAO-A and MAO-B expression may be similar in the liver, but MAO-A predominates in the intestine. Thus, any effects of MAO-A inhibition in the intestine could be concerning. When other dietary compounds are substrates of MAO and their presystemic metabolism is blocked resulting in higher systemic exposure, MAO inhibition may be problematic. One example is tyramine. Interactions between food constituents and drugs are complicated with various conditions and difficult to predict. When patients take irreversible MAO inhibitors, tyramine-rich foods are to be avoided.

Other assays for MAO activity are available, including peroxidase- and luciferase-based assays. However, antioxidant phenolics can interfere with peroxidase-based assays by quenching the hydrogen peroxide formed [58]. In our lab, resveratrol strongly quenched luminescence in the MAO-glo assay (Promega, Madison, WI; Tamoor Hassan, unpublished data). The metabolic production of 4-hydroxyquinoline could avoid these interferences, but only for compounds which do not interfere with its detection. Thus, the kynuramine-based assay with chromatographic separation offers a solution to avoid interferences. Assays for kynuramine and 4-hydroxyquinoline have been previously reported, and Herraiz et al. showed that antioxidants can indeed interfere with Amplex Red assays, while this interference is avoided by HPLC analysis of 4-hydroxyquinoline formation [18]. The quantitative analysis could be simply achieved by fluorometric assay [59]. The phenolic compounds tested in this study have very strong fluorescence, which may interfere with the fluorescent signal from 4-hydroxyquinoline if measured in a microplate reader. Therefore, a fluorometric microplate assay may not be selective



for the detection of 4-hydroxyquinoline and thus chromatographic separation of 4-hydroxyquinoline and the phenolic compounds are required. Other analyses are accomplished by HPLC with UV and fluorescence detection as well as LC-MS/MS [21, 34, 60, 61]. Since 4-hydroxyquinoline has very good fluorescence and kynuramine can be detected by UV detection, HPLC methods with UV and fluorescence detectors are found to be quite adequate for analysis in *in vitro* enzyme kinetic studies. In order to avoid analytical interferences, Herraiz et al. developed a reversed-phase HPLC method by gradient elution with 50 mM ammonium phosphate buffer at pH 3 and 20% of this buffer in acetonitrile [21, 60]. Also, in their HPLC method for 4-hydroxyquinoline, Parikh et al. used a mobile phase containing 0.2mM perchloric acid [23]. In order to avoid the potential for damage to our HPLC system, we modified the mobile phase as discussed in the method section.

The HPLC method for quantitative analysis of kynuramine and 4-hydroxyquinoline used 6.5 mM triethylamine and 13 mM trifluoroacetic acid in water as its aqueous phase, which has a pH value around 2. The estimated most basic pKa value for kynuramine is 8.4, making it cationic in the mobile phase [26]. The estimated most acidic and most basic pKa values for 4-hydroxyquinoline are 4.3 and 11.1, respectively [26]. Hence 4-hydroxyquinoline is also cationic in the mobile phase. At high concentration, trifluoroacetic acid can act as an ion-pairing agent for cations, which can improve kynuramine and 4-hydroxyquinoline retention. When using the aqueous mobile phase with only TFA at 0.05%, there was a tailing problem with the peak shape. This can be caused by the ions like sodium and potassium bound to silanol exchanging with ionized basic analytes at low pH. As an additive in the mobile phase, triethylamine can fix the tailing problem on the column. Excess triethylamine in the mobile phase can replace the ions instead of basic analytes. Therefore, triethylamine can reduce the peak tailing [62].

## 5. Conclusions

In conclusion, we applied a previously validated kynuramine-based MAO activity assay with HPLC separation and fluorescence detection for determining the inhibition and selectivity of several phenolic compounds. Among the compounds tested, resveratrol was potent and selective for MAO-A inhibition, while pterostilbene was potent and selective for MAO-B inhibition. Both compounds appeared to be competitive, time-independent inhibitors. Our calculations suggest that high doses of resveratrol have the potential to inhibit MAO-A in the gastrointestinal tract. Human pharmacokinetic studies with oral dosing of pterostilbene will facilitate future predictions of its clinical potential to interact with MAO-B in the gastrointestinal tract, liver, or systemic circulation. The anti-aging potential of these compounds is worth further investigations.

## Data Availability

The data used to support the findings of this study are available from the corresponding author upon request.

## Conflicts of Interest

The authors declare that there are no conflicts of interest regarding the publication of this paper.

## Acknowledgments

This work was submitted by Zhenxian Zhang as a part of her PhD dissertation at the VCU School of Pharmacy. This study was supported by the VCU School of Pharmacy, the VCU Graduate School Dissertation Enhancement Award, and Pfizer Consumer Healthcare (Investigator-Initiated Research Program). The authors acknowledge Dr. Jurgen Venitz for helpful discussions regarding this project. They also acknowledge Hosoda Nutritional for their kind gift of gnetin-C.

## Supplementary Materials

Supplementary materials are available describing the HPLC method and the optimization of the enzyme incubation conditions. (*Supplementary Material*)

## References

- [1] M. Bortolato, K. Chen, and J. C. Shih, "Monoamine oxidase inactivation: from pathophysiology to therapeutics," *Advanced Drug Delivery Reviews*, vol. 60, no. 13-14, pp. 1527-1533, 2008.
- [2] L. L. Brunton, B. A. Chabner, and B. C. Knollman, *Goodman & Gilman's The Pharmacological Basis of Therapeutics*, McGraw-Hill, 2011.
- [3] D. Maggiorani, N. Manzella, D. E. Edmondson et al., "Monoamine Oxidases, Oxidative Stress, and Altered Mitochondrial Dynamics in Cardiac Ageing," *Oxidative Medicine and Cellular Longevity*, vol. 2017, Article ID 3017947, 8 pages, 2017.
- [4] B. Martín-Fernández and R. Gredilla, "Mitochondrial oxidative stress and cardiac ageing," *Clínica e Investigación en Arteriosclerosis: publicacion oficial de la Sociedad Espanola de Arteriosclerosis*, vol. 30, no. 2, pp. 74-83, 2018.
- [5] Y. Aluf, J. Vaya, S. Khatib, Y. Loboda, and J. P. Finberg, "Selective inhibition of monoamine oxidase A or B reduces striatal oxidative stress in rats with partial depletion of the nigro-striatal dopaminergic pathway," *Neuropharmacology*, vol. 65, pp. 48-57, 2013.
- [6] N. Hauptmann, J. Grimsby, J. C. Shih, and E. Cadenas, "The metabolism of tyramine by monoamine oxidase A/B causes oxidative damage to mitochondrial DNA," *Archives of Biochemistry and Biophysics*, vol. 335, no. 2, pp. 295-304, 1996.
- [7] Y. Xu, B.-S. Ku, H.-Y. Yao et al., "The effects of curcumin on depressive-like behaviors in mice," *European Journal of Pharmacology*, vol. 518, no. 1, pp. 40-46, 2005.
- [8] G. Tao, Y. Irie, D.-J. Li, and M. K. Wing, "Eugenol and its structural analogs inhibit monoamine oxidase A and exhibit antidepressant-like activity," *Bioorganic & Medicinal Chemistry*, vol. 13, no. 15, pp. 4777-4788, 2005.
- [9] L. D. Kong, C. H. K. Cheng, and R. X. Tan, "Inhibition of MAO a and B by some plant-derived alkaloids, phenols and anthraquinones," *Journal of Ethnopharmacology*, vol. 91, no. 2-3, pp. 351-355, 2004.
- [10] S. Yoshino, A. Hara, H. Sakakibara et al., "Effect of quercetin and glucuronide metabolites on the monoamine oxidase-A reaction

- in mouse brain mitochondria," *Nutrition Journal*, vol. 27, no. 7-8, pp. 847–852, 2011.
- [11] Y. Bandaruk, R. Mukai, T. Kawamura, H. Nemoto, and J. Terao, "Evaluation of the inhibitory effects of quercetin-related flavonoids and tea catechins on the monoamine oxidase-A reaction in mouse brain mitochondria," *Journal of Agricultural and Food Chemistry*, vol. 60, no. 41, pp. 10270–10277, 2012.
  - [12] S. Y. Ryu, Y. N. Han, and B. H. Han, "Monoamine oxidase-A inhibitors from medicinal plants," *Archives of Pharmacal Research*, vol. 11, no. 3, pp. 230–239, 1988.
  - [13] S. Carradori, M. D'Ascenzio, P. Chimenti, D. Secci, and A. Bolasco, "Selective MAO-B inhibitors: A lesson from natural products," *Molecular Diversity*, vol. 18, no. 1, pp. 219–243, 2014.
  - [14] M. C. Gidaro, C. Astorino, A. Petzer et al., "Kaempferol as Selective Human MAO-A Inhibitor: Analytical Detection in Calabrian Red Wines, Biological and Molecular Modeling Studies," *Journal of Agricultural and Food Chemistry*, vol. 64, no. 6, pp. 1394–1400, 2016.
  - [15] S. Carradori, M. C. Gidaro, A. Petzer et al., "Inhibition of Human Monoamine Oxidase: Biological and Molecular Modeling Studies on Selected Natural Flavonoids," *Journal of Agricultural and Food Chemistry*, vol. 64, no. 47, pp. 9004–9011, 2016.
  - [16] F. Sjöqvist, "Psychotropic drugs (2). Interaction between monoamine oxidase (MAO) inhibitors and other substances," *Proceedings of the Royal Society of Medicine*, vol. 58, no. 11, pp. 967–978, 1965.
  - [17] M. J. Rand and F. R. Trinker, "The mechanism of the augmentation of responses to indirectly acting sympathomimetic amines by monoamine oxidase inhibitors," *British Journal of Pharmacology*, vol. 33, no. 2, pp. 287–303, 1968.
  - [18] T. Herraiz, A. Flores, and L. Fernández, "Analysis of monoamine oxidase (MAO) enzymatic activity by high-performance liquid chromatography-diode array detection combined with an assay of oxidation with a peroxidase and its application to MAO inhibitors from foods and plants," *Journal of Chromatography B*, vol. 1073, pp. 136–144, 2018.
  - [19] D. Uesugi, H. Hamada, K. Shimoda, N. Kubota, S. Ozaki, and N. Nagatani, "Synthesis, oxygen radical absorbance capacity, and tyrosinase inhibitory activity of glycosides of resveratrol, pterostilbene, and pinostilbene," *Bioscience, Biotechnology, and Biochemistry*, vol. 81, no. 2, pp. 226–230, 2016.
  - [20] D. Sato, N. Shimizu, Y. Shimizu et al., "Synthesis of glycosides of resveratrol, pterostilbene, and piceatannol, and their anti-oxidant, anti-allergic, and neuroprotective activities," *Bioscience, Biotechnology, and Biochemistry*, vol. 78, no. 7, pp. 1123–1128, 2014.
  - [21] T. Herraiz and C. Chaparro, "Analysis of monoamine oxidase enzymatic activity by reversed-phase high performance liquid chromatography and inhibition by  $\beta$ -carboline alkaloids occurring in foods and plants," *Journal of Chromatography A*, vol. 1120, no. 1-2, pp. 237–243, 2006.
  - [22] Z. Yan, G. W. Caldwell, B. Zhao, and A. B. Reitz, "A high-throughput monoamine oxidase inhibition assay using liquid chromatography with tandem mass spectrometry," in *Rapid Communications in Mass Spectrometry*, vol. 18, pp. 834–840, 2004.
  - [23] S. Parikh, S. Hanscom, P. Gagne, C. Crespi, and C. Patten, "A fluorescent-based, high-throughput assay for detecting inhibitors of human monoamine oxidase A and B," *Drug Metabolism Reviews*, vol. 34, p. 164, 2002.
  - [24] K. F. Tipton, G. Davey, and M. Motherway, "Monoamine Oxidase Assays," *Current Protocols in Pharmacology*, vol. 9, no. 1, pp. 3.6.1–3.6.42, 2000.
  - [25] R. S. Obach, O. A. Fahmi, and R. L. Walsky, "Inactivation of human cytochrome P450 enzymes and drug-drug interactions," in *Enzyme- and Transporter-Based Drug-Drug Interactions: Progress and Future Challenges*, K. S. Pang, A. D. Rodrigues, and R. M. Peter, Eds., pp. 473–495, Springer, New York, NY, USA, 2010.
  - [26] SciFinder, "Chemical Abstracts Service," 2019, <https://www.cas.org/products/scifinder>.
  - [27] T. Kuge, T. Shibata, and M. S. Willett, "Wood Creosote, the Principal Active Ingredient of Seirogan, an Herbal Antidiarrheal Medicine: A Single-Dose, Dose-Escalation Safety and Pharmacokinetic Study," *Pharmacotherapy*, vol. 23, no. 11, pp. 1391–1400, 2003.
  - [28] N. Ogata, N. Matsushima, and T. Shibata, "Pharmacokinetics of wood creosote: Glucuronic acid and sulfate conjugation of phenolic compounds," *Pharmacology*, vol. 51, no. 3, pp. 195–204, 1995.
  - [29] U.S. Food and Drug Administration, "Substances Added to Food (formerly EAFUS)," Updated 10/10/2018, U.S. Department of Health and Human Services, <https://www.accessdata.fda.gov/scripts/fdccc/?set=FoodSubstances>.
  - [30] U.S. Food and Drug Administration, "GRAS Notices," Updated 12/20/2018, U.S. Department of Health and Human Services, <https://www.accessdata.fda.gov/scripts/fdccc/index.cfm?set=GRASNotices>.
  - [31] M. S. Bobka, "The 21 CFR (Code of Federal Regulations) online database: Food and Drug Administration regulations full-text," *Medical Reference Services Quarterly*, vol. 12, pp. 7–15, 1993.
  - [32] G. Burdock, *Fenaroli's Handbook of Flavor Ingredients*, CRC Press, Boca Raton, FL, USA, 5th edition, 2005.
  - [33] M. Yáñez, N. Fraiz, E. Cano, and F. Orallo, "Inhibitory effects of *cis*- and *trans*-resveratrol on noradrenaline and 5-hydroxytryptamine uptake and on monoamine oxidase activity," *Biochemical and Biophysical Research Communications*, vol. 344, no. 2, pp. 688–695, 2006.
  - [34] Z. Yan, G. W. Caldwell, B. Zhao, and A. B. Reitz, "A high-throughput monoamine oxidase inhibition assay using liquid chromatography with tandem mass spectrometry," *Rapid Communications in Mass Spectrometry*, vol. 18, no. 8, pp. 834–840, 2004.
  - [35] M. Naoi, Y. Nomura, R. Ishiki, H. Suzuki, and T. Nagatsu, "4-(O-Benzylphenoxy)-N-Methylbutylamine (Bifemelane) and Other 4-(O-Benzylphenoxy)-N-Methylalkylamines as New Inhibitors of Type A and B Monoamine Oxidase," *Journal of Neurochemistry*, vol. 50, no. 1, pp. 243–247, 1988.
  - [36] R. A. Copeland, *Evaluation Of Enzyme Inhibitors In Drug Discovery: A Guide For Medicinal Chemists And Pharmacologists*, Wiley-Interscience: City, 2005.
  - [37] P. Anand, A. B. Kunnumakkara, R. A. Newman, and B. B. Aggarwal, "Bioavailability of curcumin: problems and promises," *Molecular Pharmaceutics*, vol. 4, no. 6, pp. 807–818, 2007.
  - [38] A. L. Cheng, C. H. Hsu, J. K. Lin et al., "Phase I clinical trial of curcumin, a chemopreventive agent, in patients with high-risk or pre-malignant lesions," *Anticancer Research*, vol. 21, pp. 2895–2900, 2001.
  - [39] S. P. Hong, A. F. Fuciarelli, J. D. Johnson et al., "Toxicokinetics of Isoeugenol in F344 rats and B6C3F," *Xenobiotica*, vol. 43, no. 11, pp. 1010–1017, 2013.

- [40] L. Almeida, M. Vaz-da-Silva, A. Falcão et al., "Pharmacokinetic and safety profile of trans-resveratrol in a rising multiple-dose study in healthy volunteers," *Molecular Nutrition & Food Research*, vol. 53, no. 1, pp. S7–S15, 2009.
- [41] D. J. Boocock, G. E. S. Faust, K. R. Patel et al., "Phase I dose escalation pharmacokinetic study in healthy volunteers of resveratrol, a potential cancer chemopreventive agent," *Cancer Epidemiology, Biomarkers & Prevention*, vol. 16, no. 6, pp. 1246–1252, 2007.
- [42] H. S. Lin, B. D. Yue, and P. C. Ho, "Determination of pterostilbene in rat plasma by a simple HPLC-UV method and its application in pre-clinical pharmacokinetic study," *Biomedical Chromatography*, vol. 23, no. 12, pp. 1308–1315, 2009.
- [43] I. M. Kapetanovic, M. Muzzio, Z. Huang, T. N. Thompson, and D. L. McCormick, "Pharmacokinetics, oral bioavailability, and metabolic profile of resveratrol and its dimethylether analog, pterostilbene, in rats," *Cancer Chemotherapy and Pharmacology*, vol. 68, no. 3, pp. 593–601, 2011.
- [44] G. Garcea, D. P. Berry, D. J. L. Jones et al., "Consumption of the putative chemopreventive agent curcumin by cancer patients: assessment of curcumin levels in the colorectum and their pharmacodynamic consequences," *Cancer Epidemiology, Biomarkers & Prevention*, vol. 14, no. 1, pp. 120–125, 2005.
- [45] C. Ireson, S. Orr, D. J. L. Jones et al., "Characterization of metabolites of the chemopreventive agent curcumin in human and rat hepatocytes and in the rat in vivo, and evaluation of their ability to inhibit phorbol ester-induced prostaglandin E<sub>2</sub> production," *Cancer Research*, vol. 61, no. 3, pp. 1058–1064, 2001.
- [46] C. R. Ireson, D. J. L. Jones, S. Orr et al., "Metabolism of the cancer chemopreventive agent curcumin in human and rat intestine," *Cancer Epidemiology, Biomarkers & Prevention*, vol. 11, no. 1, pp. 105–111, 2002.
- [47] D. A. Badger, R. L. Smith, J. Bao, R. K. Kuester, and I. G. Sipes, "Disposition and metabolism of isoeugenol in the male Fischer 344 rat," *Food and Chemical Toxicology*, vol. 40, no. 12, pp. 1757–1765, 2002.
- [48] P. Vitaglione, S. Sforza, G. Galaverna et al., "Bioavailability of trans-resveratrol from red wine in humans," *Molecular Nutrition & Food Research*, vol. 49, no. 5, pp. 495–504, 2005.
- [49] V. Aumont, S. Krisa, T. Richard et al., "Regioselective and stereospecific glucuronidation of trans- and cis-resveratrol in human," *Archives of Biochemistry and Biophysics*, vol. 393, no. 2, pp. 281–289, 2001.
- [50] M. Miksits, A. Maier-Salamon, S. Aust et al., "Sulfation of resveratrol in human liver: Evidence of a major role for the sulfotransferases SULT1A1 and SULT1E1," *Xenobiotica*, vol. 35, no. 12, pp. 1101–1119, 2005.
- [51] C. M. Remsberg, J. A. Yáñez, Y. Ohgami, K. R. Vega-Villa, A. M. Rimando, and N. M. Davies, "Pharmacometrics of pterostilbene: preclinical pharmacokinetics and metabolism, anticancer, antiinflammatory, antioxidant and analgesic activity," *Phytotherapy Research*, vol. 22, no. 2, pp. 169–179, 2008.
- [52] A. Burkon and V. Somoza, "Quantification of free and protein-bound trans-resveratrol metabolites and identification of trans-resveratrol-C/O-conjugated diglucuronides—two novel resveratrol metabolites in human plasma," *Molecular Nutrition & Food Research*, vol. 52, no. 5, pp. 549–557, 2008.
- [53] S.-M. Huang, R. Temple, D. C. Throckmorton, and L. J. Lesko, "Drug interaction studies: Study design, data analysis, and implications for dosing and labeling," *Clinical Pharmacology & Therapeutics*, vol. 81, no. 2, pp. 298–304, 2007.
- [54] P. Wang and S. Sang, "Metabolism and pharmacokinetics of resveratrol and pterostilbene," *BioFactors*, vol. 44, no. 1, pp. 16–25, 2018.
- [55] D. M. Riche, C. L. McEwen, K. D. Riche et al., "Analysis of Safety from a Human Clinical Trial with Pterostilbene," *Journal of Toxicology*, vol. 2013, Article ID 463595, 5 pages, 2013.
- [56] R. W. Dellinger, S. R. Santos, M. Morris et al., "Repeat dose NRPT (nicotinamide riboside and pterostilbene) increases NAD<sup>+</sup> levels in humans safely and sustainably: a randomized, double-blind, placebo-controlled study," *npj Aging and Mechanisms of Disease*, vol. 3, no. 17, 2017.
- [57] M. Nishimura and S. Naito, "Tissue-specific mRNA expression profiles of human phase I metabolizing enzymes except for cytochrome P450 and phase II metabolizing enzymes," *Drug Metabolism and Pharmacokinetics*, vol. 21, no. 5, pp. 357–374, 2006.
- [58] C. Carpéné, M. Hasnaoui, B. Balogh et al., "Dietary Phenolic Compounds Interfere with the Fate of Hydrogen Peroxide in Human Adipose Tissue but Do Not Directly Inhibit Primary Amine Oxidase Activity," *Oxidative Medicine and Cellular Longevity*, vol. 2016, Article ID 2427618, 15 pages, 2016.
- [59] T. Matsumoto, O. Suzuki, T. Furuta et al., "A sensitive fluorometric assay for serum monoamine oxidase with kynuramine as substrate," *Clinical Biochemistry*, vol. 18, no. 2, pp. 126–129, 1985.
- [60] T. Herraiz and C. Chaparro, "Human monoamine oxidase enzyme inhibition by coffee and  $\beta$ -carboline norharman and harman isolated from coffee," *Life Sciences*, vol. 78, no. 8, pp. 795–802, 2006.
- [61] C. K. Jones, M. Bubser, A. D. Thompson et al., "The metabotropic glutamate receptor 4-positive allosteric modulator VU0364770 produces efficacy alone and in combination with L-DOPA or an adenosine 2A antagonist in preclinical rodent models of Parkinson's disease," *The Journal of Pharmacology and Experimental Therapeutics*, vol. 340, no. 2, pp. 404–421, 2012.
- [62] L. R. Snyder, J. J. Kirkland, and J. L. Glajch, *Practical HPLC Method Development*, John Wiley & Sons, 2012.



## Research Article

# Effect of Chemotherapeutics and Tocopherols on MCF-7 Breast Adenocarcinoma and KGN Ovarian Carcinoma Cell Lines *In Vitro*

Daniela Figueroa , Mohammad Asaduzzaman, and Fiona Young

Department of Medical Biotechnology, College of Medicine and Public Health, Flinders University, Adelaide, SA, 5052, Australia

Correspondence should be addressed to Daniela Figueroa; [daniela.figueroagonzalez@flinders.edu.au](mailto:daniela.figueroagonzalez@flinders.edu.au)

Received 7 June 2018; Revised 28 November 2018; Accepted 30 December 2018; Published 15 January 2019

Guest Editor: Claudio Tabolacci

Copyright © 2019 Daniela Figueroa et al. This is an open access article distributed under the Creative Commons Attribution License, which permits unrestricted use, distribution, and reproduction in any medium, provided the original work is properly cited.

The combination of doxorubicin and cyclophosphamide commonly used to treat breast cancer can cause premature ovarian failure and infertility.  $\alpha$ -Tocopherol is a potent antioxidant whereas  $\gamma$ -tocopherol causes apoptosis in a variety of cancer models *in vitro* including breast cancer. We hypothesised that the combination of doxorubicin (Dox) and 4-hydroperoxycyclophosphamide (4-Cyc) would be more cytotoxic *in vitro* than each agent alone, and that  $\alpha$ -tocopherol would reduce and  $\gamma$ -tocopherol would augment the cytotoxicity of the combined chemotherapeutics. Human MCF-7 breast cancer and KGN ovarian cells were exposed to Dox, 4-Cyc, combined Dox and 4-Cyc,  $\alpha$ -tocopherol,  $\gamma$ -tocopherol, or a combination of Dox and 4-Cyc with  $\alpha$ -tocopherol or  $\gamma$ -tocopherol. Cell viability was assessed using a crystal violet assay according to four schedules: 24h exposure, 24h exposure + 24h culture in medium, 24h exposure + 48h culture in medium, or 72h continuous exposure. Supernatants from each separate KGN culture experiment ( $n=3$ ) were examined using an estradiol ELISA. Dox was cytotoxic to both MCF-7 and KGN cells, but 4-Cyc only killed MCF-7 cells.  $\gamma$ -Tocopherol significantly decreased MCF-7 but not KGN cell viability. The combined chemotherapeutics and  $\gamma$ -tocopherol were more cytotoxic to MCF-7 than KGN cells, and  $\alpha$ -tocopherol reduced the cytotoxicity of the combined chemotherapeutics towards KGN ovarian cells, but not MCF-7 cells. The addition of both  $\gamma$ -tocopherol and  $\alpha$ -tocopherol to the chemotherapeutic combination of Dox and cyclophosphamide has the potential to increase *in vitro* chemotherapeutic efficacy against breast cancer cells whilst decreasing cytotoxicity towards ovarian granulosa cells.

## 1. Introduction

In Asia, approximately 25% of all breast cancer patients are premenopausal and younger than 35 years old [1]. Worldwide, up to 90% of breast cancer patients can survive for 5 years following diagnosis [2, 3] but it was found that chemotherapy-induced premature ovarian failure and infertility reduce the survivors quality of life [4–10].

Many types of breast cancer are treated with a combination of chemotherapeutic agents such as doxorubicin (adriamycin) and cyclophosphamide [3, 11, 12]. Clinical administration [13, 14] resulted in plasma concentrations of  $1.8 \pm 0.4 \mu\text{M}$  doxorubicin within 24h of infusion [15] and serum concentrations of 4-hydroxycyclophosphamide to be approximately  $0.02 \mu\text{M}$  2–4h after administration [16].

Cyclophosphamide, an alkylating agent, requires hepatic activation to form 4-hydroxycyclophosphamide and

aldophosphamide, which coexist in equilibrium and diffuse freely into cells. Aldophosphamide is metabolised into phosphoramidate mustard [17, 18] which causes intra- and interstrand crosslinking in DNA. This interferes with DNA replication [19] and stimulates apoptosis [17]. A synthetic compound, 4-hydroperoxycyclophosphamide (4-Cyc), is metabolised to 4-hydroxycyclophosphamide *in vitro* [13, 20] and *in vivo* [21, 22]. Aldehyde dehydrogenase oxidises aldophosphamide to an inactive metabolite instead of the active phosphoramidate mustard, and hence cells with different levels of aldehyde dehydrogenase respond differently to 4-Cyc [18].

Doxorubicin (Dox), an anthracycline agent, intercalates at double strand DNA breaks in a topoisomerase-II dependent manner and inhibits DNA replication, synthesis, and mitosis [23, 24]. Dox also induces the production of reactive



oxygen species (ROS) which cause lipid peroxidation and apoptosis [25]. The combined administration of both drugs caused therapeutic synergism in a mouse model [26] that was attributed to these different mechanisms of action: cyclophosphamide crosslinking of DNA strands and Dox prevention of DNA repair [27].

The chemotherapeutic combination of Dox and cyclophosphamide causes premature ovarian failure in premenopausal breast cancer patients [10, 18, 28]. Ovaries contain follicles, a spherical structure consisting of a single oocyte (egg) surrounded by layers of dividing granulosa cells. Granulosa cells produce anti-Müllerian hormone (AMH) which inhibits activation of small, quiescent primordial follicles [29]. It is thought that chemotherapeutics cause granulosa cell death [30, 31], which reduces AMH and results in the activation of primordial follicles [10]. The granulosa cells in the activated follicles proliferate and the follicles grow, but subsequent cycles of Dox and cyclophosphamide therapy cause granulosa cell death and loss of these follicles [32, 33]. Hence chemotherapy to treat breast cancer reduces serum concentrations of AMH, depletes the ovary of its reservoir of quiescent primordial follicles, and advances infertility through premature ovarian failure [10, 34]. The administration of cyclophosphamide to rodents caused a dose-dependent loss of small follicles [32, 35, 36] with DNA double strand breaks in the oocytes [37]. Dox caused apoptosis in mature murine oocytes [38, 39] and the *in vivo* administration of Dox to mice significantly reduced the numbers of follicles, whilst increasing ovarian apoptosis [40, 41]. It is clear that cyclophosphamide alone, or Dox alone, has adverse effects on the follicular granulosa cells of the ovary, but there are no reports describing the cytotoxic effects of the combined regime (which is used to treat breast cancer patients) on ovarian granulosa cells.

Dox-induced ROS damage was significantly lower in mice administered vitamin E [42, 43], and vitamin E decreased the toxicity of Dox without reducing its effectiveness as chemotherapeutic agent [44–49]. Vitamin E consists of eight structurally distinct compounds classified as tocopherols (alpha, beta, gamma, and delta) and tocotrienols (alpha, beta, gamma, and delta) [50–53]. Tocopherols have antioxidant activity against ROS-induced lipid peroxidation [54, 55], and gamma tocopherol ( $\gamma$ Toc) is the prominent form in the human diet [56].

The administration of  $\alpha$ -tocopherol ( $\alpha$ Toc) to 21 breast cancer patients prior to chemotherapy significantly elevated serum concentrations of  $\alpha$ Toc but did not augment efficacy of the chemotherapeutics and did not decrease toxic side-effects, although ovarian function was not assessed in this study [57]. It seems that long-term dietary supplementation with antioxidant vitamins reduces the incidence, but not the severity, of cancer [58, 59]. Klein et al. [60] reported that  $\alpha$ Toc did not have anticancer properties *in vivo*, but when the human breast cancer MCF-7 cell line was used to generate tumours in mice, the dietary administration of either  $\alpha$ Toc or  $\gamma$ Toc reduced tumour growth [53]. Delta and  $\gamma$ Toc increased the levels of proapoptotic proteins, inhibited expression of antiapoptotic proteins *in vivo*, and also had antitumour activity in animal models of colon and prostate

cancer [52].  $\gamma$ Toc inhibited the proliferation of human breast cancer cells *in vitro* [52, 61], delayed the formation of breast cancer tumours in rodent models [52], and induced apoptosis in breast cancer cells via upregulation of DR5 expression [60]. Estrogen metabolism can generate ROS and this may contribute to the pathogenesis of breast cancer [53]. This also suggests that antioxidant tocopherols may have more anticancer activity *in vivo* than in estrogen-free *in vitro* systems.

We hypothesised that the combination of Dox and cyclophosphamide would be more cytotoxic *in vitro* to the human MCF-7 breast cancer cell line and the human ovarian granulosa tumour-derived KGN cell line than each chemotherapeutic agent alone [26]. Both alpha and gamma tocopherol are antioxidants with the potential to reduce chemotherapeutic-induced ROS damage and consequently reduce cytotoxicity, but  $\gamma$ Toc additionally has anticancer activity. We therefore hypothesised that  $\gamma$ Toc, but not  $\alpha$ Toc, would augment the cytotoxic activity of the combined Dox and cyclophosphamide regime *in vitro*.

## 2. Materials and Methods

**2.1. Chemicals and Reagents.** All chemicals and reagents used in this study were obtained from Sigma-Aldrich (Australia), unless specified otherwise.

**2.2. Preparation of Solutions.** Stock solutions of 100  $\mu$ M doxorubicin (Dox) and 1000  $\mu$ M 4-hydroperoxycyclophosphamide (4-Cyc, ThermoFisher Scientific, Victoria, Australia) were prepared in RPMI media and 10% foetal calf serum (FCS, DKSH, Victoria, Australia) for MCF-7 cells or in DMEM/F12 media and 10% FCS for KGN cells. These solutions were kept at 4°C and -20°C, respectively, for a maximum of 3 months and were diluted immediately before use, because these conditions maintain activity and stability [62, 63]. Stock solutions of alpha and gamma tocopherol ( $\alpha$ Toc and  $\gamma$ Toc) were prepared by diluting the compounds in dimethyl sulfoxide (DMSO) to yield solutions of 1000  $\mu$ M. These were stored for a maximum of 3 months at 4°C. Further dilutions in the appropriate cell culture medium were prepared immediately before use, and cells were exposed to 0.8% DMSO. The 0.5% crystal violet stain was prepared in a 50% methanol (99.9% pure). 100% acetic acid was diluted to 33% with demineralised water, to be used as a destaining solution in the crystal violet assay.

**2.3. Cell Culture.** The MCF-7 human epithelial breast adenocarcinoma cell line was obtained from the American Type Culture Collection (ATCC) and maintained in RPMI media, supplemented with 10% FCS and 1% v/v of 10,000 units/mL penicillin + 10mg/mL streptomycin. Media were replaced every 2–3 days and cells were harvested with 0.1% trypsin/EDTA solution and subcultured twice a week. The KGN human granulosa carcinoma cell line [64] was kindly donated by Dr. Theresa Hickey, Research Centre for Reproductive Health, Department of Obstetrics and Gynaecology, University of Adelaide, and maintained in DMEM/F12 supplemented with insulin (5  $\mu$ g/mL), transferrin (5  $\mu$ g/mL), selenium (5ng/mL,

TABLE 1: Concentrations of chemotherapeutics and tocopherols. Dox: doxorubicin, 4-Cyc: 4-hydroperoxycyclophosphamide,  $\alpha$ Toc:  $\alpha$ -tocopherol,  $\gamma$ Toc:  $\gamma$ -tocopherol.

(a)		
Single agents		Concentrations ( $\mu$ M)
Dox		0.5, 10, 25
4-Cyc		0, 0.5, 1, 2.5
$\alpha$ Toc		0, 50, 75, 100
$\gamma$ Toc		0, 50, 75, 100
(b)		
Combined agents		Concentrations ( $\mu$ M)
Dox + 4-Cyc	Low	10 (Dox) + 1 (4-Cyc)
Dox + 4-Cyc	High	25 (Dox) + 2.5 (4-Cyc)
Dox + 4-Cyc + $\alpha$ Toc	Low	10 (Dox) + 1 (4-Cyc) + 75 ( $\alpha$ Toc)
Dox + 4-Cyc + $\alpha$ Toc	High	25 (Dox) + 2.5 (4-Cyc) 75 ( $\alpha$ Toc)
Dox + 4-Cyc + $\gamma$ Toc	Low	10 (Dox) + 1 (4-Cyc) + 75 ( $\gamma$ Toc)
Dox + 4-Cyc + $\gamma$ Toc	High	25 (Dox) + 2.5 (4-Cyc) + 75 ( $\gamma$ Toc)

ITS), 10% FCS, and 1% v/v of 10,000 units/mL penicillin + 10mg/mL streptomycin. Although the KGN cell line was derived from an ovarian granulosa cell carcinoma, it can be used as a model for human ovarian granulosa cell growth, apoptosis, and steroid hormone production [64]. Media were replaced every 2-3 days and both cell lines were subcultured twice a week. Cell culture flasks containing 80% confluent cells in exponential growth phase were used for all experiments.

2.4. *Effect of Doxorubicin, 4-Hydroperoxycyclophosphamide, and  $\alpha$ - and  $\gamma$ -Tocopherol on MCF-7 and KGN Cell Viability.* MCF-7 cells (20,000 cells per well) and KGN cells (25,000 cells per well) were added to 96-well microplates. After a 24h adherence period, supernatants were removed and cells were exposed to 100 $\mu$ L of chemotherapeutics or tocopherols (Table 1). The chemotherapeutic doses selected for this *in vitro* study bracket the clinical, *in vivo* serum concentrations of Dox [15] and 4-hydroxycyclophosphamide [16] (Table 1). Cells were exposed to chemotherapeutics and tocopherols according to four different schedules: 24h exposure, 24h exposure + 24h culture in media, 24h exposure + 48h culture in media, or 72h continuous exposure where reagents in medium + 10% FCS were replenished every 24h. After exposure to chemotherapeutics and tocopherols, media containing reagents were collected and frozen, and the cell viability was assessed by the crystal violet (CV) assay. Each test condition was examined in three replicate wells and each experiment was repeated on 3 separate occasions (n=3) for the two cell types.

2.5. *Crystal Violet (CV) Cell Viability Assay.* Cell culture supernatants were replaced with 50 $\mu$ L of crystal violet stain (0.5%). The cells were stained and fixed for 10min at room temperature. Excess stain was rinsed away with demineralised water, and cells were left to air-dry overnight. 50 $\mu$ L of destaining solution was added for 10min. The optical density was read at 570nm with correction at 630nm [65].

A crystal violet standard plot was produced in each replicate experiment in which MCF-7 cell densities ranged from 0 to 80,000 and KGN cell densities from 0 to 100,000 cells per well in replicates of 6 for each cell density. Absorbance readings were plotted against cell densities with an average linear correlation of  $R^2 = 0.99$  (n=3) replicate experiments for MCF-7 cells and  $R^2 = 0.97$  (n=3) replicate experiments for KGN cells. Numbers of viable cells after exposure to chemotherapeutics and/or tocopherols were determined by comparison with the CV standard curve for the same experimental replicate.

2.6. *Estradiol Enzyme-Linked Immunosorbent Assay (ELISA).* Supernatants from each KGN culture experiment (n=3) were examined in a competitive estradiol ELISA (Cayman Chemical ELISA, Ann Arbor, MI, USA) that uses a mouse anti-rabbit IgG and an acetylcholinesterase estradiol tracer. Detection ranges from 6.6 to 4000 pg/mL, and the intra-assay coefficient of variation (CoV) ranges from 7.8 to 18.8%. For this study, the estradiol standard was diluted in the DMEM/F12 cell culture medium to give concentrations that ranged from 6.6 to 4000 pg/mL. A separate standard plot was constructed for each experimental replicate (n=3) and the lowest  $R^2$  value was 0.99. Concentration of estrogen was determined by comparison with the standard curve. Estrogen/cell concentration was calculated by dividing pg/mL of estrogen for each culture well by the numbers of viable cells in the same well.

3. Statistical Analysis

To examine the dose-dependent effect of chemotherapeutics and/or tocopherols, a one-way ANOVA with Tukey HSD and Bonferroni post hoc was conducted. To examine the effect of the four different exposure schedules on cell viability, an ANOVA was conducted that used the periods of culture as independent factors. Statistical significance was assessed by Tukey HSD and Bonferroni post hoc tests. A one-way ANOVA with Tukey HSD post hoc was conducted

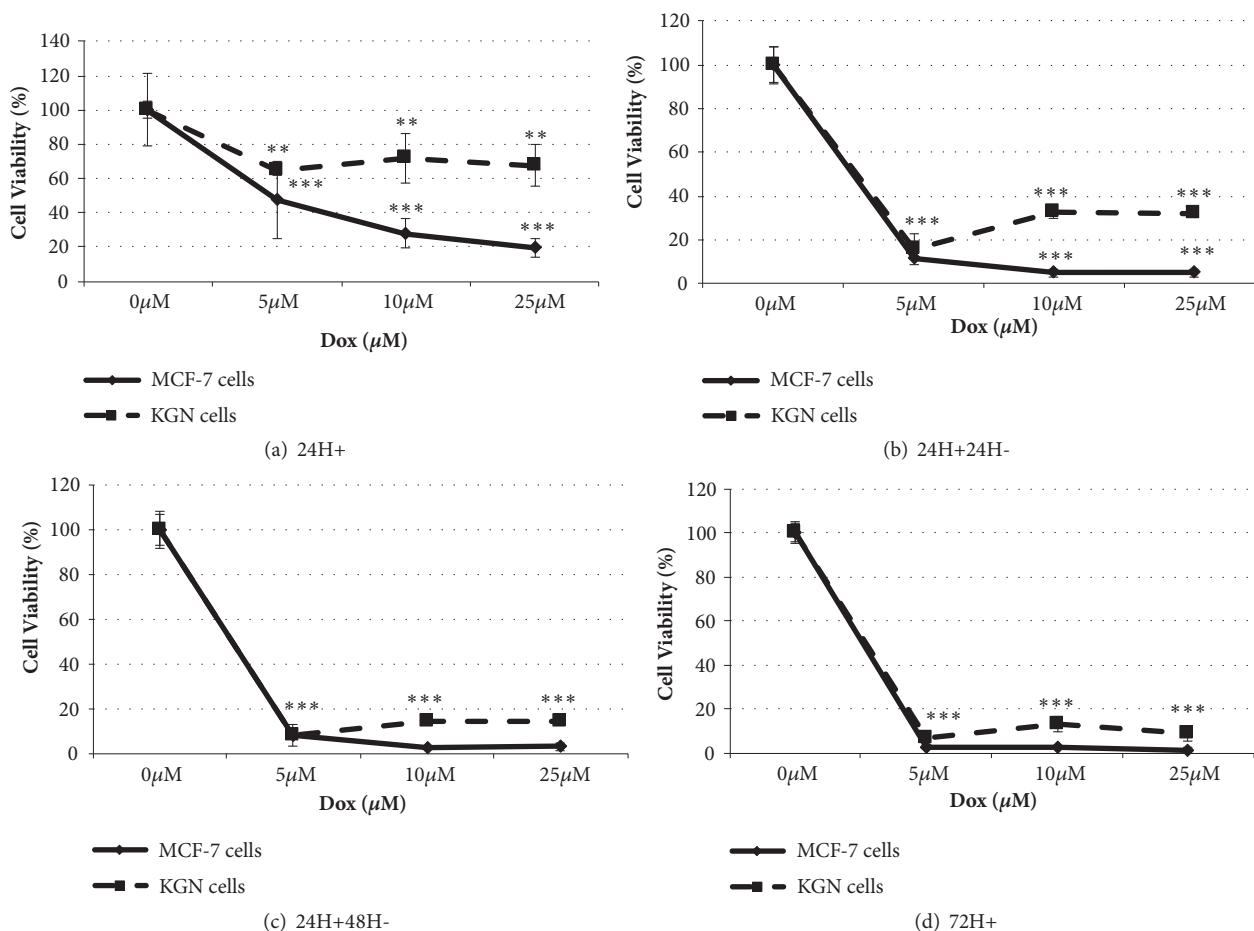


FIGURE 1: Doxorubicin-induced cytotoxicity. MCF-7 and KGN cells were exposed to Dox 0, 5, 10, 25 μM for (a) 24h (24H+), (b) 24h exposure and 24h culture with medium (24H+24H-), (c) 24h exposure and 48h culture with medium (24H+48H-), or (d) 72h continuous exposure (72H+). Complete RPMI (MCF-7) or DMEM/F12 (KGN) without Dox (0 μM) was used as a control. Cell viability was assessed by a crystal violet assay, in which cell number was obtained by comparison with a standard curve and % cell viability was calculated from medium control. Means  $\pm$  SD of 3 independent experiments shown. Data analysed by one-way ANOVA with Tukey's post hoc test. \*  $p \leq 0.05$ ; \*\*  $p \leq 0.01$ , \*\*\*  $p \leq 0.0001$  compared to control.

to examine estrogen production. These statistical analyses were performed using SPSS statistics software (V22.0 IBM, Australia). Statistical significance was set at  $p \leq 0.05$ . All experiments were performed as three independent replicates, and all data expressed as mean  $\pm$  standard deviation.

#### 4. Results

KGN (25,000) and MCF-7 (20,000) cells were added to each well, and after 24h adherence and 24h culture in control conditions, there were  $113,600 \pm 15,600$  KGN cells/well and  $38,100 \pm 4400$  MCF-7 cells/well. After 24h adherence and 72h in culture there were  $119072 \pm 8750$  KGN and  $83383 \pm 13546$  MCF-7 cells per well in control medium.

Doxorubicin killed both MCF-7 and KGN cells (Figure 1). A 24h exposure to 5 μM Dox significantly decreased MCF-7 to  $46 \pm 22\%$  ( $p < 0.0001$ ) and KGN to  $65 \pm 3\%$  ( $p < 0.01$ ) percent of control ( $n=3$ , Figure 1(a)). Cells were exposed to Dox for 24h, then the cells were washed and cultured for an additional 24 or 48h in medium alone (Figures 1(b) and 1(c))

with media replenished at 24h intervals. There was a time-dependent decrease in the numbers of viable cells during the subsequent 48h culture (Figures 1(b) and 1(c)). There were similar numbers of viable cells after 72h continuous exposure to Dox (with media replenishment every 24h, Figure 1(d)) as those after 24h exposure and a further 48h culture (Figure 1(c)).

4-Cyc had no effect on KGN cell viability (Figure 2(a)) and only the longest 72h exposure to the highest concentration (2.5 μM) of 4-Cyc significantly reduced the numbers of viable MCF-7 cells to  $56354 \pm 1657$  cells per well ( $p < 0.05$ ).

Exposure to  $\alpha$ Toc had no significant effect on MCF-7 or KGN cell viability (Figure 3) but  $\gamma$ -Toc was significantly more cytotoxic to MCF-7 cells than to KGN cells (Figure 4). A dose- and time-dependent decrease in MCF-7 cell viability were observed after a 24h or a 72h continuous exposure to  $\gamma$ Toc (Figure 4), but increasing concentrations of  $\gamma$ Toc had no significant effects on KGN cell viability compared to the vehicle control (Figure 4). The percentage of viable KGN cells after 24h exposure to 100 μM  $\gamma$ Toc was  $113 \pm 16\%$  per cells/well,

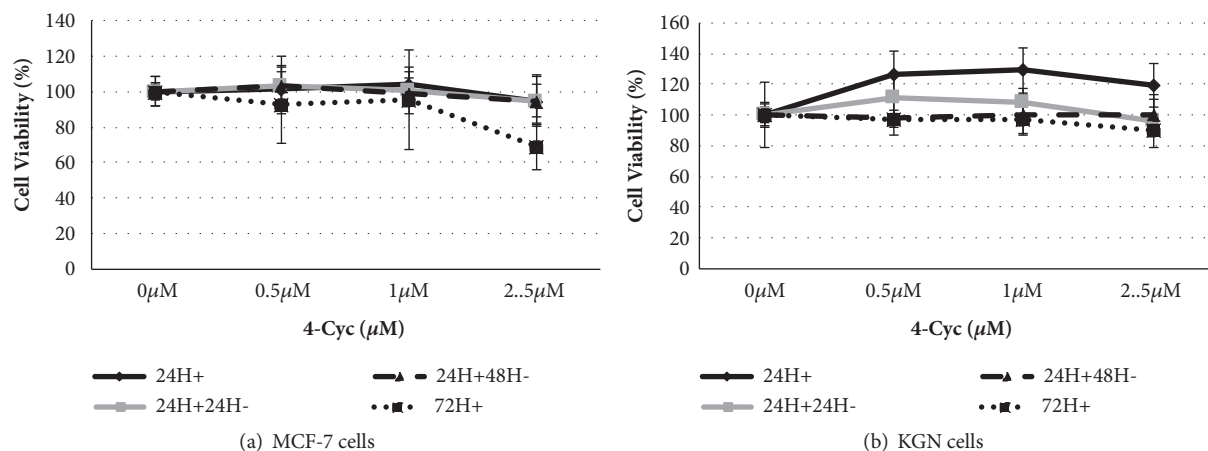


FIGURE 2: Effect of 4-Cyc on cell viability. (a) MCF-7 and (b) KGN cells were exposed to 4-Cyc 0, 0.5, 1, 2.5  $\mu\text{M}$  for 24h exposure (24H+), 24h exposure and 24h culture with media (24H+24H-), 24h exposure and 48h culture with media (24H+48H-), or 72h continuous exposure (72H+). Complete RPMI or DMEM/F12 without 4-Cyc (0  $\mu\text{M}$ ) was used as a control. Cell viability was assessed by a crystal violet assay, in which cell number was obtained by comparison with a standard curve and % cell viability was calculated from medium control. Means  $\pm$  SD of 3 independent experiments shown. Data analysed by one-way ANOVA with Tukey's post hoc test.

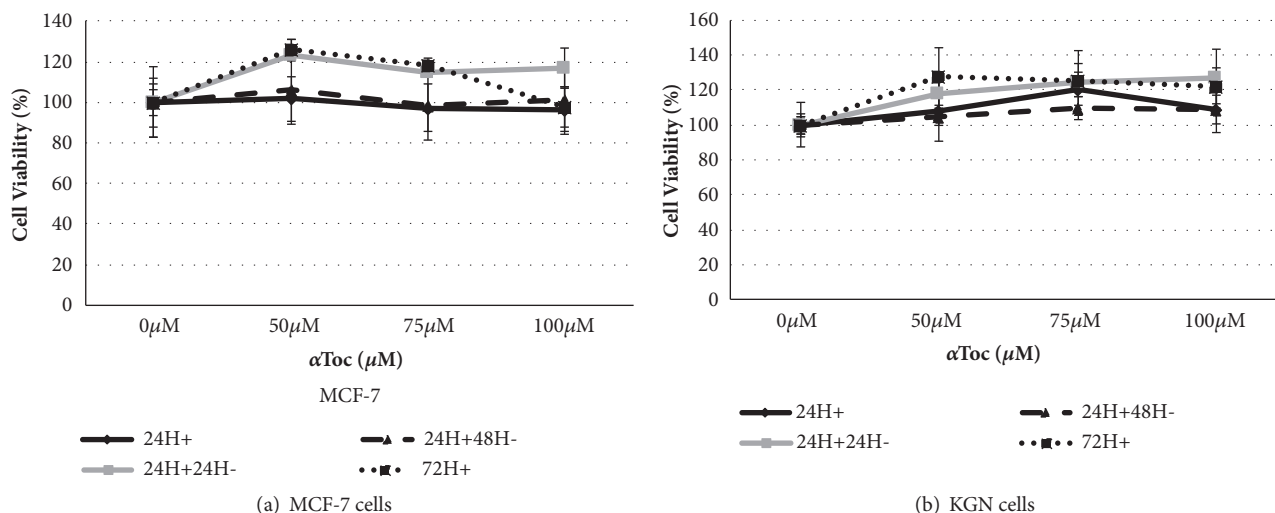


FIGURE 3: Effect of  $\alpha\text{Toc}$  on cell viability. MCF-7 and KGN cells were exposed to  $\alpha\text{Toc}$  0, 50, 75, 100  $\mu\text{M}$  for 24h exposure (24H+), 24h exposure and 24h culture with media (24H+24H-), 24h exposure and 48h culture with media (24H+48H-), or 72h continuous exposure (72H+). Culture media containing 0.8% DMSO was used as a control. Cell viability was assessed by a crystal violet assay, in which cell number was obtained by comparison with a standard curve and % cell viability was calculated from vehicle control. Means  $\pm$  SD of 3 independent experiments shown. Data analysed by one-way ANOVA with Tukey's post hoc test.

similar to the percentage of viable cells after exposure to the same concentration of  $\alpha\text{Toc}$  ( $109 \pm 13\%$  cells/well, Figure 3).

The viability of MCF-7 cells was reduced to  $31 \pm 7\%$  percent of control by a 24h exposure to the low concentration combination of Dox ( $10 \mu\text{M}$ ) and 4-Cyc ( $1 \mu\text{M}$ ), similar to that observed with the same ( $10 \mu\text{M}$ ) concentration of Dox alone (data not shown). When the MCF-7 cells were exposed to the combination of higher concentrations of Dox ( $25 \mu\text{M}$ ) and 4-Cyc ( $2.5 \mu\text{M}$ ) for 24h, the combination also had the same effect as Dox ( $25 \mu\text{M}$ ) alone; viable MCF-7 cells were reduced to  $16 \pm 6\%$  of control (Figure 5(a)). Adding  $\alpha\text{Toc}$  to this combination had no effect on cell viability ( $23 \pm 7\%$  of control), but the addition of  $\gamma\text{Toc}$  ( $75 \mu\text{M}$ ) to the combination

decreased MCF-7 cell viability to  $9 \pm 3\%$  cells per well after 24h exposure, significantly lower than Dox alone ( $p < 0.05$ , Figure 5(a)) or 4-Cyc alone ( $2.5 \mu\text{M}$ , Figure 2(a),  $95 \pm 13\%$  of control), or compared to the combination of Dox and 4-Cyc (Figure 5(a)).

The combination of Dox ( $25 \mu\text{M}$ ) and 4-Cyc ( $2.5 \mu\text{M}$ ) caused significantly more KGN cell death than Dox alone (Figure 5(b)). After 72h exposure to this combination there were  $1763 \pm 1494$  KGN cells per well ( $1.4 \pm 1\%$  of control, Figure 5(b)), significantly lower than those after a 72h exposure to Dox alone ( $10555 \pm 4797$ ,  $p < 0.01$ ), equivalent to  $8.7 \pm 3.4$  percent of control (Figure 5(b)). The addition of  $\alpha\text{Toc}$  to this combination reduced KGN cell death so that it was the similar



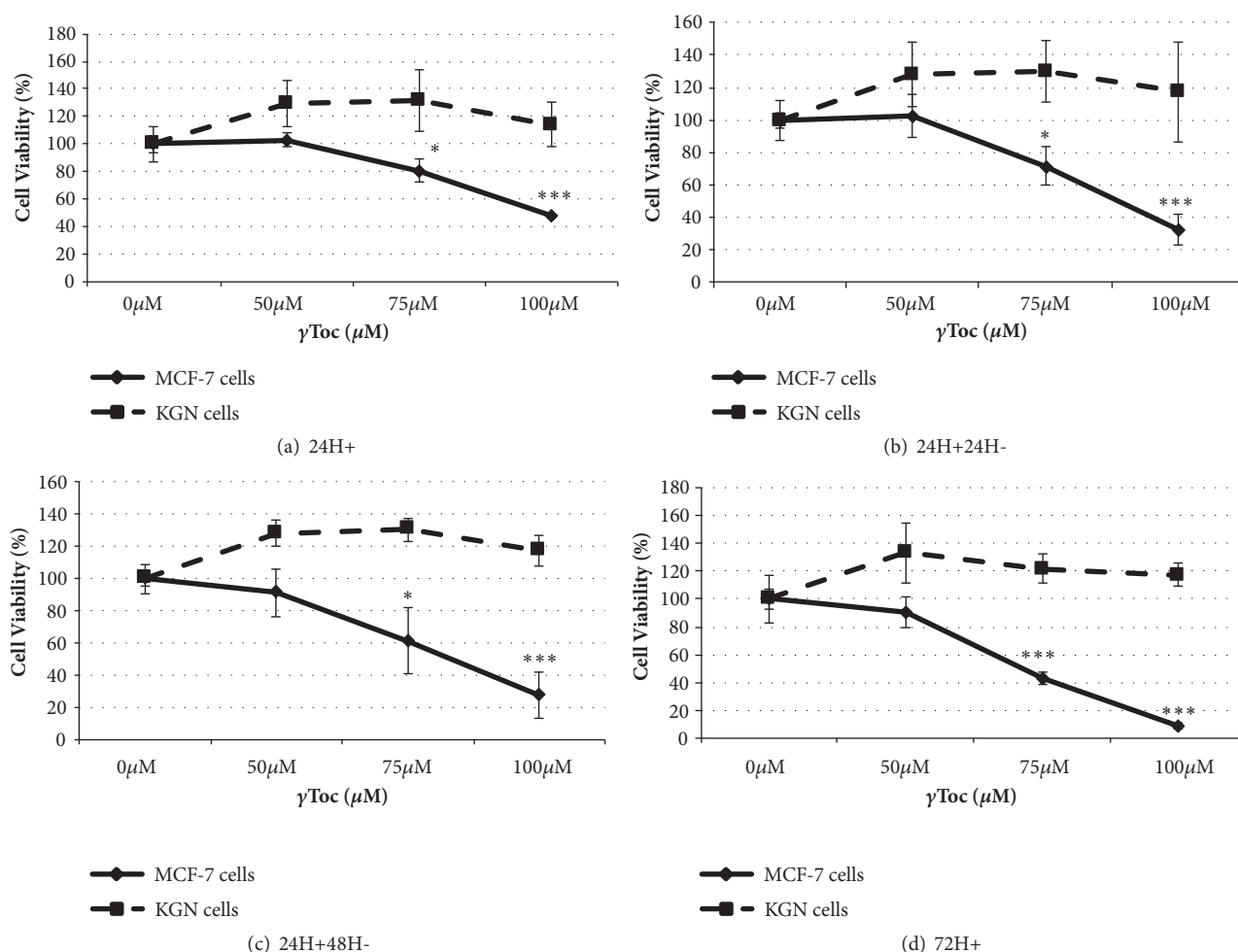


FIGURE 4: Effect of  $\gamma$ Toc on cell viability. MCF-7 and KGN cells were exposed to  $\gamma$ Toc 0, 50, 75, 100  $\mu$ M for 24h exposure (24H+), 24h exposure and 24h culture with media (24H+24H-), 24h exposure and 48h culture with media (24H+48H-), or 72h continuous exposure (72H+). 0.8% DMSO in RPMI or DMEM/F12 was used as a control. Cell viability was assessed by a crystal violet assay, in which cell number was obtained by comparison with a standard curve and % cell viability was calculated from vehicle control. Means  $\pm$  SD of 3 independent experiments shown. Data analysed by one-way ANOVA with Tukey's post hoc test. \* $p \leq 0.05$ ; \*\* $p \leq 0.01$ ; \*\*\* $p \leq 0.0001$  compared to control.

to Dox alone,  $7305 \pm 1823$  cells per well, equivalent to  $7.9 \pm 1$  percent of control (Figure 5(b)). The addition of  $\gamma$ Toc to the combination did not augment the cytotoxicity of Dox and 4-Cyc in KGN cells (Figure 5(a)). Overall,  $\gamma$ Toc combined with Dox and 4-Cyc was more cytotoxic towards MCF-7 than KGN cells in the first 24h of culture (Figure 5).

After 24h culture KGN cells produced  $1.2 \pm 0.1$  pg/cell of estrogen and  $0.8 \pm 0.08$  pg/cell in the last 24h of a 72h culture under control conditions (Figures 6(a) and 6(b)). A 24h exposure to 5  $\mu$ M Dox significantly reduced KGN cell viability (Figure 1(a)) but had no effect on estrogen per cell production, which was  $1.2 \pm 0.03$  pg/cell (Figure 6(a)). However, a continuous 72h exposure to Dox, during which media were replenished every 24h and the number of viable cells decreased (Figure 1(d)), caused a significant increase to  $13 \pm 3$  pg/cell ( $p < 0.01$ , Figure 6(a)) in the last 24h culture period. The same 72h continuous exposure to 2.5  $\mu$ M 4-Cyc had no effect on cell viability (Figure 2(b)) and no effect on

estrogen production, which was  $0.81 \pm 0.08$  pg/cell in the last 24h culture period (Figure 6(b)).

When KGN cells were exposed to tocopherols, the 24h+48h<sup>-</sup> control KGN cells were exposed to almost the same conditions as the 72h+ control cells, 72h *in vitro* with media replenished every 24h. The only difference was that the 72h+ continuously exposed cells were cultured with 0.8% DMSO throughout, whereas the 24h+48h<sup>-</sup> control KGN cells were only cultured in the presence of 0.8% DMSO for the first 24h. The 72h+ exposure to 0.8% DMSO did not significantly affect KGN cell viability (Figure 3(b)), but it stimulated significantly more estrogen production ( $1.32 \pm 0.07$  pg/cell) in the last 24h period of culture than the 24h+48h<sup>-</sup> exposure which supported production of  $0.76 \pm 0.14$  pg/cell ( $p < 0.05$ , Figures 6(c) and 6(d)).

KGN cells in the 0.8% DMSO control produced  $1.1 \pm 0.4$  pg/cell after 24h *in vitro*. The same 24h exposure to  $\alpha$ Toc had no effect on estrogen per cell production (Figure 6(c))

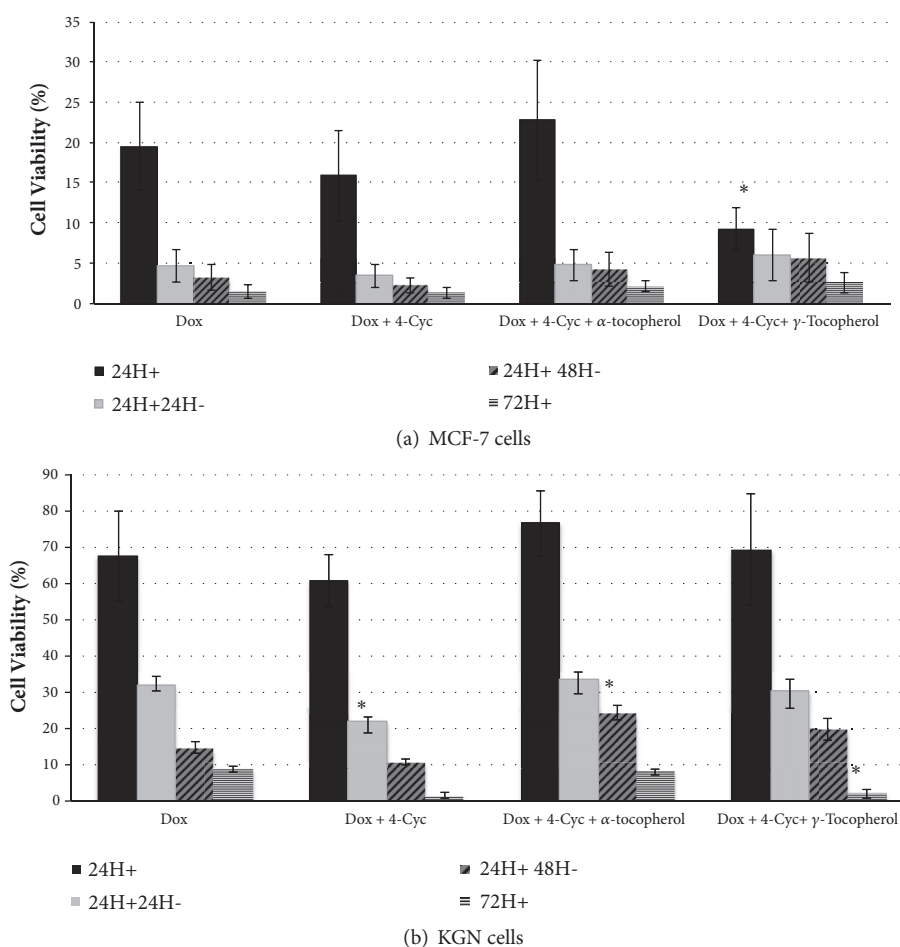


FIGURE 5: Cytotoxicity of combined chemotherapeutic regime. (a) MCF-7 and (b) KGN cells were exposed to a combination of chemotherapeutics (25 $\mu$ M Dox + 2.5 $\mu$ M 4-Cyc), or a combination of chemotherapeutics + 75 $\mu$ M  $\alpha$ Toc, or a combination of chemotherapeutics + 75 $\mu$ M  $\gamma$ Toc for 24h (24H+); 24h exposure and 24h culture with media (24H+24H-); 24h exposure and 48h culture with media (24H+48H-); or 72h continuous exposure (72H+). Cell viability was assessed by a crystal violet assay, in which cell number was obtained by comparison with a standard cue and % cell viability was calculated from vehicle control. Means  $\pm$  SD of 3 independent experiments shown. Data analysed by one-way ANOVA with Tukey's post hoc test. \* $p \leq 0.05$ ; \*\*  $p \leq 0.01$ , \*\*\*  $p \leq 0.0001$  compared to control same concentration of doxorubicin alone (25 $\mu$ M).

whereas 100 $\mu$ M  $\gamma$ Toc stimulated the production of  $1.6 \pm 0.5$  pg/cell (Figure 6(d)). A 72h continuous exposure to either  $\alpha$ Toc or  $\gamma$ Toc significantly reduced estrogen per cell production compared to control medium containing 0.8% DMSO (Figures 6(c) and 6(d)). The highest (100 $\mu$ M) concentration of  $\alpha$ Toc and  $\gamma$ Toc supported higher levels of estrogen synthesis than the lowest (50 $\mu$ M) concentrations of the tocopherols.

A continuous 72h exposure to the combination of Dox and 4-Cyc reduced cell viability (Figure 5(b)) but stimulated the highest recorded estrogen per cell production;  $39 \pm 22$  pg/cell in the last 24h culture period (Figure 7). This was also higher than the estrogen per cell concentration caused by 72h exposure to Dox alone (Figure 6(a)). The addition of  $\alpha$ Toc or  $\gamma$ Toc to the combination of Dox and 4-Cyc had no statistically significant effect on estrogen per cell production (Figure 7), although it was noted that 72h exposure to the combination of Dox and 4-Cyc with 75 $\mu$ M  $\alpha$ Toc resulted in  $13 \pm 2$  pg/cell.

## 5. Discussion

The combination of Dox and cyclophosphamide has been used as a standard chemotherapy option for breast cancer patients since 1975 [3, 66]. Although it is a successful treatment for breast cancer [2], it causes premature ovarian failure and infertility [10]. This study showed for the first time that the combination of Dox and 4-Cyc caused the same cytotoxicity to MCF-7 breast cancer cells *in vitro* as Dox alone, but there were different cytotoxic effects towards the KGN ovarian granulosa cell line; the Dox and 4-Cyc combination was significantly more cytotoxic than Dox alone. Similarly,  $\gamma$ Toc affected the two cell lines differently; it augmented the cytotoxicity of the Dox and 4-Cyc combination towards MCF-7 cells but did not affect cytotoxicity of the combination towards the KGN cells.

Breast cancer patients are administered multiple cycles of Dox and cyclophosphamide [3], and although this can result

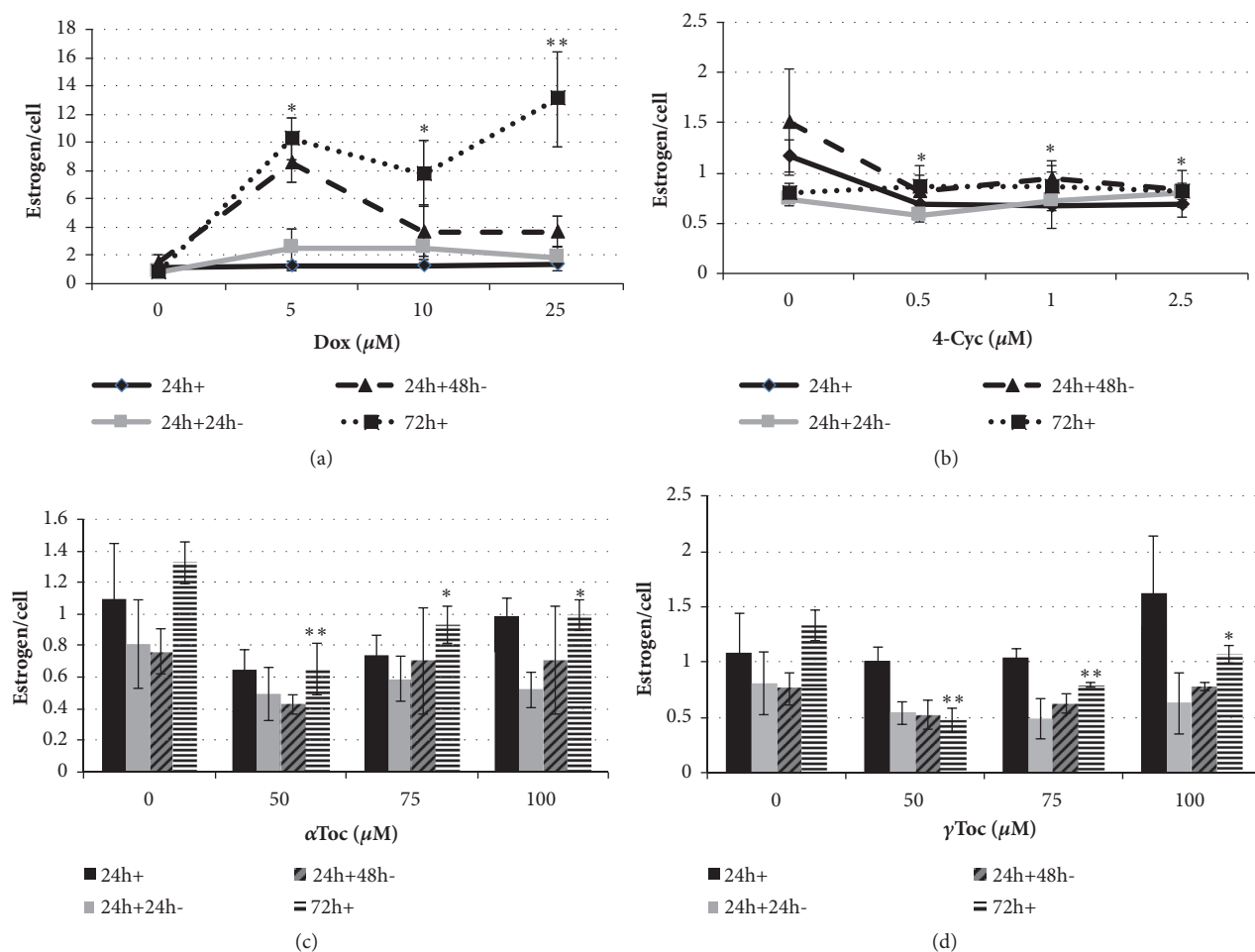


FIGURE 6: Effect of chemotherapeutics and tocopherols on estrogen production. KGN cells were exposed to Dox (0, 5, 10, 25 μM), 4-Cyc (0, 0.5, 1, 2.5 μM), αToc (0, 50, 75, 100 μM) or γToc (0, 50, 75, 100 μM) for 24h exposure (24h+), 24h exposure and 24h culture with fresh DMEM/F-12 complete medium (24h+24h-), 24h exposure and 48h culture with DMEM/F-12 complete medium (24h+48h-), or 72h continuous exposure where reagents in medium + 10% FCS were replenished every 24h (72h+). Estrogen production was assessed in supernatant at the end of each exposure using an estradiol Enzyme-Linked Immunoassay, in which concentration of estrogen (pg/mL) was obtained by comparison with a standard curve, and estrogen/cell concentration was calculated by dividing pg/mL of estrogen by the number of viable cells in the same well. Means ± SD of 3 independent experiments shown. Data analysed by one-way ANOVA with Tukey's post hoc test. \*p ≤ 0.05; \*\* p ≤ 0.01, \*\*\* p ≤ 0.0001 compared to the same exposure control.

in 90% survival for 5y [2], chemotherapeutic-resistant cells are known to cause recurrence of the cancer. The exposure and culture schedules used in this *in vitro* study resulted in only 54% of MCF-7 and 35% of KGN cells being killed in the first 24h of exposure. In our *in vitro* model 'viable' meant cells were adherent to the floor of the culture vessel, whereas nonadherent dead cells were washed away. Cells with damaged DNA may still function and adhere to the culture vessel, and it is likely that DNA damage is only manifested as cell death or loss in the crystal violet assay when the cell attempts to go through mitosis. Since the doubling time for MCF-7 is 29h [67] and was originally reported as being 46h for the KGN cell line [64], we expected to see further cell loss in the 48–72h following removal of the chemotherapeutics, and this proved to be the case; fewer than 10% of the cells were viable after 72h *in vitro*. We conclude that additional time in culture, sufficient for the MCF-7 to undergo mitosis,

would be needed to be able to determine if this surviving ≤10% would give rise to Dox-resistant cells or if these would also die. Further development is required to determine if this *in vitro* system can be used to derive chemoresistant cells.

Resistance or sensitivity to chemotherapeutics *in vivo* is affected by a number of interacting factors including the hepatic clearance of the chemotherapeutics and intracellular levels of metabolising enzymes such as glutathione S-transferase [68] or aldehyde dehydrogenase, which *in vitro* metabolises 4-Cyc to its inactive form [18]. KGN cells were more sensitive to Dox but less sensitive to 4-Cyc than MCF-7 cells. We concluded this because a 72h continuous exposure to 4-Cyc reduced the number of viable MCF-7 cells but had no effect on KGN cells. It is possible that KGN cells express higher levels of aldehyde dehydrogenase than MCF-7 cells and hence metabolised 4-Cyc to its inactive form [62].

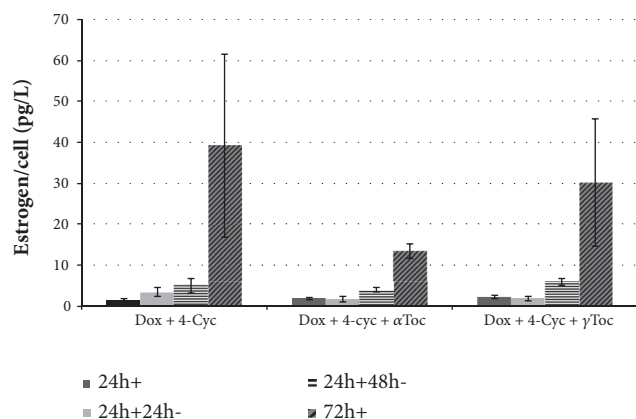


FIGURE 7: Effect of chemotherapeutics and tocopherols on estrogen production. Combined chemotherapeutic regime (25 $\mu$ M Dox with 2.5 $\mu$ M 4-Cyc), combined regime + 75 $\mu$ M  $\alpha$ Toc, or combined regime + 75 $\mu$ M  $\gamma$ Toc for 24h exposure (24h+), 24h exposure and 24h culture with fresh DMEM/F-12 complete medium (24h+24h-), 24h exposure and 48h culture with DMEM/F-12 complete medium (24h+48h-), or 72h continuous exposure where reagents in medium + 10% FCS were replenished every 24h (72h+). Estrogen production was assessed in supernatant at the end of each exposure by using an estradiol ELISA, in which concentration of estrogen (pg/mL) was obtained by comparison with a standard curve, and estrogen/cell concentration was calculated by dividing pg/mL of estrogen by the number of viable cells in the same well. Means  $\pm$  SD of 3 independent experiments shown. Data analysed by one-way ANOVA with Tukey's post hoc test. \* $p \leq 0.05$ ; \*\* $p \leq 0.01$ , \*\*\* $p \leq 0.0001$  compared to control same concentration of doxorubicin alone (10 $\mu$ M).

A relatively short 24h *in vitro* exposure to 2.5 $\mu$ M 4-Cyc had no effect on MCF-7 cells, although this concentration is two orders of magnitude higher than the plasma concentration (0.02 $\mu$ M) of the pharmacologically equivalent 4-hydroxycyclophosphamide 2-24h after administration of cyclophosphamide *in vivo*. The pharmacokinetics of cyclophosphamide has been well characterised [69–71], but much less is known about the kinetics of the metabolites of cyclophosphamide. The hepatic metabolite 4-hydroxycyclophosphamide has a plasma half-life of only a few minutes *in vivo* [71] because it undergoes spontaneous alteration into phosphoramidate mustard [17, 18]. However, phosphoramidate mustard may be ionised at physiological pH with a consequent reduction in cytotoxicity, and the oxidation of 4-hydroxycyclophosphamide can produce inactive metabolites [71]. Therefore, the clinically relevant dose of cyclophosphamide necessary to treat breast cancer patients might differ from the *in vitro* effective concentration.

Dox was more cytotoxic to MCF-7 cells than 4-Cyc. Although 2.5 $\mu$ M 4-Cyc did kill MCF-7 cells after 72h continuous exposure, when the same 2.5 $\mu$ M concentration of 4-Cyc was combined with Dox for 72h, the numbers of surviving cells were comparable to those recorded after exposure to Dox alone, suggesting that in this *in vitro* model 4-Cyc did not potentiate the *in vitro* effect of Dox in the MCF-7 cells. Corbett et al. [26] found that the growth of murine mammary adenocarcinomas *in vivo* was slower after

administration of Dox as a single agent than after cyclophosphamide alone, meaning that the Dox was more cytotoxic than cyclophosphamide *in vivo*. However, the combination of Dox and cyclophosphamide delayed the *in vivo* development of mammary adenocarcinomas for longer than after the administration of each single agent [26] which suggested therapeutic synergism between the two chemotherapeutics *in vivo*.

The combination of Dox and 4-Cyc reduced MCF-7 viability by 85% whereas exposure to 75 $\mu$ M  $\gamma$ Toc for 24h caused a 20% reduction in viable cell numbers. The addition of 75 $\mu$ M  $\gamma$ Toc to Dox and 4-Cyc for 24h reduced cell viability by 91%, less than the amount of cytotoxicity predicted by adding the activity of  $\gamma$ Toc to Dox and 4-Cyc. More studies using lower concentrations of reagents are needed to determine if there are synergistic interactions between  $\gamma$ Toc, Dox, and 4-Cyc.

A long 72h continuous exposure to 2.5 $\mu$ M 4-Cyc had no effect on KGN cell viability nor estrogen per cell production, a 72h exposure to Dox was cytotoxic, and exposure to the combination of Dox and 2.5 $\mu$ M 4-Cyc was more cytotoxic than exposure to Dox alone. This result suggested synergism between Dox and 4-Cyc, but a mechanism for that synergism cannot be deduced from this study. It is possible that 4-Cyc caused DNA crosslinking [18], but this damage was repaired in KGN cells exposed to 4-Cyc alone, whereas the addition of Dox to 4-Cyc prevented the damage from being repaired [27] and hence caused KGN cell death.

In a previous study, KGN cells incubated with androstenedione for 72h synthesised and secreted significant amounts of estrogen into the culture medium [64]. In the present study, a 24h culture in DMEM/F-12 medium containing 10% FCS and ITS resulted in the production of  $1.2 \pm 0.1$  pg/cell, and that rate of production was maintained for 72h when the culture medium was replenished every 24h. Foetal calf serum is rich in fatty acids and cholesterol, the substrate for the whole steroidogenic pathway [72]. Fatty acids, like arachidonic acid, play an essential role in StAR protein expression [73] and the *in vitro* synthesis of steroid hormones such as progesterone and estrogen. In this study, the use of DMEM/F12 with 10% FCS and ITS was enough to support steroidogenesis; androstenedione was not required to support estrogen synthesis and secretion.

Bak et al. [53] reported that estrogen induced the expression of cyclin D1 and c-myc and hence increased mitosis in MCF-7 cells *in vitro*, and that  $\gamma$ Toc, but not  $\alpha$ Toc, inhibited expression of these cell-cycle genes and reduced estrogen-stimulated MCF-7 cell proliferation. The MCF-7 cells in our study were not exposed to estrogen; therefore this was not the cause of the significant cell death caused by  $\gamma$ Toc in our study, suggesting that  $\gamma$ Toc is cytotoxic through another estrogen-independent mechanism of action. Lee et al. [61] showed that  $\gamma$ Toc was cytotoxic to breast cancer cells because it enhanced the transactivation of PPAR $\gamma$  which caused apoptosis and inhibited cell-cycle progression.  $\gamma$ Toc has also shown anti-cancer activity in numerous cancer models, including colon [74], prostate [75], and lung cancer [76] in the absence of estrogen. KGN cells synthesised estrogen, which raises the possibility that there may have been interactions between estrogen and  $\gamma$ Toc, but  $\gamma$ Toc alone did not cause cytotoxicity



towards KGN cells in the presence of 75 to 183 pg/mL estrogen, and neither did  $\gamma$ Toc increase the cytotoxicity of the combination of Dox and 4-Cyc, which suggests that the proapoptotic effect that Bak et al. [53] reported in estrogen-stimulated MCF-7 exposed to  $\gamma$ Toc does not apply to KGN cells.

Exposure to Dox for 72h caused significant KGN cell death and, counterintuitively, also caused a significant increase in estrogen production per KGN cell. This effect has been reported in other steroid hormone-synthesising reproductive cell lines *in vitro*. An extract from a marine snail was significantly cytotoxic to a human Jar choriocarcinoma placental cell line. As the number of viable cells decreased, secreted progesterone increased [77]. Gross et al. [78] also described dying primary-derived granulosa cells increasing progesterone production. It is possible that the cytotoxic mechanisms of action in these cases disrupted membranes and dysregulated steroidogenesis, resulting in massive overproduction of steroid hormones. This confounding effect might be avoided in future by measuring production of another nonsteroid hormone, AMH, which is important for fertility.

Four test reagents ( $\gamma$ Toc,  $\alpha$ Toc, Dox, and 4-Cyc) were each tested at several different concentrations in four exposure schedules. This generated a relatively high number of test conditions which justified the use of human cell lines. Further studies examining ROS generation and cell death will support the selection of a reduced number of test conditions. At this point MCF-7 cells could be replaced with heterogeneous populations of primary-derived breast cancer cells from different tumour types, and the KGNS could be replaced with 3D primary-derived ovarian follicle culture [79] to better model the effects of chemotherapeutics with or without tocopherols on breast cancer and the ovary.

In summary, 4-Cyc was active because a 72h continuous exposure killed MCF-7 cells and reduced KGN estrogen per cell production. Both  $\gamma$ Toc and Dox (applied as single agents) significantly reduced the numbers of viable MCF-7 and KGN cells within 24h of exposure, whilst  $\alpha$ Toc reduced the cytotoxic effects of the Dox and 4-Cyc combination in KGN cells. The 4-Cyc concentration, despite two orders of magnitude higher than effective clinical plasma concentrations, may have been too low for this *in vitro* model; hence we do not exclude the possibility of therapeutic synergism of the Dox and 4-Cyc combination in MCF-7 cells too. Our hypotheses were partially supported: although the Dox and 4-Cyc combination was not more cytotoxic than Dox alone towards MCF-7 cells, the combination displayed therapeutic synergism towards the ovarian KGN granulosa cells.  $\gamma$ Toc, but not  $\alpha$ Toc, augmented the cytotoxic activity of Dox and 4-Cyc in the MCF-7 cells, but not the KGN cells. This study supports further work to explore the potential of  $\gamma$ Toc to increase the chemotherapeutic efficacy of Dox and 4-Cyc against breast cancer cells *in vitro*.

## Abbreviations

Dox: Doxorubicin

4-Cyc: 4-Hydroperoxycyclophosphamide

ROS: Reactive oxygen species

AMH: Anti-Müllerian hormone

$\alpha$ Toc: Alpha tocopherol

$\gamma$ Toc: Gamma tocopherol.

## Data Availability

The raw data for cell viability assay and ELISA, used to support the findings of this study, may be released upon reasonable request to the corresponding author, who can be contacted at daniela.figueroa@flinders.edu.au. The graphs used to support the findings of this study are included within the article.

## Conflicts of Interest

The authors declare that they have no conflicts of interest.

## Authors' Contributions

Daniela Figueroa and Mohammad Asaduzzaman contributed equally to this work.

## References

- [1] V. Tiong, A. M. Rozita, N. A. Taib, C. H. Yip, and C. H. Ng, "Incidence of chemotherapy-induced ovarian failure in premenopausal women undergoing chemotherapy for breast cancer," *World Journal of Surgery*, vol. 38, no. 9, pp. 2288–2296, 2014.
- [2] J. Ferlay, I. Soerjomataram, R. Dikshit et al., "Cancer incidence and mortality worldwide: sources, methods and major patterns in GLOBOCAN 2012," *International Journal of Cancer*, vol. 136, no. 5, 2015.
- [3] D. A. Yardley, E. R. Arrowsmith, B. R. Daniel et al., "TITAN: phase III study of doxorubicin/cyclophosphamide followed by ixabepilone or paclitaxel in early-stage triple-negative breast cancer," *Breast Cancer Research and Treatment*, vol. 164, no. 3, pp. 649–658, 2017.
- [4] V. Mor, M. Malin, and S. Allen, "Age differences in the psychosocial problems encountered by breast cancer patients," *Journal of the National Cancer Institute Monographs*, no. 16, pp. 191–197, 1994.
- [5] P. A. Ganz, J. H. Rowland, K. Desmond, B. E. Meyerowitz, and G. E. Wyatt, "Life after breast cancer: understanding women's health-related quality of life and sexual functioning," *Journal of Clinical Oncology*, vol. 16, no. 2, pp. 501–514, 1998.
- [6] P. A. Ganz, G. A. Greendale, L. Petersen, B. Kahn, and J. E. Bower, "Breast cancer in younger women: Reproductive and late health effects of treatment," *Journal of Clinical Oncology*, vol. 21, no. 22, pp. 4184–4193, 2003.
- [7] P. A. Ganz, "Breast cancer, menopause, and long-term survivorship: Critical issues for the 21st century," *American Journal of Medicine*, vol. 118, no. 12, pp. 136–141, 2005.
- [8] D. H. Baucom, L. S. Porter, J. S. Kirby, T. M. Gremore, and F. J. Keefe, "Psychosocial issues confronting young women with breast cancer," *Breast Disease*, vol. 23, pp. 103–113, 2005.
- [9] A. B. Mariotto, J. H. Rowland, L. A. G. Ries, S. Scoppa, and E. J. Feuer, "Multiple cancer prevalence: A growing challenge

- in long-term survivorship," *Cancer Epidemiology, Biomarkers & Prevention*, vol. 16, no. 3, pp. 566–571, 2007.
- [10] S. Morgan, R. A. Anderson, C. Gourley, W. H. Wallace, and N. Spears, "How do chemotherapeutic agents damage the ovary?" *Human Reproduction Update*, vol. 18, no. 5, pp. 525–535, 2012.
  - [11] J.-M. Nabholz, C. Falkson, D. Campos et al., "Docetaxel and doxorubicin compared with doxorubicin and cyclophosphamide as first-line chemotherapy for metastatic breast cancer: results of a randomized, multicenter, phase III trial," *Journal of Clinical Oncology*, vol. 21, no. 6, pp. 968–975, 2003.
  - [12] J. Bray, J. Sludden, M. J. Griffin et al., "Influence of pharmacogenetics on response and toxicity in breast cancer patients treated with doxorubicin and cyclophosphamide," *British Journal of Cancer*, vol. 102, no. 6, pp. 1003–1009, 2010.
  - [13] E. Claire Dees, S. O'Reilly, S. N. Goodman et al., "A prospective pharmacologic evaluation of age-related toxicity of adjuvant chemotherapy in women with breast cancer," *Cancer Investigation*, vol. 18, no. 6, pp. 521–529, 2000.
  - [14] S. E. Jones, M. A. Savin, F. A. Holmes et al., "Phase III trial comparing doxorubicin plus cyclophosphamide with docetaxel plus cyclophosphamide as adjuvant therapy for operable breast cancer," *Journal of Clinical Oncology*, vol. 24, no. 34, pp. 5381–5387, 2006.
  - [15] C. E. Swenson, L. E. Bolcsak, G. Batist et al., "Pharmacokinetics of doxorubicin administered i.v. as Myocet (TLC D-99; liposome-encapsulated doxorubicin citrate) compared with conventional doxorubicin when given in combination with cyclophosphamide in patients with metastatic breast cancer," *Anti-Cancer Drugs*, vol. 14, no. 3, pp. 239–246, 2003.
  - [16] R. F. Struck, D. S. Alberts, K. Horne, J. G. Phillips, Y.-M. Peng, and D. J. Roe, "Plasma Pharmacokinetics of Cyclophosphamide and Its Cytotoxic Metabolites after Intravenous versus Oral Administration in a Randomized, Crossover Trial," *Cancer Research*, vol. 47, no. 10, pp. 2723–2726, 1987.
  - [17] A. V. Boddy and S. M. Yule, "Metabolism and pharmacokinetics of oxazaphosphorines," *Clinical Pharmacokinetics*, vol. 38, no. 4, pp. 291–304, 2000.
  - [18] A. Emadi, R. J. Jones, and R. A. Brodsky, "Cyclophosphamide and cancer: golden anniversary," *Nature Reviews Clinical Oncology*, vol. 6, no. 11, pp. 638–647, 2009.
  - [19] Q. Dong, D. Barskt, M. E. Colvin et al., "A structural basis for a phosphoramidate mustard-induced DNA interstrand cross-link at 5'-d(GAC)," *Proceedings of the National Academy of Sciences of the United States of America*, vol. 92, no. 26, pp. 12170–12174, 1995.
  - [20] H. Ozer, J. W. Cowens, M. Colvin, A. Nussbaum-Blumenson, and D. Sheedy, "In vitro effects of 4-hydroperoxycyclophosphamide on human immunoregulatory T subset function. I. Selective effects on lymphocyte function in T-B cell collaboration," *The Journal of Experimental Medicine*, vol. 155, no. 1, pp. 276–290, 1982.
  - [21] B. A. Teicher, S. A. Holden, D. A. Goff, J. E. Wright, O. Tretyakov, and L. J. Ayash, "Antitumor efficacy and pharmacokinetic analysis of 4-hydroperoxycyclophosphamide in comparison with cyclophosphamide  $\pm$  hepatic enzyme effectors," *Cancer Chemotherapy and Pharmacology*, vol. 38, no. 6, pp. 553–560, 1996.
  - [22] A. Yuksel, G. Bildik, F. Senbabaoglu et al., "The magnitude of gonadotoxicity of chemotherapy drugs on ovarian follicles and granulosa cells varies depending upon the category of the drugs and the type of granulosa cells," *Human Reproduction*, vol. 30, no. 12, pp. 2926–2935, 2015.
  - [23] K. M. Tewey, T. C. Rowe, L. Yang, B. D. Halligan, and L. F. Liu, "Adriamycin-induced DNA damage mediated by mammalian DNA topoisomerase II," *Science*, vol. 226, no. 4673, pp. 466–468, 1984.
  - [24] C. F. Thorn, C. Oshiro, S. Marsh et al., "Doxorubicin pathways: pharmacodynamics and adverse effects," *Pharmacogenetics and Genomics*, vol. 21, no. 7, pp. 440–446, 2011.
  - [25] D. A. Gewirtz, "A critical evaluation of the mechanisms of action proposed for the antitumor effects of the anthracycline antibiotics adriamycin and daunorubicin," *Biochemical Pharmacology*, vol. 57, no. 7, pp. 727–741, 1999.
  - [26] T. H. Corbett, D. P. Griswold, J. G. Mayo, W. R. Laster, and F. M. Schabel, "Cyclophosphamide-Adriamycin Combination Chemotherapy of Transplantable Murine Tumors," *Cancer Research*, vol. 35, no. 6, pp. 1568–1573, 1975.
  - [27] J. S. Tobias, L. M. Parker, M. H. Tattersall, and E. Frei, "Adriamycin/cyclophosphamide and adriamycin/melphalan in advanced L1210 leukaemia," *British Journal of Cancer*, vol. 32, no. 2, pp. 199–207, 1975.
  - [28] D. Meirrow, H. Biederman, R. A. Anderson, and W. H. B. Wallace, "Toxicity of chemotherapy and radiation on female reproduction," *Clinical Obstetrics and Gynecology*, vol. 53, no. 4, pp. 727–739, 2010.
  - [29] A. L. L. Durlinger, P. Kramer, B. Karels et al., "Control of primordial follicle recruitment by anti-mullerian hormone in the mouse ovary," *Endocrinology*, vol. 140, no. 12, pp. 5789–5796, 1999.
  - [30] S. M. Downs and A. M. Utecht, "Metabolism of radiolabeled glucose by mouse oocytes and oocyte-cumulus cell complexes," *Biology of Reproduction*, vol. 60, no. 6, pp. 1446–1452, 1999.
  - [31] X.-J. Zhao, Y.-H. Huang, Y.-C. Yu, and X.-Y. Xin, "GnRH antagonist cetrorelix inhibits mitochondria-dependent apoptosis triggered by chemotherapy in granulosa cells of rats," *Gynecologic Oncology*, vol. 118, no. 1, pp. 69–75, 2010.
  - [32] O. Oktem and K. Oktay, "Quantitative assessment of the impact of chemotherapy on ovarian follicle reserve and stromal function," *Cancer*, vol. 110, no. 10, pp. 2222–2229, 2007.
  - [33] R. Soleimani, E. Heytens, Z. Darzynkiewicz, and K. Oktay, "Mechanisms of chemotherapy-induced human ovarian aging: double strand DNA breaks and microvascular compromise," *AGING*, vol. 3, no. 8, pp. 782–793, 2011.
  - [34] M. S. Yucebilgin, M. C. Terek, A. Ozsaran et al., "Effect of chemotherapy on primordial follicular reserve of rat: An animal model of premature ovarian failure and infertility," *Australian and New Zealand Journal of Obstetrics and Gynaecology*, vol. 44, no. 1, pp. 6–9, 2004.
  - [35] D. Meirrow, H. Lewis, D. Nugent, and M. Epstein, "Subclinical depletion of primordial follicular reserve in mice treated with cyclophosphamide: Clinical importance and proposed accurate investigative tool," *Human Reproduction*, vol. 14, no. 7, pp. 1903–1907, 1999.
  - [36] P. Desmeules and P. J. Devine, "Characterizing the ovotoxicity of cyclophosphamide metabolites on cultured mouse ovaries," *Toxicological Sciences*, vol. 90, no. 2, pp. 500–509, 2006.
  - [37] S. K. Petrillo, P. Desmeules, T.-Q. Truong, and P. J. Devine, "Detection of DNA damage in oocytes of small ovarian follicles following phosphoramidate mustard exposures of cultured rodent ovaries in vitro," *Toxicology and Applied Pharmacology*, vol. 253, no. 2, pp. 94–102, 2011.
  - [38] G. I. Perez, C. M. Knudson, L. Leykin, S. J. Korsmeyer, and J. L. Tilly, "Apoptosis-associated signaling pathways are required for

- chemotherapy- mediated female germ cell destruction," *Nature Medicine*, vol. 3, no. 11, pp. 1228–1232, 1997.
- [39] A. Jurisicova, H.-J. Lee, S. G. D'Estaing, J. Tilly, and G. I. Perez, "Molecular requirements for doxorubicin-mediated death in murine oocytes," *Cell Death & Differentiation*, vol. 13, no. 9, pp. 1466–1474, 2006.
- [40] I. Ben-Aharon, H. Bar-Joseph, G. Tzarfaty et al., "Doxorubicin-induced ovarian toxicity," *Reproductive Biology and Endocrinology*, vol. 8, article no. 20, 2010.
- [41] E. C. Roti Roti, S. K. Leisman, D. H. Abbott, and S. M. Salih, "Acute doxorubicin insult in the mouse ovary is cell- and follicle-type dependent," *PLoS ONE*, vol. 7, no. 8, Article ID e42293, 2012.
- [42] Y. Nagata, J. Takata, A. Yoshiharu Karube, and Y. Matsushima, "Effects of a water-soluble prodrug of vitamin E on doxorubicin-induced toxicity in mice," *Biological & Pharmaceutical Bulletin*, vol. 22, no. 7, pp. 698–702, 1999.
- [43] M. I. Thabrew, N. Samarawickrema, L. G. Chandrasena, and S. Jayasekera, "Effect of oral supplementation with vitamin E on the oxido-reductive status of red blood cells in normal mice and mice subject to oxidative stress by chronic administration of Adriamycin," *Annals of Clinical Biochemistry*, vol. 36, no. 2, pp. 216–220, 1999.
- [44] C. E. Myers, W. McGuire, and R. Young, "Adriamycin: amelioration of toxicity by  $\alpha$  tocopherol," *Cancer Treatment Reports*, vol. 60, no. 7, pp. 961–962, 1976.
- [45] W. Krivit, "Adriamycin cardiotoxicity amelioration by  $\alpha$ -tocopherol," *Journal of Pediatric Hematology/Oncology*, vol. 1, no. 2, pp. 151–153, 1979.
- [46] W. C. Lubawy, J. Whaley, and L. H. Hurley, "Coenzyme Q10 or  $\alpha$ -tocopherol reduce the acute toxicity of anthramycin in mice," *Research Communications in Chemical Pathology and Pharmacology*, vol. 24, no. 2, pp. 401–404, 1979.
- [47] E. H. Herman and V. J. Ferrans, "Influence of vitamin E and ICRF-187 on chronic doxorubicin cardiotoxicity in miniature swine," *Laboratory Investigation*, vol. 49, no. 1, pp. 69–77, 1983.
- [48] J. Milei, A. Boveris, S. Llesuy et al., "Amelioration of adriamycin-induced cardiotoxicity in rabbits by prenylamine and vitamins A and E," *American Heart Journal*, vol. 111, no. 1, pp. 95–102, 1986.
- [49] A. Geetha, R. Sankar, T. Marar, and C. S. Shyamala Devi, " $\alpha$ -Tocopherol reduces doxorubicin-induced toxicity in rats - histological and biochemical evidences," *Indian Journal of Physiology and Pharmacology*, vol. 34, no. 2, pp. 94–100, 1990.
- [50] R. Brigelius-Flohé, F. J. Kelly, J. T. Salonen, J. Neuzil, J. Zingg, and A. Azzi, "The European perspective on vitamin E: current knowledge and future research," *American Journal of Clinical Nutrition*, vol. 76, no. 4, pp. 703–716, 2002.
- [51] G. Lu, H. Xiao, G.-X. Li et al., "A  $\gamma$ -tocopherol-rich mixture of tocopherols inhibits chemically induced lung tumorigenesis in A/J mice and xenograft tumor growth," *Carcinogenesis*, vol. 31, no. 4, pp. 687–694, 2010.
- [52] A. K. Smolarek and N. Suh, "Chemopreventive activity of vitamin e in breast cancer: A focus on  $\gamma$ - and  $\delta$ -tocopherol," *Nutrients*, vol. 3, no. 11, pp. 962–986, 2011.
- [53] M. J. Bak, S. Das Gupta, J. Wahler et al., "Inhibitory Effects of  $\gamma$ - and  $\delta$ -Tocopherols on Estrogen-Stimulated Breast Cancer," *Cancer Prevention Research*, vol. 10, no. 3, pp. 188–197, 2017.
- [54] M. G. Traber, "Vitamin E regulatory mechanisms," *Annual Review of Nutrition*, vol. 27, no. 1, pp. 347–362, 2007.
- [55] M. G. Traber and J. Atkinson, "Vitamin E, antioxidant and nothing more," *Free Radical Biology & Medicine*, vol. 43, no. 1, pp. 4–15, 2007.
- [56] R. B.-F. Brigelius-Flohé and M. G. Traber, "Vitamin E: function and metabolism," *The FASEB Journal*, vol. 13, no. 10, pp. 1145–1155, 1999.
- [57] S. S. Legha, R. S. Benjamin, B. Mackay et al., "Reduction of doxorubicin cardiotoxicity by prolonged continuous intravenous infusion," *Annals of Internal Medicine*, vol. 96, no. 2, pp. 133–139, 1982.
- [58] N. E. Day and S. A. Blngham, "Re: Nutrition intervention trials in linxian, China: Supplementation with specific vitamin/mineral combinations, cancer incidence, and disease-specific mortality in the general population," *Journal of the National Cancer Institute*, vol. 86, no. 21, pp. 1645–1646, 1994.
- [59] O. P. Heinonen, D. Albanes, J. Virtamo et al., "Prostate cancer and supplementation with  $\alpha$ -tocopherol and  $\beta$ -carotene: incidence and mortality in a controlled trial," *Journal of the National Cancer Institute*, vol. 90, no. 6, pp. 440–446, 1998.
- [60] E. A. Klein, I. M. Thompson Jr., C. M. Tangen et al., "Vitamin E and the risk of prostate cancer: the selenium and vitamin E cancer prevention trial (SELECT)," *Journal of the American Medical Association*, vol. 306, no. 14, pp. 1549–1556, 2011.
- [61] J. L. Hong, J. Ju, S. Paul et al., "Mixed tocopherols prevent mammary tumorigenesis by inhibiting estrogen action and activating PPAR- $\gamma$ ," *Clinical Cancer Research*, vol. 15, no. 12, pp. 4242–4249, 2009.
- [62] D. M. Hoffman, D. D. Grossano, L. Damin, and T. M. Woodcock, "Stability of refrigerated and frozen solutions of doxorubicin hydrochloride," *American Journal of Health-System Pharmacy*, vol. 36, no. 11, pp. 1536–1538, 1979.
- [63] E. Ulukaya, F. Ozdikicioglu, A. Y. Oral, and M. Demirci, "The MTT assay yields a relatively lower result of growth inhibition than the ATP assay depending on the chemotherapeutic drugs tested," *Toxicology in Vitro*, vol. 22, no. 1, pp. 232–239, 2008.
- [64] Y. Nishi, T. Yanase, Y.-M. Mu et al., "Establishment and characterization of a steroidogenic human granulosa-like tumor cell line, KGN, that expresses functional follicle-stimulating hormone receptor," *Endocrinology*, vol. 142, no. 1, pp. 437–445, 2001.
- [65] K. J. Reid, K. Lang, S. Frosio, A. J. Humpage, and F. M. Young, "Undifferentiated murine embryonic stem cells used to model the effects of the blue-green algal toxin cylindrospermopsin on preimplantation embryonic cell proliferation," *Toxicon*, vol. 106, article no. 5192, pp. 79–88, 2015.
- [66] T. Younis, D. Rayson, and C. Skedgel, "The cost-utility of adjuvant chemotherapy using docetaxel and cyclophosphamide compared with doxorubicin and cyclophosphamide in breast cancer," *Current Oncology*, vol. 18, no. 6, pp. e288–e296, 2011.
- [67] R. L. Sutherland, R. E. Hall, and I. W. Taylor, "Cell Proliferation Kinetics of MCF-7 Human Mammary Carcinoma Cells in Culture and Effects of Tamoxifen on Exponentially Growing and Plateau-Phase Cells," *Cancer Research*, vol. 43, no. 9, pp. 3998–4006, 1983.
- [68] A. T. McGown and B. W. Fox, "A proposed mechanism of resistance to cyclophosphamide and phosphoramidate mustard in a Yoshida cell line in vitro," *Cancer Chemotherapy and Pharmacology*, vol. 17, no. 3, pp. 223–226, 1986.
- [69] L. B. Grochow and M. Colvin, "Clinical Pharmacokinetics of Cyclophosphamide," *Clinical Pharmacokinetics*, vol. 4, no. 5, pp. 380–394, 1979.

- [70] M. J. Moore, "Clinical Pharmacokinetics of Cyclophosphamide," *Clinical Pharmacokinetics*, vol. 20, no. 3, pp. 194–208, 1991.
- [71] M. E. De Jonge, A. D. R. Huitema, S. Rodenhuis, and J. H. Beijnen, "Clinical pharmacokinetics of cyclophosphamide," *Clinical Pharmacokinetics*, vol. 44, no. 11, pp. 1135–1164, 2005.
- [72] W. L. Miller and H. S. Bose, "Early steps in steroidogenesis: Intracellular cholesterol trafficking," *Journal of Lipid Research*, vol. 52, no. 12, pp. 2111–2135, 2011.
- [73] X. Wang, L. P. Walsh, A. J. Reinhart, and D. M. Stocco, "The role of arachidonic acid in steroidogenesis and steroidogenic acute regulatory (StAR) gene and protein expression," *The Journal of Biological Chemistry*, vol. 275, no. 26, pp. 20204–20209, 2000.
- [74] S. E. Campbell, W. L. Stone, S. Lee et al., "Comparative effects of RRR- $\alpha$ - and RRR- $\gamma$ -tocopherol on proliferation and apoptosis in human colon cancer cell lines," *BMC Cancer*, vol. 6, no. 1, article no 13, 2006.
- [75] Q. Jiang, J. Wong, and B. N. Ames, " $\gamma$ -Tocopherol Induces Apoptosis in Androgen-Responsive LNCaP Prostate Cancer Cells via Caspase-Dependent and Independent Mechanisms," *Annals of the New York Academy of Sciences*, vol. 1031, no. 1, pp. 399–400, 2004.
- [76] G. Li, M. Lee, A. B. Liu et al., " $\delta$ -Tocopherol Is More Active than  $\alpha$ - or  $\gamma$ -Tocopherol in Inhibiting Lung Tumorigenesis In Vivo," *Cancer Prevention Research*, vol. 4, no. 3, pp. 404–413, 2011.
- [77] V. Edwards, E. Markovic, J. Matisons, and F. Young, "Development of an in vitro reproductive screening assay for novel pharmaceutical compounds," *Biotechnology and Applied Biochemistry*, vol. 51, no. 2, pp. 63–71, 2008.
- [78] S. A. Gross, J. M. Newton, and J. Hughes F.M., "Decreased intracellular potassium levels underlie increased progesterone synthesis during ovarian follicular atresia," *Biology of Reproduction*, vol. 64, no. 6, pp. 1755–1760, 2001.
- [79] M. Asaduzzaman, D. F. Gonzalez, and F. Young, "Ovarian Follicle Disaggregation to Assess Granulosa Cell Viability," *International Journal of Clinical Medicine*, vol. 09, no. 05, pp. 377–399, 2018.



## Research Article

# The Effects of Korea Red Ginseng on Inflammatory Cytokines and Apoptosis in Rat Model with Chronic Nonbacterial Prostatitis

Sang Wook Kang <sup>1</sup>, Je-Hoon Park,<sup>2</sup> Hosik Seok,<sup>1</sup> Hae Jeong Park,<sup>1</sup> Joo-Ho Chung <sup>1</sup>,  
Chang-Ju Kim,<sup>1,3</sup> Young Ock Kim,<sup>4</sup> Young Rok Han,<sup>5</sup> DongWhan Hong,<sup>5</sup>  
Young Sik Kim,<sup>6</sup> and Su Kang Kim <sup>7</sup>

<sup>1</sup>Kohwang Medical Research Institute, School of Medicine, Kyung Hee University, Seoul, Republic of Korea

<sup>2</sup>Department of Surgery, International St. Mary's Hospital, College of Medicine, Catholic Kwandong University, Incheon, Republic of Korea

<sup>3</sup>Department of Physiology, College of Medicine, Kyung Hee University, Seoul, Republic of Korea

<sup>4</sup>Development of Bio-Environmental Chemistry, College of Agriculture and Life Sciences, Chungnam National University, Daejeon, Republic of Korea

<sup>5</sup>Department of Physical Medicine & Rehabilitation, Graduate School, Kyung Hee University, Seoul, Republic of Korea

<sup>6</sup>Management Research Institute, Kyung Hee University, Seoul, Republic of Korea

<sup>7</sup>Department of Biomedical Laboratory Science, Catholic Kwandong University, Gangneung, Republic of Korea

Correspondence should be addressed to Su Kang Kim; [skkim7@khu.ac.kr](mailto:skkim7@khu.ac.kr)

Received 10 July 2018; Revised 24 October 2018; Accepted 27 December 2018; Published 14 January 2019

Guest Editor: Francesco Facchiano

Copyright © 2019 Sang Wook Kang et al. This is an open access article distributed under the Creative Commons Attribution License, which permits unrestricted use, distribution, and reproduction in any medium, provided the original work is properly cited.

Chronic prostatitis typically occurs in aging men, and its symptoms include frequent and painful urination. In recent study, several studies have shown that Korean red ginseng (KRG) can be used in the prevention and treatment of various diseases. The objective of this study is to investigate whether KRG can play a role in repressing the development of chronic nonbacterial prostatitis (CNP) in male Wistar rats. To induce CNP, rats were castrated and beta-estradiol (0.25 mg/kg) was subcutaneously (s.c.) injected daily. 7-week-old male Wistar rats were divided into 5 groups (the normal group, CNP group, positive group, and KRG group (0.25g/kg) and another KRG (0.50g/kg) group. After 4 weeks, all rats were sacrificed and their prostate and serum were analyzed. Compared to the positive group, the KRG groups (0.25g/kg and 0.50g/kg) showed similar protective properties on CNP based on the histopathologic morphology of the prostate and the inflammation cytokines in the prostate tissue. Also, results of the immunohistochemistry staining showed that expression levels of vascular endothelial growth factor A (VEGFA), interleukin 6 (IL6), interleukin 1 beta (IL-1 $\beta$ ), tumor necrosis factor (TNF- $\alpha$ ), and cytochrome c oxidase subunit II (COX2) were also decreased in KRG group (0.25g/kg) and KRG group (0.50g/kg). These results suggested that KRG inhibited the development of CNP and might a useful herbal treatment or functional food for CNP.

## 1. Introduction

Chronic prostatitis is a common disease in aged men [1]. The disease causes a diverse range and degree of symptoms, including voiding irritation, pelvic region discomfort, and sexual dysfunctions [2–4].

Chronic prostatitis is classified as acute, chronic, bacterial, and nonbacterial prostatitis. More than 90% of all

prostatitis patients are affected by chronic nonbacterial prostatitis (CNP) [5]. Despite the high incidence of CNP, the cause of the disease has not been verified, and it is known to be difficult to treat. It is a morbid illness that causes mental dissatisfaction and negatively impacts an individual's daily quality of life.

The disease is characterized by chronic pelvic pain and possibly voiding symptoms with no evidence of urinary tract

infection [4]. Although it is not an infection, it may cause pathologic changes including dysmorphic prostatic glandular ducts, gland atrophy, interstitial fibrosis, and infiltrations of polymorphonuclear neutrophils, lymphocytes, and monocytes. CNP is an inflammatory disease in which inflammatory cells are found in microscopic examinations of the prostate gland with our any detection of a causative organism [1].

Inflammation is a biologic defense reaction against a stimulant substance. Various cytokines are involved in inflammatory reactions. Expressions of proinflammatory cytokine such as tumor necrosis factor- $\alpha$  (TNF- $\alpha$ ), vascular endothelial growth factor A (VEGFA), interleukin 6 (IL6), and interleukin 1 beta (IL-1 $\beta$ ) are induced in the macrophage inflammatory response by external stimulation. Nitric oxide (NO) is produced by stimulating the expression of inducible nitric oxide synthase (iNOS) and cyclooxygenase-2 (COX-2) [6].

Korea red ginseng (KRG) has been used safely in human for a long time. KRG has been traditionally used in Korea and East Asian countries for treatment of diverse diseases [7]. It is a heat-modified product of the Ginseng Radix (*Panax ginseng*) root. KRG was originally developed for the sole purpose of improving the long-term preservation of the root, but it was found to contain the active elements of ginseng saponins or ginsenosides, of which the original root does not [8]. These elements are known to increase the efficacy of ginseng. The KRG known so far has been reported to be effective as an antioxidant, antibacterial agent, anti-inflammatory action agent, blood circulation enhancer, cancer preventing agent, and infectious defense and immunity enhance [9–13]. KRG is also commonly used for male rejuvenation [14, 15] and, to treat urinary discomfort in the elderly, as it is known in Korea as a herb that improves vigor and stamina [16, 17].

The aim of the present study is to investigate the effects of orally administrated KRG in CNP rat model based on the histopathologic morphology of the prostate and inflammation cytokines in the prostate tissue.

## 2. Methods

**2.1. Preparation of the KRG.** The material of KRG was provided from Korea Ginseng Corp (KGC, Korea).

**2.2. Animals.** The animals used in this study were 7-week-old male Wistar rats (RaonBio Inc., Korea) with an average body weight of 250 $\pm$ 10g. The animal room was maintained at 22 $\pm$ 2°C with 40–70% relative humidity. The room lighting consisted of 12h/12h of light and dark. All experiments were carried out according to the protocols approved by the Animal Care Committee of the Animal Center at Kyung Hee University in accordance with guidelines from the Korean National Health Institute of Health Animal Facility (KHUASP-16-019).

**2.3. Induction of CNP and Treatments.** After the orchietomy, rats that were injected with beta estradiol (0.25 mg/kg, Sigma-Aldrich Co., St. Louis, MO, USA) (20 mg/kg) for 4 weeks were shown to have prostatitis. The rats were then divided into five

groups ( $n = 5$ ): (A) a normal control group; (B) a CNP group: CNP that induced 17 $\beta$ -estradiol group through subcutaneous injection; (C) a positive group: CNP that induced 17 $\beta$ -estradiol group through subcutaneous injection + testosterone, injected subcutaneously; (D) a KRG (0.25g/kg) group: CNP that induced 17 $\beta$ -estradiol group through subcutaneous injection + KRG (0.25g/kg); (E) and another KRG (0.50g/kg) group: CNP that induced 17 $\beta$ -estradiol group through subcutaneous injection + KRG (0.50g/kg), administered orally. The experiment was performed with the drug administration and subcutaneous injection for 4 weeks. After 4 weeks, drug administration and subcutaneous injection were stopped.

**2.4. Blood Collection and Biochemical Analysis.** To collect blood, rats were anesthetized and blood was drawn from their hearts into the serum separate tube (SST) tubes. The serum was separated from the blood by centrifuge at 3,000 rpm. Serum was gathered immediately and stored at -70°C. The level of glutamic oxaloacetic transaminase (GOT), glutamic pyruvic transaminase (GPT), blood urea nitrogen (BUN), creatinine, and  $\gamma$ -GTP in serum were tested by Greenlab (Seoul, Korea).

**2.5. Tunnel Assay in Prostate Tissue.** The prostate tissues in each group were dewaxed with xylenes and rehydrated through an ethanol series. Tunnel reactions were performed with the In Situ Cell Death Detection POD Kit (Roche USA) according to the manufacturer's protocol. The prostate tissues after the Tunnel reactions were dehydrated, mounted, and examined under a microscope.

**2.6. Nitric Oxide (NO) Assay in Serum.** NO accumulation was used as an indicator of NO production. Its level in serum was determined using the Griess reagent (Promega, USA, Griess Reagent system). Briefly, serum (50 $\mu$ l) was mixed with the same volume of Griess reagent (1% sulfanilamide and 0.1% N-(1-naphthyl)-ethylenediamine dihydrochloride in 5% phosphoric acid) for 10 min, and absorbance was measured at 520 nm.

**2.7. RNA Extraction and Reverse Transcriptase-Polymerase Chain Reaction (RT-PCR).** Total RNA was isolated from the prostate tissues of each mouse using Trizol (Invitrogen, CA, USA), according to the manufacturer's instructions. An aliquot of total RNA was reverse transcribed using MMuLV reverse transcriptase and Taq DNA polymerase (Promega, Madison, WI, USA), respectively. Primers for VEGFA, IL6, IL-1 $\beta$ , TNF- $\alpha$ , and COX2 were designed in reverse transcription (RT-PCR) according to previous studies [18, 19].

**2.8. Immunohistochemistry (IHC).** Immunohistochemistry (IHC) staining was performed for prostate tissue section at thickness of 10 $\mu$ m. First, paraffin was removed from slides through a deparaffinization process. To avoid endogenous peroxidase activity, slides were incubated with 3% of H<sub>2</sub>O<sub>2</sub> solution in methanol at room temperature for 15 minutes and then washed with PBS for 3 times (5 minutes each). Slides were prerestrained with normal goat or rabbit serum

TABLE 1: Analysis of GOT, GPT, BUN, creatinine, and  $\gamma$ -GTP level in serum level.

Group	GOT (IU/L)	GPT (IU/L)	BUN (mg/dl)	Creatinine (mg/dl)	$\gamma$ -GTP (U/L)
Normal	77.0 $\pm$ 9.2	28.0 $\pm$ 10.1	18.0 $\pm$ 1.0	0.49 $\pm$ 0.07	<3
CNP	75.6 $\pm$ 3.3	41.5 $\pm$ 9.6	19.3 $\pm$ 2.5	0.55 $\pm$ 0.04	<3
Positive	76.0 $\pm$ 10.3	26.2 $\pm$ 4.9	16.7 $\pm$ 1.5	0.59 $\pm$ 0.02	<3
KRG (0.25g/kg)	100.1 $\pm$ 13.1 <sup>#</sup>	34.7 $\pm$ 16.8	22.0 $\pm$ 1.0	0.50 $\pm$ 0.04	<3
KRG (0.50g/kg)	91.1 $\pm$ 13.7	38.6 $\pm$ 20.1	16.7 $\pm$ 3.2	0.48 $\pm$ 0.07	<3

Data are presented as mean  $\pm$  SE ( $n=6$ ).

<sup>#</sup>P < 0.05, compared with the CNP group.

for 1hr. In primary antibody reaction stage, slides were incubated carefully with anti-VEGFA, anti-TNF-alpha, anti-IL1 $\beta$ , anti-IL-6, and anti-COX2 (Santa Cruz Biotechnology Inc., Santa Cruz, CA, USA) in a 1:500 dilution for a night at 4°C and washed with PBS for 3 times, 5 minutes each. For second antibody reaction, the slides were incubated with biotinylated secondary antibodies (1:1000) at room temperature for 1h and washed with PBS three times, five minutes each. Finally, diaminobenzidine tetrahydrochloride substrate (DAB) staining with streptavidin-HRP was performed to visualize antigen-antibody reaction. For each section, three different random fields were examined at least  $\times 100$  magnification.

**2.9. Statistical Analyses.** All values were presented as the mean $\pm$ standard error (SE). Significant differences among the groups were statistically analyzed by using the one-way analysis of variances (ANOVA), followed by a nonparametric post-Tukey test. All  $p$  values were two-tailed. A  $p$  value of less than 0.05 was considered statistically significant. All statistical analyses were performed using SPSS 22.0 for Windows.

### 3. Results

**3.1. Effect of KRG on Weight Change.** The changes in body weight are shown in Figure 1. Final body weight was measured at 30 days after treatment. The final body weights in each group (CNP, positive, and KRG groups) had decreased compared to that in the normal group. However, differences among CNP, positive, and KRG groups were not significant ( $p>0.05$ ).

**3.2. Effect of KRG on Levels of GOT, GPT, BUN, Creatinine, and  $\gamma$ -GTP in Serum.** Serum levels of GOT, GPT, BUN, creatinine, and  $\gamma$ -GTP are shown in Table 1. Levels of GOT in the normal, CNP, positive, KRG (0.25g/kg), and KRG (0.50g/kg) groups were 77.0 $\pm$ 9.2, 75.6 $\pm$ 3.3, 76.0 $\pm$ 10.3, 100.1 $\pm$ 13.1, and 91.1 $\pm$ 13.7 IU/L, respectively. Levels of GPT in the normal, CNP, positive, KRG (0.25g/kg), and KRG (0.50g/kg) groups were 28.0 $\pm$ 10.1, 41.5 $\pm$ 9.6, 26.2 $\pm$ 4.9, 34.7 $\pm$ 16.8, and 38.6 $\pm$ 20.1 IU/L, respectively. Levels of BUN in the normal, CNP, positive, KRG (0.25g/kg), and KRG (0.50g/kg) groups were 18.0 $\pm$ 1.0, 19.3 $\pm$ 2.5, 16.7 $\pm$ 1.5, 22.0 $\pm$ 1.0, and 16.7 $\pm$ 3.2 mg/dl,

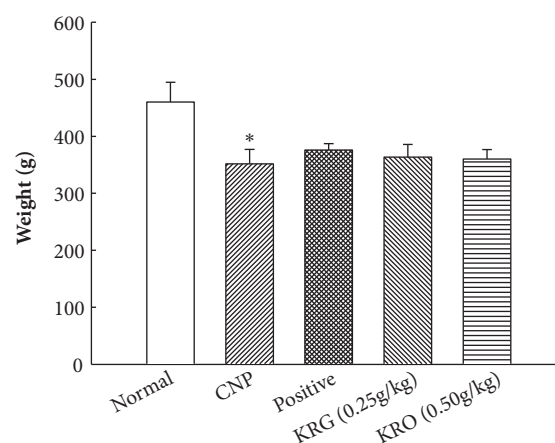
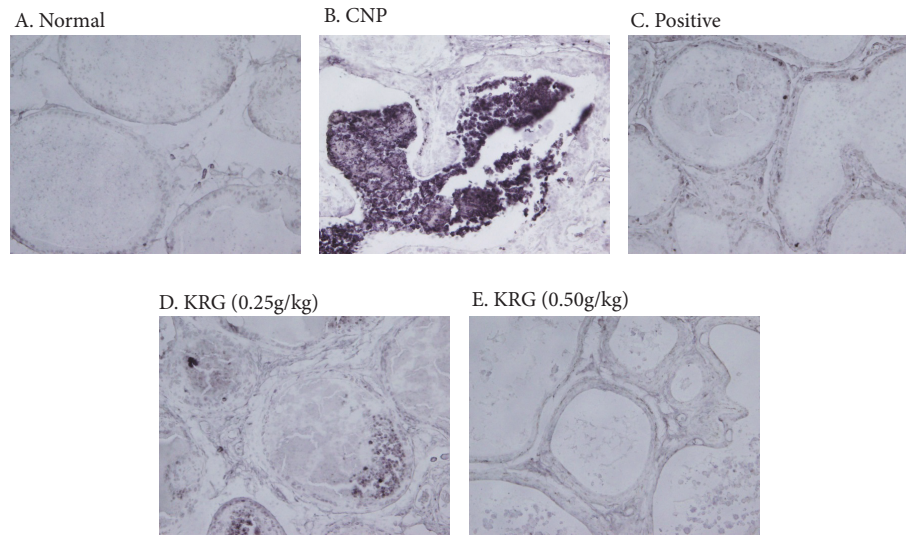


FIGURE 1: Effects of Korea red ginseng (KRG) on body weight in each group. Normal, normal group; CNP, chronic nonbacterial prostatitis group; Positive, estradiol induced CNP with testosterone; KRG (0.25g/kg), beta-estradiol induced CNP with KRG (0.25g/kg); KRG (0.5g/kg), estradiol induced CNP with KRG (0.5g/kg). \* P < 0.05, compared with the normal group and # P < 0.05, compared with the CNP group.

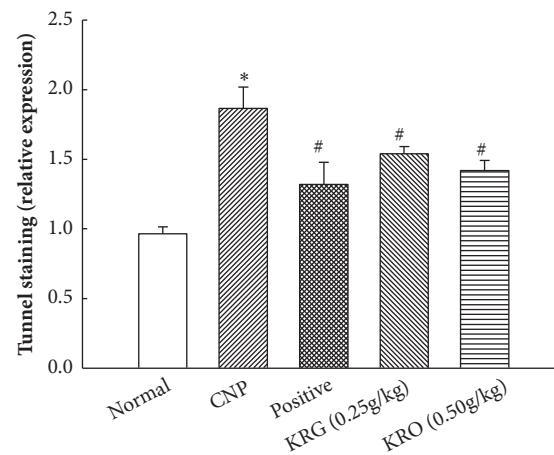
respectively. Levels of creatinine in the normal, CNP, positive, KRG (0.25g/kg), and KRG (0.50g/kg) groups were 0.49 $\pm$ 0.07, 0.55 $\pm$ 0.04, 0.59 $\pm$ 0.02, 0.50 $\pm$ 0.04, and 0.48 $\pm$ 0.07 mg/dl, respectively. And levels of  $\gamma$ -GTP were less than 3 IU/L in all groups. Differences among groups were not statistically significant ( $p>0.05$ ). These results indicated that KRG did not have toxicity in the animal model.

**3.3. Effects of KRG on Apoptosis in Prostate Tissue Using Tunnel Assay.** As shown in Figures 2(a) and 2(b), apoptosis of the prostate tissue among the groups was examined. The apoptosis of prostate tissue had significantly increased in the CNP group. The apoptosis of prostate tissue in the positive and KRG (0.25g/kg and 0.50g/kg) groups had significantly decreased compared to that in the CNP group ( $p<0.05$ ).

**3.4. Effects of KRG on Nitric Oxide Level in Serum.** Serum levels of NO in the normal, CNP, positive, KRG (0.25g/kg), and KRG (0.50g/kg) groups were 19.89 $\pm$ 9.7, 98.6 $\pm$ 4.7, 42.2 $\pm$ 18.5, 70.0 $\pm$ 16.1, and 48.9 $\pm$ 16.4  $\mu$ M (Figure 3). The level of NO in the CNP group was significantly higher compared to that in the



(a)



(b)

**FIGURE 2: Tunnel staining in prostate tissue in each group (x100).** Normal, normal group; CNP, chronic nonbacterial prostatitis group; Positive, estradiol induced CNP with testosterone; KRG (0.25g/kg), beta-estradiol induced CNP with KRG (0.25g/kg); KRG (0.5g/kg), estradiol induced CNP with KRG (0.5g/kg). \*  $P < 0.05$ , compared with the normal group and #  $P < 0.05$ , compared with the CNP group.

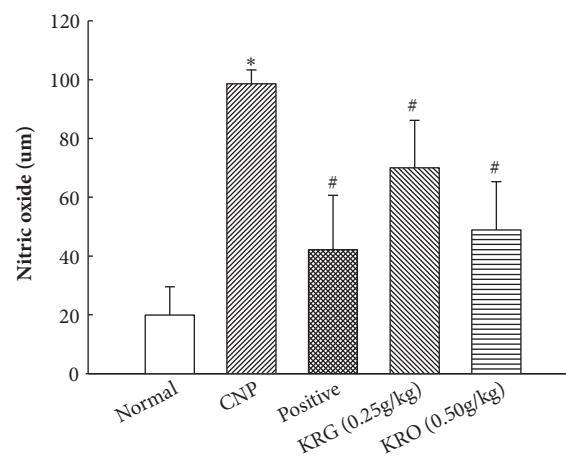


**FIGURE 3: Analysis of nitric oxide (NO) in serum in each group.** Normal, normal group; CNP, chronic nonbacterial prostatitis group; Positive, estradiol induced CNP with testosterone; KRG (0.25g/kg), beta-estradiol induced CNP with KRG (0.25g/kg); KRG (0.5g/kg), estradiol induced CNP with KRG (0.5g/kg). \*  $P < 0.05$ , compared with the normal group and #  $P < 0.05$ , compared with the CNP group.



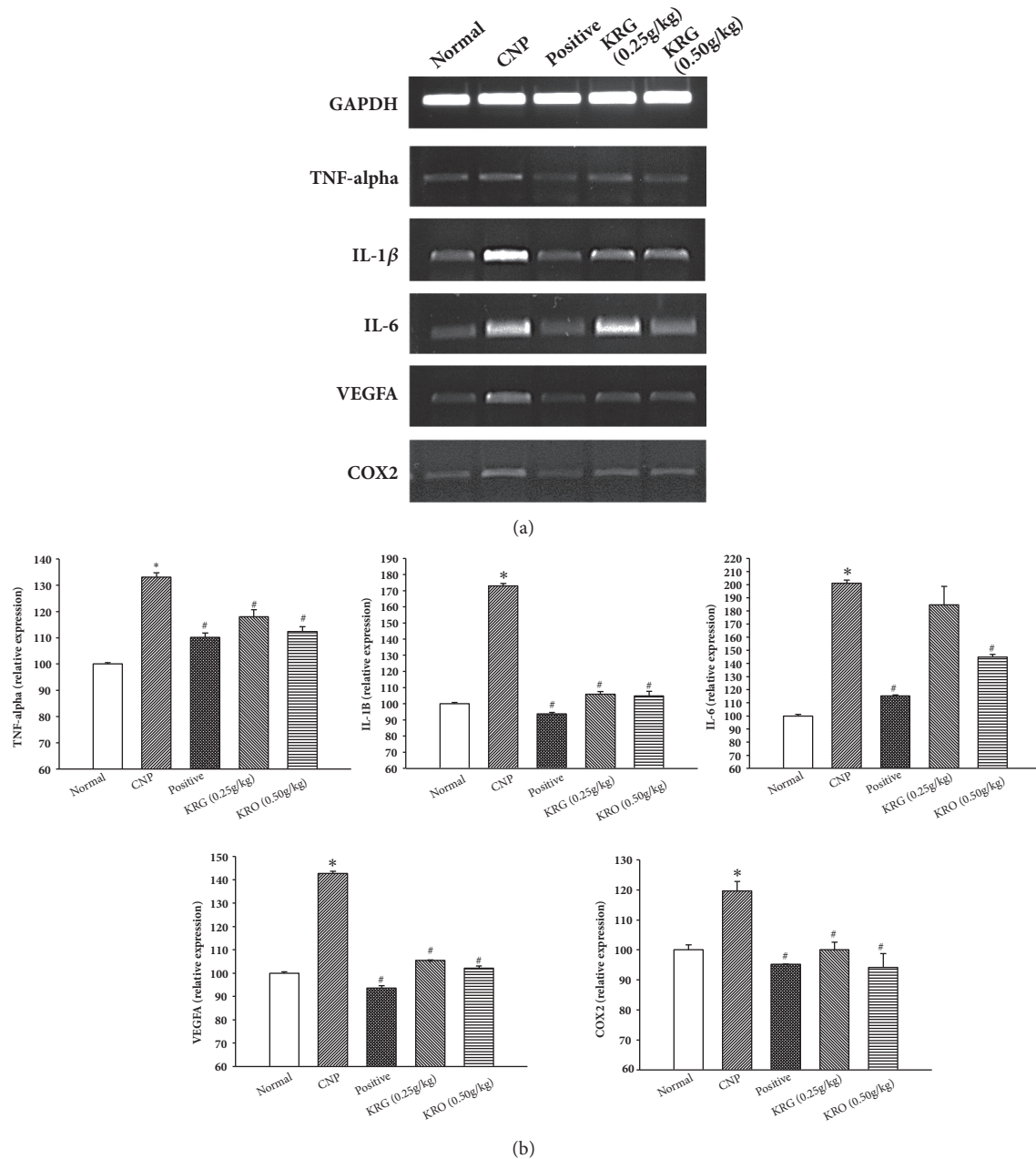


**FIGURE 4: The expressions of TNF-alpha, IL-1β, IL-6, VEGFA, and COX2 by RT-PCR in each group.** Normal, normal group; CNP, chronic nonbacterial prostatitis group; Positive, estradiol induced CNP with testosterone; KRG (0.25g/kg), beta-estradiol induced CNP with KRG (0.25g/kg); KRG (0.5g/kg), estradiol induced CNP with KRG (0.5g/kg). \*  $P < 0.05$ , compared with the normal group and #  $P < 0.05$ , compared with the CNP group.

normal group ( $p < 0.05$ ). And the levels of NO in the positive and KRG groups (0.25 g/kg and 0.5 g/kg) were significantly lower than those in the CNP group ( $p < 0.05$ ).

**3.5. Effect of KRG on mRNA Expression Levels of Inflammation Cytokines in Prostate Tissue Using RT-PCR.** The measurements of mRNA expression levels of VEGFA, TNF-alpha, IL-1β, IL-6, and COX2 were performed using RT-PCR. The mRNAs of VEGFA, TNF-alpha, IL-1β, IL-6, and COX2 were amplified by RT-PCR. As shown in Figure 4, mRNA

expression levels of VEGFA, TNF-alpha, IL1β, IL-6, and COX2 in the CNP group at 4 weeks were higher than those of the normal group (Figure 4(a)). In the positive and KRG (0.25g/kg and 0.50g/kg) groups at 4 weeks, mRNA expression levels of VEGFA, TNF-alpha, IL1β, IL-6, and COX2 had significantly decreased compared to those in the CNP group ( $p < 0.05$ ) (Figure 4(b)).

**3.6. Effect of KRG on Expression of Inflammation Cytokines in Prostate Tissue Using IHC.** To examine the effects of

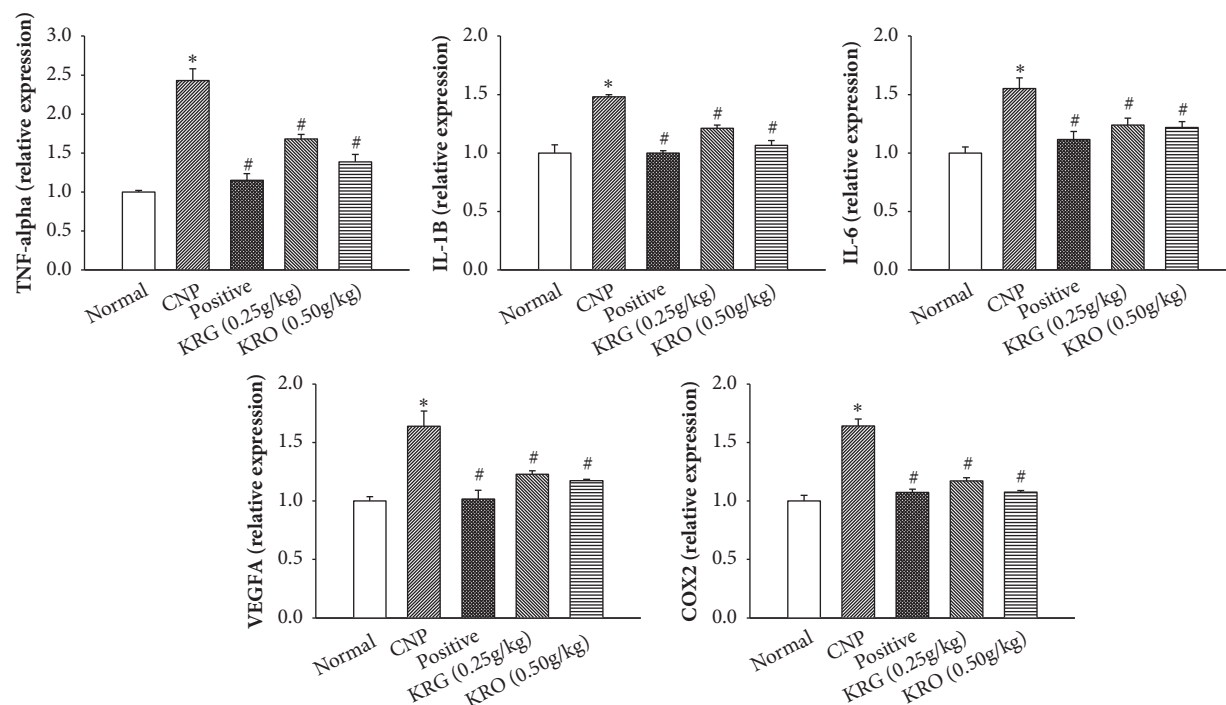


FIGURE 5: **The expressions of TNF-alpha, IL-1 $\beta$ , IL-6, VEGFA, and COX2 by immunohistochemistry in each group.** Normal, normal group; CNP, chronic nonbacterial prostatitis group; Positive, estradiol induced CNP with testosterone; KRG (0.25g/kg), beta-estradiol induced CNP with KRG (0.25g/kg); KRG (0.5g/kg), estradiol induced CNP with KRG (0.5g/kg). \*  $P < 0.05$ , compared with the normal group, and #  $P < 0.05$ , compared with the CNP group.

KRG on expression of inflammation cytokines (VEGFA, TNF-alpha, IL-1 $\beta$ , IL-6, and COX2) in prostate tissue, IHC was performed. As shown in Figure 5, expression levels of inflammation cytokines (VEGFA, TNF-alpha, IL-1 $\beta$ , IL-6, and COX2) in the CNP group were higher than those in the normal group ( $p < 0.05$ ). Proteins expression levels of VEGFA, TNF-alpha, IL-1 $\beta$ , IL-6, and COX2 in both positive and KRG (0.25g/kg and 0.50g/kg) groups had decreased compared to those in the CNP group ( $p < 0.05$ ).

#### 4. Discussion

In this study, we examined the effect of KRG on CNP using the E2-induced CNP animal model. Our results showed the effects of KRG on the inflammation and morphology of prostate tissue in case of the CNP.

Weight loss was the first difference observed when comparing the normal group against the other groups. Weight difference between the normal and E2 induced prostatitis groups, however, has already been reported in previous studies. These studies suggest that E2 may be causative or that prostatitis itself may play a role in such reduction in body weight [20, 21]. In our study, positive and the KRG groups also showed weight loss, which is E2 or prostatitis.

To examine the effect of KRG on hepatotoxicity, the serum levels of GOT, GPT, BUN, creatinine, and  $\gamma$ -GTP were measured. Most of the serum levels in the CNP, positive, and the KRG groups were not significantly different from those in the normal group. The only GOT level in of the

KRG (0.25g/kg) group was statistically higher than that in the other groups but it was within the normal range [22]. These results suggest that KRG has no toxicity in the CNP animal model.

The results of TUNEL staining show clear differences among the groups. The infiltration of inflammatory cells, destruction of prostate gland tissue, and a lot of apoptotic cells were observed in the CNP group. In the KRG group, it was observed that these changes of prostate tissue were significantly reduced. At higher concentrations of KRG, tissue changes and apoptotic cells were hardly observed. In the relative expression analysis, evidence of apoptosis had significantly increased in the CNP group and decreased in the positive and KRG groups compared with that in the CNP group. This result suggests that KRG has an antiapoptotic and anti-inflammatory effects on CNP.

To investigate the anti-inflammatory effect of KRG, levels of NO and proinflammatory cytokines were analyzed. NO is considered as a proinflammatory mediator [23]. The level of NO was significantly increased in the CNP group and decreased in the other groups compared with that in the CNP group. The results of RT-PCR and IHC for the proinflammatory cytokine showed a similar tendency. The mRNA and protein expression levels of TNF-alpha, IL-1 $\beta$ , IL-6, VEGFA, and COX2 in positive and the KRG groups were significantly lower than those in the CNP group. In addition, higher concentrations of KRG showed more effective anti-inflammatory responses in all cytokines (TNF-alpha, IL-1 $\beta$ , IL-6, VEGFA, and COX2).

Many previous studies have revealed that KRG has anti-inflammatory and antiapoptotic properties through various pathways. Red ginseng attenuated inflammatory responses through inhibition of the MAPKs/NF- $\kappa$ B/c-Fos pathways in the lung tissue [24]. In atopic dermatitis animal model, inflammatory responses were reduced through the suppression of the p70 ribosomal protein S6 kinase pathway by red ginseng [25]. In a previous study of FK506-induced nephrotoxicity in LLC-PK1 cells, KRG was also shown to play a protective role. KRG was showed antiapoptotic properties via the inhibition of p38 phosphorylation and activation of caspase, as well as an anti-inflammatory property via the inhibition of TLR-4 expression. Our results are consistent with these previous studies [26]. We showed the antiapoptotic effect of KRG using TUNEL assay and the anti-inflammatory effect of KRG by confirming the reduction of inflammatory mediator NO and the decrease of proinflammatory cytokine using RT-PCR and IHC.

## 5. Conclusions

Our results suggest that KRG plays protective effects against CNP in rat model via the suppressing expression of TNF- $\alpha$ , IL-1 $\beta$ , IL6, VEGFA, and COX2. In conclusion, KRG could be a useful agent for the prevention or treatment of CNP.

## Data Availability

The data used to support the findings of this study are included within the article.

## Disclosure

This manuscript has been posted at Georg Thieme Verlag KG Stuttgart.

## Conflicts of Interest

The authors declare no conflicts of interest.

## Authors' Contributions

The first two authors have equally contributed to this article.

## Acknowledgments

This work was supported by the 2016 grant from the Korean Society of Ginseng.

## References





- [1] J. N. Krieger, S. O. Ross, D. E. Riley et al., "Chronic prostatitis: Epidemiology and role of infection," *Urology*, vol. 60, no. 6, pp. 8–13, 2002.
- [2] V. Magri, E. Marras, A. Restelli, F. M. E. Wagenlehner, and G. Perletti, "Multimodal therapy for category III chronic prostatitis/chronic pelvic pain syndrome in UPOINTs phenotyped patients," *Experimental and Therapeutic Medicine*, vol. 9, no. 3, pp. 658–666, 2015.
- [3] C. N. Tran and D. A. Shoskes, "Sexual dysfunction in chronic prostatitis/chronic pelvic pain syndrome," *World Journal of Urology*, vol. 31, no. 4, pp. 741–746, 2013.
- [4] J. C. Nickel, D. A. Shoskes, and F. M. E. Wagenlehner, "Management of chronic prostatitis/chronic pelvic pain syndrome (CP/CPPS): the studies, the evidence, and the impact," *World Journal of Urology*, vol. 31, no. 4, pp. 747–753, 2013.
- [5] F. U. Khan, A. U. Ihsan, H. U. Khan et al., "Comprehensive overview of prostatitis," *Biomedicine & Pharmacotherapy*, vol. 94, pp. 1064–1076, 2017.
- [6] M. Higuchi, N. Higashi, H. Taki, and T. Osawa, "Cytolytic mechanisms of activated macrophages: Tumor necrosis factor and L-arginine-dependent mechanisms act synergistically as the major cytolytic mechanisms of activated macrophages," *The Journal of Immunology*, vol. 144, no. 4, pp. 1425–1431, 1990.
- [7] N.-H. Lee and C.-G. Son, "Systematic review of randomized controlled trials evaluating the efficacy and safety of ginseng," *JAMS Journal of Acupuncture and Meridian Studies*, vol. 4, no. 2, pp. 85–97, 2011.
- [8] M. He, X. Huang, S. Liu et al., "The Difference between White and Red Ginseng: Variations in Ginsenosides and Immunomodulation," *Planta Medica*, vol. 84, no. 12–13, pp. 845–854, 2018.
- [9] Q. L. Pham, H.-J. Jang, and K.-B. Kim, "Anti-wrinkle effect of fermented black ginseng on human fibroblasts," *International Journal of Molecular Medicine*, vol. 39, no. 3, pp. 681–686, 2017.
- [10] H. Lee, J. Choi, S. Shik Shin, and M. Yoon, "Effects of Korean red ginseng (Panax ginseng) on obesity and adipose inflammation in ovariectomized mice," *Journal of Ethnopharmacology*, vol. 178, pp. 229–237, 2016.
- [11] J. H. Lee, O. Shehzad, S. K. Ko, Y. S. Kim, and H. P. Kim, "Matrix metalloproteinase-13 downregulation and potential cartilage protective action of the Korean Red Ginseng preparation," *Journal of Ginseng Research*, vol. 39, no. 1, pp. 54–60, 2015.
- [12] C. Tian, Y. J. Kim, H. J. Lim, Y. S. Kim, H. Y. Park, and Y.-H. Choung, "Red ginseng delays age-related hearing and vestibular dysfunction in C57BL/6 mice," *Experimental Gerontology*, vol. 57, pp. 224–232, 2014.
- [13] S. Kim, Y. Lee, and J. Cho, "Korean red ginseng extract exhibits neuroprotective effects through inhibition of apoptotic cell death," *Biological & Pharmaceutical Bulletin*, vol. 37, no. 6, pp. 938–946, 2014.
- [14] D.-J. Jang, M. S. Lee, B.-C. Shin, Y.-C. Lee, and E. Ernst, "Red ginseng for treating erectile dysfunction: a systematic review," *British Journal of Clinical Pharmacology*, vol. 66, no. 4, pp. 444–450, 2008.
- [15] L. L. Murphy and T. J. Lee, "Ginseng, sex behavior, and nitric oxide," *Annals of the New York Academy of Sciences*, vol. 962, pp. 372–377, 2002.
- [16] S. K. Kim, J.-H. Chung, B.-C. Lee, S. W. Lee, K. H. Lee, and Y. O. Kim, "Influence of Panax ginseng on alpha-adrenergic receptor of benign prostatic hyperplasia," *International Neurourology Journal*, vol. 18, no. 4, pp. 179–186, 2014.
- [17] J.-S. Bae, H.-S. Park, J.-W. Park, S.-H. Li, and Y.-S. Chun, "Red ginseng and 20(S)-Rg3 control testosterone-induced prostate hyperplasia by deregulating androgen receptor signaling," *Journal of Natural Medicines*, vol. 66, no. 3, pp. 476–485, 2012.
- [18] M. Li, T. Han, W. Zhang, W. Li, Y. Hu, and S. K. Lee, "Simulated altitude exercise training damages small intestinal mucosa

- barrier in the rats,” *Journal of Exercise Rehabilitation*, vol. 14, no. 3, pp. 341–348, 2018.
- [19] M. Tunc-Ata, G. Turgut, M. Mergen-Dalyanoglu, and S. Turgut, “Examination of levels pentraxin-3, interleukin-6, and C-reactive protein in rat model acute and chronic exercise,” *Journal of Exercise Rehabilitation*, vol. 13, no. 3, pp. 279–283, 2017.
- [20] H. Akdere, I. Oztekin, E. Arda, T. Aktoz, F. N. Turan, and K. M. Burgazli, “Analgesic effects of oligonol, acupuncture and quantum light therapy on chronic nonbacterial prostatitis,” *Iranian Red Crescent Medical Journal*, vol. 17, no. 4, Article ID e26006, 2015.
- [21] M. M. Said and M. C. Bosland, “The anti-inflammatory effect of montelukast, a cysteinyl leukotriene receptor-1 antagonist, against estradiol-induced nonbacterial inflammation in the rat prostate,” *Naunyn-Schmiedeberg's Archives of Pharmacology*, vol. 390, no. 2, pp. 197–205, 2017.
- [22] T. Matsuzawa, M. Nomura, and T. Unno, “Clinical pathology reference ranges of laboratory animals. Working Group II, Nonclinical Safety Evaluation Subcommittee of the Japan Pharmaceutical Manufacturers Association,” *Journal of Veterinary Medical Science*, vol. 55, no. 3, pp. 351–362, 1993.
- [23] J. N. Sharma, A. Al-Omran, and S. S. Parvathy, “Role of nitric oxide in inflammatory diseases,” *Inflammopharmacology*, vol. 15, no. 6, pp. 252–259, 2007.
- [24] J. H. Lee, D. S. Min, C. W. Lee, K. H. Song, Y. S. Kim, and H. P. Kim, “Ginsenosides from Korean Red Ginseng ameliorate lung inflammatory responses: inhibition of the MAPKs/NF- $\kappa$ B/c-Fos pathways,” *Journal of Ginseng Research*, vol. 42, no. 4, pp. 476–484, 2018.
- [25] M. Osada-Oka, S. Hirai, Y. Izumi et al., “Red ginseng extracts attenuate skin inflammation in atopic dermatitis through p70 ribosomal protein S6 kinase activation,” *Journal of Pharmacological Sciences*, vol. 136, no. 1, pp. 9–15, 2018.
- [26] D. Lee, K. S. Kang, J. S. Yu et al., “Protective effect of Korean red ginseng against FK506-induced damage in LLC-PK1 cells,” *Journal of Ginseng Research*, vol. 41, no. 3, pp. 284–289, 2017.



## Clinical Study

# Effects of a New Combination of Medical Food on Endothelial Function and Lipid Profile in Dyslipidemic Subjects: A Pilot Randomized Trial

Francesco Landi <sup>1,2</sup>, Anna Maria Martone,<sup>1</sup> Sara Salini,<sup>1</sup> Beatrice Zazzara,<sup>1</sup> Riccardo Calvani <sup>1</sup>, Emanuele Marzetti <sup>1</sup>, Antonio Nesci,<sup>3</sup> Angela Di Giorgio,<sup>3</sup> Bianca Giupponi,<sup>4</sup> Luca Santoro <sup>3</sup> and Angelo Santoliquido<sup>2,3</sup>

<sup>1</sup>Department of Geriatrics, Neurosciences and Orthopedics, Fondazione Policlinico Gemelli IRCCS, Roma, Italy

<sup>2</sup>Università Cattolica del Sacro Cuore, Roma, Italy

<sup>3</sup>Division of Vascular Medicine, Department of Medicine-Fondazione Policlinico Universitario A. Gemelli IRCCS, Roma, Italy

<sup>4</sup>Medicina d'Urgenza e Pronto Soccorso, Fondazione Policlinico Universitario A. Gemelli IRCCS, Roma, Italy

Correspondence should be addressed to Luca Santoro; [luca.santoro@policlinicogemelli.it](mailto:luca.santoro@policlinicogemelli.it)

Received 10 July 2018; Revised 21 November 2018; Accepted 13 December 2018; Published 6 January 2019

Guest Editor: Claudio Tabolacci

Copyright © 2019 Francesco Landi et al. This is an open access article distributed under the Creative Commons Attribution License, which permits unrestricted use, distribution, and reproduction in any medium, provided the original work is properly cited.

Nutritional approaches to improve dyslipidemias have been recently developed, but evidences on different medical foods are often incomplete. The main aim of our study was to evaluate the effects on endothelial function, lipid profile, and glucose metabolism of two different combinations of nutraceuticals, first one containing Bergavit (200 mg Citrus bergamia), Omega-3 (400 mg), Crominex 3+ (10 mcg trivalent chromium), and red yeast rice (100 mg; 5 mg monacolin K) and second one containing red yeast rice (200 mg; 3 mg monacolin K), Berberine (500 mg), Astaxanthin (0.5 mg), folic acid (200 mcg), Coenzyme Q10 (2 mg), and Policosanol (10 mg). Fifty subjects affected by dyslipidemia not requiring statin treatment were enrolled in this randomized, blind, controlled trial and submitted to blood sampling for lipid and glucose profiles and instrumental evaluation of endothelial function before and after 6 weeks of treatment with nutraceuticals. Both nutraceutical combinations improved the lipid profile; the nutraceutical containing 5 mg of monacolin K, 200 mg of the extract *Citrus bergamia*, 400 mg of Omega-3, and 10 mcg of trivalent chromium entailed a significant improvement of endothelial function with enhanced cholesterol lowering effect. In conclusion, this study confirms the positive effect of functional food on lipid profile and endothelial function in absence of major undesirable effects.

## 1. Introduction

Cardiovascular (CV) disease is one of the most important public health problems of our time, in both Europe and the rest of the world, accounting for the largest expenditure in the healthcare budgets of many countries [1]. Despite the prevention strategies adopted in the last decades and the growing therapeutic options, CV disease remains the principal cause of disability, morbidity, and mortality [2, 3]. Whereas prevention strategies continue to address individuals who has experienced a major CV event or presented one or more CV risk factors, primordial prevention has been recommended for reaching CV well-being on healthy population [4, 5].

When discussing about major CV risk factors, experts widely recognize important contributions from observational and epidemiological studies, which demonstrate that higher cholesterol levels are associated with greater risks of atherosclerotic CV events [6–8]. In this respect, new nutritional approaches to improve dyslipidemias have been recently developed [9–11]; these products are founded on both amending some potentially dangerous foods and encouraging the intake of specific ‘healthy’ medical foods or nutritional supplements. With regard to medical food cholesterol lowering treatment, some evidences suggest that combinations that include more components, recruiting numerous specific mechanisms, are able to better increase the lipid pathway. However, even though these nutraceuticals can

be utilized either as substitutions or in addition to drugs [12], the existing evidence on these medical foods is inconclusive.

The present study was, therefore, undertaken to compare the effects of two specific mixtures of nutraceuticals on the control of lipid profile, glucose metabolism and endothelial function among subjects suffering from high levels of serum cholesterol not requiring statin. Our results offer new evidences about the positive effect of functional food on lipid profile and endothelial function.

## 2. Subjects and Methods

We conducted a randomized controlled trial (6-week follow-up) during which participants assumed deferent combination of nutraceuticals (Nutraceutical “A” or Nutraceutical “B”) according to a randomization procedure. All participants gave written informed consent before being enrolled in the study for the prerandomization assessment and at the baseline of intervention for follow-up assessments and treatment.

**2.1. Study Sample.** For the enrollment in the study, we screened individuals admitted to the national campaign, named “Longevity Check-up 7+” (Look-up 7+) and promoted by the Catholic University of Rome [13]. The Catholic University of Sacred Heart Ethical Committee ratified this study protocol within the context of the National Campaigns for CV prevention [14].

The inclusion criteria for the present study were higher level of serum cholesterol not needing statins or statin intolerant, age between 18 and 75 years. The exclusion criteria were the potential side effects to nutraceuticals products, pregnant status, previous prescription of lipid lowering drugs during (6 weeks), and/or severe hypertriglyceridemia (500 mg/dl). Furthermore, we excluded subjects with diseases impairing endothelial function (i.e., uncontrolled diabetes and chronic inflammatory disorders), presence of CV diseases, and subjects treated with vasoactive drugs. Of the total of 75 subjects screened, 17 were excluded for the presence of CV diseases and 3 subjects with uncontrolled diabetes. Five subjects refused to be part of the study protocol. Hence, 67% of the screened subjects ( $n=50$ ) were fully eligible and entered the study. Finally, three subjects, one in the nutraceutical “A” and two in the nutraceutical “B” group, were missing at the end of the study.

**2.2. Study Design.** Baseline assessments were completed before randomization. After the baseline assessment, participants received nutritional counseling, according to their medical conditions. At the end of this run-in period, participants were randomly stratified according to age and gender by a computer-generated list into two groups assigned to receive Nutraceutical “A” or Nutraceutical “B” for 6 weeks.

Nutraceutical A contained the following: Bergavit (200 mg Citrus bergamia), Omega-3 (400 mg), Crominex 3+ (10 mcg trivalent chromium), and red yeast rice (100 mg; 5 mg monacolin K) (Riscal Plus, Errekappa Euroterapici).

Nutraceutical B contained the following: Policosanol (10 mg), red yeast rice (200 mg; 3 mg monacolin K), Berberine

(500 mg), Astaxanthin (0.5 mg), folic acid (200 mcg), and Coenzyme Q10 (2 mg) (Armolidip Plus, RottapharmSpA).

Both nutraceutical “A” and “B” are tablets that were taken by the participants once a day, preferably in the evening. Nutraceutical “A” was chosen as it represents a new combination on the Italian market with an excellent biological plausibility of its main components. At the same time, nutraceutical “B” should be considered the “gold standard”. In fact, this combination has been extensively investigated in several randomized control trials, seven of which were placebo-controlled. Recently, Barrios and colleagues [15], in their review of the clinical evidences, concluded that nutraceutical “B” (Armolidip Plus) has proved to be able to achieve significant reductions in total cholesterol (11-21%) and in LDL-C (15-31%) levels, which is equivalent to expectations from low dose statins.

The primary endpoint was the statistically significant reduction of endothelial dysfunction; secondary endpoints were the modifications in triglycerides, serum total cholesterol (HDL and LDL), blood glucose, and insulin sensitivity index (HOMA index).

**2.3. Data Collection.** All participants enrolled in the study received a dedicated visit comprising an anamnestic questionnaire, the measurement of objective CV health metrics, and the assessment of anthropometric parameters. In particular, the baseline and follow-up assessment were designed to obtain the following data: informed consent, age, gender, lifestyle evaluation (smoking, eating habits, and physical activity), blood pressure measurement, weight and height assessment, waist circumference, lipids measurement and fasting glucose measurements, and plasma level of insulin; furthermore, we estimated the HOMA index using the Matthews’ formula [16].

Endothelial function was assessed by evaluating flow-mediated dilation (FMD) of brachial artery that measures the nitric oxide-mediated vasodilation after a period of ischemia (endothelium-dependent vasodilation), in accordance with actual guidelines [17].

All participants were asked to fast and to avoid exercise and vasoactive substances (i.e., drugs, tobacco, and coffee) for at least 12 hours before the examination.

**2.4. Statistical Analyses.** Sample power was previously calculated based on FMD, considering a power of 80% and an  $\alpha$ -error of 5% with an expected positive result among participants receiving product “A” of 90%, compared to 40% of the subjects in the control group (product “B”). Based on this estimation, 40 subjects were needed to have 80% probability of finding a positive result for the primary outcome from 90% in the subjects taking nutraceutical “A” to 40% in the subjects taking nutraceutical “B”.

Variables were shown as mean values ( $\pm$ SD). Differences in characteristics between control and treatment groups were examined in numerous ways. Quantitative outcomes were analyzed by the Student *t*-test after a previous test for variance homogeneity. The Mann-Whitney analysis was utilized when the normality assumption was not realistic.

TABLE 1: Characteristics of study population according to gender \*.

Characteristics	Total Sample (n=47)	Nutraceutical A (n=24)	Nutraceutical B (n=23)	<i>p</i>
Age (years)	58.7± 8.7	58.0± 8.9	59.5± 8.5	0.55
Gender (male)	33 (70)	16 (67)	17 (74)	0.41
Smoking	7 (14)	4 (16)	3 (13)	0.45
Healthy diet	25 (53)	13 (54)	12 (52)	0.77
Physically active	19 (40)	10 (41)	9 (39)	0.65
BMI (Kg/m <sup>2</sup> )	27.3± 4.6	28.0± 5.1	26.5± 5.9	0.28
Systolic blood pressure (mmHg)	122.9± 14.0	125.8± 14.4	119.8± 13.2	0.14
Diastolic blood pressure (mmHg)	75.4± 9.9	76.4± 10.9	74.3± 8.9	0.47
Total cholesterol (mg/dl)	239.1± 26.3	234.9± 10.0	243.6± 36.1	0.29
HDL cholesterol (mg/dl)	47.0± 3.2	46.9± 2.0	47.2± 4.2	0.46
LDL cholesterol (mg/dl)	143.8± 25.6	141.3± 15.3	146.4± 33.3	0.49
Triglycerides (mg/dl)	105.4± 34.3	104.3± 40.3	106.5± 27.6	0.83
Fasting plasma glucose (mg/dl)	91.1± 6.4	90.2± 7.6	91.9± 5.0	0.38
Insulin (IU/ml)	8.8 ± 5.3	9.4 ± 5.8	8.1 ± 4.8	0.43

\*Data are given as number (percent) for gender, smoking, healthy diet, and physical activity; for all the other variables, means ± SD are reported.

Healthy diet: consumption of at least three portions of fruit and/or vegetables per day.

Physically active: physical exercise at least twice a week.

BMI: body mass index.

TABLE 2: Unadjusted and adjusted means of flow-mediated dilation (FMD) measures (dependentvariable) according to different treatments.

Characteristics	Nutraceutical A (n=24)	Nutraceutical B (n=23)	<i>p</i>
Baseline	5.19 ± 2.25	4.74 ± 1.67	0.14
Follow-up (unadjusted)	7.55 ± 3.38	5.75 ± 2.09	0.04
Follow up (adjusted) *	7.48 ± 0.58	5.58 ± 0.59	0.05

\* ANCOVA: analysis adjusted for age, gender, and baseline value.

The Fisher exact test was used for categorical variables. The analysis of covariance (ANCOVA) adjusted for age, gender, and baseline values was used to examine the result of different intervention on lipid pathway and FMD at the end of follow-up period.

All analyses were completed using the SPSS software (SPSS Inc., Chicago, IL, version 11.0).

The funding sources had no part in any phase of study procedures (collection, analysis, and data interpretation).

### 3. Results

Mean age of 47 subjects participating the study was 58.7 (standard deviation 8.7, range from 42 to 75 years) years, and 33 (70%) were men. Characteristics of the study population according to the treatments are summarized in Table 1. At baseline assessment, no differences in life style habits, BMI, and systolic and diastolic blood pressure were observed. Total serum cholesterol, HDL-c and LDL-c, triglycerides, glucose, and insulin were similar between the different groups. None of the participants in the study groups reported difficulty in taking the tablet regarding size, taste, and palatability.

Treatment compliance was excellent in both groups and no adverse events were reported.

Mean values of FMD assessment are shown in Table 2. At baseline, FMD were similar between nutraceutical “A” and nutraceutical “B” groups ( $p=0.14$ ); after the 6 weeks of treatment, FMD in the subjects receiving nutraceutical “A” significantly increases in comparison with subjects receiving nutraceutical “B” ( $p=0.04$ ). After adjusting for age, gender, and baseline values, FMD value was higher among participants in nutraceutical “A” group compared with subjects in nutraceutical “B” group ( $p=0.05$ ).

Figure 1 shows lipid profile at 6-week follow-up after treatment with nutraceutical “A” and nutraceutical “B”. It is important to highlight that both nutraceuticals produce a noteworthy decrease of serum levels of total and LDL cholesterol, triglycerides, and an improvement of HDL with respect to baseline values (all  $p<0.01$ ). However, this improvement was more significant in subjects treated with nutraceutical “A” compared with participants receiving nutraceutical “B”.

For these measurements, we considered the percentage change found by both nutraceuticals associations versus the baseline values (Figure 2). Nutraceutical “A” reduced the total and LDL cholesterol more than nutraceutical “B”;

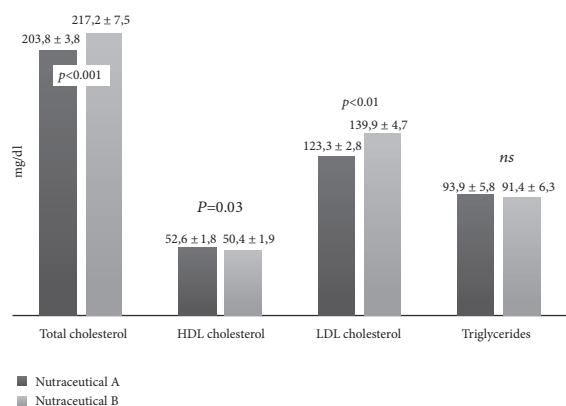


FIGURE 1: Lipid profile at the end of the study period (ANCOVA analysis adjusted for age, gender, and the baseline values); data are presented as mean ± standard errors values.

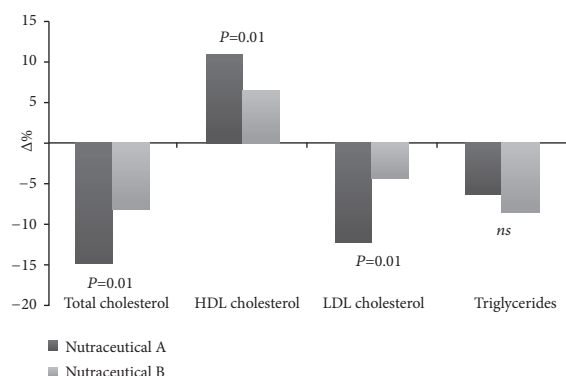


FIGURE 2: Percentage changes in lipid profile between baseline and follow-up.

similarly, participants in nutraceutical “A” group showed a higher improvement in HDL cholesterol level. On the contrary, no statistically significant modification was noted in the percentage changes of triglycerides between the two nutraceuticals mixtures.

Furthermore, according to ESC/EAS guideline [12], the rate of participants showing a reduction of LDL cholesterol below 115 mg/dl at the end of treatment periods has been calculated.

A greater number of subjects with a normal value of LDL cholesterol with nutraceutical “A” were observed as compared to nutraceutical “B” (59.6% versus 40.4 %, p=0.04) (Figure 3).

Finally, no statistically significant difference was observed for glucose, insulin, and HOMA index recorded throughout the study.

#### 4. Discussion

This randomized study corroborates that treatment with specific nutraceutical combination (actually approved in Italy) is able to ameliorate the lipid profile among subjects with high levels of cholesterol not specifically needing statins.

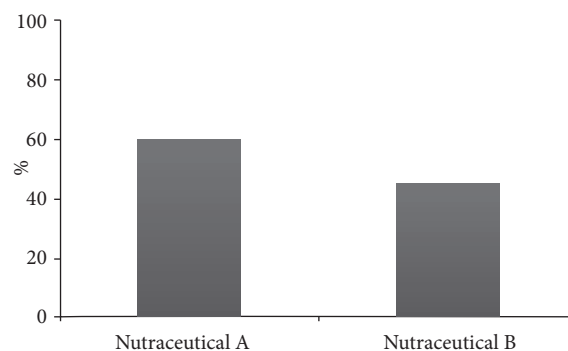


FIGURE 3: Percentage of subjects with LDL<130 mg/dl at the end of follow-up.

Moreover, it suggests that the nutraceutical containing 5 mg of monacolin K, 200 mg of the extract *Citrus bergamia*, 400 mg of Omega-3, and 10 mcg of trivalent chromium entailed a cholesterol lowering effect with a significant improvement of endothelial function. This last effect is very important, in particular considering that endothelial dysfunction is considered an early event of atherosclerosis that precedes structural atherosclerotic changes in the vascular wall [18] and several studies have demonstrated that impaired FMD predicts CV morbidity and mortality independently of traditional CV risk factors and the Framingham risk score [19, 20]. These findings have been recently confirmed also in young population, in absence of CV disease [21].

As recommended by the 2016 ESC/EAS guidelines for the management of dyslipidaemias, nutraceuticals containing purified red yeast rice may be considered in subjects with elevated plasma cholesterol levels who do not qualify for treatment with statins in view of their global CV risk [20]. The bioactive ingredient of red yeast rice is the monacolin K. Effects of monacolin K on lipid profile are correlated to a statin-like action with the inhibition of hydroxymethylglutaryl-coenzyme A (HMG-CoA) reductase. Diverse nutraceutical combinations have different concentrations of monacolin K, while a clinically relevant effect on cholesterol levels (up to a 20% reduction) is observed with preparations providing a daily dose of monacolin K between 2.5 to 10 mg [22–24]. The higher concentration of monacolin K in the mixture “A” may in part explain the better results obtained in the control of lipid profile and on the endothelial function. However, it is possible to hypothesize that these better results may be explained by the presence of other specific ingredients, too.

The extract of bergamot (*Citrus bergamia*) is rich in flavonoids that have antioxidant, anti-inflammatory, as well as lipid-lowering properties [25]. The hydroxy methylglutaryl-flavonones contained in the *Citrus bergamia*, such as hesperetin, naringenin bruteridine, and melitidine, have specific effects on lipid profile inhibiting, as the statin, the enzyme HMG-CoA reductase, and the activity of AcylCo-enzymeA Cholesterol-Acyl-Transferase (ACAT), then reducing the assembly of VLDL and LDL lipoproteins [26]. Furthermore, as regards the potential effect on the endothelium, the flavonoids contained in the *Citrus bergamia* limit the



production of oxygen free radicals in the vessel wall, improve the endothelial production of nitric oxide, and also modulate the inflammatory response. In particular, by inhibiting the activation of NF- $\kappa$ B, they reduce the expression of the inflammatory cytokines, such as IL-6, IL-1b, TNF- $\alpha$ , and therefore have antiproliferative effects on the smooth muscle cells and contribute to the prevention of atherosclerosis [27]. *Citrus bergamia* can therefore play an important role in preventing vascular damage due to proliferation of smooth muscle cells and dysfunction of endothelial cells. A study of an angioplasty model in rats showed that pretreatment with *Citrus bergamia* reduced neointima proliferation, free radical formation, and LDL-ox receptor expression [25]. Toth and colleagues [28] recently investigated the effects of *Citrus bergamia* flavonoids supplementation on cardio-metabolic risk in dyslipidemic subjects, demonstrating that this supplementation significantly reduced plasma lipids and improved the lipoprotein profile. Carotid intima-media thickness was also reduced significantly over a relatively short time frame of 6 months [28].

Trivalent chromium (Cr3+) is classified as an essential micronutrient for optimal carbohydrate and lipid metabolism. Although evidence relating Cr3+ deficiency and CV disease is incomplete, deficit has been associated with lower levels of HDL cholesterol. Sealls and colleagues [28] demonstrated that Cr3+ reversed hyperinsulinemia-induced cellular cholesterol accrual and associated defects in cholesterol transporter ABCA1 trafficking and apolipoprotein A1-mediated cholesterol efflux. These findings suggest a mechanism of Cr3+ action that fits with long-standing claims of its role in cholesterol homeostasis [29].

The lipid-lowering action of omega-3 polyunsaturated fatty has been clearly demonstrated in numerous clinical trials and meta-analyses [30, 31]. Nutraceuticals with omega-3 have a number of other beneficial effects on biomarker parameters that justify their use in subjects with metabolic syndrome [32]. In fact, they also stimulate the formation of prostaglandins, inhibit the activity of the enzyme to convert angiotensin, reduce the formation of angiotensin II and increase that of nitric oxide, and reduce the formation of homocysteine [33–35].

So, we can speculate that the final beneficial effect of nutraceutical “A” (*Citrus bergamia*, Omega-3 Crominex 3+, monacolin K; Riscol Plus, Errekappa Euroterapici) is the result of a series of synergies that are created between different nutrients. For these reasons, the components present in this nutraceutical should not be seen in an exclusively lipid profile optics, but rather for the anti-inflammatory, antioxidant, and vasodilation actions that they are able to perform.

Albeit dealing with a highly relevant result, our study presents several limitations that need to be discussed. First, this study should be considered a pilot trial showing a significant improvement of endothelial function and lipid profile; however, it is important to highlight that the small number of participants enrolled needs validation in a larger sample. The short follow-up limits the probability to observe positive results on insulin and glycemic levels, which needs a longer time of follow-up to assess the differences. Nevertheless, our

preliminary data are promising and could be the base for a larger clinical trial.

Apart from these limitations, this study offers new evidence about the positive effect of functional food on lipid profile and endothelial function with a good compliance and the absence of significant side effects. Dietary recommendations should always take into account healthy food choices; however, innovative nutritional strategies to improve dyslipidaemias, such as nutraceutical combinations, should be promoted [35, 36]. In this respect it is important to highlight that the two formulations considered in the present study are very different in composition. This means that no specific conclusion regarding one or more compounds may be definitively reached and, as a consequence, a larger study specifically designed for this purpose will be needed.

## Data Availability

The data used to support the findings of this study are available from the corresponding author upon request.

## Conflicts of Interest

The authors declare that they have no conflicts of interest.

## Authors' Contributions

All of the authors participated in conceiving, designing, and writing the manuscript. All authors read and approved the final manuscript.

## Acknowledgments

The study was supported by grant from Errekappa Euroterapici.

## References

- [1] K. K. Ray, J. J. P. Kastelein, S. M. Boekholdt et al., “The ACC/AHA 2013 guideline on the treatment of blood cholesterol to reduce atherosclerotic cardiovascular disease risk in adults: the good the bad and the uncertain: a comparison with ESC/EAS guidelines for the management of dyslipidaemias 2011,” *European Heart Journal*, vol. 35, no. 15, pp. 960–968, 2014.
- [2] M. Laaksonen, K. Talala, T. Martelin et al., “Health behaviours as explanations for educational level differences in cardiovascular and all-cause mortality: A follow-up of 60 000 men and women over 23 years,” *European Journal of Public Health*, vol. 18, no. 1, pp. 38–43, 2008.
- [3] V. L. Roger, A. S. Go, D. M. Lloyd-Jones et al., “Executive summary: heart disease and stroke statistics–2012 update: a report from the American Heart Association,” *Circulation*, vol. 125, pp. 188–197, 2012.
- [4] D. Ose, J. Rochon, S. M. Campbell et al., “Health-related quality of life and risk factor control: The importance of educational level in prevention of cardiovascular diseases,” *European Journal of Public Health*, vol. 24, no. 4, pp. 679–684, 2014.
- [5] GBD 2015 Eastern Mediterranean Region Cardiovascular Disease Collaborators, “Burden of cardiovascular diseases in the


- Eastern Mediterranean Region, 1990-2015: findings from the Global Burden of Disease 2015 study," *International Journal of Public Health*, vol. 3, pp. 137-149, 2018.
- [6] E. Upmeyer, S. Lavonius, A. Lehtonen, M. Viitanen, H. Isoaho, and S. Arve, "Serum lipids and their association with mortality in the elderly: A prospective cohort study," *Aging Clinical and Experimental Research*, vol. 21, no. 6, pp. 424-430, 2009.
  - [7] M. Hamer, G. O'Donovan, and E. Stamatakis, "High-Density Lipoprotein Cholesterol and Mortality: Too Much of a Good Thing?" *Arteriosclerosis, Thrombosis, and Vascular Biology*, vol. 38, no. 3, pp. 669-672, 2018.
  - [8] C. Zoccali and F. Mallamaci, "Cholesterol: Another Salty Pathway to Cardiovascular Disease?" *Arteriosclerosis, Thrombosis, and Vascular Biology*, vol. 37, no. 3, pp. 383-384, 2017.
  - [9] F. Liu, M. Prabhakar, J. Ju, H. Long, and H.-W. Zhou, "Effect of inulin-type fructans on blood lipid profile and glucose level: A systematic review and meta-analysis of randomized controlled trials," *European Journal of Clinical Nutrition*, vol. 71, no. 1, pp. 9-20, 2017.
  - [10] M. R. Wofford, C. M. Rebholz, K. Reynolds et al., "Effect of soy and milk protein supplementation on serum lipid levels: A randomized controlled trial," *European Journal of Clinical Nutrition*, vol. 66, no. 4, pp. 419-425, 2012.
  - [11] H. Gylling and P. Simonen, "Phytosterols, phytosteranols, and lipoprotein metabolism," *Nutrients*, vol. 7, no. 9, pp. 7965-7977, 2015.
  - [12] A. L. Catapano, I. Graham, G. De Backer et al., "2016 ESC/EAS Guidelines for the Management of Dyslipidaemias," *European Heart Journal*, vol. 37, no. 39, pp. 2999-3058, 2016.
  - [13] F. Landi, R. Calvani, A. Picca et al., "Cardiovascular health metrics, muscle mass and function among Italian community-dwellers: the Lookup 7+ project," *European Journal of Public Health*, vol. 28, no. 4, pp. 766-772, 2018.
  - [14] D. L. Vetrano, A. M. Martone, S. Mastropaolo et al., "Prevalence of the seven cardiovascular health metrics in a Mediterranean country: Results from a cross-sectional study," *European Journal of Public Health*, vol. 23, no. 5, pp. 858-862, 2013.
  - [15] V. Barrios, C. Escobar, A. F. G. Cicero et al., "A nutraceutical approach (Armolid Plus) to reduce total and LDL cholesterol in individuals with mild to moderate dyslipidemia: Review of the clinical evidence," *Atherosclerosis Supplements*, vol. 24, pp. 1-15, 2017.
  - [16] D. R. Matthews, J. P. Hosker, A. S. Rudenski, B. A. Naylor, D. F. Treacher, and R. C. Turner, "Homeostasis model assessment: Insulin resistance and  $\beta$ -cell function from fasting plasma glucose and insulin concentrations in man," *Diabetologia*, vol. 28, no. 7, pp. 412-419, 1985.
  - [17] D. H. J. Thijssen, M. A. Black, K. E. Pyke et al., "Assessment of flow-mediated dilation in humans: a methodological and physiological guideline," *American Journal of Physiology-Heart and Circulatory Physiology*, vol. 300, no. 1, pp. H2-H12, 2011.
  - [18] R. Ross, "Atherosclerosis—an inflammatory disease," *The New England Journal of Medicine*, vol. 340, no. 2, pp. 115-126, 1999.
  - [19] J. Grewal, S. Chan, J. Frohlich, and G. B. Mancini, "Assessment of a novel risk factors in patients at low risk for cardiovascular events based on Framingham risk stratification," *Clinical and Investigative Medicine*, vol. 36, pp. 158-165, 2003.
  - [20] S. Y. Chan, G. B. J. Mancini, L. Kuramoto, M. Schulzer, J. Frohlich, and A. Ignaszewski, "The prognostic importance of endothelial dysfunction and carotid atheroma burden in patients with coronary artery disease," *Journal of the American College of Cardiology*, vol. 42, no. 6, pp. 1037-1043, 2003.
  - [21] L. Santoro, F. D'Onofrio, S. Campo et al., "Endothelial dysfunction but not increased carotid intima-media thickness in young European women with endometriosis," *Human Reproduction*, vol. 27, no. 5, pp. 320-326, 2012.
  - [22] A. L. Catapano, I. Graham, G. De Backer et al., "2016 ESC/EAS Guidelines for the Management of Dyslipidaemias," *Revista Española de Cardiología*, vol. 70, no. 2, article 115, 2017.
  - [23] T. Heinz, J. P. Schuchardt, K. Möller, P. Hadji, and A. Hahn, "Low daily dose of 3 mg monacolin K from RYR reduces the concentration of LDL-C in a randomized, placebo-controlled intervention," *Nutrition Research*, vol. 36, no. 10, pp. 1162-1170, 2016.
  - [24] G. Derosa, A. D'Angelo, D. Romano, and P. Maffioli, "Effects of a combination of berberis aristata, silybum marianum and monacolin on lipid profile in subjects at low cardiovascular risk; a double-blind, randomized, placebo-controlled trial," *International Journal of Molecular Sciences*, vol. 18, no. 2, 2017.
  - [25] V. Mollace, S. Ragusa, I. Sacco et al., "The protective effect of bergamot oil extract on lecithine-like oxylDL receptor-1 expression in balloon injury-related neointima formation," *Journal of Cardiovascular Pharmacology and Therapeutics*, vol. 13, no. 2, pp. 120-129, 2008.
  - [26] V. Spigoni, P. Mena, F. Fantuzzi et al., "Bioavailability of Bergamot (Citrus bergamia) Flavanones and Biological Activity of Their Circulating Metabolites in Human Pro-Angiogenic Cells," *Nutrients*, vol. 9, no. 12, p. 1328, 2017.
  - [27] R. Risitano, M. Currò, S. Cirmi et al., "Flavonoid fraction of bergamot juice reduces LPS-induced inflammatory response through SIRT1-mediated NF- $\kappa$ B inhibition in THP-1 monocytes," *PLoS ONE*, vol. 9, Article ID e107431, 2014.
  - [28] P. P. Toth, A. M. Patti, D. Nikolic et al., "Bergamot reduces plasma lipids, atherogenic small dense LDL, and subclinical atherosclerosis in subjects with moderate hypercholesterolemia: A 6 Months Prospective Study," *Frontiers in Pharmacology*, vol. 6, no. Article no. 299, 2016.
  - [29] W. Sealls, B. A. Penque, and J. S. Elmendorf, "Evidence that chromium modulates cellular cholesterol homeostasis and ABCA1 functionality impaired by hyperinsulinemia-brief report," *Arteriosclerosis, Thrombosis, and Vascular Biology*, vol. 1, pp. 1139-1140, 2011.
  - [30] M. Y. Wei and T. A. Jacobson, "Effects of eicosapentaenoic acid versus docosahexaenoic acid on serum lipids: A systematic review and meta-analysis," *Current Atherosclerosis Reports*, vol. 13, no. 6, pp. 474-483, 2011.
  - [31] T. L. Schumacher, T. L. Burrows, M. E. Rollo, L. G. Wood, R. Callister, and C. E. Collins, "Comparison of fatty acid intakes assessed by a cardiovascular-specific food frequency questionnaire with red blood cell membrane fatty acids in hyperlipidaemic Australian adults: A validation study," *European Journal of Clinical Nutrition*, vol. 70, no. 12, pp. 1433-1438, 2016.
  - [32] L. Laubertová, K. Koňariková, H. Gbelcová et al., "Fish oil emulsion supplementation might improve quality of life of diabetic patients due to its antioxidant and anti-inflammatory properties," *Nutrition Research*, vol. 46, pp. 49-58, 2017.
  - [33] S. L. Dawson, S. J. Bowe, and T. C. Crowe, "A combination of omega-3 fatty acids, folic acid and B-group vitamins is superior at lowering homocysteine than omega-3 alone: A meta-analysis," *Nutrition Research*, vol. 36, pp. 499-508, 2016.
  - [34] M. Zanetti, G. G. Cappellari, D. Barbeta, A. Semolic, and R. Barazzoni, "Omega 3 polyunsaturated fatty acids improve

endothelial dysfunction in chronic renal failure: Role of eNOS activation and of oxidative stress,” *Nutrients*, vol. 9, p. E895, 2017.

- [35] A. Poli, C. M. Barbagallo, A. F. G. Cicero et al., “Nutraceuticals and functional foods for the control of plasma cholesterol levels. An intersociety position paper,” *Pharmacological Research*, vol. 134, pp. 51–60, 2018.
- [36] A. F. G. Cicero, A. Colletti, G. Bajraktari et al., “Lipid-lowering nutraceuticals in clinical practice: position paper from an International Lipid Expert Panel,” *Nutrition Reviews*, vol. 75, no. 9, pp. 731–767, 2017.

## Research Article

# Natural Compound Oridonin Inhibits Endotoxin-Induced Inflammatory Response of Activated Hepatic Stellate Cells

Claire B. Cummins,<sup>1</sup> Xiaofu Wang,<sup>1</sup> Christian Sommerhalder,<sup>1</sup>  
Frederick J. Bohanon,<sup>1</sup> Omar Nunez Lopez,<sup>1</sup> Hong-Yan Tie,<sup>2</sup> Victoria G. Rontoyanni,<sup>3</sup>  
Jia Zhou,<sup>4</sup> and Ravi S. Radhakrishnan<sup>1</sup> 

<sup>1</sup>Department of Surgery, University of Texas Medical Branch, Galveston, Texas, 77555, USA

<sup>2</sup>Department of Anatomy, College of Basic Medicine, Zhengzhou University, Zhengzhou 450066, China

<sup>3</sup>Department of Surgery, Shriners Hospitals for Children, Galveston, Texas, 77555, USA

<sup>4</sup>Department of Pharmacology and Toxicology, University of Texas Medical Branch, Galveston, Texas, 77555, USA

Correspondence should be addressed to Ravi S. Radhakrishnan; rsradhak@utmb.edu

Received 28 June 2018; Revised 16 September 2018; Accepted 9 December 2018; Published 30 December 2018

Academic Editor: Ravirajsinh N. Jadeja

Copyright © 2018 Claire B. Cummins et al. This is an open access article distributed under the Creative Commons Attribution License, which permits unrestricted use, distribution, and reproduction in any medium, provided the original work is properly cited.

Hepatic stellate cells (HSCs) play an important role in hepatic fibrogenesis and inflammatory modulation. Endotoxin is dramatically increased in portal venous blood after serious injury and can contribute to liver damage. However, the mechanism underlying endotoxin's effects on HSCs remains largely unknown. Oridonin is a bioactive diterpenoid isolated from *Rabdosia rubescens* that exhibits anti-inflammatory properties in different tissues. In the present study, we determined the effects of oridonin on endotoxin-induced inflammatory response and signaling pathways *in vitro*. The production of proinflammatory cytokines in activated human HSCs line LX-2 was measured by ELISA and Western blots. Immunofluorescence and nuclear fractionation assay were used to determine NF- $\kappa$ B activity. Oridonin treatment significantly inhibited LPS-induced proinflammatory cytokines IL-1 $\beta$ , IL-6, and MCP-1 production as well as cell adhesion molecules ICAM-1 and VCAM-1. Additionally, oridonin blocked LPS-induced NF- $\kappa$ B p65 nuclear translocation and DNA binding activity. Oridonin prevented LPS-stimulated NF- $\kappa$ B regulator IKK $\alpha$ / $\beta$  and I $\kappa$ B $\alpha$  phosphorylation and I $\kappa$ B $\alpha$  degradation. Combined treatment of oridonin and an Hsp70 substrate binding inhibitor synergistically suppressed LPS-stimulated proinflammatory cytokines and NF- $\kappa$ B pathway activation. Therefore, oridonin inhibits LPS-stimulated proinflammatory mediators through IKK/I $\kappa$ B $\alpha$ /NF- $\kappa$ B pathway. Oridonin could be a promising agent for a hepatic anti-inflammatory.

## 1. Introduction

*Rabdosia rubescens*, a Chinese medicinal herb, contains the active diterpenoid compound oridonin. For hundreds of years, *Rabdosia rubescens* has been used in Chinese traditional medicine as an antitumor, antimicrobial, anti-inflammatory, and antioxidant agent. It has been used to treat a variety of ailments including stomach aches, pharyngitis, cough and sport-related injuries, as well as multiple cancer types, such as esophageal, breast, liver, and prostate [1, 2]. Oridonin was identified in the late 1960s as the active compound in *Rabdosia rubescens* and was able to be synthesized in early 1970s. Today, it remains one of the most important

compounds isolated from traditional Chinese herbs. Oridonin has been shown to have multiple biological activities. Oridonin has been shown to interfere with several pathways involved in cell proliferation, cell cycle arrest, and apoptosis, which contribute to its chemopreventative and antitumor effects. [3, 4]. Recently, several research papers have demonstrated that oridonin also has immunomodulatory effects on the immune system and proinflammatory mediators. For example, in murine primary splenocytes, oridonin significantly inhibited both IL-2 (Th1) and IL-10 (Th2) cytokine production at the same time, suggesting that this terpenoid compound has anti-inflammatory potential through the inhibition of T-cell immune responses [5]. The NF- $\kappa$ B pathway



has been well established as playing a prominent role in inflammatory processes. Oridonin was found to inhibit NF- $\kappa$ B activity in different cell types [6, 7]. Importantly, Zhou and colleagues [8] reported that oridonin showed significant antileukemic and organ protective effects without obvious adverse reaction. Their results revealed that oridonin treatment markedly reduced disseminated disease and prevented the destruction of tissue architecture caused by leukemia in both the liver and the spleen, indicating that oridonin exerts a protective effect on the liver. Multiple studies have further demonstrated the ability of oridonin to block inflammatory signaling in other tissue such as renal cortex tissue, colonic tissue, hippocampal tissue, BxPC-3 pancreatic cancer cells, and U937 human histocytic lymphoma cells [9–13]. However, the effect of oridonin on liver inflammation remains largely unknown, and our study is the first to examine its role in hepatic stellate cells (HSCs).

Quiescent HSCs are nonproliferative and are typically localized within the space of Disse and function as the principal storage site of retinoids in the liver. Upon activation, HSCs proliferate, and are primarily characterized as the main effector cells for liver fibrosis, due to their capacity to trans-differentiate into collagen-producing myofibroblasts. More recent studies have elucidated the fundamental role of HSCs not only in hepatic fibrogenesis but also in liver immunology. HSCs have been reported to respond to many immunological triggers via toll-like receptors (TLR) (e.g., TLR4, TLR9) as well as transduction signals through pathways and mediators traditionally found in immune cells, such as NF- $\kappa$ B and the Hedgehog (Hh) pathways or inflammasome activation [14–16]. Activated HSCs are identified as a versatile source of many soluble immunologically active factors including cytokines and chemokines and may act as antigen presenting cells. After liver injury, HSCs are important sensors of altered tissue integrity and initiators of innate immune cell activation [17]. Previously, our group demonstrated the antifibrogenic effects of oridonin and its analogs in activated HSC lines via inhibition of cell proliferation and suppression of extracellular matrix expression, such as collagen type I and fibronectin [18–20]. In the present study, we determined the immunomodulatory effects of oridonin with the activated human HSC line LX-2. Our main objective was to examine the effects and molecular mechanism of oridonin on proinflammatory mediators and adhesion molecules stimulated by lipopolysaccharide (LPS), which is dramatically increased in portal venous blood after serious injuries. We hypothesized that oridonin would inhibit the LPS-induced inflammatory response in HSCs.

## 2. Materials and Methods

**2.1. Reagents.** All cell culture mediums and trypsin were purchased from Life Technology Corp. (Carlsbad, CA). We purchased oridonin from Sigma-Aldrich (St. Louis, MO). Hsp70 substrate binding inhibitor PES-CI was from EMD Millipore (Now is Millipore Sigma). The following primary antibodies were used: rabbit anti- NF- $\kappa$ B p65 (#8242), rabbit anti- I $\kappa$ B $\alpha$  (#4814), rabbit anti- IKK- $\beta$  (#8943), rabbit anti- IKK $\alpha$  (#11930), rabbit anti-phospho I $\kappa$ B $\alpha$  Ser32 (Cat#2859),

and rabbit anti-Glyceraldehyde 3-phosphate dehydrogenase (GADPH) (#5174) were from Cell Signaling Technology Inc., Danvers, MA); mouse anti-IL-1 $\beta$  (sc-7884), mouse anti-ICAM-1 (sc-8439), VCAM-1(sc-8304), and goat anti-Lamin A (sc-71481) were from Santa Cruz Biotechnology(Santa Cruz, CA); mouse anti-Topo II  $\beta$  (#3611492) was from BD Bioscience (San Jose, CA); rabbit anti-phospho IKK $\alpha$ / $\beta$  (ab195907) was abcam (Cambridge, MA).

**2.2. Cell Culture.** As described in previous publications, the human immortalized HSC line LX-2 immortalized HSC line was a gift from Dr. Scott Friedman (Mount Sinai Medical Center, New York) and cultured at 37°C with 5% CO<sub>2</sub> in Dulbecco's modified Eagle's medium (DMEM) with a high glucose concentration (4.5 g/L) supplemented with 5% fetal bovine serum (FBS) and 1% penicillin/streptomycin. [20, 21]. Within 6 weeks of culture from liquid nitrogen, all experiments were performed.

**2.3. Nuclear Protein Extraction and NF- $\kappa$ B p65 DNA-Binding Activity.** Nuclear protein was isolated with NE-PER nuclear and cytoplasmic extraction reagent (Pierce Biotechnology; Rockford, IL) according to the instructions of the manufacturer. The Trans-AM NF- $\kappa$ B p65 Transcription Factor kit was purchased from Active Motif North America (Carlsbad, CA) and the manufacturer's instructions were followed in order to quantify the DNA binding activity of NF- $\kappa$ B. The wild-type consensus oligonucleotide was used as a competitor for NF- $\kappa$ B binding, as according to the instructions. This competition assay confirms that the protein subunits binding to the plate are specific for the NF- $\kappa$ B consensus binding sequence and is used as a control for each cell type studied. The samples were analyzed in duplicate and repeated at least three times.

**2.4. Western Immunoblotting.** As described in previous publications [20, 21], RIPA buffer (Thermo Fischer Scientific, Inc., Waltham, MA) with 1% Halt protease inhibitor cocktail and 1% Halt phosphatase inhibitor cocktails (Thermo Fischer Scientific, Inc., Waltham, MA) was used to prepare whole cell extracts. NE-PER nuclear and cytoplasmic extraction reagent (Pierce Biotechnology) were used to prepare nuclear extracts. The Bradford method was used to measure and quantify the protein concentration. 10-30 g of protein were fractionated by sodium dodecyl sulfate-polyacrylamide gel electrophoresis (SDS-PAGE) (Life Technologies Corporation, Grand Island, NY) under denaturing conditions and then electro-transferred to a polyvinylidene fluoride (PVDF) membrane. After being blocked with Blocking buffer (LI-COR, Inc., Lincoln, NE) the membrane was probed with the indicated primary antibody (Ab) diluted with blocking buffer. Membranes were washed three times with Phosphate buffered saline with 0.1% Tween 20 (PBST) and incubated 1h with IRDye 680-conjugated anti-mouse or IRDye 800-conjugated anti-rabbit Ab (LI-COR, Inc., Lincoln, NE). Finally, the membranes were washed three times with PBST, and signals were scanned and visualized by Odyssey Infrared Imaging System (LI-COR, Inc., Lincoln, NE). Densitometric analysis

was performed on the proteins of interest and normalized to GAPDH by LI-COR Image Studio software (LICOR, Inc., Lincoln, NE).

**2.5. Immunofluorescence Staining.** After indicated treatments, the cells were fixed with 4% paraformaldehyde in PBS for 20 min, and permeabilized with 0.3% Triton-100 in PBS, followed by incubation in blocking buffer (5% goat serum, 0.1% triton X-100 in PBS) and incubated with primary antibodies in incubation buffer (0.1% triton X-100 and 1% goat serum in PBS) overnight at 4°C. After three times washing with PBS, cells were stained with Alexa Fluor 488-conjugated Goat anti-rabbit IgG (Invitrogen) in incubation buffer for 1 h. After removing secondary antibody, the cells were fixed and counterstained with DAPI. The cells were visualized by Nikon fluorescence LSM510 confocal microscope at 20X magnification.

**2.6. Enzyme-Linked Immunosorbent Assay (ELISA).** Twenty-four hours after cell treatment, the culture supernatant was corrected for subsequent measurement of cytokines secretion. The supernatants were measured using commercially available human IL-6 ELISA kit (#KHC0061) and human MCP-1 ELISA kit (#KHC1011) from Life Technologies (Frederick, MD) according to the instructions of the manufacturer. The total amount IL-6 and MCP-1 in the cell medium was normalized to the total amount of protein in the viable cell pellets. The samples were analyzed in duplicate and repeated at least three times.

**2.7. Statistical Analysis.** Statistical analysis was performed with GraphPad Prism 7.0 from GraphPad Software Inc. (La Jolla, CA, USA) as previously described [21]. Where indicated, one-way ANOVA with Sidak's multiple comparisons test were used. All figures are presented as mean  $\pm$  SEM, with the following significance denotation \*:  $P < 0.05$ , \*\*:  $P < 0.01$ , and \*\*\*:  $P < 0.001$ .

### 3. Results

**3.1. Ordonin Inhibits LPS-Induced Inflammatory Cytokines and Cell Adhesion Molecules.** To test the anti-inflammatory effects of oridonin in human activated HSCs, we treated LX-2 cells with either LPS alone, or with LPS and varying concentrations of oridonin. The concentrations of oridonin used are 2.5, 5, and 7.5  $\mu$ M because those concentrations represent the upper dose limit before cell viability in LX-2 cells is affected and the concentrations at which cell viability begins to be affected [18]. In addition, the dose associated with significant levels of apoptosis in LX-2 cells is 6  $\mu$ M [18]. ELISA was used to determine proinflammatory cytokines secretion. Ordonin significantly decreased LPS-induced IL-6 and MCP-1 secretion in a dose-dependent manner, with significantly decreased levels of IL-6 and MCP-1 for all concentrations of oridonin ( $P < 0.001$ ). (Figures 1(a) and 1(b)). The effect of oridonin on LPS-stimulated IL-1 $\beta$  expression was determined by Western blot. As shown in Figure 1(c), LPS increased IL-1 $\beta$  protein in a time-dependent

fashion and oridonin treatment inhibited LPS-stimulated IL-1 $\beta$  expression in a dose-dependent manner. LPS-induced levels of IL-1 $\beta$  were significantly increased compared to control at 9 hours ( $P < 0.05$ ). LPS-induced levels of IL-1 $\beta$  at 9 hours were significantly decreased with addition of oridonin 7.5  $\mu$ M ( $P < 0.05$ ).

It has been reported that HSCs are involved in liver inflammation via upregulation of cell surface leukocyte adhesion molecules expression in response to proinflammatory stimulators [22]. To assess the expression of the adhesion molecules ICAM-1 and VCAM-1, total protein was extracted from LPS and oridonin treated LX-2 cells and Western blot was performed. ICAM-1 and VCAM-1 are transmembrane proteins expressed on vascular endothelial cells that serve as a ligand for integrins on immune cells such as lymphocytes, monocytes, eosinophils, and basophils. They serve to promote adhesion and migration of these inflammatory cells from the vasculature into tissues. As shown in Figure 1(d), LPS-induced expression of ICAM-1 and VCAM-1 was significantly increased compared to control ( $P < 0.05$  and  $P < 0.001$ , respectively). Pretreatment with oridonin 7.5  $\mu$ M significantly decreased LPS-induced expression of ICAM-1 ( $P < 0.05$ ) and pretreatment with oridonin 5.0  $\mu$ M and 7.5  $\mu$ M significantly reduced LPS-induced expression of VCAM-1 ( $P < 0.01$ ). In addition, our data demonstrated TLR4 inhibitor TAK-244 and NF- $\kappa$ B chemical inhibitors Bortezomib and MG132 blocked LPS-stimulated proinflammatory mediators in LX-2 cells, suggesting the TLR4/NF- $\kappa$ B pathway is involved (data not shown).

**3.2. Ordonin Blocks LPS-Induced NF- $\kappa$ Bp65 Nuclear Translocation and DNA Binding Activity.** NF- $\kappa$ B has been demonstrated to be a key component of inflammatory mediator production and plays an important role in liver inflammation. The nuclear translocation of NF- $\kappa$ B subunit p65 is a crucial step in NF- $\kappa$ B pathway activation. Thus, we determined the effects of oridonin on NF- $\kappa$ B p65 translocation from cytoplasm to nucleus with isolated nuclear protein of LX-2 cells. As shown in Figure 2(a), the expression of p65 was markedly increased in the nucleus after 1  $\mu$ g/mL of LPS treatment for 30 min and reverted to near normal levels with pretreatment with oridonin. This finding was confirmed by immunofluorescence assay, as shown in Figure 2(b). NF- $\kappa$ B p65 sub-cellular localization demonstrated that LPS administration caused NF- $\kappa$ B p65 nuclear translocation and it was prevented by pretreatment with oridonin. To examine whether oridonin affected LPS-induced NF- $\kappa$ B DNA binding activity, we conducted the TransAM NF- $\kappa$ B p65 ELISA assay. As shown in Figure 2(c), LPS-induced NF- $\kappa$ B subunit p65 DNA binding activity was significantly increased compared to control ( $P < 0.001$ ). Pretreatment with oridonin significantly decreased NF- $\kappa$ B p65 DNA binding activity ( $P < 0.001$ ).

**3.3. Ordonin Affected LPS-Stimulated IKKs/I $\kappa$ B $\alpha$ /NF- $\kappa$ B Pathway.** To further elucidate how NF- $\kappa$ B is affected by oridonin, the protein levels of upstream signaling molecules IKK $\alpha$ / $\beta$  and I $\kappa$ B were measured. First, we investigated the effects of oridonin on I $\kappa$ B $\alpha$  turnover in response to

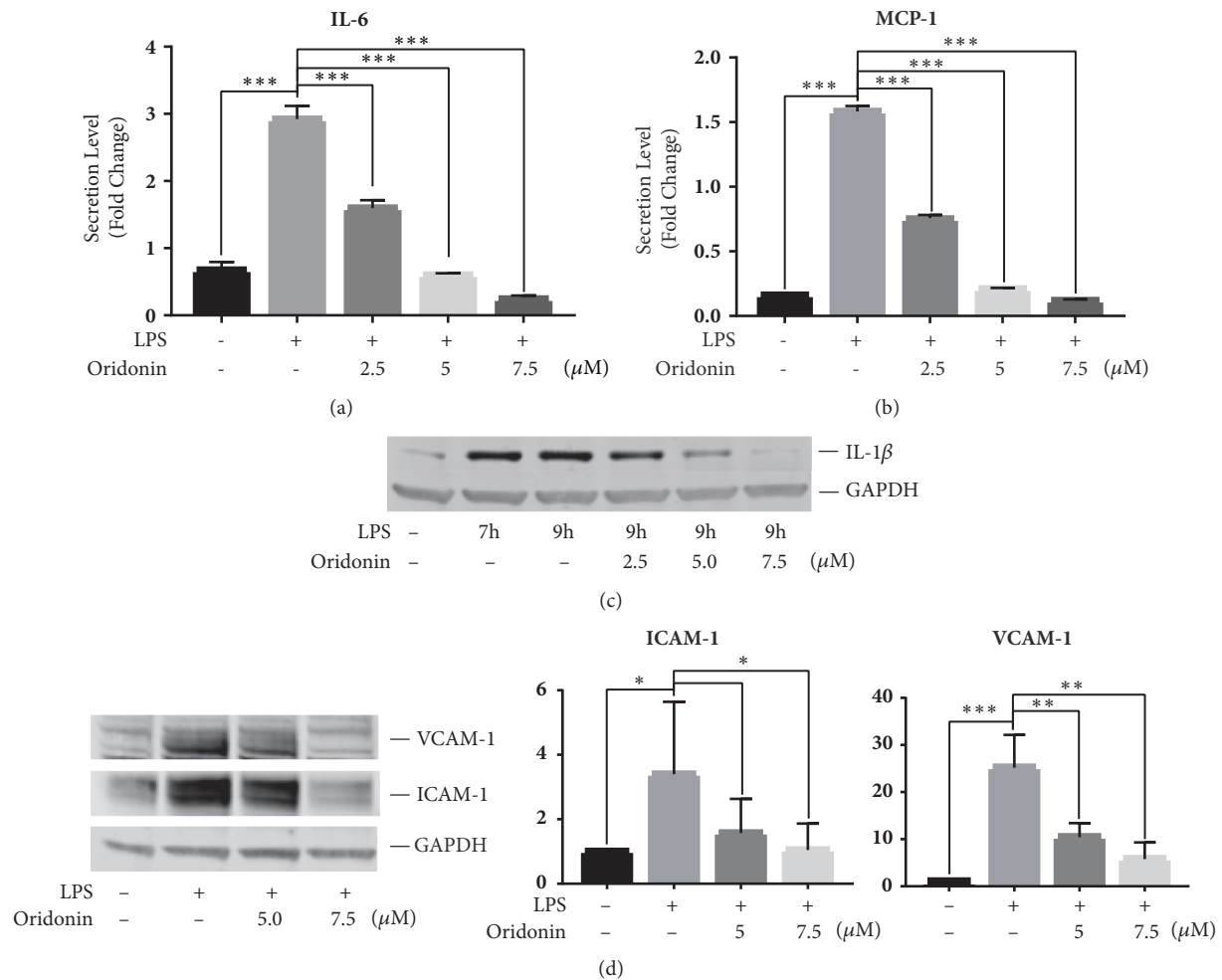


FIGURE 1: Oridonin inhibits LPS-induced pro-inflammatory cytokines and cell adhesion molecules. LX-2 cells were pretreated with oridonin (2.5, 5, or 7.5 μM) for 1 h, then stimulated with LPS (1 μg/mL) for 24 h. Cell culture medium was collected for ELISA of IL-6 (a) and MCP-1 (b). Cells were pretreated with oridonin at different concentrations for 1 h and then incubated with LPS (1 μg/mL) for 7 or 9 h and total proteins were examined by Western blots with antibody of IL-1β (c), or ICAM-1, VCAM-1 (d). GAPDH was used as internal control. Densitometric analyses of bands were quantified and data expressed as fold of control normalized to GAPDH. All Western blot pictures are the representative of at least 3.

LPS. As shown in Figure 3(a), LPS treatment for 30 min promoted an increase in the phosphorylation of IκBα with a concomitant reduction in cellular IκBα protein levels. Pretreatment with oridonin prevented LPS-mediated IκBα phosphorylation, while cellular IκBα protein level was maintained.

As shown in Figure 3(b), the level of total IKKα/β was high in all conditions and the basal level of phospho-IKKα/β(p-IKKα/β) was very low. LPS stimulation markedly increased the level of p-IKKα/β, but oridonin treatment suppressed LPS-stimulated the level of p-IKKα/β.

**3.4. Oridonin and PES-CI Synergistically Inhibited LPS-Induced Proinflammatory Cytokines.** It has been established that heat shock protein (Hsp70) is involved in the LPS-induced inflammatory response. A small molecular compound 2-phenylethanesulfonamide (PES), an inhibitor of

Hsp70 substrate binding activity, has been reported to attenuate the induction of proinflammatory factors and prevents LPS-induced liver injury [23]. PES-CI is a derivative of PES that demonstrates improved anticancer activity [24, 25]. In the current study, we combined oridonin with PES-CI to treat LX-2 cells at a relatively low concentration (2.5 μM). As shown in Figures 4(a) and 4(b), both oridonin 2.5 μM alone and PES-CI 2.5 μM alone significantly decreased LPS-induced IL-6 and MCP-1 secretion ( $P < 0.001$ ). Combination treatment with both PES-CI 2.5 μM and oridonin 2.5 μM significantly reduced IL-6 and MCP-1 secretion compared to either treatment alone ( $P < 0.001$ ).

**3.5. The Inhibitory Effects of PES-CI on LPS-Induced NF-κB Signaling Were Enhanced by Oridonin.** To evaluate the effect of combined treatment of oridonin and PES-CI on IKKs/IκBα/NF-κB pathway, LX-2 cells were treated with

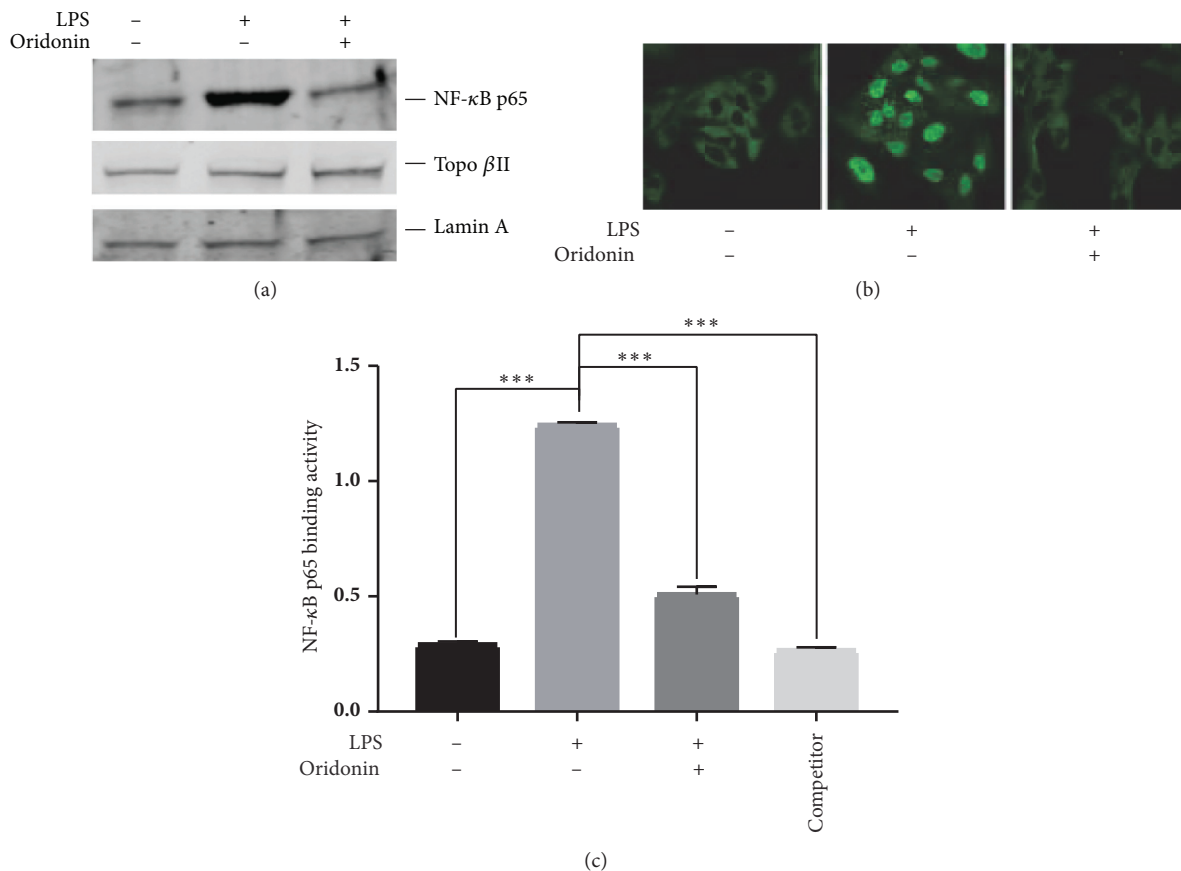


FIGURE 2: Oridonin suppresses LPS-induced NF-κB p65 nuclear translocation and DNA binding. LX-2 cells were pretreated with 7.5 μM of oridonin for 1 h, then stimulated with LPS (1 μg/mL) for 30 min. Nuclear protein was isolated for Western blot assay using NF-κB p65 antibody. Lamin A and Topo βII were used as internal control to normalize the nuclear p65 protein (a). The subcellular translocation of NF-κB p65 was imaged by immunofluorescence assay (b). DNA binding activity of NF-κB p65 was analyzed by TransAM p65 ELISA kit with 10 μg of nuclear proteins (c) and 20 pmol of the wild-type NF-κB oligonucleotide as competitor (lane 4). Data are representative of 3 independent experiments.

PES-CI at 2.5 μM alone or in combination with oridonin. As shown in Figure 5(a), PES-CI treatment attenuated LPS-induced nuclear NF-κB p65 accumulation; combined treatment markedly enhanced the effects of PES-CI. This observation was confirmed by immunofluorescence staining assay (Figure 5(b)). NF-κB DNA binding activity was determined by TransAM NF-κB p65 DNA binding ELISA. As shown in Figure 5(c), both oridonin (2.5 μM) alone and PES-CI (2.5 μM) alone significantly decreased LPS-induced p65 DNA binding ( $P < 0.001$ ). Combination treatment with both PES-CI (2.5 μM) and oridonin (2.5 μM) led to further significant decreases in p65 DNA binding activity compared to either treatment alone ( $P < 0.001$ ). Interestingly, treatment with either oridonin or PES-CI alone partially recovered LPS-induced IκBα degradation. However, total recovery was found with combined treatment (Figure 5(d)). Furthermore, single-agent treatment suppressed LPS-induced pIKKβ and partially inhibited LPS-induced pIKKα, while combined treatment blocked both LPS-induced pIKKα and pIKKβ (Figure 5(d)).

#### 4. Discussion

There is increasing evidence showing HSCs not only play an important role in hepatic fibrosis but also contribute to liver inflammation. Activated HSCs promote hepatic inflammation by production of potent chemokines, such as MCP-1 [26]. Endotoxin, such as LPS, was reported to induce IL-8, MCP-1, and MIP-2 in activated HSCs. HSCs also contribute to hepatic inflammation by induction of cell surface of leukocyte adhesion molecules ICAM-1 and VCAM-1 in response to proinflammatory stimulators [22]. Thus, HSCs may participate in hepatic inflammation via enhancement of monocyte and neutrophil transmigration out of the hepatic sinusoid and into the liver parenchyma with endotoxin-involved liver injury. Oridonin, a major ingredient of the traditional Chinese medicinal herb *Rabdosia rubescens*, has anti-inflammatory activity in a variety of cell types. Oridonin has been shown to form a covalent bond with cysteine 279 of the NLRP3 inflammasome, thereby specifically inhibiting NLRP3 inflammasome activation and



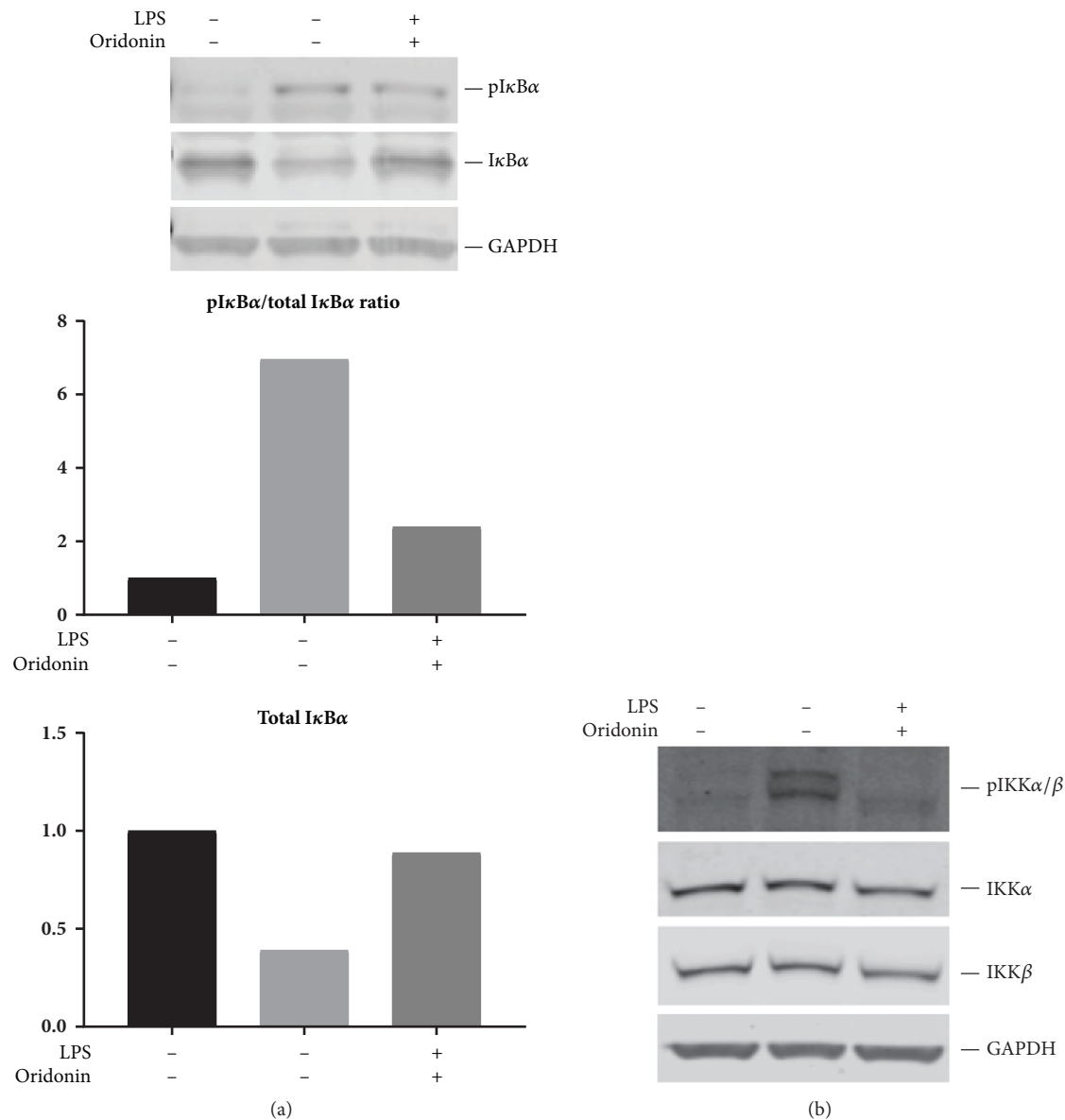


FIGURE 3: Oridonin affected LPS-stimulated IKKα/β and IκBα phosphorylation and IκBα degradation. LX-2 cells were treated with 7.5 μM of oridonin for 1 h followed by LPS (1 μg/mL) for 30 min. Total proteins were examined by western blots using antibody pIκBα and IκBα (a), or pIKKα/β, IKKα and IKKβ (b). GAPDh was used as internal control. Densitometric analyses of bands were quantified and data expressed as fold of control normalized to GAPDH. All Western blot pictures are the representative of at least 3 independent experiments.

assembly and suppressing NLRP3-dependent inflammation [27]. NLRP3 is a central inhibitor of innate immunity and inflammation and has been shown to mediate NF-κB activation, making this interaction the likely mechanism of action [28]. Our previous work has focused on the antifibrogenic properties of oridonin and its analogues; however, its anti-inflammatory properties have not yet been fully elucidated in HSCs [18–20]. These previous studies focused on the effect of oridonin on HSC apoptosis, apoptotic markers, and cell-cycle arrest markers without exploring the mechanism of

action or hepatic inflammation in response to injury. In the present study, our data revealed that oridonin inhibits LPS-induced proinflammatory mediators MCP-1, IL-6, and IL-1β production and adhesion molecules ICAM-1 and VCAM-1 expression in the activated human HSC line LX-2. Simultaneously, we demonstrated that oridonin inhibited LPS-induced NF-κB p65 nuclear translocation and DNA binding activity, while suppressing LPS-stimulated phosphorylation of IKKα/β and IκBα as well as preventing cellular IκBα degradation. These results suggest that oridonin not

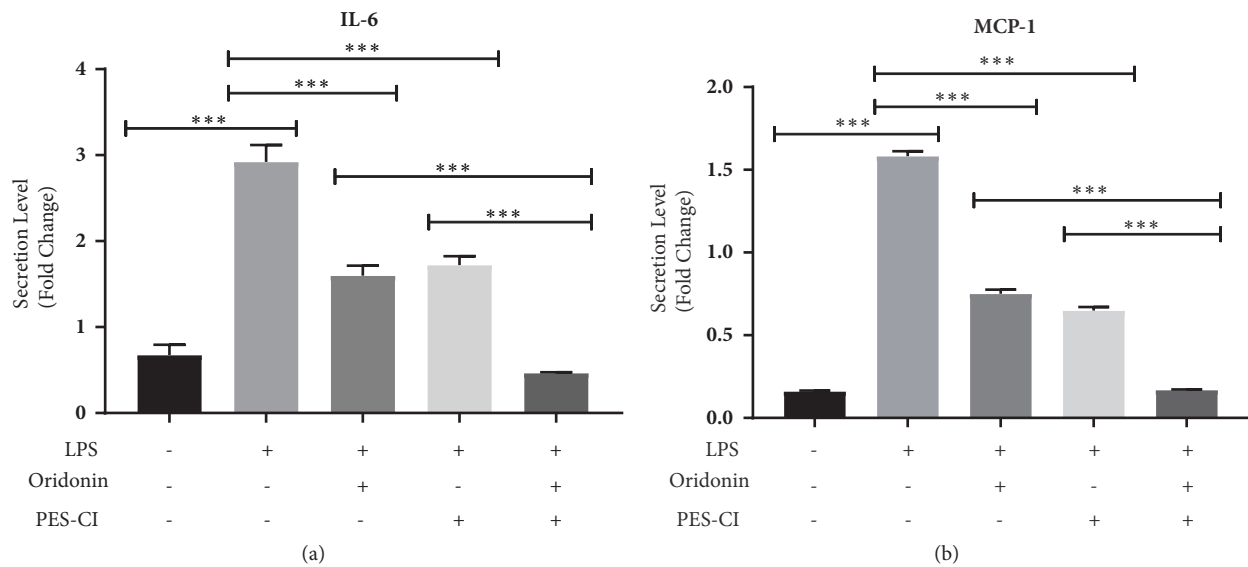


FIGURE 4: *Oridonin and PES-CI synergistically inhibit LPS-induced proinflammatory cytokines.* LX-2 cells were pretreated with oridonin (2.5  $\mu$ M), or PES-CI (2.5  $\mu$ M) or combination of two agents for 1 h, then stimulated with LPS (1  $\mu$ g/mL) for 24 h. Cell culture medium was collected for ELISA of IL-6 (a) and MCP-1 (b). Data are representative of 3 independent experiments.

only has potent antifibrogenetic properties but also has effective anti-inflammatory activity in the liver through inhibition of the NF- $\kappa$ B pathway.

Liver injury induced by septic shock is characterized by monocyte and neutrophil infiltration within the parenchymal space. MCP-1, IL-6, and IL-1 $\beta$  are potent activators for monocytes and neutrophils. The recruitment of leukocytes to the site of inflammation not only involves chemoattractant factors, such as MCP-1, but also requires adhesion molecules such as ICAM-1 to anchor the leukocytes at the site. Together, these chemokines and adhesion molecules coordinate the migration of leukocytes to the sites of inflammation and injury. Therefore, the inhibitory effects of oridonin for both LPS-induced MCP-1 and ICAM-1 production indicate that oridonin may be an effective compound for treatment of liver injury. A recent paper from Huang et al. confirmed our findings demonstrating that oridonin blocks inflammation via inhibition of NF- $\kappa$ B and MAPK [29]. Their results also demonstrated the blockage of ICAM-1 and VCAM-1. This work was done in human umbilical vein endothelial cells, and our study remains the only one that demonstrates these effects in HSCs. Further studies are necessary to determine the effects of oridonin on other cell types in liver, such as Kupffer cells, hepatocytes, and sinusoidal endothelial cells.

Stimulation with endotoxin leads to activation of NF- $\kappa$ B and production of proinflammatory cytokines. Oridonin is considered to be a natural inhibitor of NF- $\kappa$ B in different cell lines, including Jurkat, RAW264.7 [6], human CD4(+) T cells [30], rat primary microglia [7], and others. Generally, activation of NF- $\kappa$ B involves two important steps: (a) phosphorylation and subsequent degradation of I $\kappa$ B $\alpha$  by I $\kappa$ B kinases (IKKs), which releases of NF- $\kappa$ B, and (b) nuclear translocation of the activated NF- $\kappa$ B subunit p65 and its binding to the target genes' promoter which regulates

gene expression. The molecular mechanisms for oridonin's inhibition of NF- $\kappa$ B activity are still not fully understood. It was reported that oridonin interfered with NF- $\kappa$ B DNA binding activity in a number of cell types. Notably, oridonin has an impact on the DNA binding activity and nuclear translocation of NF- $\kappa$ B without affecting I $\kappa$ B $\alpha$  phosphorylation and degradation after TNF $\alpha$  treatment in HepG2 cells [31]. In addition, oridonin inhibited NF- $\kappa$ B DNA binding without affecting its nuclear translocation, I $\kappa$ B phosphorylation, and degradation in Jurkat cells [6]. In MCF-10A cells, decreases in p65 or p50 forms of NF- $\kappa$ B and I $\kappa$ B were found; however these changes were not seen in MCF-7 cells [32]. All these findings suggest that oridonin regulates NF- $\kappa$ B pathway components in a cell type specific manner. Our data demonstrated that oridonin suppressed LPS-induced NF- $\kappa$ B p65 nuclear translocation and DNA binding, while impairing LPS-induced IKK/I $\kappa$ B $\alpha$ /NF- $\kappa$ B signaling in LX-2 cells. The more detailed molecular mechanism of how oridonin regulates the NF- $\kappa$ B pathway should be further evaluated.

The results of the current study showed that a combination treatment with oridonin and PES-CI at relatively low dosage (2.5  $\mu$ M) synergistically inhibited LPS-induced proinflammatory cytokines, suggesting that combined treatment with oridonin and PES-CI could be a useful therapeutic approach for liver inflammation. Moreover, combined treatment significantly increased the suppression of LPS-induced NF- $\kappa$ B p65 nuclear translocation and DNA binding activity compared to each compound alone. Interestingly, each agent only inhibited LPS-induced phosphorylation of IKK $\beta$ , while combination treatment inhibited LPS-induced phosphorylation of both IKK $\alpha$  and IKK $\beta$ .

The inhibitory effect of oridonin on the NF- $\kappa$ B pathway in LX-2 cells suggests that oridonin has a potent

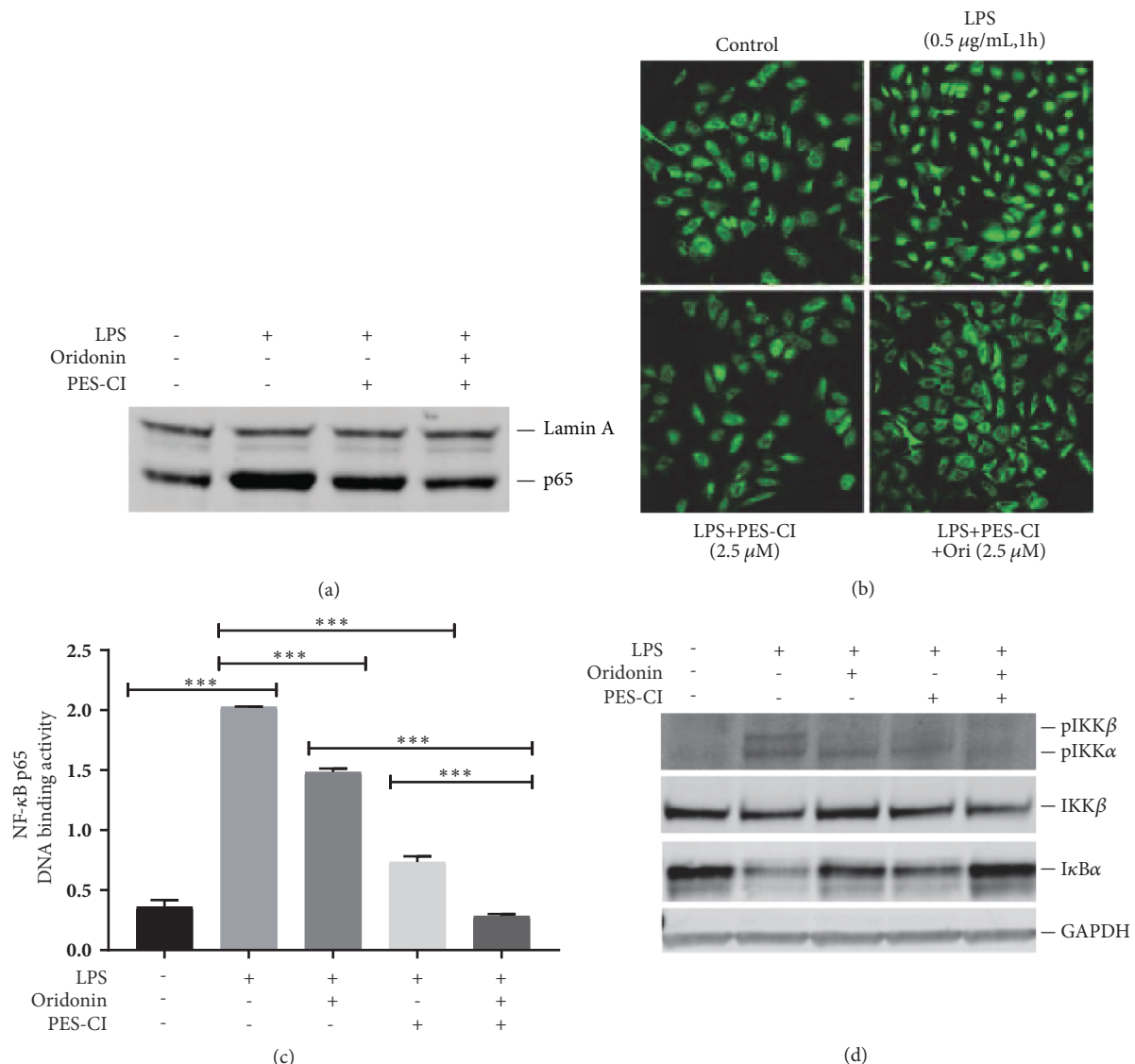


**FIGURE 5: The inhibitory effects of PES-CI on LPS-induced NF- $\kappa$ B signaling was enhanced by oridonin.** LX-2 cells were pretreated with 2.5  $\mu$ M of oridonin, PES-CI or combination of two agents for 1 h, then stimulated with LPS (1  $\mu$ g/mL) for 30 min. Nuclear protein was isolated for Western blot assay using NF- $\kappa$ B p65 antibody. Lamin A was used as internal control to normalize the nuclear p65 protein (a). The subcellular translocation of NF- $\kappa$ B p65 was imaged by immunofluorescence assay (b). DNA binding activity of NF- $\kappa$ B p65 was analyzed by TransAM p65 ELISA kit with 10  $\mu$ g of nuclear proteins (c). Total proteins were examined by Western blots using antibody pIKK $\beta$ , I $\kappa$ B $\alpha$ , or pIKK $\alpha$ / $\beta$  (d). Densitometric analyses of bands were quantified and data expressed as fold of control normalized to GAPDH. Data are representative of 3 independent experiments.

anti-inflammatory effect in the liver. Oridonin therefore represents a potential drug candidate for a hepatic anti-inflammatory.

### Data Availability

The data used to support the findings of this study are available from the corresponding author upon request.

### Conflicts of Interest

None of the authors has financial interest in any of the products, devices, or drugs mentioned in this manuscript.

### Authors' Contributions

Claire B. Cummins and Xiaofu Wang contributed equally to this work.

### Acknowledgments

Christian Sommerhalder and Frederick J. Bohanon were supported by a training grant from the National Institutes of Health (T32 GM008256), and Omar Nunez Lopez and Claire B. Cummins were supported by a fellowship award from the Department of Surgery at the University of Texas Medical Branch. These studies were also supported in part by

a research award made to Ravi S. Radhakrishnan from the Department of Surgery at the University of Texas Medical Branch.

## References

- [1] Q. B. Han, W. L. Xiao, Y. H. Shen, and H. D. Sun, "Ent-Kaurane Diterpenoids from *Isodon rubescens* var. *rubescens*," *Chemical and Pharmaceutical Bulletin*, vol. 52, no. 6, pp. 767–769, 2004.
- [2] W. Xu, J. Sun, T.-T. Zhang et al., "Pharmacokinetic behaviors and oral bioavailability of oridonin in rat plasma," *Acta Pharmacologica Sinica*, vol. 27, no. 12, pp. 1642–1646, 2006.
- [3] C. Li, E. Wang, Y. Cheng, and J. Bao, "Oridonin: an active diterpenoid targeting cell cycle arrest, apoptotic and autophagic pathways for cancer therapeutics," *The International Journal of Biochemistry & Cell Biology*, vol. 43, no. 5, pp. 701–704, 2011.
- [4] W. Tian and S.-Y. Chen, "Recent advances in the molecular basis of anti-neoplastic mechanisms of oridonin," *Chinese Journal of Integrative Medicine*, vol. 19, no. 4, pp. 315–320, 2013.
- [5] A.-P. Hu, J.-M. Du, J.-Y. Li, and J.-W. Liu, "Oridonin promotes CD4<sup>+</sup>/CD25<sup>+</sup> Treg differentiation, modulates Th1/Th2 balance and induces HO-1 in rat splenic lymphocytes," *Inflammation Research*, vol. 57, no. 7, pp. 163–170, 2008.
- [6] T. Ikezoe, Y. Yang, K. Bandobashi et al., "Oridonin, a diterpenoid purified from *Rabdosiarubescens*, inhibits the proliferation of cells from lymphoid malignancies in association with blockade of the NF-kappa B signal pathways," *Molecular Cancer Therapeutics*, vol. 4, no. 4, pp. 578–586, 2005.
- [7] Y. Xu, Y. Xue, Y. Wang, D. Feng, S. Lin, and L. Xu, "Multiple-modulation effects of Oridonin on the production of proinflammatory cytokines and neurotrophic factors in LPS-activated microglia," *International Immunopharmacology*, vol. 9, no. 3, pp. 360–365, 2009.
- [8] G.-B. Zhou, H. Kang, L. Wang et al., "Oridonin, a diterpenoid extracted from medicinal herbs, targets AML1-ETO fusion protein and shows potent antitumor activity with low adverse effects on t(8;21) leukemia in vitro and in vivo," *Blood*, vol. 109, no. 8, pp. 3441–3450, 2007.
- [9] L. Zang, Q. Xu, Y. Ye et al., "Autophagy enhanced phagocytosis of apoptotic cells by oridonin-treated human histocytic lymphoma U937 cells," *Archives of Biochemistry and Biophysics*, vol. 518, no. 1, pp. 31–41, 2012.
- [10] R.-Y. Chen, B. Xu, S.-F. Chen et al., "Effect of oridonin-mediated hallmark changes on inflammatory pathways in human pancreatic cancer (BxPC-3) cells," *World Journal of Gastroenterology*, vol. 20, no. 40, pp. 14895–14903, 2014.
- [11] S. Wang, H. Yang, L. Yu et al., "Oridonin Attenuates A $\beta$ 1–42-Induced Neuroinflammation and Inhibits NF- $\kappa$ B Pathway," *PLoS ONE*, vol. 9, no. 8, p. e104745, 2014.
- [12] Q. Q. Liu, H. L. Wang, K. Chen et al., "Oridonin derivative ameliorates experimental colitis by inhibiting activated T-cells and translocation of nuclear factor-kappa B," *Journal of Digestive Diseases*, vol. 17, no. 2, pp. 104–112, 2016.
- [13] J. Li, L. Bao, D. Zha et al., "Oridonin protects against the inflammatory response in diabetic nephropathy by inhibiting the TLR4/p38-MAPK and TLR4/NF- $\kappa$ B signaling pathways," *International Immunopharmacology*, vol. 55, pp. 9–19, 2018.
- [14] B. Schnabl, K. Brandl, M. Fink et al., "A TLR4/MD2 fusion protein inhibits LPS-induced pro-inflammatory signaling in hepatic stellate cells," *Biochemical and Biophysical Research Communications*, vol. 375, no. 2, pp. 210–214, 2008.
- [15] H. Wang, S. Liu, Y. Wang, B. Chang, and B. Wang, "Nod-like receptor protein 3 inflammasome activation by *Escherichia coli* RNA induces transforming growth factor beta 1 secretion in hepatic stellate cells," *Bosnian Journal of Basic Medical Sciences*, vol. 16, pp. 126–131, 2016.
- [16] H. Wobser, C. Dorn, T. S. Weiss et al., "Lipid accumulation in hepatocytes induces fibrogenic activation of hepatic stellate cells," *Cell Research*, vol. 19, no. 8, pp. 996–1005, 2009.
- [17] S. Kumar, J. Wang, S. K. Shanmukhappa, and C. R. Gandhi, "Toll-like receptor 4-independent carbon tetrachloride-induced fibrosis and lipopolysaccharide-induced acute liver injury in mice: role of hepatic stellate cells," *The American Journal of Pathology*, vol. 187, no. 6, pp. 1356–1367, 2017.
- [18] F. J. Bohanon, X. Wang, C. Ding et al., "Oridonin inhibits hepatic stellate cell proliferation and fibrogenesis," *Journal of Surgical Research*, vol. 190, no. 1, pp. 55–63, 2014.
- [19] F. J. Bohanon, X. Wang, B. M. Graham et al., "Enhanced effects of novel oridonin analog CYD0682 for hepatic fibrosis," *Journal of Surgical Research*, vol. 199, no. 2, pp. 441–449, 2015.
- [20] F. J. Bohanon, X. Wang, B. M. Graham et al., "Enhanced anti-fibrogenic effects of novel oridonin derivative CYD0692 in hepatic stellate cells," *Molecular and Cellular Biochemistry*, vol. 410, no. 1–2, pp. 293–300, 2015.
- [21] C. Cummins, X. Wang, O. Nunez Lopez et al., "Luteolin-mediated inhibition of hepatic stellate cell activation via suppression of the STAT3 pathway," *International Journal of Molecular Sciences*, vol. 19, no. 6, 2018.
- [22] T. Knittel, C. Dinter, D. Kobold et al., "Expression and regulation of cell adhesion molecules by hepatic stellate cells (HSC) of rat liver: involvement of HSC in recruitment of inflammatory cells during hepatic tissue repair," *The American Journal of Pathology*, vol. 154, no. 1, pp. 153–167, 1999.
- [23] C. Huang, J. Wang, Z. Chen, Y. Wang, and W. Zhang, "2-phenylethanesulfonamide prevents induction of pro-inflammatory factors and attenuates LPS-induced liver injury by targeting NHE1-Hsp70 complex in mice," *PLoS ONE*, vol. 8, no. 6, Article ID e67582, 2013.
- [24] A. Budina-Kolomets, G. M. Balaburski, A. Bondar, N. Beeharry, T. Yen, and M. E. Murphy, "Comparison of the activity of three different HSP70 inhibitors on apoptosis, cell cycle arrest, autophagy inhibition, and HSP90 inhibition," *Cancer Biology & Therapy*, vol. 15, no. 2, pp. 194–199, 2014.
- [25] G. M. Balaburski, J. I.-J. Leu, N. Beeharry et al., "A modified HSP70 inhibitor shows broad activity as an anticancer agent," *Molecular Cancer Research*, vol. 11, no. 3, pp. 219–229, 2013.
- [26] H. Sprenger, A. Kaufmann, H. Garn, B. Lahme, D. Gerns, and A. M. Gressner, "Differential expression of monocyte chemoattractant protein-1 (MCP-1) in transforming rat hepatic stellate cells," *Journal of Hepatology*, vol. 30, no. 1, pp. 88–94, 1999.
- [27] H. He, H. Jiang, Y. Chen et al., "Oridonin is a covalent NLRP3 inhibitor with strong anti-inflammasome activity," *Nature Communications*, vol. 9, article 2550, 2018.
- [28] T. Kinoshita, R. Imamura, H. Kushiya, T. Suda, and D. M. Ojcius, "NLRP3 Mediates NF- $\kappa$ B Activation and Cytokine Induction in Microbially Induced and Sterile Inflammation," *PLoS ONE*, vol. 10, no. 3, Article ID e0119179, 2015.
- [29] W. Huang, M. Huang, H. Ouyang, J. Peng, and J. Liang, "Oridonin inhibits vascular inflammation by blocking NF-kappaB and MAPK activation," *European Journal of Pharmacology*, vol. 826, pp. 133–139, 2018.



- [30] M.-L. Cho, Y.-M. Moon, Y.-J. Heo et al., "NF- $\kappa$ B inhibition leads to increased synthesis and secretion of MIF in human CD4+ T cells," *Immunology Letters*, vol. 123, no. 1, pp. 21–30, 2009.
- [31] C. H. Leung, S. P. Grill, W. Lam, Q. B. Han, H. D. Sun, and Y. C. Cheng, "Novel mechanism of inhibition of nuclear factor-kappa B DNA-binding activity by diterpenoids isolated from *Isodon rubescens*," *MolPharmacol*, vol. 68, pp. 286–297, 2005.
- [32] T. Hsieh, E. K. Wijeratne, J. Liang, A. L. Gunatilaka, and J. M. Wu, "Differential control of growth, cell cycle progression, and expression of NF- $\kappa$ B in human breast cancer cells MCF-7, MCF-10A, and MDA-MB-231 by ponacidin and oridonin, diterpenoids from the chinese herb *Rabdosia rubescens*," *Biochemical and Biophysical Research Communications*, vol. 337, no. 1, pp. 224–231, 2005.

## Research Article

# Degalactotigonin, a Steroidal Glycoside from *Solanum nigrum*, Induces Apoptosis and Cell Cycle Arrest via Inhibiting the EGFR Signaling Pathways in Pancreatic Cancer Cells

Hoang Le Tuan Anh,<sup>1</sup> Phuong Thao Tran<sup>1</sup>,<sup>2</sup> Do Thi Thao,<sup>3</sup>  
Duong Thu Trang,<sup>4</sup> Nguyen Hai Dang<sup>1</sup>,<sup>4</sup> Pham Van Cuong,<sup>4</sup>  
Phan Van Kiem,<sup>4</sup> Chau Van Minh,<sup>4</sup> and Jeong-Hyung Lee<sup>2</sup>

<sup>1</sup>Mien Trung Institute for Scientific Research, Vietnam Academy of Science and Technology (VAST), 321 Huynh Thuc Khang, Hue city, Thua Thien Hue 531600, Vietnam

<sup>2</sup>Department of Biochemistry, College of Natural Sciences, Kangwon National University, Chuncheon, Gangwon-Do 200-701, Republic of Korea

<sup>3</sup>Institute of Biotechnology, VAST, 18 Hoang Quoc Viet, Cau Giay, Hanoi, Vietnam

<sup>4</sup>Advanced Center for Bio-Organic Chemistry, Institute of Marine Biochemistry, VAST, 18 Hoang Quoc Viet, Cau Giay, Hanoi, Vietnam

Correspondence should be addressed to Nguyen Hai Dang; [nguyenhd@imbc.vast.vn](mailto:nguyenhd@imbc.vast.vn) and Jeong-Hyung Lee; [jhlee36@kangwon.ac.kr](mailto:jhlee36@kangwon.ac.kr)

Received 11 September 2018; Accepted 4 November 2018; Published 16 December 2018

Guest Editor: Cinzia Forni

Copyright © 2018 Hoang Le Tuan Anh et al. This is an open access article distributed under the Creative Commons Attribution License, which permits unrestricted use, distribution, and reproduction in any medium, provided the original work is properly cited.

Degalactotigonin (1) and three other steroidal compounds solasodine (2), O-acetyl solasodine (3), and soladulcoside A (4) were isolated from the methanolic extract of *Solanum nigrum*, and their chemical structures were elucidated by spectroscopic analyses. The isolated compounds were evaluated for cytotoxic activity against human pancreatic cancer cell lines (PANC1 and MIA-PaCa2) and lung cancer cell lines (A549, NCI-H1975, and NCI-H1299). Only degalactotigonin (1) showed potent cytotoxicity against these cancer cell lines. Compound 1 induced apoptosis in PANC1 and A549 cells. Further study on its mechanism of action in PANC1 cells demonstrated that 1 significantly inhibited EGF-induced proliferation and migration in a concentration-dependent manner. Treatment of PANC1 cells with degalactotigonin induced cell cycle arrest at G0/G1 phase. Compound 1 induced downregulation of cyclin D1 and upregulation of p21 in a time- and concentration-dependent manner and inhibited EGF-induced phosphorylation of EGFR, as well as activation of EGFR downstream signaling molecules such as Akt and ERK.

## 1. Introduction

Pancreatic cancer is the 12th most common cancer worldwide and is the most seventh deathly related-cancer. Surgical resection and chemotherapeutics are the traditional treatment of pancreatic cancer. The recent success of chemotherapy treatments is based on the inhibition of tumor-associated specific pathways and commonly referred to as targeted agents [1]. For instances, some inhibitors of the epidermal growth factor receptors (EGFR) were approved by FDA for

the treatment of several cancer types including pancreatic cancer [2–4]. However, these commonly used techniques are frequently challenged in view of metastasis and other pathological changes. Therefore, the search for new antipancreatic cancer agents is important to reduce the mortality rate.

Overexpression of growth factors and their receptors, inactivation of tumor suppressor gene, or activation of oncogene is the stimulators for the growth of an aggressive cancer [5]. EGFR and its family members are the main components of a complex signaling cascade that regulates proliferation,

growth, migration, differentiation, and survival of cancer cells [6]. Thirteen known ligands that can activate the EGFR family include epidermal growth factor (EGF), amphiregulin (AR), betacellulin (BTC), transforming growth factor alpha (TGF- $\alpha$ ), epiregulin (EPR), epigen (EPG), neuregulins 1–6 (NRG), and heparin-binding EGF-like growth factor (HB-EGF) [7]. The activation of EGFR leads to the phosphorylation of specific tyrosine residues on the intracellular cytoplasmic tail, which results in the activation of corresponding signaling cascades critically in cell proliferation, survival, migration, and angiogenesis. EGFR then undergoes endocytosis to recycle or direct to lysosomes for degradation, resulting in the downregulation of EGFR signaling [8]. Receptor tyrosine kinases including EGFR, PDGFR $\alpha$  (platelet-derived growth factor receptor- $\alpha$ ), and VEGFR (vascular endothelial growth factor receptor) have been detected to be activated in pancreatic cancer. Noteworthy, overexpression of EGFR is found up to 90% in pancreatic cancer cells [9]. Though EGFR expression has been supported to growth and metastatic stages of cancer [10], its effects on survival is still a debate [11, 12]. Overall, EGFR is an emerging candidate for further research in pancreatic cancer therapy.

*Solanum nigrum* L. (Solanaceae) has been used in traditional medicine for the treatment of edema, diuretic, inflammation, mastitis, and hepatic cancer [13]. Recent studies showed that the aqueous extract of *S. nigrum* leaves induced autophagy and enhanced cytotoxicity of some chemotherapy drugs in HT-29 human colorectal carcinoma cells [14]. The antitumor properties of extracts from various parts of this plant have been reported [15–18]. Furthermore, the anti-inflammatory, antinociceptive, antineoplastic, antiulcerogenic, and antiviral activities of extracts and compounds of *S. nigrum* were demonstrated [19–25]. Studies on the chemical properties of this plants revealed that alkaloids, glycoproteins, flavonoids, and steroidal glycosides are the major contents, among which, the cytotoxicity of alkaloids and glycoproteins of *S. nigrum* were reported [26–30]. It is assumed that these contents mostly contribute to the antitumor properties of this plant [30–36]. The previous studies indicated that steroidal glycosides from *S. nigrum* are also the major constituents with potential anticancer activities [37–39]. Degalactotigonin, a steroidal glycoside of this plant, showed potent cytotoxicity against multiple cell lines [40]. This compound is considered to be the most cytotoxic steroidal glycoside isolated from *S. nigrum* to date. A recent report demonstrated that this compound suppressed the growth and metastasis of osteosarcoma [41]. In this study, we presented the isolation of some steroidal glycoside from the leaves of *S. nigrum* and evaluated their cytotoxic properties on human lung and pancreatic cell lines. We also investigated for the first time the mechanism of action of cytotoxic degalactotigonin in human pancreatic cancer cell line PANC1.

## 2. Materials and Methods

**2.1. Plant Materials.** The plant *S. nigrum* was collected in August 2015 at Thaibinh province, Vietnam, and was identified by Dr. Do Thanh Tuan, Thaibinh University of

Medicine and Pharmacy. The voucher specimen (TB16.2015) was deposited at the Herbarium of Mientrung Institute for Scientific Research (VAST) and Thaibinh University of Medicine and Pharmacy.

**2.2. Isolation of Compounds 1–4 from *Solanum nigrum*.** The whole plant of *S. nigrum* was air dried, ground to powder, and extracted with methanol at 50°C with the aid of ultrasonic (3 times x 1 h each). The organic layer was filtered and removed under vacuum to obtain the crude extract of methanol. This crude extract was suspended in hot distilled water (1.5 L) and successively partitioned with dichloromethane and ethyl acetate (3 times x 1.5 L each) to yield corresponding extracts, dichloromethane (SND, 30 g), ethyl acetate (SNE, 32 g), and water-soluble layer (SNW). The SNW layer was passed through a Diaion HP-20 column, washed with distilled water, and eluted with increasing volume of methanol in water (25%, 50%, 75%, and 100% of methanol) to obtain four subfractions, SNW1–SNW4. The subfraction SNW3 (2.5 g) was chromatographed on a silica gel column and eluted with solvent system of dichloromethane/methanol/water (2.0/1.0/0.1, v/v/v) to obtain four smaller fractions, SNW1A–SNW1D. The fraction SNW1B (0.6 g) was chromatographed on a silica gel column and eluted with dichloromethane/methanol (3.0/1.0, v/v) and then was further purified on an RP-18 reversed phase column and eluted with acetone/water (1.0/2.0, v/v) to yields **2** (11.0 mg) and **3** (14.0 mg). The fraction SNW1D (1.2 g) was separated into 2 fractions, SNW2A – SNW2B, on a silica gel column eluting with solvent system dichloromethane/methanol/water (4.0/1.0/0.1, v/v/v). The fraction SNW2A (0.2 g) was further purified on a silica gel column and eluted with dichloromethane/methanol/water (2.0/1.0/0.1, v/v/v) to yield **4** (7.0 mg). Compound **1** (50.0 mg) was obtained from fraction SNW2B (0.4 g) on a silica gel column eluting with dichloromethane/acetone/water (1.5/1.0/0.1, v/v/v).

**2.3. Antibodies and Reagents.** EGF was purchased from Invitrogen (Carlsbad, CA, USA). Antibodies including anti-EGFR, anticyclin D1, and anti-p21 were obtained from Santa Cruz Biotechnology (Santa Cruz, CA, USA). Anti-phospho-EGFR, anti-Akt, anti-phospho Akt (Ser473), anti-ERK, and anti-phospho-ERK antibodies were from Cell Signaling Technology (Danvers, MA, USA).

**2.4. Cell Culture.** All cell lines used in this study were obtained from the American Type Culture Collection (Manassas, VA, USA). A549, NCI-H1975, and NCI-H1299 cells were maintained in RPMI 1640 medium. PANC1 and MIA-PaCa2 cells were maintained in DMEM. All media were supplemented with 10% fetal bovine serum (Hyclone, Logan, UT, USA) and streptomycin-penicillin (Invitrogen, Carlsbad, CA, USA). Cultures were maintained in a CO<sub>2</sub> incubator humidified atmosphere 5% CO<sub>2</sub> at 37°C.

**2.5. Cell Viability Assay.** The cytotoxic activity of **1–4** was determined by MTT [3-(4,5-dimethylthiazol-2-yl)-2,5-diphenyltetrazolium bromide]-based colorimetric assay [42]. MTT was purchased from Sigma, MO, USA. In brief, 2 x

$10^5$  cells/mL were seeded into 96-well plate and incubated for overnight. The compounds were treated to each well with various concentrations (0, 1, 3, 10, and 30  $\mu$ M). After incubation for 48 h, the MTT solution (0.5 mg/mL) was added to each well and further incubated for 3 h. Cell viability was calculated as a percentage compared to the vehicle-only treated control sample and performed in triplicate. The  $IC_{50}$  values were calculated using nonlinear regression analysis (percentage survival versus concentration).

**2.6. Western Blot Analysis.** Cells were harvested and lysed in a lysis buffer [150 mM NaCl, 50 mM Tris-HCl, pH 7.4, 1 mM EDTA, and 1% NP-40, 5 mM sodium orthovanadate, and protease inhibitors cocktail (BD Biosciences)] and then centrifuged for 10 min at 4°C and 15,000 rpm. An equal amount of protein was separated onto SDS-PAGE (sodium dodecyl sulfate polyacrylamide gel electrophoresis) and transferred to a Hybond-P membrane (Amersham Biosciences, Buckinghamshire, UK). Membranes were blocked in 5% nonfat skim milk for 1 h at room temperature, probed with the appropriate primary antibodies (1:1,000 dilution), washed, and then incubated with the corresponding secondary antibody (1:2,000 dilution). The signal was detected using the ECL (enhanced chemiluminescence) system (Intron, Seongnam, Korea).

**2.7. Annexin V and PI Double Staining Assay.** Annexin V and PI (propidium iodide) staining for apoptosis detection was performed using an Annexin V-FLOUS kit according to the manufacturer's instructions (BD Biosciences, CA, USA). Briefly, cells were treated with various concentrations of **1** and incubated for 24 h. The cells were then collected by trypsinization, washed 2 times with cold PBS, suspended in 100  $\mu$ L of a binding buffer (dilute from 10X binding buffer), and stained with 5  $\mu$ L PI (stock solution 50  $\mu$ g/mL) and 5  $\mu$ L FITC-labeled Annexin V in the dark for 15 min at room temperature. The cells were analyzed by FACS Calibur (Becton Dickinson, CA, USA). The percentages of Annexin V+/PI- (apoptosis cells), Annexin V /PI- (living cells), and Annexin V+ /PI+ (necrotic cells) staining were determined after marking for the positive and negative population.

**2.8. Cell Cycle Analysis.** Cells were seeded into 60 mm culture dishes and serum-starved in DMEM containing 0.5% FBS for 24 h. The cells were treated with indicated concentrations of **1** for 30 min and then stimulated by EGF (100 ng/mL) for 24 h. The cells were harvested by trypsinization, washed two times with cold PBS, and then centrifuged. The collected cells were fixed in 70% ethanol (v/v) for at least 2 hours at 4°C, washed once with PBS, and then suspended in cold propidium iodide (PI) solution (50  $\mu$ g/mL) containing RNase A (0.1  $\mu$ g/mL) in PBS (pH 7.4) in the dark for 15 min at room temperature. Flow cytometry analyses were performed using FACS Calibur (Becton Dickinson, CA, USA). The data were analyzed using the Cell Quest software (Becton Dickinson, CA, USA).

**2.9. Cell Migration Assay.** Cell migration assays were performed by following the Boyden chamber method using polycarbonate membranes with an 8  $\mu$ m pore size. In brief,  $10^5$  cells were seeded onto the upper chamber in 200  $\mu$ L of

DMEM containing 0.5% FBS, and then the upper chamber was put onto the 24-well plate with 800  $\mu$ L of the same media with or without EGF (100 ng/mL). The various concentrations of **1** (0, 0.1, 0.3, and 1  $\mu$ M) were treated in the upper chamber. After 12 h incubation, the migrated cells on the lower surface of the filter were fixed in methanol and then stained with H&E (hematoxylin and eosin). The cotton swabs were used to remove the cells which did not migrate through the pore. The migrated cells were counted in at least five randomly selected microscopic fields ( $\times 100$ ) per filter.

**2.10. Statistical Analysis.** Data was expressed as the mean  $\pm$  standard deviations (SD). Statistical significance was assessed by the two-tailed unpaired Student's *t*-test and P values less than 0.05 was considered statistically significant.

### 3. Results and Discussion

**3.1. Isolation and Identification of Compounds 1-4.** Compounds **1-4** were isolated from the methanolic extracts of *S. nigrum* by using various chromatographic techniques. Their structures were elucidated by using spectroscopic data (Supplementary Data (available here)) and by comparison with the reported data [39, 43, 44]. The compounds were determined as degalactotigonin (**1**), solasodine (**2**), O-acetyl solasodine (**3**), and soladulcoside A (**4**) (Figure 1).

**3.2. Degalactotigonin Induces Apoptosis in PANC1 and A549 Cells.** Cytotoxic activities of the isolated compounds on five human cancer cell lines (lung cancer cell lines: A549, NCI-H1975 and NCI-H1299; pancreatic cancer lines: PANC1 and MIA-PaCa2) were evaluated by an MTT method. As a result, compound **1** showed to be the most active compound against all tested cell lines (Table 1). The results were in accordance with those of previous reports in which degalactotigonin showed the cytotoxicity against various cancer cell lines including PC-12 (human lung carcinoma), HCT-116 (human colon carcinoma), NCI-H460 (human lung carcinoma), HepG2 (human liver carcinoma), MCF-7 (human breast carcinoma), and SF-268 (human glioma) [39, 40]. Further studies demonstrated that this compound induced apoptosis in MCF-7 cells and suppressed the growth and metastasis of human osteosarcoma through modulation of GSK-3 $\beta$  inactivation-mediated repression of the Hedgehog/Gli1 pathway [41, 45].

We determined apoptosis-inducing activity of **1** in PANC1 and A549 cells by Annexin V/PI double staining assays. Treatment with **1** increased the ration of apoptotic cells (Annexin V positive) in a concentration-dependent manner in these cells and PANC1 cells were more sensitive to apoptosis induced by **1** than A549 cells (Figures 2(a) and 2(b)). Since PANC1 cells were the most sensitive to **1** (Table 1) and expressed the highest level of EGFR compared to other tested cell lines (Figure 2(c)), we further investigated on the mechanism of action of **1** in PANC1 cells.

**3.3. Degalactotigonin Inhibits EGF-Induced Cell Cycle Progression of PANC1 Cells.** EGF acts as a regulator of cell proliferation, growth and migration by binding to its receptor EGFR



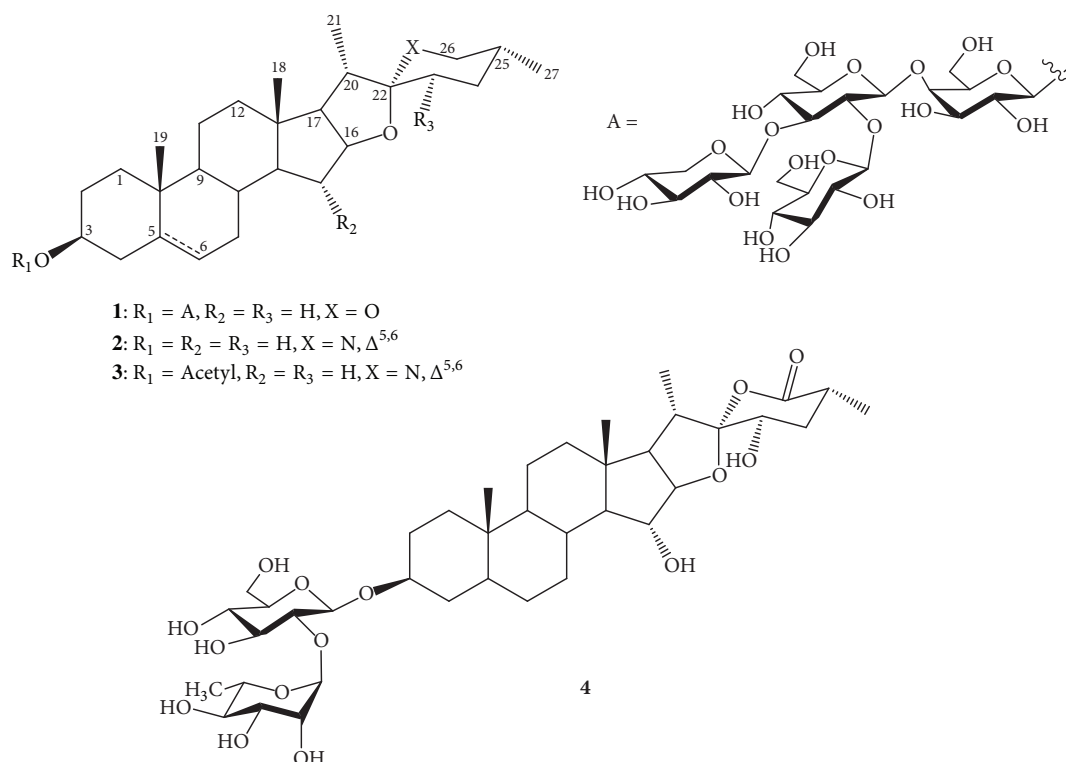


FIGURE 1: The structures of compounds (1-4) from *Solanum nigrum*.

[46]. We determined whether **1** inhibits EGF-induced cell cycle progression of PANC1 cells. Serum starvation of PANC1 cells for 24 h resulted in approximately 55.% synchronization of the cell cycle at the  $G_0/G_1$  phase. The percentage of S phase cells increased from 5.8% to 11.2% after treatment with EGF (100 ng/mL) for 24 h. In contrast, treatment with **1** at 0.3  $\mu\text{M}$  significantly induced cell cycle arrest at  $G_0/G_1$  phase by increasing the percentage of cells up to 52.2% and reducing the S phase to 9.0% (Figure 3(a)), suggesting that **1** could inhibit EGF-induced cell cycle progression via inhibiting EGFR signaling pathway. However, treatment with higher concentration of **1** (1  $\mu\text{M}$  and 3  $\mu\text{M}$ ) induced cell death due to its cytotoxicity in serum-starved condition.

Cyclin D1 and p21 are two important regulators in the  $G_1/S$  phase progression and downstream target genes of the EGFR signaling pathway. p21 (also known as Waf1/Cip1), a well-known cyclin-dependent kinase inhibitor, is involved in regulation of the cell cycle and acts as a mediator of cell survival as well as inhibiting DNA synthesis [47, 48]. Over-expression of p21 can potentially inhibit cyclin D1/CDK4 complex and suppress the catalytic activity of this complex, leading to cell cycle arrest at G1 phase [49]. Western blot analyses revealed that stimulation of PANC1 cells with EGF increased the expression levels of cyclin D1 and p21 in a time-dependent manner (Figure 3(b)). Treatment of PANC1 cells with **1** inhibited EGF-induced expression of cyclin D1 (Figure 3(c)), suggesting that **1** could inhibit EGFR signaling pathway. However, treatment with **1** further increased the expression level of p21 in PANC1 cells (Figure 3(c)). In osteosarcoma cancer cells, **1** increases p21 mRNA and protein

expression through undefined mechanisms and induces cell cycle arrest [41]. Thus, it is likely that **1** induces p21 expression via EGFR-independent signaling pathway and the induction of p21 by **1** may significantly contribute to the inhibition of EGF-induced cell cycle progression.

**3.4. Degalactotigonin Suppresses EGF-Induced Activation of EGFR in PANC1 Cells.** After EGF binding to EGFR in the cell membrane, EGFR is autophosphorylated, endocytosis, and recycled or directed to lysosomes for degradation [50]. We determined whether **1** regulates EGFR activation in response to EGF stimulation. Serum-starved PANC1 cells were treated with **1** at different concentrations for 30 min followed by EGF stimulation for 5 min. Treatment with **1** significantly reduced the level of EGFR phosphorylation (Y1068) (Figure 4(a)), suggesting that **1** may inhibit EGFR activation. Next, we examined whether **1** inhibits the activation of EGFR downstream signaling molecules such as Akt and ERK (extracellular signal-regulated kinase) [33]. The PI3K (phosphatidylinositol 3-kinase)/Akt pathway is activated in many cancers, and inhibition of the PI3K/Akt pathway induces cell apoptosis [51]. The activation of Ras/Raf/ERK by growth factor triggers the synthesis of D-type cyclins which bind with Cdk4 or Cdk6 to regulate cell cycle progression [52]. Treatment of PANC1 cells with **1** inhibited EGF-induced Akt (Ser473) and ERK (Thr202/Tyr204) phosphorylation (Figures 4(b) and 4(c)) in a concentration-dependent manner. Taken together, these results suggested that **1** may inhibit EGF-mediated activation of EGFR and subsequent EGFR downstream signaling molecules such as Akt and ERK.

TABLE 1: Cytotoxic activities of steroidal glycosides from *S. nigrum* on five cancer cell lines.

Compounds	IC <sub>50</sub> (μM) <sup>a</sup>				
	A549	H1975	H1299	PANCI	MIA-PaCa2
<b>1</b>	4.9 ± 1.0	5.5 ± 0.6	6.3 ± 0.8	2.9 ± 0.2	6.4 ± 0.4
<b>2</b>	>30	>30	>30	>30	>30
<b>3</b>	>30	>30	27.9 ± 3.0	>30	>30
<b>4</b>	28.4 ± 3.1	>30	>30	>30	>30
Camptothecin <sup>b</sup>	1.5 ± 0.9	0.16 ± 0.1	0.24 ± 0.1	4.7 ± 0.5	3.3 ± 0.2

<sup>a</sup>The IC<sub>50</sub> values were calculated in a triplicate experiment.

<sup>b</sup>Camptothecin used as positive control.

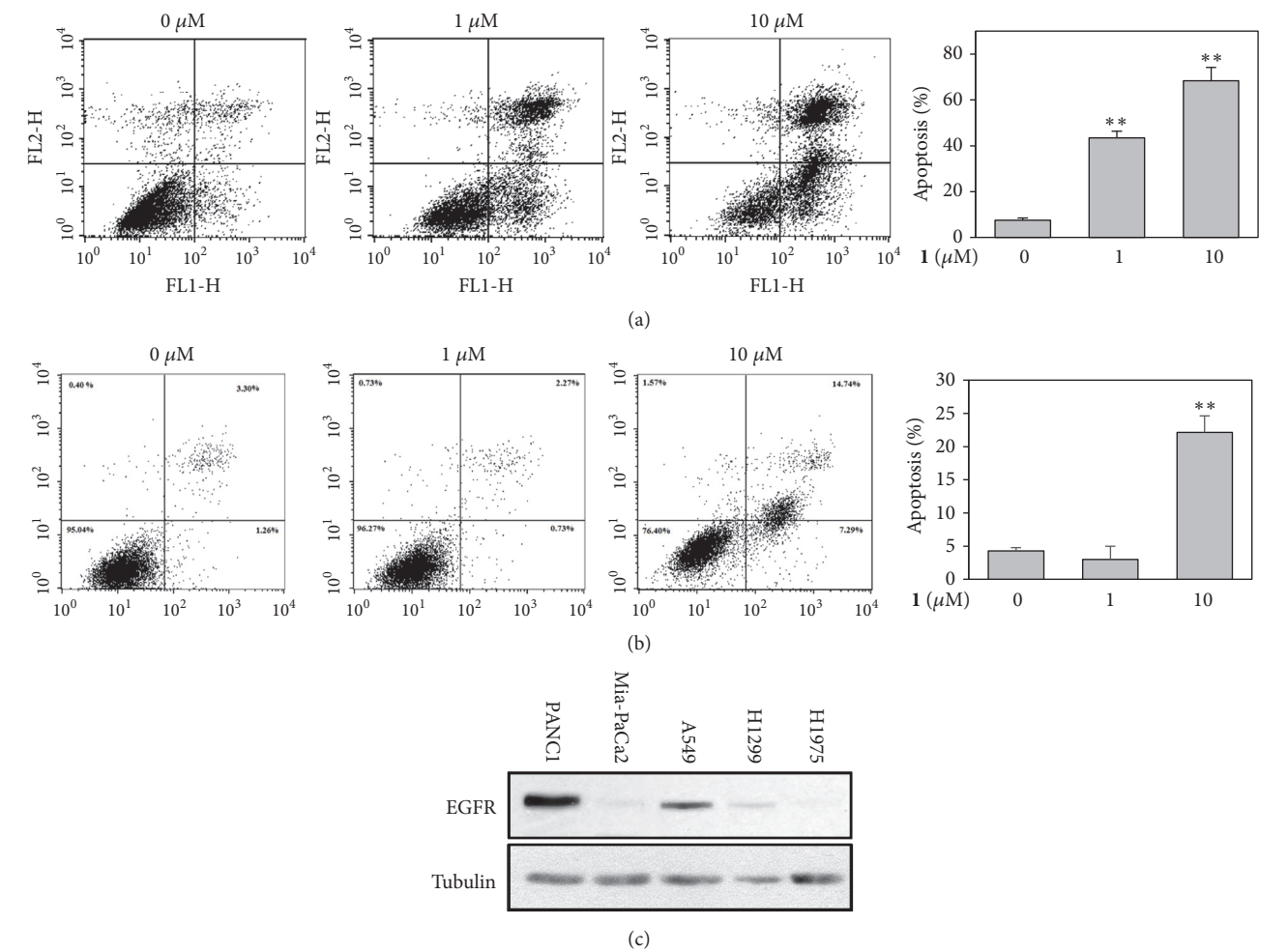


FIGURE 2: Effect of **1** on apoptosis of PANC1 and A549 cells. (a) PANC1 or (b) A549 cells were treated with the indicated concentrations of **1** (0-10 μM) for 12 h, and subsequently stained with Annexin V-FITC and PI. The percentage of Annexin V-FITC positive apoptotic cells was analyzed by flow cytometry. The results were presented in three independent experiments and described as the mean ± SD. \*, P<0.05; \*\*, P<0.01 versus vehicle-treated control. (c) Expression of EGFR in PANC1, MIA-PaCa2, A549, NCI-H1975, and NCI-H1299 cell lines. Whole cell lysates from these cell lines were probed with the indicated antibodies. α-Tubulin was used as a loading control.

**3.5. Degalactotigonin Attenuates EGF-Induced Migration of PANC1 Cells.** In the tumor progression, acquisition of the invasive and metastatic capability is important characteristics, which correlate with poor clinical prognosis and become the barrier to successful treatment [53]. EGF is a well-known growth factor that promotes cancer cell migration

and motility [54–56]. To further investigate the inhibitory effect of **1** on EGF-induced signaling, we determined whether **1** inhibits EGF-induced migration of PANC1 cells by transwell migration assay. The results showed that **1** markedly decreased the migration of PANC1 cells induced by EGF in a dose-dependent manner (Figure 5), suggesting that **1**



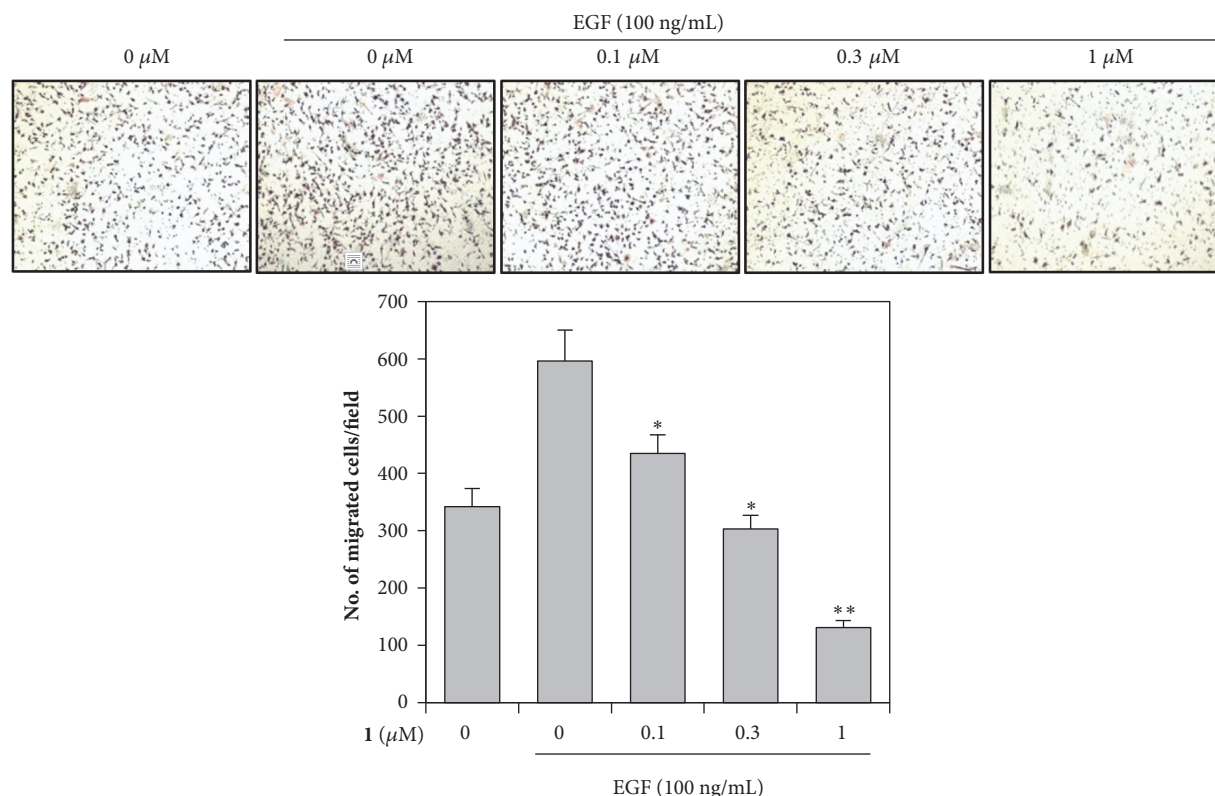


FIGURE 5: Effect of **1** on EGF-induced migration of PANC1 cells. PANC1 cells were treated with the indicated concentrations of **1** and then underwent a transwell invasion assay in the absence or presence of EGF (100 ng/mL) for 12 h. Representative images were shown (top). The graphs represented quantification of migrated PANC1 cells (bottom) and the mean  $\pm$  SD of three independent experiments was expressed. \* $P < 0.05$ , \*\* $P < 0.01$  versus EGF only treated control.

effectively suppressed EGF-mediated migration of PANC1 cells via inhibiting EGFR signaling pathway.

Pancreatic cancer is one of the most common deathly cancers in the Western world [57]. Overexpression of EGFR has been detected up to 90% in this cancer [9]. Gefitinib and erlotinib were the first EGFR tyrosine kinase inhibitors to be developed. Both of them target blocking EGFR signaling downstream pathways as competitive inhibitors of ATP for the tyrosine kinase domain [58]. Degalactotigonin (**1**), a saponin isolated from *Solanum nigrum*, has chemopreventive effects on various cancer types [45]. However, the anticancer effects of **1** and its mode of action mechanism in pancreatic cancer cells have not been investigated yet. In this study, we demonstrated that **1** induced apoptosis in PANC cells. Notably, compound **1** reduced EGF-induced phosphorylation of EGFR and its downstream signaling molecules such as Akt and ERK and suppressed the EGF-induced proliferation and migration of PANC1 cells in a dose-dependent manner.

Taken together, this study showed that **1** not only suppressed proliferation and migration of PANC1 cells, but also induced cell cycles arrest at G0/G1 phase and apoptosis via inhibiting EGF-mediated EGFR activation. These results might clarify a novel biological mechanism for **1** in anti-tumor therapy targeted on EGFR-overexpressing pancreatic cancer.

## Data Availability

The data used to support the findings of this study are included within the supplementary information file.

## Conflicts of Interest

The authors declare no competing financial interest.

## Authors' Contributions

Hoang Le Tuan Anh and Phuong Thao Tran make equal contributions to this work.

## Acknowledgments

This research is funded by the Vietnam National Foundation for Science and Technology Development (NAFOSTED) under Grant no. 106.02-2017.20 and Kangwon National University.

## Supplementary Materials

The spectroscopic data of the isolated compounds used to support the findings of this study are included within the supplementary information file. (*Supplementary Materials*)



## References

- [1] S. A. Danovi, H. H. Wong, and N. R. Lemoine, "Targeted therapies for pancreatic cancer," *British Medical Bulletin*, vol. 87, no. 1, pp. 97–130, 2008.
- [2] C. J. Bruns, M. T. Harbison, D. W. Davis et al., "Epidermal growth factor receptor blockade with C225 plus gemcitabine results in regression of human pancreatic carcinoma growing orthotopically in nude mice by antiangiogenic mechanisms," *Clinical Cancer Research*, vol. 6, no. 5, pp. 1936–1948, 2000.
- [3] C. Bangard, A. Gossmann, A. Papyan, S. Tawadros, M. Hellmich, and C. J. Bruns, "Magnetic resonance imaging in an orthotopic rat model: Blockade of epidermal growth factor receptor with EMD72000 inhibits human pancreatic carcinoma growth," *International Journal of Cancer*, vol. 114, no. 1, pp. 131–138, 2005.
- [4] M. H. Kulke, L. S. Blaszkowsky, D. P. Ryan et al., "Capecitabine plus erlotinib in gemcitabine-refractory advanced pancreatic cancer," *Journal of Clinical Oncology*, vol. 25, no. 30, pp. 4787–4792, 2007.
- [5] S. J. Zunino, Y. Zhang, N. P. Seeram, and D. H. Storms, "Berry fruit extracts inhibit growth and induce apoptosis of high-risk acute lymphoblastic leukemia cells in vitro," *Journal of Functional Foods*, vol. 2, no. 3, pp. 187–195, 2010.
- [6] D. S. Salomon, R. Brandt, F. Ciardiello, and N. Normanno, "Epidermal growth factor-related peptides and their receptors in human malignancies," *Critical Review in Oncology/Hematology*, vol. 19, no. 3, pp. 183–232, 1995.
- [7] S. R. Hubbard and W. T. Miller, "Receptor tyrosine kinases: mechanisms of activation and signaling," *Current Opinion in Cell Biology*, vol. 19, no. 2, pp. 117–123, 2007.
- [8] P. Seshacharyulu, M. P. Ponnusamy, D. Haridas, M. Jain, A. K. Ganti, and S. K. Batra, "Targeting the EGFR signaling pathway in cancer therapy," *Expert Opinion on Therapeutic Targets*, vol. 16, no. 1, pp. 15–31, 2012.
- [9] A. Citri and Y. Yarden, "EGF-ERBB signalling: towards the systems level," *Nature Reviews Molecular Cell Biology*, vol. 7, no. 7, pp. 505–516, 2006.
- [10] K. Tobita, H. Kijima, S. Dowaki et al., "Epidermal growth factor receptor expression in human pancreatic cancer: significance for liver metastasis," *International Journal of Molecular Medicine*, vol. 11, no. 3, pp. 305–309, 2003.
- [11] K. Uegaki, Y. Nio, Y. Inoue et al., "Clinicopathological significance of epidermal growth factor and its receptor in human pancreatic cancer," *Anticancer Research*, vol. 17, no. 5 B, pp. 3841–3847, 1997.
- [12] Y. Zhang, S. Banerjee, Z.-W. Wang, D. J. Marciniak, A. P. N. Majumdar, and F. H. Sarkar, "Epidermal growth factor receptor-related protein inhibits cell growth and induces apoptosis of BxPC3 pancreatic cancer cells," *Cancer Research*, vol. 65, no. 9, pp. 3877–3882, 2005.
- [13] R. Jain, A. Sharma, S. Gupta, I. P. Sarethy, and R. Gabrani, "*Solanum nigrum*: current perspectives on therapeutic properties," *Alternative Medicine Review*, vol. 16, no. 1, pp. 78–85, 2011.
- [14] C. J. Tai, C. K. Wang, C. J. Tai et al., "Aqueous extract of solanum nigrum leaves induces autophagy and enhances cytotoxicity of cisplatin, doxorubicin, docetaxel, and 5-fluorouracil in human colorectal carcinoma cells," *Evidence-Based Complementary and Alternative Medicine*, vol. 2013, Article ID 514719, 12 pages, 2013.
- [15] H. C. Wang, P. J. Chung, C. H. Wu, K. P. Lan, M. Y. Yang, and C. J. Wang, "*Solanum nigrum* L. polyphenolic extract inhibits hepatocarcinoma cell growth by inducing G2/M phase arrest and apoptosis," *Journal of the Science of Food and Agriculture*, vol. 91, no. 1, pp. 178–185, 2011.
- [16] H. M. Lin, H. C. Tseng, C. J. Wang et al., "Induction of autophagy and apoptosis by the extract of *Solanum nigrum* Linn in HepG2 cells," *Journal of Agricultural and Food Chemistry*, vol. 55, no. 9, pp. 3620–3628, 2007.
- [17] J. Li, Q. Li, T. Feng et al., "Antitumor activity of crude polysaccharides isolated from *Solanum nigrum* Linne on U14 cervical carcinoma bearing mice," *Phytotherapy Research*, vol. 21, no. 9, pp. 832–840, 2007.
- [18] J. Li, Q.-W. Li, D.-W. Gao, Z.-S. Han, and K. Li, "Antitumor effects of total alkaloids isolated from *Solanum nigrum* in vitro and in vivo," *Die Pharmazie*, vol. 63, no. 7, pp. 534–538, 2008.
- [19] Z. A. Zakaria, H. K. Gopalan, and H. Zainal, "Antinociceptive, anti-inflammatory and antipyretic effects of *Solanum nigrum* chloroform extract in animal models," *Yakugaku Zasshi*, vol. 126, no. 11, pp. 1171–1178, 2006.
- [20] H. Kang, H.-D. Jeong, and H.-Y. Choi, "The chloroform fraction of solanum nigrum suppresses nitric oxide and tumor necrosis factor- $\alpha$  in LPS-stimulated mouse peritoneal macrophages through inhibition of p38, JNK and ERK1/2," *American Journal of Chinese Medicine*, vol. 39, no. 6, pp. 1261–1273, 2011.
- [21] F.-P. Liu, X. Ma, M.-M. Li et al., "Hepatoprotective effects of *Solanum nigrum* against ethanol-induced injury in primary hepatocytes and mice with analysis of glutathione S-transferase A1," *Journal of the Chinese Medical Association*, vol. 79, no. 2, pp. 65–71, 2016.
- [22] L. Xiang, Y. Wang, X. Yi, and X. He, "Anti-inflammatory steroidal glycosides from the berries of *Solanum nigrum* L. (European black nightshade)," *Phytochemistry*, vol. 148, pp. 87–96, 2018.
- [23] L. Zhao, L. Wang, S. Di et al., "Steroidal alkaloid solanine A from *Solanum nigrum* Linn. exhibits anti-inflammatory activity in lipopolysaccharide/interferon  $\gamma$ -activated murine macrophages and animal models of inflammation," *Biomedicine & Pharmacotherapy*, vol. 105, pp. 606–615, 2018.
- [24] K. Hu, H. Kobayashi, A. Dong, Y. Jing, S. Iwasaki, and X. Yao, "Antineoplastic agents III: steroidal glycosides from solanum nigrum," *Planta Medica*, vol. 65, no. 1, pp. 35–38, 1999.
- [25] T. Javed, U. A. Ashfaq, S. Riaz, S. Rehman, and S. Riazuddin, "In-vitro antiviral activity of *Solanum nigrum* against Hepatitis C Virus," *Virology Journal*, vol. 8, article 26, 2011.
- [26] X. Ding, F. Zhu, Y. Yang, and M. Li, "Purification, antitumor activity in vitro of steroidal glycoalkaloids from black nightshade (*Solanum nigrum* L.)," *Food Chemistry*, vol. 141, no. 2, pp. 1181–1186, 2013.
- [27] L. An, J. T. Tang, X. M. Liu, and N. N. Gao, "Review about mechanisms of anti-cancer of *Solanum nigrum*," *Journal of Chinese Materia Medica*, vol. 31, no. 15, pp. 1225–1226, 1260.
- [28] F. Kalalinia and I. Karimi-Sani, "Anticancer properties of solamargine: a systematic review," *Phytotherapy Research*, vol. 31, no. 6, pp. 858–870, 2017.
- [29] B. Pan, W. Zhong, Z. Deng et al., "Inhibition of prostate cancer growth by solanine requires the suppression of cell cycle proteins and the activation of ROS/P38 signaling pathway," *Cancer Medicine*, vol. 5, no. 11, pp. 3214–3222, 2016.
- [30] Y. Yi, X. Jia, J. Wang, J. Chen, H. Wang, and Y. Li, "Solanine induced apoptosis and increased chemosensitivity to Adriamycin in T-cell acute lymphoblastic leukemia cells," *Oncology Letters*, vol. 15, no. 5, pp. 7383–7388, 2018.

- [31] K.-S. Heo and K.-T. Lim, "Glycoprotein isolated from *Solanum nigrum* L. modulates the apoptotic-related signals in 12-O-tetradecanoylphorbol 13-acetate-stimulated MCF-7 cells," *Journal of Medicinal Food*, vol. 8, no. 1, pp. 69–77, 2005.
- [32] S.-J. Lee and K.-T. Lim, "150 kDa glycoprotein isolated from *Solanum nigrum* Linne stimulates caspase-3 activation and reduces inducible nitric oxide production in HCT-116 cells," *Toxicology in Vitro*, vol. 20, no. 7, pp. 1088–1097, 2006.
- [33] S.-J. Lee, P.-S. Oh, J.-H. Ko, K. Lim, and K.-T. Lim, "A 150-kDa glycoprotein isolated from *Solanum nigrum* L. has cytotoxic and apoptotic effects by inhibiting the effects of protein kinase C alpha, nuclear factor-kappa B and inducible nitric oxide in HCT-116 cells," *Cancer Chemotherapy and Pharmacology*, vol. 54, no. 6, pp. 562–572, 2004.
- [34] K.-T. Lim, "Glycoprotein isolated from *Solanum nigrum* L. kills HT-29 cells through apoptosis," *Journal of Medicinal Food*, vol. 8, no. 2, pp. 215–226, 2005.
- [35] X. Ding, F.-S. Zhu, M. Li, and S.-G. Gao, "Induction of apoptosis in human hepatoma SMMC-7721 cells by solamargine from *Solanum nigrum* L.," *Journal of Ethnopharmacology*, vol. 139, no. 2, pp. 599–604, 2012.
- [36] I. K. Sani, S. H. Marashi, and F. Kalalinia, "Solamargine inhibits migration and invasion of human hepatocellular carcinoma cells through down-regulation of matrix metalloproteinases 2 and 9 expression and activity," *Toxicology in Vitro*, vol. 29, no. 5, pp. 893–900, 2015.
- [37] T. Ikeda, H. Tsumagari, and T. Nohara, "Steroidal oligoglycosides from *Solanum nigrum*," *Chemical & Pharmaceutical Bulletin*, vol. 48, no. 7, pp. 1062–1064, 2000.
- [38] M. Ohno, K. Murakami, M. El-Aasr et al., "New spirostanol glycosides from *Solanum nigrum* and *S. jasminoides*," *Journal of Natural Medicines*, vol. 66, no. 4, pp. 658–663, 2012.
- [39] X. Zhou, X. He, G. Wang et al., "Steroidal saponins from *Solanum nigrum*," *Journal of Natural Products*, vol. 69, no. 8, pp. 1158–1163, 2006.
- [40] T. Ikeda, H. Tsumagari, T. Honbu, and T. Nohara, "Cytotoxic activity of steroidal glycosides from *solanum* plants," *Biological & Pharmaceutical Bulletin*, vol. 26, no. 8, pp. 1198–1201, 2003.
- [41] Z. Zhao, Q. Jia, M. Wu et al., "Degalactotigonin, a Natural Compound from ,", *Clinical Cancer Research*, vol. 24, no. 1, pp. 130–144, 2018.
- [42] T. Mosmann, "Rapid colorimetric assay for cellular growth and survival: application to proliferation and cytotoxicity assays," *Journal of Immunological Methods*, vol. 65, no. 1-2, pp. 55–63, 1983.
- [43] X. Zha, H. Sun, J. Hao, and Y. Zhang, "Efficient synthesis of solasodine, O-acetylsolasodine, and soladulcidine as anticancer steroidal alkaloids," *Chemistry & Biodiversity*, vol. 4, no. 1, pp. 25–31, 2007.
- [44] T. Yamashita, T. Matsumoto, S. Yahara, N. Yoshida, and T. Nohara, "Structures of Two New Steroidal Glycosides, Soladulcosides a and B From *Solanum dulcamara*," *Chemical and Pharmaceutical Bulletin*, vol. 39, no. 6, pp. 1626–1628, 1991.
- [45] D. Chakraborty, C. K. Jain, A. Maity et al., "Chenopodium album metabolites act as dual topoisomerase inhibitors and induce apoptosis in the MCF7 cell line," *MedChemComm*, vol. 7, no. 5, pp. 837–844, 2016.
- [46] N. Normanno, A. de Luca, C. Bianco et al., "Epidermal growth factor receptor (EGFR) signaling in cancer," *Gene*, vol. 366, no. 1, pp. 2–16, 2006.
- [47] Y. Li, D. Dowbenko, and L. A. Lasky, "AKT/PKB phosphorylation of p21Cip/WAF1 enhances protein stability of p21Cip/WAF1 and promotes cell survival," *The Journal of Biological Chemistry*, vol. 277, no. 13, pp. 11352–11361, 2002.
- [48] A. Karimian, Y. Ahmadi, and B. Yousefi, "Multiple functions of p21 in cell cycle, apoptosis and transcriptional regulation after DNA damage," *DNA Repair*, vol. 42, pp. 63–71, 2016.
- [49] M. Fu, C. Wang, Z. Li, T. Sakamaki, and R. G. Pestell, "Minireview: Cyclin D1: Normal and abnormal functions," *Endocrinology*, vol. 145, no. 12, pp. 5439–5447, 2004.
- [50] A. Tomas, C. E. Futter, and E. R. Eden, "EGF receptor trafficking: consequences for signaling and cancer," *Trends in Cell Biology*, vol. 24, no. 1, pp. 26–34, 2014.
- [51] L. Rössig, A. S. Jadidi, C. Urbich, C. Badorff, A. M. Zeiher, and S. Dimmeler, "Akt-dependent phosphorylation of p21Cip1 regulates PCNA binding and proliferation of endothelial cells," *Molecular and Cellular Biology*, vol. 21, no. 16, pp. 5644–5657, 2001.
- [52] K. M. Regula, M. J. Rzeszutek, D. Baetz, C. Seneviratne, and L. A. Kirshenbaum, "Therapeutic opportunities for cell cycle re-entry and cardiac regeneration," *Cardiovascular Research*, vol. 64, no. 3, pp. 395–401, 2004.
- [53] Z. Lu, G. Jiang, P. Blume-Jensen, and T. Hunter, "Epidermal growth factor-induced tumor cell invasion and metastasis initiated by dephosphorylation and downregulation of focal adhesion kinase," *Molecular and Cellular Biology*, vol. 21, no. 12, pp. 4016–4031, 2001.
- [54] J. T. Price, H. M. Wilson, and N. E. Haites, "Epidermal growth factor (EGF) increases the in vitro invasion, motility and adhesion interactions of the primary renal carcinoma cell line, A704," *European Journal of Cancer Part A: General Topics*, vol. 32, no. 11, pp. 1977–1982, 1996.
- [55] E. M. Rosen and I. D. Goldberg, "Protein factors which regulate cell motility," *In Vitro Cellular & Developmental Biology*, vol. 25, no. 12, pp. 1079–1087, 1989.
- [56] T. Shibata, T. Kawano, H. Nagayasu et al., "Enhancing effects of epidermal growth factor on human squamous cell carcinoma motility and matrix degradation but not growth," *Tumor Biology*, vol. 17, no. 3, pp. 168–175, 1996.
- [57] D. Hariharan, A. Saied, and H. M. Kocher, "Analysis of mortality rates for pancreatic cancer across the world," *HPB*, vol. 10, no. 1, pp. 58–62, 2008.
- [58] B. A. Chan and B. G. Hughes, "Targeted therapy for non-small cell lung cancer: current standards and the promise of the future," *Translational Lung Cancer Research*, vol. 4, no. 1, pp. 36–54, 2015.

## Review Article

# ***Cannabis sativa* L. and Nonpsychoactive Cannabinoids: Their Chemistry and Role against Oxidative Stress, Inflammation, and Cancer**

**Federica Pellati** <sup>1</sup>, **Vittoria Borgonetti**,<sup>2</sup> **Virginia Brighenti**,<sup>1</sup> **Marco Biagi**,<sup>2</sup> **Stefania Benvenuti**,<sup>1</sup> and **Lorenzo Corsi** <sup>1</sup>

<sup>1</sup>Department of Life Sciences, University of Modena and Reggio Emilia, Via G. Campi 103/287, 41125 Modena, Italy

<sup>2</sup>Department of Physical Sciences, Earth and Environment, University of Siena, Strada Laterina 8, 53100 Siena, Italy

Correspondence should be addressed to Lorenzo Corsi; [corsi.lorenzo@unimore.it](mailto:corsi.lorenzo@unimore.it)

Received 7 September 2018; Revised 14 November 2018; Accepted 22 November 2018; Published 4 December 2018

Guest Editor: Claudio Tabolacci

Copyright © 2018 Federica Pellati et al. This is an open access article distributed under the Creative Commons Attribution License, which permits unrestricted use, distribution, and reproduction in any medium, provided the original work is properly cited.

In the last decades, a lot of attention has been paid to the compounds present in medicinal *Cannabis sativa* L., such as  $\Delta^9$ -tetrahydrocannabinol ( $\Delta^9$ -THC) and cannabidiol (CBD), and their effects on inflammation and cancer-related pain. The National Cancer Institute (NCI) currently recognizes medicinal *C. sativa* as an effective treatment for providing relief in a number of symptoms associated with cancer, including pain, loss of appetite, nausea and vomiting, and anxiety. Several studies have described CBD as a multitarget molecule, acting as an adaptogen, and as a modulator, in different ways, depending on the type and location of disequilibrium both in the brain and in the body, mainly interacting with specific receptor proteins CB<sub>1</sub> and CB<sub>2</sub>. CBD is present in both medicinal and fibre-type *C. sativa* plants, but, unlike  $\Delta^9$ -THC, it is completely nonpsychoactive. Fibre-type *C. sativa* (hemp) differs from medicinal *C. sativa*, since it contains only few levels of  $\Delta^9$ -THC and high levels of CBD and related nonpsychoactive compounds. In recent years, a number of preclinical researches have been focused on the role of CBD as an anticancer molecule, suggesting CBD (and CBD-like molecules present in the hemp extract) as a possible candidate for future clinical trials. CBD has been found to possess antioxidant activity in many studies, thus suggesting a possible role in the prevention of both neurodegenerative and cardiovascular diseases. In animal models, CBD has been shown to inhibit the progression of several cancer types. Moreover, it has been found that coadministration of CBD and  $\Delta^9$ -THC, followed by radiation therapy, causes an increase of autophagy and apoptosis in cancer cells. In addition, CBD is able to inhibit cell proliferation and to increase apoptosis in different types of cancer models. These activities seem to involve also alternative pathways, such as the interactions with TRPV and GRP55 receptor complexes. Moreover, the finding that the acidic precursor of CBD (cannabidiolic acid, CBDA) is able to inhibit the migration of breast cancer cells and to downregulate the proto-oncogene *c-fos* and the cyclooxygenase-2 (COX-2) highlights the possibility that CBDA might act on a common pathway of inflammation and cancer mechanisms, which might be responsible for its anticancer activity. In the light of all these findings, in this review we explore the effects and the molecular mechanisms of CBD on inflammation and cancer processes, highlighting also the role of minor cannabinoids and noncannabinoids constituents of  $\Delta^9$ -THC deprived hemp.

## **1. The Chemistry of *Cannabis sativa* L.**

*Cannabis sativa* L. is a dioicous plant of the Cannabaceae family and it is widely distributed all over the world [1]. It has been used as a psychoactive drug, as a folk medicine ingredient, and as a source of textile fibre since ancient times [2]. The taxonomic classification of this plant has always been difficult, due to its genetic variability [1, 3]. Firstly, the

genus *Cannabis* has been divided into three main species [1, 3, 4]: a fibre-type one, named *C. sativa* L., a drug-type one, characterised by high levels of the psychoactive compound  $\Delta^9$ -tetrahydrocannabinol ( $\Delta^9$ -THC), named *C. indica* Lam., and another one with intermediate properties, named *C. ruderalis* Janisch. Due the easy crossbreeding of these species to generate hybrids, a monotypic classification has been preferred, in which one species (*C. sativa*) is recognised



and it is divided into different chemotypes [1, 3, 4]. On the basis of their cannabinoid profiles, five chemotypes have been recognised: chemotype I comprises drug type plants with a predominance of  $\Delta^9$ -THC-type cannabinoids; chemotypes III and IV are fibre-type plants containing high levels of nonpsychoactive cannabinoids and very low amounts of psychoactive ones; chemotype II comprises plants with intermediate characteristics between drug-type and fibre-type plants; chemotype V is composed of fibre-type plants which contains almost no cannabinoids [5].

For both medicinal and forensic purposes, the most important classification of *Cannabis* types is that into the drug-type and the fibre-type: the drug-type *Cannabis*, which is rich in psychoactive  $\Delta^9$ -THC, is used for medicinal or recreational purposes; the fibre-type *Cannabis*, rich of cannabidiol (CBD) or related compounds and almost devoid of  $\Delta^9$ -THC, is used for textile or food purposes [3]. Indeed, the well-known pharmacological activity of psychoactive cannabinoid  $\Delta^9$ -THC makes drug-type *Cannabis* one of the most investigated medicinal plants [3]. Fibre-type *Cannabis* (also known as hemp or industrial hemp) is at the moment underemployed for pharmacological purposes, while drug-type *C. sativa* is used in several diseases as a palliative therapy or in coadministration with primary therapy [1]. However, there has also been a growing interest in fibre-type *C. sativa* varieties in recent years [1], and those approved for commercial use by the European Community are 69 [5]. Many European countries have recognized the commercial value of hemp and a legal limit of 0.2-0.3%  $\Delta^9$ -THC is usually applied [1].

*C. sativa* is characterized by a complex chemical composition, including terpenes, carbohydrates, fatty acids and their esters, amides, amines, phytosterols, phenolic compounds, and the specific compounds of this plant, namely, the cannabinoids [2]. Cannabinoids are meroterpenoids (specifically  $C_{21}$  or  $C_{22}$  terpenophenolic compounds), obtained from the alkylation of an alkyl resorcinol with a monoterpene unit [3]. They are mainly synthesized in glandular trichomes, which are more abundant in female inflorescences [2]. More than 100 cannabinoids have been isolated, characterised, and divided into 11 chemical classes [4, 6]. Usually, the most abundant cannabinoids present in drug-type plants are  $\Delta^9$ -tetrahydrocannabinolic acid ( $\Delta^9$ -THCA) and  $\Delta^9$ -THC, while fibre-type plants are known to contain mainly cannabinoic acids, such as cannabidiolic acid (CBDA) and cannabigerolic acid (CBGA), followed by their decarboxylated forms, namely, cannabidiol (CBD) and cannabigerol (CBG) (Figure 1) [7, 8]. Other minor cannabinoids include cannabichromenic acid (CBCA), cannabichromene (CBC), cannabinolic acid (CBNA), and cannabinol (CBN), with the last two being the oxidative degradation products of  $\Delta^9$ -THCA and  $\Delta^9$ -THC, respectively, present in aged *Cannabis* (Figure 1) [1, 3, 4, 7-10].  $\Delta^9$ -THC can also be transformed by isomerization to  $\Delta^8$ -THC (Figure 1), which is an artefact. It should be pointed out that cannabinoids are biosynthesized in the acid form in plant tissues; then, they can generate their decarboxylated counterparts under the action of heat and

light, by means of a spontaneous decarboxylation [1, 3, 4, 7-10].

Many of the psychoactive effects of  $\Delta^9$ -THC are mediated by  $CB_1$  receptors, while nonpsychoactive cannabinoids, such as CBD, have low affinity for both  $CB_1$  and  $CB_2$  receptors [3]. The interaction with  $CB_1$  receptors is responsible for the analgesic effect of  $\Delta^9$ -THC, due to their role in the transmission of the nociceptive information in various tissues [3].  $CB_2$  receptors are highly expressed in some cells of the immune system and they are believed to have a role in the immune cell function, thus explaining the immunomodulatory properties of  $\Delta^9$ -THC.  $CB_2$  receptors are also considered to be involved in neuroinflammation, atherosclerosis, and bone remodelling [3].

In the ambit of nonpsychoactive compounds, CBD represents the most valuable one from the pharmaceutical point of view, since it has been found to possess a high antioxidant and anti-inflammatory activity, together with antibiotic, neuroprotective, anxiolytic, and anticonvulsant properties [1, 3, 11-14]. CBDA has antimicrobial and antinausea properties [1, 11, 13], while CBG has anti-inflammatory, antimicrobial, and analgesic activities [1, 11, 13, 15]. Thanks to its lack of psychoactivity, CBD is one of the most interesting compounds, with many reported pharmacological effects in various models of pathologies, from inflammatory and neurodegenerative diseases, to epilepsy, autoimmune disorders like multiple sclerosis, arthritis, schizophrenia, and cancer [16]. In the presence of  $\Delta^9$ -THC, CBD is able to antagonize  $CB_1$  at low concentration; this supports its regulatory properties on  $\Delta^9$ -THC adverse effects like tachycardia, anxiety, sedation, and hunger in animals and humans [16]. CBD has also been found to be a negative allosteric modulator of the  $CB_1$  receptors and an inverse agonist of  $CB_2$  receptors, the second activity partly explaining its anti-inflammatory activity [16]. Different targets have been described in the literature for nonpsychoactive cannabinoids, including the transient potential vanilloid receptor type-1 (TPVR-1) channels, the peroxisome proliferator-activated receptor  $\gamma$  (PPAR $\gamma$ ) GPR55, the 5-hydroxytryptamine receptor subtype 1A (5-HT $1A$ ), glycine  $\alpha 1$  and  $\alpha 1\beta$  receptors, the adenosine membrane transporter phospholipase A $2$ , lipoxygenase (LO) and cyclooxygenase-2 (COX-2) enzymes, and  $Ca^{2+}$  homeostasis [11, 16].

Concerning other phenolics present in *C. sativa*, several flavonoids have been identified, belonging mainly to flavones and flavonols, together with cannflavins A and B, which are *C. sativa* typical methylated isoprenoid flavones [17]. *Cannabis* flavonoids exert several biological effects, including properties possessed also by cannabinoids and terpenes [2]. Anti-inflammatory, neuroprotective, and anti-cancer activities have been described for these compounds [2]. In particular, cannflavin A and B are known to possess an anti-inflammatory action [2]. Microsomal prostaglandin  $E_2$  synthase (mPGES-1) and 5-LO have been identified as the molecular targets of cannflavins A and B [18]. An antimicrobial and antileishmanial activity has also been demonstrated for cannflavin B [17]. Cannflavin A has shown a good antileishmanial activity and a moderate antioxidant action [17]. In the ambit of *Cannabis* phenolics, canniprene,



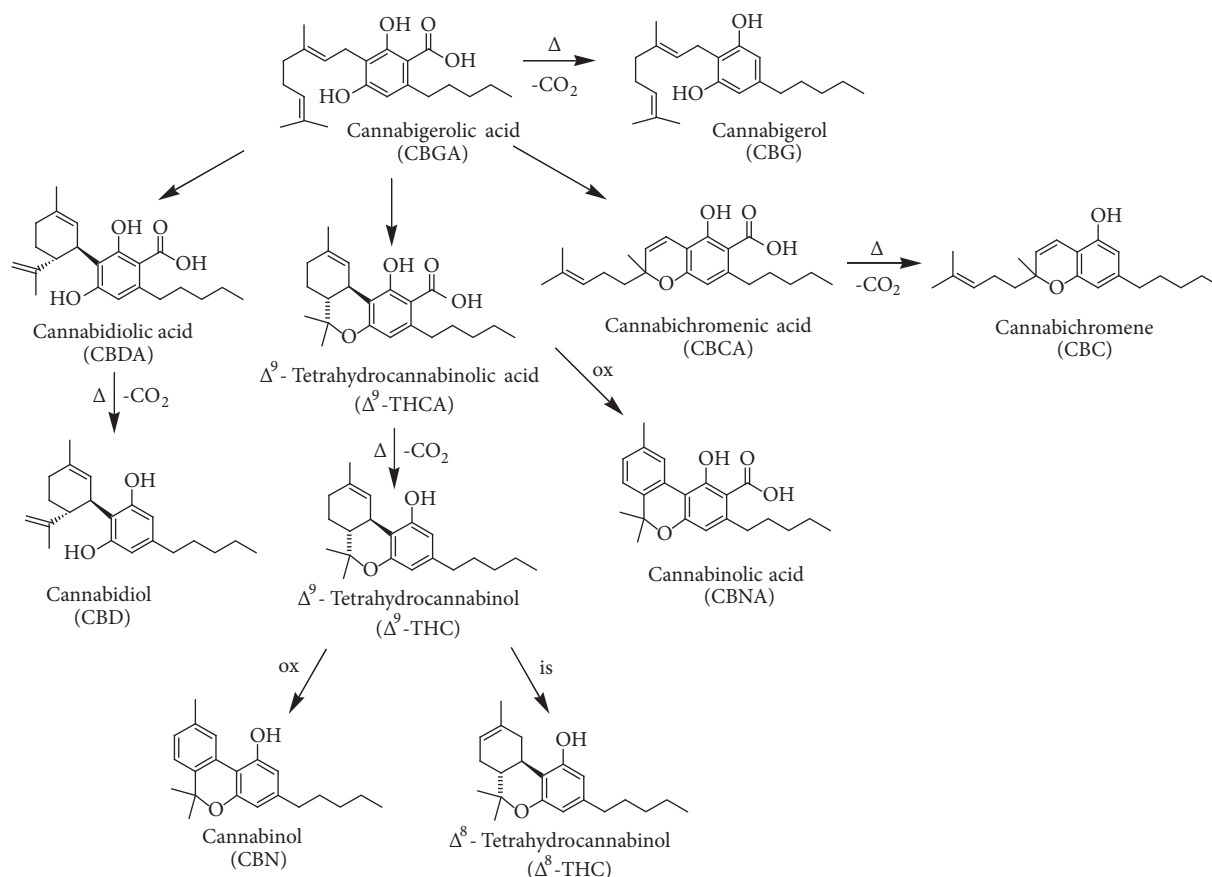


FIGURE 1: Chemical structures of main cannabinoids present in *Cannabis sativa* L. Abbreviation:  $\Delta$  = heating; ox = oxidation; is = isomerization.

which is a dihydrostilbene unique to *C. sativa*, represents an interesting compound [19]. If compared with cannflavin A, which is the most potent cannflavin, canniprene has been found to be superior at inhibiting 5-LO, but it is less effective for mPGES-1 inhibition [19].

As regards the other compounds present in *C. sativa*, terpenes are responsible for the characteristic scent of the plant. Both mono- and sesquiterpenes have been detected in roots and aerial parts of *Cannabis* and they are mainly produced in secretory glandular hairs [2]. In the ambit of monoterpenes,  $\beta$ -myrcene is known to possess anti-inflammatory, analgesic, and anxiolytic properties [2]. As for sesquiterpenes,  $\beta$ -caryophyllene has anti-inflammatory and gastric cytoprotector activities; it is also able to bind to the CB<sub>2</sub> receptors and, in this context, it is considered as a phytocannabinoid [2].

Several interactions between *Cannabis* secondary metabolites have been described in the literature [2]. In addition to the capacity of CBD to reduce  $\Delta^9$ -THC side effects, terpenes are able to increase blood-brain barrier permeability, thus affecting  $\Delta^9$ -THC pharmacokinetics; they can also influence the affinity of  $\Delta^9$ -THC for CB<sub>1</sub> receptors and interact with neurotransmitter receptors, thus contributing to cannabinoid-mediated analgesic and psychotic effects [2]. Finally, also flavonoids may modulate the pharmacokinetics

of  $\Delta^9$ -THC, by means of the inhibition of hepatic P450 enzymes (3A11 and 3A4) [2].

**1.1. Cannabidiol (CBD).** Many studies have expanded the concept that inflammation is a critical component of tumour progression [20]. Indeed, several cancers originate from infection, chronic irritation, and inflammation [20]. Tumour microenvironment, which is largely regulated by inflammatory cells, displays a key role in the neoplastic process, fostering proliferation, survival, and migration [20]. In addition, cancer cells have co-opted some of the signalling molecules of the innate immune system for invasion, migration, and metastasis [20].

By focusing the attention on hemp nonpsychoactive cannabinoids, CBD has been demonstrated to be useful in the treatment of different inflammatory ailments, including bowel diseases (e.g., Crohn's and ulcerative colitis), neuronal diseases (e.g., Parkinson and Alzheimer), and a wide range of inflammatory skin diseases (e.g., atopic dermatitis and psoriasis) [21].

As regards cancer, CBD has exhibited antiproliferative and proapoptotic activities, thus demonstrating modulating the tumorigenesis in different types of cancer, including breast, lung, colon, brain, and others [21].

In this context, this review is focused on the effects and the molecular mechanisms of CBD and related compounds

on inflammation and cancer processes, highlighting also the role of other related nonpsychoactive cannabinoids and noncannabinoids constituents of fibre-type hemp. Although it has been reported that CBD is able to bind several protein complexes, such as PPAR $\gamma$  and 5HT $_1$ , their role in CBD-mediated anticancer activity is still poor documented. For this reason, the attention is focused mainly on the interaction between CBD and three putative molecular targets such CB $_2$ , GPR55, and TRPV1/2 protein receptors, where there is an extensive literature and several molecular mechanisms have been proposed.

## 2. The Role of the Endocannabinoid System in Peripheral Inflammation

Endocannabinoids and their metabolic enzymes and receptors have been identified in monocytes, macrophages, basophils, lymphocytes, and dendritic cells. In these cells their role is to modulate immune function in an autocrine and paracrine way [22].

In human peripheral blood cells, CB $_1$  are expressed by B cells, NK cells, neutrophils, CD8+ T cells, monocytes, and CD4+ T cells, in a decreasing rank order, whereas CB $_2$  mRNA is expressed by human B cells, NK cells, monocytes, neutrophils, and T cells, in a decreasing rank order [23].

CB $_2$  expression in human B cells increases after the activation by anti-CD40 antibody. However, differentiation of B cells is accompanied by decreased expression of CB $_2$ . CB $_2$  levels in macrophages undergo changes correlated with cell activation or with inflammation. Indeed, macrophages express higher levels of CB $_2$ ; so, the functions of macrophages in these states of activation may be the most sensitive to the actions of cannabinoids. These data suggest a physiological role of the endocannabinoid system in the functions of immune cells with respect to inflammation [24].

Both 2-arachidonylglycerol (2-AG) and anandamide (AEA) play an immunomodulatory role through their activity on CB $_2$ . CB $_2$  activation typically inhibits the functions of immune cells with intracellular signaling mechanisms, including the inhibition of adenylate cyclase activity by Gi/o proteins and activation of MAPKs. Indeed, CB $_2$  are able to inhibit the production of proinflammatory cytokines, like TNF- $\alpha$ , IL-6, and IL-8 in human monocytes and macrophages, and to reduce the release of TNF- $\alpha$ , IL-2, and IFN- $\gamma$  in activated human peripheral lymphocytes.

Moreover, a relationship between the endocannabinoid system and toll-like receptors (TLR) has been reported, with TLR activation enhancing the production of endocannabinoids and cannabinoids suppressing TLR-induced inflammatory response [25].

**2.1. Nonpsychoactive Cannabinoids and Peripheral Inflammation.** The study of the anti-inflammatory effects of cannabinoids from *C. sativa* L. is of current interest [26, 27]. Although  $\Delta^9$ -THC has been reported to possess anti-inflammatory in a plethora of *in vitro* and *in vivo* models [28–38], a number of reports have highlighted the role of nonpsychoactive cannabinoids in inflammatory processes (Figure 2).

CBD anti-inflammatory effect may be mediated by cannabinoid receptors (CB $_r$ ), adenosine A $_2$ A receptors, TRPV1 receptors, GPR55 receptors, and CB $_2$ /5HT(1A) heterodimerization [27]. *In vivo*, CBD has been able to reduce inflammation in a murine model of colitis, even if  $\Delta^9$ -THC was more effective [28]. In a carrageenan-induced inflammation model in rats, CBD reduced PGE $_2$ , nitric oxide (NO), and malondialdehyde production, together with COX activity [39]. CBDA has been found to possess a dual inhibitory effect on COX, through downregulation [40] and enzyme inhibition [35]. CBD has also completely inhibited the production of TNF- $\alpha$  in LPS-stimulated RAW264.7 macrophages [41]. Moreover, a reduction of IL-1 $\beta$  and TNF- $\alpha$  levels has been observed in mitogen-activated human PBMC [42]. More recently, CBD has been found to significantly reduce cytokines production in an *in vitro* model of allergic contact dermatitis, using HaCaT cells [43].

The ability to activate and desensitize TRPV4 channels is linked to the reduction of NO production exerted by CBG in LPS-stimulated macrophages [44]. Moreover, CBG and CBGA resulted in inhibiting COX activity, even at high micromolar concentrations [35].

CBC has reduced nitrites production, IL-10 and IFN- $\gamma$  levels in murine macrophages, without influencing CB $_r$  [25]. Moreover, CBC has decreased intestinal hypermotility in mice, in a manner not dependent on CB $_r$  and TRPA1 receptors [45].

Concerning the effect of other *C. sativa* constituents, cannflavins anti-inflammatory activity has been poorly investigated, but it seems to be related to the reduction of PGE $_2$  and the inhibition of 5-lipoxygenase [18, 46].

As regards terpenes, myrcene and limonene are able to reduce cytokines production and inhibit NF- $\kappa$ B and MAPK in LPS-stimulated murine macrophages [47].  $\beta$ -Caryophyllene reduced TNF- $\alpha$  and IL-1 $\beta$  production by downregulating MAPK and reducing ERK phosphorylation in LPS-stimulated PBMC [48].

As far as peripheral inflammation is concerned, *C. sativa* has been used medicinally for centuries to treat a variety of disorders, including those associated with the gastrointestinal tract. Recent investigations have highlighted the involvement of the endocannabinoid system in the physiology of the gastrointestinal function and its possible deregulation in gastrointestinal pathology [49]. The precise mechanisms across tissue departments that are under the regulatory control of the endocannabinoid system have not been fully understood [49].

Cannabinoids have been found to modulate intestinal permeability in an *in vitro* model. Both  $\Delta^9$ -THC and CBD are able to restore the increased permeability induced by either EDTA or endocannabinoids whether applied to the apical or basolateral membrane of Caco-2 cells [50]. These data suggest that endocannabinoids may play a role in the modulation of gut permeability and that *Cannabis*-based medicines may possess therapeutic benefit in a variety of gastrointestinal diseases characterized by abnormal intestinal permeability, such as inflammatory bowel disease (IBD) and shock [50].

These findings have been further confirmed in another *in vitro* model of intestinal inflammation. In particular,

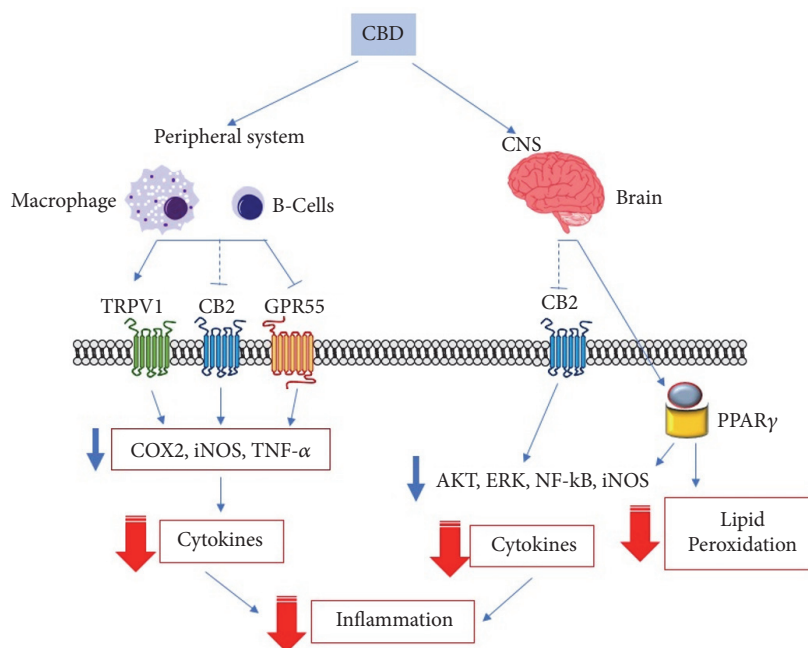


FIGURE 2: General representation of the signaling pathways involved in CBD anti-inflammatory effects. Cannabinoids reduce peripheral inflammation by acting at TRPV1, CB<sub>2</sub>, and GPR55 receptors; these interactions lead to downregulation of enzymes involved in the production of prostaglandins, reactive oxygen species, and cytokines. MAPK inhibition and NF-κB downregulation, together with PPARγ-mediated reduction of lipid peroxidation, are also involved in the anti-inflammatory effects of cannabinoids in the CNS. Abbreviations: CBD, cannabidiol; CNS, central nervous system, CB<sub>2</sub>, cannabinoid receptor 2; TRPV1, receptor potential channel subfamily V member 1; GPR55, orphan G-protein coupled receptor 55; Akt, protein kinase B; ERK, extracellular signal-regulated kinases; NF-κB nuclear factor kappa-light-chain-enhancer of activated B cells; iNOS, inducible nitric oxide synthase; COX2, cyclooxygenase 2; TNF-α, tumor necrosis factor alpha; PPARγ, peroxisome proliferator-activated receptor gamma.

endocannabinoids caused further increases in Caco-2 cell permeability in the presence of cytokines, whereas both Δ<sup>9</sup>-THC and CBD restored increased permeability induced by cytokines [51]. The effects of cytokines on increased permeability were inhibited by a CB<sub>1</sub> receptor antagonist and a 2-AG synthesis inhibitor and were enhanced by inhibitors of the degradation of AEA or 2-AG, suggesting that local production of endocannabinoids activating CB<sub>1</sub> may play a role in the modulation of gut permeability during inflammation [51].

CBD anti-inflammatory effects on the acutely inflamed human colon have also been investigated in combination with palmitoylethanolamide (PEA) in cultured cell lines and this effect was compared with experimentally inflamed explant human colonic tissue [52]. In particular, Caco-2 cells and human colonic explants collected from elective bowel cancer, inflammatory bowel disease (IBD), or acute appendicitis resections were used. CBD and PEA were able to prevent cytokine production in human colonic explant tissue via PPARα, CB<sub>2</sub>, and TRPV1, but not in Caco-2 cells [52]. These effects extend into chronic inflammatory processes, such as IBD, but also acute inflammatory conditions, such as appendicitis. Since these two compounds are well tolerated in humans with few side effects, their clinical use in treating IBD can be very useful [52].

In another study, CBD has been demonstrated to improve *Clostridium difficile* toxin A-induced damage in Caco-2

cells, by inhibiting the apoptotic process and restoring the intestinal barrier integrity, through the involvement of CB<sub>1</sub> receptors [53]. *Clostridium difficile* infection is the leading cause of hospital-acquired diarrhea and pseudomembranous colitis. *Clostridium difficile* toxin A significantly affects enterocytes permeability leading to apoptosis and colonic mucosal damage. Given the absence of any significant toxic effect in humans, CBD may ideally represent an effective adjuvant treatment for *Clostridium difficile*-associated colitis [53].

In addition to the protective role of *Cannabis* components on the inflamed intestine, an additional positive aspect is their potential role in preventing imbalances of gut microbiota. This aspect not only is relevant for the treatment of several gastrointestinal disorders, such as IBD and obesity, but also has implications for the treatment of colorectal cancer (CRC). The impact of the endocannabinoid system on gut microbiota is a relatively new and emerging field wherein the interplay between cannabinoids and metabolic syndrome has been the focus so far. Recent data have suggested that Δ<sup>9</sup>-THC prevents further exacerbation of the Firmicutes:Bacteroidetes ratio typically found in obesity, resulting in weight-loss, indicating that *Cannabis* may play a role in CRC prevention as well [54]. Further studies are needed to determine whether CBD has the same effect on gut microbiota with respect to the balance of Firmicutes:Bacteroidetes to evaluate its application in halting the progression of the obese microbiota profile

present in CRC, with the hopes of delaying this disease onset [54].

### 3. The Role of the Endocannabinoid System in Neuroinflammation

CB<sub>1</sub> receptors are much more expressed in the brain if compared to CB<sub>2</sub> [55]. However, CB<sub>2</sub> can be upregulated under neuroinflammatory conditions and as a result of the invasion of peripheral cells expressing CB<sub>2</sub> [56].

The neuroprotective effect of endocannabinoids involves the suppression of proinflammatory cytokines and the increase of anti-inflammatory cytokines production. This altered expression is mainly mediated by the activation of the MAPKs pathway and regulated primarily by MKP-1 [23].

A decrease of TNF- $\alpha$ , IL-6, IL-1 $\beta$ , and IL-12 levels in rats brain has been observed after treatment with LPS in several studies. Nevertheless, cannabinoids have been found to increase the production of cytokines, including TNF- $\alpha$ , IL-6, IL-1 $\beta$ , and IL-10, when administered alone [57].

Cytokines may regulate the normal activity of the endocannabinoid system in different ways: for example, IL-4 and IL-10 are able to stimulate FAAH activity, whereas IFN- $\gamma$  and IL-12 decrease FAAH expression, resulting in an increase of AEA levels [58, 59]. TNF- $\alpha$  and IL-6 are the major cytokines which can regulate CBR activity. Indeed, these cytokines have pro- and anti-inflammatory properties, depending on a variety of factors. Recent studies have shown that TNF- $\alpha$  provides a crucial signal for stem cells migration through CB<sub>1</sub>/CB<sub>2</sub> signaling. The activation of TNF- $\alpha$  receptor then leads to 2AG synthesis, which may act on CB<sub>1</sub> and CB<sub>2</sub>. This activity leads to a promotion of stem cells proliferation and migration that might have important implications for brain self-repairing processes [60].

The cannabinoid system and cytokine network are directly related. CB<sub>1</sub> and CB<sub>2</sub> expression is significantly induced by the presence of TNF- $\alpha$ . This occurs, at least in part, through the activation of NF- $\kappa$ B, which could be induced by stimulation of TNF receptor. Upon activation, NF- $\kappa$ B translocates into the nucleus, where it binds DNA and triggers the transcription of target genes, some of which encode inflammatory proteins and may include the CBR genes [61].

**3.1. Nonpsychoactive Cannabinoids and Neuroinflammation.** Evidences suggest that controlled neuroinflammation is crucial for tissue repair within the brain [62, 63]. However, prolonged exposure to inflammatory conditions in the brain has been linked with the development of neurodegenerative diseases, such as the Alzheimer's and Parkinson's diseases, and multiple sclerosis [64]. In Alzheimer's disease, misfolded and aggregated proteins are recognized by microglia and activate an innate immune response characterized by the release of inflammatory mediators, contributing to the disease progression and severity [65]. The role of neuroinflammation in the pathogenesis of Parkinson's diseases is supported by several experimental evidences, even if it remains unclear whether the inflammatory processes are involved in the initiation of the disease or are secondary consequences of the brain injury [66, 67]. Regarding multiple sclerosis,

inflammation appears to be mediated by T-helper 1 cells, with enhanced presence of Th1/Th17 cells being found in central nervous system (CNS) tissue, cerebrospinal fluid (CSF), and blood of patients [68, 69].

*C. sativa* and its constituents have been reported to be promising candidates for the management of several neuroinflammatory conditions (Figure 2) [70]. CBD, similarly to  $\Delta^9$ -THC, has been able to reduce neurotoxicity in SH-SY5Y neuronal cells exposed to LPS-conditioned BV2 microglial cells medium, by modulating BV2 morphological plasticity and cytokines signaling through the activation of GPR18 receptors [71].

In an *in vitro* model of neuroinflammation using LPS-stimulated rat microglia, CBD has suppressed TNF- $\alpha$ , IL-1 $\beta$ , and IL-6 release, by reducing NF- $\kappa$ B phosphorylation, together with COX and iNOS activation, in a CB<sub>2</sub> dependent manner [72, 73]. Interestingly, CBD has caused a downregulation of Akt and ERK pathways in human glioma cells [74]. The inhibition of ATP-induced intracellular calcium increase, together with the inhibition of NO production, has been suggested as a mechanism by which CBD can reduce microglia activation [75]. In cultured rat primary astrocytes, CBD has reduced the A $\beta$ -induced release of NO, IL-1 $\beta$ , and TNF- $\alpha$ , by activating PPAR $\gamma$  and inhibiting NF- $\kappa$ B nuclear translocation [76]. In another work, CBD has also inhibited the neurotoxic effects of protease-resistant prion protein (PrPres) and it has affected PrPres-induced microglial cell migration in a concentration-dependent manner; so, it may protect neurons against the multiple molecular and cellular factors involved in the different steps of the neurodegenerative process, which takes place during prion infection [77]. More recently, the neuroprotection of fibre-type hemp extracts and CBD was assessed in human neuroblastoma SH-SY5Y and microglial BV-2 cell lines in the presence of rotenone as the toxic agent, also in serum-free conditions [78]. The decarboxylated hemp extract has shown a mild neuroprotective activity on BV-2 cells treated with rotenone, higher than that of pure CBD [78]. As regards serum-free experiments, the nondecarboxylated hemp extract was the most effective neuroprotective agent toward SH-SY5Y cells, while BV-2 cells were better protected from the toxic insult by the decarboxylated extract and CBD [78].

Concerning other cannabinoids, the anti-inflammatory properties of CBG have been described in an *in vitro* model of neuroinflammation, using NSC motor neurons conditioned with the medium of LPS-stimulated murine macrophages. CBG treatment in macrophages has prevented neuronal cytotoxicity by reducing inflammation, (i.e., IL-1 $\beta$ , TNF- $\alpha$ , and IFN- $\gamma$  production, together with PPAR $\mu$  protein levels) and oxidative stress, reducing nitrotyrosine, SOD1, and iNOS protein levels and restoring Nrf-2 levels [79].

As regards other *C. sativa* components,  $\beta$ -caryophyllene is able to reduce the production of IL-1 $\beta$ , TNF- $\alpha$ , IL-6, and ROS, through the inhibition of NF- $\kappa$ B nuclear translocation in murine microglial cells, after hypoxic exposure [80].

In the ambit of CNS pathology and, in particular, regarding Alzheimer's disease, studies in rodents have demonstrated the ability of CBD to reduce reactive gliosis and



neuroinflammatory response as well as to promote neurogenesis [81]. Moreover, in an *in vitro* model using SH-SY5Y human neuroblastoma cells, CBD has been able to induce ubiquitination of APP protein, reducing  $\beta$ -amyloid peptide production and neuronal apoptosis through activation of PPAR $\gamma$  [82]. These results are consistent with those obtained by Hughes and coworkers, who have observed a PPAR $\gamma$  mediated neuroprotective effect of CBD in the hippocampus of C57Bl/6 mice [83].

#### 4. Inflammation and Cancer

Cancer is the second leading cause of death worldwide, and it accounts for about 8.8 million deaths in 2015 (GHO 2018 data); nearly 1 of 6 deaths is due to cancer. Cancer is a multistep disease characterized by a formation of a preneoplastic lesion (initiation processes) which, by time, progresses into malignant tumor. Generally, cell transformation is a combination of intrinsic genetic factors and external exposure to physical, chemical, and biological carcinogens. However, it must be underlined that ageing and life style are others fundamental factors for the development of the disease. Indeed, the incidence of cancer rises dramatically with age, probably due to the decreased efficacy of cellular repair mechanisms, while tobacco, alcohol, unhealthy diet, and physical inactivity are the major global cancer risks. A number of evidences pointed out that chronic inflammation, independently of the triggering agent, could be responsible of almost 20% of human cancers [84]. As described above, inflammation *per se* is not dangerous, since it protects the body by increasing host defense and it is self-limiting. However, persistent and deregulated inflammation is associated with an increased risk of malignant diseases [85]. Cells and mediators of the innate immune system have been detected in many cancers, even when inflammation is not implicated in tumor development [85, 86]. This finding suggests that inflammatory conditions and carcinogenesis might share common pathways, such as proliferation, increased cell survival, and migration, where cytokines and growth factors play a pivotal and fundamental role. Therefore, not only can inflammation cause cancer, but also cancer causes inflammation [87]. Thus, in the tumor microenvironment, inflammatory mediators regulate a number of proinflammatory responses, acting in an autocrine and/or paracrine manner, leading to either an antiproliferative response or an increase of cancer promotion through the inhibition of protective immune response [88]. In this context, it has been shown that the activation of the proinflammatory NF- $\kappa$ B pathway has a tumor prosurvival effect, giving chemotherapy resistance to cancer cells in an Akt-independent pathway, but involving the epidermal growth factor (EGF) activating signaling [89]. This interesting link between inflammation and growth factors, such as EGF/EGFR, configures an intriguing perspective in the study of the possible correlation between inflammatory processes and aberrant cell growth. Studies carried out on liver cancer have shown that chronic tissue damage and inflammation in liver result in a sustained overexpression and overstimulation of the EGFR pathway and that the deregulated EGFR signaling has been reported to play an

important role in the development of liver cancer [89]. Proinflammatory stimuli activated by EGFR promote the release of EGFR ligands, such as heparin-binding-EGF (HB-EGF), from liver cancer cells and endothelial cells, which stimulate the proliferation of initiated hepatocytes [89], and further potentiate their aggressive behavior [90]. Moreover, the finding that CBD suppresses the activation of EGF/EGFR signaling transduction pathway and its downstream targets Akt, ERK, and NF- $\kappa$ B suggests that the effect of *C. sativa* extract might play an important in the modulation on the intricate relationship between growth factors, inflammation, and cell growth [90]. Indeed, the ability to inhibit proinflammatory pathways, as described in the previous chapter, strongly indicates that cannabinoids are antiproliferative compounds by possibly interfering with NF- $\kappa$ B/EGF/EGFR pathway. This hypothesis has been further supported by Elbaz et al. [91], who have demonstrated that CBD, acting on its receptors, changes cytokine secretion, such as CCL3, GM-CSF, and MIP-2 proteins, from 4T1.2 tumor cells compared to vehicle-treated cells, thus decreasing the recruitment of macrophages to the tumor microenvironment and, therefore, suppressing both angiogenesis and the invasive potential of cancer cells. In addition, the presence of GPR55 receptor, which is able to bind CBD, on NK cells, represents a possible novel modulatory activity of NK cell responsiveness [92]. Noteworthy, the noncanonical cannabinoid receptor G coupled receptor GPR55-mediated NK cell stimulation and/or inhibition is of particular importance in tumor immune-surveillance, since these cells play a pivotal role in the recognition and elimination of malignant cells.

#### 5. The Role of the Endocannabinoid System in Cancer

The role of the endocannabinoid system in cancer biology is a controversial matter. Indeed, if on one hand an increase, although with a different pattern and extent, of endocannabinoid receptors CB<sub>1</sub> and CB<sub>2</sub> in various types of cancers has been observed, on the other hand the endocannabinoid system seems to play a tumor suppressing role on colon carcinoma in a genetic modified mouse model, carrying a knockdown of CB<sub>1</sub> gene [93]. However, the majority of researches have reported an increase of CB<sub>1</sub> and CB<sub>2</sub> in different types of cancer. In particular, CB<sub>1</sub> receptor has been found to be upregulated in cellular hepatocarcinoma [94] and in Hodgkin lymphoma cells [95], and its expression correlates with the severity of the disease in human epithelial ovarian cancer [96], whereas CB<sub>2</sub> has been found to be overexpressed in human breast adenocarcinomas associated with HER2+ [97] and in glioma [98]. Moreover, CB<sub>1</sub> and CB<sub>2</sub> expression has been proposed to be a factor of bad prognosis following surgery in stage IV of colorectal cancer [99]. All these findings support the hypothesis that cannabinoids might interfere with cancer biology, acting on CB<sub>1</sub> and CB<sub>2</sub> receptors in a wide range of cancer types, in particular for  $\Delta^9$ -tetrahydrocannabinavarin ( $\Delta^9$ -THCV), which is a homologue of  $\Delta^9$ -THC with a propyl side chain instead of a pentyl group. However, since nonpsychoactive cannabinoids, such

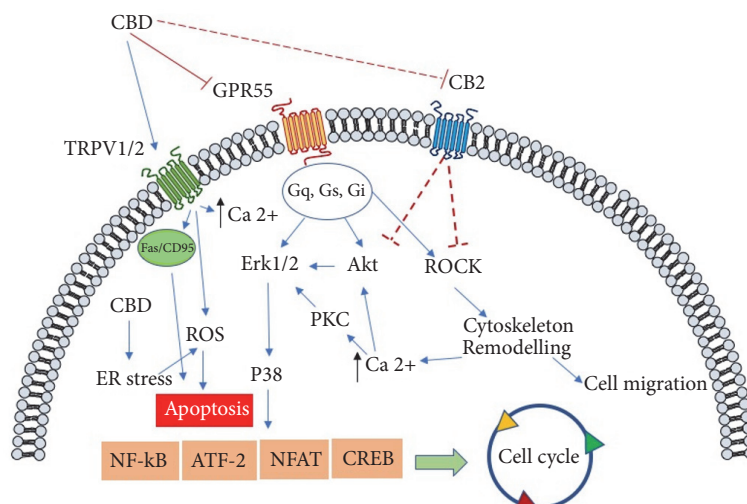


FIGURE 3: General representation of the signaling pathways involved in CBD anticancer mediated effects. Cannabinoid-induced apoptosis relies on the stimulation of endoplasmic reticular (ER) stress and through stimulation of TRPV channel. The signaling route involving the arrest of cell proliferation is mediated by the antagonism mainly on GPR55, which causes an inhibition of the activation of ERK pathway; in addition, the block of ROCK activation might be responsible for the antimigratory effect elicited by cannabidiol. CBD, cannabidiol; CB<sub>2</sub>, cannabinoid receptor 2; TRPV1/2, receptor potential channel subfamily V members 1 and 2; GPR55, orphan G-protein coupled receptor 55; ROS, reactive oxygen species; ER, endoplasmic reticulum; p8, protein p8 (Nuclear Protein 1, NUPR1); CHOP, CCAAT/-enhancer-binding protein homologous protein; ATF2, activating transcription factor 2; CREB, cAMP response element-binding protein; Akt, protein kinase B; ROCK Rho-associated protein kinase; NFAT, nuclear factor of activated T-cells; NF-κB, nuclear factor kappa-light-chain-enhancer of activated B cells; PKC, protein kinase C; P38, mitogen-activated protein kinases.

as CBD, do not bind with high affinity to both CB<sub>1</sub> and CB<sub>2</sub>, alternative pathways should be considered in order to analyze the molecular mechanisms of CBD anticancer activity (Figure 3).

**5.1. Nonpsychoactive Cannabinoids and Cancer.** In cancer treatment, cannabinoids, such as dronabinol (synthetic Δ<sup>9</sup>-THC) and nabilone (a synthetic cannabinoid similar to Δ<sup>9</sup>-THC), are mainly used in association with chemotherapy in order to decrease its side effects such as pain, weight loss, nausea, and vomiting, although their use is still limited due to their psychoactive side effects [100]. However, incoming evidences have suggested that their activity could not be ascribed solely to these “palliative” effects, but rather the compounds could possess some interesting properties in terms of inhibition of tumor cell proliferation.

The first evidence of the ability of cannabinoids, and in particular Δ<sup>9</sup>- and Δ<sup>8</sup>-THC (Figure 1), to reduce the growth of lung adenocarcinoma both *in vitro* and *in vivo* has been reported by Munson et al. in 1975 [101]. As mentioned above, in recent years a number of researches have been made to evaluate the antiproliferative and proapoptotic effects of cannabinoids in both *in vitro* and *in vivo* models and in different cancer types, such as glioma, breast, pancreas, prostate, colorectal and lung carcinoma, and lymphoma [102–109]. These results prompted up the research of the possible molecular mechanism involved in the effects mediated by cannabinoids, together with the discovery of new activities elicited by these compounds, such as the interference with angiogenesis, cancer cell migration, and invasion [110]. All

these findings strongly reinforce the idea that these compounds are able to control the cell survival/death fate and, therefore, they could be good candidates in cancer therapies.

**5.2. Nonpsychoactive Cannabinoids and GPR55.** GPR55 is a, so-called, orphan receptor protein, constituted by 319 amino acids, and it is present in the chromosome 2q37 [111]. GPR55 has been identified for the first time in 1999, and it belongs to the δ group of rhodopsin-like G protein coupled receptors (GPCRs) [112]. GPR55 possesses different biological functions based upon its localization: it controls the motility of the gastrointestinal tract, angiogenesis, and neuropathic pain; it modulates the inflammatory processes and it is involved in intracellular signaling involving the upstream signaling of RhoA, ROCK, ERK, and p38 mitogen activated protein kinase pathways, and Ca<sup>2+</sup> release, which in turn modulate the downstream, cell motility and stiffness and the transcription factors nuclear factor activated T cell (NFAT), nuclear-factor-kB (NF-κB), cAMP response elements binding protein (CREB), and the activating transcription factor-2 (ATF2) [113–115]. The modulation of these important biological determinants indicates that GPR55 is a possible pharmacological target in a number of diseases where these pathways are deregulated, such as cancer. Increased expression of GPR55 and severity and malignancy of the disease has been reported in different cancer types, such as the human pancreatic ductal adenocarcinoma, the squamous cell carcinomas human astrocytoma, the melanoma, the B lymphoblastoma [116–118], and the hepatocellular carcinoma as well [94]. Although the pharmacology of GPR55 remains

controversial, a number of evidences have suggested that it is a non- $CB_1/CB_2$  receptor able to bind nonpsychoactive cannabinoids and CBD in particular is its putative ligand, acting as an antagonist [119, 120]. In this view, Shrivastava et al. [121] have demonstrated that CBD is able to kill breast cancer cells by inducing ER stress, enhancing ROS generation and inhibiting mTOR signaling. In addition, CBD has been found to regulate the balance between autophagy and mitochondria-mediated apoptosis. This latter effect could be mediated by the antagonistic effect of CBD to GPR55, since its inhibition with anandamide allows the recruitment of the death receptor Fas into cell membrane through the activation of protein  $G\alpha_{12}$  and Jun N-terminal kinase [113]. Moreover, Solinas et al. [74] have shown the antiproliferative and anti-invasive effects of CBD in U87-MG cells in a  $CB_1/CB_2$  independent manner, and these effects have been extended to T98G glioma cells, a  $\Delta^9$ -THC-resistant lineage, thus suggesting a possible alternative pathway from that involving  $CB_1/CB_2$  receptors. CBD effects are mediated by a significant downregulation of ERK and PI3K/Akt kinases, which are fundamental for cell survival and proliferation (Figure 3). The finding that stable overexpression of this GPR55 in HEK293 cells led to increased levels of phosphorylated extracellular signal-regulated kinase (ERK) [117] involved in cell proliferation strongly indicates that GPR55 is a target for CBD-mediated anticancer activity. Moreover, the fact that CBD downregulates the expression of angiogenic related proteins both *in vitro* and *in vivo*, such as matrix metalloproteinase 9 (MMP9), tissue inhibitor of metalloproteinases 1 (TIMP1), serpinE1-plasminogen activator inhibitor type-1 (PAI-1), CXCL16, ET-1, PDGF-AA, and IL-8 [74], reinforces the hypothesis that CBD might exert its antiangiogenic activity through the interaction with GPR55. Indeed, a clear relationship between GPR55 and angiogenesis has been reported by Zhang et al. [122], where the endothelial vascular cells regulate GPR55-mediated angiogenesis through the autocrine release of LPI; once GPR55 was downregulated in primary human microvascular endothelial cells, a decrease in angiogenesis was observed. Even if all these data clearly indicate that the antagonism of CBD on GPR55 activity inhibits cancer cell proliferation and angiogenesis and increases apoptosis, further studies are necessary, in order to better understand and to complete the portrait of the relation between CBD, GPR55, and cancer biology both in *in vitro* and *in vivo* models. Moreover, other protein receptors may be able to bind CBD, and in turn they can be of importance in the modulation of cancer growth.

**5.3. Cannabinoids and TRPVs.** Beside the discussed GPR55 receptors for nonpsychoactive cannabinoids, another non- $CB_1/CB_2$  receptor system, i.e., the transient receptor protein of vanilloid types 1 and 2 (TRPV1, TRPV2), has been proposed to bind either endocannabinoid or phytocannabinoids. The TRP receptors control mainly body temperature perception, thermal pain, and noxious stimuli and they are involved in several biological functions, such as cell proliferation [123].

In particular, the TRPV vanilloid channels belong to a superfamily of channels called "Transient Receptor Potential" (TRP), which promote calcium entry into the cells. The

most extensively studied receptor in the ambit of the TRPV family is represented by TRPV1. TRPV1 and TRPV2 are ubiquitously expressed throughout the body, with a particular abundance in the central nervous system (CNS), and they differ both in the activities that they mediate and in their pharmacological profiles [124]. TRPV1 is activated by heat and, once activated, it allows the entrance of calcium and magnesium into the cells. Upon activation, the channel undergoes a rapid desensitization in a Ca-dependent manner.

TRPV1 is modulated by a number of bioactive compounds, such as capsaicin, piperine, camphor, CBD, and the endocannabinoid anandamide, which activate the channel. TRPV2 is not modulated by pungent-tasting compounds, such as capsaicin or piperine, but it shares with TRPV1 the activation elicited by CBD, related cannabinoids, and probenecid. It differs also from TRPV1 for its role in various osmo- or mechanosensory activities rather than noxious heat stimuli [125]. So, both TRPV1 and TRPV2 receptors are activated by CBD [126, 127], allowing an increase of intracellular  $Ca^{2+}$  [128]. The activation and the subsequent desensitization of these receptor proteins, which are involved in transducing acute inflammatory and chronic pain (especially TRPV1), might be responsible for the antihyperalgesic actions of CBD [127]. Interestingly, the results found on prostate and skin cancers cells have shown that both TRPV1 and TRPV2 are involved in cancer progression, thanks to their ability to interact with G-proteins and, therefore, to interfere with intracellular signaling and to modulate intracellular  $Ca^{2+}$  [129, 130]. Protein receptors are differently up- and downregulated in cancer tissues, thus indicating a possible different role in cancer progression. In particular, TRPV1 is upregulated in glioma, prostate, and pancreas cancers, whereas it is downregulated in hepatocellular carcinoma (HCC), bladder, and skin cancer [123]. TRPV2 is upregulated in bladder, prostate, and HCC, while it is downregulated in glioma cancer cells [123]. In this context, it has been demonstrated that the concomitant overexpression of TRPV2 and insulin-like growth factor 1 (IGF-1) suggests that TRPV2 might control the urothelial cancer cell growth and progression through the modulation of IGF-1 pathway [131]. In U87MG glioblastoma/astrocytoma cell line, TRPV2 decreases cell malignancy and cell survival in an ERK dependent manner [123]. In addition, TRPV1 has been found to be colocalized with the proapoptotic protein Fas/CD95, and, when stimulated with the agonist capsaicin, it causes a cell cycle arrest in G0/G1 in RT4 and apoptosis in urothelial cancer cells [132]. So, the interaction with an agonist on TRPV1 or TRPV2 receptors could originate different biological responses, depending on the distribution of TRPV, together with the fine interactions with other molecular complexes. In this view, CBD has been found to inhibit the multidrug resistance (MDR), by interacting with TRPV1 and  $CB_2$  at the same time (Figure 3). Indeed, in the MDR CEM/VLB100 cell model, Arnold et al. have reported that the treatment with CBD caused a downregulation of P-glycoprotein (P-gp) expression and an increase of the cytotoxic effects of vinblastine, whose P-gp is the substrate [133]. However, this effect was mediated both by the cooperation of CBD with TRPV1 and by  $CB_2$  receptors,



indicating once more the intricate complexity of interaction between biological pathways. Moreover, the ability of CBD to increase the cytotoxic activity of anticancer agents, such as temozolomide, doxorubicin, and carmustine in U87MG cancer cells, allowed Nabissi et al. [134] to discover that this effect was due to the interaction of CBD with TRPV2 receptor, which resulted in an increase of drug uptake. This interesting finding could be of relevance also in the management of glioma cancer stem cells (GSCs). Indeed, it has been reported that TRPV2 activation led to a GSCs differentiation and, therefore, to an inhibition of their proliferation [135]. This effect could be due, at least in part, to the ability of CBD to upregulate the prodifferentiation factor ID2 and to downregulate the metastatic factor ID1 [136], since both these proteins play an important role in spreading neuroblastoma cells [137]. Taking into account the fact that GSCs are the major factor responsible for glioma recurrence, the use of CBD could also be a valuable tool against the proliferation of the GSCs subpopulations present in glioma/glioblastoma cancers.

## 6. Hemp Extracts and CBD between Present and Future

This review is mainly focused on the role of CBD and related nonpsychoactive compounds in the modulation of the inflammatory processes linked to the degenerative diseases and, in particular, to cancer. From a pharmaceutical point of view, CBD represents at the moment the most promising compound present in *C. sativa*. Although this component is well-known mainly for its antioxidant and anti-inflammatory activities, a number of researches pointed out its ability to interfere with cell proliferation apoptosis and cancer growth. If we consider also that cancer biology and inflammation share several common pathways in some stages of their biological processes, CBD might be a potential important tool in the control of cancer spread and growth.

It is important however to consider also other issues regarding cannabinoids and their use, comprising the poor availability of the plant material, the uncertainties on the quality of the products, and the safety of CBD. For these reasons, CBD is under scrutiny at many levels, ranging from national health organizations to FDA and WHO. Up to now, many clinical trials have been performed on Sativex®, which is a combination of  $\Delta^9$ -THC and CBD, or on Epidiolex®, which is currently in phase three, with encouraging results against a severe form of epilepsy in children.

However, one of the main points under debate is whether cannabinoids and CBD, in particular, are safe for consumers at the doses found to be active in the experimental conditions, by taking into account the fact that there is only limited knowledge about the long-term effects of chronic use and drug-drug interactions between CBD and other medications, although human studies have indicated that CBD is very well tolerated even at high doses. Another important issue is whether or not *Cannabis* extracts or CBD are simply a food supplement, a pharmaceutical product, or other. If on one hand this perplexity is justified by the need for a reliable

evaluation of the balance between efficacy and side effects, on the other hand it must be recognized that, in some cases, an unconscious prejudice seems to hover on *C. sativa*, mainly because of its history of drug of abuse.

We believe that although an important number of studies regarding the therapeutic effects of CBD have been performed in the last decade, there is no solid clinical evidence yet to support that cannabinoids can effectively and safely treat cancer in humans. However, by taking into account the fact that hemp extracts with low  $\Delta^9$ -THC concentration but rich in nonpsychoactive compounds are still poorly studied from a pharmacological and molecular point of view, we think that they could be a precious resource for future treatment of both acute and chronic diseases. In addition, by considering the availability of specific cultivars containing different amounts of active compounds, such as flavonoids and terpenes, it might be possible to select the appropriate variety enriched of a specific class of compounds to be used for a specific disease. Moreover, if we consider that the treatment of most degenerative diseases is still far from achieving full success, the research on hemp and CBD extracts is strongly encouraged in order to have enough data for a rational clinical application.

## Conflicts of Interest

The authors declare that they have no conflicts of interest.

## References

- [1] J. A. Hartsel, J. Eades, B. Hickory, and A. Makriyannis, "Cannabis sativa and Hemp," *Nutraceuticals: Efficacy, Safety and Toxicity*, pp. 735–754, 2016.
- [2] C. M. Andre, J. Hausman, and G. Guerriero, "Cannabis sativa: The Plant of the Thousand and One Molecules," *Frontiers in Plant Science*, vol. 7, 2016.
- [3] G. Appendino, G. Chianese, and O. Tagliatalata-Scafati, "Cannabinoids: Occurrence and medicinal chemistry," *Current Medicinal Chemistry*, vol. 18, no. 7, pp. 1085–1099, 2011.
- [4] B. F. Thomas and M. A. ElSohly, "The analytical chemistry of *Cannabis*: quality assessment, assurance and regulation of medicinal marijuana and cannabinoid preparations," Elsevier, Amsterdam, 1st edition, 2015.
- [5] "European Commission, Food safety, plant variety catalogues, databases and information systems," 2018, [https://ec.europa.eu/food/plant/plant\\_propagation\\_material/plant\\_variety\\_catalogues-databases.en](https://ec.europa.eu/food/plant/plant_propagation_material/plant_variety_catalogues-databases.en).
- [6] L. O. Hanuš, S. M. Meyer, E. Muñoz, O. Tagliatalata-Scafati, and G. Appendino, "Phytocannabinoids: A unified critical inventory," *Natural Product Reports*, vol. 33, no. 12, pp. 1357–1392, 2016.
- [7] V. Brighenti, F. Pellati, M. Steinbach, D. Maran, and S. Benvenuti, "Development of a new extraction technique and HPLC method for the analysis of non-psychoactive cannabinoids in fibre-type *Cannabis sativa* L. (hemp)," *Journal of Pharmaceutical and Biomedical Analysis*, vol. 143, pp. 228–236, 2017.
- [8] F. Pellati, V. Brighenti, J. Sperlea, L. Marchetti, D. Bertelli, and S. Benvenuti, "New Methods for the Comprehensive Analysis of Bioactive Compounds in *Cannabis sativa* L. (hemp)," *Molecules*, vol. 23, no. 10, 2018.



- [9] M. A. ElSohly and D. Slade, "Chemical constituents of marijuana: the complex mixture of natural cannabinoids," *Life Sciences*, vol. 78, no. 5, pp. 539–548, 2005.
- [10] B. De Backer, B. Debrus, P. Lebrun et al., "Innovative development and validation of an HPLC/DAD method for the qualitative and quantitative determination of major cannabinoids in cannabis plant material," *Journal of Chromatography B*, vol. 877, no. 32, pp. 4115–4124, 2009.
- [11] A. A. Izzo, F. Borrelli, R. Capasso, V. Di Marzo, and R. Mechoulam, "Non-psychoactive plant cannabinoids: new therapeutic opportunities from an ancient herb," *Trends in Pharmacological Sciences*, vol. 30, no. 10, pp. 515–527, 2009.
- [12] J. Fernández-Ruiz, M. Moreno-Martet, C. Rodríguez-Cueto et al., "Prospects for cannabinoid therapies in basal ganglia disorders," *British Journal of Pharmacology*, vol. 163, no. 7, pp. 1365–1378, 2011.
- [13] S. P. H. Alexander, "Therapeutic potential of cannabis-related drugs," *Progress in Neuro-Psychopharmacology & Biological Psychiatry*, vol. 64, pp. 157–166, 2016.
- [14] A. C. Campos, M. V. Fogaça, A. B. Sonego, and F. S. Guimarães, "Cannabidiol, neuroprotection and neuropsychiatric disorders," *Pharmacological Research*, vol. 112, pp. 119–127, 2016.
- [15] R. Brenneisen, "Chemistry and analysis of phytocannabinoids and other Cannabis constituents," in *Marijuana and the Cannabinoids*, M. A. ElSohly, Ed., 49, p. 17, Marijuana and the cannabinoids, Humana Press Inc., Totowa, NJ, USA, 2007.
- [16] S. Pisanti, A. M. Malfitano, E. Ciaglia et al., "Cannabidiol: State of the art and new challenges for therapeutic applications," *Pharmacology & Therapeutics*, vol. 175, pp. 133–150, 2017.
- [17] F. Pollastro, A. Minassi, and L. G. Fresu, "Cannabis Phenolics and their Bioactivities," *Current Medicinal Chemistry*, vol. 25, no. 10, pp. 1160–1185, 2018.
- [18] O. Werz, J. Seegers, A. M. Schaible et al., "Cannflavins from hemp sprouts, a novel cannabinoid-free hemp food product, target microsomal prostaglandin E2 synthase-1 and 5-lipoxygenase," *PharmaNutrition*, vol. 2, no. 3, pp. 53–60, 2014.
- [19] G. Allegrone, F. Pollastro, G. Magagnini et al., "The Bibenzyl Canniprene Inhibits the Production of Pro-Inflammatory Eicosanoids and Selectively Accumulates in Some Cannabis sativa Strains," *Journal of Natural Products*, vol. 80, no. 3, pp. 731–734, 2017.
- [20] S. I. Grivennikov, F. R. Greten, and M. Karin, "Immunity, Inflammation, and Cancer," *Cell*, vol. 140, no. 6, pp. 883–899, 2010.
- [21] D. Namdar and H. Koltai, "Medical Cannabis for the treatment of inflammation," *Nat. Prod. Commun*, vol. 13, pp. 249–254, 2018.
- [22] K. Mackie and N. Stella, "Cannabinoid receptors and endocannabinoids: evidence for new players," *The AAPS Journal*, vol. 8, no. 2, article 34, pp. E298–E306, 2006.
- [23] L. Jean-Gilles, M. Braithe, M. L. Latif et al., "Effects of pro-inflammatory cytokines on cannabinoid CB1 and CB2 receptors in immune cells," *Acta Physiol*, vol. 214, pp. 63–74, 2015.
- [24] K. Fijal and M. Filip, "Clinical/therapeutic approaches for cannabinoid ligands in central and peripheral nervous system diseases: Mini review," *Clinical Neuropharmacology*, vol. 39, no. 2, pp. 94–101, 2016.
- [25] K. L. McCoy, "Interaction between Cannabinoid System and Toll-Like Receptors Controls Inflammation," *Mediators of Inflammation*, vol. 2016, Article ID 5831315, 18 pages, 2016.
- [26] P. Nagarkatti, R. Pandey, S. A. Rieder, V. L. Hegde, and M. Nagarkatti, "Cannabinoids as novel anti-inflammatory drugs," *Future Medicinal Chemistry*, vol. 1, no. 7, pp. 1333–1349, 2009.
- [27] S. Burstein, "Cannabidiol (CBD) and its analogs: A review of their effects on inflammation," *Bioorganic & Medicinal Chemistry*, vol. 23, no. 7, pp. 1377–1385, 2015.
- [28] J. M. Jamontt, A. Molleman, R. G. Pertwee, and M. E. Parsons, "The effects of  $\Delta^9$ -tetrahydrocannabinol and cannabidiol alone and in combination on damage, inflammation and in vitro motility disturbances in rat colitis," *British Journal of Pharmacology*, vol. 160, no. 3, pp. 712–723, 2010.
- [29] D. de Filippis, G. Esposito, C. Cirillo et al., "Cannabidiol reduces intestinal inflammation through the control of neuroimmune axis," *PLoS ONE*, vol. 6, no. 12, 2011.
- [30] J. M. Sido, A. R. Jackson, P. S. Nagarkatti, and M. Nagarkatti, "Marijuana-derived  $\Delta^9$ -tetrahydrocannabinol suppresses Th1/Th17 cell-mediated delayed-type hypersensitivity through microRNA regulation," *Journal of Molecular Medicine*, vol. 94, no. 9, pp. 1039–1051, 2016.
- [31] E. Berdyshev, E. Boichot, M. Corbel, N. Germain, and V. Lagente, "Effects of cannabinoid receptor ligands on LPS-induced pulmonary inflammation in mice," *Life Sciences*, vol. 63, no. 8, pp. 125–129, 1998.
- [32] M. D. Roth, J. T. Castaneda, and S. M. Kiertscher, "Exposure to  $\Delta^9$ -tetrahydrocannabinol impairs the differentiation of human monocyte-derived dendritic cells and their capacity for T cell activation," *Journal of Neuroimmune Pharmacology*, vol. 10, no. 2, pp. 333–343, 2015.
- [33] T. Ngaotepprutaram, B. L. Kaplan, and N. E. Kaminski, "Impaired NFAT and NF $\kappa$ B activation are involved in suppression of CD40 ligand expression by  $\Delta^9$ -tetrahydrocannabinol in human CD4+ T cells," *Toxicology and Applied Pharmacology*, vol. 273, no. 1, pp. 209–218, 2013.
- [34] Y.-H. Chang, S. T. Lee, and W.-W. Lin, "Effects of cannabinoids on LPS-stimulated inflammatory mediator release from macrophages: involvement of eicosanoids," *Journal of Cellular Biochemistry*, vol. 81, no. 4, pp. 715–723, 2001.
- [35] L. R. Ruhaak, J. Felth, P. C. Karlsson, J. J. Rafter, R. Verpoorte, and L. Bohlin, "Evaluation of the cyclooxygenase inhibiting effects of six major cannabinoids isolated from Cannabis sativa," *Biological & Pharmaceutical Bulletin*, vol. 34, no. 5, pp. 774–778, 2011.
- [36] S. C. Shivers, C. Newton, H. Friedman, and T. W. Klein, " $\Delta^9$ -tetrahydrocannabinol (THC) modulates IL-1 bioactivity in human monocyte/macrophage cell lines," *Life Sciences*, vol. 54, no. 17, pp. 1281–1289, 1994.
- [37] C. Lombard, M. Nagarkatti, and P. S. Nagarkatti, "Targeting cannabinoid receptors to treat leukemia: Role of cross-talk between extrinsic and intrinsic pathways in  $\Delta^9$ -tetrahydrocannabinol (THC)-induced apoptosis of Jurkat cells," *Leukemia Research*, vol. 29, no. 8, pp. 915–922, 2005.
- [38] W. Jia, V. L. Hegde, N. P. Singh et al., " $\Delta^9$ -tetrahydrocannabinol-induced apoptosis in Jurkat leukemia T cells is regulated by translocation of bad to mitochondria," *Molecular Cancer Research*, vol. 4, no. 8, pp. 549–562, 2006.
- [39] B. Costa, M. Colleoni, S. Conti et al., "Oral anti-inflammatory activity of cannabidiol, a non-psychoactive constituent of cannabis, in acute carrageenan-induced inflammation in the rat paw," *Naunyn-Schmiedeberg's Archives of Pharmacology*, vol. 369, no. 3, pp. 294–299, 2004.
- [40] S. Takeda, H. Okazaki, E. Ikeda et al., "Down-regulation of cyclooxygenase-2 (cox-2) by cannabidiolic acid in human

- breast cancer cells," *Journal of Toxicological Sciences*, vol. 39, no. 5, pp. 711–716, 2014.
- [41] S. Ben-Shabat, L. O. Hanuš, G. Katzavian, and R. Gallily, "New cannabidiol derivatives: Synthesis, binding to cannabinoid receptor, and evaluation of their antiinflammatory activity," *Journal of Medicinal Chemistry*, vol. 49, no. 3, pp. 1113–1117, 2006.
  - [42] B. Watzl, P. Scuderi, and R. R. Watson, "Marijuana components stimulate human peripheral blood mononuclear cell secretion of interferon-gamma and suppress interleukin-1 alpha in vitro," *International Journal of Immunopharmacology*, vol. 13, no. 8, pp. 1091–1097, 1991.
  - [43] S. Petrosino, R. Verde, M. Vaia, M. Allarà, T. Iuvone, and V. Di Marzo, "Anti-inflammatory Properties of Cannabidiol, a Nonpsychotropic Cannabinoid, in Experimental Allergic Contact Dermatitis," *The Journal of Pharmacology and Experimental Therapeutics*, vol. 365, no. 3, pp. 652–663, 2018.
  - [44] F. Borrelli, I. Fasolino, B. Romano et al., "Beneficial effect of the non-psychotropic plant cannabinoid cannabigerol on experimental inflammatory bowel disease," *Biochemical Pharmacology*, vol. 85, no. 9, pp. 1306–1316, 2013.
  - [45] A. A. Izzo, R. Capasso, G. Aviello et al., "Inhibitory effect of cannabichromene, a major non-psychotropic cannabinoid extracted from *Cannabis sativa*, on inflammation-induced hypermotility in mice," *British Journal of Pharmacology*, vol. 166, no. 4, pp. 1444–1460, 2012.
  - [46] M. L. Barrett, D. Gordon, and F. J. Evans, "Isolation from *cannabis sativa* L. of cannflavin-a novel inhibitor of prostaglandin production," *Biochemical Pharmacology*, vol. 34, no. 11, pp. 2019–2024, 1985.
  - [47] W.-J. Yoon, N. H. Lee, and C.-G. Hyun, "Limonene suppresses lipopolysaccharide-induced production of nitric oxide, prostaglandin E2, and pro-inflammatory cytokines in RAW 264.7 macrophages," *Journal of Oleo Science*, vol. 59, no. 8, pp. 415–421, 2010.
  - [48] J. Gertsch, M. Leonti, S. Raduner et al., "Beta-caryophyllene is a dietary cannabinoid," *Proceedings of the National Academy of Sciences of the United States of America*, vol. 105, no. 26, pp. 9099–9104, 2008.
  - [49] N. V. DiPatrizio, "Endocannabinoids in the Gut," *Cannabis and Cannabinoid Research*, vol. 1, no. 1, pp. 67–77, 2016.
  - [50] A. Alhamoruni, A. C. Lee, K. L. Wright, M. Larvin, and S. E. O'Sullivan, "Pharmacological effects of cannabinoids on the Caco-2 cell culture model of intestinal permeability," *The Journal of Pharmacology and Experimental Therapeutics*, vol. 335, no. 1, pp. 92–102, 2010.
  - [51] A. Alhamoruni, K. L. Wright, M. Larvin, and S. E. O'Sullivan, "Cannabinoids mediate opposing effects on inflammation-induced intestinal permeability," *British Journal of Pharmacology*, vol. 165, no. 8, pp. 2598–2610, 2012.
  - [52] D. G. Couch, C. Tasker, E. Theophilidou, J. N. Lund, and S. E. O'Sullivan, "Cannabidiol and palmitoylethanolamide are anti-inflammatory in the acutely inflamed human colon," *Clinical Science*, vol. 131, no. 21, pp. 2611–2626, 2017.
  - [53] S. Gigli, L. Seguela, M. Pesce et al., "Cannabidiol restores intestinal barrier dysfunction and inhibits the apoptotic process induced by *Clostridium difficile* toxin A in Caco-2 cells," *United European Gastroenterology Journal*, vol. 5, no. 8, pp. 1108–1115, 2017.
  - [54] R.-V. Kalaydina, B. Qorri, and M. R. Szewczuk, "Preventing negative shifts in gut microbiota with *Cannabis* therapy: implications for colorectal cancer," *Adv. Res. Gastroentero. Hepatol*, vol. 7, pp. 1–5, 2017.
  - [55] K. Mackie, Y. Lai, R. Westenbroek, and R. Mitchell, "Cannabinoids activate an inwardly rectifying potassium conductance and inhibit Q-type calcium currents in AtT20 cells transfected with rat brain cannabinoid receptor," *The Journal of Neuroscience*, vol. 15, no. 10, pp. 6552–6561, 1995.
  - [56] K. Maresz, G. Pryce, E. D. Ponomarev et al., "Direct suppression of CNS autoimmune inflammation via the cannabinoid receptor CB1 on neurons and CB2 on autoreactive T cells," *Nature Medicine*, vol. 13, no. 4, pp. 492–497, 2007.
  - [57] T. W. Klein, B. Lane, C. A. Newton, and H. Friedman, "The cannabinoid system and cytokine network," *Proceedings of the Society for Experimental Biology and Medicine*, vol. 225, no. 1, pp. 1–8, 2000.
  - [58] L. Thors, A. Bergh, E. Persson et al., "Fatty acid amide hydrolase in prostate cancer: Association with disease severity and outcome, CB1 receptor expression and regulation by IL-4," *PLoS ONE*, vol. 5, no. 8, Article ID e12275, 2010.
  - [59] M. Maccarrone, H. Valensise, M. Bari, N. Lazzarin, C. Romanini, and A. Finazzi-Agrò, "Progesterone up-regulates anandamide hydrolase in human lymphocytes: Role of cytokines and implications for fertility," *The Journal of Immunology*, vol. 166, no. 12, pp. 7183–7189, 2001.
  - [60] A. Rubio-Araiz, Á. Arévalo-Martín, O. Gómez-Torres et al., "The endocannabinoid system modulates a transient TNF pathway that induces neural stem cell proliferation," *Molecular and Cellular Neuroscience*, vol. 38, no. 3, pp. 374–380, 2008.
  - [61] M. Rajesh, P. Mukhopadhyay, S. Bátkai et al., "CB2-receptor stimulation attenuates TNF- $\alpha$ -induced human endothelial cell activation, transendothelial migration of monocytes, and monocyte-endothelial adhesion," *American Journal of Physiology-Heart and Circulatory Physiology*, vol. 293, no. 4, pp. H2210–H2218, 2007.
  - [62] S. Vivekanantham, S. Shah, R. Dewji, A. Dewji, C. Khatri, and R. Ologunde, "Neuroinflammation in Parkinson's disease: Role in neurodegeneration and tissue repair," *International Journal of Neuroscience*, vol. 125, no. 10, pp. 717–725, 2015.
  - [63] T. Koudriavtseva and C. Mainero, "Neuroinflammation, neurodegeneration and regeneration in multiple sclerosis: Inter-correlated manifestations of the immune response," *Neural Regeneration Research*, vol. 11, no. 11, pp. 1727–1730, 2016.
  - [64] R. Gordon and T. M. Woodruff, "Neuroinflammation as a therapeutic target in neurodegenerative diseases," in *Disease-modifying targets in neurodegenerative disorders*, V. Baekelandt and E. Lobbestael, Eds., pp. 49–80, Academic Press, Cambridge, 2017.
  - [65] M. T. Heneka, M. J. Carson, J. El. Khoury et al., "Neuroinflammation in Alzheimer's disease," *The Lancet Neurology*, vol. 14, no. 4, pp. 388–405, 2015.
  - [66] Géraldine Gelders, Veerle Baekelandt, and Anke Van der Perren, "Linking Neuroinflammation and Neurodegeneration in Parkinson's Disease," *Journal of Immunology Research*, vol. 2018, Article ID 4784268, 12 pages, 2018.
  - [67] E. C. Hirsch, S. Vyas, and S. Hunot, "Neuroinflammation in Parkinson's disease," *Parkinsonism & Related Disorders*, vol. 18, no. 1, pp. S210–S212, 2012.
  - [68] T. Chitnis, "The Role of CD4 T Cells in the Pathogenesis of Multiple Sclerosis," *International Review of Neurobiology*, vol. 79, pp. 43–72, 2007.
  - [69] B. J. Kaskow and C. Baecher-Allan, "Effector T Cells in Multiple Sclerosis," *Cold Spring Harbor Perspectives in Medicine*, vol. 8, no. 4, p. a029025, 2018.

- [70] V. Borgonetti, P. Governa, M. Montopoli, and M. Biagi, "Cannabis sativa L. constituents and their role in neuroinflammation," *Curr. Bioact. Compd*, 2018.
- [71] E. Janefjord, J. L. V. Mååg, B. S. Harvey, and S. D. Smid, "Cannabinoid effects on  $\beta$  amyloid fibril and aggregate formation, neuronal and microglial-activated neurotoxicity in vitro," *Cellular and Molecular Neurobiology*, vol. 34, no. 1, pp. 31–42, 2014.
- [72] E. Kozela, M. Pietr, A. Juknat, N. Rimmerman, R. Levy, and Z. Vogel, "Cannabinoids delta(9)-tetrahydrocannabinol and cannabidiol differentially inhibit the lipopolysaccharide-activated NF-kappaB and interferon-beta/STAT proinflammatory pathways in BV-2 microglial cells," *The Journal of Biological Chemistry*, vol. 285, no. 3, pp. 1616–1626, 2010.
- [73] S. A. Hunter and S. H. Burstein, "Receptor mediation in cannabinoid stimulated arachidonic acid mobilization and anandamide synthesis," *Life Sciences*, vol. 60, no. 18, pp. 1563–1573, 1997.
- [74] M. Solinas, P. Massi, V. Cinquina et al., "Cannabidiol, a Non-Psychoactive Cannabinoid Compound, Inhibits Proliferation and Invasion in U87-MG and T98G Glioma Cells through a Multitarget Effect," *PLoS ONE*, vol. 8, no. 10, Article ID e76918, 2013.
- [75] A. M. Martín-Moreno, D. Reigada, B. G. Ramírez et al., "Cannabidiol and other cannabinoids reduce microglial activation in vitro and in vivo: Relevance to alzheimer's disease," *Molecular Pharmacology*, vol. 79, no. 6, pp. 964–973, 2011.
- [76] G. Esposito, C. Scuderi, M. Valenza et al., "Cannabidiol reduces A $\beta$ -induced neuroinflammation and promotes hippocampal neurogenesis through PPAR $\gamma$  involvement," *PLoS ONE*, vol. 6, no. 12, Article ID e28668, 2011.
- [77] S. Dirikoc, S. A. Priola, M. Marella, N. Zsürger, and J. Chabry, "Nonpsychoactive cannabidiol prevents prion accumulation and protects neurons against prion toxicity," *The Journal of Neuroscience*, vol. 27, no. 36, pp. 9537–9544, 2007.
- [78] L. Corsi, F. Pellati, V. Brighenti, N. Plessi, and S. Benvenuti, "Chemical composition and in vitro neuroprotective activity of fibre-type Cannabis sativa L. (hemp)," *Current Bioactive Compounds*, vol. 14, 2018.
- [79] A. Gugliandolo, F. Pollastro, G. Grassi, P. Bramanti, and E. Mazzon, "In Vitro Model of Neuroinflammation: Efficacy of Cannabigerol, a Non-Psychoactive Cannabinoid," *International Journal of Molecular Sciences*, vol. 19, no. 7, article E1992, 2018.
- [80] K. Guo, X. Mou, J. Huang, N. Xiong, and H. Li, "Transcaryophyllene suppresses hypoxia-induced neuroinflammatory responses by inhibiting NF- $\kappa$ B activation in microglia," *Journal of Molecular Neuroscience*, vol. 54, no. 1, pp. 41–48, 2014.
- [81] G. Watt and T. Karl, "In vivo evidence for therapeutic properties of cannabidiol (CBD) for Alzheimers Disease," *Front. Pharmacol*, vol. 8, article 20, 2017.
- [82] C. Scuderi, L. Steardo, and G. Esposito, "Cannabidiol promotes amyloid precursor protein ubiquitination and reduction of beta amyloid expression in SHSY5YAPP+ cells through PPAR $\gamma$  involvement," *Phytotherapy Research*, vol. 28, no. 7, pp. 1007–1013, 2014.
- [83] B. Hughes and C. E. Herron, "Cannabidiol Reverses Deficits in Hippocampal LTP in a Model of Alzheimer's Disease," *Neurochemical Research*, 2018.
- [84] K. Kundu and Y. J. Surh, "Inflammation: gearing the journey to cancer," *Mutat. Res*, vol. 659, pp. 15–30, 2008.
- [85] A. Mantovani, P. Allavena, A. Sica, and F. Balkwill, "Cancer-related inflammation," *Nature*, vol. 454, no. 7203, pp. 436–444, 2008.
- [86] H. F. Dvorak, "Tumors: wounds that do not heal: similarities between tumor stroma generation and wound healing," *The New England Journal of Medicine*, vol. 315, no. 26, pp. 1650–1659, 1986.
- [87] S. M. Crusz and F. R. Balkwill, "Inflammation and cancer: advances and new agents," *Nature Reviews Clinical Oncology*, vol. 12, pp. 584–596, 2015.
- [88] S. I. Grivnenkov and M. Karin, "Inflammation and oncogenesis: a vicious connection," *Curr. Opin. Genet. Dev*, vol. 20, pp. 65–71, 2010.
- [89] K. Tanaka, I. Babic, D. Nathanson et al., "Oncogenic EGFR signaling activates an mTORC2-NF- $\kappa$ B pathway that promotes chemotherapy resistance," *Cancer Discovery*, vol. 1, no. 6, pp. 524–538, 2011.
- [90] C. Berasain, M. J. Perugorria, M. U. Latasa et al., "The Epidermal Growth Factor Receptor: A Link Between Inflammation and Liver Cancer," *Experimental Biology and Medicine*, vol. 234, no. 7, pp. 713–725, 2009.
- [91] M. Elbaz, M. W. Nasser, J. Ravi et al., "Modulation of the tumor microenvironment and inhibition of EGF/EGFR pathway: Novel anti-tumor mechanisms of Cannabidiol in breast cancer," *Molecular Oncology*, vol. 9, no. 4, pp. 906–919, 2015.
- [92] V. Chiurchiù, M. Lanuti, M. De Bardi, L. Battistini, and M. MacCarrone, "The differential characterization of GPR55 receptor in human peripheral blood reveals a distinctive expression in monocytes and NK cells and a proinflammatory role in these innate cells," *International Immunology*, vol. 27, no. 3, pp. 153–160, 2015.
- [93] D. Wang, H. Wang, W. Ning, M. G. Backlund, S. K. Dey, and R. N. DuBois, "Loss of cannabinoid receptor 1 accelerates intestinal tumor growth," *Cancer Research*, vol. 68, no. 15, pp. 6468–6476, 2008.
- [94] B. Mukhopadhyay, K. Schuebel, P. Mukhopadhyay et al., "Cannabinoid receptor 1 promotes hepatocellular carcinoma initiation and progression through multiple mechanisms," *Hepatology*, vol. 61, no. 5, pp. 1615–1626, 2015.
- [95] A. H. Benz, C. Renné, E. Maronde et al., "Expression and functional relevance of cannabinoid receptor 1 in hodgkin lymphoma," *PLoS ONE*, vol. 8, no. 12, Article ID e81675, 2013.
- [96] E. M. Messalli, F. Grauso, R. Luise, A. Angelini, and R. Rossiello, "Cannabinoid receptor type 1 immunoreactivity and disease severity in human epithelial ovarian tumors," *American Journal of Obstetrics & Gynecology*, vol. 211, no. 3, pp. 234–e6, 2014.
- [97] E. Pérez-Gómez, C. Andradas, and S. Blasco-Benito, "Role of Cannabinoid Receptor CB2 in HER2 Pro-oncogenic Signaling in Breast Cancer," *JNCI: Journal of the National Cancer Institute*, vol. 107, no. 6, 2015.
- [98] C. A. Dumitru, I. E. Sandalcioğlu, and M. Karsak, "Cannabinoids in Glioblastoma Therapy: New Applications for Old Drugs," *Frontiers in Molecular Neuroscience*, vol. 11, article 159, 2018.
- [99] C. K. Jung, W. K. Kang, J. M. Park et al., "Expression of the cannabinoid type I receptor and prognosis following surgery in colorectal cancer," *Oncology Letters*, vol. 5, no. 3, pp. 870–876, 2013.
- [100] F. K. Engels, F. A. de Jong, R. H. J. Mathijssen, J. A. Erkens, R. M. Herings, and J. Verweij, "Medicinal cannabis in oncology," *European Journal of Cancer*, vol. 43, no. 18, pp. 2638–2644, 2007.



- [101] A. E. Munson, L. S. Harris, M. A. Friedman, W. L. Dewey, and R. A. Carchman, "Antineoplastic Activity of Cannabinoids2," *JNCI: Journal of the National Cancer Institute*, vol. 55, no. 3, pp. 597–602, 1975.
- [102] I. Galve-Roperh, C. Sánchez, M. L. Cortés, T. G. Del Pulgar, M. Izquierdo, and M. Guzmán, "Anti-tumoral action of cannabinoids: Involvement of sustained ceramide accumulation and extracellular signal-regulated kinase activation," *Nature Medicine*, vol. 6, no. 3, pp. 313–319, 2000.
- [103] C. Sánchez, M. L. de Ceballos, T. Gomez del Pulgar et al., "Inhibition of glioma growth in vivo by selective activation of the CB2 cannabinoid receptor," *Cancer Res*, vol. 61, pp. 5784–5789, 2001.
- [104] M. L. Casanova, C. Blázquez, J. Martínez-Palacio et al., "Inhibition of skin tumor growth and angiogenesis in vivo by activation of cannabinoid receptors," *The Journal of Clinical Investigation*, vol. 111, no. 1, pp. 43–50, 2003.
- [105] C. Blázquez, A. Carracedo, L. Barrado et al., "Cannabinoid receptors as novel targets for the treatment of melanoma," *The FASEB journal: official publication of the Federation of American Societies for Experimental Biology*, vol. 20, no. 14, pp. 2633–2635, 2006.
- [106] A. Carracedo, M. Gironella, M. Lorente et al., "Cannabinoids induce apoptosis of pancreatic tumor cells via endoplasmic reticulum stress-related genes," *Cancer Research*, vol. 66, no. 13, pp. 6748–6755, 2006.
- [107] F. Ciani, L. Papucci, N. Schiavone et al., "Cannabinoid receptor activation induces apoptosis through tumor necrosis factor alpha-mediated ceramide de novo synthesis in colon cancer cells," *Clinical Cancer Research*, vol. 14, no. 23, pp. 7691–7700, 2008.
- [108] M. Bifulco and V. Di Marzo, "Targeting the endocannabinoid system in cancer therapy: A call for further research," *Nature Medicine*, vol. 8, no. 6, pp. 547–550, 2002.
- [109] M. Bifulco, C. Laezza, S. Pisanti, and P. Gazerro, "Cannabinoids and cancer: Pros and cons of an antitumour strategy," *British Journal of Pharmacology*, vol. 148, no. 2, pp. 123–135, 2006.
- [110] N. Freimuth, R. Ramer, and B. Hinz, "Antitumorigenic effects of cannabinoids beyond apoptosis," *The Journal of Pharmacology and Experimental Therapeutics*, vol. 332, no. 2, pp. 336–344, 2010.
- [111] M. Sawzdargo, T. Nguyen, D. K. Lee et al., "Identification and cloning of three novel human G protein-coupled receptor genes GPR52, GPR53 and GPR55: GPR55 is extensively expressed in human brain," *Brain Research*, vol. 64, no. 2, pp. 193–198, 1999.
- [112] R. Fredriksson, M. C. Lagerström, L.-G. Lundin, and H. B. Schiöth, "The G-protein-coupled receptors in the human genome form five main families. Phylogenetic analysis, paralogon groups, and fingerprints," *Molecular Pharmacology*, vol. 63, no. 6, pp. 1256–1272, 2003.
- [113] D. Leyva-Illades and S. DeMorrow, "Orphan G protein receptor GPR55 as an emerging target in cancer therapy and management," *Cancer Management and Research*, vol. 5, no. 1, pp. 147–155, 2013.
- [114] C. M. Henstridge, N. A. Balenga, R. Schröder et al., "GPR55 ligands promote receptor coupling to multiple signalling pathways," *British Journal of Pharmacology*, vol. 160, no. 3, pp. 604–614, 2010.
- [115] J. E. Lauckner, J. B. Jensen, H.-Y. Chen, H.-C. Lu, B. Hille, and K. Mackie, "GPR55 is a cannabinoid receptor that increases intracellular calcium and inhibits M current," *Proceedings of the National Academy of Sciences of the United States of America*, vol. 105, no. 7, pp. 2699–2704, 2008.
- [116] S. Oka, S. Kimura, T. Toshida, R. Ota, A. Yamashita, and T. Sugiura, "Lysophosphatidylinositol induces rapid phosphorylation of p38 mitogen-activated protein kinase and activating transcription factor 2 in HEK293 cells expressing GPR55 and IM-9 lymphoblastoid cells," *The Journal of Biochemistry*, vol. 147, no. 5, pp. 671–678, 2010.
- [117] C. Andradas, M. M. Caffarel, E. Pérez-Gómez et al., "The orphan G protein-coupled receptor GPR55 promotes cancer cell proliferation via ERK," *Oncogene*, vol. 30, no. 2, pp. 245–252, 2011.
- [118] E. Pérez-Gómez, C. Andradas, J. M. Flores et al., "The orphan receptor GPR55 drives skin carcinogenesis and is upregulated in human squamous cell carcinomas," *Oncogene*, vol. 32, no. 20, pp. 2534–2542, 2013.
- [119] E. Ryberg, N. Larsson, S. Sjögren et al., "The orphan receptor GPR55 is a novel cannabinoid receptor," *British Journal of Pharmacology*, vol. 152, no. 7, pp. 1092–1101, 2007.
- [120] A. Kapur, P. Zhao, H. Sharir et al., "Atypical responsiveness of the orphan receptor GPR55 to cannabinoid ligands," *The Journal of Biological Chemistry*, vol. 284, no. 43, pp. 29817–29827, 2009.
- [121] A. Shrivastava, P. M. Kuzontkoski, J. E. Groopman, and A. Prasad, "Cannabidiol Induces Programmed Cell Death in Breast Cancer Cells by Coordinating the Cross-talk between Apoptosis and Autophagy," *Molecular Cancer Therapeutics*, vol. 10, no. 7, pp. 1161–1172, 2011.
- [122] X. Zhang, Y. Maor, J. F. Wang, G. Kunos, and J. E. Groopman, "Endocannabinoid-like N-arachidonoyl serine is a novel pro-angiogenic mediator," *British Journal of Pharmacology*, vol. 160, no. 7, pp. 1583–1594, 2010.
- [123] G. Santoni, V. Farfariello, and C. Amantini, "TRPV Channels in Tumor Growth and Progression," in *Transient Receptor Potential Channels*, vol. 704 of *Advances in Experimental Medicine and Biology*, pp. 947–967, Springer Netherlands, Dordrecht, 2011.
- [124] R. Vennekens, G. Owsianik, and B. Nilius, "Vanilloid transient receptor potential cation channels: An overview," *Current Pharmaceutical Design*, vol. 14, no. 1, pp. 18–31, 2008.
- [125] A. Perálvarez-Marín, P. Doñate-Macian, and R. Gaudet, "What do we know about the transient receptor potential vanilloid 2 (TRPV2) ion channel?" *FEBS Journal*, vol. 280, no. 21, pp. 5471–5487, 2013.
- [126] T. Bisogno, L. Hanuš, L. De Petrocellis et al., "Molecular targets for cannabidiol and its synthetic analogues: Effect on vanilloid VR1 receptors and on the cellular uptake and enzymatic hydrolysis of anandamide," *British Journal of Pharmacology*, vol. 134, no. 4, pp. 845–852, 2001.
- [127] N. Qin, M. P. Nepper, Y. Liu, T. L. Hutchinson, M. L. Lubin, and C. M. Flores, "TRPV2 is activated by cannabidiol and mediates CGRP release in cultured rat dorsal root Ganglion neurons," *The Journal of Neuroscience*, vol. 28, no. 24, pp. 6231–6238, 2008.
- [128] A. Ligresti, A. S. Moriello, K. Starowicz et al., "Antitumor activity of plant cannabinoids with emphasis on the effect of cannabidiol on human breast carcinoma," *The Journal of Pharmacology and Experimental Therapeutics*, vol. 318, no. 3, pp. 1375–1387, 2006.
- [129] M. Flourakis and N. Prevarskaya, "Insights into Ca<sup>2+</sup> homeostasis of advanced prostate cancer cells," *Biochimica et Biophysica Acta (BBA) - Molecular Cell Research*, vol. 1793, no. 6, pp. 1105–1109, 2009.



- [130] A. M. Bode, Y.-Y. Cho, D. Zheng et al., "Transient receptor potential type vanilloid 1 suppresses skin carcinogenesis," *Cancer Research*, vol. 69, no. 3, pp. 905–913, 2009.
- [131] M. A. Rochester, N. Patel, B. W. Turney et al., "The type 1 insulin-like growth factor receptor is over-expressed in bladder cancer," *BJU International*, vol. 100, no. 6, pp. 1396–1401, 2007.
- [132] C. Amantini, P. Ballarini, S. Caprodossi et al., "Triggering of transient receptor potential vanilloid type 1 (TRPV1) by capsaicin induces Fas/CD95-mediated apoptosis of urothelial cancer cells in an ATM-dependent manner," *Carcinogenesis*, vol. 30, no. 8, pp. 1320–1329, 2009.
- [133] J. C. Arnold, P. Hone, M. L. Holland, and J. D. Allen, "CB2 and TRPV1 receptors mediate cannabinoid actions on MDR1 expression in multidrug resistant cells," *Pharmacological Reports*, vol. 64, no. 3, pp. 751–757, 2012.
- [134] M. Nabissi, M. B. Morelli, M. Santoni, and G. Santoni, "Triggering of the TRPV2 channel by cannabidiol sensitizes glioblastoma cells to cytotoxic chemotherapeutic agents," *Carcinogenesis*, vol. 34, no. 1, pp. 48–57, 2013.
- [135] M. B. Morelli, M. Nabissi, C. Amantini et al., "The transient receptor potential vanilloid-2 cation channel impairs glioblastoma stem-like cell proliferation and promotes differentiation," *International Journal of Cancer*, vol. 131, no. 7, pp. E1067–E1077, 2012.
- [136] S. D. McAllister, R. Murase, R. T. Christian et al., "Pathways mediating the effects of cannabidiol on the reduction of breast cancer cell proliferation, invasion, and metastasis," *Breast Cancer Research and Treatment*, vol. 129, no. 1, pp. 37–47, 2011.
- [137] J. Perk, A. Iavarone, and R. Benezra, "Id family of helix-loop-helix proteins in cancer," *Nature Reviews Cancer*, vol. 5, no. 8, pp. 603–614, 2005.

## Research Article

# Gallic Acid Attenuates Dimethylnitrosamine-Induced Liver Fibrosis by Alteration of Smad Phosphoisoform Signaling in Rats

Yuxin Chen <sup>1</sup>, Ziping Zhou,<sup>1</sup> Qigui Mo,<sup>1</sup> Gao Zhou,<sup>1</sup> and Youwei Wang <sup>1,2</sup>

<sup>1</sup>Institute of TCM and Natural Products, School of Pharmaceutical Sciences, Wuhan University, Wuhan 430071, China

<sup>2</sup>MOE Key Laboratory of Combinatorial Biosynthesis and Drug Discovery, Wuhan University, Wuhan 430072, China

Correspondence should be addressed to Youwei Wang; [wyw@whu.edu.cn](mailto:wyw@whu.edu.cn)

Received 31 August 2018; Revised 31 October 2018; Accepted 8 November 2018; Published 2 December 2018

Academic Editor: Ravirajsinh N. Jadeja

Copyright © 2018 Yuxin Chen et al. This is an open access article distributed under the Creative Commons Attribution License, which permits unrestricted use, distribution, and reproduction in any medium, provided the original work is properly cited.

Dimethylnitrosamine (DMN) is a potent hepatotoxin, carcinogen, and mutagen. In our previous study, a candidate gallic acid (GA) that widely exists in food and fruit was selected for its capability to alleviate DMN toxicity *in vivo*. We aimed to investigate the therapeutic potential of GA against DMN-induced liver fibrosis. During the first four weeks, DMN was administered to rats via intraperitoneal injection every other day, except the control group. GA or silymarin was given to rats by gavage once daily from the second to the sixth week. GA significantly reduced liver damage in serum parameters and improved the antioxidant capacity in liver and kidney tissues. Cytokines involved in liver fibrosis were measured at transcriptional and translational levels. These results indicate that GA exhibits robust antioxidant and antifibrosis effects and may be an effective candidate natural medicine for liver fibrosis treatment.

## 1. Introduction

Chronic liver disease is one of the major health problems, with liver cirrhosis and drug-induced liver damage being the ninth leading cause of death, in western and developing countries [1]. Liver fibrosis is a critical stage in the pathogenesis of liver damage to cirrhosis or a tumor, because liver fibrosis can be reversed, but liver cirrhosis and liver cancer cannot be reversed [2]. Therefore, conducting some drug treatments is critical to avoid deterioration during the stage of liver fibrosis. In recent years, the molecular mechanism of antifibrosis has attracted scholars, and many excellent *in vivo* models have been established for the study of liver fibrosis regulation. These models induced by toxins such as dimethylnitrosamine (DMN), CCl<sub>4</sub>, acetaminophen, or thioacetamide can represent chronic or acute/fulminant hepatitis [3]. DMN is a potent hepatotoxin, carcinogen, and mutagen. A minimal dose of 20 mg/kg DMN can cause hepatocellular necrosis and death in many species [4]. Repeated exposure to lower doses of DMN resulted in a subacute or chronic liver injury with varying degrees of necrosis, fibrosis, and nodular

regeneration [5]. The DMN-induced fibrosis model is a good model to use since it has many of the similar characteristics observed in human liver fibrosis, such as an initial central hemorrhagic necrosis of the liver with rapid formation of septa and fully established micronodular cirrhosis [6]. The model also has the advantage of producing progressive and significant pathological changes, high fibrogenesis rates, and low mortality of experimental animals [7]. Therefore, our study selected DMN as the inducer of liver fibrosis.

Countries, such as China, Japan, and India, have had their own medical theories and systems, in which they become accustomed to using a variety of plants with or without current medicines in order to treat various illnesses. Recently, the beneficial effects of compounds derived from plants for the prevention and treatment of liver fibrosis have attracted extensive attention. Ramalin, an antioxidant compound derived from Antarctic lichen, has been reported to be able to prevent progression of liver fibrosis induced by DMN in rats, potentially via the Nrf2/ARE pathway [8]. Curcumin, which is a yellow pigment found in the rhizome of the spice turmeric, has shown amelioration of liver

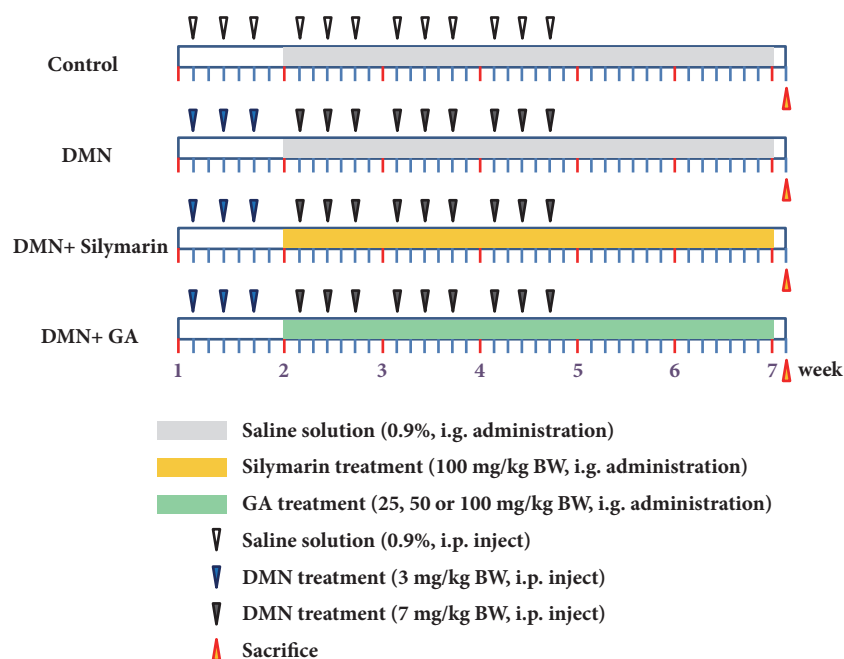


FIGURE 1: Schematic illustration for animal experiment design. DMN at 3 mg/kg BW is injected three times on the first week (blue triangle), and DMN at 7 mg/kg BW is injected three times per week from the second to the fourth week (black triangle) to all the rats except the rats in control group. Saline is injected as a control under the same regime (hollow triangle). Subsequently, GA (green column) or silymarin (yellow column) is suspended in saline and administered daily by intragastric gavage (i.g.) from the second to the sixth week. Saline is administered as a control under the same regime (gray column). Rats were weighed and sacrificed six weeks after first DMN injection (red triangle).  $n = 8$  animals/group.

cirrhosis via its anti-inflammatory effect and suppression of HSC activity [9]. Silymarin, a clinical antifibrotic agent, is widely accepted and used for treating liver diseases. It downregulates TIMP metalloproteinase inhibitor 1 (TIMP-1) and transforming growth factor beta 1 (TGF- $\beta$ 1) expressions and suppresses collagen synthesis [10]. Silymarin is a unique flavonoid complex containing silybin, silydianin, and silychristin derived from the milk thistle plant [11]. Currently, silymarin remains the most widely clinical used antifibrotic agent in China. So we selected silymarin as the positive control in our study.

In previous study, we proved that the ethyl acetate fraction (EF) from the fruit of *Terminalia bellirica* has an antifibrotic effect in vitro [12]. Mass spectrometry analysis shows that the main components of EF are gallic acid (GA) and ellagic acid (unpublished data). GA, a type of phenolic acid with strong antioxidant effect, can be found in white, red, and black mulberry, blackberry, raspberry, strawberry, dragon fruit, guava, mangosteen, papaya, tea leaves, and other plants [13–15]. Since GA is a major component of EF, we hypothesize that GA is a major contributor to the antifibrotic effects of EF.

In this study, we aim to prove that GA has the capability to reverse liver fibrosis by using an animal model of liver fibrosis induced by DMN and to investigate biomarkers altered by GA treatment after the liver of the rat suffers subchronic injury.

## 2. Materials and Methods

**2.1. Chemicals.** All chemical reagents and commercial kits used are referred to in Supplementary Table 1.

**2.2. Animals.** A total of 48 male Sprague Dawley rats (180–200 g) were purchased from the Laboratory Animal Center of Wuhan University (Wuhan, China). They were housed in a 12 h light–dark cycle at  $25 \pm 2^\circ\text{C}$  and at a relative humidity of 50%–70%. Animals were fed ad libitum with a standard diet of pellets and water. Animals were allowed to acclimate to housing conditions for three days prior to experimentation. This study secured clearance from the Institutional Animal Care and Use Committee (IACUC) at Center for Animal Experiment, Wuhan University, China.

**2.3. Study Design.** The rats were divided into six groups consisting of eight animals per group and underwent six weeks of treatment. The design of the animal work refers to Su et al. [16] and slightly modified. The schematic for DMN induction of liver fibrosis and for GA treatment refers to Figure 1. Group I was administered 0.9% saline solution as control; Group II was administered 3 mg/kg and 7 mg/kg DMN dissolved in 0.9% saline solution; Group III was the positive control group and administered silymarin, 100 mg/kg BW; Group IV was the low-dose GA group administered 25 mg/kg BW; Group V was the medium-dose GA group administered 50 mg/kg BW; and Group VI was the high-dose GA group administered 100 mg/kg BW.

**2.4. Determination of Body and Organ Weights.** The body weights were recorded before the rats were sacrificed by spine dislocation. After the rats were sacrificed, livers, kidneys, and spleens were extracted and weighed immediately.

TABLE 1: Effects of GA on body and organ weight in rats with DMN-induced liver fibrosis (n = 8).

Group	Weight (g)			
	Body	Liver	Kidney	Spleen
Group I control	442.38±16.72 a	15.58±0.90 a	2.85±0.15 a	1.09±0.09 a
Group II DMN	383.08±9.24 bc	12.81±0.45 b	2.44±0.09 b	0.98±0.05 a
Group III silymarin 100 (mg/kg)	368.78±12.94 b	11.66±0.74 b	2.46±0.13 b	0.99±0.07 a
Group IV GA 25 (mg/kg)	399.90±7.14 c	14.01±0.68 ab	2.64±0.10 ab	1.12±0.04 a
Group V GA 50 (mg/kg)	384.88±8.03 bc	12.66±0.45 b	2.47±0.09 b	1.11±0.06 a
Group VI GA 100 (mg/kg)	361.94±10.38 b	12.03±0.40 b	2.45±0.09 b	1.02±0.05 a

Values are Mean ± SEM., “a, b, c” means values in the same column with different letters are significantly different from each other (p<0.05).



**2.5. Determination of Serum Biomarkers.** At the end of the experiment, all rats were fasted overnight and sacrificed the next day. Blood was extracted from the heart and coagulated. The serum was obtained by centrifugation at 1000g for 10 min and stored at  $-20^{\circ}\text{C}$  until use. Alanine aminotransferase (ALT), aspartate aminotransferase (AST), alkaline phosphatase (ALP), and total bilirubin (TB) were determined by the commercial kits consistent with the instructions of the manufacturers.

**2.6. Oxidative Stress Assessment in Liver and Kidney.** After the livers and kidneys were extracted and weighed, 10% liver or kidney tissue homogenate was prepared with 50 mM sodium phosphate buffer (pH 7.4) and centrifuged at 5000g for 10 min at  $4^{\circ}\text{C}$ . The supernatants were transferred into new tubes and stored at  $-80^{\circ}\text{C}$  for subsequent experiments. The total protein content was determined using the Bradford method. The activities of superoxide dismutase (SOD) and catalase (CAT) and the levels of glutathione (GSH) and malondialdehyde (MDA) were determined by commercial kits, following the steps indicated in the kit manuals.

**2.7. Hematoxylin–Eosin and Masson's Trichrome Staining.** For each rat, a piece of liver tissue was fixed in 10% formalin for at least 24 h, embedded in paraffin, and cut into  $5\ \mu\text{m}$  thick sections using a rotary microtome. The sections were stained with hematoxylin–eosin and Masson's trichrome dye, and then the slides were observed under a microscope (IX51, Olympus, Japan) to detect histopathological changes in the liver.

**2.8. ELISA.** The supernatants obtained from 10% liver homogenates were diluted in appropriate concentrations for each ELISA kit according to the range determined from the standard curve. Transforming growth factor beta 1 (TGF- $\beta$ 1), epidermal growth factor (EGF), and hydroxyproline were quantified by the corresponding assay kit consistent with the instructions of the manufacturers.

**2.9. RNA Extraction and Real-Time Polymerase Chain Reaction.** After the rats were sacrificed, the liver was quickly extracted and a small piece was ground in liquid nitrogen. After grinding in liquid nitrogen with RNase-free instrumentation, TRIzol reagent was quickly added to the ground samples. Real-time PCR was subsequently performed to detect the gene expression of alpha smooth muscle actin ( $\alpha$ -SMA), platelet-derived growth factor receptor (PDGFR), TIMP-1, and tissue inhibitor of metalloproteinases 2 (TIMP-2) in triplicate using the CFX384 Touch Real-Time PCR Detection System (Bio-Rad, China). All mRNA quantification data were normalized to glyceraldehyde 3-phosphate dehydrogenase (GAPDH). For the primers, refer to Supplementary Table 2. For the amplification condition of the PCR, refer to Chen et al. [12].

**2.10. Western Blot.** The protein concentrations of the supernatants from 10% homogenate were determined by the Bradford method. Equal protein amount of supernatant from each sample was fractionated by gradient sodium dodecyl sulfate-polyacrylamide gel electrophoresis. 5% stacking gel and 12%

separating gel were used for collagen I, and 5% stacking gel and 15% separating gel were used for Smad2, Smad3, p-Smad2, p-Smad3, and  $\beta$ -actin protein. The separated proteins were then transferred to polyvinylidene difluoride (PVDF) blotting membranes. Nonspecific binding was blocked by 5% nonfat milk or 5% bovine serum albumin (BSA) in TBST for 2 h and then incubated overnight at  $4^{\circ}\text{C}$  with the respective primary antibodies. The membranes were then washed and incubated with horseradish peroxidase-conjugated secondary antibodies for 1 h at room temperature. Immunoreactive bands were visualized using a chemiluminescent reagent and then exposed to X-Omat Blue XB-1 Film (Kodak, Rochester, NY) for autoradiography. The gray density of each blot was analyzed by ImageJ software (NIH, Bethesda, MD, USA).

**2.11. Statistical Analysis.** All data are shown as mean  $\pm$  SEM corresponding to three replicates. IBM SPSS Statistics 20.0 was used for data analysis. Statistical differences were analyzed by one-way ANOVA, and the LSD test was performed to evaluate the significant differences of means at  $p < 0.05$  level.

### 3. Results

**3.1. Effect of GA on Rat Body and Organ Weights.** Table 1 displays the body, liver, kidney, and spleen weights of the rats after 6 weeks of treatment. From the changes in body weight, we can see that the weight of rats in the DMN model group (Group II) decreased significantly ( $p < 0.01$ ) compared with the control group (Group I). The silymarin-treated (Group III) and all GA-treated groups (Groups IV–VI) had no significant effect on body weight gain compared to Group II. With increasing GA dose, the body weight gradually decreased. Hence, we hypothesize that GA has potential pharmacological effects on weight loss. The liver weight of the control group was significantly different from that of the other groups, except Group IV, and no significant difference was observed among Groups II, III, V, and VI. The statistical analysis of the kidney weights shows a similar trend with that of the liver. No statistically significant difference was observed in the spleen weights among the groups.

**3.2. Effect of GA on Determining the Serum Biomarker.** After treatment with GA for six weeks, serum levels of ALT, TB, ALP, and AST increased by 1.4-, 1.5-, 1.6-, and 1.7-fold, respectively, compared to control (Figures 2(b), 2(d), 2(c), and 2(a)). GA treatment with 50 or 100 mg/kg BW significantly prevented these biomarkers from elevating ( $p < 0.05$ ) compared to the DMN model group. The lowest dose of GA (25 mg/kg BW) had a comparable effect with silymarin (100 mg/kg BW) on reversing the elevation of AST and ALP levels induced by DMN (Figures 2(a) and 2(c)). For ALT and TB levels (Figures 2(b) and 2(d)), the effect of the low-dose GA was better than that of silymarin. These results show that GA has a protective effect on liver injury induced by the long-term administration of DMN in a dose-dependent manner.

**3.3. Effect of GA on the Oxidative Stress Assessment in Liver and Kidney.** In liver tissue, SOD, and CAT activities and GSH

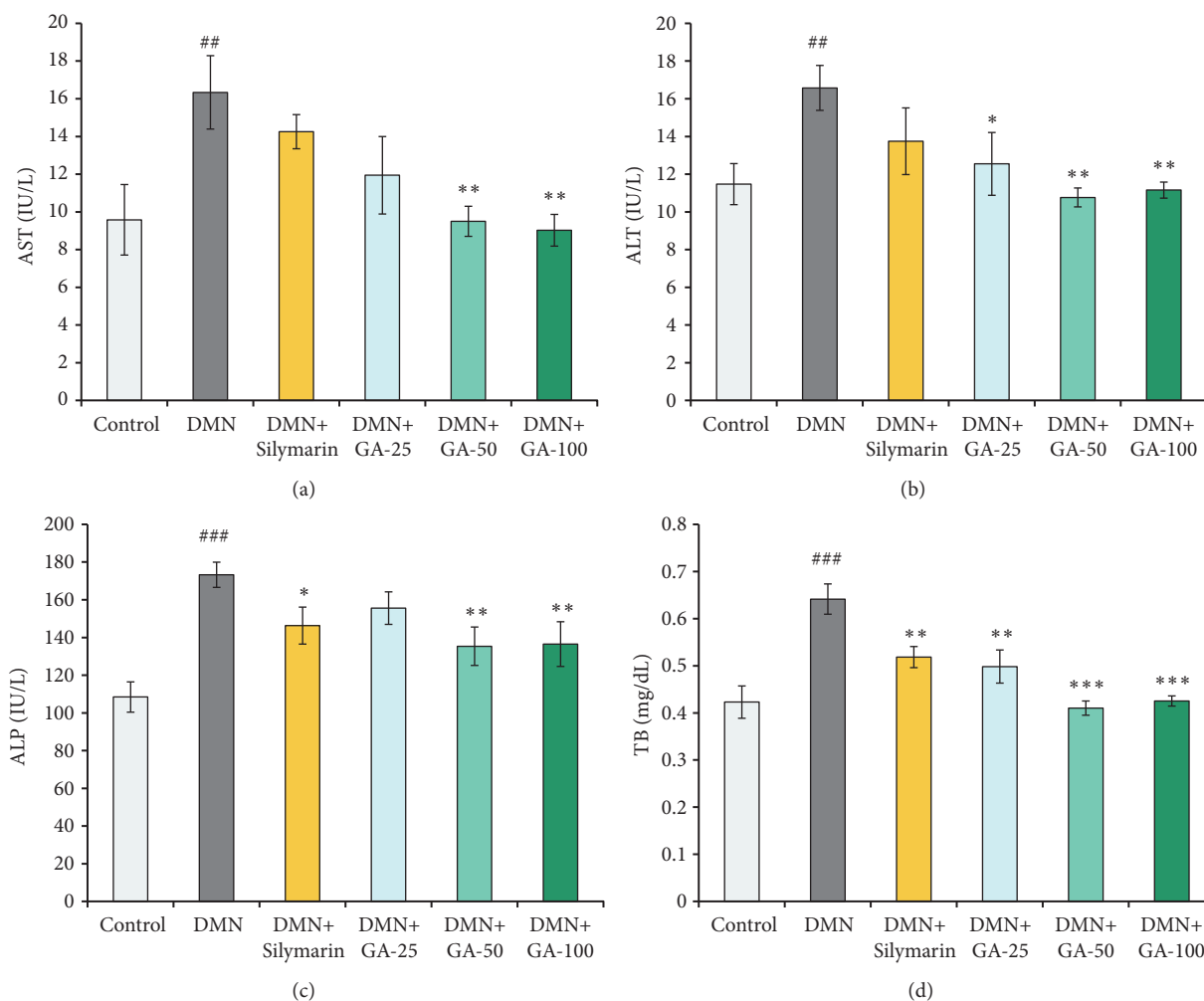


FIGURE 2: Effects of EF on the (a) AST, (b) ALT, (c) and ALP activities, and (d) the level of TB in the serum of rats with DMN-induced liver fibrosis (n = 8). The statistically significant differences are indicated by symbols (#  $p < 0.05$ , ##  $p < 0.01$ , and ###  $p < 0.001$  compared with the control group; \*  $p < 0.05$ , \*\*  $p < 0.01$ , and \*\*\*  $p < 0.001$  compared with the DMN-induced group).

level in the DMN model groups were significantly ( $p < 0.01$ ,  $p < 0.001$ ,  $p < 0.05$ , respectively) lower than their control groups, whereas the level of MDA was significantly ( $p < 0.001$ ) increased compared to the control group. This observation was significantly ( $p < 0.05$ ,  $p < 0.001$ ,  $p < 0.05$ , and  $p < 0.001$ ) reversed by the high-dose GA (100 mg/kg BW) treatment (Figures 3(a)–3(d)). Although the values showed that the silymarin and low- and medium-dose GA groups affect the reversal of the changes of SOD, CAT, GSH, and MDA shown in the DMN groups, statistically significant differences were not observed. The results obtained from the four biomarkers showed that the highest dose of GA had the best effect on liver protection. Although the highest doses of GA and silymarin shared the same dose (100 mg/kg), the effect of GA was much better than the effect of silymarin.

In the kidney tissue, compared with the control groups, the DMN model significantly ( $p < 0.05$  and  $p < 0.001$ ) reduced the activities of SOD and CAT (Figures 3(a) and 3(b)), while it significantly ( $p < 0.001$ ) elevated the MDA level (Figure 3(d)). After GA treatment (25, 50, and 100

mg/kg BW) and silymarin treatment, SOD activities were not significantly increased compared with the model group, but the values were slightly higher than that of the model group (Figure 3(a)). Compared to the model group, CAT activities increased significantly after treatment with the medium and high doses of GA and silymarin ( $p < 0.01$  and  $p < 0.01$ ) (Figure 3(b)). The three doses of GA and silymarin significantly lowered the MDA levels ( $p < 0.05$ ,  $p < 0.001$ ,  $p < 0.001$ , and  $p < 0.01$ , respectively) when compared to the value of model group (Figure 3(d)). Notably, the DMN model did not statistically significantly affect GSH levels (Figure 3(c)). However, the value of the model group remains the lowest, whereas the value of the highest dose GA group is closest to that of the control group. Hence, the highest dose of GA had the best protective effect on the kidney.

**3.4. Effects of GA on the Histopathological Changes.** Hematoxylin–eosin staining (Figure 4) of the DMN group (Figure 4(b)) showed sinus fibrosis and hyperplastic wire mesh-like collagen fibers around the liver cells (black circle). A

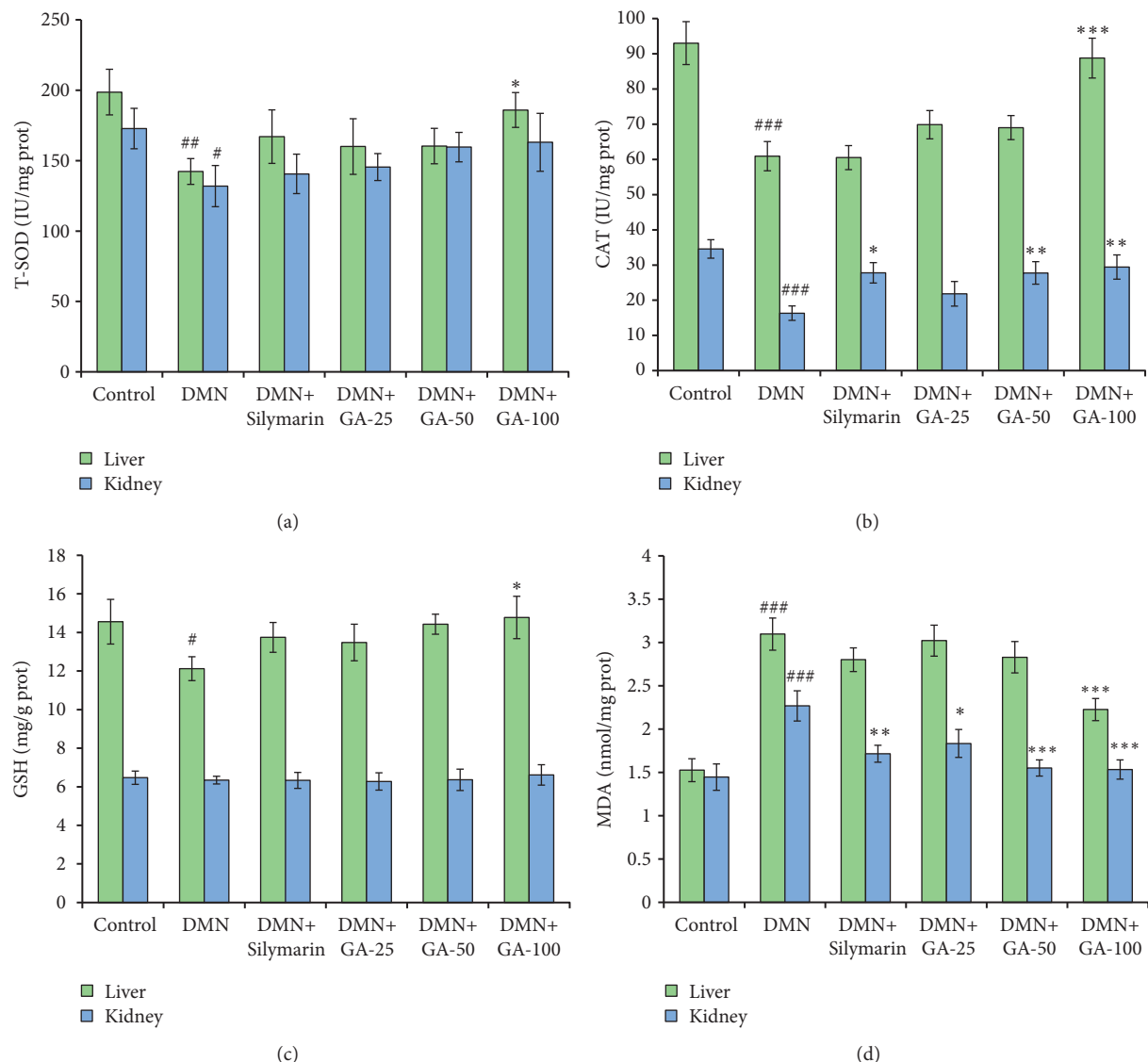


FIGURE 3: Effects of EF on the (a) SOD activity, (b) CAT activity, and the levels of (c) GSH and (d) MDA in the liver and kidney of DMN-induced liver fibrosis rats ( $n = 8$ ). The statistically significant differences are indicated by symbols (<sup>#</sup> $p < 0.05$ , <sup>##</sup> $p < 0.01$ , and <sup>###</sup> $p < 0.001$  compared with control group; <sup>\*</sup> $p < 0.05$ , <sup>\*\*</sup> $p < 0.01$ , and <sup>\*\*\*</sup> $p < 0.001$  compared with DMN-induced group).

large number of inflammatory cell infiltration (white arrow) and congestion in the extracellular matrix (black arrow) were found in the DMN group compared to control group (Figure 4(a)). GA treatment reversed these phenomena in a dose-dependent manner, which indicated that the highest dose of GA has the best liver protection effect (Figures 4(d)–4(f)).

We employed Masson trichrome staining that contains three dyes selectively to stain muscle, collagen fibers, fibrin, and erythrocytes. From Figure 5, we can see that black spots represent nuclei, red stains represent cytoplasm, muscle, erythrocytes, and blue stains represent collagen. Masson trichrome staining showed that majority of fibrous septa formed in the DMN group (Figure 5(b)). Bridging fibrosis formed a broad interval (black arrow) separating the liver parenchyma. GA treatments reversed this observation in a

dose-dependent manner (Figures 5(d)–5(f)). The high dose of GA was more effective in protecting the liver from DMN damage (Figure 5(f)) compared to the low- or medium-dose GA treatment (Figures 5(d) and 5(e)). The silymarin-treated group showed constricted and reduced fibrous septa (Figure 5(c)), but the number of fibrous septa remained much more than that in the medium- or high-dose GA-treated group. Therefore, the effect of silymarin-reversing liver fibrosis was lower than the GA at the same dose.

**3.5. Effects of GA on the Growth Factor Expression.** Compared to the control group, DMN treatment induced a significant ( $p < 0.001$ ) approximately 2-fold increase in TGF- $\beta 1$  level (Figure 6(a)). After treatment with the medium/high dose of GA (50 and 100 mg/kg) or silymarin, the levels of TGF- $\beta 1$  were significantly decreased ( $p < 0.05$ ,  $p < 0.001$ , and



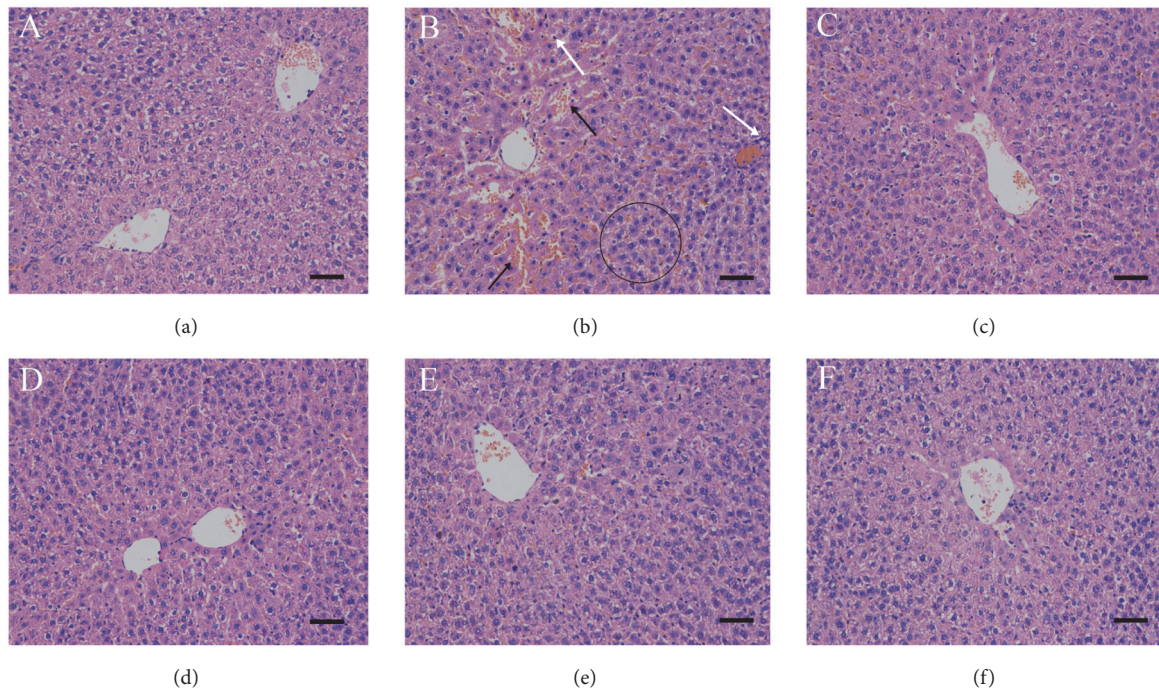


FIGURE 4: Effects of GA on the liver histological structure of rats with DMN-induced liver fibrosis (hematoxylin-eosin staining, 200 $\times$ ),  $n = 8$  animals/group, scale bar: 50  $\mu\text{m}$ . The treatments were as follows: (a) control group, (b) DMN (3 mg/kg; 7 mg/kg), (c) DMN + silymarin (100 mg/kg), (d) DMN + GA (25 mg/kg), (e) DMN + GA (50 mg/kg), and (f) DMN + GA (100 mg/kg). Hyperplastic wire mesh-like collagen fibers around the liver cells (black circle), inflammatory cell infiltration (white arrow), and congestion in ECM (black arrow) were found in the DMN group.

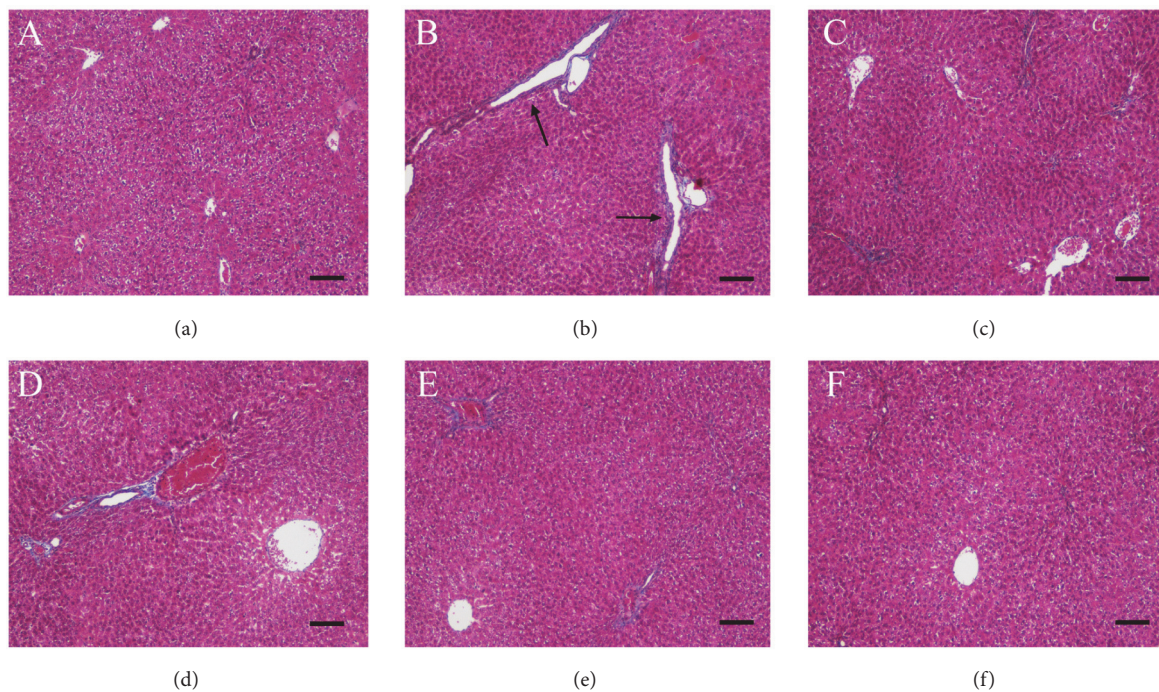


FIGURE 5: Effects of GA on the liver histological structure of rats with DMN-induced liver fibrosis (Masson staining, 100 $\times$ ),  $n = 8$  animals/group, scale bar: 100  $\mu\text{m}$ . The treatments were as follows: (a) control group, (b) DMN (3 mg/kg; 7 mg/kg), (c) DMN + silymarin (100 mg/kg), (d) DMN + GA (25 mg/kg), (e) DMN + GA (50 mg/kg), and (f) DMN + GA (100 mg/kg). Bridging fibrosis, which formed a broad interval (black arrow) separating the liver parenchyma, was found in the DMN group.



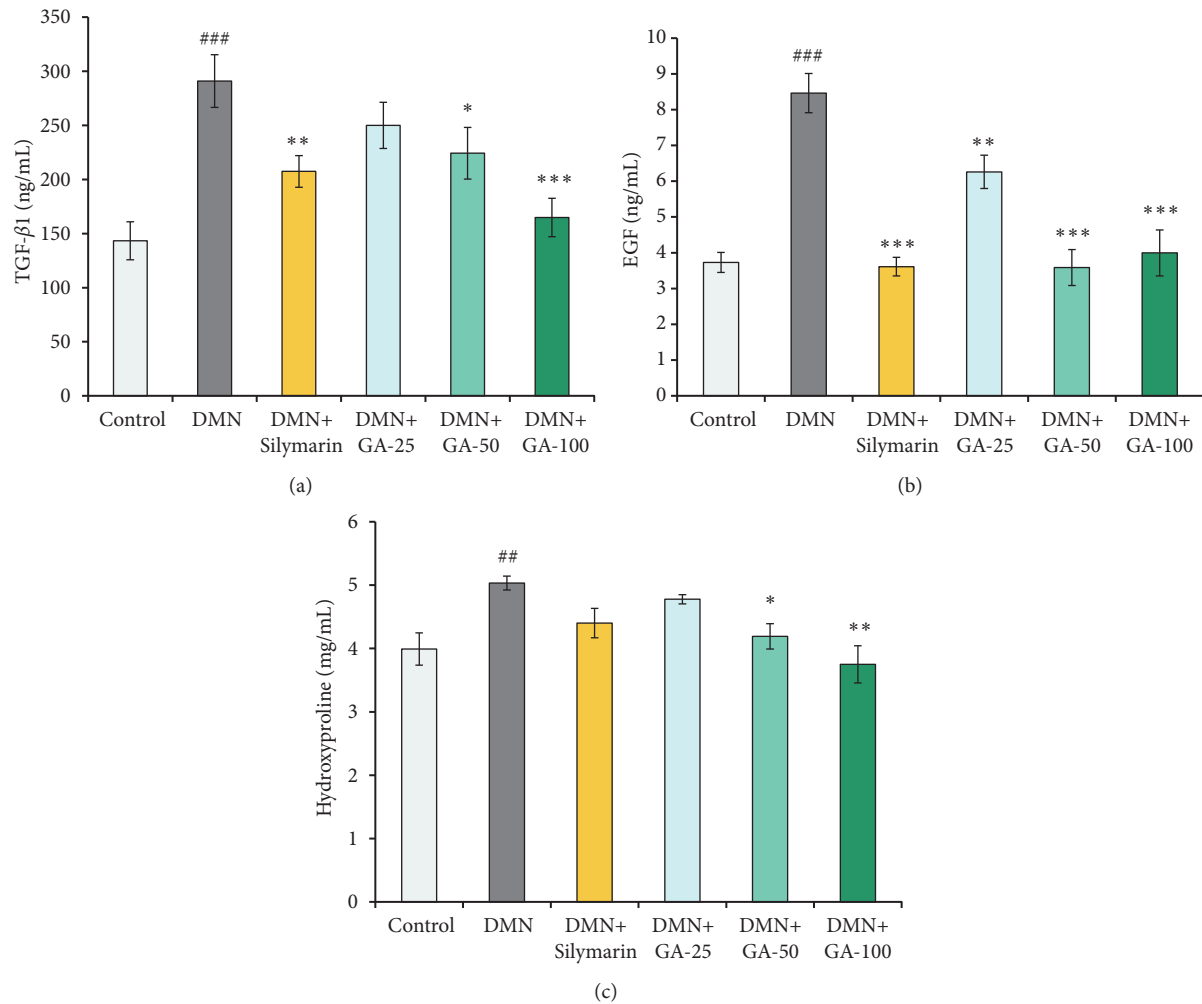


FIGURE 6: Effects of GA on the (a) TGF- $\beta$ 1, (b) EGF, and (c) hydroxyproline content in DMN-treated rat liver ( $n = 8$ ). The statistically significant differences are indicated by symbols ( $^{\#}p < 0.05$ ,  $^{\#\#}p < 0.01$ , and  $^{\#\#\#}p < 0.001$  compared with the control group;  $^*p < 0.05$ ,  $^{**}p < 0.01$ , and  $^{***}p < 0.001$  compared with the DMN-induced group).

$p < 0.01$ , respectively) compared to the model group. The highest dose of GA enabled the level of TGF- $\beta$ 1 to nearly revert to the control group level. Compared with the control group, the DMN treatment significantly ( $p < 0.001$ ) increased the content of GA (Figure 6(b)). After treatment with the three doses of GA (25, 50, and 100 mg/kg) or silymarin, the content of GA decreased significantly ( $p < 0.01$ ,  $p < 0.001$ ,  $p < 0.001$ , and  $p < 0.001$ , respectively) compared with the model group. The medium- and high-dose GA and silymarin treatment could significantly ( $p < 0.001$ ) reverse the level of GA elevated by DMN to the control group level. Compared to the control group, the hydroxyproline content was significantly ( $p < 0.01$ ) increased by the DMN modeling (Figure 6(c)), which was increased by nearly fourfold. The hydroxyproline content was decreased significantly ( $p < 0.05$  and  $p < 0.01$ ) after being treated with a medium or high dose of GA (50 and 100 mg/kg) compared to the DMN group. The high dose of GA has the best effect on reversing the abnormal increase of hydroxyproline content induced by DMN. The silymarin and low-dose GA treatment groups did not show

a good inhibitory effect on hydroxyproline synthesis, which is consistent with the results shown in Figures 5(c) and 5(d). Hydroxyproline is the substrate of collagen synthesis, and fibrous septa contain large amounts of collagen; thus, hydroxyproline content is closely related to the fibrous septa formation.

**3.6. Effects of GA on  $\alpha$ -SMA, PDGFR, TIMP-1, and TIMP-2 Gene Expression.** Compared to the control group, the DMN modeling significantly ( $p < 0.05$ ) upregulated the mRNA expression of  $\alpha$ -SMA by 1.4-fold (Figure 7(a)), and the mRNA expressions of  $\alpha$ -SMA were downregulated by treating with various concentrations of GA. However, only the mRNA expression of  $\alpha$ -SMA from the high-dose GA group showed a significant difference with the value obtained from the DMN model group ( $p < 0.05$ ). Evidently, silymarin did not significantly downregulate the expression of the  $\alpha$ -SMA gene, and its effect was comparable with the medium-dose GA. We then analyzed the response of the liver to GA by measuring mRNA expression of PDGFR (Figure 7(b)). A decrease in

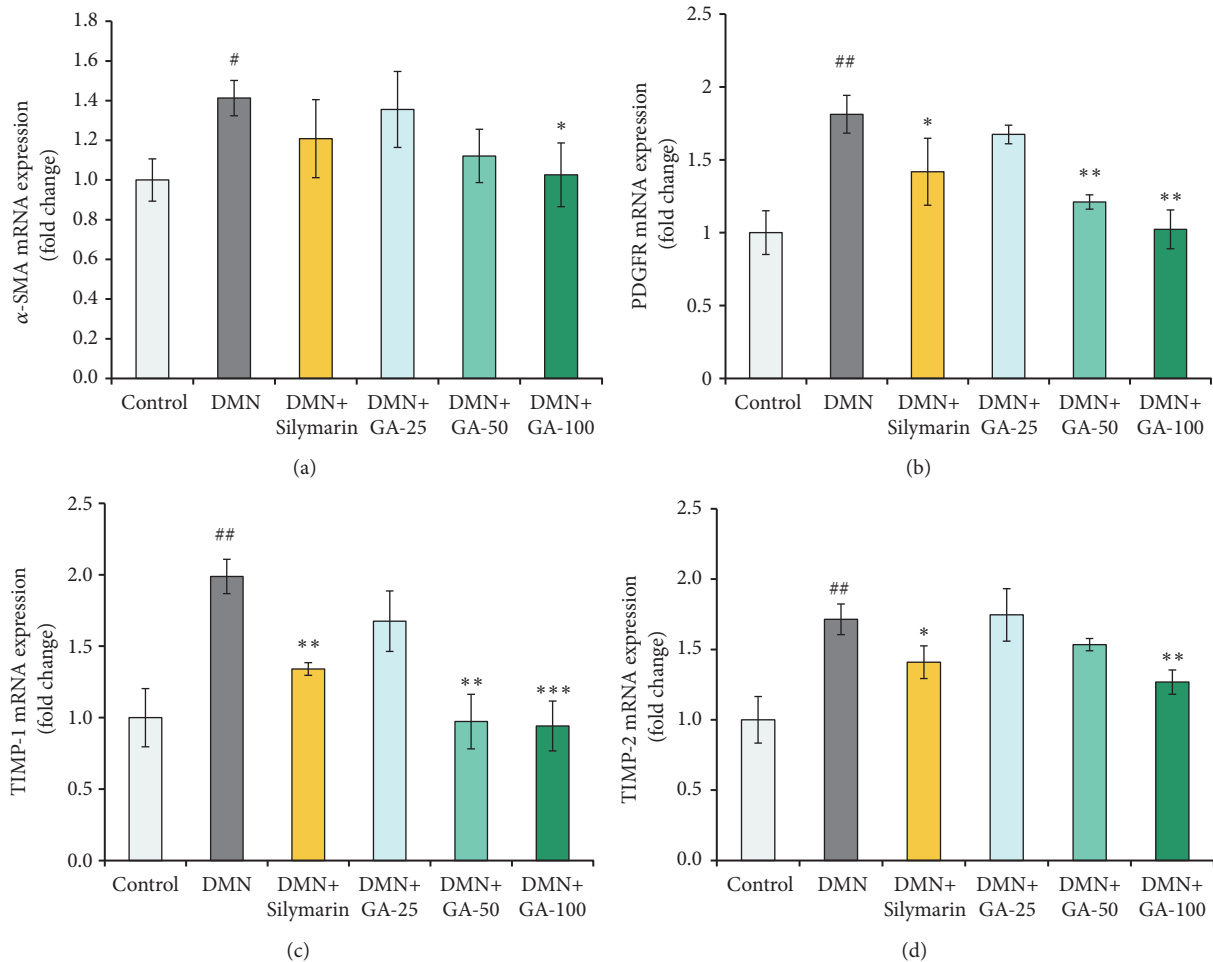


FIGURE 7: Effects of GA on the (a)  $\alpha$ -SMA, (b) PDGFR, (c) TIMP-1, and (d) TIMP-2 gene expressions were measured in the DMN-treated rat liver ( $n = 8$ ). The results are presented as relative changes normalized to GAPDH. The statistically significant differences are indicated by symbols (#  $p < 0.05$ , ##  $p < 0.01$ , and ###  $p < 0.001$  compared with the control group; \*  $p < 0.05$ , \*\*  $p < 0.01$ , and \*\*\*  $p < 0.001$  compared with the DMN-induced group).

gene expression of PDGFR will reduce the response to PDGF in liver cells, further reducing the signs of liver fibrosis. The gene expression of PDGFR was significantly ( $p < 0.01$ ) elevated by DMN treatment, but the medium- and high-dose GA or silymarin treatment played a role in reversing the PDGFR gene expression significantly ( $p < 0.01$ ,  $p < 0.01$ , and  $p < 0.05$ , respectively). The mRNA levels of TIMP-1 and TIMP-2 (Figures 7(c) and 7(d)) were significantly ( $p < 0.01$  and  $p < 0.01$ ) higher (1.9- and 1.7-fold, respectively) in the DMN model group than those in the control group. The mRNA expression level of TIMP-1 was downregulated by GA treatment in a dose-dependent manner compared with the DMN group, but only 50 or 100 mg/kg GA treatment has a significant ( $p < 0.01$  and  $p < 0.001$ ) reversal effect on inhibiting the upregulation of TIMP-1 mRNA expression. Silymarin treatment could also significantly ( $p < 0.01$ ) downregulate the expression of TIMP-1, but the effect was not as good as the medium- and high-dose GA treatment (Figure 7(c)). The mRNA expression levels of TIMP-2 were significantly ( $p < 0.01$  and  $p < 0.05$ ) decreased by the high-dose GA and

silymarin treatment. The medium-dose GA treatment has a mild effect on reversing the elevation of the expression of TIMP-2 caused by DMN, but the mRNA expression of TIMP-2 was not nearly decreased by the low-dose GA treatment compared to the DMN group (Figure 7(d)).

**3.7. Western Blot Analysis.** Oxidative stress could alter signal transduction pathways and consequently activate key stress receptors, such as Smad2 and Smad3. The Smad protein family plays an important role in regulating cell proliferation and death in response to oxidative stress. In the present study, we analyzed the expression of Smads and p-Smads after injured liver cells were treated with silymarin and the three doses of GA (Figure 8(a)). These treatments to an extent reduced the phosphorylation-dependent activation of signaling components, such as p-Smad2 and p-Smad3 compared to that in the model group ( $p < 0.05$ ).

The result of quantitative analysis showed that the expression of collagen I significantly ( $p < 0.05$ ) increased in DMN group when compared to control, and silymarin and

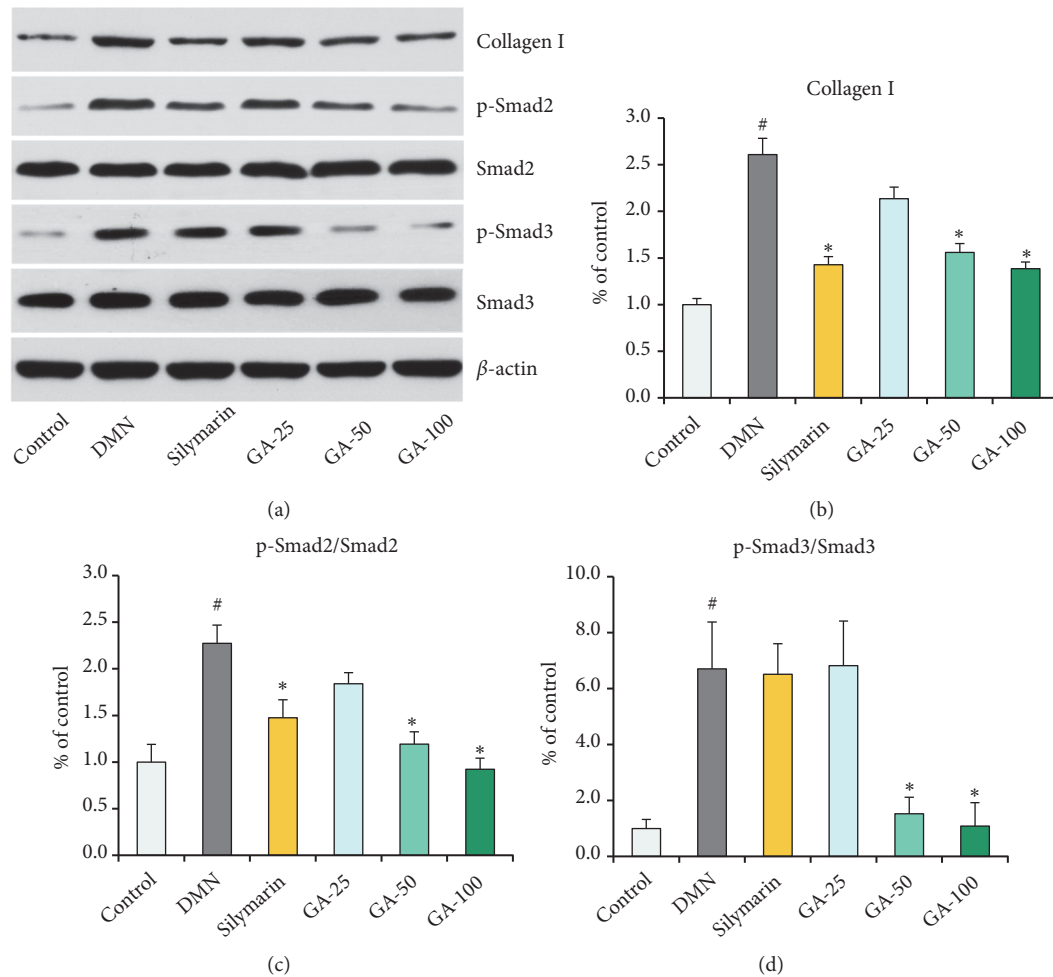


FIGURE 8: Expressions of extracellular matrix key protein and TGF- $\beta$ /Smad signaling pathway key protein in liver. Error bars indicate the standard deviation of three independent repeats. (a) Protein expressions of collagen I, p-Smad2, Smad2, p-Smad3, and Smad3.  $\beta$ -actin as loading controls. The gray density scanning analysis of (b) Collagen I, (c) p-Smad2/Smad2, and (d) p-Smad3/Smad3 by ImageJ software. DMN, dimethylnitrosamine; GA, gallic acid. \* $p < 0.05$ , compared with the model group. # $p < 0.05$ , compared with the control group.

medium- and high-dose GA treatment groups significantly ( $p < 0.001$ ) reduced the expression of collagen I (Figure 8(b)). Collagen I protein is a cell constitutive protein, continuously expressed without the induction by DMN. However, the DMN treatment induced hepatic stellate cells activation in the liver, which is the principal cellular source of collagen I protein that would be detected by Western blot [17]. Our results verified that additional collagen I was synthesized after DMN treatment (Figures 8(a) and 8(b)).

To better understand the molecular mechanism of the inhibitory effects of GA in DMN-induced liver fibrosis, we investigated the possible involvement of key TGF- $\beta$ /Smad pathway. The results demonstrated that DMN could significantly ( $p < 0.05$ ) activate the TGF- $\beta$ /Smad pathway by the phosphorylation of Smad2 and Smad3 proteins. There was no significant change between the groups in terms of Smad2 or Smad3 expression, but the level of phosphorylated Smad2 or Smad3 was markedly decreased ( $p < 0.05$ ) after treatment with silymarin and medium- and high-dose GA compared to the model group. Among the three treatments, the effect

of the high-dose GA treatment group was the best, which reversed the phosphorylation level of Smad2 or Smad3 to almost normal levels (Figures 8(c) and 8(d)).

#### 4. Discussion

In recent years, antifibrosis studies of plant extracts or plant-derived compounds have received increasing attention. Puerarin, naringenin, chlorogenic acid, and a variety of other compounds derived from plants have been proven to have antiliver fibrosis effect on in vivo and in vitro experiments [18–20]. GA is widely found in food and fruit, and its antifibrosis effect was investigated in the present study. The DMN-induced body weight losses of rats were clearly observed in Table 1. The body weight had a decreasing trend with treatment of increasing GA doses; thus we hypothesized that GA has a weight loss effect. This hypothesized GA function is consistent with a previous report that investigated GA as an effective and safe treatment for weight loss in an animal trial [21]. Liver and kidney weights have the corresponding

change with body weight after DMN, silymarin, or GA treatments. Hence, the ratio of organ and body weight is nearly unchanged among the six groups. GA has no effect on the physiological index of the organ.

A blood test for AST is used to detect liver damage. AST is often ordered with ALT, another liver enzyme, or as part of a liver comprehensive metabolic panel to screen for and/or help diagnose liver disorders [22]. Detecting increasing enzymes levels of AST, ALT, and ALP in the serum indicates liver cell damage because large quantities of these enzymes are leaked in to the serum after liver damage. This process is usually associated with alterations in the levels of many other serum parameters, such as bilirubin, albumin, glucose, and cholesterol. The bilirubin level is an independent predictor that indicates the lack of antioxidant protection and is a possible molecular determinant for the progression of liver injury.

The primary protective mechanisms of some antifibrotic agents result from their antioxidative capabilities [23]. In this study, a series of parameters was used to measure the oxidative stress in rats. SOD is the primary enzymatic defense in the liver against the damaging effects of  $O_2^{\cdot-}$ , by converting  $O_2^{\cdot-}$  into  $H_2O_2$ , which is a substrate for CAT and glutathione peroxidase (GPx) [24]. If SOD activity is low, then  $O_2^{\cdot-}$  can interact with  $\cdot NO$  to form peroxynitrite ( $ONOO^{\cdot-}$ ), which can react to form the potent  $\cdot OH$  and nitrogen dioxide ( $NO_2\cdot$ ) radicals. These radicals are highly damaging to cell proteins, lipids, and DNA [25]. We observed decreases in the activities of SOD and CAT in the DMN groups, in contrast to the control group. However, these effects were reversed by the GA treatment in a dose-dependent manner. GSH is catalyzed by GPx to reduce hydroperoxides and can effectively remove free radicals in the body to protect cells from oxidative damage. Consequently, GA enhanced the activities of antioxidant enzymes, which can lead to the increase in antioxidant capacity. The data obtained in the oxidative stress state of the liver of DMN-exposed rats show that DMN treatment leads to the accumulation of MDA as high as 2-fold of controls. Cell membranes can be modified by lipid peroxidation products, such as trans-4-hydroxy-2-nonenal, 4-hydroperoxy-2-nonenal, and MDA [26]. Lipid peroxidation products can also modulate signaling molecules and alter functions of enzymes and proteins involved in inflammation [27], which was confirmed by hematoxylin–eosin staining. We observed a large number of inflammatory cell infiltration in the DMN group. GA can help relieve the elevating trend of the level of lipid peroxidation caused by DMN. Rats treated with the higher concentration of GA had lower concentration of MDA in the liver cells.

In the kidney, we observed alarmingly low levels of SOD and CAT with DMN treatment, which can show the sensitivity of the kidney to these toxins and its inefficacy to clear reactive oxygen species (ROS). Figure 2 shows a trend that GA at increasing doses can restore the SOD activity, but this increase was insignificant. The mechanism of GA for improving the SOD activity is unknown, but we hypothesize that GA initiates the expressions of some genes to enhance the SOD activity. The CAT activities increased significantly after being treated with various concentrations of GA compared

to the DMN-treated group, which shows that GA is a good assistance for the CAT activity, possibly by enhancing the expression of the CAT gene. DMN treatment cannot significantly affect GSH levels compared to the control group. GSH is mainly synthesized in the liver and is transported to the kidney through the intestinal liver cycle. After glomerular filtration, GSH can be hydrolyzed into amino acids by the degrading enzymes located in the brush-like edge of the renal tubular cell. This process provides a reasonable explanation for the stable GSH levels we observed in the GSH content assay. In our study, various doses of GA can significantly reduce the MDA content in the kidney after DMN induction. Hence, GA is a strong reducing agent, which could reduce oxygen free radicals that can further reduce MDA formation.

The implications of this damage to an organ like the liver is extreme because this damage can hinder the capacity of the tissue to detoxify the body, leading to further exacerbated damage by the DMN toxins and leading to metabolic diseases, such as hepatic fibrosis. The increase in the number of fibrous septa by DMN treatment was confirmed by Masson trichrome staining. Collectively, these fibrous septa indicate a massive state of fibrosis occurring in response to the DMN exposure. However, this phenomenon requires at least a medium-dose GA treatment, because low-dose GA treatment did not show significant differences compared to the DMN-treated group.

The EGF family and its receptors play an important role in cell proliferation, tissue repair, and stability of normal cells. One of the main pathological features of liver fibrosis is the proliferation of fibroblasts stimulated by various growth factors. TGF- $\beta$ 1 and its receptor can stimulate fibroblast proliferation and play an important role in the pathogenesis of liver fibrosis [28]. Samarakoon et al. [29] have shown that induction of renal fibrotic genes by TGF- $\beta$ 1 requires EGF receptor (EGFR) activation, which is essential for the expression of TGF- $\beta$ 1-induced fibrotic target genes. Fuchs et al. [30] have reported that the small-molecule EGFR inhibitor, erlotinib, inhibits the activation of myofibroblastic HSCs, prevents the progression of cirrhosis, and regresses fibrosis in some animals. GA could reduce the level of EGF significantly after the animal was induced with liver fibrosis; however, whether GA is an EGFR inhibitor has yet to be determined. Hydroxyproline is an important amino acid for collagen synthesis and currently used to characterize collagens. From our study, we found that GA could significantly reduce the accumulation of hydroxyproline content in the fibrotic liver. To confirm the effects on collagen, we next measured collagen I because originally the collagen content was estimated from the hydroxyproline content of acid hydrolysates of tissue, not collagen directly [31]. Collagen I is the most abundant and ubiquitous connective tissue protein and through Western blot showed that GA could effectively reduce the deposition of collagen I in liver tissue.

The mRNA level of  $\alpha$ -SMA was also markedly suppressed by the medium- and high-dose GA treatments. Hinz et al. [32] reported that accumulation of biologically active TGF- $\beta$ 1 is one of the three local events are needed to generate  $\alpha$ -SMA-positive differentiated myofibroblasts. Similarly, GA significantly suppressed the mRNA level of PDGFR. Liver



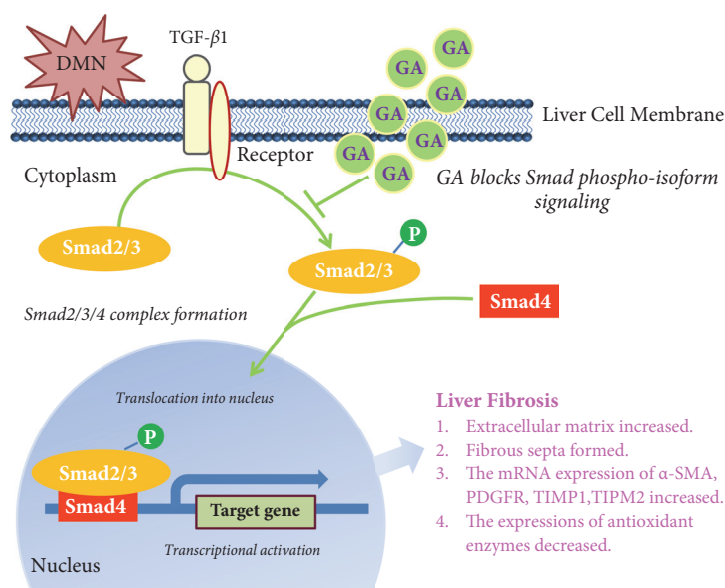


FIGURE 9: Schematic of DMN-induced liver fibrosis through activating the TGF- $\beta$ /Smad signaling pathway and GA attenuate liver fibrosis through blocking Smad phosphorylation in liver cell.

fibrosis is a complex dynamic process mediated by the death of hepatocytes and activation of HSCs. The generation of ROS, tumor necrosis factor- $\alpha$ , TGF- $\beta$ , and PDGF can be implicated as a cause of hepatic fibrosis [33, 34]. The matrix metalloproteinases (MMPs) family is a major group of enzymes responsible for extracellular matrix (ECM) degradation and their activity is regulated by protein inhibitors called TIMPs [35]. Liver fibrosis, a chronic hepatic injury, is characterized by an excessive production of ECM. The balance between the activity of MMPs and the inhibitory role of TIMPs plays a key role in degrading ECM in fibrosis. After GA treatment, TIMPs had significantly altered mRNA expression compared to the DMN-treated group, suggesting that GA may be involved in the transcription of TIMP-1 and TIMP-2. The reduction in expression could lead to a reduction of their protein levels, attenuating their inhibitory effects on MMPs. Eventually, ECM degradation by MMPs was resumed to the normal activity under GA treatment.

The Smad proteins 2, 3, 4, and 7 and their roles in fibrosis have been described in some in vivo and in vitro experiments [36–38]. Angiotensin-converting enzyme (ACE) inhibitor therapy has also been shown to have an antifibrosis effect, partly because of their capability to prevent type II angiotensin-induced Smad2 nuclear translocation and inhibit transcriptional activity. Angiotensin receptor antagonists can block this important pathway and have a similar effect [39]. In response to TGF- $\beta$ , the TGF- $\beta$  receptor phosphorylates serine residues on the C-terminus of Smad2 and Smad3. Han et al. reported that hepcidin suppresses liver fibrosis by impeding TGF- $\beta$ 1-induced Smad3 phosphorylation in HSCs, which depends on AKT activated by a deficiency of ferroportin [40]. TGF- $\beta$  is considered to be the major factor regulating liver carcinogenesis and accelerating liver fibrosis. Smad2 and Smad3 act as the intracellular mediators of TGF- $\beta$  signal transduction pathway (Figure 9).

Ma et al. (2014) have reported that GA is able to attenuate DMN-induced acute liver injury in mice, suggesting the potential mechanism is that increasing the expression level of hemoxygenase-1 (HO-1) and glutathione-s-transferase alpha 3 (GSTA3) can enhance the detoxification ability of liver tissue [41]. However, in our paper, we established a subchronic toxicity model by DMN for studying liver fibrosis rather than acute liver injury and shed light on another possible mechanism of GA reversing the detrimental effect caused by DMN, involvement of key TGF- $\beta$ /Smad pathway. In summary, our study focused on alteration of Smad phosphoisoform signaling suggesting that the Smad protein could be a potential therapeutic target for liver fibrosis.

## 5. Conclusion

The present study provides the first evidence that GA can reduce the DMN-induced liver fibrosis in rats relying on its superior antioxidant capacity and take part in the regulation of cytokines expression. Moreover, this study provides an attractive alternative strategy against liver fibrosis, because GA widely exists in plants and food.

## Data Availability

The data used to support the findings of this study are available from the corresponding author upon request.

## Conflicts of Interest

The authors declare that there are no conflicts of interest.

## Acknowledgments

We thank Jane Hannah Kim from Department of Molecular, Cell and Systems Biology, University of California, Riverside,

USA, for the language editing of this article. This work was supported by the Project of the National Twelve-Five Year Research Program of China (2012BAI29B03), the Commonwealth Specialized Research Fund of China Agriculture (201103016), and the Nanjing 321 plan for Bringing in technological leading talents (2013A12011).

## Supplementary Materials

Table S1. Reagents and Chemicals Manufacturer List. Table S2. Real-Time PCR Primers for Analysis. (Supplementary Materials)

## References

- [1] T. S. Mohamed Saleem, S. Madhusudhana Chetty, S. Ramkanth, V. S. T. Rajan, K. Mahesh Kumar, and K. Gauthaman, "Hepatoprotective herbs—a review," *International Journal of Research in Pharmaceutical Sciences*, vol. 1, no. 1, pp. 1–5, 2010.
- [2] S. L. Friedman and M. B. Bansal, "Reversal of hepatic fibrosis—fact or fantasy?" *Hepatology*, vol. 43, no. 2, pp. S82–S88, 2006.
- [3] B. Spee, *Regenerative and Fibrotic pathways in Canine Liver Disease [Ph.D. thesis]*, Faculty of Veterinary Medicine, Utrecht University, 2006.
- [4] N. Hashimoto, Y. Ishikawa, and J. Utsunomiya, "Effects of portacaval shunt, transposition, and dimethylnitrosamine-induced chronic liver injury on pancreatic hormones and amino acids in dog," *Journal of Surgical Research*, vol. 46, no. 1, pp. 35–40, 1989.
- [5] V. Rani, Y. Verma, K. Rana, and S. V. Rana, "Zinc oxide nanoparticles inhibit dimethylnitrosamine induced liver injury in rat," *Chemico-Biological Interactions*, vol. 295, pp. 84–92, 2018.
- [6] A. M. Jézéquel, R. Mancini, M. L. Rinaldesi et al., "Dimethylnitrosamine-induced cirrhosis. Evidence for an immunological mechanism," *Journal of Hepatology*, vol. 8, no. 1, pp. 42–52, 1989.
- [7] X. Liu, R. Dai, M. Ke, I. Suheryani, W. Meng, and Y. Deng, "Differential Proteomic Analysis of Dimethylnitrosamine (DMN)-Induced Liver Fibrosis," *Proteomics*, vol. 17, no. 22, 2017.
- [8] M. Kim, M. A. Kim, J. H. Yim, D. Lee, S. K. Cho, and S. Yang, "Ramalin, an antioxidant compound derived from Antarctic lichen, prevents progression of liver fibrosis induced by dimethylnitrosamine (DNM) in rats," *Biochemical and Biophysical Research Communications*, vol. 504, no. 1, pp. 25–33, 2018.
- [9] E. J. Kyung, H. B. Kim, E. S. Hwang, S. Lee, B. K. Choi, J. W. Kim et al., "Evaluation of Hepatoprotective Effect of Curcumin on Liver Cirrhosis Using a Combination of Biochemical Analysis and Magnetic Resonance-Based Electrical Conductivity Imaging," *Mediators of Inflammation*, vol. 2018, Article ID 5491797, 9 pages, 2018.
- [10] J.-D. Jia, M. Bauer, J. J. Cho et al., "Antifibrotic effect of silymarin in rat secondary biliary fibrosis is mediated by downregulation of procollagen alpha 1(I) and TIMP-1," *Journal of Hepatology*, vol. 35, no. 3, pp. 392–398, 2001.
- [11] B. Sharma, U. Chaube, and B. M. Patel, "Beneficial Effect of Silymarin in Pressure Overload Induced Experimental Cardiac Hypertrophy," *Cardiovascular Toxicology*, 2018.
- [12] Y.-X. Chen, J. Tong, L.-L. Ge, B.-X. Ma, J.-S. He, and Y.-W. Wang, "Ethyl acetate fraction of Terminalia bellirica fruit inhibits rat hepatic stellate cell proliferation and induces apoptosis," *Industrial Crops and Products*, vol. 76, pp. 364–373, 2015.
- [13] S. Ercisli and E. Orhan, "Chemical composition of white (*Morus alba*), red (*Morus rubra*) and black (*Morus nigra*) mulberry fruits," *Food Chemistry*, vol. 103, no. 4, pp. 1380–1384, 2007.
- [14] S. Y. Wang and H. Lin, "Antioxidant activity in fruits and leaves of blackberry, raspberry, and strawberry varies with cultivar and developmental stage," *Journal of Agricultural and Food Chemistry*, vol. 48, no. 2, pp. 140–146, 2000.
- [15] Y. Y. Lim, T. T. Lim, and J. J. Tee, "Antioxidant properties of several tropical fruits: a comparative study," *Food Chemistry*, vol. 103, no. 3, pp. 1003–1008, 2007.
- [16] L. J. Su, C. C. Chang, C. H. Yang et al., "Graptopetalum paraguayense ameliorates chemical-induced rat hepatic fibrosis in vivo and inactivates stellate cells and Kupffer cells in vitro," *PLoS ONE*, vol. 8, no. 1, Article ID e53988, 2013.
- [17] A. Galli, D. W. Crabb, E. Ceni et al., "Antidiabetic thiazolidinediones inhibit collagen synthesis and hepatic stellate cell activation in vivo and in vitro," *Gastroenterology*, vol. 122, no. 7, pp. 1924–1940, 2002.
- [18] L. Xu, N. Zheng, Q. He, R. Li, K. Zhang, and T. Liang, "Puerarin, isolated from *Pueraria lobata* (Willd.), protects against hepatotoxicity via specific inhibition of the TGF-beta1/Smad signaling pathway, thereby leading to anti-fibrotic effect," *Phytomedicine*, vol. 20, no. 13, pp. 1172–1179, 2013.
- [19] M.-H. Lee, S. Yoon, and J.-O. Moon, "The flavonoid naringenin inhibits dimethylnitrosamine-induced liver damage in rats," *Biological & Pharmaceutical Bulletin*, vol. 27, no. 1, pp. 72–76, 2004.
- [20] H. Shi, L. Dong, Y. Bai, J. Zhao, Y. Zhang, and L. Zhang, "Chlorogenic acid against carbon tetrachloride-induced liver fibrosis in rats," *European Journal of Pharmacology*, vol. 623, no. 1–3, pp. 119–124, 2009.
- [21] A. T. Roberts, C. K. Martin, Z. Liu et al., "The safety and efficacy of a dietary herbal supplement and gallic acid for weight loss," *Journal of Medicinal Food*, vol. 10, no. 1, pp. 184–188, 2007.
- [22] W. R. Kim, S. L. Flamm, A. M. Di Bisceglie, and H. C. Bodenheimer, "Serum activity of alanine aminotransferase (ALT) as an indicator of health and disease," *Hepatology*, vol. 47, no. 4, pp. 1363–1370, 2008.
- [23] B.-J. Ke and C.-L. Lee, "Cordyceps cicadae NTTU 868 mycelium prevents CCl4-induced hepatic fibrosis in BALB/c mice via inhibiting the expression of pro-inflammatory and pro-fibrotic cytokines," *Journal of Functional Foods*, vol. 43, pp. 214–223, 2018.
- [24] C. J. Weydert and J. J. Cullen, "Measurement of superoxide dismutase, catalase and glutathione peroxidase in cultured cells and tissue," *Nature Protocols*, vol. 5, no. 1, pp. 51–66, 2010.
- [25] A. Rahal, A. Kumar, V. Singh et al., "Oxidative stress, prooxidants, and antioxidants: the interplay," *BioMed Research International*, vol. 2014, Article ID 761264, 19 pages, 2014.
- [26] I. A. Blair, "DNA adducts with lipid peroxidation products," *The Journal of Biological Chemistry*, vol. 283, no. 23, pp. 15545–15549, 2008.
- [27] H. Bartsch and J. Nair, "Chronic inflammation and oxidative stress in the genesis and perpetuation of cancer: role of lipid peroxidation, DNA damage, and repair," *Langenbeck's Archives of Surgery*, vol. 391, no. 5, pp. 499–510, 2006.
- [28] Y. L. Zhou, S. Yang, and P. Zhang, "Effect of Exogenous Fetuin-A on TGF-beta/Smad Signaling in Hepatic Stellate Cells," *BioMed Research International*, vol. 2016, Article ID 8462615, 6 pages, 2016.

- [29] R. Samarakoon, A. D. Dobberfuhr, C. Cooley, J. M. Overstreet, S. Patel, R. Goldschmeding et al., "Induction of renal fibrotic genes by TGF-beta 1 requires EGFR activation, p53 and reactive oxygen species," *Cellular Signalling*, vol. 25, no. 11, pp. 2198–2209, 2013.
- [30] B. C. Fuchs, Y. Hoshida, T. Fujii, L. Wei, S. Yamada, G. Y. Lauwers et al., "Epidermal Growth Factor Receptor Inhibition Attenuates Liver Fibrosis and Development of Hepatocellular Carcinoma," *Hepatology*, vol. 59, no. 4, pp. 1577–1590, 2014.
- [31] X. P. Tian, C. H. Zhao, J. B. Guo, S. R. Xie, F. R. Yin, X. X. Huo et al., "Carvedilol Attenuates the Progression of Hepatic Fibrosis Induced by Bile Duct Ligation," *BioMed Research International*, vol. 2017, Article ID 4612769, 10 pages, 2017.
- [32] B. Hinz, S. H. Phan, V. J. Thannickal, A. Galli, M.-L. Bochaton-Piallat, and G. Gabbiani, "The myofibroblast: one function, multiple origins," *The American Journal of Pathology*, vol. 170, no. 6, pp. 1807–1816, 2007.
- [33] Y. Xu, Z. X. Peng, W. D. Ji, X. Li, X. J. Lin, L. Q. Qian et al., "A Novel Matrine Derivative WM130 Inhibits Activation of Hepatic Stellate Cells and Attenuates Dimethylnitrosamine-Induced Liver Fibrosis in Rats," *BioMed Research International*, vol. 2015, Article ID 203978, 13 pages, 2015.
- [34] H. M. Eltahir and M. H. Nazmy, "Esomeprazole ameliorates CCl4 induced liver fibrosis in rats via modulating oxidative stress, inflammatory, fibrogenic and apoptotic markers," *Biomedicine & Pharmacotherapy*, vol. 97, pp. 1356–1365, 2018.
- [35] S. Ghatak, A. Biswas, G. K. Dhali, A. Chowdhury, J. L. Boyer, and A. Santra, "Oxidative stress and hepatic stellate cell activation are key events in arsenic induced liver fibrosis in mice," *Toxicology and Applied Pharmacology*, vol. 251, no. 1, pp. 59–69, 2011.
- [36] Y. Wang, R. Hong, Y. Xie, and J. Xu, "Melatonin Ameliorates Liver Fibrosis Induced by Carbon Tetrachloride in Rats via Inhibiting TGF-beta1/Smad Signaling Pathway," *Current Medical Science*, vol. 38, no. 2, pp. 236–244, 2018.
- [37] Y. He, C. Huang, X. Sun, X.-R. Long, X.-W. Lv, and J. Li, "MicroRNA-146a modulates TGF-beta1-induced hepatic stellate cell proliferation by targeting SMAD4," *Cellular Signalling*, vol. 24, no. 10, pp. 1923–1930, 2012.
- [38] F. Yu, Y. Guo, B. Chen, P. Dong, and J. Zheng, "MicroRNA-17-5p activates hepatic stellate cells through targeting of Smad7," *Laboratory Investigation*, vol. 95, no. 7, pp. 781–789, 2015.
- [39] Y. Kamada, S. Tamura, S. Kiso, K. Fukui, Y. Doi, N. Ito et al., "Angiotensin II stimulates the nuclear translocation of Smad2 and induces PAI-I mRNA in rat hepatic stellate cells," *Hepatology Research*, vol. 25, no. 3, pp. 296–305, 2003.
- [40] C. Y. Han, J. H. Koo, S. H. Kim et al., "Hepcidin inhibits Smad3 phosphorylation in hepatic stellate cells by impeding ferroportin-mediated regulation of Akt," *Nature Communications*, vol. 7, Article ID 13817, 2016.
- [41] S. H. Ma, L. Lv, Q. Lu, Y. B. Li, F. Zhang, M. Lin et al., "Gallic acid attenuates dimethylnitrosamine-induced acute liver injury in mice through Nrf2-mediated induction of heme oxygenase-1 and glutathione-s-transferase alpha 3," *Medicinal Chemistry*, vol. 4, no. 9, pp. 663–669, 2014.

## Review Article

# Natural Compounds for the Management of Parkinson's Disease and Attention-Deficit/Hyperactivity Disorder

Juan Carlos Corona 

*Laboratory of Neurosciences, Hospital Infantil de México Federico Gómez, Mexico*

Correspondence should be addressed to Juan Carlos Corona; [jcorona@himfg.edu.mx](mailto:jcorona@himfg.edu.mx)

Received 28 June 2018; Revised 31 October 2018; Accepted 11 November 2018; Published 22 November 2018

Guest Editor: Francesco Facchiano

Copyright © 2018 Juan Carlos Corona. This is an open access article distributed under the Creative Commons Attribution License, which permits unrestricted use, distribution, and reproduction in any medium, provided the original work is properly cited.

Parkinson's disease (PD) is the second most common neurodegenerative disorder with an unknown aetiology. The pathogenic mechanisms include oxidative stress, mitochondrial dysfunction, protein dysfunction, inflammation, autophagy, apoptosis, and abnormal deposition of  $\alpha$ -synuclein. Currently, the existing pharmacological treatments for PD cannot improve fundamentally the degenerative process of dopaminergic neurons and have numerous side effects. On the other hand, attention-deficit/hyperactivity disorder (ADHD) is the most common neurodevelopmental disorder of childhood and is characterised by hyperactivity, impulsivity, and inattention. The aetiology of ADHD remains unknown, although it has been suggested that its pathophysiology involves abnormalities in several brain regions, disturbances of the catecholaminergic pathway, and oxidative stress. Psychostimulants and nonpsychostimulants are the drugs prescribed for the treatment of ADHD; however, they have been associated with increased risk of substance use and have several side effects. Today, there are very few tools available to prevent or to counteract the progression of such neurological disorders. Thus, therapeutic approaches with high efficiency and fewer side effects are needed. This review presents a brief overview of the two neurological disorders and their current treatments, followed by a discussion of the natural compounds which have been studied as therapeutic agents and the mechanisms underlying the beneficial effects, in particular, the decrease in oxidative stress.

## 1. Introduction

For many years, natural compounds have provided an efficient resource for the discovery of potential therapeutic agents. Among them, many natural products possess antioxidative, antiapoptotic and anti-inflammatory activities. In this review, we summarize the role of natural compounds and their therapeutic use for the management of dopamine-related diseases, divided into part 1 for Parkinson's disease and part 2 for attention-deficit/hyperactivity disorder. In addition, the current knowledge of the mechanisms underlying the potential beneficial effects of diverse natural compounds capable of counteracting the progression of this type of diseases is reviewed, as demonstrated by their antioxidative effects.

## 2. Parkinson's Disease

Parkinson's disease (PD) is the second most common progressive and chronic neurodegenerative disorder,

characterised by the progressive loss of dopaminergic neurons in the substantia nigra (SN) and their projections to the striatum. Thus, the function of the nigrostriatal pathway becomes reduced and causes the development of movement disorder [1]. The basic characteristics of PD include tremor, rigidity, bradykinesia, and impaired balance; depression is also present in patients, affecting the quality of life. One of the pathological features of PD is the presence of Lewy bodies, which are intraneuronal proteinaceous cytoplasmic inclusions and include  $\alpha$ -synuclein, ubiquitin, and neurofilaments found in all affected brain regions [2]. The pathogenic mechanisms of PD include oxidative stress, mitochondrial dysfunction, protein dysfunction, inflammation, autophagy, and apoptosis [3]. PD occurs 95 % as a sporadic form, while familial forms involve mutations in proteins that include PINK1, DJ-1, PARKIN, FBXO7, and LRRK2 [4], even though pesticides, chemicals, and metals may increase the risk of developing PD. Currently, the treatment of PD includes drugs such as L-DOPA, which is catalysed primarily by dopa decarboxylase in the brain and is



converted into dopamine, producing its therapeutic effects. Another treatment includes anticholinergic drugs that can block striatal cholinergic receptors inhibiting the excitability of cholinergic nerves; it has also been demonstrated that they can inhibit dopamine reuptake to enhance the function of dopaminergic neurons [5]. At present, there are also other drugs in Phase III clinical trials. Nevertheless, the current drugs used for the PD treatment have some side effects, limiting their clinical applications [6]. Drugs used for the PD treatment and their side effects are shown in Table 1. Thus, the growing interest in alternative therapies for neurodegenerative disorders, including PD, has focused on the neuroprotective and antioxidant effects of natural products that may provide alternatives, since they can have high efficiency and fewer side effects. Natural compounds used as alternative therapies for the management of PD are shown in Table 2.

**2.1. *Ginkgo biloba*.** *Ginkgo biloba* is an ancient tree native to China and has been extensively used in traditional Chinese medicine to manage symptoms associated with dysfunctions of the heart and lungs. *G. biloba* usually contains three ingredients, which include flavonoids, terpenoids, and ginkgolic acid [81]. Ginkgolides well-known plant extracts obtained from leaves from *G. biloba*, especially in the preparation EGb761, which contains ginkgolide B and bilobalide, have emerged as natural therapeutic compounds, in part due to their antioxidant activity. These effects have been observed in the 1-methyl-4-phenyl-1,2,3,6-tetrahydropyridine- (MPTP-) treated mouse model of PD, where chronic ingestion of EGb761 prevented MPTP-induced reduction in the dopaminergic nerve endings [9]. In addition, EGb761 administered before or after MPTP treatment protected against MPTP-induced dopaminergic neurotoxicity [10]. Moreover, EGb761 attenuated the neurotoxic effect of levodopa in the 6-hydroxydopamine (6-OHDA) model of PD, indicated that levodopa is neurotoxic and that EGb761 may decrease this toxicity [11]. The neuroprotective effects of EGb761 were demonstrated in the 6-OHDA rat model, as indicated by the reduction in the behavioural deficit in the rat [12]. Paraquat is a pesticide that has been linked to PD, and it has been demonstrated that EGb761 protects against paraquat-induced apoptosis of PC12 cells by increasing bcl-2 activation, maintaining of mitochondrial membrane potential ( $\Delta \Psi_m$ ) and decreasing caspase-3 activation through the mitochondria-dependent pathway [13]. The neuroprotective effect of EGb761 against MPTP neurotoxicity is associated with the blockade of lipid peroxidation, reduction of oxidative stress, and attenuation of MPTP-induced neurodegeneration of the nigrostriatal pathway [14]. Also, it was demonstrated in an extensive review that EGb761 may exert therapeutic actions in an animal model of PD via the antioxidant effects [82]. Ginkgetin, a natural biflavonoid isolated from leaves of *G. biloba*, protected against 1-methyl-4-phenylpyridinium ion- (MPP<sup>+</sup>-) induced cell damage in vitro by decreasing the levels of intracellular reactive oxygen species (ROS) and by maintaining  $\Delta \Psi_m$  and also improved the sensorimotor coordination in a mouse PD model induced by MPTP, suggesting that the neuroprotective mechanism of ginkgetin occurs via regulating

iron homeostasis [16]. In low-dose whole-body  $\gamma$ -irradiation in the reserpine model of PD, EGb761 was protective by ameliorating the reserpine-induced state of oxidative stress, mitochondrial dysfunction, and apoptosis in the brain [15]. The pretreatment with ginkgolide B or bilobalide protected SH-SY5Y cells against  $\alpha$ -synuclein-induced cell injury and apoptosis [17]. Ultimately, the *G. biloba* extract treatment improved locomotor activity, decreased oxidative damage, maintained the dopamine homeostasis, and inhibited the development of PD in A53T  $\alpha$ -synuclein transgenic mice [18].

**2.2. *Ginseng*.** Ginseng is a traditional Chinese herb containing more than 30 ginsenosides, the active ingredients of ginseng. Ginsenosides Rb1 and Rg1 are regarded as the main compounds responsible for the therapeutic actions of ginseng. Previous studies have shown that, in SN-K-SH cells, both ginsenosides Rb1 and Rg1 reversed MPTP-induced cell death [19]. The protective effect of Rg1 against MPTP-induced apoptosis was attributed to enhancing Bcl-2 and Bcl-xl expression, reducing Bax and iNOS expression, and inhibiting activation of caspase-3 [20]. The ginseng extract G115 significantly blocked tyrosine hydroxylase- (TH-) positive cell loss in the SN and reduced the appearance of locomotor dysfunction in two rodent models of PD [21]. Pretreatments of Rg1 or N-acetylcysteine were found to protect against MPTP-induced SN neuron loss by preventing glutathione (GSH) reduction, attenuate the phosphorylations of JNK and c-Jun, and activate superoxide dismutase (SOD) [22]. MPP<sup>+</sup>-induced cytotoxicity in SH-SY5Y was inhibited by water extract of ginseng, as demonstrated by the inhibitory effect on cell death, overproduction of ROS, elevated Bax/Bcl-2 ratio, release of cytochrome c, and activation of caspase-3 expression [23]. It was demonstrated that ginsenosides protect by reducing intracellular ROS levels, enhancing antioxidant activity, preserving the activity of complex I, stabilising the  $\Delta \Psi_m$ , and increasing intracellular ATP levels. Rg1 treatment restored motor functions in MPTP-treated mice and these behavioural ameliorations were accompanied by restoration of dopaminergic neurons in the SN and striatum [24]. Additionally, the ginsenoside Rb1 exhibited a strong ability to disaggregate fibrils and to inhibit the polymerisation of  $\alpha$ -synuclein [25]. Rg1 treatment inhibited the activation of microglia and reduced the infiltration of CD3+ and T cells and also protected TH-positive cells in the SN and reduced the serum concentrations of proinflammatory cytokines TNF $\alpha$ , IFN $\gamma$ , IL-1 $\beta$ , and IL-6 in MPTP mouse models [26]. Also, using in vivo and in vitro models of PD, it was demonstrated that ginsenoside Rg1 may exert therapeutic effects on PD via the Wnt/ $\beta$ -catenin signalling pathway [27]. In the MPTP-probenecid mouse model, the oral treatment with Rg1 significantly attenuated MPTP-induced mortality, behaviour defects, and loss of dopaminergic neurons. The protective effect of Rg1 may be mediated by reducing aberrant  $\alpha$ -synuclein-mediated neuroinflammation [28]. The neurotoxin rotenone is an inhibitor of complex I and has been widely used in vivo and in vitro to model PD. Thus, cotreatment with ginsenosides Rd and Re inhibited the increased intracellular ROS production and lipid peroxidation accumulation caused by rotenone. Besides, the major ginsenosides Rd and Re

TABLE 1: Drugs used in PD and ADHD and their side effects.

Drugs for PD [7]	Mechanism	Side effects
L-DOPA and Carbidopa	A precursor to dopamine, combined with carbidopa, which blocks aromatic amino acid decarboxylase	Nausea, vomiting, insomnia, psychosis, hallucinations, hypotension, arrhythmia, somnolence, nightmares
Selegiline, Rasagiline, Saffinamide	Monoamine oxidase B inhibitors (MAO-B); increase the synaptic availability of dopamine; safinamide also inhibits glutamate release	Abnormal movements, dizziness, nausea, vomiting, dry mouth, persistent diarrhoea, constipation, weight loss
Entacapone and Tolcapone	Catechol-O-methyltransferase inhibitors (COMT); Increase CNS L-DOPA bioavailability by decreasing peripheral L-DOPA metabolism	Dyskinesia, nausea, sleep disturbances, arterial hypotension, liver toxicity, vomiting, dizziness
Pramipexole, Ropinirole, Rotigotine, Apomorphine	Dopamine agonists; stimulate the action of dopamine at postsynaptic receptors	Nausea, dyskinesia, hallucinations, sleepiness, sleep attacks, confusion, ankle oedema, orthostatic hypotension, constipation
Trihexyphenidyl and Benztropine	Anticholinergics; block acetylcholine in the striatum	Dry mouth, urine retention, hallucinations, dry eyes, constipation, blurred vision, loss of memory, and confusion, somnolence, dizziness
Amantadine	Is an antagonist of the NMDA type glutamate receptor and also stimulates dopamine release	Oedema, hallucinations, insomnia, confusion
Drugs For ADHD [8]	Mechanism	Side effects
Methylphenidate	Inhibits reuptake of dopamine and norepinephrine	Anxiety, agitation, insomnia, decrease appetite, weight loss, irritability, hypertension, headache, stomach pain, numbness
Amphetamines	Inhibit reuptake of dopamine and norepinephrine	Decrease appetite, weight loss, irritability, hypertension, anxiety, agitation, nervousness, depression
Atomoxetine	Selective norepinephrine reuptake inhibitor	Dry mouth, sedation, fatigue, increased sweating, hypertension, decrease appetite, dizziness, drowsiness, insomnia, itching, impotence, unusually fast or irregular heartbeat, increased suicidality
Imipramine, Nortriptyline, Amitriptyline, Desipramine	Tricyclic antidepressants; Inhibit reuptake of dopamine and norepinephrine	Dry mouth, sweating abnormalities, drowsiness/sedation, increased suicidality
Clonidine and Guanfacine	Agonists of the $\alpha$ -2 and $\alpha$ -2A adrenergic receptors in the prefrontal cortex	Dry mouth, fatigue, dizziness, profound withdrawal effects

TABLE 2: Effects of natural compounds used as an alternative therapy for PD.

Source	Compound	Action mechanism	Refs
Ginkgo biloba	EGb761	Antioxidant, inhibited toxic effect of levodopa, inhibited MAO activity, ↓behavioural deficit, anti-apoptotic, maintain $\Delta\Psi_m$ , ↑bcl-2, ↓caspase-3, ↓lipid peroxidation, ↓oxidative stress	[9–15]
Ginkgo biloba	Ginkgetin	↓ROS, maintain $\Delta\Psi_m$	[16]
Ginkgo biloba	Ginkgolide B and Bilobalide	↓ $\alpha$ -synuclein, anti-apoptotic	[17]
Ginkgo biloba	Ginkgo biloba extract	↑SOD, ↑GHS, ↓malondialdehyde	[18]
Ginseng	Ginsenosides Rb1 and Rg1	Antioxidant, anti-apoptotic, ↑bcl-2, ↓Bax, ↓iNOS, ↓caspase-3, ↑SOD, ↑GHS, ↓ $\alpha$ -synuclein fibrils, ↓TNF- $\alpha$ , ↓JFN- $\gamma$ , ↓JL-1 $\beta$ , ↓JL-6, ↑Wnt-1, ↑ $\beta$ -catenin, ↑GSK-3 $\beta$ , maintain $\Delta\Psi_m$ , ↓cytochrome c release	[19–28]
Ginseng	Ginsenosides Rd and Re	Antioxidant, anti-apoptotic, improved mitochondrial function	[29, 30]
Flavonoid	Baicalein	↓lipid peroxidation, ↑serotonin, ↓dopamine levels, ↓oxidative stress, ↓ $\alpha$ -synuclein aggregation, ↑DJ-1, ↓NF- $\kappa$ B, ↓JERK, ↓JNK	[31–40]
Flavonoid	Luteolin	↓Inflammation, ↓ROS, ↓oxidative stress	[41–43]
Flavonoid	Quercetin	Antioxidant, ↑SOD, ↑GPx, ↓oxidative stress, ↑ATPase, ↑catalase, ↑complex I activity, ↑PKD1, ↑Akt, ↑CREB, ↑BDNF	[44–47]
Flavonoid	Kaempferol	↑SOD, ↑GHS, ↓lipid peroxidation, ↑autophagy	[48, 49]
Flavonoid	Rutin	↓oxidative stress, ↑SOD, ↑GPx, ↓oxidative stress, ↓lipid peroxidation, ↑catalase	[50, 51]
Flavonoid	Isoquercitrin	↓oxidative stress	[52]
Flavonoid	Apigenin	↓Inflammation, ↓ROS	[43, 53]
Flavonoid	Troloxerutin	↓lipid peroxidation, ↓ROS, ↓DNA fragmentation	[54]
Flavonoid	Hesperidin	Antioxidant	[55, 56]
Valeriana officinalis	Extract of valerian	Normalised SOD and catalase mRNAs	[57]
Valeriana wallichii	Valeriana wallichii	↓ROS, ↓Inflammation, ↓lipid peroxidation	[58]
Passiflora incarnata	Extract of passion flower	Antioxidant	[59]
Passiflora cincinnata	Passiflora cincinnata	Antioxidant	[60]
Hypericum perforatum	Extract of St. John's wort	Antioxidant, anti-apoptotic, ↑GHS, ↑catalase, ↓malondialdehyde, ↓DNA fragmentation	[61, 62]

upregulate SOD and aconitase activities, and GSH also attenuates the depolarisation of  $\Delta \Psi_m$  and restores  $Ca^{2+}$  levels and moreover prevents apoptosis by modulating Bax and Bcl-2 and inhibiting cytochrome c release and caspase-3 activation [29]. Additionally, ginsenoside Rd reversed the loss of TH-positive cells in SN in vivo and in vitro PD models, which may involve its antioxidant effects and mitochondrial function preservation [30].

**2.3. Flavonoids.** Flavonoids are part of a large group of natural polyphenol phytochemicals with a long history of use as therapeutic agents. Baicalin, a flavonoid isolated from *Scutellaria baicalensis*, is the main metabolite of baicalein. The neuroprotective efficacy of baicalein has been shown in an in vivo model of PD using the neurotoxin 6-OHDA, where the protective effects on dopaminergic dysfunction and lipid peroxidation were seen [31]. Other reports showed that baicalein prevented abnormal behaviour by increasing dopaminergic neurons and dopamine and serotonin levels in the striatum and also inhibited oxidative stress and astroglial response [32]. Luteolin and apigenin are flavones with similar structure; luteolin is found in celery, broccoli, parsley, thyme, and olive oil, and apigenin is present in vegetables, several fruits, and herbs. Luteolin protects dopaminergic neurons against inflammation-induced neurotoxicity by inhibiting microglial activation [41]. Moreover, baicalein exerts protective effects in vivo and in vitro against 6-OHDA [33]. In addition, baicalein protects cells against the toxicity of a point mutation in  $\alpha$ -synuclein [34]. Baicalein also inhibited the formation of  $\alpha$ -synuclein oligomers and consequently prevents its oligomerisation [35]. Quercetin is the aglycone form of a number of other flavonoid glycosides, such as rutin and quercitrin, and is found in citrus fruit, onions, and grains. In the 6-OHDA rat model, treatment of quercetin increased levels of antioxidant and striatal dopamine and reduced dopaminergic neuronal loss [44]. Kaempferol is a natural flavonoid which has been found in grapefruit, and other plant sources. It improves motor coordination, raises striatal dopamine and its metabolite levels, increases SOD and GSH activity, and reduces the content of lipid peroxidation, also preventing the loss of TH-positive neurons induced by MPTP [48]. There is also evidence of neuroprotection by kaempferol by autophagy in SH-SY5Y cells and primary neurons against rotenone toxicity [49]. It has been demonstrated that rutin protects dopaminergic neurons against oxidative stress induced by 6-OHDA [50]. Furthermore, it has been shown that quercetin protects against oxidative stress and increases activities of glutathione peroxidase (GPx), SOD, ATPase, AchE, and dopamine depletion in MPTP-treated mice [45]. The bioflavonoid rutin inhibits 6-OHDA-induced neurotoxicity in PC12 cells by activation of SOD, catalase, GPx, and total GSH and by inhibition of lipid peroxidation [51]. Moreover, in a rotenone model, quercetin has been shown to upregulate mitochondrial complex I activity and increase catalase and SOD activity [46]. Mitochondrial dysfunction in SH-SY5Y cells and upregulation of DJ-1 protein expression induced by 6-OHDA is prevented by baicalein [36]. The flavonol isoquercitrin protects PC12 cells against 6-OHDA-induced oxidative stress [52]. Baicalein downregulates the activation

of NF- $\kappa$ B, ERK, and JNK and attenuates astrocyte activation in MPTP mice [37]. Baicalein inhibits the upregulation of proinflammatory cytokines in the SN and striatum in PD mice models [38]. Luteolin also reduces cytotoxicity induced by 6-OHDA and ROS production in neuronal PC12 cells by modulating changes in the stress response pathway [42]. In MPTP-treated mice, luteolin and apigenin protect dopaminergic neurons by reducing oxidative damage, neuroinflammation, and microglial activation and also improve muscular and locomotor activity [43]. The flavonoids and their metabolites can interact with neuronal receptors and modulate kinase signalling pathways, transcription factors, and gene and/or protein expression, which control memory and learning processes in the hippocampus [83]. Naringin is a flavonoid glycoside that is contained abundantly in the skin of grapefruit and orange and is the origin of their bitterness. It protects dopaminergic neurons by induction of the activation of mammalian target of rapamycin complex 1 (mTORC1) and inhibited microglial activation in the SN of the mouse treated with 6-OHDA [84]. In a rotenone mouse model, baicalein prevented the progression of  $\alpha$ -synuclein accumulation and protected dopaminergic neurons and also inhibited the formation of  $\alpha$ -synuclein oligomers [39]. It has been shown that baicalein inhibits  $\alpha$ -synuclein aggregates and autophagy in rats treated with  $MPP^+$  [40]. Besides, in the same model, apigenin ameliorated dopaminergic neuronal loss and improved behavioural, biochemical, and mitochondrial enzyme activities; such effects were associated with the suppression of oxidative stress and neuroinflammation [53]. Recently, it was demonstrated that quercetin improved mitochondrial biogenesis and induced the activation of two major cell survival kinases, PKD1, and Akt and also enhanced CREB and BDNF (a CREB target gene) in MN9D cells against 6-OHDA-induced neurotoxicity, and in the MitoPark transgenic mouse model of PD, quercetin improved behavioural deficits and reduced TH cell loss [47]. Troxerutin (also known as vitamin P4) is a natural derivative of the bioflavonoid rutin that is present in coffee, cereal grains, tea, and vegetables. The neuroprotective effects of troxerutin were reported in a 6-OHDA rat model to reduce striatal lipid peroxidation, ROS, GFAP, and DNA fragmentation. Meanwhile, troxerutin was capable of preventing loss of TH-positive neurons in the SN [54]. The bioflavonoid hesperidin is a specific flavonoid glycoside frequently found in oranges and lemons. Hesperidin protects against iron-induced oxidative damage and dopamine depletion in *Drosophila melanogaster* model of PD [55]. In addition, in 6-OHDA-treated mice, hesperidin protects by reducing oxidative damage, increasing the dopamine levels and also improving the behavioural parameters [56].

**2.4. Valeriana officinalis.** Valeriana officinalis (Valerian) is a plant with sedative and antispasmodic effect, traditionally used in the treatment of insomnia, anxiety, and restlessness. The effects of valerian on rotenone-induced cell death in SH-SY5Y cells have been demonstrated [85]. Moreover, extract of valerian was effective in reducing the toxicity induced by rotenone in *Drosophila melanogaster*, as confirmed by the normalisation in the expression of SOD and catalase mRNAs,



suggesting that the effects of valerian are, at least in part, associated with the antioxidant properties of the plant due to its phenolic and flavonoid constituents [57]. Valeriana wallichii, also known as Indian valerian or Tagar-Ganthoda, belongs to the family Valerianaceae and is considered as an important Asian counterpart of the European valerian. Thus, valeriana wallichii treatment significantly recuperated the altered behaviour, striatal dopamine levels, increased GFAP expression, and the histopathological changes observed in mice treated with MPTP. Likewise, it ameliorated the increased levels of ROS, inflammatory cytokines and lipid peroxidation and also ameliorated the diminished levels of antioxidants [58].

**2.5. Passion Flower.** Passion flower, commonly known as *Passiflora incarnata* (Passifloraceae), contains flavonoids, glycosides, alkaloids, and phenolic compounds. Also, it has been used for the treatment of anxiety, insomnia, epilepsy, muscular spasms, and other diseases [86]. Therefore, the biological effects of passion flower have been investigated in PD. The extract of passion flower reduced the number of jaw movements induced by tacrine, which is a widely used animal model of PD tremors. In addition, the model showed cognitive improvement, with significantly reduced duration of haloperidol-induced catalepsy. The passion flower possesses antioxidant activity, as shown by its significant scavenging ability [59]. *Passiflora cincinnata* is a Brazilian native species of passion flower and its possible biological effects have been investigated. Thus, in a model of PD induced by reserpine, *Passiflora cincinnata* extract prevented the decrease in TH in the SN induced by reserpine, delayed the onset of motor impairments, and prevented the occurrence of increased catalepsy behaviour. However, the extract did not modify reserpine-induced cognitive impairments [60].

**2.6. St. John's Wort.** The use of St. John's wort, known as *Hypericum perforatum*, dates back to the time of the ancient Greeks. Active compounds of St. John's wort have been identified and include naphthodianthrones, phloroglucinols, and flavonoids (such as phenylpropanes, flavonol glycosides, and biflavones), as well as essential oils. Therefore, the active compounds provide antioxidant and neuroprotective effects [87]. Two standardised extracts of St. John's wort have been tested on the neurodegeneration induced by chronic administration of rotenone in rats. Accordingly, St. John's wort reduced neuronal damage and inhibited the apoptotic cascade by decreasing Bax levels [61]. Besides, intrastriatal 6-OHDA-lesioned rats were treated with an the extract of St. John's wort and showed lowered striatal level of malondialdehyde, enhanced catalase activity, reduced GSH content, normalised expression of GFAP and TNF $\alpha$ , lowered DNA fragmentation and prevention of damage to dopaminergic neurons [62].

### 3. Attention-Deficit/Hyperactivity Disorder

Attention-deficit/hyperactivity disorder (ADHD) is the most common neurodevelopmental disorder in childhood and

is characterised by inattention, impulsivity, and hyperactivity. The worldwide prevalence of ADHD in children and adolescents is 5.3% [88]; across cultures the prevalence is estimated to range from 5% to 7% [88, 89]. ADHD has high impact on school performance and causes impairments in personal, social, or occupational function, leading to isolation, poorer grades, and in adolescence there is increased risk of depression, delinquent and antisocial behaviour, incurring comorbid conditions, and later substance abuse [90]. ADHD has been associated with deregulation of the catecholaminergic pathway in the brain [91], although extensive data point to oxidative stress as potential contributor to the pathophysiology in ADHD [92]. Currently, ADHD treatment is pharmacologic and improves the attention, reducing distractibility and impulsive behaviour. Pharmacologic agents used for the treatment of ADHD increase levels of catecholamines in the brain, alleviating ADHD symptoms, and can be divided into two: psychostimulants and nonpsychostimulants [93]. Methylphenidate (MPH) is a psychostimulant that increases extracellular dopamine and norepinephrine levels, thereby correcting the underlying abnormalities in catecholaminergic functions and restoring neurotransmitter imbalance [94]. Atomoxetine (ATX) is a nonpsychostimulant, a norepinephrine specific reuptake inhibitor that increases catecholamine levels in the brain resulting in behavioural improvement [94, 95]. ADHD is a heterogeneous disorder and is categorized into three subtypes: hyperactive/impulsive, inattentive, and the combined subtype [89, 90]. There may be also differences in terms of treatment responses, for example, the hyperactive/impulsive subtype responds well to MPH, the inattentive subtype responds better to ATX, and the combined type responds well to ATX and MPH, although controversy still persists about which is the best treatment for each subtype. However, it has been demonstrated that the pharmacological treatments to improve ADHD symptoms have some side effects, which include nausea, headache, insomnia, abdominal pain, decreased appetite, and motor tics [96]. Drugs used for the ADHD treatment and their side effects are shown in Table 1. Moreover, the use of psychostimulant medications in ADHD has been also associated with increased risk of substance use disorder [97]. Thus, there has been growing interest in alternative treatments for ADHD, including natural compounds because of their antioxidant properties [98]. Natural compounds used as alternative therapies for the management of ADHD are shown in Table 3.

**3.1. Ginkgo biloba.** The extract from *G. biloba* leaves has been used as a herbal medicine for dementia [81, 99]. Therefore, several reports indicate that *G. biloba* may have therapeutic benefits in ADHD, given that the cotreatment with *G. biloba* and ginseng were found to alleviate ADHD symptoms in children, with minor side effects observed [63]. Moreover, in a double-blind, randomised trial the administration of *G. biloba* was less effective than MPH in the treatment of ADHD [64]. *G. biloba* extract treatment at a maximal dosage of 240 mg improved the behavioural ratings of ADHD symptoms and the electrical brain activity in children, suggesting that *G. biloba* extract seems to be well tolerated in the short term

TABLE 3: Effects of natural compounds used as an alternative therapy for ADHD.

Compound	Outcome	Refs
Ginkgo biloba	Alleviates ADHD symptoms in children and has minor side effects	[63]
Ginkgo biloba	Double blind, randomised trial; was less effective than MPH in children with ADHD	[64]
Ginkgo biloba	Improved behavioural ratings of ADHD symptoms and the electrical brain activity in children	[65]
Ginkgo biloba	Randomised, placebo-controlled trial; the response rate was higher	[66]
Ginseng	Open trial, improved the inattention and hyperactive/impulsive score in children with ADHD	[67]
Ginseng	Observational clinical study, improved inattentiveness in children with ADHD	[68]
Ginseng	Double-blind randomised placebo-controlled trial; ↓inattention and hyperactivity scores in children with ADHD	[69]
Ginsenoside Rg3 and Ginkgo biloba	↓ROS, ↑BDNF levels, ↑p-TrkB, ↑BDNF, ↑dopamine transporter, ↑norepinephrine transporter	[70]
Flavonoid	↓hyperactivity, improved attention and visual-motor coordination and concentration of children with ADHD	[71]
Flavonoid	Randomised, double-blind and placebo controlled study; normalised total antioxidant status, ↓oxidative damage to DNA and improved attention in children with ADHD	[72]
Flavonoid	Randomised, double-blind controlled design; ↓hyperactivity, normalised catecholamine concentrations and ↓oxidative stress in children with ADHD	[73]
Flavonoid	↑dopaminergic neurotransmission, improved synaptosomal ATPase, regulated motor ability, learning and memory, ↓hyperactivity, inattention and impulsivity in the SHR model	[74–76]
Valeriana officinalis	double-blind, placebo-controlled pilot study; improved ADHD symptoms	[77]
Passiflora incarnata	Randomised study, alleviated ADHD symptoms and has tolerable side effect	[78]
Hypericum perforatum	Randomised controlled trial; did not improve symptoms in children with ADHD	[79]
Hypericum perforatum	A preliminary study; improved some symptoms in ADHD patients	[80]

and may be a useful treatment [65]. Lately, in a randomised, placebo-controlled trial the response rate was higher with *G. biloba* treatment compared to placebo. Thus, *G. biloba* could be an effective complementary treatment for ADHD [66].

**3.2. Ginseng.** Ginseng contains a class of phytochemicals called ginsenosides, which are known as potent antioxidants and for their neuroprotective properties. Ginseng has been shown to alleviate effectively symptoms of ADHD. In an open trial, ginseng medication improved the inattention and hyperactive/impulsive score in children with ADHD [67]. Indeed, an observational clinical study showed that ginseng, given at 1000 mg for 8 weeks, improved inattentiveness in children with ADHD [68]. A double-blind randomised, placebo-controlled trial reported that ginseng decreased inattention and hyperactivity scores in children with ADHD [69]. Hence, ginseng has the potential to be used as an alternative therapy for ADHD. On the ADHD-like condition induced by Aroclor1254, YY162, which consists of terpenoid-strengthened *G. biloba* and ginsenoside Rg3, attenuated the increase in ROS and decrease in BDNF levels in SH-SY5Y cells. Moreover, YY162 attenuated reductions in p-TrkB, BDNF, dopamine transporter, and norepinephrine transporter expression [70].

**3.3. Flavonoids.** Pycnogenol is a herbal dietary supplement extracted from French maritime pine bark whose main ingredient is procyanidin. Procyanidins are members of the proanthocyanidin a class of flavonoids and are powerful antioxidants also found in food such as grapes, berries, pomegranates, red wine, and nuts. The treatment of 1-month pycnogenol administration resulted in a significant reduction in hyperactivity, improved attention, and visual-motor coordination and concentration in children with ADHD [71]. Moreover, pycnogenol reduced oxidative damage to DNA, normalised total antioxidant status, and improved attention, as demonstrated in a randomised, double-blind, placebo-controlled study [72]. Also, the administration of pycnogenol in children with ADHD, normalised catecholamine concentrations, leading to less hyperactivity, and reduced oxidative stress, in a randomised, double-blind, controlled design [73]. St. John's wort and pycnogenol have been tested as therapeutic alternatives to treat ADHD. A significant increase of SH-SY5Y cell survival was induced by pycnogenol, which did not cause any cytotoxic effect when used in therapeutically relevant concentrations; also, treatment with St. John's wort significantly increased ATP levels [100]. Oroxylin A is a flavonoid isolated from the root of *Scutellaria baicalensis* Georgi, a herb found in East Asia. It has been observed that oroxylin A is an antagonist of the GABA-A receptor and its neuroprotective actions include antioxidant, anti-inflammatory, and memory-enhancing effects. On the other hand, spontaneously hypertensive rats (SHRs) display some symptoms of ADHD, which makes them a model of the disorder. It was demonstrated that oroxylin A improved ADHD-like behaviours via enhancement of dopaminergic neurotransmission and not the modulation of the GABA pathway in the SHR [74]. Furthermore, an oroxylin A analogue reduced hyperactivity, sustained inattention, and

impulsivity in the SHR [75]. Baicalin regulated the motor ability and learning and memory abilities in the SHR and thus controlled the core symptoms of ADHD [76]. Also, baicalin improved synaptosomal ATPase and LDH activities in the SHR, suggesting that baicalin exerts its therapeutic effect by upregulating the AC/cAMP/PKA signalling pathway [101]. A randomised, double-blind trial to investigate the therapeutic benefit of pycnogenol in ADHD patients is in progress [102].

**3.4. Valeriana officinalis.** The efficacy of valerian has been evaluated in a double-blind, placebo-controlled pilot study, where valerian showed improvement in ADHD symptoms, in particular, sustained inattention, anxiety and impulsivity, and/or hyperactivity [77]. The GABA- A receptors are the substrate for the anxiolytic action of valerenic acid, a major constituent of valerian root extracts [103]. GABA is the main inhibitory neurotransmitter in the CNS, and its deficiency causes anxiety, restlessness, and obsessive behaviour, symptoms often seen in ADHD. The European Medicine Agency deemed that root extracts of valerian could be used for the relief of mild nervous tension and sleep disorders. However, more research is required to support the efficacy of valerian in the treatment ADHD.

**3.5. Passion Flower.** The effect of passion flower in alleviating ADHD symptoms was tested in a randomised study. In addition, a tolerable side effect profile may be considered as one of the advantages of passion flower as compared with MPH [78]. It seems that the mechanism of action of passion flower is mediated via modulation of the GABA-A and GABA-B receptors and its effects on GABA uptake [104]. Although the passion flower has shown pharmacological activity in preclinical experiments, including sedative, anxiolytic, antitussive, antiasthmatic, and antidiabetic activities, its supposed efficacy does not appear to be adequately corroborated in the literature, since clinical studies often present methodologies and procedures with weaknesses [105].

**3.6. St. John's Wort.** St. John's wort produces its therapeutic effects by involving inhibition of the reuptake of dopamine, serotonin, and norepinephrine [106]. In a randomised controlled trial, the use of St. John's wort for the treatment of ADHD over the course of eight weeks did not improve symptoms [79]. However, a preliminary study reported that treatment with St. John's wort improved some symptoms in ADHD patients [80]. Because of findings that St. John's wort has no adverse effects, more studies are required to determine efficacy in the treatment of ADHD.

## 4. Conclusions

The natural compounds discussed in this review appear to be promising for the treatment of PD and ADHD. Therefore, these compounds can lay the foundation for a new therapeutic approach for the treatment of these disorders. Natural compounds are more easily accepted by patients, since they are considered healthier than synthetic drugs. Although the use of natural compounds for the neurological

disorders has been considered as a safe approach, they are still far from being standard treatments, due to the lack of controlled clinical studies that could corroborate both their high efficacy and safety. Hence, better designed and more rigorous clinical trials are required before they can be established as therapeutic compounds. Neither PD nor ADHD, until today, have a therapeutic option capable of counteracting the progression of the disease, and natural compounds are often able to modulate the progression of this type of disorder, as demonstrated by their decreasing of oxidative stress.

## Conflicts of Interest

The author declares that there are no conflicts of interest.

## Acknowledgments

This work was supported by Fondos Federales HIM 2015/022 SSA 1160.

## References

- [1] W. Dauer and S. Przedborski, "Parkinson's disease: mechanisms and models," *Neuron*, vol. 39, no. 6, pp. 889–909, 2003.
- [2] C. W. Olanow, D. R. Wakeman, and J. H. Kordower, "Peripheral alpha-synuclein and Parkinson's disease," *Movement Disorders*, vol. 29, no. 8, pp. 963–966, 2014.
- [3] J. C. Corona and M. R. Duchen, "PPARgamma and PGC-1alpha as therapeutic targets in Parkinson's," *Neurochemical Research*, vol. 40, no. 2, pp. 308–316, 2015.
- [4] H. Deng, P. Wang, and J. Jankovic, "The genetics of Parkinson disease," *Ageing Research Reviews*, vol. 42, pp. 72–85, 2018.
- [5] L. Brichta, P. Greengard, and M. Flajolet, "Advances in the pharmacological treatment of Parkinson's disease: targeting neurotransmitter systems," *Trends in Neurosciences*, vol. 36, no. 9, pp. 543–554, 2013.
- [6] B. K. Young, R. Camicioli, and L. Ganzini, "Neuropsychiatric adverse effects of antiparkinsonian drugs. Characteristics, evaluation and treatment," *Drugs & Aging*, vol. 10, no. 5, pp. 367–383, 1997.
- [7] H. Homayoun, "Parkinson Disease," *Annals of Internal Medicine*, vol. 169, no. 5, pp. ITC33–ITC48, 2018.
- [8] R. D. White, G. D. Harris, and M. E. Gibson, "Attention Deficit Hyperactivity Disorder and Athletes," *Sports Health*, vol. 6, no. 2, pp. 149–156, 2014.
- [9] C. Ramassamy, F. Clostre, Y. Christen, and J. Costentin, "Prevention by a Ginkgo biloba Extract (GBE 761) of the Dopaminergic Neurotoxicity of MPTP," *Journal of Pharmacy and Pharmacology*, vol. 42, no. 11, pp. 785–789, 1990.
- [10] W.-R. Wu and X.-Z. Zhu, "Involvement of monoamine oxidase inhibition in neuroprotective and neurorestorative effects of Ginkgo biloba extract against MPTP-induced nigrostriatal dopaminergic toxicity in C57 mice," *Life Sciences*, vol. 65, no. 2, pp. 157–164, 1999.
- [11] F. Cao, S. Sun, and E. T. Tong, "Experimental study on inhibition of neuronal toxic effect of levodopa by ginkgo biloba extract on Parkinson disease in rats," *Journal of Huazhong University of Science and Technology - Medical Sciences*, vol. 23, no. 2, pp. 151–153, 2003.
- [12] M.-S. Kim, J.-I. Lee, W.-Y. Lee, and S.-E. Kim, "Neuroprotective effect of Ginkgo biloba L. extract in a rat model of parkinson's disease," *Phytotherapy Research*, vol. 18, no. 8, pp. 663–666, 2004.
- [13] X. Kang, J. Chen, Z. Xu, H. Li, and B. Wang, "Protective effects of Ginkgo biloba extract on paraquat-induced apoptosis of PC12 cells," *Toxicology in Vitro*, vol. 21, no. 6, pp. 1003–1009, 2007.
- [14] P. Rojas, N. Serrano-García, J. J. Mares-Sámano, O. N. Medina-Campos, J. Pedraza-Chaverri, and S. O. Ögren, "EGb761 protects against nigrostriatal dopaminergic neurotoxicity in 1-methyl-4-phenyl-1,2,3, 6-tetrahydropyridine-induced Parkinsonism in mice: Role of oxidative stress," *European Journal of Neuroscience*, vol. 28, no. 1, pp. 41–50, 2008.
- [15] M. A. El-Ghazaly, N. A. Sadik, E. R. Rashed, and A. A. Abd-El-Fattah, "Neuroprotective effect of EGb761(R) and low-dose whole-body gamma-irradiation in a rat model of Parkinson's disease," *Toxicology & Industrial Health*, vol. 31, no. 12, pp. 1128–1143, 2015.
- [16] Y. Q. Wang, M. Y. Wang, X. R. Fu et al., "Neuroprotective effects of ginkgetin against neuroinjury in Parkinson's disease model induced by MPTP via chelating iron," *Free Radical Research*, vol. 49, no. 9, pp. 1069–1080, 2015.
- [17] J. Hua, N. Yin, B. Yang et al., "Ginkgolide B and bilobalide ameliorate neural cell apoptosis in  $\alpha$ -synuclein aggregates," *Biomedicine & Pharmacotherapy*, vol. 96, pp. 792–797, 2017.
- [18] S. Kuang, L. Yang, Z. Rao et al., "Effects of Ginkgo Biloba Extract on A53T  $\alpha$ -Synuclein Transgenic Mouse Models of Parkinson's Disease," *Canadian Journal of Neurological Sciences*, vol. 45, no. 2, pp. 182–187, 2018.
- [19] M. Rudakewich, F. Ba, and C. G. Benishin, "Neurotrophic and neuroprotective actions of ginsenosides Rb(1) and Rg(1)," *Planta Medica*, vol. 67, no. 6, pp. 533–537, 2001.
- [20] X.-C. Chen, Y. Chen, Y.-G. Zhu, F. Fang, and L.-M. Chen, "Protective effect of ginsenoside Rg1 against MPTP-induced apoptosis in mouse substantia nigra neurons," *Acta Pharmacologica Sinica*, vol. 23, no. 9, pp. 829–834, 2002.
- [21] J. Van Kampen, H. Robertson, T. Hagg, and R. Drobitch, "Neuroprotective actions of the ginseng extract G115 in two rodent models of Parkinson's disease," *Experimental Neurology*, vol. 184, no. 1, pp. 521–529, 2003.
- [22] X.-C. Chen, Y.-C. Zhou, F. Fang, Y. Chen, Y.-G. Zhu, and L.-M. Chen, "Ginsenoside Rg1 reduces MPTP-induced substantia nigra neuron loss by suppressing oxidative stress," *Acta Pharmacologica Sinica*, vol. 26, no. 1, pp. 56–62, 2005.
- [23] S. Hu, R. Han, S. Mak, and Y. Han, "Protection against 1-methyl-4-phenylpyridinium ion (MPP<sup>+</sup>)-induced apoptosis by water extract of ginseng (*Panax ginseng* C.A. Meyer) in SH-SY5Y cells," *Journal of Ethnopharmacology*, vol. 135, no. 1, pp. 34–42, 2011.
- [24] W. Jiang, Z. Wang, Y. Jiang, M. Lu, and X. Li, "Ginsenoside Rg1 ameliorates motor function in an animal model of Parkinson's disease," *Pharmacology*, vol. 96, no. 1-2, pp. 25–31, 2015.
- [25] M. T. Ardah, K. E. Paleologou, G. Lv et al., "Ginsenoside Rb1 inhibits fibrillation and toxicity of alpha-synuclein and disaggregates preformed fibrils," *Neurobiology of Disease*, vol. 74, pp. 89–101, 2015.
- [26] T.-T. Zhou, G. Zu, X. Wang et al., "Immunomodulatory and neuroprotective effects of ginsenoside Rg1 in the MPTP(1-methyl-4-phenyl-1,2,3,6-tetrahydropyridine) -induced mouse model of Parkinson's disease," *International Immunopharmacology*, vol. 29, no. 2, pp. 334–343, 2015.



- [27] T. Zhou, G. Zu, X. Zhang et al., "Neuroprotective effects of ginsenoside Rg1 through the Wnt/ $\beta$ -catenin signaling pathway in both in vivo and in vitro models of Parkinson's disease," *Neuropharmacology*, vol. 101, no. 5, pp. 480–489, 2016.
- [28] Y. Heng, Q.-S. Zhang, Z. Mu, J.-F. Hu, Y.-H. Yuan, and N.-H. Chen, "Ginsenoside Rg1 attenuates motor impairment and neuroinflammation in the MPTP-probenecid-induced parkinsonism mouse model by targeting  $\alpha$ -synuclein abnormalities in the substantia nigra," *Toxicology Letters*, vol. 243, pp. 7–21, 2016.
- [29] E. González-Burgos, C. Fernández-Moriano, R. Lozano, I. Iglesias, and M. P. Gómez-Serranillos, "Ginsenosides Rd and Re co-treatments improve rotenone-induced oxidative stress and mitochondrial impairment in SH-SY5Y neuroblastoma cells," *Food and Chemical Toxicology*, vol. 109, pp. 38–47, 2017.
- [30] Y. Liu, R.-Y. Zhang, J. Zhao et al., "Ginsenoside Rd protects SH-SY5Y cells against 1-methyl-4-phenylpyridinium induced injury," *International Journal of Molecular Sciences*, vol. 16, no. 7, pp. 14395–14408, 2015.
- [31] H.-I. Im, W. S. Joo, E. Nam, E.-S. Lee, Y.-J. Hwang, and Y. S. Kim, "Baicalein prevents 6-hydroxydopamine-induced dopaminergic dysfunction and lipid peroxidation in mice," *Journal of Pharmacological Sciences*, vol. 98, no. 2, pp. 185–189, 2005.
- [32] Y. Cheng, G. He, X. Mu et al., "Neuroprotective effect of baicalein against MPTP neurotoxicity: Behavioral, biochemical and immunohistochemical profile," *Neuroscience Letters*, vol. 441, no. 1, pp. 16–20, 2008.
- [33] X. Mu, G. He, Y. Cheng, X. Li, B. Xu, and G. Du, "Baicalein exerts neuroprotective effects in 6-hydroxydopamine-induced experimental parkinsonism in vivo and in vitro," *Pharmacology Biochemistry & Behavior*, vol. 92, no. 4, pp. 642–648, 2009.
- [34] M. Jiang, Y. Porat-Shliom, Z. Pei et al., "Baicalein reduces E46K  $\alpha$ -synuclein aggregation in vitro and protects cells against E46K  $\alpha$ -synuclein toxicity in cell models of familial Parkinsonism," *Journal of Neurochemistry*, vol. 114, no. 2, pp. 419–429, 2010.
- [35] J.-H. Lu, M. T. Ardah, S. S. K. Durairajan et al., "Baicalein Inhibits Formation of  $\alpha$ -Synuclein Oligomers within Living Cells and Prevents A $\beta$  Peptide Fibrillation and Oligomerisation," *ChemBioChem*, vol. 12, no. 4, pp. 615–624, 2011.
- [36] Y.-H. Wang, H.-T. Yu, X.-P. Pu, and G.-H. Du, "Baicalein prevents 6-hydroxydopamine-induced mitochondrial dysfunction in SH-SY5Y cells via inhibition of mitochondrial oxidation and up-regulation of DJ-1 protein expression," *Molecules*, vol. 18, no. 12, pp. 14726–14738, 2013.
- [37] E. Lee, H. R. Park, S. T. Ji, Y. Lee, and J. Lee, "Baicalein attenuates astroglial activation in the 1-methyl-4-phenyl-1,2,3,4-tetrahydropyridine-induced Parkinson's disease model by downregulating the activations of nuclear factor- $\kappa$ B, ERK, and JNK," *Journal of Neuroscience Research*, vol. 92, no. 1, pp. 130–139, 2014.
- [38] X. Xue, H. Liu, L. Qi et al., "Baicalein ameliorated the upregulation of striatal glutamatergic transmission in the mice model of Parkinson's disease," *Brain Research Bulletin*, vol. 103, pp. 54–59, 2014.
- [39] Q. Hu, V. N. Uversky, M. Huang et al., "Baicalein inhibits alpha-synuclein oligomer formation and prevents progression of alpha-synuclein accumulation in a rotenone mouse model of Parkinson's disease," *Biochim Biophys Acta*, vol. 1862, no. 10, pp. 1883–1890, 2016.
- [40] K.-C. Hung, H.-J. Huang, Y.-T. Wang, and A. M.-Y. Lin, "Baicalein attenuates  $\alpha$ -synuclein aggregation, inflammasome activation and autophagy in the MPP<sup>+</sup>-treated nigrostriatal dopaminergic system in vivo," *Journal of Ethnopharmacology*, vol. 194, pp. 522–529, 2016.
- [41] H.-Q. Chen, Z.-Y. Jin, X.-J. Wang, X.-M. Xu, L. Deng, and J.-W. Zhao, "Luteolin protects dopaminergic neurons from inflammation-induced injury through inhibition of microglial activation," *Neuroscience Letters*, vol. 448, no. 2, pp. 175–179, 2008.
- [42] L. Hu, J. Yen, Y. Shen, K. Wu, M. Wu, and Y. Ho, "Luteolin Modulates 6-Hydroxydopamine-Induced Transcriptional Changes of Stress Response Pathways in PC12 Cells," *PLoS ONE*, vol. 9, no. 5, p. e97880, 2014.
- [43] S. P. Patil, P. D. Jain, J. S. Sancheti, P. J. Ghumatkar, R. Tambe, and S. Sathaye, "Neuroprotective and neurotrophic effects of Apigenin and Luteolin in MPTP induced parkinsonism in mice," *Neuropharmacology*, vol. 86, pp. 192–202, 2014.
- [44] N. Haleagrahara, C. J. Siew, N. K. Mitra, and M. Kumari, "Neuroprotective effect of bioflavonoid quercetin in 6-hydroxydopamine-induced oxidative stress biomarkers in the rat striatum," *Neuroscience Letters*, vol. 500, no. 2, pp. 139–143, 2011.
- [45] C. Lv, T. Hong, Z. Yang et al., "Effect of quercetin in the 1-methyl-4-phenyl-1, 2, 3, 6-tetrahydropyridine-induced mouse model of parkinson's disease," *Evidence-Based Complementary and Alternative Medicine*, vol. 2012, Article ID 928643, 6 pages, 2012.
- [46] S. S. Karuppagounder, S. K. Madathil, M. Pandey, R. Haobam, U. Rajamma, and K. P. Mohanakumar, "Quercetin up-regulates mitochondrial complex-I activity to protect against programmed cell death in rotenone model of Parkinson's disease in rats," *Neuroscience*, vol. 236, pp. 136–148, 2013.
- [47] M. Ay, J. Luo, M. Langley et al., "Molecular mechanisms underlying protective effects of quercetin against mitochondrial dysfunction and progressive dopaminergic neurodegeneration in cell culture and MitoPark transgenic mouse models of Parkinson's Disease," *Journal of Neurochemistry*, vol. 141, no. 5, pp. 766–782, 2017.
- [48] S. Li and X.-P. Pu, "Neuroprotective effect of kaempferol against a 1-methyl-4-phenyl-1,2,3,6-tetrahydropyridine-induced mouse model of Parkinson's disease," *Biological & Pharmaceutical Bulletin*, vol. 34, no. 8, pp. 1291–1296, 2011.
- [49] G. Filomeni, I. Graziani, D. de Zio et al., "Neuroprotection of kaempferol by autophagy in models of rotenone-mediated acute toxicity: possible implications for Parkinson's disease," *Neurobiology of Aging*, vol. 33, no. 4, pp. 767–785, 2012.
- [50] M. M. Khan, S. S. Raza, H. Javed et al., "Rutin protects dopaminergic neurons from oxidative stress in an animal model of Parkinson's disease," *Neurotoxicity Research*, vol. 22, no. 1, pp. 1–15, 2012.
- [51] K. B. Magalingam, A. Radhakrishnan, and N. Haleagrahara, "Rutin, a bioflavonoid antioxidant protects rat pheochromocytoma (PC-12) cells against 6-hydroxydopamine (6-OHDA)-induced neurotoxicity," *International Journal of Molecular Medicine*, vol. 32, no. 1, pp. 235–240, 2013.
- [52] K. B. Magalingam, A. Radhakrishnan, and N. Haleagrahara, "Protective effects of flavonol isoquercitrin, against 6-hydroxydopamine (6-OHDA)-induced toxicity in PC12 cells," *BMC Research Notes*, vol. 7, p. 49, 2014.
- [53] C. Anusha, T. Sumathi, and L. D. Joseph, "Protective role of apigenin on rotenone induced rat model of Parkinson's disease: Suppression of neuroinflammation and oxidative stress mediated apoptosis," *Chemico-Biological Interactions*, vol. 269, pp. 67–79, 2017.
- [54] T. Baluchnejadmojarad, N. Jamali-Raeufy, S. Zabihnejad, N. Rabiee, and M. Roghani, "Trolox exerts neuroprotection

- in 6-hydroxydopamine lesion rat model of Parkinson's disease: Possible involvement of PI3K/ER $\beta$  signaling," *European Journal of Pharmacology*, vol. 801, pp. 72–78, 2017.
- [55] M. R. Poetini, S. M. Araujo, M. Trindade de Paula et al., "Hesperidin attenuates iron-induced oxidative damage and dopamine depletion in *Drosophila melanogaster* model of Parkinson's disease," *Chemico-Biological Interactions*, vol. 279, pp. 177–186, 2018.
- [56] M. S. Antunes, A. T. R. Goes, S. P. Boeira, M. Prigol, and C. R. Jesse, "Protective effect of hesperidin in a model of Parkinson's disease induced by 6-hydroxydopamine in aged mice," *Nutrition Journal*, vol. 30, no. 11-12, pp. 1415–1422, 2014.
- [57] J. H. Sudati, F. A. Vieira, and S. S. Pavin, "*Valeriana officinalis* attenuates the rotenone-induced toxicity in *Drosophila melanogaster*," *NeuroToxicology*, vol. 37, pp. 118–126, 2013.
- [58] S. Sridharan, K. Mohankumar, S. P. Jeepipalli et al., "Neuroprotective effect of *Valeriana wallichii* rhizome extract against the neurotoxin MPTP in C57BL/6 mice," *NeuroToxicology*, vol. 51, pp. 172–183, 2015.
- [59] S. Ingale and S. Kasture, "Protective effect of standardized extract of *Passiflora incarnata* flower in parkinson's and alzheimer's disease," *Ancient Science of Life*, vol. 36, no. 4, pp. 200–206, 2017.
- [60] L. E. M. Brandão and D. Nôga, "*Passiflora cincinnata* extract delays the development of motor signs and prevents dopaminergic loss in a mice model of parkinson's disease," *Evidence-Based Complementary and Alternative Medicine*, vol. 2017, Article ID 8429290, 11 pages, 2017.
- [61] M. A. Gómez del Rio, M. I. Sánchez-Reus, I. Iglesias et al., "Neuroprotective properties of standardized extracts of hypericum perforatum on rotenone model of parkinson's disease," *CNS and Neurological Disorders - Drug Targets*, vol. 12, no. 5, pp. 665–679, 2013.
- [62] Z. Kiasalari, T. Baluchnejadmojarad, and M. Roghani, "Hypericum perforatum hydroalcoholic extract mitigates motor dysfunction and is neuroprotective in intrastriatal 6-hydroxydopamine rat model of parkinson's disease," *Cellular and Molecular Neurobiology*, vol. 36, no. 4, pp. 521–530, 2016.
- [63] M. R. Lyon, J. C. Cline, J. T. De Zepetnek, J. J. Shan, P. Pang, and C. Benishin, "Effect of the herbal extract combination *Panax quinquefolium* and *Ginkgo biloba* on attention-deficit hyperactivity disorder: a pilot study," *Journal of Psychiatry & Neuroscience*, vol. 26, no. 3, pp. 221–228, 2001.
- [64] B. Salehi, R. Imani, M. R. Mohammadi et al., "Ginkgo biloba for attention-deficit/hyperactivity disorder in children and adolescents: a double blind, randomized controlled trial," *Progress in Neuro-Psychopharmacology & Biological Psychiatry*, vol. 34, no. 1, pp. 76–80, 2010.
- [65] H. Uebel-von Sandersleben, A. Rothenberger, B. Albrecht, L. G. Rothenberger, S. Klement, and N. Bock, "Ginkgo biloba extract EGb 761 in children with ADHD," *Zeitschrift für Kinder- und Jugendpsychiatrie und Psychotherapie*, vol. 42, no. 5, pp. 337–347, 2014.
- [66] F. Shakibaei, M. Radmanesh, E. Salari, and B. Mahaki, "Ginkgo biloba in the treatment of attention-deficit/hyperactivity disorder in children and adolescents. A randomized, placebo-controlled, trial," *Complementary Therapies in Clinical Practice*, vol. 21, no. 2, pp. 61–67, 2015.
- [67] H. Niederhofer, "Panax ginseng may improve some symptoms of attention-deficit hyperactivity disorder," *Journal of Dietary Supplements*, vol. 6, no. 1, pp. 22–27, 2009.
- [68] S. H. Lee, W. S. Park, and M. H. Lim, "Clinical effects of korean red ginseng on attention deficit hyperactivity disorder in children: an observational study," *Journal of Ginseng Research*, vol. 35, no. 2, pp. 226–234, 2011.
- [69] H.-J. Ko, I. Kim, J.-B. Kim et al., "Effects of Korean red ginseng extract on behavior in children with symptoms of inattention and hyperactivity/impulsivity: a double-blind randomized placebo-controlled trial," *Journal of Child and Adolescent Psychopharmacology*, vol. 24, no. 9, pp. 501–508, 2014.
- [70] Y. Nam, E.-J. Shin, S. W. Shin et al., "YY162 prevents ADHD-like behavioral side effects and cytotoxicity induced by Aroclor1254 via interactive signaling between antioxidant potential, BDNF/TrkB, DAT and NET," *Food and Chemical Toxicology*, vol. 65, pp. 280–292, 2014.
- [71] J. Trebatícká, S. Kopasová, Z. Hradečná et al., "Treatment of ADHD with French maritime pine bark extract, Pycnogenol," *European Child and Adolescent Psychiatry*, vol. 15, no. 6, pp. 329–335, 2006.
- [72] Z. Chovanová, J. Muchová, M. Sivoňová et al., "Effect of polyphenolic extract, Pycnogenol, on the level of 8-oxoguanine in children suffering from attention deficit/hyperactivity disorder," *Free Radical Research*, vol. 40, no. 9, pp. 1003–1010, 2006.
- [73] M. Dvořáková, M. Sivoňová, J. Trebatícká et al., "The effect of polyphenolic extract from pine bark, Pycnogenol, on the level of glutathione in children suffering from attention deficit hyperactivity disorder (ADHD)," *Redox Report*, vol. 11, no. 4, pp. 163–172, 2006.
- [74] S. Y. Yoon, I. D. Peña, S. M. Kim et al., "Oroxylin A improves attention deficit hyperactivity disorder-like behaviors in the spontaneously hypertensive rat and inhibits reuptake of dopamine in vitro," *Archives of Pharmacol Research*, vol. 36, no. 1, pp. 134–140, 2013.
- [75] I. C. Dela Peña, S. Y. Yoon, Y. Kim et al., "5,7-Dihydroxy-6-methoxy-4'-phenoxyflavone, a derivative of oroxylin A improves attention-deficit/hyperactivity disorder (ADHD)-like behaviors in spontaneously hypertensive rats," *European Journal of Pharmacology*, vol. 715, no. 1–3, pp. 337–344, 2013.
- [76] R. Zhou, X. Han, J. Wang, and J. Sun, "Effect of baicalin on behavioral characteristics of rats with attention deficit hyperactivity disorder," *Zhongguo Dang Dai Er Ke Za Zhi*, vol. 19, no. 8, pp. 930–937, 2017.
- [77] R. Razlog, J. Pellow, and S. J. White, "A pilot study on the efficacy of *Valeriana officinalis* mother tincture and *Valeriana officinalis* 3X in the treatment of attention deficit hyperactivity disorder," *Health SA Gesondheid*, vol. 17, no. 1, pp. 1–7, 2012.
- [78] S. Akhondzadeh, M. R. Mohammadi, and F. Momeni, "*Passiflora incarnata* in the treatment of attention-deficit hyperactivity disorder in children and adolescents," *Therapy*, vol. 2, no. 4, pp. 609–614, 2005.
- [79] W. Weber, A. Vander Stoep, R. L. McCarty, N. S. Weiss, J. Biederman, and J. McClellan, "Hypericum perforatum (St John's Wort) for attention-deficit/hyperactivity disorder in children and adolescents: a randomized controlled trial," *The Journal of the American Medical Association*, vol. 299, no. 22, pp. 2633–2641, 2008.
- [80] H. Niederhofer, "St. John's wort may improve some symptoms of attention-deficit hyperactivity disorder," *Natural Product Research*, vol. 24, no. 3, pp. 203–205, 2010.
- [81] F. V. DeFeudis and K. Driew, "Ginkgo biloba extract (EGb 761) and CNS functions: basic studies and clinical applications," *Current Drug Targets*, vol. 1, no. 1, pp. 25–58, 2000.

- [82] P. Rojas, P. Montes, C. Rojas, N. Serrano-García, and J. C. Rojas-Castañeda, "Effect of a phytopharmaceutical medicine, Ginkgo biloba extract 761, in an animal model of Parkinson's disease: Therapeutic perspectives," *Nutrition Journal*, vol. 28, no. 11-12, pp. 1081–1088, 2012.
- [83] C. Rendeiro, J. S. Rhodes, and J. P. E. Spencer, "The mechanisms of action of flavonoids in the brain: Direct versus indirect effects," *Neurochemistry International*, vol. 89, pp. 126–139, 2015.
- [84] H. D. Kim, K. H. Jeong, U. J. Jung, and S. R. Kim, "Naringin treatment induces neuroprotective effects in a mouse model of Parkinson's disease in vivo, but not enough to restore the lesioned dopaminergic system," *The Journal of Nutritional Biochemistry*, vol. 28, pp. 140–146, 2016.
- [85] D. M. de Oliveria, G. Barreto, D. V. G. de Andrade et al., "Cytoprotective effect of valeriana officinalis extract on an in vitro experimental model of parkinson disease," *Neurochemical Research*, vol. 34, no. 2, pp. 215–220, 2009.
- [86] K. Dhawan, S. Dhawan, and A. Sharma, "Passiflora: a review update," *Journal of Ethnopharmacology*, vol. 94, no. 1, pp. 1–23, 2004.
- [87] J. Barnes, L. A. Anderson, and J. D. Phillipson, "St John's wort (*Hypericum perforatum* L.): a review of its chemistry, pharmacology and clinical properties," *Journal of Pharmacy and Pharmacology*, vol. 53, no. 5, pp. 583–600, 2001.
- [88] G. Polanczyk, M. S. de Lima, B. L. Horta, J. Biederman, and L. A. Rohde, "The worldwide prevalence of ADHD: a systematic review and meta-regression analysis," *The American Journal of Psychiatry*, vol. 164, no. 6, pp. 942–948, 2007.
- [89] E. G. Willcutt, "The prevalence of DSM-IV attention-deficit/hyperactivity disorder: a meta-analytic review," *Neurotherapeutics*, vol. 9, no. 3, pp. 490–499, 2012.
- [90] S. V. Faraone, P. Asherson, T. Banaschewski et al., "Attention-deficit/hyperactivity disorder," *Nature Reviews Disease Primers*, vol. 1, p. 15020, 2015.
- [91] J. Prince, "Catecholamine dysfunction in attention-deficit/hyperactivity disorder: an update," *Journal of Clinical Psychopharmacology*, vol. 28, no. 3, suppl 2, pp. S39–S45, 2008.
- [92] A. L. Lopresti, "Oxidative and nitrosative stress in ADHD: possible causes and the potential of antioxidant-targeted therapies," *ADHD Attention Deficit and Hyperactivity Disorders*, vol. 7, no. 4, pp. 237–247, 2015.
- [93] L. Briars and T. Todd, "A review of pharmacological management of attention-deficit/hyperactivity disorder," *The Journal of Pediatric Pharmacology and Therapeutics*, vol. 21, no. 3, pp. 192–206, 2016.
- [94] J. Biederman, T. Spencer, and T. Wilens, "Evidence-based pharmacotherapy for attention-deficit hyperactivity disorder," *The International Journal of Neuropsychopharmacology*, vol. 7, no. 1, pp. 77–97, 2004.
- [95] V. A. Reed, J. K. Buitelaar, E. Anand et al., "The safety of atomoxetine for the treatment of children and adolescents with attention-deficit/hyperactivity disorder: a comprehensive review of over a decade of research," *CNS Drugs*, vol. 30, no. 7, pp. 603–628, 2016.
- [96] J. Lee, N. Grizenko, V. Bhat, S. Sengupta, A. Polotskaia, and R. Joobar, "Relation between therapeutic response and side effects induced by methylphenidate as observed by parents and teachers of children with ADHD," *BMC Psychiatry*, vol. 11, p. 70, 2011.
- [97] T. E. Wilens, A. Kwon, S. Tanguay et al., "Characteristics of adults with attention deficit hyperactivity disorder plus substance use disorder: The role of psychiatric comorbidity," *American Journal on Addictions*, vol. 14, no. 4, pp. 319–327, 2005.
- [98] H. R. Searight, K. Robertson, T. Smith, S. Perkins, and B. K. Searight, "Complementary and Alternative Therapies for Pediatric Attention Deficit Hyperactivity Disorder: A Descriptive Review," *ISRN Psychiatry*, vol. 2012, Article ID 804127, 8 pages, 2012.
- [99] P. L. Le Bars, M. M. Katz, N. Berman, T. M. Itil, A. M. Freedman, and A. F. Schatzberg, "A placebo-controlled, double-blind, randomized trial of an extract of Ginkgo biloba for dementia. North American EGB Study Group," *The Journal of the American Medical Association*, vol. 278, no. 16, pp. 1327–1332, 1997.
- [100] A. J. Schmidt, J.-C. Krieg, U. M. Hemmeter et al., "Impact of plant extracts tested in attention-deficit/hyperactivity disorder treatment on cell survival and energy metabolism in human neuroblastoma SH-SY5Y cells," *Phytotherapy Research*, vol. 24, no. 10, pp. 1549–1553, 2010.
- [101] R.-Y. Zhou, J.-J. Wang, Y. You et al., "Effect of baicalin on ATPase and LDH and its regulatory effect on the AC/cAMP/PKA signaling pathway in rats with attention deficit hyperactivity disorder," *Zhongguo Dang Dai Er Ke Za Zhi*, vol. 19, no. 5, pp. 576–582, 2017.
- [102] A. A. J. Verlaet, B. Ceulemans, H. Verhelst et al., "Effect of Pycnogenol(R) on attention-deficit hyperactivity disorder (ADHD): study protocol for a randomised controlled trial," *Trials*, vol. 18, no. 1, p. 145, 2017.
- [103] D. Benke, A. Barberis, S. Kopp et al., "GABAA receptors as in vivo substrate for the anxiolytic action of valerenic acid, a major constituent of valerian root extracts," *Neuropharmacology*, vol. 56, no. 1, pp. 174–181, 2009.
- [104] K. Appel, T. Rose, B. Fiebich, T. Kammler, C. Hoffmann, and G. Weiss, "Modulation of the  $\gamma$ -aminobutyric acid (GABA) system by Passiflora incarnata L.," *Phytotherapy Research*, vol. 25, no. 6, pp. 838–843, 2011.
- [105] M. Miroddi, G. Calapai, M. Navarra, P. L. Minciullo, and S. Gangemi, "Passiflora incarnata L.: ethnopharmacology, clinical application, safety and evaluation of clinical trials," *Journal of Ethnopharmacology*, vol. 150, no. 3, pp. 791–804, 2013.
- [106] V. Butterweck, "Mechanism of action of St John's wort in depression: what is known?" *CNS Drugs*, vol. 17, no. 8, pp. 539–562, 2003.

## Research Article

# Plumbagin-Loaded Nanoemulsion Drug Delivery Formulation and Evaluation of Antiproliferative Effect on Prostate Cancer Cells

Adrian Chrastina , Veronique T. Baron, Parisa Abedinpour, Gaelle Rondeau, John Welsh, and Per Borgström

Vaccine Research Institute of San Diego (VRISD), San Diego Science Center, San Diego, California, USA

Correspondence should be addressed to Adrian Chrastina; [achrastina@vrisd.org](mailto:achrastina@vrisd.org)

Received 12 June 2018; Revised 19 September 2018; Accepted 24 October 2018; Published 11 November 2018

Guest Editor: Claudio Tabolacci

Copyright © 2018 Adrian Chrastina et al. This is an open access article distributed under the Creative Commons Attribution License, which permits unrestricted use, distribution, and reproduction in any medium, provided the original work is properly cited.

**Background.** Plumbagin, a medicinal plant-derived 5-hydroxy-2-methyl-1,4-naphthoquinone, is an emerging drug with a variety of pharmacological effects, including potent anticancer activity. We have previously shown that plumbagin improves the efficacy of androgen deprivation therapy (ADT) in prostate cancer and it is now being evaluated in phase I clinical trial. However, the development of formulation of plumbagin as a compound with sparing solubility in water is challenging. **Methods.** We have formulated plumbagin-loaded nanoemulsion using pneumatically controlled high pressure homogenization of oleic acid dispersions with polyoxyethylene (20) sorbitan monooleate as surfactant. Nanoemulsion formulations were characterized for particle size distribution by dynamic light scattering (DLS). The kinetics of *in vitro* drug release was determined by equilibrium dialysis. Anticancer activity toward prostate cancer cells PTEN-P2 was assessed by MTS (Owen's reagent) assay. **Results.** Particle size distribution of nanoemulsions is tunable and depends on the surfactant concentration. Nanoemulsion formulations of plumbagin with 1-3.5% (w/w) of surfactant showed robust stability of size distribution over time. Plumbagin-loaded nanoemulsion with average hydrodynamic diameter of 135 nm showed exponential release of plumbagin with a half-life of 6.1 h in simulated gastric fluid, 7.0 h in simulated intestinal fluid, and displayed enhanced antiproliferative effect toward prostate cancer cells PTEN-P2 compared to free plumbagin. **Conclusion.** High drug-loading capacity, retention of nanoparticle size, kinetics of release under simulated physiological conditions, and increased antiproliferative activity indicate that oleic-acid based nanoemulsion formulation is a suitable delivery system of plumbagin.

## 1. Introduction

Plumbagin (5-hydroxy-2-methyl-1,4-naphthoquinone, Figure 1) is a plant-derived secondary metabolite found in plant families such as Plumbaginaceae, Ebenaceae, Dioncophyllaceae, Anastrocladaceae, and Droseraceae [1]. Plumbagin possesses multiple pharmacological activities, such as anticancer, antiatherosclerotic, antidiabetic, anti-inflammatory, antimicrobial, hypolipidemic, and neuroprotective activities [2, 3]. Recently, significant research effort was developed to evaluate antitumor effects of plumbagin. Plumbagin showed potent anti-tumor activity in various tumor models, including breast cancer [4], Ehrlich ascites carcinoma [5], esophageal cancer [6], lung cancer [7], melanoma [8],

ovarian cancer [9], promyelocytic leukemia [10], and prostate cancer [11–13]. Plumbagin exhibits these anticancer effects via interaction with multiple targets and modulation of various molecular signaling pathways, including AMPK, CDK1/CDC2, cyclin B1, cyclin D1, NF- $\kappa$ B, p53, p21 Waf1/Cip1, p27 Kip1, Nrf2/ARE, PI3K/AKT/mTOR, Ras, STAT3/PLK1/AKT, and Wnt [3], resulting in induction of apoptosis and autophagy, cell cycle arrest, inhibition of invasion, and metastasis, as well as antiangiogenic activities [2].

Great progress has recently been made regarding its use in prostate cancer. For example, experiments from Dr. Verma's laboratory demonstrated that plumbagin administered by intraperitoneal injection strongly inhibited tumor growth



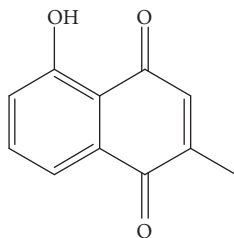


FIGURE 1: Chemical structure of plumbagin (5-hydroxy-2-methyl-1,4-naphthoquinone or 5-hydroxy-2-methyl-1,4-naphthalenedione,  $C_{11}H_8O_3$ ).

or delayed disease progression in several models of prostate cancer including subcutaneous xenografts, hormone-independent orthotopic tumors, transgenic TRAMP/FVB, and knock-out PTEN<sup>-/-</sup> mouse models [14–16]. It also decreased the occurrence of metastases and therefore may be effective for the treatment of metastatic castration-resistant prostate cancer [15]. In addition, plumbagin considerably improved the efficacy of castration and chemical ADT in hormone-sensitive models of prostate cancer, causing tumor regression and increasing mouse survival when used in combination [11, 12]. IND-enabling preclinical studies were completed, leading to the first-in-human clinical trial for the combination of plumbagin and ADT in prostate cancer patients (NCT03137758).

Translation of plumbagin into clinical application unfortunately is made difficult by its poor water solubility. Drug solubility fundamentally influences its pharmacokinetics, its rate and extent of absorption, and its bioavailability after peroral administration [17], and thus essentially its therapeutic efficacy. As the drug advances into the clinic, it becomes critical to develop a formulation that considerably increases its solubility while potentially reducing systemic toxicity. Indeed, a better formulation would improve the patient's quality of life and achieve optimal therapeutic potential. Here, we describe the development and characterization of a nanoemulsion formulation of plumbagin. Nanoemulsions are kinetically stable, optically isotropic, biphasic dispersions of oil-in-water stabilized by an interfacial film of amphiphilic surfactant [18]. These nanoparticle systems have droplets within submicron size range, typically 5–200 nm. Nanoemulsions have multiple potential advantages for oral delivery of active pharmaceutical ingredients, including high encapsulation capacity for poorly water soluble drugs, robust stability to separation, flocculation and coalescence, and potentially improved absorption and bioavailability of encapsulated drugs [19, 20]. We have formulated nanoemulsions using biocompatible components, with oleic acid as an oil phase and polyoxyethylene (20) sorbitan monooleate (polysorbate 80) as an emulsifier. High plumbagin-loading capacity, kinetics of release in simulated physiological environments, and enhancement of antiproliferative activity toward prostate cancer cells suggest that oleic-acid based nanoemulsion formulation of plumbagin is a suitable delivery system.

## 2. Materials and Methods

**2.1. Materials.** Plumbagin, polysorbate 80, oleic acid and all other chemicals were supplied by Sigma (St. Louis, MO, USA) unless otherwise stated.

**2.2. Preparation of Plumbagin-Loaded Nanoemulsion.** To find the optimal composition for a formulation of plumbagin-loaded nanoemulsions, series of samples with increasing concentrations of surfactant were processed by high-pressure homogenization. Briefly, coarse emulsions of oleic acid (10% w/w) saturated with plumbagin, prepared in 0.25–4.0% (w/w) polysorbate 80 in deionized water, were homogenized using high speed homogenizer (Biospec Products, Inc.) at 30,000 rpm for 5 min. Emulsions were then processed by high-pressure homogenization using pneumatically controlled EmulsiFlex-C3 (Avestin) 10 cycles at 5000 psi.

**2.3. Particle Size Analysis.** Nanoemulsion formulations at the time of production and at different time points afterwards were analyzed for particle size distribution and polydispersity by dynamic light scattering (DLS) method using noninvasive back scatter (NIBS) detection at 173° angle and at 25°C on Zetasizer Nano-ZS (Malvern Instruments) equipped with 4 mW He-Ne, 633 nm laser.

**2.4. Physical Stability of Nanoemulsions.** Plumbagin-loaded nanoemulsions were evaluated for any particle size change over time, or after incubation in 0.1M HCl or 0.01M sodium phosphate buffer pH 6.8 or pH 7.5, simulating physiological conditions. Particle size distribution was analyzed at designated time-points using Zetasizer Nano-ZS (Malvern Instruments) as described above.

**2.5. In Vitro Drug Release.** *In vitro* plumbagin release from nanoemulsion formulation was performed using membrane dialysis (MW cutoff 8–10 kDa) against simulated gastric fluid (0.1M HCl, 0.05% (w/v) Tween 80) or simulated intestinal fluid (0.01M sodium phosphate buffer pH 7.5, 0.05% (w/v) Tween 80) at 37°C. At designed time intervals, the concentration of plumbagin was determined by UV-VIS spectrometry from four independent measurements (n=4) as described below. To analyze kinetics of release, the data were fitted by one phase exponential nonlinear regression using GraphPad PRISM 6.

**2.6. Determination of Plumbagin Concentration.** Concentration of plumbagin in nanoemulsions was estimated by UV-VIS spectrophotometry. Briefly, nanoemulsions were dispersed in methanol (200–3000 X dilution) vortexed for 10 sec and then concentration of plumbagin was determined spectrophotometrically (DU-640, Beckman Coulter) at 410 nm ( $\epsilon_\lambda = 3,800 \text{ dm}^3 \cdot \text{mol}^{-1} \cdot \text{cm}^{-1}$ ).

**2.7. Cell Culture.** PTEN-P2 murine prostate cancer cells were kindly provided by the Wu laboratory and have been previously described [21]. The cells were grown in RPMI-1640 medium (Sigma) supplemented with 10% (v/v) heat-inactivated fetal bovine serum, 2 mM L-glutamine, 100

U/ml penicillin, 100 µg/ml streptomycin, insulin-selenium-transferrin (5 µg/ml insulin), and  $10^{-8}$  M dihydrotestosterone. Cultures were passaged by dissociation using trypsin (0.05%) and maintained at 37°C in a humidified atmosphere with 5% CO<sub>2</sub>.

**2.8. In Vitro Cytotoxicity Assay.** The antiproliferative properties of plumbagin nanoemulsion were examined by MTS tetrazolium compound (Owen's reagent) based assay. Briefly, the PTEN-P2 cells were plated at density of  $8 \times 10^3$  cells per well of 96-well plates in four replicates. 24 h later, the medium was replaced with medium containing increasing concentration of plumbagin or nanoemulsion formulation of plumbagin corresponding to the range of 0-10 µM plumbagin. Control nanoemulsion formulation without drug was tested at the same concentration range but without plumbagin. After 24 h exposure, the cytotoxicity was determined using a CellTiter 96AQueous on solution cell proliferation assay (MTS) kit according to manufacturer's instructions (Promega, Madison, WI) by measuring conversion of (3-(4,5-dimethylthiazol-2-yl)-5-(3-carboxymethoxyphenyl)-2-(4-sulfophenyl)-2H-tetrazolium, inner salt) to formazan product. IC<sub>50</sub> values were then determined from cytotoxicity curves as a concentration that induced 50% inhibition of the cell growth.

**2.9. Data Analysis.** Particle size (Z-average, intensity-weighted mean size) and polydispersity index (PDI) were determined by method of cumulants (defined by ISO standards 13321 and 22412) of autocorrelation function generated by DLS instrument. Drug release and cytotoxicity studies were performed in replicates (n=4) and the %cumulative release and %cytotoxicity values are expressed as means from these measurements with corresponding standard deviations.

### 3. Results

**3.1. Formulation of Plumbagin-Loaded Nanoemulsions.** Our preformulatory tests of various excipients identified oleic acid to be a good solubilizer of plumbagin (51.8 mg/ml at 25°C). Therefore, we proceeded to optimize the formulation of plumbagin nanoemulsions using oleic acid as the oil phase. Dispersions of oleic acid saturated with plumbagin were generated by high-pressure homogenization of coarse emulsions with variable contents of polysorbate 80 as surfactant. Particle size analysis by DLS showed a decrease of hydrodynamic diameter with increasing concentration of surfactant, as indicated by intensity-based particle size distribution profiles (Figure 2). Dispersions with concentrations of polysorbate 80 equal to or less than 0.5% (w/w) showed high polydispersity index as also indicated by the wide range of particle size distribution (Figure 3). Furthermore, these dispersions were unstable over time, showing multimodal distribution patterns with presence of particles with a diameter higher than 1000 nm (Figure 3). Progressive increase in surfactant concentration above 1.0% (w/w) stabilized dispersions. Nanoemulsions with surfactant content

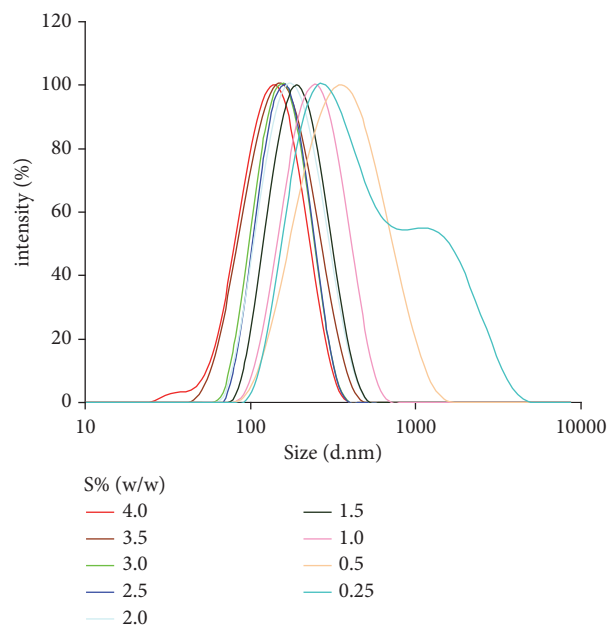


FIGURE 2: Particle size distribution profile of plumbagin-loaded nanoemulsions is tunable and depends on surfactant concentration (S% (w/w)) during processing of emulsion by high pressure homogenization. Particle size is indicated as intensity-based Z-average hydrodynamic diameter (nm) determined from DLS measurements.

in the range of 1.0-3.5% (w/w) showed narrow particle size distribution profiles and high stability over time (Figure 3). Dispersions with higher concentrations of polysorbate 80 (4.0% w/w) showed the smallest average radius, although we observed the presence of ~ 30 nm surfactant micelles in these formulations. Therefore, a surfactant content in the range of 1.0-3.5% yielded uniform plumbagin-loaded nanoemulsions with an average particle size that can be controlled by the concentration of surfactant during high-pressure homogenization.

**3.2. Stability of Nanoemulsions.** Nanoemulsions with narrow polydispersity and diameter (Z-average, 135 nm, 3.5% (w/w) polysorbate 80) were selected for further characterization. This formulation of plumbagin-loaded nanoemulsions and the same formulation without plumbagin showed nearly identical particle size immediately after preparation (Figure 4). Both plumbagin-loaded and control (empty) nanoemulsions showed good retention of size distribution over three months of storage at 25°C (Figure 4), with only a moderate increase of diameter of the plumbagin-loaded nanoemulsions. Furthermore, both the control nanoemulsion and the plumbagin-loaded nanoemulsion, when dispersed in acidic media that simulate the physiological environment of stomach acid and intestinal fluids, showed retention of particle size (Table 1). A moderate increase in the hydrodynamic diameter of both empty- and plumbagin-loaded nanoemulsions was observed in the slightly alkaline environment of phosphate buffer (pH 7.5) (Table 1).

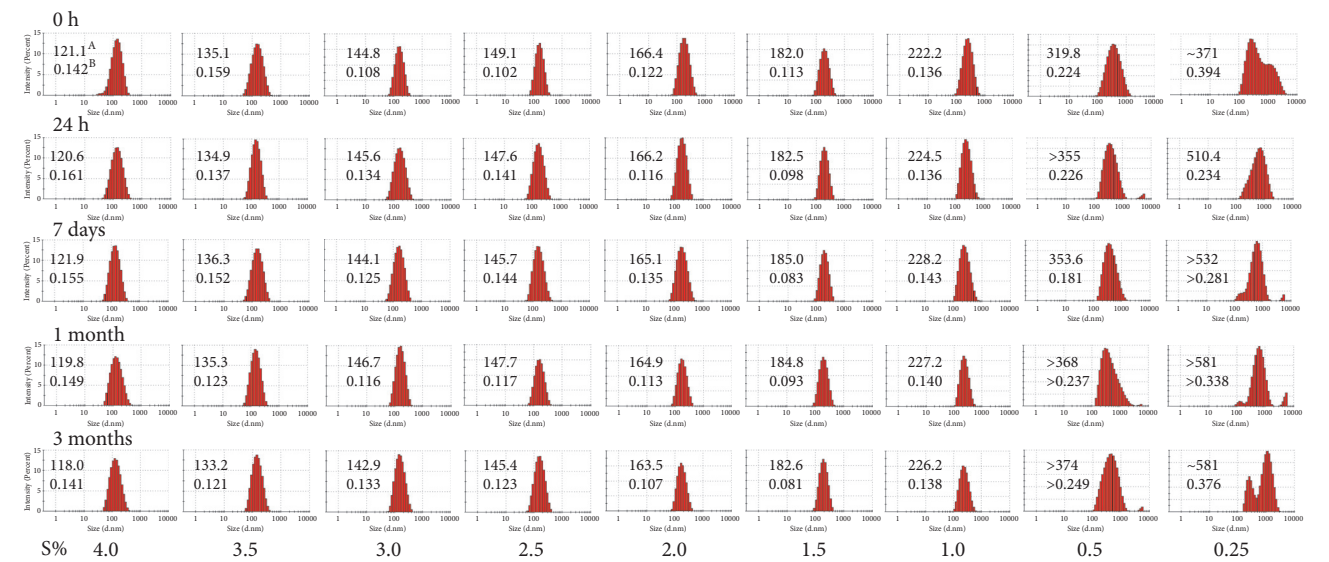


FIGURE 3: Time-dependent intensity-based particle size distribution profiles of plumbagin-loaded microemulsions at different surfactant concentrations (S%, w/w). A: particle size is indicated as Z-average hydrodynamic diameter (nm) determined by cumulants fit analysis from DLS measurements. B: heterogeneity of size distribution is indicated by polydispersity index (PDI).

TABLE 1: Changes in particle size distribution after dispersion of nanoemulsions in media simulating physiological conditions. Control, empty (NE), and plumbagin-loaded (NE-PL) nanoemulsions (3.5% polysorbate 80) were dispersed in indicated media (1000 x dilution) and incubated for 24 h at 37°C. The particle size distribution was determined by DLS. PDI values are indicated in brackets.

	Water	HCl 0.1 M	0.01 M NaH <sub>2</sub> PO <sub>4</sub> /Na <sub>2</sub> HPO <sub>4</sub>	
			pH 6.8	pH 7.5
NE, empty	134.5 (0.111)	134.2 (0.115)	126.6 (0.127)	158.8 (0.177)
NE-PL, loaded	135.1 (0.166)	135.2 (0.101)	135.7 (0.088)	185.7 (0.149)

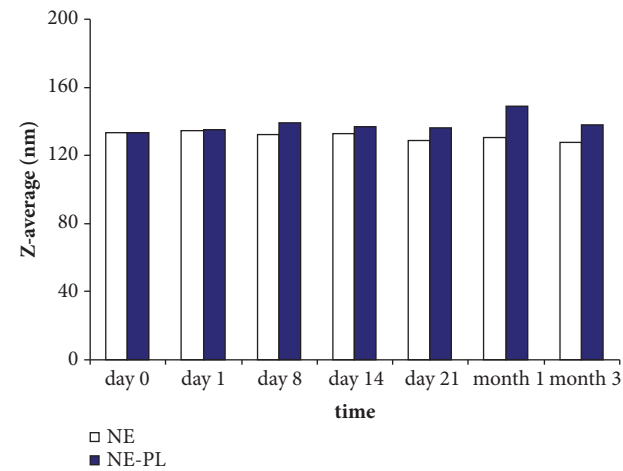


FIGURE 4: Stability of size distribution profile of oleic acid-based nanoemulsions (polysorbate 80 (3.5%) without plumbagin (NE) and plumbagin-loaded (NE-PL) nanoemulsion formulation at 25°C over time.

**3.3. In Vitro Release of Plumbagin.** The plumbagin-loaded formulation (Z-average, 135 nm) was further studied for *in vitro* release in media mimicking physiological conditions: simulated gastric fluid (SGF) and simulated intestinal fluid (SIF). The plumbagin-loaded nanoemulsion showed a one

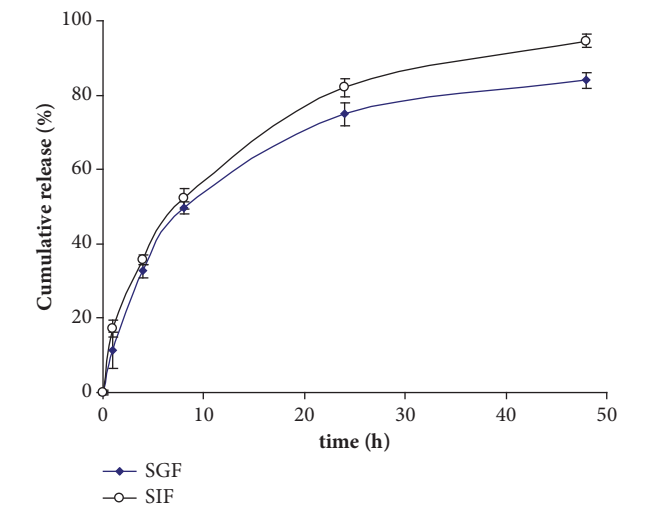


FIGURE 5: *In vitro* release of plumbagin from oleic acid-based nanoemulsion (polysorbate 80 (3.5%) as a function of time. SGF, simulated gastric fluid (SGF), and simulated intestinal fluid (SIF) at 37°C was used as release media.

phase exponential release profile of plumbagin with a half-life of 6.1 h in simulated gastric fluid (SGF) and 7.0 h in simulated intestinal fluid (SIF) (Figure 5). Release trends

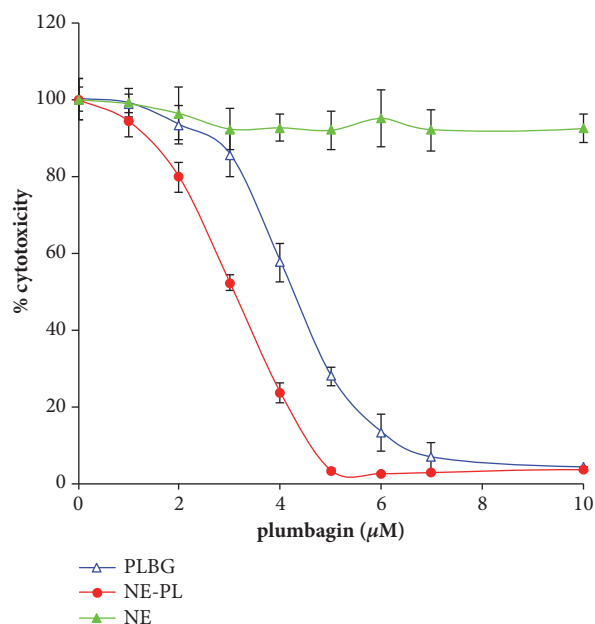


FIGURE 6: Plumbagin-loaded nanoemulsion shows increased antiproliferative activity. Cytotoxicity of free plumbagin (PLBG), plumbagin-loaded nanoemulsions (NE-PL), and control empty nanoemulsions (NE) toward PTEN-P2 cells. For control NE, the cells were exposed to the same concentration of nanoemulsion. PTEN-P2 cells were incubated with increasing dilutions of formulations for 24 h and then cytotoxicity was determined by cell proliferation assay (MTS).

showed a slightly higher span and plateau for SIF compared to SGF, corresponding to the higher ionization of the phenolic hydroxyl group of plumbagin leading to facilitated release in media with higher pH.

**3.4. In Vitro Cytotoxicity of Plumbagin-Loaded Nanoemulsion.** The antiproliferative effect of the plumbagin-loaded nanoemulsion formulation was evaluated using prostate cancer PTEN-P2 cells *in vitro*. Plumbagin-loaded nanoemulsion and free plumbagin inhibited PTEN-P2 proliferation in dose-dependent manner. However, the plumbagin-loaded nanoemulsion showed increased cytotoxicity toward PTEN-P2 cells compared to free plumbagin,  $IC_{50}$  ( $\mu M$ ) 3.1 versus 4.3 after 24 hr exposure (Figure 6). These observations correspond to microscopic assessment, where plumbagin-loaded nanoemulsion apparently caused more cellular damage to PTEN-P2 cells compared to free plumbagin (Figure 7). Besides a decrease in cell density, morphological changes included cell detachment and shrinkage (Figure 7). Control nanoemulsions without plumbagin did not show significant cytotoxicity (Figures 6 and 7).

## 4. Discussion

It is well recognized that the aqueous solubility of a drug is a fundamental property that controls the rate and extent of its absorption and bioavailability [17]. Therefore, as a limiting factor of bioavailability, it essentially influences the

pharmacokinetic profile and the pharmacodynamics of the drug after oral administration. Since the majority of the drug candidates in drug discovery show poor aqueous solubility [22], this is a significant challenge. To address this issue, several approaches have been developed, including formulation of poorly soluble drugs in nanoparticle-based drug delivery systems (polymeric micelles, liposomes, nanoemulsions, solid lipid nanoparticles, etc.). Among these, nanoemulsions provide the documented advantage of increased absorption and bioavailability, enhanced penetration via biological membranes, and lower inter- and intraindividual variability in drug pharmacokinetics [19, 20].

We have generated plumbagin-loaded oleic-acid based nanoemulsions using high pressure homogenization of oleic acid emulsion with polysorbate 80 as emulsifying agent. Polysorbate 80, a nonionic surfactant with a high hydrophilic-lipophilic balance (HLB=15.0), was chosen to ensure immediate formation of oil-in-water droplets during production. Depending on surfactant content (1.0-3.5% (w/w)), the high pressure homogenization process yielded plumbagin-loaded nanoemulsions with stable size distribution profiles in the range of 135-220 nm. High pressure homogenization methodology is implemented on a large scale in the pharmaceutical industry and established procedures will provide a distinctive advantage when production of higher quantities of nanoemulsions is needed.

The plumbagin-loaded nanoemulsion (135 nm Z-average, 10% (w/w) oleic acid, 3.5% (w/w) polysorbate 80) which had a good retention of size distribution over time and polydispersity was selected for further studies of drug release, stability in simulated physiological fluids, and *in vitro* cytotoxicity against prostate cancer cells. The plumbagin-loaded nanoemulsion showed good retention of nanoparticle size after dispersion in water or media simulating physiological environment. Furthermore, drug release studies showed exponential release of plumbagin from nanoemulsion with half-lives that would permit optimal absorption of plumbagin from the gastrointestinal tract. Plumbagin-loaded nanoemulsion exhibited higher antiproliferative activity on PTEN-P2 cells compared to free plumbagin. Of note, there is no reason to think that plumbagin released from the nanoemulsion would act differently in prostate cancer cells compared to other types of cancer cells; therefore it is expected that once released, plumbagin will have the same effects as have been extensively described in the literature. Increased cytotoxicity of plumbagin-loaded nanoemulsion was not due to an additive effect, because the control nanoemulsion (without plumbagin) did not show apparent cytotoxicity at the equivalent dose of components. Therefore, the increased cytotoxicity of plumbagin in the nanoemulsion formulation could be attributed either to increased cellular uptake of plumbagin in the nanoparticulate form or to a stabilizing effect of nanoemulsions on plumbagin or both. The high particle surface area [20] associated with small diameter of nanodispersion (surface to mass ratio) could lead to increased reactivity with cellular surface and thus increased uptake of plumbagin by PTEN-P2 cells. Moreover, plumbagin as an electrophilic compound has a propensity to react with various nucleophiles in the extracellular environment.



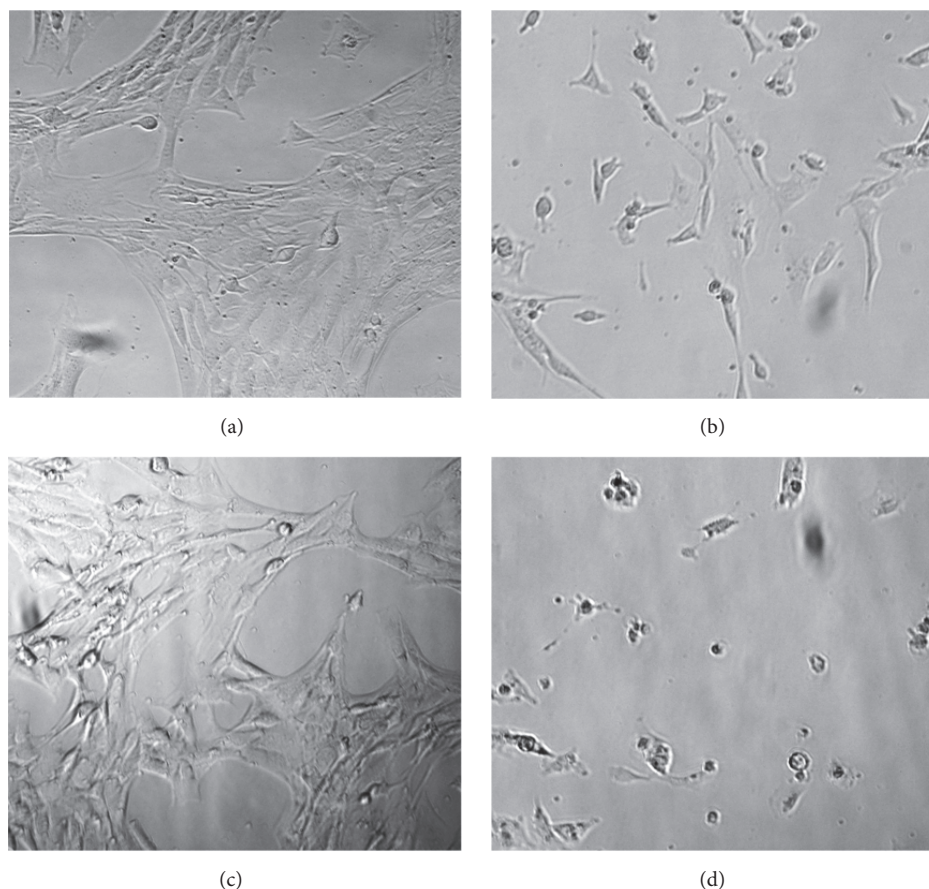


FIGURE 7: Bright field microscopy images of PTEN-P2 cells. Images show untreated control (a), and cells exposed for 24 h to free plumbagin  $4\ \mu\text{M}$  (b), empty nanoemulsion (c), and plumbagin-loaded ( $4\ \mu\text{M}$ ) nanoemulsion (d).

The shielding of plumbagin in the hydrophobic core of the nanoemulsion would therefore decrease its exposure and potential interaction with nucleophiles before reaching cellular targets. This stabilizing effect would be expected to improve the pharmacokinetic/pharmacodynamic behavior of plumbagin when administered using a nanoemulsion formulation.

The nanoemulsion described here was formulated using oil and surfactant components that are biocompatible and generally recognized as safe (GRAS). Additionally, the oleic acid is an FDA-approved excipient and penetration enhancer. High loading capacity for active pharmaceutical ingredient of interest (plumbagin), retention of nanoparticle size over time, kinetics of plumbagin release under simulated physiological conditions, and antiproliferative activity all indicate that the oleic acid-based nanoemulsion formulation is a promising drug delivery system for plumbagin.

## Abbreviations

DLS: Dynamic light scattering  
HLB: Hydrophilic-lipophilic balance  
S: Surfactant  
NE: Nanoemulsions  
NE-PL: Plumbagin-loaded nanoemulsions

PDI: Polydispersity index  
PLBG: Plumbagin  
SGF: Simulated gastric fluid  
SIF: Simulated intestinal fluid.

## Data Availability

All data are available at Vaccine Research Institute of San Diego, San Diego Science Center, San Diego, CA.

## Disclosure

Neither the funding agency nor any outside organization has participated in study design or has any conflicts of interest. Pellfibre Pharmaceuticals, Inc., had final approval of the manuscript.

## Conflicts of Interest




Borgström P, Chrastina A, and Baron VT are inventors on a patent in relation to this work. Borgström P is also CEO of PellFiCure Pharmaceuticals, Inc. Chrastina A and Baron VT are consultants for PellFiCure Pharmaceuticals, Inc.

## References

- [1] S. Padhye, P. Dandawate, M. Yusufi, A. Ahmad, and F. H. Sarkar, "Perspectives on medicinal properties of plumbagin and its analogs," *Medicinal Research Reviews*, vol. 32, no. 6, pp. 1131–1158, 2012.
- [2] Y. Liu, Y. Cai, C. He, M. Chen, and H. Li, "Anticancer Properties and Pharmaceutical Applications of Plumbagin: A Review," *American Journal of Chinese Medicine*, vol. 45, no. 03, pp. 423–441, 2017.
- [3] P. Panichayupakaranant and M. I. Ahmad, "Plumbagin and Its Role in Chronic Diseases," in *Drug Discovery from Mother Nature*, vol. 929 of *Advances in Experimental Medicine and Biology*, pp. 229–246, Springer International Publishing, Cham, 2016.
- [4] W. Yan, T.-Y. Wang, Q.-M. Fan et al., "Plumbagin attenuates cancer cell growth and osteoclast formation in the bone microenvironment of mice," *Acta Pharmacologica Sinica*, vol. 35, no. 1, pp. 124–134, 2014.
- [5] R. A. Raja Naresh, N. Udupa, and P. Uma Devi, "Niosomal Plumbagin with Reduced Toxicity and Improved Anticancer Activity in BALB/C Mice," *Journal of Pharmacy and Pharmacology*, vol. 48, no. 11, pp. 1128–1132, 1996.
- [6] Y. Cao, J. Yu, T. Liu et al., "Plumbagin inhibits the proliferation and survival of esophageal cancer cells by blocking STAT3-PLK1-AKT signaling," *Cell Death & Disease*, vol. 9, no. 2, 2018.
- [7] C. G. Kang, E. Im, H.-J. Lee, and E.-O. Lee, "Plumbagin reduces osteopontin-induced invasion through inhibiting the Rho-associated kinase signaling pathway in A549 cells and suppresses osteopontin-induced lung metastasis in BalB/c mice," *Bioorganic & Medicinal Chemistry Letters*, vol. 27, no. 9, pp. 1914–1918, 2017.
- [8] M. R. Sunil Kumar, B. Kiran Aithal, N. Udupa et al., "Formulation of plumbagin loaded long circulating pegylated liposomes: In vivo evaluation in C57BL/6J mice bearing B16F1 melanoma," *Drug Delivery*, vol. 18, no. 7, pp. 511–522, 2011.
- [9] S. Sinha, K. Pal, A. Elkhanany et al., "Plumbagin inhibits tumorigenesis and angiogenesis of ovarian cancer cells in vivo," *International Journal of Cancer*, vol. 132, no. 5, pp. 1201–1212, 2013.
- [10] K.-H. Xu and D.-P. Lu, "Plumbagin induces ROS-mediated apoptosis in human promyelocytic leukemia cells *in vivo*," *Leukemia Research*, vol. 34, no. 5, pp. 658–665, 2010.
- [11] P. Abedinpour, V. T. Baron, A. Chrastina et al., "Plumbagin improves the efficacy of androgen deprivation therapy in prostate cancer: A pre-clinical study," *The Prostate*, vol. 77, no. 16, pp. 1550–1562, 2017.
- [12] P. Abedinpour, V. T. Baron, A. Chrastina, J. Welsh, and P. Borgström, "The combination of plumbagin with androgen withdrawal causes profound regression of prostate tumors in vivo," *The Prostate*, vol. 73, no. 5, pp. 489–499, 2013.
- [13] G. Rondeau, P. Abedinpour, A. Chrastina, J. Pelayo, P. Borgstrom, and J. Welsh, "Differential gene expression induced by anti-cancer agent plumbagin is mediated by androgen receptor in prostate cancer cells," *Scientific Reports*, vol. 8, no. 1, 2018.
- [14] B. B. Hafeez, W. Zhong, J. W. Fischer et al., "Plumbagin, a medicinal plant (*Plumbago zeylanica*)-derived 1,4-naphthoquinone, inhibits growth and metastasis of human prostate cancer PC-3M-luciferase cells in an orthotopic xenograft mouse model," *Molecular Oncology*, vol. 7, no. 3, pp. 428–439, 2013.
- [15] B. B. Hafeez, W. Zhong, A. Mustafa, J. W. Fischer, O. Witkowsky, and A. K. Verma, "Plumbagin inhibits prostate cancer development in TRAMP mice via targeting PKC $\epsilon$ , Stat3 and neuroendocrine markers," *Carcinogenesis*, vol. 33, no. 12, Article ID bgs291, pp. 2586–2592, 2012.
- [16] B. B. Hafeez, J. W. Fischer, A. Singh et al., "Plumbagin inhibits prostate carcinogenesis in intact and castrated pten knockout mice via targeting PKC, Stat3, and epithelial-to-mesenchymal transition markers," *Cancer Prevention Research*, vol. 8, no. 5, pp. 375–386, 2015.
- [17] G. L. Amidon, H. Lennernäs, V. P. Shah, and J. R. Crison, "A Theoretical Basis for a Biopharmaceutic Drug Classification: The Correlation of in Vitro Drug Product Dissolution and in Vivo Bioavailability," *Pharmaceutical Research*, vol. 12, pp. 413–420, 1995.
- [18] A. Gupta, H. B. Eral, T. A. Hatton, and P. S. Doyle, "Nanoemulsions: formation, properties and applications," *Soft Matter*, vol. 12, no. 11, pp. 2826–2841, 2016.
- [19] X. Wang, Y. Jiang, Y.-W. Wang, M.-T. Huang, C.-T. Ho, and Q. Huang, "Enhancing anti-inflammation activity of curcumin through O/W nanoemulsions," *Food Chemistry*, vol. 108, no. 2, pp. 419–424, 2008.
- [20] L. Salvia-Trujillo, R. Soliva-Fortuny, M. A. Rojas-Graü, D. J. McClements, and O. Martín-Belloso, "Edible Nanoemulsions as Carriers of Active Ingredients: A Review," *Annual Review of Food Science and Technology*, vol. 8, pp. 439–466, 2017.
- [21] J. Jiao, S. Wang, R. Qiao et al., "Murine cell lines derived from Pten null prostate cancer show the critical role of PTEN in hormone refractory prostate cancer development," *Cancer Research*, vol. 67, no. 13, pp. 6083–6091, 2007.
- [22] Y. Kawabata, K. Wada, M. Nakatani, S. Yamada, and S. Onoue, "Formulation design for poorly water-soluble drugs based on biopharmaceutics classification system: basic approaches and practical applications," *International Journal of Pharmaceutics*, vol. 420, no. 1, pp. 1–10, 2011.

## Research Article

# Analysis of *In Vitro* Cyto- and Genotoxicity of Barbatimão Extract on Human Keratinocytes and Fibroblasts

Neida L. Pellenz,<sup>1</sup> Fernanda Barbisan ,<sup>2</sup> Veronica F. Azzolin,<sup>1</sup> Thiago Duarte,<sup>1</sup> Aline Bolignon,<sup>3</sup> Moisés H. Mastella,<sup>2</sup> Cibele F. Teixeira ,<sup>1</sup> Euler E. Ribeiro,<sup>4</sup> Ivana B. Mânica da Cruz ,<sup>1,2</sup> and Marta M. M. F. Duarte<sup>1,5</sup>

<sup>1</sup>Postgraduate Program of Pharmacology, Federal University of Santa Maria, Santa Maria, RS, Brazil

<sup>2</sup>Postgraduate Program of Gerontology, Federal University of Santa Maria, Santa Maria, RS, Brazil

<sup>3</sup>Phytochemical Research Laboratory, Department of Industrial Pharmacy, Federal University of Santa Maria, Santa Maria, RS, Brazil

<sup>4</sup>Third Age Open University, University of Amazonas State, Manaus, AM, Brazil

<sup>5</sup>Brazilian Lutheran University (ULBRA), Santa Maria, RS, Brazil

Correspondence should be addressed to Ivana B. Mânica da Cruz; [ivana.ufsm@gmail.com](mailto:ivana.ufsm@gmail.com)

Received 30 April 2018; Revised 24 August 2018; Accepted 13 September 2018; Published 8 October 2018

Guest Editor: Francesco Facchiano

Copyright © 2018 Neida L. Pellenz et al. This is an open access article distributed under the Creative Commons Attribution License, which permits unrestricted use, distribution, and reproduction in any medium, provided the original work is properly cited.

Barbatimão (*Stryphnodendron adstringens*, Mart.) is a native Brazilian species used in traditional medicine and some commercial preparations owing to its strong wound-healing activity. However, controversy regarding its use due to safety concerns over the potential genotoxic effect of this plant remains. In order to clarify this issue, the effect of hydroalcoholic extract of barbatimão *in vitro* on cell viability, DNA damage, and induction of apoptosis in two commercial cell lines of keratinocytes (HaCaT) and fibroblasts (HFF-1) was evaluated. Barbatimão stem bark hydroalcoholic extract (70% ethanol) was obtained and lyophilized for subsequent use in all experiments. The main bioactive molecules quantified by HPLC were gallic acid, caffeic acid, quercetin, catechin, and epigallocatechin gallate (EGCG). Barbatimão (0.024 to 1.99 mg/mL) was found to decrease cellular mortality as compared to the control group. GEMO assay, a noncellular DNA protocol that uses H<sub>2</sub>O<sub>2</sub>-exposed calf thymus DNA, revealed not only a genotoxic effect of barbatimão, but also a potential genoprotective action against H<sub>2</sub>O<sub>2</sub>-triggered DNA fragmentation. These results indicated that barbatimão at concentrations of 0.49 and 0.99 mg/mL, which are near to the levels found in commercial preparations, exerted an *in vitro* genoprotective effect on cells by decreasing the levels of DNA oxidation quantified by 8-hydroxy-2'-deoxyguanosine (8-OHdG) and reactive oxygen species (ROS) levels. Gene and protein apoptotic markers, quantified by qRT-PCR (*BAX/Bcl-2* genes) and immunoassays (Caspases 3 and 8), respectively, also indicated a decrease in apoptotic events in comparison with control cells. Collectively, the results suggest that barbatimão could exert genoprotective and antiapoptotic effects on human keratinocytes and fibroblasts.

## 1. Introduction

Many studies have described potential effectiveness of phenolic compounds in medicine due to their antioxidant, anti-inflammatory, antimicrobial, and proliferative properties [1, 2]. Some of these polyphenol molecules have been described in plants such as *Stryphnodendron adstringens* (Mart.), a Brazilian species popularly known as “barbatimão,” with strong wound-healing activity [3, 4]. Barbatimão is a native species of the Savanah Biomes (Cerrado and Caatinga), where a bark extract is used by traditional communities

as a wound-healing natural product [5–9]. Prior investigations have described potential causal mechanisms associated with the healing efficacy of barbatimão, such as antioxidant, anti-inflammatory, and antimicrobial activities [6, 10–13].

Considering that barbatimão is effective and inexpensive, this bark extract has been included in some commercial Brazilian medicines. Its inclusion as a phytotherapeutic plant is also based on complementary studies that have described low acute and chronic toxicity in barbatimão experimental models [14–17].



However, there are some aspects of the plant that need to be studied for the safe use of barbatimão as a drug, such as its cito- and genotoxic potential. Therefore, it is necessary to perform complementary investigations to evaluate the effect of barbatimão on human cellular DNA damage modulation. The present study evaluated the modulation of genotoxicity and apoptosis as an indicator of the effect of a commercial barbatimão extract on DNA damage in human keratinocytes and dermal fibroblast commercial cell lines.

## 2. Materials and Methods

**2.1. Reagents.** Chemical reagents including acetonitrile, formic acid (purity > 98%), gallic acid (purity > 98%), and caffeic acid (purity > 98%) were purchased from Merck (Darmstadt, FRM, Germany), and quercetin (purity > 98%), catechin (purity > 98%), rutin (purity > 98%), and kaempferol (purity > 98%) used as reference molecules were obtained from Sigma (Saint Louis, MI, United States). High-pressure liquid chromatography with a diode array detector (HPLC-DAD) was performed using Shimadzu Prominence Auto Sampler (SIL-20A) high-pressure liquid chromatography (HPLC) system (Shimadzu, Kyoto, Japan), equipped with Shimadzu LC-20AT reciprocating pumps connected to a DGU 20A5 degasser with a CBM 20A integrator, SPD-M20A diode array detector, and LC solution 1.22 SP1 software. Materials used in cell culture were purchased from Vitrocell Embriolife (Campinas, SP, Brazil) and Gibco-Life Technologies (Carlsbad, CA, United States). Molecular biology reagents were obtained from QIAGEN (Hilden, NW, Germany), Invitrogen (Carlsbad, CA, United States), and Bio-Rad Laboratories (Hercules, CA, United States).

Biochemical reagent protocols for performing the spectrophotometry assays were obtained from Sigma-Aldrich (St. Louis, MI, United States). The apoptotic and genotoxic markers marked by an ELISA immunoassay kit were obtained from Abcam (Cambridge, MA, United States). The equipment used included a SpectraMax i3x Multimode microplate reader (Molecular Devices, Sunnyvale, CA, United States) and Rotor-Gene Q 5plex HRM System (QIAGEN biotechnology, Hilden, NW, Germany).

**2.2. Good In Vitro Methods Practices and Experimental Design.** The *in vitro* protocols performed in the present investigation are according to presumptions described in OECD Guidelines for the Testing of Chemicals and in a draft of guidance document on Good *In vitro* Methods Practices (GIVIMP) organized by Griesinger [18]. The followed standard procedures were used in the present study to guarantee high data quality: (1) reagents and plastics of high quality and origin were used; (2) ATCC commercial lineages and standardized conditions described by the ATCC were used; (3) all experiments were initialized with cells at of  $1 \times 10^5$  concentration; (4) all experiments were carried out at controlled culture times identified in the results and/figures; (5) experiments conducted in 96-well plates were just in the internal wells in order to attenuate problems related to the evaporation of

the medium which can cause large intravariation of the data; (6) in the 96-well plates each treatment was repeated at least five times; (7) all experiments were replicated at different moments, at least three times. In each replication, at least five repetitions of each treatment were tested; (8) details of data analysis used in GIVIMP were also followed and are presented in statistical section of this study.

General analysis performed in the present investigation is synthetized in Figure 1. Further, details of assays used in the present study will be detailed. Initially, to test potential toxicological effect of barbatimão on human cell lines, a hydroalcoholic extract using bark samples of this plant collected in Manaus, Amazonas State, Brazil (-3.10719S, -60.0261 3° 6' 26''W), and voucher specimens were deposited at the Herbarium of the Biological Sciences Course, Federal University of Santa Maria, RS, Brazil (Figure 1(A)). Main bioactive molecules present in the barbatimão extract were quantified by HPLC-DAD analyses (Figure 1(B)).

Before *in vitro* analyses, the noncellular GEMO assay was performed to identify potential genotoxic and/or genoprotective barbatimões's capacity according to different concentrations (Figure 1(C)). The principle of this assay previously developed and validated by Cadoná et al. [19] is to verify the effect of some extract-test on fragmentation of double-strand (ds) DNA molecule that is concomitantly exposed to  $H_2O_2$ , an oxidative molecule. Therefore, if an extract-test has genotoxic capacity, dsDNA fragmentation triggered by  $H_2O_2$  exposure will be more intense than negative control group with just dsDNA in the solution. On the contrary, if an extract-test has a genoprotective capacity, dsDNA fragmentation will be less intense than positive control group with dsDNA plus  $H_2O_2$ . GEMO assay is performed using a highly specific dsDNA dye (PicoGreen®), as a basic reagent. This dye is an ultrasensitive fluorescent reagent that allows quantification in the solution, just dsDNA, but not single DNA molecules and nucleotides. Therefore, high dsDNA concentration is associated to high fluorescence levels quantified by fluorimeter (Figure 1(C-1)). When dsDNA is fragmented by the presence of oxidant molecules, such as  $H_2O_2$ , fluorescence drops in comparison with negative non- $H_2O_2$  exposed control (Figure 1(C-2)). Therefore, the effect of some extract-test on this reaction can indicate its genotoxic or genoprotective effect. Genoprotective capacity is detected when fluorescence increases significantly in a solution containing dsDNA,  $H_2O_2$ , and extract-test in comparison with a solution containing just dsDNA plus  $H_2O_2$ . On the contrary, if fluorescence decreases significantly with addition of extract-test in the same solution, this result indicates genotoxic capacity of the extract. Therefore, this assay was used as preliminary indication of genoprotective and/or genotoxic (Figure 1(C-3)) capacity of barbatimão extract at different concentrations.

All *in vitro* protocols were performed using two cell commercial lines of keratinocytes (HaCaT) and dermal fibroblasts (HFF-1) in 24 h cell cultures (Figure 1(D)). First protocol determined if similar concentrations tested in the GEMO assay could present some cytotoxic effects on these cell lines. Therefore, cell cultures were supplemented with barbatimão at 10 different concentrations (0.012, 0.024, 0.049, 0.099, 0.12,



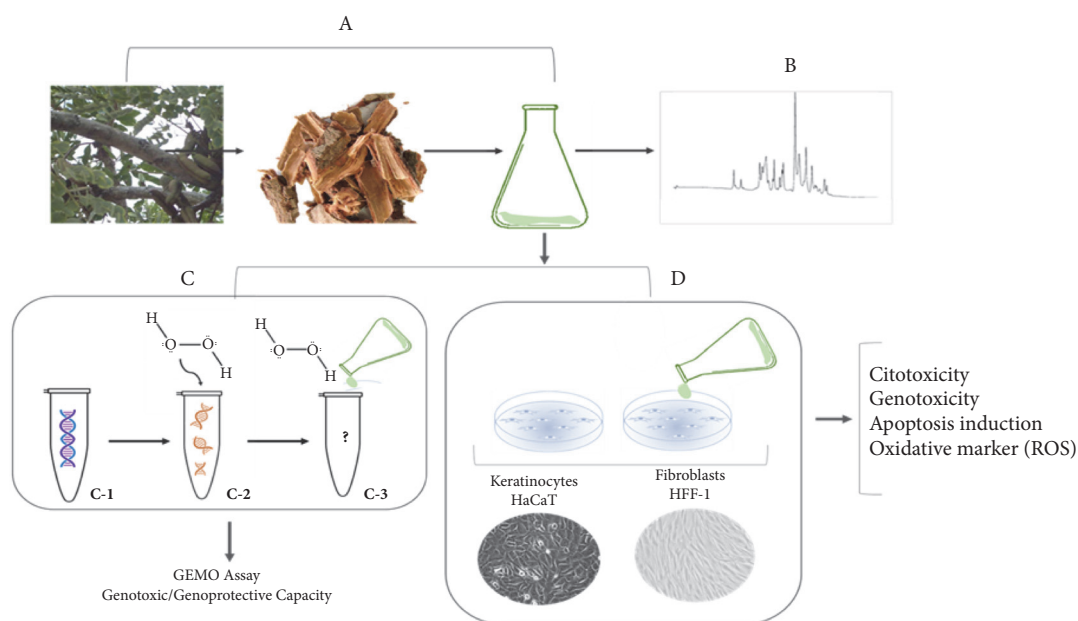


FIGURE 1: General experiment design. (A) Initially was obtained a hydroalcoholic extract using barbatimão bark samples. (B) Main bioactive compounds were quantified by HPLC-DA. (C) An exploratory noncellular GEMO assay was conducted to determine if barbatimão at 10 different concentrations could present some genotoxic or genoprotective capacity of the extract. (D) The *in vitro* protocols were performed in two commercial human cell lines of keratinocytes (HaCaT) and dermal fibroblasts (HFF-1). Additional protocols were conducted to evaluate barbatimão effects on DNA oxidation by quantification of DNA-8-OHdG levels and by intrinsic or extrinsic apoptosis induction by quantification and comparison with negative control group of gene BAX/Bcl-2 ratio and CASP 3 and 8 protein levels. Details of experimental design and assays used in this study are presented in Methods section.

0.24, 0.49, 0.99, 1.99, and 3.92). From these results, two barbatimão concentrations estimated to be found in Brazilian commercial wound-healing barbatimão products described in pharmaceutical package were used in the complementary protocols (0.49 and 0.99 mg/mL).

These protocols evaluated if barbatimão extract could induce cellular *in vitro* genotoxicity by quantification of 8-deoxyguanosine (DNA-8-OHdG) levels. This molecule is formed when DNA is oxidized and is considered a good biomarker of oxidative stress and oxidative DNA damage [20]. Extensive cellular and DNA damage can trigger apoptotic events on the cells. The intrinsic apoptotic events are triggered by increase of p53 protein levels, which are able to detect no-repaired DNA lesions and induce overexpression of Bcl-2-associated X protein (BAX gene), an apoptotic regulator. On the contrary, p53 protein induces downregulation of B-cell lymphoma 2 (Bcl-2) that plays a crucial role in promoting cellular survival and proliferation. Therefore, BAX/Bcl-2 ratio has been used as marker of intrinsic apoptosis events (when ratio is  $\geq 1.0$ ) in a large number of studies, such as performed by Bergandi et al. [21]. Upon induction of apoptosis, BAX becomes organelle membrane associated, and, in particular, mitochondrial membrane that becomes permeabilized releases cytochrome C into cytosol. The elevated cytochrome C concentration in the cytoplasm triggers caspases (CASP) pathway (including CASP 3 and 8) that regulate further apoptotic events. Moreover, caspases pathway can be triggered by an extrinsic pathway related

to binding of some molecules with dead receptors that are present in the outside of cellular membrane. In this context, concomitant quantification of BAX/Bcl-2 gene expression ratio and CASP 3 and 8 proteins can be considered informative if some extract or product triggers apoptotic events and if events involve intrinsic or extrinsic apoptosis pathways. This protocol of apoptosis induction has been used in previous studies performed by our research group [22, 23].

As barbatimão extract can be clinically tested in several days, a final protocol was performed to evaluate if the chronic cell culture exposure to barbatimão could present elevation of reactive oxygen species (ROS) levels and DNA 8-OHdG levels, which indicates DNA damage measure in 1, 3, and 5 days of cultures.

**2.3. Barbatimão Extract Obtention and HPLC-DAD Procedures.** Barbatimão hydroalcoholic extract was obtained in a manner similar to that described by Betoni et al. [24]. Barbatimão bark was dried, ground, and extracted with 70% ethanol at 4–8°C then filtered after 48 h. Filtration was done using Whatman No. 1 paper and the solvent removed using a rotary evaporator at reduced pressure, 45°C at 115 rpm. The resulting dry extract was obtained by lyophilization and stored at 20°C in a sterile flask until use. Quantification of the main bioactive molecules in the barbatimão stem bark extract was performed as previously described by Da Silva et al. [25]. Barbatimão hydroalcoholic extract at a concentration of 12 mg/mL was injected in a model SIL-20A Shimadzu Auto

sampler. Separations were carried out using Phenomenex C18 column (4.6 mm × 250 mm × 5 µm particle size). The mobile phase consisted of water with 1% formic acid (v/v) (solvent A) and HPLC grade acetonitrile (solvent B) at a flow rate of 0.6 mL/min and injection volume 40 µL. The composition gradient was 5% solvent B reaching 15% at 10 min; 30% solvent B at 20 min; 65% solvent B at 30 min; and 98% solvent B at 40 min, followed by 50 min at isocratic elution until 55 min. At 60 min, the gradient reached the initial conditions again, following the method described by Da Silva et al. [25] with small modifications. The sample and mobile phase were filtered through a 0.45 µm membrane filter (Millipore) and then degassed by ultrasonic bath prior to use. Stock solutions of standards references were prepared in acetonitrile at a concentration range of 0.030–0.500 mg/mL. Quantifications were carried out by integration of the peaks using the external standard method, at 254 nm for gallic acid, 280 nm for catechin, 327 nm for caffeic acid, and 366 nm for quercetin, rutin, and kaempferol. The chromatography peaks were confirmed by comparing retention time with those of reference standards and by DAD spectra (200 to 700 nm). All chromatography operations were carried out at ambient temperature and in triplicate.

**2.4. Cell Culture Conditions and Treatments.** The *in vitro* investigation used two commercial cell lines: immortalized human keratinocytes (HaCaT) and neonatal foreskin human dermal fibroblasts (HFF-1) obtained from American Type Culture Collection (ATCC). Cell cultures were reared in controlled conditions with Dulbecco's modified Eagle medium (DMEM) culture medium supplemented with 15% fetal bovine serum, 100 IU/mL penicillin, and 100 µg/mL streptomycin. Cells were maintained at 37°C with 5% CO<sub>2</sub> and 95% humidified atmosphere for 24 h. Potential cytotoxic effects of hydroalcoholic barbatimão extract on keratinocytes and fibroblasts were tested using ten different concentrations. The curve concentration of barbatimão analyzed here was based on a prior study by Costa et al. [15] and was used as a reference (0.012 to 3.92 mg/mL). To perform this curve, barbatimão lyophilized extract was diluted in culture medium and filtered using Whatman filter paper (2 µ) to prevent the presence of microorganisms in the solution.

Two barbatimão concentrations near to those found in commercial preparations of barbatimão extract were used to perform complementary analysis (0.49 and 0.99 mg/mL) in keratinocyte and fibroblast 24 h cell cultures. In cells exposed to these concentrations, DNA oxidative damage was evaluated by quantification of 8-hydroxy-2'-deoxyguanosine (8-OHdG) that is considered a biomarker for oxidative DNA markers and has been widely used in *in vivo* and *in vitro* studies [20]. We also evaluated potential modulation of apoptosis by barbatimão exposure via analysis of expression of two genes: *Bcl-2* (B-cell lymphoma 2) and *BAX* (bcl-2-like protein 4). *Bcl-2* gene is an inductor of cellular proliferation whereas *BAX* is an inductor of apoptotic events. Generally, *BAX/Bcl-2* gene expression ratio is used to detect if cell cultures are in apoptotic or proliferative processes [26]. In this case, values > 1 indicate an apoptotic state and potential genotoxic effect of barbatimão on cells. Quantification of two

caspase (CASP 3 and 8) protein levels was also performed to confirm the influence of barbatimão on apoptotic processes. Methods used to determine gene expression and protein quantification involved qRT-PCR and immunoassay analysis are further described in more details below.

**2.5. GEMO Assay.** Before testing the potential effect of barbatimão on the DNA of keratinocytes and fibroblasts, a GEMO assay was performed as previously described by Cadoná et al. [19], which used Quant-IT™ PicoGreen® DNA kit (Invitrogen Life Technologies, SP, Brazil). GEMO is a noncellular protocol previously described by Cadoná et al. [19] that uses exposure of calf-DNA to H<sub>2</sub>O<sub>2</sub>. This molecule is genotoxic, increasing DNA fragmentation that is detected by PicoGreen dye. If a chemical molecule in the plant extract has a genoprotective effect, DNA fragmentation will be attenuated, and fluorescence in the test group will decrease in relation to the positive control group (obtained by exposure of calf-DNA to H<sub>2</sub>O<sub>2</sub>). A 96-well plate was filled with 10 µL of calf thymus DNA (1 µg/mL plus 70 µL of TE buffer) containing varying barbatimão concentrations and 70 µL of H<sub>2</sub>O<sub>2</sub> (1M). The reaction was incubated for 30 min. After 30 min PicoGreen® DNA dye was added and the fluorescence was read (excitation at 480 nm/emission at 520 nm). The genoprotective effect was considered present when the absorbance was lower than the positive control group [19].

**2.6. Cytotoxic Assays.** Two assays were used to test the potential cytotoxic effect of barbatimão on keratinocytes and fibroblasts: trypan dye exclusion assay and cf-DNA PicoGreen assay. The cf-DNA PicoGreen assay is based on the presence of double-stranded DNA fragments that are released when cells die as the cytoplasmic and nuclear membrane rupture. The cellular mortality rate is quantified by supernatant cell-free DNA (cf-DNA) levels using PicoGreen dye®, a fluorescent marker of double-stranded DNA fragments. Therefore, high cf-DNA levels indicate high mortality rate in the cell culture [19]. This assay was performed using Invitrogen Quant-IT kit following manufacturer's instructions. Ten microliters of cell culture supernatants were collected and added in a 96-well black plate together with reagents from Quant-IT™ PicoGreen and diluted in Tris-EDTA (TE) buffer (10mM Tris-HCl, 1mM EDTA, pH 7.5). Then, 100 µL of the PicoGreen dye diluted 1:200 in TE buffer was added to the microplate to make a final volume of 200 µL per well. Following incubation in the dark for 10 min at room temperature, the fluorescent signal of the samples was measured at 480 nm excitation and 520 nm emission at room temperature using SpectraMax M2/M2e Multimode Plate Reader, Molecular Devices' equipment. Elevated cf-DNA levels indicated high cellular mortality.

**2.7. Reactive Oxygen Species (ROS) Assay.** As barbatimão is rich in antioxidant molecules, ROS levels of cell cultures were quantified using a 2,7 dichlorofluorescein diacetate (DCFH-DA) ROS production assay. DCFH-DA is hydrolysed by intracellular esterase enzymes to DCFH, which is trapped

within the cell, and the nonfluorescent molecule is then oxidized with fluorescent dichlorofluorescein (DCF) using cellular oxidants. Therefore, to quantify ROS levels, cell cultures were treated with DCF-DA (10 mM) for 60 min at 37°C. The fluorescence was measured at an excitation of 488 nm and an emission of 525 nm, and the results were obtained as pmole/mL of DCF production from 2,7 dichlorofluorescein in reaction with ROS molecules present in the samples [27]. After the data were obtained, results were converted to % of control group.

**2.8. Immunoassay Tests.** The levels of DNA 8-OHdG were used to quantify DNA damage and those of CASP 3 and 8 were measured using a Quantikine Human Kit according to the manufacturer's instructions. All reagents and working standards were prepared and the excess microplate strips were removed before adding 50 µL of the assay diluent RDIW to each well. 100 µL of standard control for the sample was added per well, after which the well was covered with an adhesive strip and incubated for 1.5 h at room temperature. Each well was subsequently aspirated and washed twice, for a total of three washes. The antiserum of each molecule analyzed here was added to each well and covered with a new adhesive strip before being incubated for 30 min at room temperature. The aspiration/wash step was repeated, and the molecule-1 conjugate (100 µL) was added to each well and incubated for 30 min at room temperature. The aspiration/wash step was repeated before adding 100 µL of substrate solution to each well, followed by incubation at room temperature for an additional 20 min. Finally, 50 µL of stop solution was added to each well and the optical density was determined within 30 min using a microplate reader set to 450 nm.

**2.9. mRNA Expression Analysis by Quantitative QT-PCR Assay.** Gene expressions of *BAX* and *Bcl-2* were analyzed in cells exposed to barbatimão extract. Total RNA was extracted using Trizol, following the manufacturer's instructions (Ludwig-Biotec, RS, Brazil). The extracted RNA was measured by a Thermo Scientific NanoDrop™ 1000 Spectrophotometer. To perform reverse transcription, 1 µg/mL RNA was added to the samples with 0.2 µL of DNase at 37°C for 5 min, followed by heating at 65°C for 10 min. The cDNA was generated with 1 µL of Iscript cDNA and 4 µL of Mix Iscript. The next steps of the reaction were 5°C for 10 min, 25°C for 5 min, and 85°C for 5 min, with a final incubation at 5°C for 60 min. The qRT-PCR was performed in the Rotor-Gene Q 5plex HRM System (QIAGEN biotechnology, NW, Germany) using QuantiFast SYBR® Green PCR Master Mix, starting with a temperature of 95°C for 3 min followed by 40 cycles of 95°C for 10 s, 60°C for 30 s and a melt curve of 60°C to 90°C in 0.5°C increments for 5 s. The reactions of each sample were made in triplicate, using 1 µM of each primer and with 2× QuantiFast SYBR® Green PCR Master Mix; the final volume was 20 µL. The beta-actin gene sense (5'TGTGGATCAGCAAGCAGGAGTA3') antisense (5'TGCGCAAGTTAGGTTTTGTCA3') was used as a housekeeping

gene; *BAX* gene sense (5'CCCTTTTCTACTTTGCCAGCA-A3') antisense (5'CCCGGAGGAAGTCCAATGT3'), *BCL-2* gene sense (5'GAGGATTGTGGCCTTCTTTGAGT3') antisense (5'AGTCATCCACAGGGCGATGT3') [23].

**2.10. Statistical Analysis.** Statistical tests were performed using Graph Pad Prism Software. Results of all experiments were replicated three times with, at least, five repetitions of each treatment. Data from repetitions were evaluated before statistical analysis and normalized by % of control group. Therefore, results were expressed as % mean ± SD (standard deviation) of the control group. This procedure is broadly used in the *in vitro* protocols (Antoneli et al., 2017) to allow comparison between results obtained on different days, by different tests, and by different laboratories. The upper and lower values of 2-SD range were considered outliers and excluded of the analysis, because generally these outliers generate relative SD > 10% indicating presence of some experimental imprecision. Treatments were statistically compared by one-way analysis of variance (ANOVA), followed by Tukey *post hoc* test. In results showed in Figures different letters identified statistical differences ( $p \leq 0.05$ ) among treatments.

### 3. Results

Details of the barbatimão tree, bark, extract preparation samples, and chemical characterization are presented in Figure 2. Barbatimão hydroalcoholic extract presented higher levels (mg/g) of gallic acid (12.48±0.05), caffeic acid (8.06±0.02), quercetin (8.16±0.04), catechin (5.93±0.01), and rutin (4.71±0.01) (Figure 2). Low levels of kaempferol and other bioactive molecules were also detected (Figure 2).

Initially potential genoprotective capacity of barbatimão extract at different concentrations was determined and results are presented in Figure 3(a). In this assay, the control group was compounded by a solution containing isolated dsDNA plus H<sub>2</sub>O<sub>2</sub> that caused extensive DNA fragmentation. When barbatimão extract was added in this solution an inverse dose-dependent action on dsDNA was observed. In this case, barbatimão at lower concentration (0.012 mg/mL) presented higher protective effect against H<sub>2</sub>O<sub>2</sub> dsDNA fragmentation than more elevated concentrations. Concentrations near to barbatimão therapeutic doses used to healing wound showed some dsDNA protection, but this effect was less intense than that observed in the other lower concentrations.

The first *in vitro* protocol performed here using keratinocytes (Figure 3(b)) and fibroblast (Figure 3(c)) cells evaluated potential barbatimão effect on viability of these cells using the same range of concentrations evaluated by GEMO assay (Figure 3(a)). Barbatimão did not present a cytotoxic effect on keratinocytes and fibroblasts when compared to control group that did not receive any additional treatment numerically represented by 0 value in the graphic. On the contrary, cell culture barbatimão extract supplementation increased viability of both cell lines when compared to no-treated control group (0). However, this



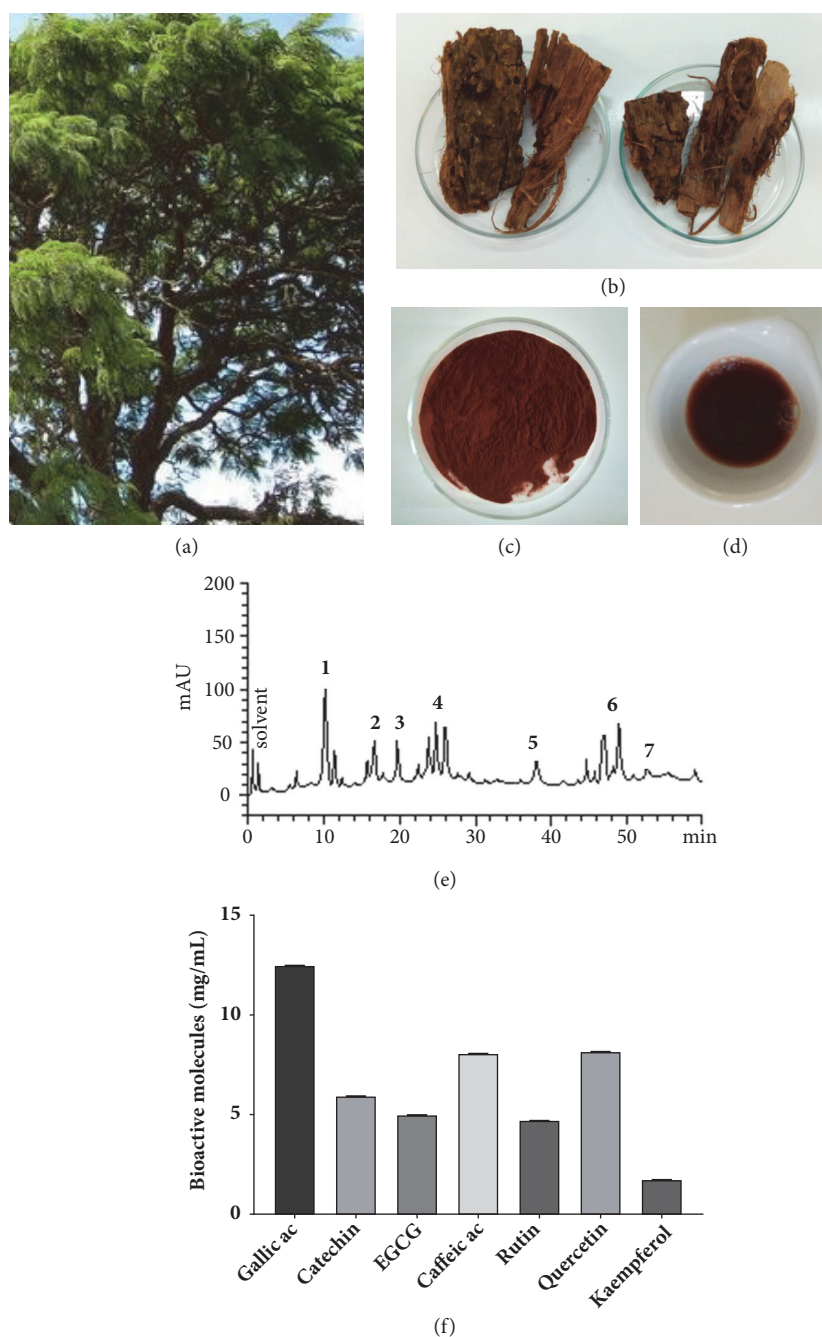


FIGURE 2: Barbatimão (*Stryphnodendron adstringens*, Mart.) components and measurement of bioactive molecules: (a) barbatimão tree; (b) stem bark used to produce barbatimão extract; (c) lyophilized barbatimão extract; (d) solution of hydroalcoholic extract of barbatimão used to treat cell cultures; and (e) representative HPLC profile of barbatimão hydroalcoholic extract. Gallic acid (peak 1), catechin (peak 2), EGCG (peak 3), caffeic acid (peak 4), rutin (peak 5), quercetin (peak 6), kaempferol (peak 7); (f) graphical representation of bioactive molecule quantification detected in barbatimão HPLC analysis.

effect was higher in cultures supplemented with intermediary concentrations (Keratinocytes: 0.099-0.49 mg/mL; fibroblasts: 0.099-0.99 mg/mL).

Two barbatimão concentrations (0.49 and 0.99 mg/mL) near to those found in commercial preparations were used to perform analysis of genotoxicity in keratinocyte and fibroblast 24 h cell cultures. In cells exposed to these concentrations,

DNA damage quantified by DNA 8-OHdG levels, *BAX/Bcl-2* gene expression ratio, and CASP 3 and 8 levels were quantified. In both barbatimão concentrations there was a significant decrease in ROS levels when 24 h keratinocyte cultures were exposed to 0.49 mg/mL ( $87.2 \pm 2.5\%$  of control group) and 0.99 mg/mL ( $74.3 \pm 3.0\%$  of control group). Similar results were also found in fibroblasts, where barbatimão



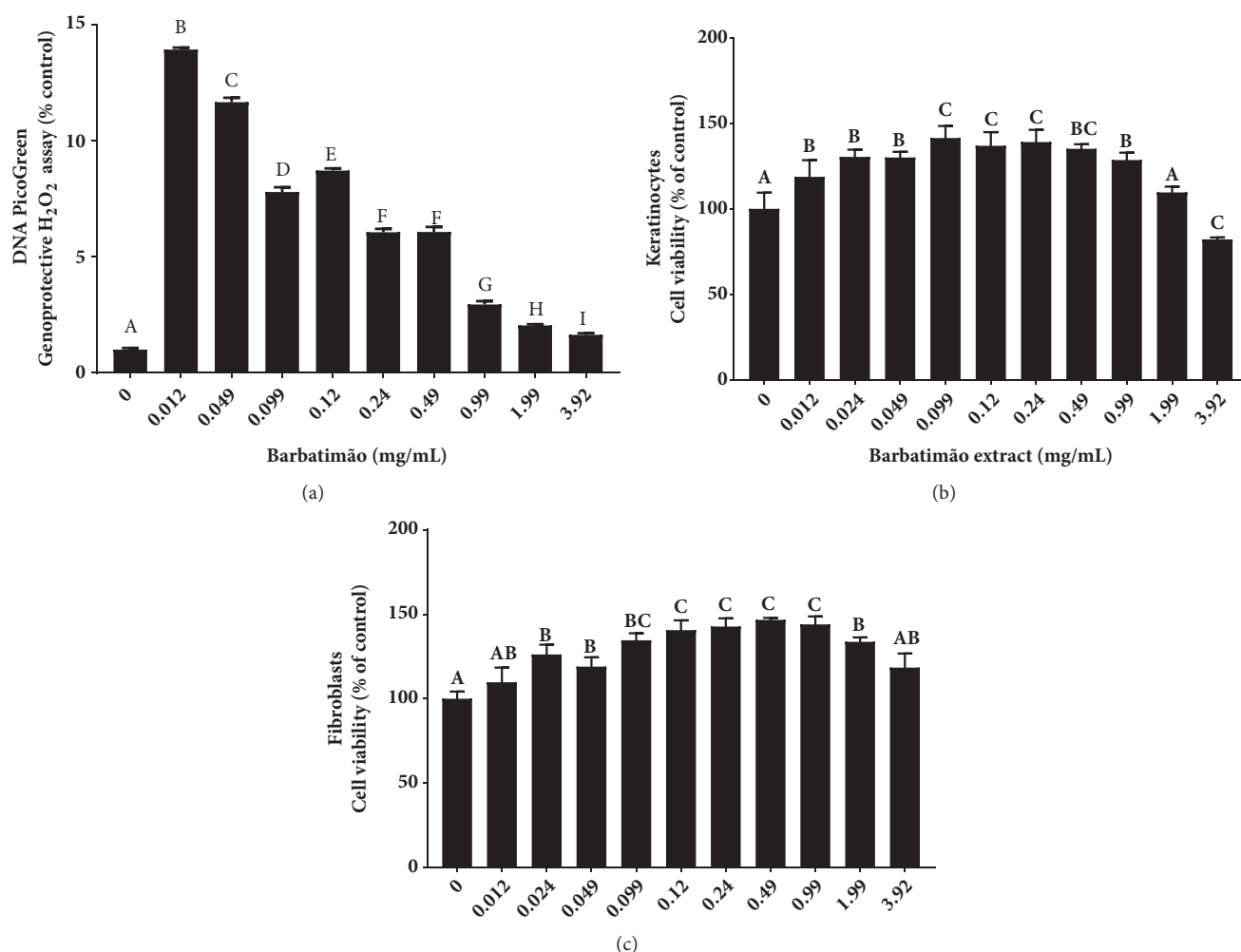


FIGURE 3: Barbatimão preliminary assays: (a) genoprotective capacity determined by GEMO noncellular assay that uses DNA PicoGreen® fluorescent dye (Cadoná et al., 2014). This dye presents specific affinity to binding with double-strand (ds) DNA levels. In GEMO assay a solution containing isolated calf dsDNA and H<sub>2</sub>O<sub>2</sub> (1M) is produced. The H<sub>2</sub>O<sub>2</sub> trigger extensive DNA fragmentation that causes decreasing in the fluorescence and here is considered the control group represented by 0 value. Cell culture supplementation with barbatimão hydroalcoholic extract at different concentrations showed significant increase in the fluorescence indicating genoprotective effect of this extract; barbatimão's viability effect on (b) keratinocytes and (c) fibroblast 24 h cell cultures measured by MTT-assay. Data were analyzed by ANOVA one-way analysis of variance followed by Tukey *post hoc* test and all statistical tests with  $p \leq 0.05$  were considered significant. Statistical differences among treatments were identified by different alphabetical letters, whereas same letters indicated no differences between each treatment compared to the others.

extract at 0.49 mg/mL reduced ROS levels to  $82.4 \pm 3.0\%$  of control group and at 0.99 mg/mL reduced ROS levels to  $69.5 \pm 3.0\%$  of control group ( $p \leq 0.001$ ).

Barbatimão treated samples also showed a decrease in DNA damage evaluated by 8-OHdG levels (Figure 4(a)) in both 24 h cell cultures tested. Analysis of apoptotic markers showed a decrease in *BAX/Bcl-2* gene expression ratio (Figure 4(b)). Moreover, barbatimão decreased CASP 3 and 8 in both keratinocyte and fibroblast cell lines (Figures 4(c) and 4(d)). However, the genoprotective and caspase lowering effect was more pronounced in fibroblasts than in keratinocytes.

Considering that the effect of barbatimão could be transient and cause subsequent triggering of an increase in ROS

levels and DNA damage in older cultures, a complementary analysis was performed in fibroblasts in order to evaluate the effect of barbatimão on 1, 3, and 5 day cell cultures. As seen in Figure 5, barbatimão maintained its antioxidant and genoprotective effect in cultures of several days old. However, this result was more pronounced in 72 h cell cultures exposed to 0.99 mg/mL concentration of barbatimão extract.

#### 4. Discussion

The present investigation evaluated potential genotoxic effects of barbatimão, a Brazilian plant used traditionally for wound healing. Most results obtained from the

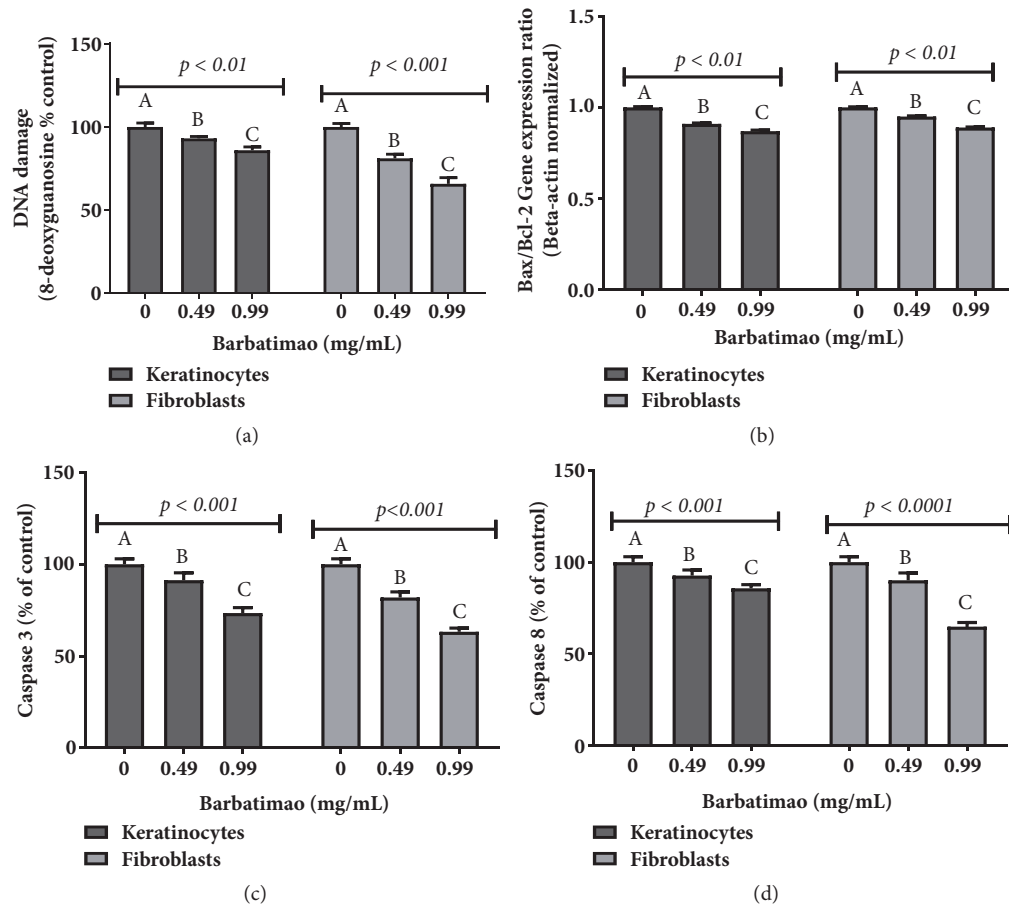


FIGURE 4: Comparison among genotoxic and apoptotic markers of keratinocytes and fibroblasts exposed to barbatimão hydroalcoholic extraction. (a) 8-OHdG levels; (b) *BAX/Bcl-2* gene expression ratio quantified by qRT-PCR, that indicates modulation of intrinsic apoptotic events; (c) caspase 3 protein levels; (d) caspase 8 protein levels. Data were compared by one-way analysis of variance (ANOVA) followed by a Tukey *post hoc* test. In each marker tested here, statistical differences at  $p \leq 0.05$  among 24 h cell cultures treatments were identified by different letters (A, B, C).

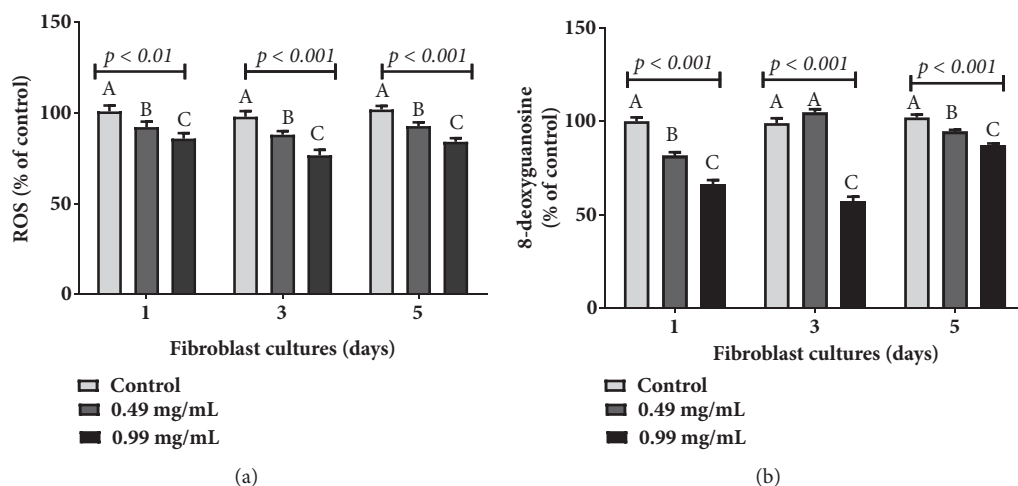


FIGURE 5: Modulation of oxidative markers on three different cell culture days of keratinocytes and fibroblasts exposed to two different hydroalcoholic barbatimão extracts to evaluate potential chronic genotoxicity of this extract on cells. (a) Reactive oxygen species (ROS) levels; (b) 8-OHdG levels. Data were compared by one-way analysis of variance (ANOVA) followed by a Tukey *post hoc* test. In each marker tested here, statistical differences at  $p \leq 0.05$  among 24 h cell cultures treatments were identified by different letters (A, B, C).

*in vitro* protocol using keratinocyte and fibroblasts indicated noncytotoxic and genoprotective effects of barbatimão extract. The genoprotective effect was estimated by a non-cellular assay, quantification of 8-deoxyguanosine levels, and gene and proteins involving in apoptosis processes in both cell lines. These results could be considered relevant since use of phytotherapeutics from traditional medicine has been considered a part of healthcare by the World Health Organization (WHO) since 2002. Barbatimão has been used as an astringent, antihemorrhagic, and antidiarrheal as well as a treatment for scurvy, genitourinary disorders, and lower airways conditions [2].

The Brazilian Official Pharmacopoeia [28] estimated that the wound-healing effect of barbatimão could be associated with the high tannin concentration in its dried bark (8%). In fact, most bioactive molecules quantified in the barbatimão extract used here were previously described in the literature, such as gallic acid [29] and catechins [3]. It is important to mention that other bioactive molecules of barbatimão such as quercetin, rutin, and kaempferol have been identified and quantified in this study and have not been described in previous chemical analyses of barbatimão. Quercetin and rutin, also called quercetin-3-O-rutinoside, are flavonoids found in several fruits and vegetables including citrus and onion. Studies on quercetin have described interesting biological effects including cell protection against UV irradiation and skin regeneration in wound healing [30].

Due to its commercial use, it is important to clarify the potential genotoxic activity of barbatimão in human cells. There are relatively few studies that evaluate potential genotoxic effect of barbatimão, leading to the controversy over the safety of this traditional medicine. Costa et al. [15] evaluated potential micronucleus induction in mice orally treated with proanthocyanidin polymer-rich fraction (F2) of the stem bark of barbatimão and did not find a genotoxic effect of these molecules. Moreover, a study involving potential somatic mutation and recombination analysis (SMART test) and chromosome damage in germ cell lines of fruit flies exposed to barbatimão bark extract did not find genotoxic effect of this plant [31]. However, when Vilar et al. [32] evaluated lyophilized solution produced from barbatimão stem bark, results indicated some cytotoxic and genotoxic effect using SOS-Inductest in *E. coli* prokaryotic model. Therefore, the authors considered it important that further *in vitro* and *in vivo* studies are performed to clarify these potentially negative results.

In this context, it is plausible to consider that triggering healing with barbatimão extract could cause some undesirable chromosomal instability associated with procarcinogenic processes. Initially, we obtained data from the GEMO assay that indicated the genoprotective activity of barbatimão extract. This validated assay was developed by Cadoná et al. [19] due to the necessity of identifying the genoprotective and genotoxic capacity of plant extracts that are generally analyzed in *in vitro* cell cultures, which are very expensive, and present some influence on testing response due to differential biochemical and molecular specifications of each cell line. Therefore, results obtained from the GEMO assay are fast and inexpensive, involving double-strand DNA (dsDNA) damage

caused by H<sub>2</sub>O<sub>2</sub> exposure that was completely reverted in the presence of barbatimão, mainly in lower concentrations of the extract.

Subsequent analysis confirmed no genotoxic effect of barbatimão by analysis of 8-OHdG levels, which decreased in the presence of this extract. This molecule is considered a biomarker of oxidative stress and oxidative DNA damage found both in physiological fluids and cells and is frequently used as a marker of exposure to oxidants as well as a potential marker of some chronic nontransmissible disease progression [33, 34]. In the presence of 0.49 and 0.99 mg/mL barbatimão 8-OHdG levels were shown to decrease, suggesting that barbatimão extract could act as genoprotective compound.

Barbatimão extract also decreased *BAX/Bcl-2* gene expression ratio, and CASP 3 and 8 protein levels. These markers are related mainly to intrinsic apoptosis triggered via accumulation of DNA lesions from genotoxic compound exposure [33].

## 5. Conclusions

Despite methodological limitations related to *in vitro* studies, our data corroborate results found in rats and fruit flies with respect to lack of genotoxicity and safety. Moreover, the results described here suggest that barbatimão could present a genoprotective and antiapoptotic effect on human keratinocytes and fibroblasts.

## Data Availability

The data used to support the findings of this study are included in the article.

## Conflicts of Interest

The authors declare that there are no conflicts of interest regarding the publication of this paper.

## Acknowledgments

The authors would like to thank the CNPq [Nos. 402325/2013-3; 490760/2013-9; 311446/2012-4], FAPERGS, FAPEAM, and CAPES for grants and fellowships.

## References

- [1] M. Działo, J. Mierziak, U. Korzun, M. Preisner, J. Szopa, and A. Kulma, "The potential of plant phenolics in prevention and therapy of skin disorders," *International Journal of Molecular Sciences*, vol. 17, no. 1, pp. 1-9, 2016.
- [2] L. M. Ricardo, B. M. Dias, F. L. B. Mügge, V. V. Leite, and M. G. L. Brandão, "Evidence of traditionality of Brazilian medicinal plants: The case studies of *Stryphnodendron adstringens* (Mart.) Coville (barbatimão) barks and *Copaifera* spp. (copaíba) oleoresin in wound healing," *Journal of Ethnopharmacology*, vol. 219, pp. 319-336, 2018.
- [3] J. Sousa, N. Pedroso, L. Borges, G. A., J. Paula, and E. Conceicao, "Optimization of Ultrasound-assisted extraction of


- polyphenols, tannins and epigallocatechin gallate from barks of *Stryphnodendron adstringens* (Mart.) Coville bark extracts," *Pharmacognosy Magazine*, vol. 10, no. 38, p. 318, 2014.
- [4] A. C. Isler, G. C. Lopes, M. L. C. Cardoso, J. C. P. De Mello, and L. C. Marques, "Development and validation of a LC-method for the determination of phenols in a pharmaceutical formulation containing extracts from *stryphnodendron adstringens*," *Química Nova*, vol. 33, no. 5, pp. 1126–1129, 2010.
  - [5] T. H. L. Bernardo, R. C. Sales Santos Veríssimo, V. Alvino et al., "Antimicrobial Analysis of an Antiseptic Made from Ethanol Crude Extracts of *P. granatum* and *E. uniflora* in Wistar Rats against *Staphylococcus aureus* and *Staphylococcus epidermidis*," *The Scientific World Journal*, vol. 2015, Article ID 751791, 7 pages, 2015.
  - [6] B. F. de Santana, R. A. Voeks, and L. S. Funch, "Ethnomedicinal survey of a maroon community in Brazil's Atlantic tropical forest," *Journal of Ethnopharmacology*, vol. 181, pp. 37–49, 2016.
  - [7] S. C. G. Pinto, F. G. Bueno, G. P. Panizzon et al., "Stryphnodendron adstringens: Clarifying Wound Healing in Streptozotocin-Induced Diabetic Rats," *Planta Medica*, vol. 81, no. 12-13, pp. 1090–1096, 2015.
  - [8] L. A. F. Silva, M. I. de Moura, C. E. Dambros, S. L. R. Freitas, L. A. Souza, and M. P. Abreu, "Stryphnodendron adstringens extract associated with the hooves trimming surgical procedure for the treatment of bovine digital dermatitis," *Tropical Animal Health and Production*, vol. 45, no. 5, pp. 1177–1181, 2013.
  - [9] L. Hernandez, L. M. da Silva Pereira, F. Palazzo, and J. C. P. de Mello, "Wound-healing evaluation of ointment from *Stryphnodendron adstringens* (barbatimão) in rat skin," *Brazilian Journal of Pharmaceutical Sciences*, vol. 46, no. 3, pp. 431–436, 2010.
  - [10] B. O. Henriques, O. Corriá, E. P. C. Azevedo et al., "In vitro TNF- $\alpha$  inhibitory activity of brazilian plants and anti-inflammatory effect of *Stryphnodendron adstringens* in an acute arthritis model," *Evidence-based Complementary and Alternative Medicine*, vol. 2016, Article ID 9872598, 15 pages, 2016.
  - [11] E. M. R. Pereira, R. T. Gomes, N. R. Freire, E. G. Aguiar, M. D. G. L. Brandão, and V. R. Santos, "In vitro antimicrobial activity of Brazilian medicinal plant extracts against pathogenic microorganisms of interest to dentistry," *Planta Medica*, vol. 77, no. 4, pp. 401–404, 2011.
  - [12] A. T. Morey, F. C. de Souza, J. P. Santos et al., "Antifungal activity of condensed tannins from *stryphnodendron adstringens*: Effect on *Candida tropicalis* growth and adhesion properties," *Current Pharmaceutical Biotechnology*, vol. 17, no. 4, pp. 365–375, 2016.
  - [13] G. M. Lanchoti Fiori, A. L. Fachin, V. S. Correa et al., "Antimicrobial Activity and Rates of Tannins in *Stryphnodendron adstringens* Mart. Accessions Collected in the Brazilian Cerrado," *American Journal of Plant Sciences*, vol. 04, no. 11, pp. 2193–2198, 2013.
  - [14] M. A. Costa, J. C. Palazzo De Mello, E. N. Kaneshima et al., "Acute and chronic toxicity of an aqueous fraction of the stem bark of *stryphnodendron adstringens* (Barbatimão) in rodents," *Evidence-Based Complementary and Alternative Medicine*, vol. 2013, Article ID 841580, 9 pages, 2013.
  - [15] M. A. Costa, K. Ishida, V. Kaplum et al., "Safety evaluation of proanthocyanidin polymer-rich fraction obtained from stem bark of *Stryphnodendron adstringens* (BARBATIMO) for use as a pharmacological agent," *Regulatory Toxicology and Pharmacology*, vol. 58, no. 2, pp. 330–335, 2010.
  - [16] M. A. Rebecca, E. L. Ishii-Iwamoto, R. Grespan et al., "Toxicological studies on *Stryphnodendron adstringens*," *Journal of Ethnopharmacology*, vol. 83, no. 1-2, pp. 101–104, 2002.
  - [17] P. Cintra, O. Malaspina, and O. C. Bueno, "Toxicity of barbatimão to *Apis mellifera* and *Scaptotrigona postica*, under laboratory conditions," *Journal of Apicultural Research*, vol. 42, no. 1-2, pp. 9–12, 2003.
  - [18] C. Griesinger, "Validation of Alternative in vitro Methods to Animal Testing: Concepts, Challenges, Processes and Tools," *Advances in Experimental Medicine and Biology*, vol. 1, pp. 1–9, 2016.
  - [19] F. C. Cadoná, M. F. Manica-Cattani, A. K. Machado et al., "Genomodifier capacity assay: A non-cell test using dsDNA molecules to evaluate the genotoxic/genoprotective properties of chemical compounds," *Analytical Methods*, vol. 6, no. 21, pp. 8559–8568, 2014.
  - [20] N. Dabrowska and A. Wiczowski, "Analytics of oxidative stress markers in the early diagnosis of oxygen DNA damage," *Advances in Clinical and Experimental Medicine*, vol. 26, no. 1, pp. 155–166, 2017.
  - [21] L. Bergandi, E. Mungo, R. Morone, B. Rolando, and S. Doublier, "Hyperglycemia Promotes Chemoresistance Through the Reduction of the Mitochondrial DNA Damage, the Bax/Bcl-2 and Bax/Bcl-XL Ratio, and the Cells in Sub-G1 Phase Due to Antitumoral Drugs Induced-Cytotoxicity in Human Colon Adenocarcinoma," *Cells*, vol. 13, p. 866, 2018.
  - [22] V. F. Azzolin, F. Barbisan, L. S. Lenz et al., "Effects of Pyridostigmine bromide on SH-SY5Y cells: An in vitro neuroblastoma neurotoxicity model," *Mutation Research - Genetic Toxicology and Environmental Mutagenesis*, vol. 8, pp. 1–10, 2018.
  - [23] F. Barbisan, J. De Rosso Motta, A. Trott et al., "Methotrexate-related response on human peripheral blood mononuclear cells may be modulated by the Ala16Val-SOD2 gene polymorphism," *PLoS ONE*, vol. 9, no. 10, Article ID e107299, 2014.
  - [24] J. E. C. Betoni, R. P. Mantovani, L. N. Barbosa, L. C. di Stasi, and A. Fernandes Jr., "Synergism between plant extract and antimicrobial drugs used on *Staphylococcus aureus* diseases," *Memórias do Instituto Oswaldo Cruz*, vol. 101, no. 4, pp. 387–390, 2006.
  - [25] E. da Silva Brum, L. da Rosa Moreira, A. R. H. da Silva et al., "Tabernaemontana catharinensis ethyl acetate fraction presents antinociceptive activity without causing toxicological effects in mice," *Journal of Ethnopharmacology*, vol. 191, pp. 115–124, 2016.
  - [26] X.-C. Xie, Y. Cao, X. Yang, Q.-H. Xu, W. Wei, and M. Wang, "Relaxin Attenuates Contrast-Induced Human Proximal Tubular Epithelial Cell Apoptosis by Activation of the PI3K/Akt Signaling Pathway In Vitro," *BioMed Research International*, vol. 2017, Article ID 2869405, 7 pages, 2017.
  - [27] V. F. Azzolin, F. C. Cadoná, A. K. Machado et al., "Superoxide-hydrogen peroxide imbalance interferes with colorectal cancer cells viability, proliferation and oxaliplatin response," *Toxicology in Vitro*, vol. 32, pp. 8–15, 2016.
  - [28] Brasil. Farmacopeia Brasileira, vol. 2, Agência Nacional de Vigilância Sanitária. Brasília: Anvisa, 546p. 2010.
  - [29] S. C. Santos, W. F. Costa, J. P. Ribeiro et al., "Tannin composition of barbatimão species," *Fitoterapia*, vol. 73, no. 4, pp. 292–299, 2002.
  - [30] T. Hatahet, M. Morille, A. Hommoss, J. M. Devoisselle, R. H. Müller, and S. Bégu, "Quercetin topical application, from conventional dosage forms to nanodosage forms," *European Journal of Pharmaceutics and Biopharmaceutics*, vol. 108, pp. 41–53, 2016.



- [31] R. Sarıkaya, K. Erciyas, M. I. Kara, U. Sezer, A. F. Erciyas, and S. Ay, "Evaluation of genotoxic and antigenotoxic effects of boron by the somatic mutation and recombination test (SMART) on *Drosophila*," *Drug and Chemical Toxicology*, vol. 39, no. 4, pp. 400–406, 2016.
- [32] J. B. Vilar, M. I. P. D'Oliveira, S. D. C. Santos, and L. C. Chen, "Cytotoxic and genotoxic investigation on barbatimão [*Stryphnodendron adstringens* (Mart.) Coville, 1910] extract," *Brazilian Journal of Pharmaceutical Sciences*, vol. 46, no. 4, pp. 687–694, 2010.
- [33] J. Chayapong, H. Madhyastha, R. Madhyastha et al., "Arsenic trioxide induces ROS activity and DNA damage, leading to G0/G1 extension in skin fibroblasts through the ATM-ATR-associated Chk pathway," *Environmental Science and Pollution Research*, vol. 24, no. 6, pp. 5316–5325, 2017.
- [34] E. A. Prokhorova, A. V. Zamaraev, G. S. Kopeina, B. Zhivotovsky, and I. N. Lavrik, "Role of the nucleus in apoptosis: Signaling and execution," *Cellular and Molecular Life Sciences*, vol. 72, no. 23, pp. 4593–4612, 2015.

## Research Article

# Protective Effects of Silymarin and Silibinin against DNA Damage in Human Blood Cells

Flávio Fernandes Veloso Borges,<sup>1</sup> Carolina Ribeiro e Silva,<sup>1</sup> Wanessa Moreira Goes,<sup>2</sup> Fernanda Ribeiro Godoy,<sup>2</sup> Fernanda Craveiro Franco,<sup>2</sup> Jefferson Hollanda Vêras,<sup>1</sup> Elisa Flávia Luiz Cardoso Bailão,<sup>3</sup> Daniela de Melo e Silva,<sup>2</sup> Clever Gomes Cardoso,<sup>1</sup> Aparecido Divino da Cruz,<sup>4</sup> and Lee Chen-Chen <sup>1</sup>

<sup>1</sup>Laboratório de Radiobiologia e Mutagênese, Instituto de Ciências Biológicas, Universidade Federal de Goiás, Campus II, Goiânia, GO, Brazil

<sup>2</sup>Laboratório de Mutagênese (LABMUT), Instituto de Ciências Biológicas, Universidade Federal de Goiás, Campus II, Goiânia, GO, Brazil

<sup>3</sup>Laboratório de Biotecnologia, Câmpus Henrique Santillo, Universidade Estadual de Goiás, Anápolis, GO, Brazil

<sup>4</sup>Núcleo de Pesquisas Replicon, Escola de Ciências Agrárias e Biológicas, Pontifícia Universidade Católica de Goiás, Goiânia, GO, Brazil

Correspondence should be addressed to Lee Chen-Chen; [chenleego@yahoo.com.br](mailto:chenleego@yahoo.com.br)

Received 11 May 2018; Revised 25 July 2018; Accepted 2 September 2018; Published 2 October 2018

Guest Editor: Claudio Tabolacci

Copyright © 2018 Flávio Fernandes Veloso Borges et al. This is an open access article distributed under the Creative Commons Attribution License, which permits unrestricted use, distribution, and reproduction in any medium, provided the original work is properly cited.

Silymarin (SM), a standardized extract derived from *Silybum marianum* (L.) Gaertn, is primarily composed of flavonolignans, with silibinin (SB) as its major active constituent. The present study aimed to evaluate the antigenotoxic activities of SM and SB using the alkaline comet assay in whole blood cells and to assess their effects on the expression of genes associated with carcinogenesis and chemopreventive processes. Different concentrations of SM or SB (1.0, 2.5, 5.0, and 7.5 mg/ml) were used in combination with the DNA damage-inducing agent methyl methanesulfonate (MMS, 800  $\mu$ M) to evaluate their genoprotective potential. To investigate the role of SM and SB in modulating gene expression, we performed quantitative real-time PCR (qRT-PCR) analysis of five genes that are known to be involved in DNA damage, carcinogenesis, and/or chemopreventive mechanisms. Treatment with SM or SB was found to significantly reduce the genotoxicity of MMS, upregulate the expression of *PTEN* and *BCL2*, and downregulate the expression of *BAX* and *ABL1*. We observed no significant changes in *ETV6* expression levels following treatment with SM or SB. In conclusion, both SM and SB exerted antigenotoxic activities and modulated the expression of genes related to cell protection against DNA damage.

## 1. Introduction

According to the World Health Organization, 70% to 95% of the world's population rely on traditional medicine for primary health care, and most health practices involve the use of plant extracts or their active components [1]. *Silybum marianum* (L.) Gaertn, popularly known as milk thistle, is one of the most widely used herbs worldwide. *S. marianum* has been well-known since ancient times and has been mostly used in traditional European and Asian medicine for treatment of liver disorders [2].

The medicinal properties of *S. marianum* are attributed to its ability to accumulate bioactive flavonolignan complexes, which are referred to as silymarin (SM). *S. marianum* contains approximately 70% to 80% flavonolignans (silymarin complex), small amounts of flavonoids, 20% to 30% fatty acids, and other polyphenolic compounds. The flavonolignan mixture present in *S. marianum* mainly consists of silibinin (SB), also known as silibinin, the major bioactive component of the extract. Milk thistle extract is currently marketed worldwide as silymarin and silibinin under various trade names, such as Siliphos, Silipide, and Legalon [3].

The effects of SM and SB have been investigated in mice, rats, rabbits, and dogs and results demonstrated that their acute, subacute, and chronic toxicities are very low. SM and SB are primarily used for the treatment of various liver disorders that are characterized by degenerative necrosis and functional impairment, such as chronic inflammatory diseases, cirrhosis, and toxic liver damage [4]. In addition, SM and SB are well documented to exhibit various biological and pharmacological activities, including antioxidant [5], antidiabetic [6], anti-inflammatory, and immunomodulatory effects [7].

The pharmacological activities and toxicological safety of SM and SB have been extensively studied both *in vitro* and *in vivo*. However, little is known about their protective effects on the genetic material. Numerous phytochemicals have been reported to interfere with specific stages of carcinogenesis, and multiple mechanisms have been shown to account for the anticarcinogenic properties of dietary constituents [8].

Analysis of genes related to DNA damage, carcinogenesis, and/or chemoprevention can help elucidate the mechanisms by which dietary supplements can exert protective effects on DNA [9–13]. Thus, given the limited knowledge of the chemopreventive effects of SM and SB, analysis of the expression patterns of the tumor suppressors genes *ETV6* and *PTEN*, the cell death regulators *BCL2* and *BAX* (pro/apoptotic processes), and the protooncogene *ABL1* can reveal the molecular basis underlying the effects of SM and SB.

Considering the biological activities presented by SM and SB, as well as their widespread use as herbal medicines, the present study aimed to evaluate the antigenotoxic activities of SM and SB using the comet assay and to evaluate the expression patterns of genes that are known to be associated with carcinogenesis and chemopreventive processes.

## 2. Material and Methods

**2.1. Chemicals.** Silymarin (SM, S0292), silibinin (SB, S0417), RPMI 1640 medium, methyl methanesulfonate (MMS), ethidium bromide, dimethyl sulfoxide (DMSO), NaCl, and Triton X-100 were purchased from Sigma-Aldrich (St. Louis, MO, USA). Low melting point agarose and normal melting point agarose were obtained from Thermo Fisher Scientific (Waltham, MA, USA). Na<sub>2</sub>EDTA, Tris base, and Tris-HCl were purchased from Bio-Rad Laboratories (Hercules, CA, USA).

**2.2. Cell Treatment.** Peripheral blood was obtained through venous puncture from three young and healthy volunteers who had no history of smoking or drinking. Our work was approved by the Human and Animal Research Ethics Committee of the Universidade Federal de Goiás (CEPMHA/HC/UFG n. 016/2011). Whole blood was treated with varying concentrations of SM or SB (1.0, 2.5, 5.0, and 7.5 mg/ml) in combination with 800  $\mu$ M MMS and subsequently incubated for 3 h at 37°C and 5% CO<sub>2</sub> in RPMI medium containing 15% (v/v) fetal calf serum. The positive (MMS) and negative (DMSO) control groups were included. The experiment was performed in triplicate. The

MMS concentration of 800  $\mu$ M used in the present study was selected based on its previously demonstrated effectiveness in inducing DNA damage [17].

**2.3. Comet Assay.** The alkaline version of the comet assay was performed according to the protocol described by Singh and coworkers [18] with slight modifications. For antigenotoxicity evaluation, cells were treated with SM and SB, concomitant with the positive control, in order to verify the possible reduction of DNA damage caused by MMS. Briefly, after cell treatment, slides coated with normal melting point agarose (1.5%) were added with a mixture containing 15  $\mu$ l of blood and 130  $\mu$ l of low melting point agarose (0.5%) and incubated at 37°C. The mixture was spread on the slides with coverslips and placed in a cold chamber. Afterwards, the coverslips were carefully removed, and the slides were immersed in lysis solution protected from light (1% Triton X-100, 10% DMSO, 2.5 M NaCl, 100 mM EDTA-Na<sub>2</sub>, and 10 mM Tris) at 4°C for 4 h. Subsequently, the slides were incubated with freshly prepared alkaline solution buffer (300 mM NaOH and 1 mM EDTA, pH > 13) at 4°C for 20 min to unwind the DNA. Samples were then subjected to electrophoresis in the same buffer at 1 V/cm and the current of 300 mA for 30 min in the dark. After electrophoresis, the slides were placed on a staining tray, covered with neutralizing buffer (0.4 M Tris-HCl, pH 7.5), and kept in the dark for 5 min. For analysis, the slides were stained with 20  $\mu$ l of ethidium bromide solution (0.02 mg/ml) and covered with a cover slip. A total of 50 nucleoids were analyzed per slide, corresponding to 100 nucleoids per sample.

The analysis was performed on a fluorescence microscopy system Axioplan-Imaging® (Carl Zeiss AG, Germany) using the Isis software with an excitation filter of 510-560 nm and a barrier filter of 590 nm under 20 $\times$  magnification. To assess genomic damage, we used the TriTek Comet Score™ software (version 1.5), in which pixels intensities are used to estimate the degree of genomic damage and are given as arbitrary units. The nucleoids with completely fragmented heads were not included in the analysis.

From the 17 parameters provided by the software, we selected the percentage of DNA in the tail for assessing DNA damage. This parameter has been proposed by several authors to be the most useful parameter because it provides a quantitative measure of DNA damage (from 0 to 100%) [19].

**2.4. Calculation of DNA Damage Reduction Percentage in Comet Test.** For antigenotoxicity assessment, the percentage of reduction in MMS-induced damage by SM and SB was calculated according to Waters et al., 1990 [20], using the following formula:

$$\% \text{ Reduction} = \left( \frac{(A - B)}{(A - C)} \right) \times 100 \quad (1)$$

where A corresponds to the DNA damage observed following treatment with MMS (positive control), B represents the group treated with SM or SB plus MMS, and C represents the negative control.

**2.5. RNA Extraction and cDNA Synthesis.** After treatment, human blood samples were transferred to tubes provided by GeneJET™ Whole Blood RNA Purification Mini Kit (Thermo Fisher Scientific, Inc., USA). RNA extraction was performed according to the manufacturer's instructions. Afterwards, the final RNA concentration was determined using a spectrophotometer NanoVuePlus™ (GE Healthcare, USA). RNA purity and integrity were assessed via 3% agarose gel electrophoresis. To ensure the purity of the RNA, the A260/A230 and A260/A280 absorbance ratios were evaluated. cDNA synthesis was performed using 1 µg of total RNA in a 10 µL sample volume using RT2 First Strand Kit® (PreAnalytix QIAGEN/BD Company, Germany) as recommended by the manufacturer. Amplified cDNA was stored at -20°C.

**2.6. Quantitative Real-Time PCR (qRT-PCR) Design and Test.** Customized qRT-PCR assay was performed using 96-well-plates. We analyzed five target genes (*ETV6*, *PTEN*, *ABLI*, *BAX*, and *BCL2*) using *GAPDH* as reference gene. In addition, the plates contained a genomic DNA control, a reverse-transcription control, and a positive PCR control.

The qRT-PCR using cDNA derived from treated human whole blood cells was performed using the RT2 SYBR Green Master Mix Kit® (PreAnalytix QIAGEN/BD Company, Germany) according to the manufacturer's instructions. Array-based qRT-PCR analysis was performed in 28 µL reaction volumes containing 1 µL of cDNA and 14 µL of RT2 SYBR Green Master Mix. Subsequently, 25 µL of PCR mix was added to each well of the RT2 Profiler PCR Array. Reactions were run on Bio-Rad's IQ5 real-time thermal cycler using the following cycling conditions: 1 cycle at 95°C for 10 min; 40 cycles of 15 s at 95°C; and 1 min at 60°C. The melting curve was performed as follows: 1 cycle of 1 min at 95°C, 2 min at 65°C, and 2 min at 65°C for 95°C. Results were obtained using iQ5® Optical System software version 2.1 and exported using Microsoft Excel (Microsoft Corporation, USA). Gene expression analysis was carried out using the comparative  $\Delta\Delta C_t$  method.

The cycle threshold ( $C_t$ ) values were exported to the PCR Array Data Analysis Web Portal (<http://dataanalysis.sabiosciences.com/pcr/arrayanalysis.php>). First, gene expression levels for each sample were normalized against those of the reference gene *GAPDH* ( $\Delta C_t$ ).  $C_t$  data was used as an input, and the web-based software will automatically perform quantification using the  $\Delta\Delta C_t$  method (using positive control MMS treatment as standard sample). The fold change was calculated for each gene for all group samples.

**2.7. Statistical Analysis.** For the comet assay, treatment and control groups were analyzed by performing one-way ANOVA, followed by Tukey's test. Statistical significance was considered at  $P < 0.05$ . All statistical analyses were conducted using GraphPad Prism 5.0.

For gene expression analysis via qRT-PCR, gene expression levels corresponding to each cotreatment (positive control + silymarin or silibinin) were compared relative to

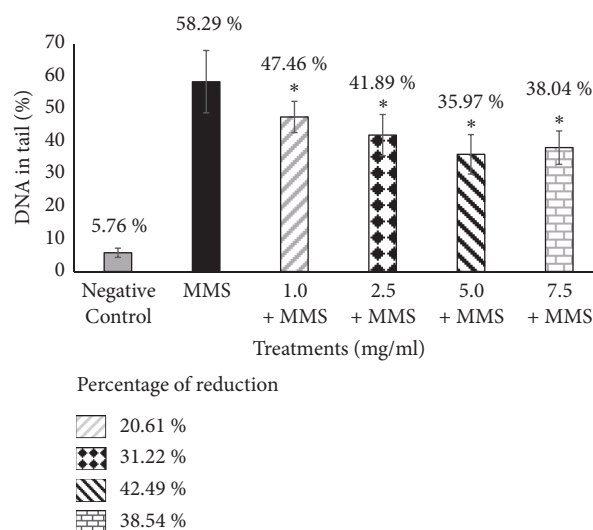


**FIGURE 1: Evaluation of the antigenotoxic effects of silymarin by comet assay.** Results are expressed as mean  $\pm$  standard deviation (SD). Percentage reduction in MMS-induced damage by SM. Negative control: 100 µL of dimethylsulfoxide (DMSO) + sterile distilled water (1:1). Positive control: methyl methanesulfonate (MMS) (800 µM). \*  $P < 0.05$  versus MMS.

the positive control (MMS) by performing the Student's  $t$ -test. The fold change values were calculated using the  $\Delta\Delta C_t$  method. A fold change  $> 2.0$  or  $P < 0.05$  was considered significant.

### 3. Results

**3.1. Modulation of MMS-Induced DNA Damage by Silymarin and Silibinin.** Assessment of the antigenotoxicity of SM and SB via the alkaline comet assay demonstrated reduced DNA damage (% DNA in tail) in cells cotreated with SM or SB and MMS relative to cells treated with the positive control MMS alone (Figures 1 and 2).

Treatment with the standardized extract (SM) significantly reduced DNA damage for all tested concentrations of the compound when combined with MMS relative to treatment with MMS alone. SB, the major active constituent of SM, also exerted significant protective effect against DNA damage induced by the genotoxic agent MMS, except at a lower concentration (1.0 mg/ml) (Figures 1 and 2). The percentage of DNA in tail ranged from 47.46% to 38.04% for SM with MMS and 49.22% to 40.32% for SB with MMS. The percent reduction in DNA damage ranged from 20.61% to 38.54% for SM with MMS and 17.26% to 34.20% for SB with MMS when compared to treatment with MMS alone (58.29% DNA in tail).

**3.2. Effects of Silymarin and Silibinin in Combination with MMS on Gene Expression in Human Blood Cells.** We evaluated the expression levels of the following five genes associated with DNA damage, carcinogenesis, and/or chemoprevention mechanisms: the tumor suppressors *ETV6* and



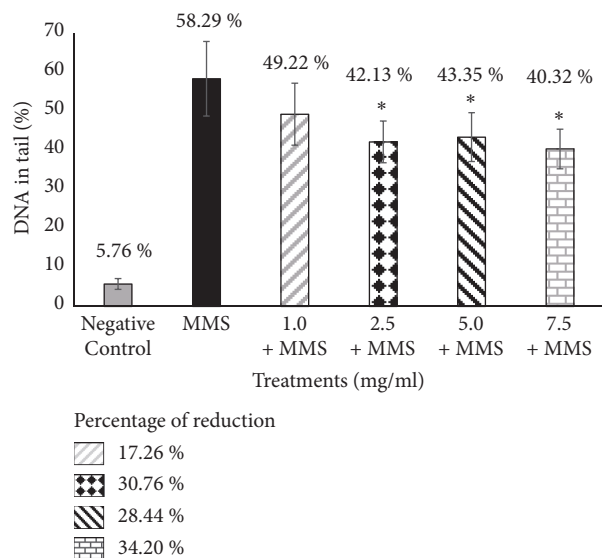


**FIGURE 2: Evaluation of the antigenotoxic effects of silibinin by the comet assay.** Results are expressed as mean  $\pm$  standard deviation (SD). Percentage reduction in MMS-induced damage by SB. Negative control: 100  $\mu$ L of dimethylsulfoxide (DMSO) + sterile distilled water (1:1). Positive control: methyl methanesulfonate (MMS) (800  $\mu$ M). \*  $P < 0.05$  versus MMS.

*PTEN*, the cell death regulators *BCL2* and *BAX* (anti- and proapoptotic, respectively), and the protooncogene *ABL1*.

Expression levels of the tumor suppressor *ETV6* gene (Figures 3 and 4) were not significantly altered in all samples treated with varying concentrations of SM + MMS or SB + MMS relative to those treated with MMS alone. However, results showed that the expression levels of the tumor suppressor gene *PTEN* were significantly upregulated following cotreatment with high SM concentrations (5.0 and 7.5 mg/ml) and the highest SB concentration (7.5 mg/ml), corresponding to fold change values of 2.71, 3.07, and 2.33, respectively (Figures 3 and 4).

Treatment with SM and SB at all concentrations was found to upregulate the expression of the antiapoptotic gene *BCL2* up to threefold relative to the positive control, similar to the expression values obtained for the negative control. In addition, expression of the proapoptotic gene *BAX* was significantly downregulated following treatment with SM at the highest concentration and SB at all tested concentrations (Figures 3 and 4).

Furthermore, results demonstrated that the expression of *ABL1*, an apoptosis promoter and cell growth inhibitor gene, was significantly downregulated when human whole blood cells were treated with the highest concentration of SB or SM (7.5 mg/ml) (Figures 3 and 4).

#### 4. Discussion

Many antioxidants are known to inhibit DNA damage by scavenging reactive oxygen species (ROS) that are generated inside the cell [21]. Several plant species have been reported as reliable sources of antioxidants, and multiple

studies have demonstrated that plant compounds promote genomic stability through various mechanisms [11–13, 22]. Silymarin (SM) and silibinin (SB) are known to exhibit strong antioxidant activities [5], and their protective effects against ROS have been demonstrated using different cell types, including mouse lymphocytes and human platelets [16, 23–25]. Furthermore, treatment with SM and SB was found to enhance the activity of endogenous antioxidant enzymes, including glutathione peroxidase [26], which in turn inhibits ROS production. Therefore, the present study aimed to evaluate the antigenotoxic activities of SM and SB using the comet assay and to assess their effects on the expression pattern of genes associated with carcinogenesis and chemopreventive processes.

To evaluate the chemopreventive effects of SB and SM on the DNA, human whole blood cells were treated with SB or SM in combination with methyl methanesulfonate (MMS). MMS is an alkylating agent that induces damage to genetic material and forms monoadducts with the nucleophilic centers of DNA [27]. Damage to the genetic material is highly associated with enhanced ROS production, as well as methylation at the N-7 position of guanine (N7MeG), at the N-3 position of adenine (N3MeA), and at the O-6 position of guanine (O6MeG) [14, 15]. A previous study on human lymphocytes and sperm cells indicated that MMS exposure promoted DNA damage based on the comet assay (increased Olive Tail Moment and % DNA in tail) and triggered the apoptotic response by upregulating the expression of *TP53* and *CDKN1A* and downregulating the expression of *BCL2* [28].

Our results showed that both the complex (SM extract) and its main active constituent (SB), cotreated with MMS, exerted protective effects by reducing the amount of DNA in the comet tail in 42.49% and 34.20% respectively, when compared to positive control (MMS). Previous studies also demonstrated the protective effects of SM and SB. In particular, SM and SB significantly decreased point mutations based on the Ames test and reduced the proportion of micronucleated polychromatic erythrocytes based on the mice bone marrow assay [29]. Furthermore, SB was demonstrated to exert protective effects against  $\gamma$ -radiation-induced strand breaks in plasmid DNA, reduce DNA damage and micronuclei formation in human lymphocytes and rat leukocytes, and reduce mouse mortality and DNA damage in blood leukocytes following whole-body  $\gamma$ -exposure in mice [16, 30].

In addition, the current findings revealed that the extract complex (SM) exerted slightly stronger antigenotoxic activity compared to the primary active constituent (SB); however, the observed difference was not statistically significant. Our current findings were consistent with those of a previous study, which demonstrated that “high purity” milk thistle extracts exerted weaker antioxidant activity relative to the complex extract [29]. The above results suggest that the SM extract contains compounds other than SB that contribute to the antioxidant potential of SM. The final response of a treatment with a plant extract is a result of synergistic, antagonistic, and other interactive effects among plant biologically active compounds present in the extract and the cell machinery [31].

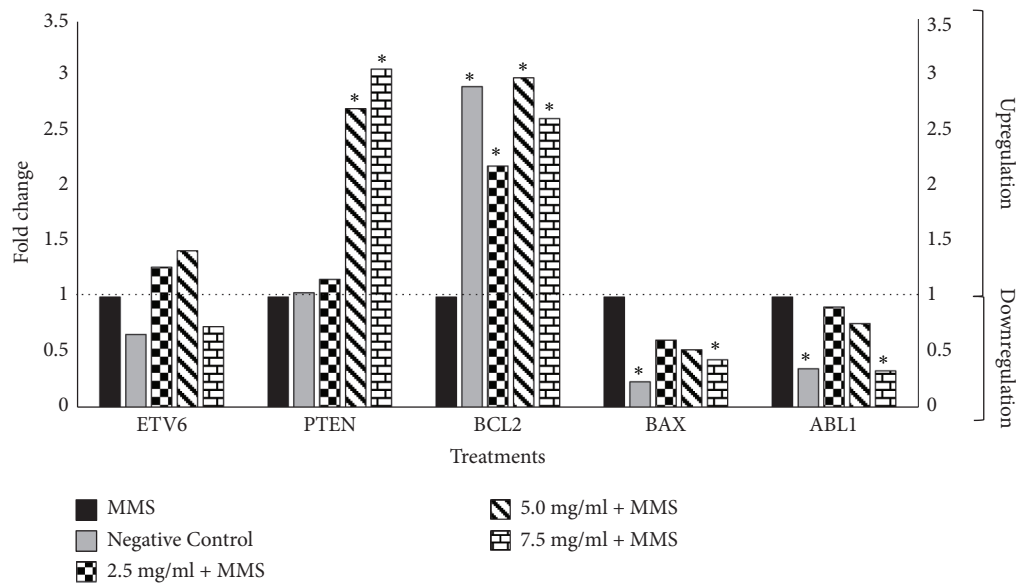


**FIGURE 3: Effects of combined treatment with MMS and silymarin on gene expression relative to MMS alone.** Positive control: methyl methanesulfonate (MMS) (800  $\mu$ M). Negative control: 100  $\mu$ L of dimethylsulfoxide (DMSO) + sterile distilled water (1:1). Expression values greater than one indicate upregulation, while expression values less than one indicate downregulation in the test sample relative to the positive control. \*  $P < 0.05$  versus MMS.

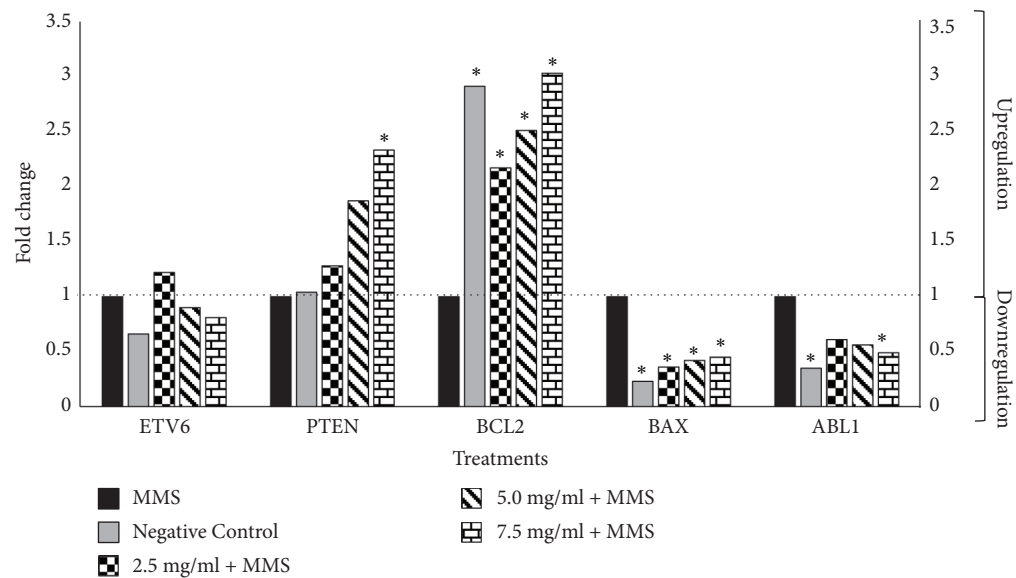


**FIGURE 4: Effects of combined treatment with MMS and silibinin on gene expression relative to MMS alone.** Positive control: methyl methanesulfonate (MMS) (800  $\mu$ M). Negative control: 100  $\mu$ L of dimethylsulfoxide (DMSO) + sterile distilled water (1:1). Expression values greater than one indicate upregulation, while expression values less than one indicate downregulation in the test sample relative to the positive control. \*  $P < 0.05$  versus MMS.

To elucidate the effects of cotreatment with MMS and SM or SB, we evaluated the expression levels of five genes that are specifically known to mediate chemoprevention and response to DNA damage.

The tumor suppressor gene *ETV6* (ets variant gene 6) encodes a protein that functions as a transcriptional regulator by binding to a specific DNA sequence. Our current findings revealed that the *ETV6* expression patterns were

not significantly altered following treatment with any tested concentration of SM and SB when compared to the positive control, indicating that SM and SB did not influence *ETV6* expression.

The *PTEN* (phosphatase and tensin homolog) gene is a tumor suppressor involved in cell migration and proliferation inhibition and participates in the modulation of cell growth and apoptosis. The essential role of nuclear PTEN in

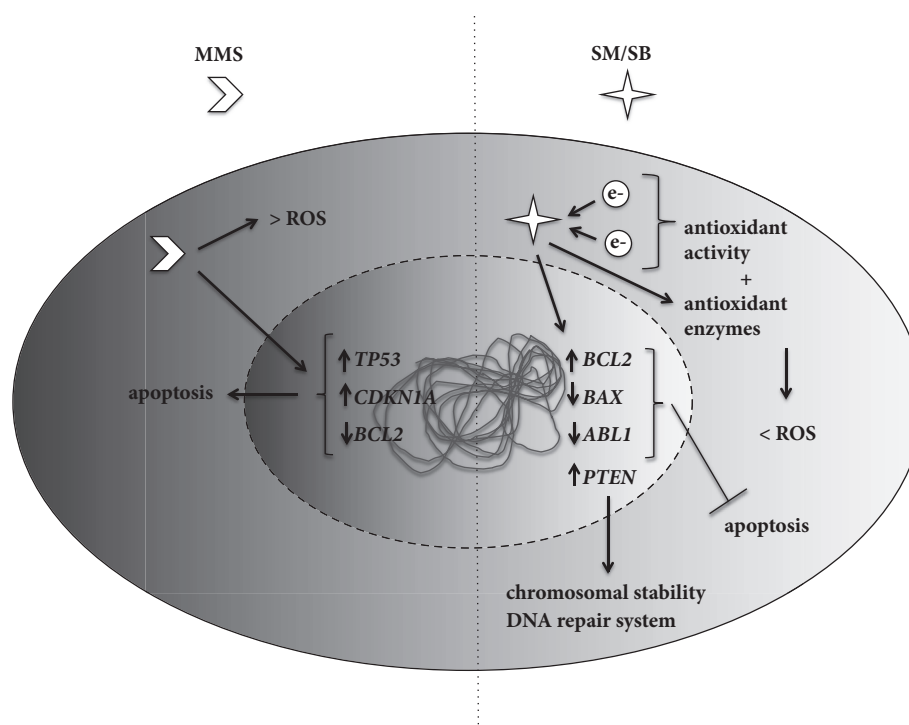


FIGURE 5: **Schematic representation of the effects of silymarin and silibinin on chemopreventive mechanisms.** While methyl methanesulfonate (MMS) is highly associated with enhanced reactive oxygen species (ROS) production [14] and apoptotic response [15], silymarin (SM) and silibinin (SB) exhibit strong antioxidant activities [5, 16] and can prevent apoptosis and influence the genomic stability and the DNA repair system.

maintaining chromosomal stability has been demonstrated in both mouse and human systems [32]. According to Yin and Shen [33], nuclear PTEN may utilize two mechanisms to maintain chromosome integrity. First, PTEN interacts with centromeres and maintains their stability through its C2 domain. Second, PTEN may be necessary for DNA repair, since loss of *PTEN* leads to a high proportion of double-strand breaks. Our results demonstrated significant upregulation of *PTEN* expression following treatment with high concentrations of SM or SB, what could contribute to explain the anticytotoxic and antigenotoxic properties of SM and SB. Also, these data allow us to infer that these protective effects may also help in the regulation and preservation of DNA in cells that are in the active process of cell division as shown in a study using mice bone marrow cells, in which SM and SB reduced the frequency of micronucleated cells [29].

The Bcl-2 family comprises proapoptotic and antiapoptotic proteins. BCL2 (B-cell lymphoma protein 2) is associated with programmed cell death inhibition in various cell types. The antiapoptotic function of BCL2 appears to be mediated by its ability to heterodimerize with other Bcl-2 family members, especially BAX (BCL-2 associated X protein). BCL2 prevents the oligomerization of BAX, which normally causes the release of several mitochondrial apoptogenic molecules [34]. Our results showed that treatment with SM or SB significantly upregulated *BCL2* expression at all tested concentrations. MMS is known to downregulate *BCL2* expression [15]; however, SM and SB can upregulate the

expression of this survival factor by interacting with the *BCL2* promoter, which harbors several putative responsive sites, or through an indirect pathway. In addition, treatment with SM or SB significantly downregulated the expression of *BAX*, thereby suggesting that SM and SB can prevent apoptosis and act as chemoprotective agents. Previous studies demonstrated the modulatory effects of SM and SB on cell survival and apoptosis via interference with the expression of cell cycle regulators and proteins involved in apoptosis [6, 35–37].

The *ABL1* gene is a protooncogene that encodes a protein tyrosine kinase known to be involved in various cellular processes, including cell division, adhesion, differentiation, and stress response. Nuclear ABL proteins modulate cellular responses induced by DNA damage and are known to participate in cell growth inhibition and apoptosis promotion [38]. In the present study, treatment with the highest tested concentration of SM and SB was found to significantly downregulate *ABL1* expression relative to treatment with MMS alone, although the lower SM and SB concentrations did not significantly alter *ABL1* expression patterns. The observed downregulation of *ABL1* expression can be associated with the repair of DNA lesions.

The decrease in DNA damage and the modulation of gene expression to protect cells against lesions suggested the roles of SM and SB in the DNA repair system (Figure 5). Thus, the protective effects of both compounds highlighted their potential clinical use as complementary treatment for cancer patients in combination with established treatments

to prevent or reduce the toxicity induced by chemotherapy and/or radiotherapy. However, further studies are required to investigate the effects of SM and SB on the DNA repair system.

## Data Availability

The data used to support the findings of this study are included within the article.

## Ethical Approval

All procedures performed in studies involving human participants were in accordance with the ethical standards of the institutional and/or national research committee and with the 1964 Helsinki declaration and its later amendments or comparable ethical standards.

## Disclosure

This work is part of a thesis made by the author Flávio Fernandes Veloso Borges [39].

## Conflicts of Interest

The authors declare that they have no conflicts of interest.

## Acknowledgments

Flávio Fernandes Veloso Borges was supported with a scholarship from Coordenação de Aperfeiçoamento de Pessoal de Nível Superior (CAPES) and Elisa Flávia Luiz Cardoso Bailão was supported by Universidade Estadual de Goiás with fellowships at the program PROBIP (Scientific Production Support Program). The authors also thank Fundação de Amparo à Pesquisa do Estado de Goiás (FAPEG) for the financial support.

## References

- [1] M. M. Robinson and X. Zhang, *The World Medicines Situation 2011 Traditional Medicines: Global Situation, Issues and Challenges*, World Heal Organ, 2011.
- [2] S. F. AbouZid, S.-N. Chen, and G. F. Pauli, "Silymarin content in *Silybum marianum* populations growing in Egypt," *Industrial Crops and Products*, vol. 83, pp. 729–737, 2016.
- [3] M. Kaur and R. Agarwal, "Silymarin and epithelial cancer chemoprevention: How close we are to bedside?" *Toxicology and Applied Pharmacology*, vol. 224, no. 3, pp. 350–359, 2007.
- [4] F. Fraschini, G. Demartini, and D. Esposti, "Pharmacology of silymarin," *Clinical Drug Investigation*, vol. 22, no. 1, pp. 51–65, 2002.
- [5] E. Köksal, I. Gülçin, S. Beyza, Ö. Sarikaya, and E. Bursal, "In vitro antioxidant activity of silymarin," *Journal of Enzyme Inhibition and Medicinal Chemistry*, vol. 24, no. 2, pp. 395–405, 2009.
- [6] R. Agarwal, C. Agarwal, H. Ichikawa, R. P. Singh, and B. B. Aggarwal, "Anticancer potential of silymarin: from bench to bedside," *Anticancer Research*, vol. 26, no. 6, pp. 4457–4498, 2006.
- [7] L. Radko and W. Cybulski, "Application of silymarin in human and animal medicine," *J Pre-Clinical Clin Res*, vol. 1, pp. 22–26, 2007.
- [8] Y. Surh, "Cancer chemoprevention with dietary phytochemicals," *Nature Reviews Cancer*, vol. 3, no. 10, pp. 768–780, 2003.
- [9] J. C. Mathers, J. M. Coxhead, and J. Tyson, "Nutrition and DNA repair - Potential molecular mechanisms of action," *Current Cancer Drug Targets*, vol. 7, no. 5, pp. 425–431, 2007.
- [10] S. Guarnieri, S. Loft, P. Riso et al., "DNA repair phenotype and dietary antioxidant supplementation," *British Journal of Nutrition*, vol. 99, no. 5, pp. 1018–1024, 2008.
- [11] R. Kotecha, A. Takami, and J. L. Espinoza, "Dietary phytochemicals and cancer chemoprevention: a review of the clinical evidence," *Oncotarget*, vol. 7, no. 32, pp. 52517–52529, 2016.
- [12] T. J. Yates, L. E. Lopez, S. D. Lokeshwar et al., "Dietary Supplement 4-Methylumbelliferone: An Effective Chemopreventive and Therapeutic Agent for Prostate Cancer," *Journal of the National Cancer Institute*, vol. 107, no. 7, Article ID djv085, 2015.
- [13] J. W. Fahey and T. W. Kensler, "Role of dietary supplements/nutraceuticals in chemoprevention through induction of cytoprotective enzymes," *Chemical Research in Toxicology*, vol. 20, no. 4, pp. 572–576, 2007.
- [14] D. Fu, J. A. Calvo, and L. D. Samson, "Balancing repair and tolerance of DNA damage caused by alkylating agents," *Nature Reviews Cancer*, vol. 12, no. 2, pp. 104–120, 2012.
- [15] A. Kitanovic, T. Walther, M. O. Loret et al., "Metabolic response to MMS-mediated DNA damage in *Saccharomyces cerevisiae* is dependent on the glucose concentration in the medium," *FEMS Yeast Research*, vol. 9, no. 4, pp. 535–551, 2009.
- [16] M. Bijak, E. Synowiec, P. Sitarek, T. Sliwiński, and J. Saluk-Bijak, "Evaluation of the cytotoxicity and genotoxicity of flavonolignans in different cellular models," *Nutrients*, vol. 9, no. 12, 2017.
- [17] Y. Jiang, S. Shan, L. Chi et al., "Methyl methanesulfonate induces necroptosis in human lung adenoma A549 cells through the PIG-3-reactive oxygen species pathway," *Tumor Biology*, vol. 37, no. 3, pp. 3785–3795, 2016.
- [18] N. P. Singh, M. T. McCoy, R. R. Tice, and E. L. Schneider, "A simple technique for quantitation of low levels of DNA damage in individual cells," *Experimental Cell Research*, vol. 175, no. 1, pp. 184–191, 1988.
- [19] A. Collins, G. Koppen, V. Valdiglesias et al., "The comet assay as a tool for human biomonitoring studies: The ComNet Project," *Mutation Research - Reviews in Mutation Research*, vol. 759, no. 1, pp. 27–39, 2014.
- [20] M. D. Waters, A. L. Brady, H. F. Stack, and H. E. Brockman, "Antimutagenicity profiles for some model compounds," *Mutation Research/Reviews in Genetic Toxicology*, vol. 238, no. 1, pp. 57–85, 1990.
- [21] A. Svobodová, A. Zdařilová, J. Mališková, H. Mikulková, D. Walterová, and J. Vostalová, "Attenuation of UVA-induced damage to human keratinocytes by silymarin," *Journal of Dermatological Science*, vol. 46, no. 1, pp. 21–30, 2007.
- [22] L. R. Ferguson, "Role of plant polyphenols in genomic stability," *Mutation Research*, vol. 475, no. 1–2, pp. 89–111, 2001.
- [23] Š. Chlopčíková, J. Psotová, P. Míketová, and V. Šimánek, "Chemoprotective Effect of Plant Phenolics against Anthracycline-induced Toxicity on Rat Cardiomyocytes. Part I. Silymarin and its Flavonolignans," *Phytotherapy Research*, vol. 18, no. 2, pp. 107–110, 2004.
- [24] A. Pietrangelo, F. Borella, G. Casalgrandi et al., "Antioxidant activity of silybin in vivo during long-term iron overload in rats," *Gastroenterology*, vol. 109, no. 6, pp. 1941–1949, 1995.



- [25] P. Tiwari, A. Kumar, M. Ali, and K. Mishra, "Radioprotection of plasmid and cellular DNA and Swiss mice by silibinin," *Mutation Research - Genetic Toxicology and Environmental Mutagenesis*, vol. 695, no. 1-2, pp. 55-60, 2010.
- [26] J. Zhao, M. Lahiri-Chatterjee, Y. Sharma, and R. Agarwal, "Inhibitory effect of a flavonoid antioxidant silymarin on benzoyl peroxide-induced tumor promotion, oxidative stress and inflammatory responses in SENCAR mouse skin," *Carcinogenesis*, vol. 21, no. 4, pp. 811-816, 2000.
- [27] D. T. Beranek, "Distribution of methyl and ethyl adducts following alkylation with monofunctional alkylating agents," *Mutation Research - Fundamental and Molecular Mechanisms of Mutagenesis*, vol. 231, no. 1, pp. 11-30, 1990.
- [28] K. Habas, M. Najafzadeh, A. Baumgartner, M. H. Brinkworth, and D. Anderson, "An evaluation of DNA damage in human lymphocytes and sperm exposed to methyl methanesulfonate involving the regulation pathways associated with apoptosis," *Chemosphere*, vol. 185, pp. 709-716, 2017.
- [29] F. F. V. Borges, C. R. Silva, J. H. Vêras, C. G. Cardoso, A. D. da Cruz, and L. C. Chen, "Antimutagenic, Antigenotoxic, and Anticytotoxic Activities of *Silybum Marianum* [L.] Gaertn Assessed by the Salmonella Mutagenicity Assay (Ames Test) and the Micronucleus Test in Mice Bone Marrow," *Nutrition and Cancer*, vol. 68, no. 5, pp. 848-855, 2016.
- [30] V. A. Toğay, T. S. Sevimli, M. Sevimli, D. A. Çelik, and N. Özçelik, "DNA damage in rats with streptozotocin-induced diabetes; protective effect of silibinin," *Mutation Research - Genetic Toxicology and Environmental Mutagenesis*, vol. 825, pp. 15-18, 2018.
- [31] T. Walle, "Absorption and metabolism of flavonoids," *Free Radical Biology & Medicine*, vol. 36, no. 7, pp. 829-837, 2004.
- [32] W. H. Shen, A. S. Balajee, J. Wang et al., "Essential Role for Nuclear PTEN in maintaining chromosomal integrity," *Cell*, vol. 128, no. 1, pp. 157-170, 2007.
- [33] Y. Yin and W. H. Shen, "PTEN: a new guardian of the genome," *Oncogene*, vol. 27, no. 41, pp. 5443-5453, 2008.
- [34] R. J. Youle and A. Strasser, "The BCL-2 protein family: opposing activities that mediate cell death," *Nature Reviews Molecular Cell Biology*, vol. 9, no. 1, pp. 47-59, 2008.
- [35] Z.-L. Bai, V. Tay, S.-Z. Guo, J. Ren, and M.-G. Shu, "Silibinin Induced Human Glioblastoma Cell Apoptosis Concomitant with Autophagy through Simultaneous Inhibition of mTOR and YAP," *BioMed Research International*, vol. 2018, Article ID 6165192, 10 pages, 2018.
- [36] H. Cui, T. Li, H. Guo et al., "Silymarin-mediated regulation of the cell cycle and DNA damage response exerts antitumor activity in human hepatocellular carcinoma," *Oncology Letters*, vol. 15, no. 1, pp. 885-892, 2018.
- [37] R. Haddadi, A. M. Nayeibi, and S. Eyvari Brooshghalan, "Silymarin prevents apoptosis through inhibiting the Bax/caspase-3 expression and suppresses toll like receptor-4 pathway in the SNC of 6-OHDA intoxicated rats," *Biomedicine & Pharmacotherapy*, vol. 104, pp. 127-136, 2018.
- [38] S. Panjarian, R. E. Iacob, S. Chen, J. R. Engen, and T. E. Smithgall, "Structure and dynamic regulation of abl kinases," *The Journal of Biological Chemistry*, vol. 288, no. 8, pp. 5443-5450, 2013.
- [39] F. F. V. Borges, *Atividades antimutagênica, antigenotóxica e anticitotóxica de Silybum marianum (L.) Gaertn e sua influência na expressão de genes de resposta a danos no DNA [Ph.D. thesis]*, Universidade Federal de Goiás, 2015.

## Research Article

# $\alpha$ -Hederin Arrests Cell Cycle at G2/M Checkpoint and Promotes Mitochondrial Apoptosis by Blocking Nuclear Factor- $\kappa$ B Signaling in Colon Cancer Cells

Dongdong Sun,<sup>1,2</sup> Weixing Shen,<sup>1,2</sup> Feng Zhang,<sup>3</sup> Huisen Fan,<sup>1,3</sup> Jiani Tan,<sup>1,2</sup> Liu Li,<sup>1,2</sup> Changliang Xu,<sup>1,2</sup> Haibin Zhang,<sup>1,3</sup> Ye Yang <sup>2,4</sup> and Haibo Cheng <sup>1,2</sup>

<sup>1</sup>The First Clinical Medical College, Nanjing University of Chinese Medicine, Nanjing 210023, China

<sup>2</sup>Key Laboratory of Famous Doctors' Proved Recipe Evaluation and Transformation under State Administration of Traditional Chinese Medicine, Jiangsu Provincial Laboratory of Proved Anticarcinoma Recipe Research and Industrialization Engineering, Jiangsu Collaborative Innovation Center of Traditional Chinese Medicine Prevention and Treatment of Tumor, Nanjing University of Chinese Medicine, Nanjing 210023, China

<sup>3</sup>College of Pharmacy, Nanjing University of Chinese Medicine, Nanjing 210023, China

<sup>4</sup>School of Medicine and Life Sciences, Nanjing University of Chinese Medicine, Nanjing 210023, China

Correspondence should be addressed to Ye Yang; yangye876@sina.com and Haibo Cheng; hbcheng\_njucm@163.com

Received 3 April 2018; Revised 8 June 2018; Accepted 12 September 2018; Published 27 September 2018

Guest Editor: Claudio Tabolacci

Copyright © 2018 Dongdong Sun et al. This is an open access article distributed under the Creative Commons Attribution License, which permits unrestricted use, distribution, and reproduction in any medium, provided the original work is properly cited.

Colon cancer represents the third most common malignancy worldwide. New drugs with high efficaciousness and safety for the treatment of colon cancer are urgently needed in clinical context. Here, we were aimed to evaluate the antitumor activity of the natural compound  $\alpha$ -hederin in human colon cancer cells. We treated SW620 cells with interleukin-6 (IL-6) *in vitro* to mimic the paracrine inflammatory microenvironment of tumor cells.  $\alpha$ -Hederin concentration dependently reduced the viability of IL-6-stimulated SW620 cells.  $\alpha$ -Hederin increased the number of IL-6-stimulated SW620 cells at the G2/M phase and reduced the mRNA and protein expression of cyclin B1 and CDK1. Moreover,  $\alpha$ -hederin induced apoptosis and loss of mitochondrial membrane potential in IL-6-stimulated SW620 cells.  $\alpha$ -Hederin downregulated Bcl-2 expression, upregulated Bax expression, and promoted cytochrome c release from mitochondria into cytoplasm. Additionally,  $\alpha$ -hederin elevated the levels of cleaved-caspase-9, cleaved-caspase-3, and cleaved-PARP, but had little effects on the levels of cleaved-caspase-8. Moreover,  $\alpha$ -hederin prevented the nuclear translocation of nuclear factor- $\kappa$ B (NF- $\kappa$ B) and reduced the phosphorylation of I $\kappa$ B $\alpha$  and IKK $\alpha$ , suggesting the blockade of NF- $\kappa$ B signaling. NF- $\kappa$ B inhibitor PDTC not only produced similar proapoptotic effects on IL-6-stimulated SW620 cells as  $\alpha$ -hederin did, but also synergistically enhanced  $\alpha$ -hederin's proapoptotic effects. Furthermore,  $\alpha$ -hederin inhibited the phosphorylation of ERK in IL-6-stimulated SW620 cells, which was involved in  $\alpha$ -hederin blockade of NF- $\kappa$ B nuclear translocation. Altogether,  $\alpha$ -hederin suppressed viability, induced G2/M cell cycle arrest, and stimulated mitochondrial and caspase-dependent apoptosis in colon cancer cells, which were associated with disruption of NF- $\kappa$ B and ERK pathways, suggesting  $\alpha$ -hederin as a promising candidate for intervention of colon cancer.

## 1. Introduction

Colon cancer represents the third most frequently diagnosed malignancy all over the world. Although the incidence has been decreased during the past decade, colon cancer still has considerably high morbidity compared with other cancers [1]. Despite the surgical resection as a primary curative management for the early stage of colon cancer,

a growing number of patients are in the advanced stage at the time of diagnosis because of the lack of effective screening [2]. Chemotherapy still serves as a common therapeutic strategy for colon cancer. Unfortunately, many patients eventually relapse, and chemotherapy resistance occurs [3]. Thus, development of novel agents with high efficaciousness and safety against colon cancer is of extreme importance.

Apoptosis is a genetically controlled cell death, playing an important role in regulation of development, cell proliferation, and stress responses [4]. Tumorigenesis has long-termly been linked to alterations of apoptotic pathways [5]. The mechanisms underlying tumor chemotherapy resistance are also largely associated with the activation of antiapoptotic pathways and the sensitivity of tumor cells to drug-induced apoptosis is determined by the balance between the anti-apoptotic and proapoptotic signals [5]. Mitochondria play a pivotal role in apoptosis. During apoptosis, some key events occur in mitochondria, including the loss of mitochondrial membrane potential (MMP), reduced ratio of Bcl-2/Bax, and release of cytochrome c (Cyt c). Particularly, MMP is a key parameter of mitochondrial apoptosis [6]. On the other hand, excessive activation of nuclear factor  $\kappa$ B (NF- $\kappa$ B) has been observed in many solid tumors, especially in colon cancer [7]. NF- $\kappa$ B with transcription activity facilitates the progression of colon cancer by regulating the expression of a range of apoptosis-related genes, including Bcl-2, Bcl-xl, Survivin, etc. NF- $\kappa$ B also mediates survival mechanisms through upregulating antiapoptotic genes. Therefore, NF- $\kappa$ B signaling is a causative factor in chemotherapy resistance [8].

Natural products provide promising candidate agents for cancer chemotherapy.  $\alpha$ -Hederin is a monodesmosidic triterpenoid saponin isolated from the leaves of *Hedera helix*. Recent studies have demonstrated that  $\alpha$ -hederin had multiple pharmacological effects such as anti-virus, anti-oxidation, anti-inflammation, etc. [9, 10]. In current study, we examined the effects of  $\alpha$ -hederin on the fate of colon cancer cells, and to explore the underlying mechanisms focusing on the NF- $\kappa$ B pathway. Because tumorigenesis and progression are commonly driven by inflammatory microenvironment, we treated colon cancer cells with interleukin 6 (IL-6, a well-known inflammatory cytokine) to mimic the inflammatory microenvironment *in vitro*.

## 2. Materials and Methods

**2.1. Reagents and Antibodies.**  $\alpha$ -Hederin of purity over 99% was provided by Shanghai Yuanye Biotechnology Co., Ltd. (Shanghai, China). NF- $\kappa$ B specific inhibitor pyrrolidine dithiocarbamate (PDTC), JAK2/STAT3 signaling specific inhibitor AG490, and ERK specific inhibitor U0126 were obtained from Selleck Chemicals (Houston, TX, USA). Dimethyl sulfoxide (DMSO) was used to dissolve the above compounds for experiments, and single treatment with DMSO was used as negative control. Recombinant human IL-6 cytokine was obtained from Solarbio Life Science (Beijing, China). The primary antibodies used for Western blot analyses against cyclin B1, CDK1, Bcl-2, Bax, Cyt c, cleaved-caspase-9, cleaved-caspase-3, cleaved-caspase-8, cleaved-PARP, NF- $\kappa$ B(p65), p-I $\kappa$ B $\alpha$ , I $\kappa$ B $\alpha$ , p-IKK $\alpha$ , IKK $\alpha$ , p-ERK, ERK, COX IV, lamin B1, and GAPDH were purchased from Bioworld Technology, Inc. (MN, USA).

**2.2. Cell Culture.** Human colon cancer HCT116 and SW620 cells were provided by the Cell Bank of Chinese Academy of Sciences (Shanghai, China). Cells were cultured in

RPMI-1640 medium incubated with 10% fetal bovine serum (FBS), 50 U/ml penicillin, and 50  $\mu$ g/ml streptomycin according to our previous methods [11]. Cells were grown at 37°C in a 5% CO<sub>2</sub> incubator.

**2.3. Cell Viability Assay.** HCT116 or SW620 cells were seeded in 96-well plates and then treated with vehicle, IL-6, and/or  $\alpha$ -hederin, or AG490 at different concentrations for 24 h. Cell Counting Kit-8 (Nanjing Enogene Biotechnology Co., Ltd., Nanjing, China) was used to evaluate cell viability according to the protocol as we previously reported [11]. The spectrophotometric absorbance at 450 nm was determined using a SPECTRAMax™ microplate spectrophotometer (Molecular Devices, Sunnyvale, CA, USA). Cell viability was presented as the percentage of control values.

**2.4. Cell Cycle Analysis by Flow Cytometry.** SW620 cells were seeded in 6-well plates and then treated with vehicle, IL-6, and/or  $\alpha$ -hederin at different concentrations for 24 h. Cells were fixed, and cell cycles were monitored using a cellular DNA flow cytometric analysis kit (Nanjing KeyGen Biotech Co., Ltd., Nanjing, China) in accordance with the protocol. Percentages of cells within the G0/G1, S, and G2/M phases were detected using flow cytometry (FACSCalibur; Becton, Dickinson and Company, Franklin Lakes, NJ, USA). Results were from triplicate experiments.

**2.5. Hoechst 33258 Staining.** SW620 cells were seeded in 6-well plates and then treated with vehicle, IL-6, and/or  $\alpha$ -hederin, or PDTC at different concentrations for 24 h. Apoptosis was evaluated using a Hoechst 33258 staining kit provided by Beyotime Institute of Biotechnology (Haimen, China) according to the protocol. Morphology of apoptotic cells was observed using a fluorescence microscope (Nikon, Tokyo, Japan). The nucleus of apoptotic cells takes up the Hoechst reagent and exhibits a bright blue fluorescence. Results were from experiments in triplicate.

**2.6. Flow Cytometry Analysis of MMP.** SW620 cells were seeded in 6-well plates and then treated with vehicle, IL-6, and/or  $\alpha$ -hederin at different concentrations for 24 h. MMP was determined using flow cytometry. Briefly, cells were incubated separately with 5 mM JC-1 dye provided by Beyotime Institute of Biotechnology (Haimen, China) at 37°C for 30 min followed by centrifugation (300 g, 5 min) and suspension in phosphate buffer solution. The fluorescence-labeled cells were monitored by flow cytometry at the excitation and emission wavelengths of 530 nm and 590 nm, respectively, using FACS Calibur Flow Cytometry System (BD Biosciences, Franklin Lakes, NJ, USA). Results were from experiments in triplicate.

**2.7. Immunofluorescence Staining.** SW620 cells were seeded in 6-well plates, and then treated with vehicle, IL-6, and/or  $\alpha$ -hederin at different concentrations for 24 h. Then, cells were incubated with the primary antibody against NF- $\kappa$ B(p65) and fluorescence-conjugated secondary antibodies in succession as we previously reported [11]. DAPI was used to stain the

TABLE 1: Primer sequences of genes for real-time PCR in this study.

Genes	Sequences	
Cyclin B1	Forward	5orwACGAAGGTCTGCGCGTGT-3'
	Reverse	5eveCCGCTGGCCATGAACTACCT-3'
CDK1	Forward	5orwardGCAGACTTTGGACTAGCCAG-3'
	Reverse	5everseCGGTACCACAGGGTCA-3'
GAPDH	Forward	5'-TGACAACAGCCTCAAGAT-3'
	Reverse	5'-GAGTCCTTCCACGATACC-3'

nucleus. Photographs were taken at random fields, and results were from experiments in triplicate.

**2.8. Real-Time PCR.** SW620 cells were treated with various reagents at different concentrations for 24 h. RNA isolation and real-time PCR were performed according to the procedures we previously described [11]. Briefly, the total RNA was isolated using TRIzol reagent (Invitrogen, Carlsbad, CA, USA), and the first-strand cDNA was synthesized with 1  $\mu$ g of total RNA using a PrimeScript RT reagent kit (TakaraBio, Tokyo, Japan). The real-time PCR was conducted using IQTM SYBR Green supermix and the iQ5 real-time detection system (Bio-Rad Laboratories, Hercules, CA, USA). The reaction mixtures contained 7.5  $\mu$ l SYBR Green I dye master mix (Quanta), 2 pM forward primers, and 2 pM reverse primers. Thermocycle conditions included initial denaturation at 50°C and 95°C (10 min each), 40 cycles at 95°C (15 s) and 60°C (1 min). Glyceraldehyde phosphate dehydrogenase (GAPDH) was used as the invariant control. Relative mRNA levels were determined by the  $2^{-\Delta\Delta CT}$  method. Sequences of primers were listed in Table 1. Results were from experiments in triplicate.

**2.9. Western Blot Analyses.** SW620 cells were treated with various reagents at different concentrations for 24 h. Protein isolation and detection were performed according to the methods as we previously reported [11]. Briefly, the whole-cell lysates were prepared using radioimmunoprecipitation analyses buffer supplemented with protease and/or phosphatase inhibitors. In some experiments, mitochondrial and cytosol proteins were extracted, respectively, using a cytosol protein extraction kit (Nanjing KeyGen Biotech Co., Ltd., Nanjing, China) for detecting the release of Cyt c from mitochondria. In another set of experiments, nuclear proteins were prepared using a Bioepitope Nuclear and Cytoplasmic Extraction Kit provided by Bioworld Technology Co., Ltd. (Saint Louis Park, MN, USA). The protein concentrations were determined using a BCA assay kit (Pierce, USA). Proteins (50  $\mu$ g/well) were separated by SDS-polyacrylamide gel, and then transferred to a PVDF membrane (Millipore, Burlington, MA, USA) followed by being blocked with 5% skim milk in Tris-buffered saline containing 0.1% Tween 20. Target proteins were monitored by their primary antibodies, and subsequently by horseradish peroxidase-conjugated secondary antibodies. Protein bands were visualized using chemiluminescence reagent (Millipore, Burlington, MA, USA). Equivalent loading was confirmed using the antibodies

against GAPDH, or COX IV, or lamin B1. The abundance of target proteins was densitometrically detected using Quantity Ones 4.4.1 (Bio-Rad Laboratories, Berkeley, CA, USA). The variation in the density of bands was presented as fold changes after normalized to GAPDH, or COX IV, or lamin B1, or the total proteins.

**2.10. Statistical Analyses.** Data were expressed as mean  $\pm$  SD, and analyzed using SPSS16.0 software. The significance of difference was determined by one-way ANOVA with the *post hoc* Dunnett's test, and values of  $P < 0.05$  were set as statistically significant.

### 3. Results

**3.1.  $\alpha$ -Hederin Arrests Cell Cycle at G2/M Checkpoint in IL-6-Stimulated SW620 Cells.** We initially examined the effects of  $\alpha$ -hederin on the viability of colon cancer cells. Our previous studies have shown that  $\alpha$ -hederin reduced the viability of SW620 cells at relatively low concentrations in a dose-dependent manner, and  $\alpha$ -hederin at the low concentration of 1  $\mu$ g/ml produced a significant inhibitory effect [11]. Herein,  $\alpha$ -hederin only at the high concentration of 10  $\mu$ g/ml significantly reduced the viability of HCT116 cells, suggesting that SW620 cells were more sensitive to  $\alpha$ -hederin treatment (Figure 1(a)). Therefore, we used SW620 cells treated with IL-6 at 6.25 ng/ml for subsequent experiments. This concentration of IL-6 was determined by our previous studies [11]. Reduced cell viability can be caused by cell cycle arrest. We used flow cytometry to analyze the cell cycle, and found that  $\alpha$ -hederin increased the number of cells at the G2/M phase, indicating that the cell cycle at the G2/M checkpoint was arrested (Figure 1(b)). Cyclins and cyclin-dependent kinases (CDKs) are known to control cell cycle, and, for the G2/M phase transition, cyclin B1 and CDK1 are critically involved [12]. We thus assumed that these two molecules might be affected by  $\alpha$ -hederin. Real-time PCR analyses showed that IL-6 significantly increased the mRNA expression of cyclin B1 and CDK1, but  $\alpha$ -hederin reduced their mRNA expression concentration dependently in IL-6-stimulated SW620 cells (Figure 1(c)). Western blot analyses consistently demonstrated that the protein levels of these molecules were also significantly elevated by IL-6, but were decreased by  $\alpha$ -hederin in a concentration-dependent manner (Figure 1(d)). Collectively, these results suggested that  $\alpha$ -hederin reduced viability and arrested cell



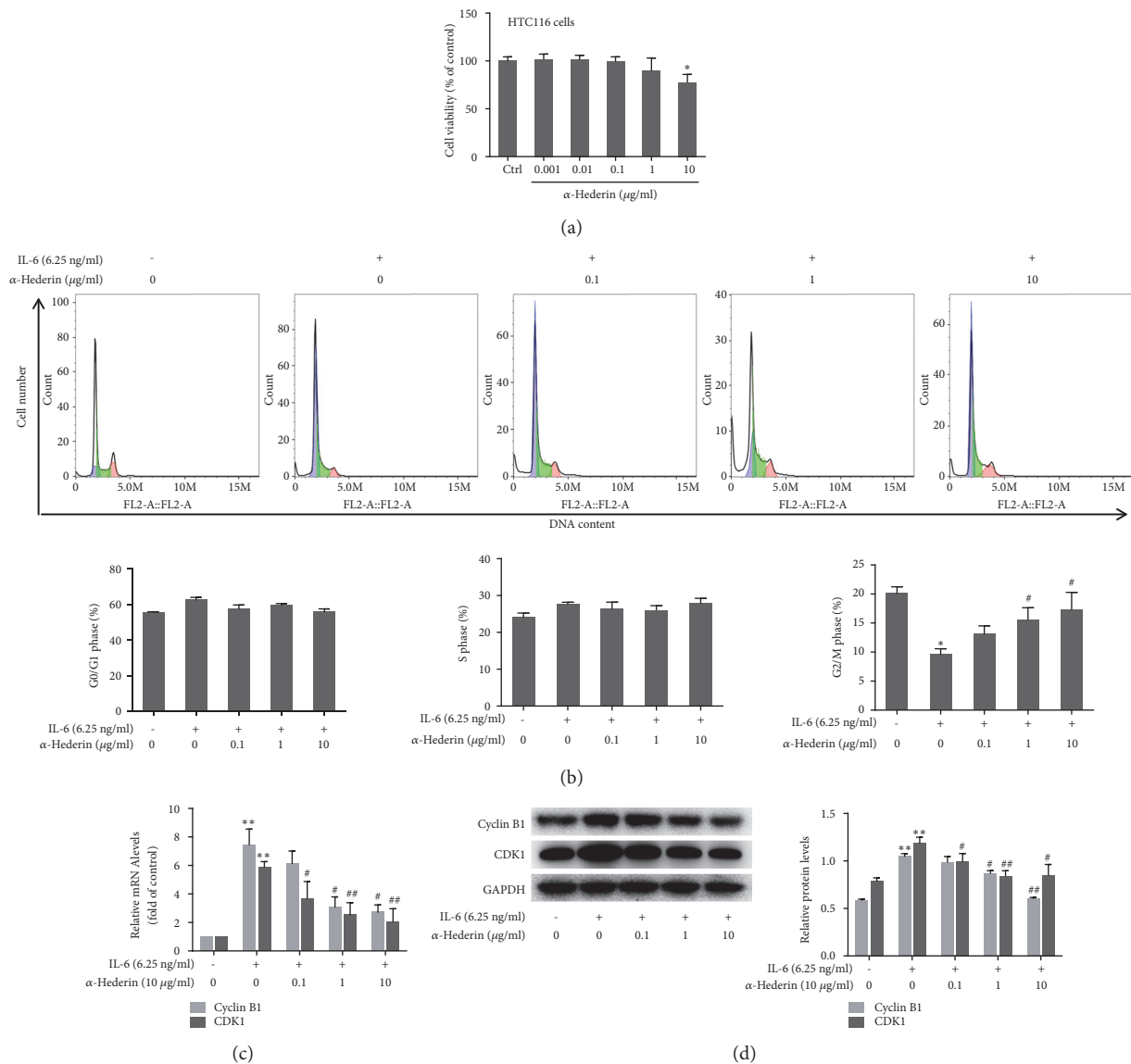


FIGURE 1:  $\alpha$ -Hederin arrests cell cycle at G2/M checkpoint in IL-6-stimulated SW620 cells. SW620 cells or HTC116 cells were treated with vehicle, IL-6, and/or  $\alpha$ -hederin at indicated concentrations for 24 h. (a) CCK-8 assay for evaluating cell viability. Cell viability was expressed as percentage of control. Significance: \* $P$ <0.05 versus control. (b) Cell cycle analysis by flow cytometry. Percentages of cell cycle distribution at the G0/G1 phase, S phase, and G2/M phase were quantified, respectively. Significance: \* $P$ <0.05 versus control, # $P$ <0.05 versus IL-6. (c) Real-time PCR analyses of mRNA expression of cyclin B1 and CDK1. Significance: \*\* $P$ <0.01 versus control, # $P$ <0.05 versus IL-6, ## $P$ <0.01 versus IL-6. (d) Western blot analyses of protein expression of cyclin B1 and CDK1 with quantification. Significance: \*\* $P$ <0.01 versus control, # $P$ <0.05 versus IL-6, ## $P$ <0.01 versus IL-6.

cycle associated with downregulation of cyclin B1 and CDK2 in colon cancer cells.

**3.2.  $\alpha$ -Hederin Induces Mitochondrial Apoptosis in IL-6-Stimulated SW620 Cells.** We next explored whether apoptosis was involved in  $\alpha$ -hederin's inhibitory effects on colon cancer cells. Hoechst staining indicated DNA condensation and fragmentation with brilliant blue staining in IL-6-treated SW620 cells in the presence of  $\alpha$ -hederin (Figure 2(a)). Flow cytometry analyses showed that  $\alpha$ -hederin concentration-dependently reduced MMP in IL-6-treated SW620 cells

(Figure 2(b)). The subsequent Western blot data demonstrated that  $\alpha$ -hederin concentration-dependently reduced the expression of the anti-apoptotic molecule Bcl-2 and increased the expression of the proapoptotic molecule Bax in IL-6-treated SW620 cells (Figure 3(a)). In addition, increased release of Cyt c from mitochondria into cytoplasm induced by  $\alpha$ -hederin was also observed (Figure 3(b)). Furthermore,  $\alpha$ -hederin concentration-dependently upregulated cleaved-caspase-9, cleaved-caspase-3, and cleaved-PARP, whereas cleaved-caspase-8 was not apparently affected (Figure 3(c)), indicating the involvement of extrinsic apoptosis. Taken

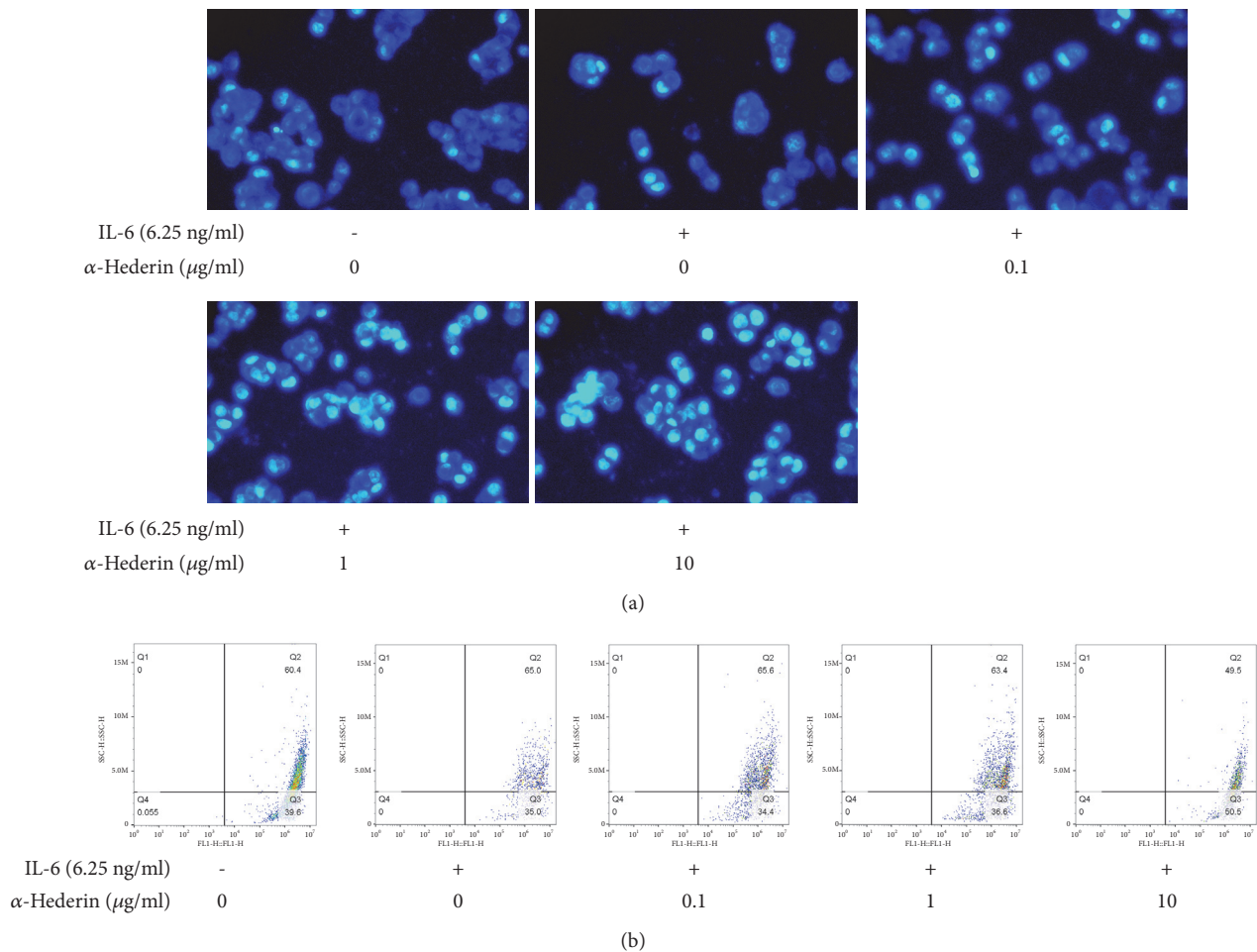


FIGURE 2:  $\alpha$ -Hederin induces mitochondrial apoptosis in IL-6-stimulated SW620 cells. SW620 cells were treated with vehicle, IL-6, and/or  $\alpha$ -hederin at indicated concentrations for 24 h. (a) Hoechst 33258 fluorescence staining. Morphologic changes of apoptotic cells were visualized under a fluorescence microscope (200 x magnification). (b) Flow cytometric analyses of MMP.

together, these findings strongly indicated that  $\alpha$ -hederin triggered mitochondrial apoptosis pathway associated with activation of caspase cascades in colon cancer cells.

**3.3. Blockade of NF- $\kappa$ B Signaling Is Required for  $\alpha$ -Hederin Induction of Mitochondrial Apoptosis in IL-6-Stimulated SW620 Cells.** We investigated the involvement of NF- $\kappa$ B signaling in order to define the mechanisms underlying  $\alpha$ -hederin-induced colon cell apoptosis. Western blot analyses of nuclear lysate showed that IL-6 increased the nuclear abundance of NF- $\kappa$ B, but  $\alpha$ -hederin concentration dependently reduced NF- $\kappa$ B nuclear abundance (Figure 4(a)). Immunofluorescence staining demonstrated consistent results, showing that  $\alpha$ -hederin at 10  $\mu$ g/ml obviously abolished IL-6-induced NF- $\kappa$ B nuclear translocation in SW620 cells (Figure 4(b)). Moreover, IL-6 apparently increased the phosphorylation of I $\kappa$ B $\alpha$  (the deactivated form of this molecule), the inhibitor of NF- $\kappa$ B; but  $\alpha$ -hederin concentration-dependently decreased I $\kappa$ B $\alpha$  phosphorylation (Figure 4(c)). IL-6 also apparently increased the phosphorylation of IKK $\alpha$  (the activated form of this molecule),

the inhibitor of IKK $\alpha$ ; but  $\alpha$ -hederin concentration dependently decreased I $\kappa$ B $\alpha$  phosphorylation (Figure 4(c)). These results clearly demonstrated that  $\alpha$ -hederin blocked NF- $\kappa$ B signaling, which could be associated with the induction of apoptosis in colon cancer cells. To validate this association, NF- $\kappa$ B selective inhibitor PDTC was used to treat SW620 cells alone or combined with  $\alpha$ -hederin. Hoechst staining results showed that PDTC induced apoptosis in SW620 cells and its combination with  $\alpha$ -hederin produced more potent effects (Figure 5(a)). Furthermore, PDTC, similar to  $\alpha$ -hederin, downregulated the Bcl-2 expression and upregulated the abundance of Bax, cleaved-caspase-9, cleaved-caspase-3, and cleaved-PARP in IL-6-treated SW620 cells, and notably, combination of PDTC and  $\alpha$ -hederin resulted in more potent regulatory effects on the protein expression of these molecules (Figure 5(b)). On the other hand, our recent studies suggested that  $\alpha$ -hederin inhibited epithelial-to-mesenchymal transition (EMT) by interrupting JAK2/STAT3 signaling in SW620 cells [11]. Here, our additional assays showed that JAK/STAT3 signaling inhibitor AG490 at 50  $\mu$ M, unlike  $\alpha$ -hederin, failed to repress the

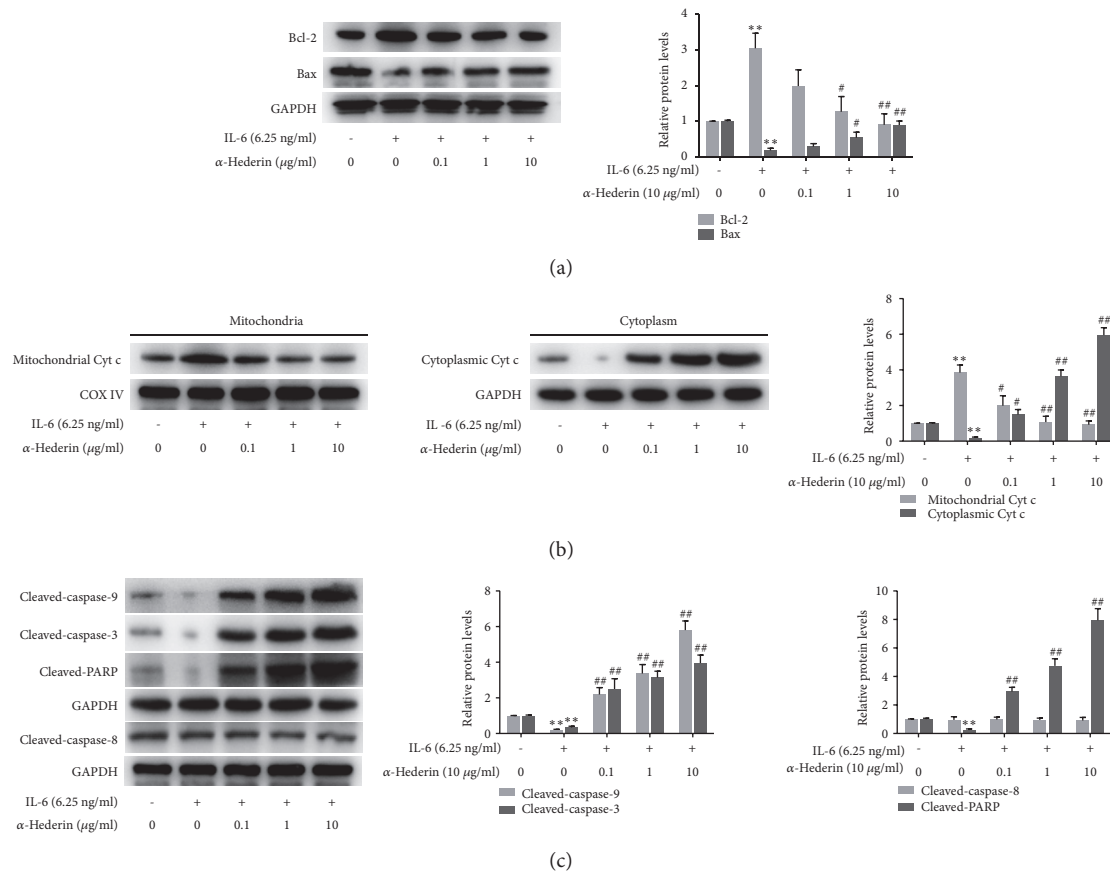


FIGURE 3:  $\alpha$ -Hederin regulates mitochondrial apoptosis-related proteins in IL-6-stimulated SW620 cells. SW620 cells were treated with vehicle, IL-6, and/or  $\alpha$ -hederin at indicated concentrations for 24 h. (a) Western blot analyses of protein expression of Bcl-2 and Bax with quantification. Significance: \*\* $P < 0.01$  versus control, # $P < 0.05$  versus IL-6, ## $P < 0.01$  versus IL-6. (b) Western blot analysis of mitochondrial and cytoplasm abundance of cytochrome c with quantification. Significance: \* $P < 0.05$  versus control, \*\* $P < 0.01$  versus control, # $P < 0.05$  versus IL-6, ## $P < 0.01$  versus IL-6. (c) Western blot analysis of protein abundance of cleaved-caspase-9, cleaved-caspase-3, cleaved-caspase-8, and cleaved-PARP with quantification. Significance: \*\* $P < 0.01$  versus control, # $P < 0.05$  versus IL-6, ## $P < 0.01$  versus IL-6.

viability of SW620 cells (Figure 6(a)), suggesting that the JAK2/STAT3 signaling might specifically regulate the EMT of colon cancer cells. Moreover, the ERK signaling plays a key role in cancer cell fate decision [13]. We here observed that  $\alpha$ -hederin reduced IL-6-induced ERK phosphorylation in SW620 cells (Figure 6(b)). ERK inhibitor U0126 at 20  $\mu$ M inhibited NF- $\kappa$ B nuclear accumulation in SW620 cells, and combination of U0126 and  $\alpha$ -hederin produced more potent inhibitory effects (Figure 6(c)), suggesting that inhibition of ERK signaling could be an upstream molecular event for  $\alpha$ -hederin-induced apoptosis in SW620 cells. Taken together, these results suggested that  $\alpha$ -hederin blockade of NF- $\kappa$ B signaling was involved in induction of mitochondrial and caspase-dependent apoptosis in colon cancer cells.

#### 4. Discussion

Increasing evidence suggests  $\alpha$ -hederin as a good candidate for cancer chemotherapy. Herein, we treated colon cancer cells with IL-6 to mimic the paracrine inflammatory microenvironment of tumor cells. We found that  $\alpha$ -hederin

significantly reduced cell viability and induced apoptosis in a concentration-dependent manner in colon cancer cells. Our study demonstrated that  $\alpha$ -hederin caused G2/M arrest in SW620 cells, resulting in decreased cell viability. Cell proliferation is controlled by cell cycle progression, which is a highly regulated process [14]. The cell cycle is constituted by four non-overlapping phases in sequence, namely, the G1, S, G2, and M phases. Each phase contains a checkpoint that can arrest cell cycle arrest and initiate repair mechanisms [14]. Normal cells commonly use the G1 checkpoint to repair DNA damage. Tumor cells, however, are more dependent on the G2 checkpoint for protecting against DNA damage [15]. These discoveries highlight the G2 checkpoint as a selective target for treatment of cancer. In addition, cell cycle is mediated by a highly conserved protein kinase family. Cyclins can activate CDKs through forming complexes with CDKs, among which the cyclin B1/CDK1 complex is critically important for the G2 to M phase transition [16]. In the present study, flow cytometric analyses showed that  $\alpha$ -hederin induced G2/M phase cell cycle arrest in colon cancer cells, and G2/M phase accumulation peaked at 24 h of treatment, suggesting

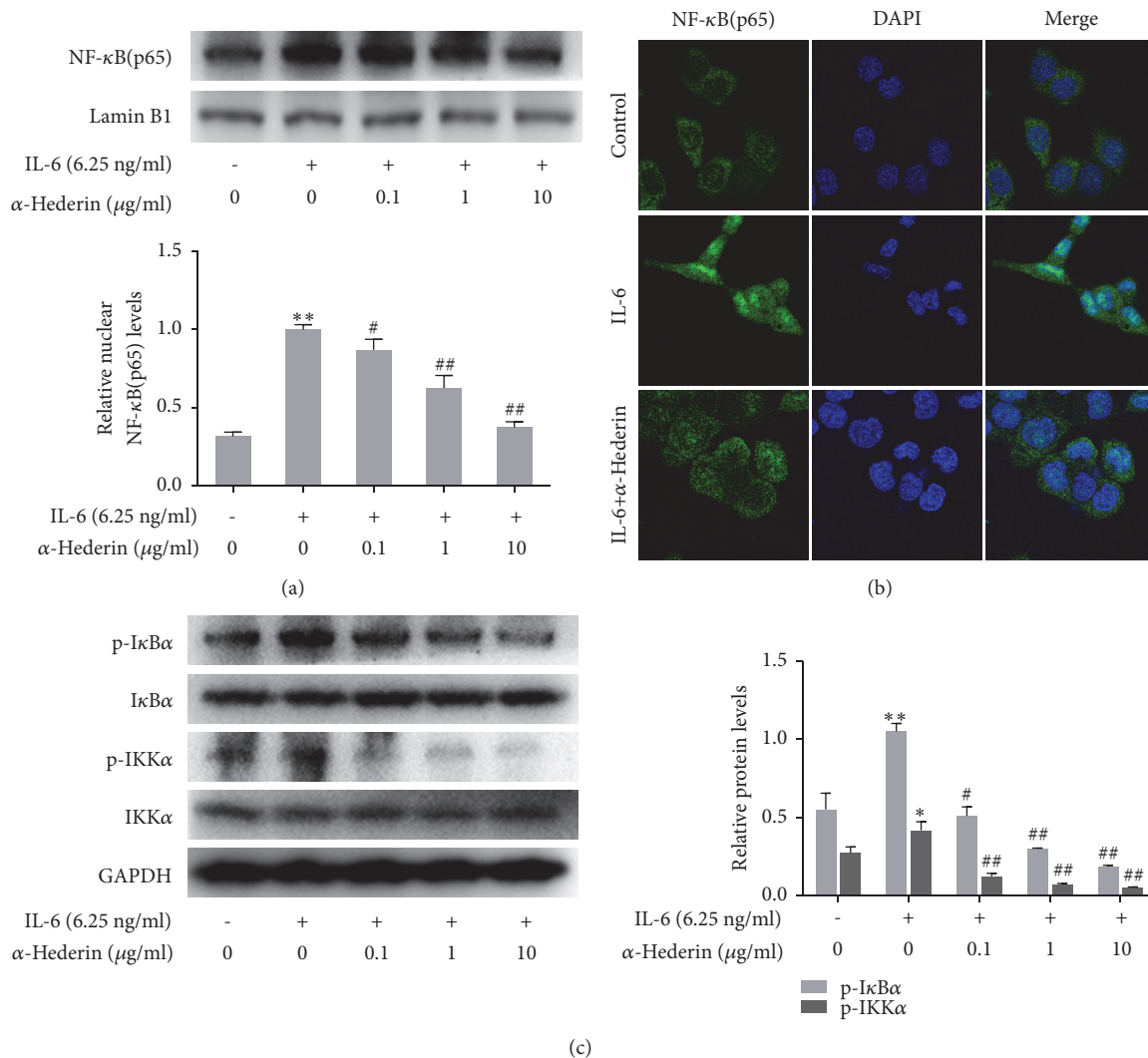


**FIGURE 4: α-Hederin inhibits NF-κB signaling in IL-6-stimulated SW620 cells.** SW620 cells were treated with vehicle, IL-6, and/or α-hederin at indicated concentrations for 24 h. (a) Western blot analysis of nuclear abundance of NF-κB with quantification. Significance: \*\* $P < 0.01$  versus control, # $P < 0.05$  versus IL-6, ## $P < 0.01$  versus IL-6. (b) Immunofluorescence analyses of the nuclear translocation NF-κB in SW620 cells treated with α-hederin at 10 μg/ml and/or IL-6 at 6.25 ng/ml (200 x magnification). (c) Western blot analysis of protein abundance of p-IκBα, IκBα, p-IKKα, and IKKα with quantification. Significance: \* $P < 0.05$  versus control, \*\* $P < 0.01$  versus control, # $P < 0.05$  versus IL-6, ## $P < 0.01$  versus IL-6.

the occurrence of sequential events of cell cycle arrest. Furthermore, G2/M phase arrest is known to be mediated by reduced formation of cyclin B1/CDK1 complex during cell cycle progression [17]. In current study, we found that α-hederin arrested SW620 cells in G2/M phase through downregulating the expression of cyclin B1 and CDK1 at both transcriptional and protein levels. This could result in reduced abundance of cyclin B1/CDK1 complex within cells. Our findings were consistent with the established molecular recognition and strongly suggested that α-hederin could be developed as a selective agent for colon cancer treatment.

To elucidate the underlying mechanism, we examined α-hederin's effects on apoptosis in colon cancer cells. Cell cycle arrest induced by drugs can cause inefficient repair, leading to apoptosis if the damage is unreparable [4]. Mitochondria

are the major organelles involved in apoptosis signaling. Mitochondrial apoptosis pathway can be initiated by intracellular stimuli and mediated by the Bcl-2 family proteins, which function as sensors to integrate the survival and death signals. The ratio of Bcl-2/Bax is a pivotal determinant, and reduced Bcl-2/Bax ratio can result in mitochondrial outer membrane permeabilization and Cyt c release, and finally activate caspase-9 and caspase-3, culminating in cellular fragmentation [18, 19]. Here, our data demonstrated that α-hederin led to decreased ratio of Bcl-2/Bax and disrupted MMP accompanied by increased release of Cyt c into cytoplasm, suggesting the initiation of mitochondrial-mediated apoptosis. In addition, caspase-9, caspase-3, and PARP-1 were all activated, indicating caspase-associated apoptosis induced by α-hederin. Interestingly, the extrinsic apoptosis pathway



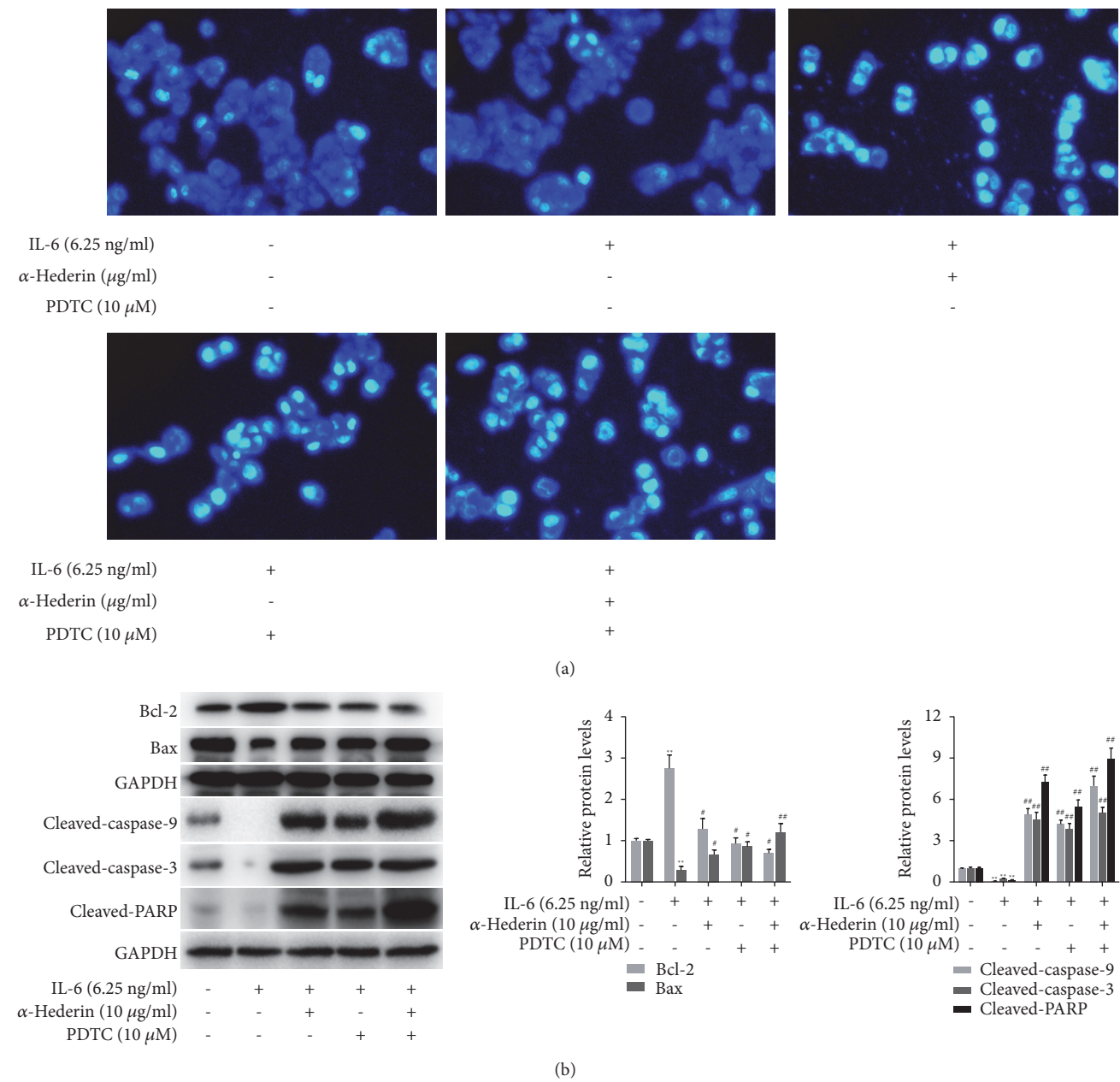


FIGURE 5: Blockade of NF- $\kappa$ B signaling is required for  $\alpha$ -hederin induction of mitochondrial apoptosis in IL-6-stimulated SW620 cells. SW620 cells were treated with vehicle, IL-6, and/or  $\alpha$ -hederin or PDTC at indicated concentrations for 24 h. (a) Hoechst 33258 fluorescence staining. Morphologic changes of apoptotic cells were visualized under a fluorescence microscope (200 x magnification). (b) Western blot analysis of protein abundance of cleaved-caspase-9, cleaved-caspase-3, and cleaved-PARP with quantification. Significance: \*\* $P$ <0.01 versus control, # $P$ <0.05 versus IL-6, ## $P$ <0.01 versus IL-6.

might not be involved, because caspase-8 was not markedly activated. Taken together, these findings suggested that  $\alpha$ -hederin selectively stimulated colon cancer cells to undergo intrinsic apoptosis dependent on caspase activation.

NF- $\kappa$ B can promote cell survival and proliferation. Increased NF- $\kappa$ B activity is positively associated with many types of cancers [20]. Thus we investigated the expression and phosphorylation of some key components in NF- $\kappa$ B pathway to further reveal the mechanisms underlying  $\alpha$ -hederin-induced apoptosis. We demonstrated that  $\alpha$ -hederin

inhibited IL-6-induced nuclear translocation of NF- $\kappa$ B. These effects could prevent NF- $\kappa$ B to transcriptionally activate the genes involved in cell proliferation. Disruption of NF- $\kappa$ B pathway by  $\alpha$ -hederin contributed to its inhibitory effects on cell cycle progression and apoptosis induction in colon cancer cells. These molecular insights could make  $\alpha$ -hederin a more valuable candidate for cancer chemotherapy, given that invasion and metastasis of tumor cell are closely related to inflammation, while NF- $\kappa$ B is exactly a pivotal player in inflammation-induced tumor progression and metastasis

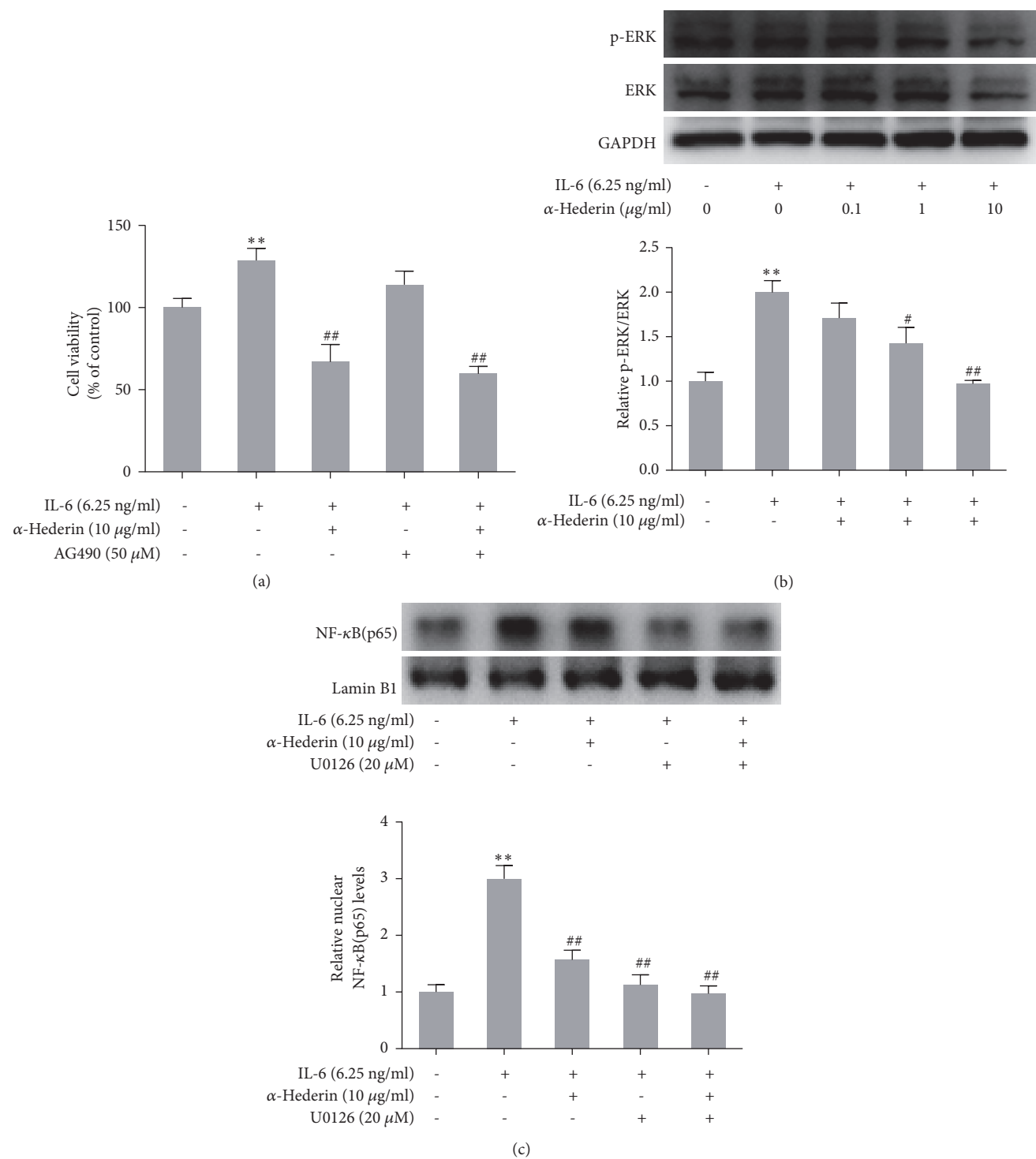


FIGURE 6: Inhibition of ERK phosphorylation is involved in  $\alpha$ -Hederin reduction of NF- $\kappa$ B nuclear translocation in IL-6 stimulated SW620 cells. SW620 cells were treated with vehicle, IL-6, and/or  $\alpha$ -hederin, or AG490, or U0126 at indicated concentrations for 24 h. (a) CCK-8 assay for evaluating cell viability. Cell viability was expressed as percentage of control. Significance: \*\* $P$ <0.01 versus control, ## $P$ <0.01 versus IL-6. (b) Western blot analysis of ERK phosphorylation with quantification. Significance: \*\* $P$ <0.01 versus control, # $P$ <0.05 versus IL-6, ## $P$ <0.01 versus IL-6. (c) Western blot analysis of nuclear abundance of NF- $\kappa$ B with quantification. Significance: \*\* $P$ <0.01 versus control, ## $P$ <0.01 versus IL-6.

[21]. Inhibition of NF- $\kappa$ B could lead to innovative approach for the treatment of cancer [20]. Our investigation demonstrated that  $\alpha$ -hederin disrupted NF- $\kappa$ B signaling in colon cancer cells, contributing to its induction of mitochondrial apoptosis. Furthermore, we preliminary explored the upstream molecule event of  $\alpha$ -hederin effects. We ruled out the role of JAK2/STAT3 signaling, because pharmacological inhibition of this pathway had little effect on the viability of SW620 cells. We turned to the ERK signaling, which has a broad array of cellular functions including proliferation, survival, apoptosis, motility, transcription, metabolism and differentiation [22]. We observed that  $\alpha$ -hederin inhibited ERK signaling contributing to the disruption of NF- $\kappa$ B signaling and presumably to the induction of apoptosis in colon cancer cells. These findings were consistent with a number of previous studies where inhibition of ERK activity led to or associated with apoptosis of colon cancer cells [23–28]. However, there were also contrast results showing that activation of ERK induced apoptosis in colon cancer cells [29, 30]. To account for the discrepancies, we will deeply investigate the distinct mechanisms underlying  $\alpha$ -hederin inhibition of ERK signaling implicated in regulation of colon cancer cell fate.

In conclusion,  $\alpha$ -hederin reduced viability, arrested cell cycle at the G2/M checkpoint, and induced mitochondrial and caspase-dependent apoptosis in SW620 cells. These effects were associated with the blockade of NF- $\kappa$ B signaling and inhibition of ERK. Our results strongly suggested  $\alpha$ -hederin as a promising candidate for colon cancer therapy.

## Data Availability

The data used to support the findings of this study are available from the corresponding author upon request.

## Conflicts of Interest

The authors of this work have no conflicts of interest to declare regarding the publication of this paper.

## Acknowledgments

This work was financially supported by the National Natural Science Foundation of China (No. 81673559, 81403079, and 81573910), the Natural Science Foundation of Jiangsu Province (No. BK20161045), the Natural Science Foundation of Colleges and Universities in Jiangsu Province (No. 16KJB360001), and a project funded by the Priority Academic Program Development of Jiangsu Higher Education Institutions.

## References

- [1] S. J. D. O'Keefe, "Diet, microorganisms and their metabolites, and colon cancer," *Nature Reviews. Gastroenterology & Hepatology*, vol. 13, no. 12, pp. 691–706, 2016.
- [2] B. K. Edwards, E. Ward, B. A. Kohler et al., "Annual report to the nation on the status of cancer, 1975–2006, featuring colorectal cancer trends and impact of interventions (risk factors, screening, and treatment) to reduce future rates," *Cancer*, vol. 116, no. 3, pp. 544–573, 2010.
- [3] J. Guo, S. Xu, X. Huang et al., "Drug Resistance in Colorectal Cancer Cell Lines is Partially Associated with Aneuploidy Status in Light of Profiling Gene Expression," *Journal of Proteome Research*, vol. 15, no. 11, pp. 4047–4059, 2016.
- [4] M. A. Savitskaya and G. E. Onishchenko, "Mechanisms of apoptosis," *Biochemistry (Moscow)*, vol. 80, no. 11, pp. 1393–1405, 2015.
- [5] L. Cao, X. B. Quan, W. J. Zeng, X. O. Yang, and M. J. Wang, "Mechanism of hepatocyte apoptosis," *Journal of Cell Death*, vol. 9, pp. 19–29, 2016.
- [6] R. W. Birkinshaw and P. E. Czabotar, "The BCL-2 family of proteins and mitochondrial outer membrane permeabilisation," *Seminars in Cell & Developmental Biology*, vol. 72, pp. 152–162, 2017.
- [7] S. Wang, Z. Liu, L. Wang, and X. Zhang, "NF-kappaB signaling pathway, inflammation and colorectal cancer," *Cellular & Molecular Immunology*, vol. 6, no. 5, pp. 327–334, 2009.
- [8] B. Hoesel and J. A. Schmid, "The complexity of NF- $\kappa$ B signaling in inflammation and cancer," *Molecular Cancer*, vol. 12, p. 86, 2013.
- [9] J. Schulte-Michels, A. Wolf, S. Aatz et al., " $\alpha$ -Hederin inhibits G protein-coupled receptor kinase 2-mediated phosphorylation of  $\beta$ 2-adrenergic receptors," *Phytomedicine*, vol. 23, no. 1, pp. 52–57, 2016.
- [10] J. H. Lorent, C. Léonard, M. Abouzi, F. Akabi, J. Quetin-Leclercq, and M.-P. Mingeot-Leclercq, " $\alpha$ -Hederin Induces Apoptosis, Membrane Permeabilization and Morphologic Changes in Two Cancer Cell Lines Through a Cholesterol-Dependent Mechanism," *Planta Medica*, vol. 82, no. 18, pp. 1532–1539, 2016.
- [11] D. Sun, W. Shen, F. Zhang et al., " $\alpha$ -Hederin inhibits interleukin 6-induced epithelial-to-mesenchymal transition associated with disruption of JAK2/STAT3 signaling in colon cancer cells," *Biomedicine & Pharmacotherapy*, vol. 101, pp. 107–114, 2018.
- [12] S. Maddika, S. R. Ande, S. Panigrahi et al., "Cell survival, cell death and cell cycle pathways are interconnected: implications for cancer therapy," *Drug Resistance Updates*, vol. 10, no. 1–2, pp. 13–29, 2007.
- [13] M. Kohno, S. Tanimura, and K.-I. Ozaki, "Targeting the extracellular signal-regulated kinase pathway in cancer therapy," *Biological & Pharmaceutical Bulletin*, vol. 34, no. 12, pp. 1781–1784, 2011.
- [14] A. Montagnoli, J. Moll, and F. Colotta, "Targeting cell division cycle 7 kinase: A new approach for cancer therapy," *Clinical Cancer Research*, vol. 16, no. 18, pp. 4503–4508, 2010.
- [15] T. Kawabe, "G2 checkpoint abrogators as anticancer drugs," *Molecular Cancer Therapeutics*, vol. 3, no. 4, pp. 513–519, 2004.
- [16] W.-J. Shangguan, H. Li, and Y.-H. Zhang, "Induction of G2/M phase cell cycle arrest and apoptosis by ginsenoside Rf in human osteosarcoma MG-63 cells through the mitochondrial pathway," *Oncology Reports*, vol. 31, no. 1, pp. 305–313, 2014.
- [17] S. Haupt, M. Berger, Z. Goldberg, and Y. Haupt, "Apoptosis—the p53 network," *Journal of Cell Science*, vol. 116, no. 20, pp. 4077–4085, 2003.
- [18] J. E. Chipuk, T. Moldoveanu, F. Llambi, M. J. Parsons, and D. R. Green, "The BCL-2 family reunion," *Molecular Cell*, vol. 37, no. 3, pp. 299–310, 2010.

- [19] C. Wang and R. J. Youle, "The role of mitochondria in apoptosis," *Annual Review of Genetics*, vol. 43, pp. 95–118, 2009.
- [20] F. H. Sarkar and Y. Li, "NF-kappaB: A potential target for cancer chemoprevention and therapy," *Frontiers in Bioscience*, vol. 13, no. 8, pp. 2950–2959, 2008.
- [21] M. O. Hengartner, "The biochemistry of apoptosis," *Nature*, vol. 407, no. 6805, pp. 770–776, 2000.
- [22] J. W. Ramos, "The regulation of extracellular signal-regulated kinase (ERK) in mammalian cells," *The International Journal of Biochemistry & Cell Biology*, vol. 40, no. 12, pp. 2707–2719, 2008.
- [23] C. Li, S. Gao, X. Li, C. Li, and L. Ma, "Procaine inhibits the proliferation and migration of colon cancer cells through inactivation of the ERK/MAPK/FAK pathways by regulation of RhoA," *Oncology Research : Featuring Preclinical and Clinical Cancer Therapeutics*, vol. 26, no. 2, pp. 209–217, 2018.
- [24] K. Li, Q. Guo, J. Yang et al., "FOX D3 is a tumor suppressor of colon cancer by inhibiting EGFR-Ras-Raf-MEK-ERK signal pathway," *Oncotarget*, vol. 8, no. 3, pp. 5048–5056, 2017.
- [25] A. A. Tahir, N. F. A. Sani, N. A. Murad, S. Makpol, W. Z. W. Ngah, and Y. A. M. Yusof, "Combined ginger extract & Gelam honey modulate Ras/ERK and PI3K/AKT pathway genes in colon cancer HT29 cells," *Nutrition Journal*, vol. 14, p. 31, 2015.
- [26] S.-A. Yang, S.-H. Paek, N. Kozukue, K.-R. Lee, and J.-A. Kim, "α-Chaconine, a potato glycoalkaloid, induces apoptosis of HT-29 human colon cancer cells through caspase-3 activation and inhibition of ERK 1/2 phosphorylation," *Food and Chemical Toxicology*, vol. 44, no. 6, pp. 839–846, 2006.
- [27] C.-H. Liao, S. Sang, C.-T. Ho, and J.-K. Lin, "Garcinol modulates tyrosine phosphorylation of FAK and subsequently induces apoptosis through down-regulation of Src, ERK, and Akt survival signaling in human colon cancer cells," *Journal of Cellular Biochemistry*, vol. 96, no. 1, pp. 155–169, 2005.
- [28] E. Im and J. D. Martinez, "Ursodeoxycholic Acid (UDCA) Can Inhibit Deoxycholic Acid (DCA)-induced Apoptosis via Modulation of EGFR/Raf-1/ERK Signaling in Human Colon Cancer Cells," *Journal of Nutrition*, vol. 134, no. 2, pp. 483–486, 2004.
- [29] H. Randhawa, K. Kibble, H. Zeng, M. P. Moyer, and K. M. Reindl, "Activation of ERK signaling and induction of colon cancer cell death by piperlongumine," *Toxicology in Vitro*, vol. 27, no. 6, pp. 1626–1633, 2013.
- [30] B. Sung, J. Ravindran, S. Prasad, M. K. Pandey, and B. B. Aggarwal, "Gossypol induces death receptor-5 through activation of the ROS-ERK-CHOP pathway and sensitizes colon cancer cells to TRAIL," *The Journal of Biological Chemistry*, vol. 285, no. 46, pp. 35418–35427, 2010.



## Research Article

# Pharmacokinetics and Bioavailability Study of Monocrotaline in Mouse Blood by Ultra-Performance Liquid Chromatography-Tandem Mass Spectrometry

Lianguo Chen,<sup>1</sup> Bin Zhang,<sup>2</sup> Jinlai Liu,<sup>1</sup> Zhehua Fan,<sup>2</sup> Ziwei Weng,<sup>2</sup> Peiwu Geng,<sup>3</sup> Xianqin Wang <sup>2</sup> and Guanyang Lin <sup>4</sup>

<sup>1</sup>The Third Clinical Institute Affiliated with Wenzhou Medical University & Wenzhou People's Hospital, Wenzhou 325000, China

<sup>2</sup>Analytical and Testing Center, School of Pharmaceutical Sciences, Wenzhou Medical University, Wenzhou 325035, China

<sup>3</sup>Laboratory of Clinical Pharmacy, The People's Hospital of Lishui, Lishui 323000, China

<sup>4</sup>The First Affiliated Hospital of Wenzhou Medical University, Wenzhou 325000, China

Correspondence should be addressed to Guanyang Lin; [guanyanglinwzmc@gmail.com](mailto:guanyanglinwzmc@gmail.com)

Received 11 April 2018; Revised 5 July 2018; Accepted 29 July 2018; Published 13 August 2018

Academic Editor: Francesco Facchiano

Copyright © 2018 Lianguo Chen et al. This is an open access article distributed under the Creative Commons Attribution License, which permits unrestricted use, distribution, and reproduction in any medium, provided the original work is properly cited.

**Background and Aims.** The present study aimed to develop a simple and sensitive method for quantitative determination of monocrotaline (MCT) in mouse blood employing ultra-performance liquid chromatography-electrospray ionization tandem mass spectrometry (UPLC-ESI/MS/MS) using rhynchophylline as an internal standard. **Methods.** Proteins present in the blood samples were precipitated using acetonitrile. MCT was separated using a 1.7- $\mu$ m ethylene bridged hybrid (BEH) C18 column (2.1 mm  $\times$  50 mm) with a gradient elution program and a constant flow rate of 0.4 mL/min. The LC mobile phase consisted of 10 mmol/L ammonium acetate (containing 0.1% formic acid) and acetonitrile. The total elution time was 4.0 min. The analytes were detected on a UPLC-ESI mass spectrometer in multiple reaction monitoring (MRM) mode and quantified. **Results.** The new method for the determination of MCT has a satisfactory linear detection range of 1-2000 ng/mL and excellent linearity ( $r = 0.9971$ ). The lower limit of quantification (LLOQ) of MCT is 1.0 ng/mL. Intra- and interassay precisions of MCT were  $\leq 13\%$  with an accuracy from 96.2% to 106.6%. The average recovery of the new method was  $>75.0\%$ , and matrix effects were between 89.0% and 94.3%. Based on the pharmacokinetics data, the bioavailability of MCT in mice was 88.3% after oral administration. **Conclusions.** The results suggest that the newly standardized method for quantitative determination of MCT in whole blood is fast, reliable, specific, sensitive, and suitable for pharmacokinetic studies of MCT after intravenous or intragastric administration.

## 1. Introduction

Monocrotaline (crotaline, MCT), a pyrrolizidine alkaloid (PA) isolated from *Crotalaria* species, induces toxicity in many tissues and causes extreme hepatic necrosis, pulmonary hypertension, and severe kidney damage [1]. MCT is considered not suitable to continuously use as a drug and is mainly used to induce pulmonary diseases in mice [2, 3]. In 1991, Mattocks et al. [4] first reported that 7-glutathionyl-dehydroretronecine (GS-DHR) given to rats was able to mimic the cardiopulmonary toxicity of MCT. In recent years, it was found that MCT exhibits dose-dependent cytotoxicity with potent antineoplastic activity [5, 6]. Thus, lower doses

of MCT may be a potent anticancer or cytotoxic agent in combination with other protective agents, which remains to be confirmed by further *in vivo* studies.

It is well known that pharmacokinetic studies play a pivotal role in drug development, as they assist in predicting a variety of efficacy- and toxicity-related events. To better understand how the toxicity and the pharmacological activity of MCT *in vivo* change with the blood concentration, a rapid, simple, and effective analytical method is necessary. Up to the present moment, only a few bioanalytical methods have been published for the detection of MCT in biological fluids. Estep et al. [7] reported the results of urinary and biliary excretion, and plasma kinetics of [ $^{14}$ C]MCT by

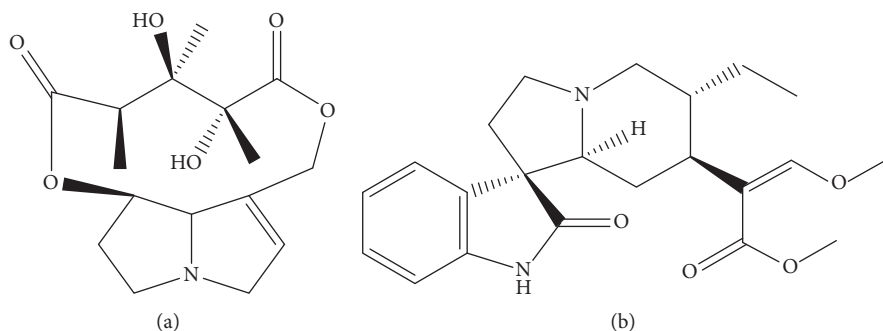


FIGURE 1: Chemical structures of (a) monocrotaline and (b) rhynchophylline.

high-performance liquid chromatography (HPLC) in 1991, but the HPLC method was less effective because of the long detection time for MCT (approximately 40 min). Glowaz and Wang et al. [8, 9] also briefly mentioned that HPLC was used for detection of a reactive pyrrole in the hepatic metabolism of MCT, metabolites formed from the metabolism of MCT, and the chromatographic peak of MCT in their research eluted at 12.4 min and 28.9 min, respectively. Unfortunately, they did not elaborate on the sample pretreatment and HPLC conditions. It is undeniable that HPLC is inexpensive and commonly used, but the weakness is also apparent: low selectivity, low sensitivity, and long detection time. Thus, Yao et al. [1] chose the HPLC/MS/MS method for detecting MCT and its metabolites in the plasma, bile, and tissues of mice for many advantages: simplified sample preparation, high sensitivity, selectivity, and reliability. Although the published studies described above provide useful information, little data are available for MCT determination. The UPLC and UPLC-MS/MS techniques have recently attracted additional interest along with the development of analysis techniques [10, 11]. Compared with HPLC-MS/MS, the advantages of UPLC-MS/MS include fast analysis, high throughput, and less solvent required [12–16].

As far as we know, there are no published data that demonstrate the validation of a sensitive assay utilizing UPLC-MS/MS for the determination of MCT in whole blood. Therefore, we standardized and validated a new and more convenient UPLC/MS/MS method in this study for the determination of the concentration of MCT, utilizing the serial blood sampling method and performing it in 4 min. After adding rhynchophylline (IS), protein precipitation was used to extract analytes. This method had been successfully applied to the pharmacokinetic study of MCT in mice after sublingual intravenous and gavage administration.

## 2. Materials and Methods

**2.1. Drugs and Reagents.** Monocrotaline (purity > 98%, Figure 1(a)) and rhynchophylline (IS, purity > 98%, Figure 1(b)) were purchased from Chengdu Mansite Pharmaceutical Co. Ltd. (Chengdu, China). HPLC-grade formic acid and organic solvents (acetonitrile and methanol) were purchased from Tedia (Ohio, USA) and Merck (Darmstadt, Germany), respectively. Purified water was obtained with a Milli-Q purification system (Millipore, Bedford, MA, USA).

**2.2. Animals.** Male ICR mice (20–22 g; n=12) were obtained from the Laboratory Animal Center of Wenzhou Medical University (Wenzhou, China). The study protocol was approved by the Animal Care Committee of Wenzhou Medical University. Mice received standard food and water *ad libitum* in a temperature-controlled room (25°C) with 12-h on and 12-h off light cycle before experiments.

**2.3. UPLC-MS/MS Conditions.** A UPLC-MS/MS system with an ACQUITY I-Class UPLC and a XEVO TQ-S micro triple quadrupole mass spectrometer (Waters Corp., Milford, MA, USA) was used for analysis. The output signal monitoring and processing were performed by MassLynx 4.1 software (Waters Corp.).

Symmetric peak performance and satisfactory retention of the analytes were accomplished on a 1.7  $\mu$ m UPLC BEH C18 (2.1 mm  $\times$  50 mm) column. Acetonitrile (solvent A) and 10 mmol/L ammonium acetate (solvent B, containing 0.1% formic acid) were selected as the mobile phase. The gradient program consisted of the following: 10% A (0–0.2 min); changing to 80% A (0.2–1.5 min); 80% A (1.5–2.0 min); changing to 10% A (2.0–2.5 min); and 10% A (2.5–4.0 min). The flow rate was set at 0.4 mL/min, the column temperature was 40°C, and the total elution time was 4.0 min.

Ionization was achieved by using electrospray in the positive ion mode (ESI+). The MRM mode was applied to monitor MCT ions at  $m/z$  326.2  $\rightarrow$  120.8. The cone voltage for MCT was set to 78 V and the collision voltage to 30 V. For IS, the MRM transition was  $m/z$  385.2  $\rightarrow$  160.0 with a cone voltage of 36 V and a collision voltage of 34 V. The capillary voltage was set to 2.1 kV for both MCT and IS. The desolvation gas (nitrogen) was set at 800 L/h with the cone gas at 50 L/h. The temperature of the ion source and desolvent was 150°C and 400°C, respectively.

**2.4. Standard Solution Samples.** Standard stock solutions of MCT and IS were prepared in methanol at 1 mg/mL. Then, these stock solutions of MCT were diluted with methanol to obtain fresh standard working solutions at several concentration levels. The standard working solution of IS was diluted with acetonitrile to the concentration of 20 ng/mL. All solutions were stored at 4°C before analysis.

**2.5. Calibration Standards (CS) and Quality Control (QC) Samples.** CS and QC samples were prepared by diluting

corresponding standard working solutions with the blank blood of mice. The concentrations of the calibration standard were 1, 5, 10, 20, 50, 100, 200, 1000, and 2000 ng/mL. Three concentrations of QC samples representing the entire range of the standard curve were prepared at 3, 180, and 1800 ng/mL: one within 3X LLOQ (low-level QC sample), one near the center (mid-level QC sample), and one near the upper boundary of the standard curve (high-level QC sample). The CS and QC samples were maintained at  $-20^{\circ}\text{C}$  until processing.

**2.6. Sample Preparation.** Frozen blood samples (20  $\mu\text{L}$ ) in 1.5-mL test tubes were brought to room temperature before adding 100  $\mu\text{L}$  acetonitrile (containing 20 ng/mL of IS). Then, these tubes were mixed on a vortexer for 60 seconds before 10 min of centrifugation (13,000 rpm,  $4^{\circ}\text{C}$ ). The supernatant (approximately 80  $\mu\text{L}$ ) was collected into a new micro-insert (clear glass, cone-shaped with a plastic stent), and then 2  $\mu\text{L}$  of the supernatant was injected into the UPLC-MS/MS system.

**2.7. Method Validation.** The method was validated for selectivity, linearity, accuracy, precision, recovery, stability, and matrix effects of samples according to the "Guideline on Bioanalytical Method Validation" recommended by the US Food and Drug Administration (FDA) in 2013 [17].

**2.7.1. Selectivity.** The selectivity was evaluated by analyzing blank mouse blood, blank blood spiked with MCT and IS, and a mouse blood sample after dosing. The method was established without interference from endogenous peaks existing at the peak region of MCT and IS in the blank blood.

**2.7.2. Linearity.** Calibration curves were generated by analyzing different concentrations of calibration samples on three consecutive days. The linear regressions of the peak area ratios (y) of each MCT to the corresponding IS versus the nominal concentration (x) of MCT were fitted over the range of 1-2000 ng/mL. Linearity was evaluated at 9 levels covering the concentration range of 1-2000 ng/mL.

**2.7.3. Precision and Accuracy.** Evaluating the intraday and interday accuracy and the precision across the quantitation range during method standardization is essential and involves analyzing QC samples at multiple concentrations across the assay range. Method validation experiments for estimating accuracy and precision should include a minimum of three levels (3, 180, 1800 ng/mL for MCT) and six independent runs conducted on the same day and three consecutive days. The precision and the accuracy were expressed by the relative standard deviation (RSD) and relative error (RE), respectively, which should be within the limits of  $\pm 15\%$  at all concentrations.

**2.7.4. Recovery and Matrix Effect.** The recovery of MCT was calculated by comparison of the peak area responses of the QC samples ( $n=6$ ) that were added before extraction and the IS that was subsequently added at three concentrations (3, 180, 1800 ng/mL), with those obtained when both the

corresponding MCT and IS were added after the extraction step.

Before evaluating the matrix effect, the stock solutions of MCT were diluted with the extracted blank blood to get new working solutions at three levels (3, 180, 1800 ng/mL). Then, matrix effects were tested by comparison of the peak areas of these new working solutions with those of the corresponding standard solutions diluted with acetonitrile: 0.1% formic acid (1:1, v/v) at equivalent concentration, and this peak area ratio was defined as the matrix effect.

**2.7.5. Stability.** The stability of MCT in mouse blood was evaluated by analyzing blood samples containing QC samples at low, medium, and high concentration levels ( $n=3$  for each concentration level). The MCT stability was tested under the following conditions: (a) storage for 12 h at room temperature in an autosampler; (b) storage for 30 days at  $-20^{\circ}\text{C}$ ; and (c) three complete freeze-thaw cycles ( $-20^{\circ}\text{C}$  to room temperature).

**2.8. Pharmacokinetic Study.** MCT was dissolved in 0.01% HCl solution for administration to mice and freshly prepared before the experiment. The mice were divided into two groups (group A and group B,  $n=6$  for each group): the mice in group A were treated with a single sublingual intravenous injection of MCT at 3 mg/kg after 12 h fasting, while the others in group B were administered an oral dose of MCT at 15 mg/kg. Blood samples (20  $\mu\text{L}$ ) were collected in 1.5-mL tubes containing heparin by tail tip bleeding at 0 (prior to dosing), 0.083, 0.5, 1, 1.5, 2, 3, 4, 8, 12, and 24 h after dosing of MCT, and stored directly at  $-20^{\circ}\text{C}$  until analysis. Blood samples were processed for UPLC-MS/MS analysis according to the method described in Sample Preparation. DAS software (version 2.0, China Pharmaceutical University, China) was used to calculate the main kinetic parameters, such as area under the concentration-time curve (AUC), the half-life ( $t_{1/2}$ ), peak blood concentrations ( $C_{\text{max}}$ ), clearance (CL), mean resident time (MRT), and volume of distribution (V). In addition, the bioavailability of MCT was examined in our study for the first time and was calculated as absolute bioavailability (%) =  $100 \times \text{AUC}_{\text{po}} \cdot D_{\text{iv}} / (\text{AUC}_{\text{iv}} \cdot D_{\text{po}})$ , where  $\text{AUC}_{\text{iv}}$  and  $\text{AUC}_{\text{po}}$  are the AUC of the drug from (0 -  $\infty$ ) after intravenous and oral administration and  $D_{\text{iv}}$  and  $D_{\text{po}}$  are a single dosage of MCT for intravenous and oral administration, respectively.

### 3. Results

#### 3.1. Method Validation

**3.1.1. Selectivity.** Figure 3 presents the ion chromatogram of a blank extract, a blank extract with MCT and IS, and an authentic sample spiked with IS. The peaks of MCT and IS appeared at 0.46 and 1.71 min, respectively. The separation of MCT and IS was satisfactory. No interfering peaks were found at or near the retention times of MCT and IS. There was increased sensitivity and selectivity when UPLC-MS/MS was used for the quantitative determination of MCT utilizing 20  $\mu\text{L}$  mouse blood as compared to the traditional HPLC

TABLE 1: The precision, accuracy, recovery, and matrix effect of MCT in mouse blood (n = 6).

Concentration (ng/mL)	Precision (RSD%)		Accuracy (%)		Found (ng/mL)		Matrix effect (%)	Recovery (%)
	Intra-day	Inter-day	Intra-day	Inter-day	Intra-day	Inter-day		
3	9.6	12.6	106.6	96.6	3.2±0.3	2.9 ±0.4	89.0±7.6	81.9 ±6.4
180	11.1	12.0	99.4	104.4	178.9±19.9	187.9 ±22.6	94.3±4.5	77.2±3.6
1800	7.3	8.2	96.2	98.4	1731.6±126.4	1771.2 ±145.2	92.2 ±4.1	75.0±4.6

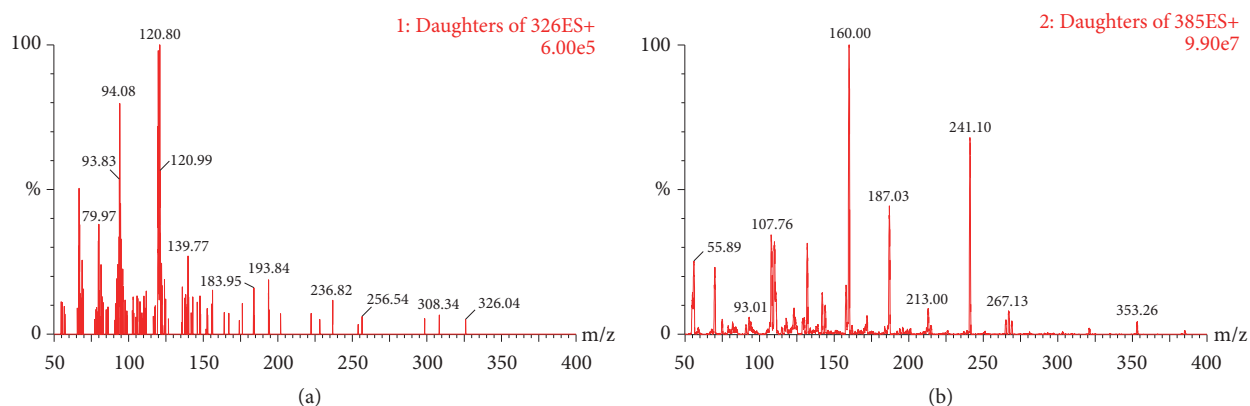


FIGURE 2: The product ion spectrum of (a) MCT and (b) IS.

method. The total runtime was 4.0 min per sample (including equilibration time), which is important for large batches of samples and faster than the LC-MS method (more than 10 min) developed by Yao et al. [1].

**3.1.2. Calibration Curve.** A linear relationship was observed in the calibration curves over the concentration range of 1-2000 ng/mL for MCT in mouse blood. The regression equation is expressed as  $y = 0.000368x - 0.000344$ ,  $r = 0.9971$ , where  $y$  represents the peak ratio of the MCT peak area to IS and  $x$  represents the concentration of MCT in mouse blood. The LLOQ was 1 ng/mL with a signal-to-noise (S/N) ratio of 9 for the determination of MCT in mouse blood, which will contribute to the assay of lower concentrations of MCT at the last time point for sample collection.

**3.1.3. Accuracy and Precision.** As shown in Table 1, the results of intra- and interday precision assessed by the relative standard deviation (RSD) were no more than 12% and 13%, respectively. The accuracy was in the range of 96.2-106.6% at each QC level. All of the recoveries were above 75.0%, and matrix effects were between 89.0% and 94.3%. These data suggest that both precision and accuracy are within the acceptable range, and the UPLC-MS/MS method established is suitable for the pharmacokinetic study of MCT.

**3.1.4. Recovery and Matrix Effects.** As can be seen from Table 1, the recovery for the method was in the range 75.0%-81.9% with matrix effect within the range of 89.0-94.3%. The results indicate reasonable recoveries with a negligible matrix effect for this method.

**3.1.5. Stability.** The stability studies for MCT in the blood of mice were performed for each concentration (3, 180, 1800 ng/mL) under the different storage conditions mentioned above (n=3). As can be seen from Table 2, the RSDs were  $\leq 14\%$  in all stability tests for MCT, which indicated reliable stability behavior for MCT under the different storage conditions.

**3.2. Pharmacokinetics.** The mean blood concentration-time curves for MCT after intravenous and intragastric administration are shown in Figures 4 and 5, respectively. The main pharmacokinetic parameters after intragastric (15 mg/kg) and sublingual intravenous (3 mg/kg) administration based on noncompartment model analysis are presented in Table 3. The high bioavailability of MCT (88.3% in this study) as well as short  $t_{max}$  (0.5 h) after oral administration indicated that MCT was quickly absorbed and less affected by the liver (or intestinal) first pass effect in animals. Thus, it would be expected that MCT could be developed for oral administration in a solid dosage form and used for treatment in the future.

## 4. Discussion

It is known that the pharmacokinetic profile and toxicity of some drugs are variable in different species [18, 19]. The mouse was chosen as the animal model in this study because it is one of the most common species for evaluating drug preclinical efficacy [20, 21], toxicology [22], biodistribution, and pharmacokinetics [23-25].



TABLE 2: Summary of stability of MCT under various storage conditions (n = 3).

Concentration (ng/mL)	Auto sampler ambient			Ambient 12 h			-20°C 30 d			Freeze-thaw		
	Found (ng/mL)	Accuracy (%)	RSD (%)	Found (ng/mL)	Accuracy (%)	RSD (%)	Found (ng/mL)	Accuracy (%)	RSD (%)	Found (ng/mL)	Accuracy (%)	RSD (%)
3	2.9± 0.1	96.6	3.5	3.1±0.2	102.9	7.6	2.8±0.4	93.6	13.8	2.7 ±0.3	88.9	13.0
180	183.4±9.7	101.9	5.3	190.8±9.2	106.0	4.8	1771±20.4	98.4	11.5	162.2 ±8.3	90.1	5.1
1800	1879.2± 54.5	104.4	2.9	1657.8±89.5	92.1	5.4	1936.8 ±108.5	107.6	5.6	1918.8±188.0	106.6	9.8

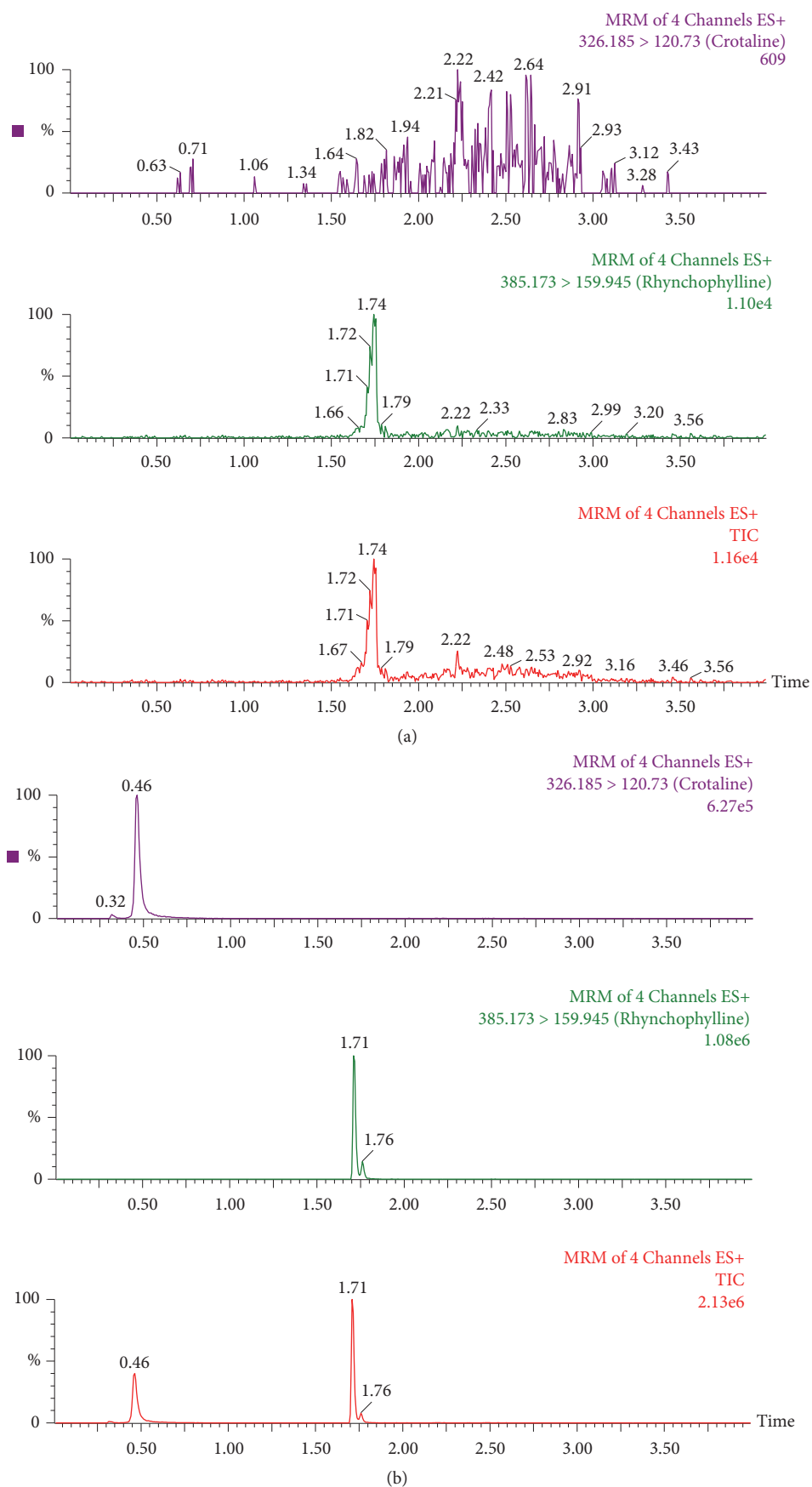


FIGURE 3: Continued.

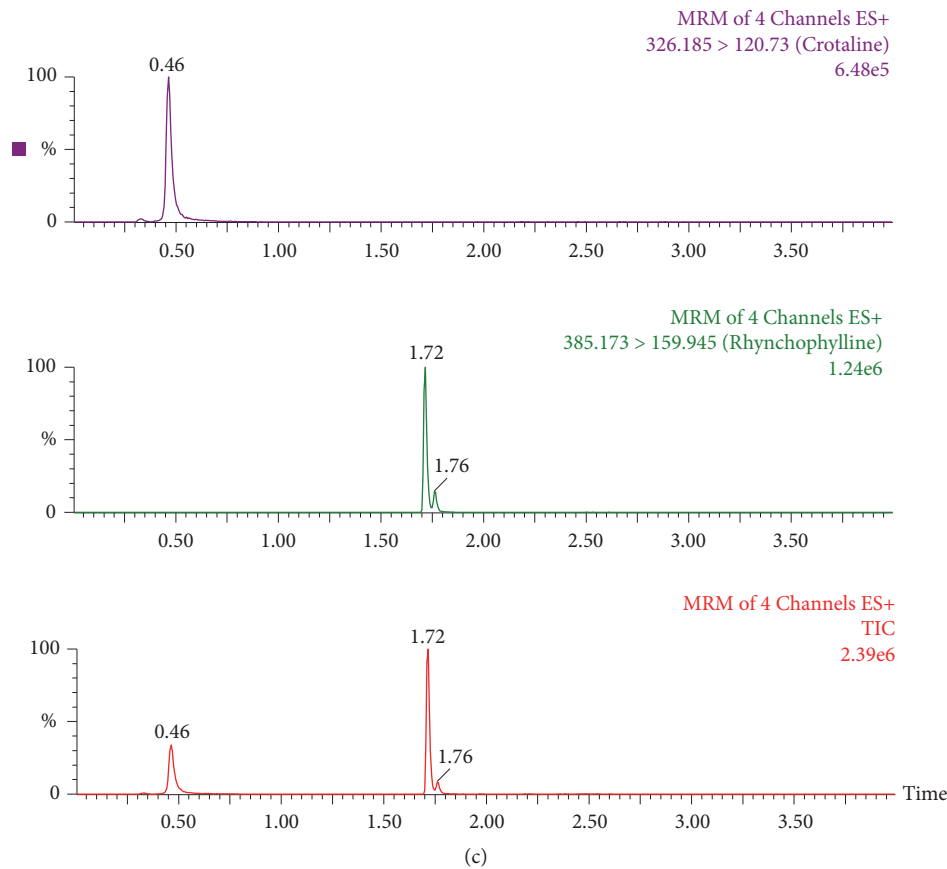


FIGURE 3: The MS/MS chromatograms of MCT and IS. (a) A blank extract, (b) a blank extract with MCT and IS, and (c) an authentic sample spiked with IS at 0.5 h after intravenous administration.

TABLE 3: The main pharmacokinetic parameters of MCT after sublingual intravenous and intragastric administration (n=6).

Parameters	Unit	iv (3 mg/kg)	po (15 mg/kg)
$AUC_{(0-t)}$	ng/mL*h	2991.9 ± 789.1	13215.0 ± 5384.2
$AUC_{(0-\infty)}$	ng/mL*h	3225.9 ± 941.9	13259.7 ± 5403.8
$MRT_{(0-t)}$	H	2.6 ± 1.2	1.6 ± 0.7
$MRT_{(0-\infty)}$	h	4.5 ± 3.3	1.6 ± 0.7
$t_{1/2z}$	h	7.1 ± 3.7	2.6 ± 1.5
$t_{max}$	h	—	0.5 ± 0.0
$CL_{z/F}$	L/h/kg	1.0 ± 0.4	1.3 ± 0.5
$V_{z/F}$	L/kg	9.3 ± 3.6	4.5 ± 3.2
$C_{max}$	ng/mL	2553.8 ± 340.2	9886.5 ± 771.3

Terminal blood sampling has been widely adopted in the pharmacokinetic evaluation of mice, but it is inappropriate for protection of animals because it requires large numbers of animals at high cost and labor. Furthermore, individual animal differences and administration errors may lead to inaccuracy of the pharmacokinetic profile [26]. A serial blood sampling method, by contrast, can reduce the number of animals needed, labor, and cost [27]. In addition, the standard deviation of pharmacokinetic parameters can be calculated based on individual drug concentrations by the serial blood sampling method, while it cannot be calculated based on

mean drug concentrations by the terminal blood sampling method. Thus, the data obtained by the serial blood sampling method are more reliable than those obtained by the terminal blood sampling method.

Small blood volume requirements for mouse pharmacokinetic evaluations support serial blood sampling and enable an entire pharmacokinetics profile to be obtained from a single mouse [20, 27]. In reality, the total blood volume of rodents is approximately 7% of their body weight [28]. Thus, the volume of a blood sample that can be collected from a mouse (approximately 20 g) is limited. Typically, blood

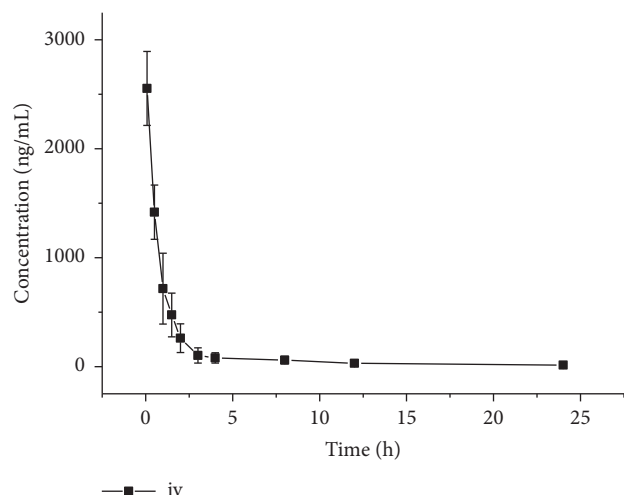


FIGURE 4: Mean blood concentration of MCT after sublingual intravenous administration at the dose of 3 mg/kg in six mice.

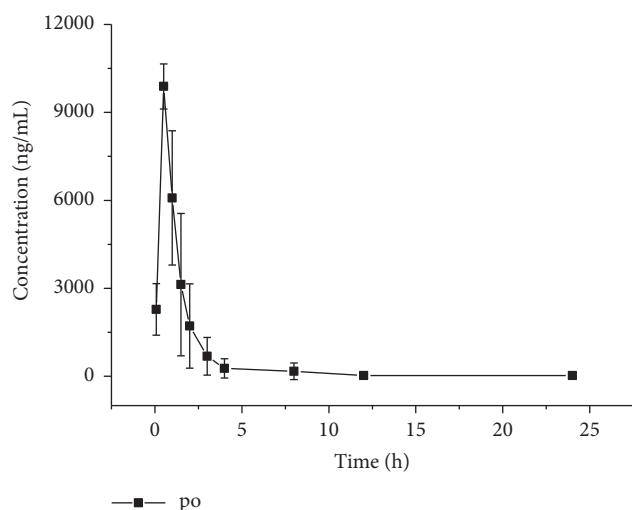


FIGURE 5: Mean blood concentration of MCT after gavage of 15 mg/kg in six mice.

samples (approximately 20-30  $\mu$ L) for 6-7 time points are withdrawn from an individual mouse, and six separate mice are used for sample collection and analysis at each time point [20]. Unfortunately, the volume of blood collected in Yao's study was not mentioned and no references were provided. Taking these factors into consideration and on the basis of previous work, we established an improved method for serially sampling the blood (11 total time points in 24 h) from one mouse with only one incision of the lateral tail vein at the first sampling time and sufficient warming of the tail at subsequent sampling times, which imparts low stress to mice and improves the quality of the pharmacokinetic study. Sufficient warming of the tail is critical for the rapid and multiple collections of blood samples from a mouse. The volume of blood sampled for each time point was only 20  $\mu$ L, and the total blood volume sampled from one mouse was approximately 10% of the total circulating blood volume.

Yao et al. briefly mentioned that HPLC/MS/MS was used for the detection of MCT in the plasma of mice. Their study, however, was focused on the relationship of the hepatic cytochrome P450s and monocrotaline-induced renal toxicity in mice. Therefore, they did not elaborate on the analytical procedure such as selectivity, accuracy, stability, quantification range, linearity, and matrix effect. The current method is an improvement to the published data by Yao et al. because the featured technique is more sensitive with a higher throughput and uses less solvent and time.

To optimize the MS conditions, positive and negative ion mode selection was often tested in the methodology. Ultimately, we chose the positive ESI mode for the detection because of the stronger and more stable responses of the analytes as compared to the negative ion mode. According to the optimized results for mass spectrometric conditions, we can see that the daughter ions  $m/z$  120.8 and  $m/z$  160.0 were the strongest and the most stable among abundant fragment ions produced by MCT and IS, respectively, which is presented in Figure 2. Thus, we selected  $m/z$  326.2  $\rightarrow$  120.8 and  $m/z$  385.2  $\rightarrow$  160.0 for MCT and IS, respectively.

Analysis of MCT with reversed phase UPLC-MS/MS was accomplished with the use of acidic mobile phases, which is more suitable for ion formation of analytes in the electrospray ionization (ESI) source [29, 30]. According to our original work and current conditions, several reversed phase columns were tested (Acquity BEH C18, Ultimate XB C18, and Hanbon Dubhe C18). We chose the Acquity BEH C18 column because of the satisfactory separation and sharper peaks. To avoid endogenous compounds appearing at the same retention times for MCT or IS, a suitable mobile phase was needed. Different acidic mobile phase compositions were tested on an Acquity BEH C18 column to obtain a perfect separation and more symmetrical peak shape, such as acetonitrile-0.1% formic acid, acetonitrile-10 mmol/L ammonium acetate (containing 0.1% formic acid), methanol-0.1% formic acid, and methanol-10 mmol/L ammonium acetate (containing 0.1% formic acid). Acetonitrile-10 mmol/L ammonium acetate (containing 0.1% formic acid) was chosen in this study for the most satisfactory resolution, peak shape, and retention time. Beyond that, gradient elution is more optimal than isocratic elution for sharper peaks and less analysis time.

Two main blood sample processing methods were used before detection: direct analysis of the blood; a sample in which the composition of the blood had been simplified by removing, for example, most of the endogenous substances and proteins. If there is a need to avoid interference or decompose drug-protein complexes, simplified samples are prepared from the blood, most frequently by extraction or by precipitation with the appropriate precipitation agents. Liquid-liquid extraction (LLE) has the advantages of a high extraction rate and low limit of quantification [30]. Yao et al. [1] reported that liquid-liquid extraction with n-butanol was used with MCT. The main disadvantage of extraction is the lengthy sample preparation due to evaporation of the extraction solvent, which results in a method that is time consuming, complicated, and expensive. Moreover, it is difficult to obtain sufficient plasma after centrifuging for liquid-liquid extraction at each point by tail vein transactional



bleeding. Thus, Yao et al. selected just 8 total time points for calculating the pharmacokinetic parameters. A one-step protein precipitation procedure for whole blood was chosen in our study following the example of previous studies [31, 32]. The supernatant obtained from the blood after precipitation and centrifugation was directly injected into the column, which significantly simplified the sample preparation and offered a high throughput assay. The precipitation method is more convenient, but only if the level of drugs in the blood is sufficiently high for detection. The LLOQ for MCT (1 ng/mL) in our study is much lower than that (5 ng/mL) achieved by Yao et al., which ensures that the level of MCT in the supernatant obtained from the blood at the last time point after protein precipitation and centrifugation is sufficiently high to be detected by UPLC-MS/MS. Thus, this assay is a modified version of a mass spectrometry assay used to determine MCT in plasma by Yao et al. and Li et al. [1, 31].

The following precipitating agents and their mixtures in different combinations and ratios were tested: methanol, acetonitrile, and acetonitrile-methanol. During the precipitation processes, the volumes of the respective precipitation agents were always the same. The results indicated that the greatest recoveries of the analytes were achieved when acetonitrile was used as the precipitating reagent. Considering that blood samples are more complex than plasma, the 20- $\mu$ L blood sample was mixed with 5 volumes of acetonitrile, which provided higher recoveries, less matrix effect, and also sufficient supernatant volume for analysis requiring multiple injections.

## 5. Conclusion

A simple, sensitive, and robust method using UPLC/MS/MS for the quantitative measurement of MCT in mouse blood was standardized and validated. The method offers sample extraction from only 20  $\mu$ L of whole blood using a simple protein precipitation procedure and was successfully applied to the pharmacokinetic investigations of MCT in mice while also meeting the requirement of high sample throughput in bioanalysis. The oral bioavailability of MCT in mice was 88.3%, which indicates that MCT is easily absorbed into the blood circulatory system through the gastrointestinal tract.

## Data Availability

The data used to support the findings of this study are included within the article.

## Conflicts of Interest

The authors declare that they have no conflicts of interest.

## Acknowledgments

This research was supported by the Science and Technology Foundation of Wenzhou (Y20160540) and a grant from the Medical Scientific Research Items of Wenzhou People's Hospital (2017ZD004).

## References

- [1] J. Yao, C.-G. Li, L.-K. Gong et al., "Hepatic cytochrome P450s play a major role in monocrotaline-induced renal toxicity in mice," *Acta Pharmacologica Sinica*, vol. 35, no. 2, pp. 292–300, 2014.
- [2] J. George and J. D'Armiento, "Transgenic expression of human matrix metalloproteinase-9 augments monocrotaline-induced pulmonary arterial hypertension in mice," *Journal of Hypertension*, vol. 29, no. 2, pp. 299–308, 2011.
- [3] J. M. Aliotta, M. Pereira, S. Wen et al., "Exosomes induce and reverse monocrotaline-induced pulmonary hypertension in mice," *Cardiovascular Research*, vol. 110, no. 3, pp. 319–330, 2016.
- [4] A. R. Mattocks, S. Croswell, R. Jukes, and R. J. Huxtable, "Identity of a biliary metabolite formed from monocrotaline in isolated, perfused rat liver," *Toxicol*, vol. 29, no. 4-5, pp. 409–415, 1991.
- [5] S. S. Kusuma, K. Tanneeru, S. Didla, B. N. Devendra, and P. Kiranmayi, "Ntineoplastic activity of monocrotaline against hepatocellular carcinoma," *Anti-Cancer Agents in Medicinal Chemistry*, vol. 14, no. 9, pp. 1237–1248, 2014.
- [6] M. J. Hartshorn, M. L. Verdonk, G. Chessari et al., "Diverse, high-quality test set for the validation of protein-ligand docking performance," *Journal of Medicinal Chemistry*, vol. 50, no. 4, pp. 726–741, 2007.
- [7] J. E. Estep, M. W. Lame, D. Morin, A. D. Jones, D. W. Wilson, and H. J. Segall, "[14C]monocrotaline kinetics and metabolism in the rat," *Drug Metabolism and Disposition*, vol. 19, no. 1, p. 135, 1991.
- [8] S. L. Glowaz, M. Michnika, and R. J. Huxtable, "Detection of a reactive pyrrole in the hepatic metabolism of the pyrrolizidine alkaloid, monocrotaline," *Toxicology and Applied Pharmacology*, vol. 115, no. 2, pp. 168–173, 1992.
- [9] Y.-P. Wang, J. Yan, R. D. Beger, P. P. Fu, and M. W. Chou, "Metabolic activation of the tumorigenic pyrrolizidine alkaloid, monocrotaline, leading to DNA adduct formation in vivo," *Cancer Letters*, vol. 226, no. 1, pp. 27–35, 2005.
- [10] J. Xiong, H. Ye, Y. Lin et al., "Determining concentrations of icotinib in plasma of rat by UPLC method with ultraviolet detection: Applications for pharmacokinetic studies," *Current Pharmaceutical Analysis*, vol. 13, no. 4, pp. 340–344, 2017.
- [11] X. Wang, S. Wang, F. Lin et al., "Pharmacokinetics and tissue distribution model of cabozantinib in rat determined by UPLC-MS/MS," *Journal of Chromatography B*, vol. 983–984, pp. 125–131, 2015.
- [12] W. Ye, R. Chen, W. Sun et al., "Determination and pharmacokinetics of engeletin in rat plasma by ultra-high performance liquid chromatography with tandem mass spectrometry," *Journal of Chromatography B*, vol. 1060, pp. 144–149, 2017.
- [13] Z. Wei, L. X. Ye, Y. Y. Jiang, Z. G. Zhang, and X. Q. Wang, "its Application to a Pharmacokinetic Study," *Latin American Journal of Pharmacy*, vol. 37, no. 3, pp. 523–528, 2018.
- [14] S. Wang, Z. Lin, K. Su et al., "Effect of curcumin and piperfenidone on toxicokinetics of paraquat in rat by UPLC-MS/MS," *Acta Chromatographica*, vol. 30, no. 1, pp. 26–30, 2018.
- [15] X. Wang, Q. Wang, Q. Hu et al., "Effect of ethanol on pharmacokinetics of ketamine in rat," *Latin American Journal of Pharmacy*, vol. 36, no. 7, pp. 1403–1407, 2017.
- [16] B. Fang, S. Bao, S. Wang et al., "Pharmacokinetic study of ardisiacrispin A in rat plasma after intravenous administration by UPLC-MS/MS," *Biomedical Chromatography*, vol. 31, no. 3, 2017.

- [17] F.a.D.A. US Department of Health and Human Services, "Guidance for Industry: Bioanalytical Method Validation," 2013.
- [18] P.-L. Toutain, A. Ferran, and A. Bousquet-Mélou, "Species differences in pharmacokinetics and pharmacodynamics," *Handbook of Experimental Pharmacology*, vol. 199, pp. 19–48, 2010.
- [19] H. Gourdeau, L. Leblond, B. Hamelin et al., "Species differences in troxacitabine pharmacokinetics and pharmacodynamics: Implications for clinical development," *Clinical Cancer Research*, vol. 10, no. 22, pp. 7692–7702, 2004.
- [20] J. Kim, J. S. Min, D. Kim et al., "A simple and sensitive liquid chromatography–tandem mass spectrometry method for trans- $\epsilon$ -viniferin quantification in mouse plasma and its application to a pharmacokinetic study in mice," *Journal of Pharmaceutical and Biomedical Analysis*, vol. 134, pp. 116–121, 2017.
- [21] S. M. Butler, M. A. Wallig, C. W. Nho et al., "A polyacetylene-rich extract from *Gymnaster koraiensis* strongly inhibits colitis-associated colon cancer in mice," *Food and Chemical Toxicology*, vol. 53, pp. 235–239, 2013.
- [22] H. Yamazaki, H. Suemizu, M. Mitsui, M. Shimizu, and F. P. Guengerich, "Combining Chimeric Mice with Humanized Liver, Mass Spectrometry, and Physiologically-Based Pharmacokinetic Modeling in Toxicology," *Chemical Research in Toxicology*, vol. 29, no. 12, pp. 1903–1911, 2016.
- [23] V. Gota, J. S. Goda, K. Doshi et al., "Biodistribution and Pharmacokinetic Study of 3,3'-Diseleno Dipropionic Acid (DSePA), A Synthetic Radioprotector, in Mice," *European Journal of Drug Metabolism and Pharmacokinetics*, vol. 41, no. 6, pp. 839–844, 2016.
- [24] G. Hallur, N. Tamizharasan, S. P. Sulochana, N. K. Saini, M. Zainuddin, and R. Mullangi, "LC-ESI-MS/MS determination of defactinib, a novel FAK inhibitor in mice plasma and its application to a pharmacokinetic study in mice," *Journal of Pharmaceutical and Biomedical Analysis*, vol. 149, pp. 358–364, 2018.
- [25] N. K. Saini, P. Suresh, M. Lella, R. K. Bhamidipati, S. Rajagopal, and R. Mullangi, "LC-MS/MS determination of tideglusib, a novel GSK-3 $\beta$  inhibitor in mice plasma and its application to a pharmacokinetic study in mice," *Journal of Pharmaceutical and Biomedical Analysis*, vol. 148, pp. 100–107, 2018.
- [26] K.-H. Diehl, R. Hull, D. Morton et al., "A good practice guide to the administration of substances and removal of blood, including routes and volumes," *Journal of Applied Toxicology*, vol. 21, no. 1, pp. 15–23, 2001.
- [27] A. Watanabe, R. Watari, K. Ogawa et al., "Using improved serial blood sampling method of mice to study pharmacokinetics and drug-drug interaction," *Journal of Pharmaceutical Sciences*, vol. 104, no. 3, pp. 955–961, 2015.
- [28] G. Lee and K. A. Goosens, "Sampling blood from the lateral tail vein of the rat," *Journal of Visualized Experiments*, vol. 2015, no. 99, Article ID e52766, 2015.
- [29] M. A. Tonon and P. S. Bonato, "Methods for the analysis of nonbenzodiazepine hypnotic drugs in biological matrices," *Bioanalysis*, vol. 4, no. 3, pp. 291–304, 2012.
- [30] E. Eliassen and L. Kristoffersen, "Quantitative determination of zopiclone and zolpidem in whole blood by liquid-liquid extraction and UHPLC-MS/MS," *Journal of Chromatography B*, vol. 971, pp. 72–80, 2014.
- [31] S. Li, Y. Chen, S. Zhang, S. S. More, X. Huang, and K. M. Giacomini, "Role of organic cation transporter 1, OCT1 in the pharmacokinetics and toxicity of cis-diammine(pyridine)chloroplatinum(II) and oxaliplatin in mice," *Pharmaceutical Research*, vol. 28, no. 3, pp. 610–625, 2011.
- [32] M. K. K. Nielsen and S. S. Johansen, "Determination of olanzapine in whole blood using simple protein precipitation and liquid chromatography-tandem mass spectrometry," *Journal of Analytical Toxicology*, vol. 33, no. 4, pp. 212–217, 2009.

## Research Article

# Antioxidant, Anti-Inflammatory, and Antitumoral Effects of Aqueous Ethanolic Extract from *Phoenix dactylifera* L. Parthenocarpic Dates

Hanen El Abed <sup>1</sup>, Mouna Chakroun,<sup>1</sup> Zaineb Abdelkafi-Koubaa,<sup>2,3</sup> Nouredine Drira,<sup>1</sup> Naziha Marrakchi,<sup>2,3</sup> Hafedh Mejdoub,<sup>1</sup> and Bassem Khemakhem <sup>1</sup>

<sup>1</sup>Laboratory of Plant Biotechnology, Sfax Faculty of Sciences, BP 1171, University of Sfax, 3038 Sfax, Tunisia

<sup>2</sup>Laboratory of Venoms and Therapeutic Biomolecules (RIIPT08), Institut Pasteur of Tunis, 13 Place Pasteur, 1002 Tunis, Tunisia

<sup>3</sup>University of Tunis el Manar, 1068 Tunis, Tunisia

Correspondence should be addressed to Hanen El Abed; hanenelabed566@hotmail.fr

Received 26 March 2018; Revised 27 June 2018; Accepted 30 July 2018; Published 6 August 2018

Academic Editor: Cinzia Forni

Copyright © 2018 Hanen El Abed et al. This is an open access article distributed under the Creative Commons Attribution License, which permits unrestricted use, distribution, and reproduction in any medium, provided the original work is properly cited.

The aim of this study was to evaluate the antioxidant, the anti-inflammatory, and the antitumoral activities of the aqueous ethanolic extract from *Phoenix dactylifera* L. parthenocarpic dates. The antioxidant activity was carried using DPPH radical scavenging activity. The result showed that parthenocarpic dates had strongly scavenging activity on DPPH reaching 94% with an  $IC_{50}$  value of  $0.15 \pm 0.011$  mg/mL ( $p < 0.05$ ). The anti-inflammatory potential was determined by the inhibitory effect of the aqueous ethanolic extract on phospholipase  $A_2$  activity as well as on carrageenan-induced paw oedema in mice. The *in vitro* study showed that the extract inhibited the phospholipase  $A_2$  activity with an  $IC_{50}$  value of 130  $\mu$ g/mL and the *in vivo* study showed a significantly decrease in the paw oedema after 1 h compared to the control group. Finally, the antiproliferative activity of the aqueous ethanolic extract was assessed by MTT test against MCF-7 and MDA-MB-231 cancer cell lines. This extract was effective in inhibiting MDA-MB-231 and MCF-7 cancer cells growth with  $IC_{50}$  values of 8 and 18 mg/mL, respectively, after 72 h treatment. These results confirm the ethnopharmacological significance of *Phoenix dactylifera* L. parthenocarpic dates, which could add support for its pharmaceutical use.

## 1. Introduction

Oxidative stress is an important risk factor in the pathogenesis of numerous chronic diseases. Free radicals and other reactive oxygen species can adversely affect various important classes of biological molecules, such as protein, deoxyribonucleic acid (DNA), and lipids causing oxidative deterioration of biomolecules [1]. This damage can lead to various human diseases, especially aging, heart disease, stroke, arteriosclerosis, diabetes, cancer, and inflammation [1].

Inflammation is considered as a primary physiologic defense mechanism against various factors such as infection, burn, toxic chemicals, allergens, and other stimuli [2]. There are many components of an inflammatory response that participate in the associated symptoms and harmful

effects to tissues. It involves a complex web of intracellular cytokine signals, which activate monocytes and/or macrophages releasing a variety of inflammatory mediators such as prostaglandins, platelet-activating factor (PAF), and arachidonic acid derivatives, which can originate locally or from cells that infiltrate in the site of inflammation [3]. Actually, nonsteroidal anti-inflammatory drugs (NSAIDs) are the most clinically important medicine used for the treatment of inflammation by inhibiting the cyclooxygenase (COX) pathway of arachidonic acid metabolism which produces prostaglandins [4]. Nevertheless, these drugs are limited in their effectiveness and cannot regulate the production of leukotrienes or PAF that continues to cause inflammation. Moreover, cyclooxygenase inhibitors could favor the appearance of thrombosis or renovascular hypertension in patients predisposed to these conditions [5]. The inhibition of

phospholipase A<sub>2</sub> (PLA<sub>2</sub>) may serve as a primary regulatory role in the development of inflammatory disorders and could deplete the sources of arachidonic acid and, therefore, its downstream metabolites and PAF, thus constituting an important strategy for the management of inflammatory disorders.

Chronic inflammation increases the risk of resistance and tumor recurrence, such as brain and breast cancer, indicating that eliminating inflammation may represent a valid strategy for cancer prevention and therapy [6]. Despite the advances in the field of anticancer drug discovery, the statistics are noteworthy; in 2012, 14.1 millions new cases of cancer were diagnosed worldwide, with 8.2 millions deaths [7]. Thus, there is still a necessity for the development of new therapies and the tumor microenvironment is an important source of multiple targets for cancer therapy, including oxidative stress and inflammation [7].

Nature has been a source of medicinal products for millennia, going along with the history of humanity. In chemotherapy field, around 75% of the anticancer agents used nowadays are derived from natural products of different origins, and plants are an important source of new promising therapies [7]. *Phoenix dactylifera* L. (date palm) is an ancient plant used in folk medicine for the treatment of various diseases and disorders [2]. Dates and their constituents act as potent antioxidant, anti-inflammatory, and antitumoral and provide a suitable alternative therapy in various diseases cure [2]. According to the Inter Professional Fruits Group (GIFruits), dates production in Tunisia reached 246.000 tons in 2015, 40% of which is disposed or recycled as animal feed [8]. These are mainly dates attacked by pests, fermented and parthenocarpic dates (Sish). The previous study has shown that the aqueous ethanolic extract from *P. dactylifera* parthenocarpic dates contains several bioactive components such as p-coumaric acid hexose, rosmadial, quercetin, quercetin-3,7-di-O-glucoside, and ganodermic acid [8]. Therefore, the objective of this study was to evaluate the antioxidant, the anti-inflammatory, and the antiproliferative activities of the aqueous ethanolic extract from *P. dactylifera* parthenocarpic dates.

## 2. Materials and Methods

**2.1. Extract Preparation.** The aqueous ethanolic extract from *P. dactylifera* parthenocarpic date was prepared using previously described protocol [8]. Briefly, the dried powdered of healthy palm parthenocarpic dates (15 g) was macerated in 100 mL 71% ethanol solution (pH = 8.5) for 24 h at 59°C under stirring condition. The hydroalcoholic crude extract was filtered and concentrated under reduced pressure. The extract was dissolved in distilled water and then preserved at 4°C.

**2.2. Storage Conditions.** The dry extract was introduced into glass bottles protected (amber) from light and stored at - 20°C according to Del-Toro-Sánchez et al. [9]. Then, the extract stability was measured before the use of the aqueous ethanolic extract by determining total phenols, flavonoids, and tannins contents as described in the previously study [8].

**2.3. Antioxidant Activity: DPPH Radical Scavenging Activity.** DPPH radical scavenging activity of the aqueous ethanolic extract from *P. dactylifera* parthenocarpic dates was determined according to the method of Kim et al. [10]. The sample stock solution (100 mg of dry extract/mL) was diluted to final concentrations of 0.05, 0.1, 0.15, 0.2, 0.25, 0.3, 0.45, and 0.6 mg of dry extract/mL in ethanol. A total of 0.5 mL of 30 mM DPPH ethanol solution was added to 0.5 mL of sample solution at different concentrations and allowed to react at room temperature. After 30 min, the absorbance (A) was measured at 520 nm.

The ability to scavenge the DPPH radical was calculated using the following equation:

**Radical Scavenging capacity (RSC, %)**

$$= 1 - \left[ \frac{(A_{\text{sample}} - A_{\text{sample blank}})}{A_{\text{control}}} \right] \times 100 \quad (1)$$

where  $A_{\text{control}}$  is the absorbance of the control (DPPH solution without sample),  $A_{\text{sample}}$  is the absorbance of the test sample (DPPH solution plus test sample), and  $A_{\text{sample blank}}$  is the absorbance of the sample only (sample without DPPH solution).

Results of DPPH radical scavenging were presented by IC<sub>50</sub> value, defined as the concentration of extract which required reducing DPPH radicals by 50%.

## 2.4. Anti-Inflammatory Activity

**2.4.1. Animals and Experimental Design.** Male albino mice of 20-25 g body masses, obtained from the Veterinary Research Institute (Sfax, Tunisia) and maintained under standard laboratory conditions (temperature 22 ± 2°C on 12 h light-dark cycle), were used in this study. Throughout the experimental period, the animals had *ad libitum* access to food and water. The experimental protocol was approved by the Medical Ethics Committee for the Care and Use of Laboratory Animals of the Pasteur Institute of Tunis (approval number: FST/LNFP/Pro 152012) and performed according to the European convention for the protection of living animals used in scientific investigations [11].

**2.4.2. In Vitro Study: Phospholipase A<sub>2</sub> Inhibition Assay.** Phospholipase inhibition assay was performed using PLA<sub>2</sub>/extract preincubation method during 1 h at room temperature in the absence of substrate [12]. Preincubation medium consisted of 10 units of PLA<sub>2</sub> and the aqueous ethanolic extract from *P. dactylifera* parthenocarpic dates with varying concentrations from 0 to 200 µg of dry extract/mL. A control sample was prepared accordingly without the aqueous ethanolic extract. The residual activity was measured titrimetrically at pH = 8 and 40°C with a pH-stat (Metrohm, Buchs, Switzerland), using 0.5% (m/v) egg yolk phosphatidylcholine as a substrate in 30 mL of 150 mM NaCl, 4 mM sodium taurodeoxycholate (NaTDC), and 8 mM CaCl<sub>2</sub>. The results were expressed as residual activity compared with the control. IC<sub>50</sub> value, defined as the sample concentration (µg/mL) at which 50% inhibition



of the enzyme activity occurs, was calculated from the graph plotting enzyme residual activity against sample concentration. All tests were carried out for three sample replications and the results were averaged.

**2.4.3. In Vivo Study: Carrageenan-Induced Mice Paw Oedema.** Mice were divided into three groups of six animals. Group 1 was served as a negative control and received saline water without the extract (solution of 0.90% (m/v) NaCl). Prior to the induction of the oedema, group 2 was injected intraperitoneally with the aqueous ethanolic extract from parthenocarpic dates (200 mg/kg), respectively. Group 3 was administered by an intraperitoneal injection of indomethacin (50 mg/kg) as a positive control. All drugs were administrated 30 min before the injection of carrageenan. Oedema was induced by injecting 0.3 mL of 2% carrageenan subcutaneously into the subplantar region of the left hind paw [13]. The paw oedema thickness was measured by using a digital micrometer (MT-045B; Shangai Metal Great Tools Co., Shangai, China) immediately before carrageenan injection and 1, 2, 3, and 4 h after carrageenan injection. Percentages of inhibition of inflammation were obtained for each group using the following ratio:

$$\text{Inhibition (\%)} = \left[ \frac{(V_t - V_0)_{\text{control}} - (V_t - V_0)_{\text{treated}}}{(V_t - V_0)_{\text{control}}} \right] \times 100 \quad (2)$$

where  $V_t$  is the average volume for each group at different hours after treatment and  $V_0$  are the average volume obtained for each group before any treatment.

## 2.5. Antitumoral Activity

**2.5.1. Cell Line and Culture Conditions.** The human tumor cell lines MDA-MB-231 (breast carcinoma) and MCF-7 (breast adenocarcinoma) were a kind gift of Dr. Khadija Essafi-Benkhadir, Institute Pasteur Tunis, Tunisia. Tumor cells were routinely maintained in Dulbecco's modified Eagle's minimum essential medium (DMEM) supplemented with 10% heat inactivated fetal bovine serum, 2 mM glutamine, 1% penicillin, and streptomycin at 37°C in a humidified atmosphere containing 5% CO<sub>2</sub>.

**2.5.2. Cell Viability Assay.** The effect of the aqueous ethanolic extract from *P. dactylifera* parthenocarpic dates on the viability of MDA-MB-231 and MCF-7 cells was assessed using the MTT (3-(4,5-dimethylthiazol-2-yl)-2,5-diphenyltetrazolium bromide) method according to Boulaaba et al. [14]. Tumor cells at optimal density were seeded in 96-well microplates (Nunc™ 96-Well Microplates-Thermo Scientific) and incubated overnight at 37°C under 5% CO<sub>2</sub> to allow them to attach. Aqueous ethanolic extract from *P. dactylifera* parthenocarpic dates at different concentrations (1 to 100 mg of dry extract/mL) was added to adhered cells and incubated for 24 h and 72 h. After the indicated time, MTT solution was added and cells were incubated for a further 4 h. The solutions were aspirated out, and DMSO was added to solubilize the formazan crystals within metabolically viable cells.

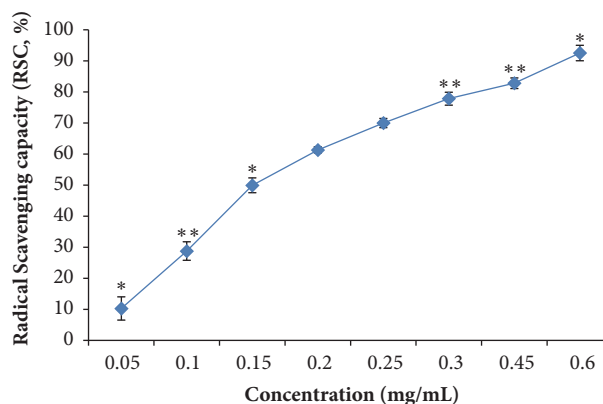


FIGURE 1: Antioxidant activities of the aqueous ethanolic extract from *Phoenix dactylifera* parthenocarpic dates. Differences in antioxidant activity were estimated by one-way analyses of variance (ANOVA) and unpaired Student's t-test compared to the control (\*p < 0.05 and \*\*p < 0.01).

Absorbance was determined by a microplate reader at 560 nm on a multidetection microplate reader (Thermo Labsystems, Franklin, MA, USA). Results were evaluated by comparing the absorbance of the treated cells with the absorbance of wells containing cell treated by the solvent control. Conventionally, cells incubated only with the medium and the solvent were considered the control with 100% viability.

All experiments were performed at least twice in triplicate. The concentration of the substance required for 50% growth inhibition (IC<sub>50</sub> value) was estimated as that resulting in 50% decrease in absorbance as compared to control incubated simultaneously without test substances.

**2.6. Statistical Analysis.** Values were expressed as the mean of triplicate analysis of the samples (n = 3) standard deviation (± SD). Statistical analysis was performed by one-way analyses of variance (ANOVA) and unpaired Student's t-test was used to determine significant differences in hyperglycemia and where appropriate. Differences were considered statistically significant if p < 0.05.

## 3. Results and Discussion

**3.1. DPPH Radical Scavenging Activity.** The antioxidant activity was defined as the mean of free radical scavenging capacity. This activity was measured using the 1,1-diphenyl-2-picrylhydrazyl free radical (DPPH), which is a stable free radical and in the presence of the total extract; it was scavenged. In this study, the antioxidant effect of the aqueous ethanolic extract from *P. dactylifera* parthenocarpic dates was examined by DPPH radical scavenging capacity. The aqueous ethanolic extract showed a potential antioxidant activity in DPPH radical scavenging with an IC<sub>50</sub> value of 0.15 ± 0.011 mg of dry extract/mL (p < 0.05) (Figure 1). The aqueous ethanolic extract was shown to scavenge 94% of superoxide radicals at 0.6 ± 0.03 mg/mL (p < 0.05). This extract had a strong free radical scavenging ability compared to the aqueous date extract (0.8 mg/mL) [15] based on the same method.

Moreover, the aqueous ethanolic extract from parthenocarpic dates exhibited high DPPH scavenging activity compared with *Diploaxis simplex* extract (0.4 mg/mL) [16] and *Aloe vera* leaf (0.635 mg/mL) [12]. These results were in line with those of Mansouri et al. [17] and Hasan et al. [18] who reported that date fruits exhibited potent DPPH scavenging capacities.

Fruits contain different antioxidant compounds. Therefore, measuring the antioxidant capacity of each compound individually becomes very difficult. Several methods have been developed to estimate the antioxidant potential of different plant materials. Usually, these methods measure the ability of antioxidants to scavenge specific radicals. The present study showed that the aqueous ethanolic extract had significant antioxidant activity toward the DPPH free radical assay. The antioxidant activity could be due to the high content of the phytochemical compounds of the aqueous ethanolic extract from parthenocarpic dates. In fact, the content of total phenols was estimated at  $513 \pm 2$  mg of GAE/g of the dry extract [8] and the extract maintains approximately up to 95% stability in phenolic content when stored at  $-20^{\circ}\text{C}$  in the dark. Moreover, the physicochemical results by liquid chromatography-tandem mass spectrometry (LC-MS/MS) analysis demonstrated that the aqueous ethanolic extract from *P. dactylifera* parthenocarpic dates contain several bioactive components acting as antioxidants, such as p-coumaric acid hexose, rosmadial, quercetin, and ganoderenic acid [8]. The antioxidant activity of phenolic compounds is a result of their redox properties, which can play an important role in absorbing and neutralizing free radicals [19].

Reactive free radicals, such as superoxide anion radical, hydroxyl radical, and hydrogen peroxide, have been implicated in the development of many diseases such as cancer, coronary heart disease, autoimmune disease, diabetes, sclerosis, cataracts, and chronic inflammation. According to the important activity on free radical scavenging, the anti-inflammatory effect of the aqueous ethanolic extract from *P. dactylifera* parthenocarpic dates was investigated *in vitro* and *in vivo*.

### 3.2. Evaluation of the Anti-Inflammatory Activity

**3.2.1. In Vitro Study: Inhibition of Phospholipase  $A_2$  Activity.** Phospholipase  $A_2$  is a class of enzyme that catalyzes the hydrolysis of membrane phospholipids releasing arachidonic acid, which serves as a substrate for proinflammatory mediators, such as prostaglandins and leukotrienes. The design of specific inhibitors for  $PLA_2$  might help in the development of new anti-inflammatory drugs.

In this study, the aqueous ethanolic extract was evaluated for their inhibitory effect on the proinflammatory  $PLA_2$  activity. The *in vitro* assay results revealed that the aqueous ethanolic extract showed a significant inhibitory activity against  $PLA_2$  activity depending on the doses of the extract (Figure 2). At a concentration of 130  $\mu\text{g}$  of dry extract/mL, the *P. dactylifera* extract reduced by 50% the activity of the enzyme in a highly significant manner ( $p < 0.001$ ). This extract exhibited a potent inhibition of  $PLA_2$  than the *Aloe vera* L. extract ( $IC_{50} = 0.22$  mg/mL) [12], *Diploaxis*

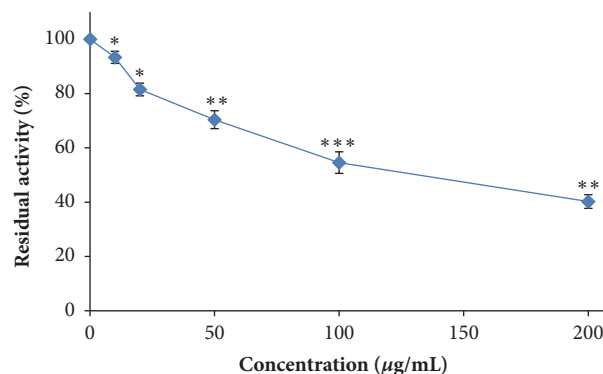


FIGURE 2: Effect of the aqueous ethanolic extract from *Phoenix dactylifera* parthenocarpic dates on phospholipase  $A_2$  activity (\* $p < 0.05$ , \*\* $p < 0.01$ , and \*\*\* $p < 0.001$ ).

*simplex* extract ( $IC_{50} = 2.97$  mg/mL) [16], and *Polygonum multiflorum* extract ( $IC_{50} = 680$   $\mu\text{g/mL}$ ) [20]. The  $PLA_2$  inhibition could be explained by the richness of the aqueous ethanolic extract in phenolic compounds, such as flavonoids, which are able to inhibit key enzymes related to inflammation process [12]. Besides, molecular modeling studies suggested that phenolic hydroxyls are linked to the amino acid Asp 49 of  $PLA_2$  and influence the capacity of this residue to participate in the coordination of the calcium atom, that is, essential to the catalytic activity [21].

#### 3.2.2. In Vivo Study: Carrageenan-Induced Mice Paw Oedema.

The carrageenan-induced paw oedema is a well-known acute model of inflammation that is widely used for screening novel anti-inflammatory compounds. Immediately after carrageenan injection, there is a cascade of mediators' release, as histamine, serotonin, bradykinin, and  $PLA_2$ . These mediators promote an increase in vascular permeability and signal for arachidonate metabolites and nitric oxide release, until the 6th hour.

Before induction of the inflammatory response, mice paw thickness was found to be  $0.20 \pm 0.01$  cm ( $p < 0.05$ ). The phlogistic agent when injected locally into the rat hind paw of the control group induced a severe inflammatory reaction, characterized by an increase in paw thickness up to  $0.27 \pm 0.01$  cm ( $p < 0.05$ ) and  $0.32 \pm 0.01$  cm ( $p < 0.01$ ) after 1 and 4 h, respectively (Table 1). The maximum peak was observed 3 h after injection when the mice paw thickness was found to be  $0.36 \pm 0.01$  cm ( $p < 0.05$ ) (Table 1). The treatment with the standard indomethacin significantly inhibited the paw thickness of carrageenan-induced mice, which reached  $0.26 \pm 0.01$  cm and  $0.22 \pm 0.02$  cm after 3 h and 4 h, respectively (Table 1). As shown in Table 1, the aqueous ethanolic extract from parthenocarpic dates showed significant anti-inflammatory activity when administered intraperitoneally, in the carrageenan-induced rat paw oedema test. The paw thickness of carrageenan-induced mice showed a decrease after 1 h ( $0.22 \pm 0.02$  cm ( $p < 0.05$ )) stronger than the indomethacin effect ( $0.24 \pm 0.01$  cm ( $p < 0.05$ )). The percentage of inhibition of oedema by the aqueous ethanolic extract, 3 h after carrageenan injection, ranged from

TABLE 1: Anti-inflammatory effect of the intraperitoneal administration of the aqueous ethanolic extract from *Phoenixdactylifera* parthenocarpic dates in Carrageenan-induced mice paw oedema test.

Treatment	Paw thickness (cm)				Inhibition (%)			
	1 h	2 h	3 h	4 h	1 h	2 h	3 h	4 h
<b>Control</b>	0.27 ± 0.01*	0.32 ± 0.02 **	0.36 ± 0.01*	0.32 ± 0.01 **	-	-	-	-
<b>Indomethacin</b>	0.26 ± 0.01*	0.26 ± 0.01 <sup>ns</sup>	0.24 ± 0.01 **	0.22 ± 0.02*	14.28	50	75	83.33
<b>Extract</b>	0.22 ± 0.02*	0.24 ± 0.02*	0.21 ± 0.01*	0.2 ± 0.02*	71.2	66.66	93.75	100

Values are expressed as mean ± SD (n=6 animals).

\*: differences were considered statistically significant if  $p < 0.05$ .

\*\*: differences were considered statistically significant if  $p < 0.01$ .

ns: not significant.

93% to 100%, whereas the reference drug produced 75% of inhibition after 3 h (Table 1). These results confirmed the anti-inflammatory activity of the aqueous ethanolic extract from *P. dactylifera* parthenocarpic dates, which could lend support for its pharmaceutical use. Similar results were observed with genus *Cystoseira* extract [1] and *Diplotaxis simplex* extract [16] which reduced the paw oedema in mice, after carrageenan injection. Moreover, Mohamed and Al-Okbi demonstrated that oral administration of methanolic or aqueous extracts of edible portion of *P. dactylifera* dates suppressed the inflammation in the foot of adjuvant arthritis rats [22].

Carrageenan rat paw oedema test produced an acute inflammation that results from the sequential action of several mediators. Histamine and serotonin were mainly released during first 1.5 h after carrageenan injection, kinin was released until 2.5 h, and at the last step, inflammation was continued until 5 h by prostaglandins. The aqueous ethanolic extract inhibited the PLA<sub>2</sub> enzymatic activity in the first phase of inflammation (arachidonate metabolites generation). The bioactive compounds, especially quercetin, present in the aqueous ethanolic extract can be the responsible for the anti-inflammatory activity [23]. In addition, the antioxidant potential observed in *P. dactylifera* extract can be also contributed for reducing inflammation. Thus, the potent anti-inflammatory activity of *P. dactylifera* parthenocarpic dates extract may be related to cumulative effects of different active compounds to reduce the synthesis, release, and action of prostaglandins or free radicals.

Increasing scientific evidence shows that polyphenols are good antioxidants and are effective in preventing inflammatory diseases and can also be used as chemopreventive agents for cancer. These molecules might act as cancer blocking agents, preventing initiation of the carcinogenic process and as cancer suppressing agents, inhibiting cancer promotion and progression [1]. Herein, we evaluated the anticancer effects of the aqueous extract on human breast cancer (MDA-MB-231 and MCF-7) cells *in vitro*.

**3.3. Evaluation of the Antitumoral Activity.** Breast cancer is the most common and leading cause of cancer-related mortality among women globally [24]. In 2012, more than 464,000 new cases were diagnosed with breast cancer in the European Union (EU) and in the United States of America (USA) [24]. It was estimated that there will be

249,260 new cases of female breast carcinoma in the year 2016 [24]. This has led to an increased interest and active search for novel anticancer agents from natural products. In the present study, we attempt to evaluate the anticancer effects of the aqueous ethanolic extract from *P. dactylifera* parthenocarpic dates on human breast carcinoma (MDA-MB-231) and adenocarcinoma (MCF-7) cells.

The effect of different concentrations (1 to 100 mg of dry extract/mL) of the aqueous ethanolic extract on tumor cell viability using the MTT method was assessed (Figure 3(a)). After 24 h incubation of MDA-MB-231 cells with the aqueous ethanolic extract, no significant inhibition of cell growth was observed at (1-25 mg/mL). However, results showed that the cytotoxic effect appeared at high concentrations (50 and 100 mg/mL), when cell viability decreased by 43.66% and 78.48%, respectively (Figure 3(a)). Similarly, results have been observed after treatment of MCF-7 with the aqueous ethanolic extract for 24 h. MCF-7 cells growth inhibition and signs of cytotoxicity were not significantly apparent until a concentration of 25 mg/mL (80% of cell viability). Then cell viability diminished with the dose of 50 and 100 mg/mL to 43.34% and 71.67%, respectively (Figure 3(a)). Interestingly, the viability of both MDA-MB-231 and MCF-7 tumor cells decreased drastically in a dose-dependent manner after 72 h of treatment with aqueous ethanolic extract with respective IC<sub>50</sub> values of  $8 \pm 0.02$  mg/mL ( $p < 0.01$ ) and  $18 \pm 0.02$  mg/mL ( $p < 0.01$ ) (Figure 3(b)).

MDA-MB-231 and MCF-7 cells viability inhibition was more pronounced after 72 h of incubation as compared to 24 h of aqueous ethanolic extract treatment. This result suggests that the inhibition of cell viability may be related to the suppression of proliferation rather than to any cytotoxic or cytolytic effects. This activity might be due to the presence of specific compounds in parthenocarpic dates, like flavonoids glucosides (quercetin), which are known by their cancer chemoprotective attributes [25]. In this context, Rahmani et al. [26] confirmed the therapeutic effects of *P. dactylifera* dates in preventing against cancer are due to its richness in polyphenolic compounds. In addition, previous studies showed that polyphenolic compounds affect cancer cell growth by inducing apoptosis in many cell lines related to breast cancer [24]. In addition, the anticancer effect of the methanolic extract of Ajwa date on human breast adenocarcinoma (MCF-7) cells was evaluated *in vitro*. MCF7 cells treated with concentrations (5, 10, 15, 20, and 25 mg/mL)

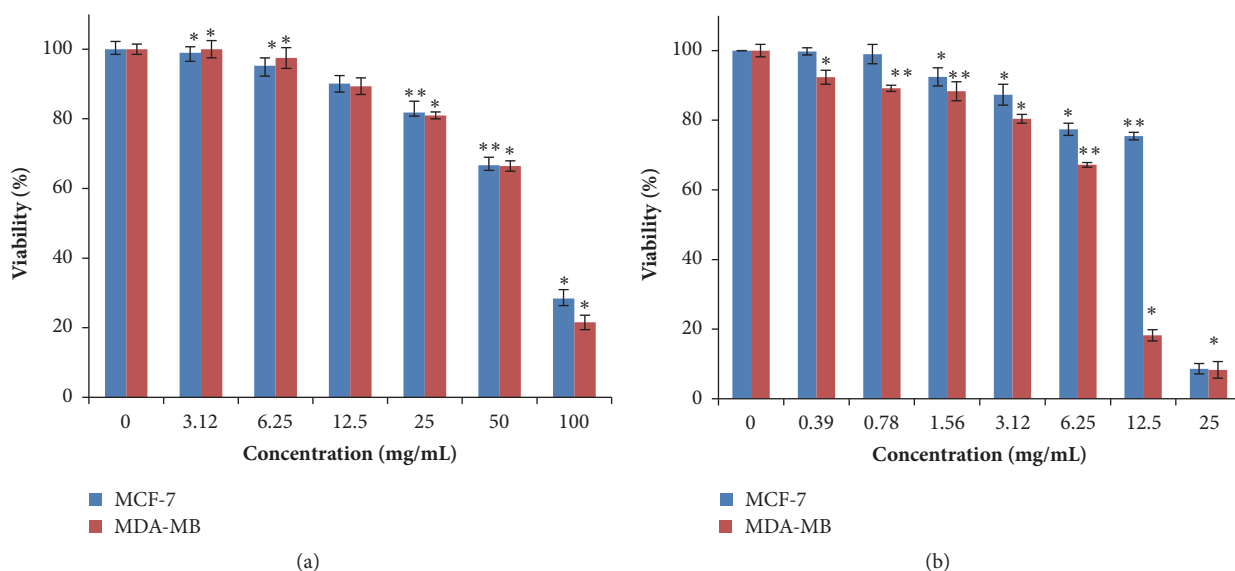


FIGURE 3: Effect of the aqueous ethanolic extract from *Phoenix dactylifera* parthenocarpic dates on MDA-MB-231 and MCF-7 cancer cell lines viability at 24 h (a) and 72 h (b). Differences between selected groups were compared to nonparametric analysis of variance (ANOVA) with Bonferroni post hoc multiple comparison test compared to the control (\* $p < 0.05$  and \*\* $p < 0.01$ ).

of methanolic Ajwa date extract inhibited the growth and the proliferation of its cells by inducing cell cycle arrest. It also induced MCF7 cell death via apoptosis in a dose and time-dependent manner by the activation and changes in genetic expression associated with apoptosis [24].

One important aspect of carcinogenesis is recognized to be the involvement of inflammation. Many studies have been conducted to treat cancers by using various anti-inflammatory agents. In fact, the use of anti-inflammatory agents can alter cancer cell and its microenvironment, potentially increasing apoptosis, and decreasing migration. Interestingly, natural phenolics could exhibit anti-inflammatory properties and also a possible role in the inhibition of cancer development through a number of basic cellular mechanisms [27].

#### 4. Conclusion

*P. dactylifera* plays an important role in social, economic, and ecological Tunisian sectors. Some date palms produce parthenocarpic fruit named Sish. This study revealed that the aqueous ethanolic extract from *P. dactylifera* parthenocarpic dates provides a strong antioxidant activity associated with an interesting anti-inflammatory activity and significant antiproliferative activity against MDA-MB-231 and MCF-7 cancer cell lines. The antitumoral effect of aqueous ethanolic extract could be attributed to a single molecule or to the synergic activity of several components of the total extract.

#### Data Availability

The data used to support the findings of this study are available from the corresponding author upon request.

#### Additional Points

(i) The aqueous ethanolic extract showed a potential antioxidant activity. (ii) The *in vitro* study showed that the extract inhibited the phospholipase  $A_2$ . (iii) The *in vivo* study showed a significantly decrease in the paw oedema in mice. (iv) The extract was effective in inhibiting MDA-MB-231 and MCF-7 cancer cell growth.

#### Conflicts of Interest

The authors declare that they have no conflicts of interest.

#### Authors' Contributions

Mouna Chakroun and Zaineb Abdelkafi-Koubaa participated equally to the work.

#### Acknowledgments

The major part of this work was accomplished at the Faculty of Sciences of Sfax and at the Institute Pasteur of Tunis. The authors gratefully acknowledge the support of Mr. El Abed Mokhles for his assistance in the project. This research was supported by the Ministry of Higher Education and Scientific Research in Tunisia.

#### References

- [1] L. Mhadhebi, A. Mhadhebi, J. Robert, and A. Bouraoui, "Antioxidant, anti-inflammatory and antiproliferative effects of aqueous extracts of three mediterranean brown seaweeds of the Genus *Cystoseira*," *Iranian Journal of Pharmaceutical Research*, vol. 13, no. 1, pp. 207–220, 2014.



- [2] A. H. Rahmani, S. M. Aly, H. Ali, A. Y. Babiker, S. Suikar, and A. A. Khan, "Therapeutic effects of date fruits (*Phoenix dactylifera*) in the prevention of diseases via modulation of anti-inflammatory, anti-oxidant and anti-tumour activity," *International Journal of Clinical and Experimental Medicine*, vol. 7, no. 3, pp. 483–491, 2014.
- [3] W. Mequanint, E. Makonnen, and K. Urga, "In vivo anti-inflammatory activities of leaf extracts of *Ocimum lamiifolium* in mice model," *Journal of Ethnopharmacology*, vol. 134, no. 1, pp. 32–36, 2011.
- [4] R. W. Blackler, B. Gemici, A. Manko, and J. L. Wallace, "NSAID-gastroenteropathy: new aspects of pathogenesis and prevention," *Current Opinion in Pharmacology*, vol. 19, pp. 11–16, 2014.
- [5] G. A. FitzGerald, "COX-2 and beyond: approaches to prostaglandin inhibition in human disease," *Nature Reviews Drug Discovery*, vol. 2, pp. 879–890, 2003.
- [6] E. R. Rayburn, S. J. Ezell, and R. Zhang, "Anti-inflammatory agents for cancer therapy," *Molecular and Cellular Pharmacology*, vol. 1, no. 1, pp. 29–43, 2009.
- [7] L. H. Iwamoto, D. B. Vendramini-Costa, P. A. Monteiro et al., "Anticancer and Anti-Inflammatory Activities of a Standardized Dichloromethane Extract from *Piper umbellatum* L. Leaves," *Evidence-Based Complementary and Alternative Medicine*, vol. 2015, Article ID 948737, 8 pages, 2015.
- [8] H. El Abed, M. Chakroun, I. Fendri et al., "Extraction optimization and in vitro and in vivo anti-postprandial hyperglycemia effects of inhibitor from *Phoenix dactylifera* L. parthenocarpic fruit," *Biomedicine & Pharmacotherapy*, vol. 88, pp. 835–843, 2017.
- [9] C. L. Del-Toro-Sánchez, M. Gutiérrez-Lomeli, E. Lugo-Cervantes et al., "Storage Effect on Phenols and on the Antioxidant Activity of Extracts from *Anemopsis californica* and Inhibition of Elastase Enzyme," *Journal of Chemistry*, vol. 2015, Article ID 602136, 8 pages, 2015.
- [10] J.-K. Kim, J. H. Noh, S. Lee et al., "The first total synthesis of 2,3,6-tribromo-4,5-dihydroxybenzyl methyl ether (TDB) and its antioxidant activity," *Bulletin of the Korean Chemical Society*, vol. 23, no. 5, pp. 661–662, 2002.
- [11] Council of European Communities, "Council instructions about the protection of living animals used in scientific investigations," *The Official Journal of the European Communities*, vol. 1986, pp. 1–18, 358.
- [12] M. Kammoun, S. Miladi, Y. B. Ali, M. Damak, Y. Gargouri, and S. Bezzine, "In vitro study of the PLA2 inhibition and antioxidant activities of Aloe vera leaf skin extracts," *Lipids in Health and Disease*, vol. 10, pp. 30–37, 2011.
- [13] A. E. Rotelli, T. Guardia, A. O. Juárez, N. E. de La Rocha, and L. E. Pelzer, "Comparative study of flavonoids in experimental models of inflammation," *Pharmacological Research*, vol. 48, no. 6, pp. 601–606, 2003.
- [14] M. Boulaaba, K. Mkadmini, S. Tsolmon et al., "In vitro antiproliferative effect of arthrocnemum indicum extracts on CACO-2 cancer cells through cell cycle control and related phenol LC-TOF-MS Identification," *Evidence-Based Complementary and Alternative Medicine*, vol. 2013, Article ID 529375, 11 pages, 2013.
- [15] S. Naskar, A. Islam, U. K. Mazumder et al., "In vitro and in vivo antioxidant potential of hydromethanolic extract of *Phoenix dactylifera* fruits," *Journal of Scientific Research*, vol. 2, pp. 144–157, 2009.
- [16] H. Jdir, B. Khemakham, H. Najjaa et al., "Anti-inflammatory and anti-proliferative activities of the wild edible cruciferous: *Diplotaxis simplex*," *Pharmaceutical Biology*, vol. 54, no. 10, pp. 2111–2118, 2016.
- [17] A. Mansouri, G. Embarek, E. Kokkalou, and P. Kefalas, "Phenolic profile and antioxidant activity of the Algerian ripe date palm fruit (*Phoenix dactylifera*)," *Food Chemistry*, vol. 89, no. 3, pp. 411–420, 2005.
- [18] N. S. Hasan, Z. H. Amom, A. Nor, N. Mokhtarrud, N. Mohd Esa, and A. Azlan, "Nutritional Composition and in vitro Evaluation of the Antioxidant Properties of Various Dates Extracts (*Phoenix dactylifera* L.) from Libya," *Asian Journal of Clinical Nutrition*, vol. 2, no. 4, pp. 208–214, 2010.
- [19] B. Mahdi-Pour, S. L. Jothy, L. Y. Latha, Y. Chen, and S. Sasidharan, "Antioxidant activity of methanol extracts of different parts of *Lantana camara*," *Asian Pacific Journal of Tropical Biomedicine*, vol. 2, no. 12, pp. 960–965, 2012.
- [20] R. W. Li, G. David Lin, S. P. Myers, and D. N. Leach, "Anti-inflammatory activity of Chinese medicinal vine plants," *Journal of Ethnopharmacology*, vol. 85, no. 1, pp. 61–67, 2003.
- [21] S. L. da Silva, A. K. Calgarotto, V. Maso et al., "Molecular modeling and inhibition of phospholipase A2 by polyhydroxy phenolic compounds," *European Journal of Medicinal Chemistry*, vol. 44, no. 1, pp. 312–321, 2009.
- [22] D. A. Mohamed and S. Y. Al-Okbi, "In vivo evaluation of antioxidant and anti-inflammatory activity of different extracts of date fruits in adjuvant arthritis," *Polish Journal of Food And Nutrition Sciences*, vol. 13, pp. 397–402, 2004.
- [23] C. Caddeo, O. Díez-Sales, R. Pons, X. Fernández-Busquets, A. M. Fadda, and M. Manconi, "Topical anti-inflammatory potential of quercetin in lipid-based nanosystems: In vivo and in vitro evaluation," *Pharmaceutical Research*, vol. 31, no. 4, pp. 959–968, 2014.
- [24] F. Khan, F. Ahmed, P. N. Pushparaj et al., "Ajwa Date (*Phoenix dactylifera* L.) extract inhibits human breast adenocarcinoma (MCF7) cells in vitro by inducing apoptosis and cell cycle arrest," *PLoS ONE*, vol. 11, no. 7, Article ID e0158963, 2016.
- [25] D. Thanekar, J. Dhodi, N. Gawali et al., "Evaluation of antitumor and anti-angiogenic activity of bioactive compounds from *Cinnamomum tamala*: In vitro, in vivo and in silico approach," *South African Journal of Botany*, vol. 104, pp. 6–14, 2016.
- [26] A. H. Rahmani, S. M. Aly, H. Ali et al., "Therapeutic effects of date fruits (*Phoenix dactylifera*) in the prevention of diseases via modulation of anti-inflammatory, anti-oxidant and anti-tumour activity," *International Journal of Clinical and Experimental Medicine*, vol. 7, no. 3, pp. 483–491, 2014.
- [27] J. Dai and R. J. Mumper, "Plant phenolics: extraction, analysis and their antioxidant and anticancer properties," *Molecules*, vol. 15, no. 10, pp. 7313–7352, 2010.

## Research Article

# *Angelica gigas* Nakai Has Synergetic Effects on Doxorubicin-Induced Apoptosis

Yong-Joon Jeon <sup>1</sup>, Jong-Il Shin <sup>1</sup>, Sol Lee,<sup>1</sup> Yoon Gyeong Lee,<sup>1</sup> Ji Beom Kim,<sup>1</sup> Hak Cheol Kwon,<sup>2</sup> Sung Hun Kim,<sup>2</sup> Inki Kim,<sup>3</sup> Kyungho Lee <sup>1,4</sup> and Ye Sun Han <sup>5</sup>

<sup>1</sup>Department of Biological Sciences, Konkuk University, Neungdong-ro 120, Gwangjin-gu, Seoul 05029, Republic of Korea

<sup>2</sup>Korea Institute of Science and Technology, Gangneung, Gangwondo 25451, Republic of Korea

<sup>3</sup>Department of Convergence Medicine, Asan Institute for Life Sciences, Asan Medical Center, Seoul 05505, Republic of Korea

<sup>4</sup>Korea Hemp Institute, Konkuk University, Konkuk University, Neungdong-ro 120, Gwangjin-gu, Seoul 05029, Republic of Korea

<sup>5</sup>Department of Advanced Technology Fusion, Konkuk University, Neungdong-ro 120, Gwangjin-gu, Seoul 05029, Republic of Korea

Correspondence should be addressed to Kyungho Lee; [kyungho@konkuk.ac.kr](mailto:kyungho@konkuk.ac.kr) and Ye Sun Han; [yshan@konkuk.ac.kr](mailto:yshan@konkuk.ac.kr)

Received 7 March 2018; Revised 11 July 2018; Accepted 24 July 2018; Published 1 August 2018

Academic Editor: Claudio Tabolacci

Copyright © 2018 Yong-Joon Jeon et al. This is an open access article distributed under the Creative Commons Attribution License, which permits unrestricted use, distribution, and reproduction in any medium, provided the original work is properly cited.

Natural products are valuable sources for drug discovery because they have a wide variety of useful chemical components and biological properties. A quick reevaluation of the potential therapeutic properties of established natural products was made possible by the recent development of the methodology and improvement in the accuracy of an automated high-throughput screening system. In this study, we screened natural product libraries to detect compounds with anticancer effects using HeLa cells. Of the 420 plant extracts screened, the extract of *Angelica gigas* Nakai (AGN) was the most effective in reducing cell viability of HeLa cells. Markers of apoptosis, such as exposure of phosphatidylserine and cleavage of caspase-7 and PARP, were increased by treatment with the AGN extract. Treatment of the AGN extract increased expression of PKR as well as ATF4 and CHOP, the unfolded protein response genes. In addition, cotreatment of doxorubicin and the AGN extract significantly increased doxorubicin-induced apoptosis in HeLa cells. Decursin and decursinol angelate, which were known to have anticancer effects, were the main components of the AGN extract. These results suggest that the extract of AGN containing, decursin and decursinol angelate, increases doxorubicin susceptibility.

## 1. Introduction

Doxorubicin (adriamycin), belonging to the anthracycline group, was initially derived from *Streptomyces peucetius* in the 1960s [1]. Owing to its wide range of anticancer effects against various types of cancers, including solid tumors and hematological malignancies, doxorubicin has occupied an important place in chemotherapy [2, 3]. The application of doxorubicin, however, has many side effects including cardiac toxicity; therefore, the dose of doxorubicin has been limited [4]. In addition, multidrug resistance or chemoresistance prompted by chemotherapy reduced doxorubicin susceptibility, further limiting its use [5]. Despite these disadvantages, doxorubicin is still an attractive chemotherapeutic drug. To use doxorubicin more efficiently, various therapies have been proposed, including the use of combination therapy as a

treatment strategy. Consequently, chemotherapy regimens using doxorubicin, such as FAC (fluorouracil, doxorubicin, and cyclophosphamide), TAC (docetaxel, doxorubicin, and cyclophosphamide), and R-CHOP (rituximab, cyclophosphamide, doxorubicin, vincristine, and prednisone), have been administered to cancer patients [6, 7].

Ever since natural products have been recognized as key components of traditional medicines, many drugs and therapies using natural products have been developed [8, 9]. Consequently, 24 natural products were developed into approved novel drugs between 1970 and 2006 [10]. However, it is very difficult to select the biologically useful natural products from among the wide diversity of natural products. Although high-throughput screening (HTS) is an efficient method for selecting various natural products, it is known to have drawbacks during natural product screening [11]. In

this study, we screened natural product libraries via HTS and applied the MTT assay to select the extract of *Angelica gigas* Nakai (AGN), which exhibited anticancer properties.

The genus *Angelica* L. belonging to the Umbelliferae family is distributed in Asia, Europe, and North America and comprises more than 60 species [12, 13]. In China, Japan, and Korea, *Angelica* L. has been used as a traditional herbal medicine for curing colds, pain, and anemia and has been known as the “female ginseng” due to its beneficial effects on female health [12, 14, 15]. *Angelica* L. contains a variety of bioactive metabolites, such as pyranocoumarins, essential oils, and polyacetylenes, which exhibit many beneficial effects, including anticancerous, anti-inflammatory, antifungal, antioxidant, and neuroprotective properties [13, 14]. Pyranocoumarins, which are known to be associated with the anticancer effect of *Angelica* L., are more abundant in the roots of the *Angelica gigas* Nakai (local name dang-gui in Korea) growing in Korea than in the species growing in China and Japan [16]. Pyranocoumarins are the major components of the alcoholic extract of AGN [17]. Decursin, decursinol angelate, and decursinol are representative pyranocoumarins in the AGN extract. Decursin, the most abundant pyranocoumarin in the AGN extract, has been reported to show anticancer effects in various cancer cells [13, 14]. In addition, the alleviation of neurotoxicity and nephrotoxicity via its antioxidant properties is the other beneficial effect of decursin [18, 19]. As neurotoxicity and nephrotoxicity are some of the side effects of doxorubicin [20], the combination of doxorubicin and the AGN extract could offer a strategy for increasing the effectiveness of doxorubicin.

Integrated stress response (ISR) is a cellular stress response induced by various stress stimuli, leading to the phosphorylation of eukaryotic translation initiation factor 2 alpha (eIF2 $\alpha$ ). The phosphorylation of eIF2 $\alpha$  is mediated by four kinases, General Control Nondepressible protein 2 (GCN2), Protein Kinase R (PKR), PKR-like ER localized eIF2 $\alpha$  Kinase (PERK), and Heme-Regulated Inhibitor kinase (HRI) [21, 22]. Although each kinase recognizes different stimuli, ISR is initiated by very diverse stress stimuli via the four kinases and prompts a cellular response for determining cell fate. The upregulation of eIF2 $\alpha$  phosphorylation attenuates global protein translation to reduce cellular stress [21]. However, the rates of translation of mRNAs including the second 5'-uORF such as activating transcription factor 4 (ATF4) are further increased by eIF2 $\alpha$  phosphorylation [23]. ATF4 activates the expression of genes that regulate cellular homeostasis in order to protect cells or increases the expression of downstream transcription factors such as C/EBP-homologous protein (CHOP) [24]. In conditions of severe stress, ATF4 and CHOP induce cell death by activating downstream death factors or by producing ROS via increased protein synthesis [24, 25]. Therefore, ISR is an important mechanism for determining cell fate by inducing a cellular response by various cellular stimuli via the eIF2 $\alpha$ -ATF4 pathway.

In this study, the AGN extract effectively induced apoptosis in HeLa cells. As the cell death induced by doxorubicin was related to eIF2 $\alpha$  phosphorylation, we investigated the synergetic effect between doxorubicin and the AGN extract.

The administration of the AGN extract enhanced ATF4 and CHOP expression in doxorubicin-treated HeLa cells, resulting in an increase in doxorubicin-induced apoptosis.

## 2. Materials and Methods

Doxorubicin was purchased from Sigma-Aldrich (St. Louis, MO). The PKR inhibitor C16 was purchased from Calbiochem (La Jolla, CA). The anti-phospho eIF2 $\alpha$ , anti-eIF2 $\alpha$ , and anti-CHOP antibodies were purchased from Cell Signaling Technology (Beverly, MA). The anti-GAPDH, anti-actin, anti-caspase-3, anti-PKR, anti-Bcl-2, and anti-PARP antibodies were purchased from Santa Cruz Biotechnology (Santa Cruz, CA). The annexin V probe was purchased from Bioacts (Korea). Hoechst 33342 was purchased from Invitrogen (Carlsbad, CA).

**2.1. Cell Culture.** The HeLa cell line was obtained from the Korean Cell Line Bank (KCLB). The HeLa cells were cultured in Dulbecco's modified Eagle's media (Welgene, Daegu, Korea) supplemented with 10% heat-activated fetal bovine serum (Biowest, Nuaillé, France) and 1% penicillin or streptomycin mixtures (GIBCO, ThermoFisher, MA, USA). The HeLa cells were incubated in a humidified atmosphere at a CO<sub>2</sub> concentration of 5% and a temperature of 37°C.

**2.2. Cell Viability Assay.** The cells were seeded in 48-well plates and incubated for 16 h. The cells were treated with different concentrations of doxorubicin for 24 h. Cell survival was measured using the MTT [3-(4, 5-dimethylthiazol-2-yl)-2, 5-diphenyltetrazolium bromide] assay (Sigma-Aldrich, St. Louis, MO). In brief, PBS containing 5 mg/ml MTT was diluted with the media at a concentration of 0.5 mg/ml and incubated in a humidified chamber containing CO<sub>2</sub> for 2 h. The medium was aspirated from each well and 200  $\mu$ l DMSO was added to dissolve the Formazan crystals. The absorbance of each well was measured using a UVM 340 plate reader at a wavelength of 570 nm.

**2.3. Immunoblot Analyses.** The cells were harvested using RIPA lysis buffer [containing 150 mM NaCl, 1% Triton X-100, 1% sodium deoxycholate, 0.1% SDS, 50 mM Tris-HCl, and 2 mM EDTA] along with 1% phosphatase inhibitor and protease inhibitor cocktail (Roche Diagnostics, Germany). The protein concentration was quantified using the Pierce BCA protein assay kit (Thermo Scientific, Australia). Proteins boiled in 1x sample buffer [containing 500 mM Tris-HCl (pH 6.8), 10% SDS, 20% glycerol, 0.05% bromophenol blue, and 1%  $\beta$ -mercaptoethanol] for 5 minutes at 100°C were separated on SDS-polyacrylamide gels. The proteins were electrotransferred to Immobilon-P membranes (Millipore, Temecula, CA) and blotted with the indicated antibodies at 4°C overnight in Tris-Buffered saline containing 0.08% Tween 20 (TBST) and 1% nonfat milk. The membranes were then incubated with horseradish peroxidase-conjugated antibodies at room temperature for 2 h, and the band signal was detected using a LAS-3000 Luminescent Image Analyzer (Fujifilm, Japan). To determine the equal loading of samples, the blots were stripped in stripping buffer [containing



TABLE 1: EC50 values of the natural products.

Natural product extract	#478	#622	#1114	#1197
EC 50 value	46.77	10.36	29.12	43.26

100 mM  $\beta$ -mercaptoethanol, 2% SDS, and 62.5 mM Tris-HCl (pH 6.8)] at 50°C for 20 minutes, followed by washing twice with TBST buffer for 15 minutes each time, and reprobed with an antibody specific for  $\beta$ -actin or GAPDH.

**2.4. Measurement of Apoptosis.** The cells were cultured in a confocal dish and treated with doxorubicin and/or the AGN extract for 24 h. The cells were washed with PBS and binding buffer (20 mM Hepes at pH 7.4, 150 mM NaCl, and 2.5 mM  $\text{CaCl}_2$ ). The staining solution was prepared by diluting the annexin V probe and Hoechst 33342 with the binding buffer at concentration ratios of 1:200 and 1:5000, respectively. The cells were stained with the staining solution for 20 minutes. The stained cells were observed using a confocal microscope (Zeiss LSM 800, Carl Zeiss).

**2.5. Preparation of Crude Extract.** The crude extract samples used in this study were provided by Natural Product Library of Korea Institute of Science and Technology, Gangneung Institute, Gangneung, Korea. The natural product library was made from Korean native plants. The preparation of *A. gigas* extract is as follows. The roots of *A. gigas* were purchased in a local oriental medicine market in Bonghwa, Korea, in 2015. The plant materials were authenticated by Professor DS Jang at College of Korean Medicine at Kyung Hee University. The specimen was deposited in KIST Natural Product Library (Deposit number: #BS0622A1). The dried materials (100 g) were cut and extracted twice with 1 L of ethanol by reflux at 60°C for 2 hours. Thereafter, the extract was filtered and concentrated using a rotary evaporator under vacuum at 35°C.

**2.6. Chemical Composition of the AGN Extract.** To investigate the chemical constituents of the AGN extract, LC/MS analyses were performed on an Agilent 1200 HPLC system equipped with UV and ESI-MS detection, using a Phenomenex Luna C18 column (150  $\times$  4.6 mm, 5  $\mu\text{m}$ ). The mobile phase used was a linear gradient of 10-100% acetonitrile in water (containing 0.05% formic acid) for over 30 minutes at a flow rate of 0.7 ml/min. The HPLC chromatogram was monitored at a UV wavelength of 254 nm. Mass analysis was performed using the positive-ion mode. After analyses, the peaks in the HPLC chromatogram were identified by comparing the obtained UV spectra and mass spectra with those of compounds previously reported from *A. gigas*.

**2.7. Quantitative Real-Time PCR.** Quantitative real-time PCR was accomplished with HiPi Real-Time PCR 2 $\times$  Master Mix SYBR Green (ELPiS Biotechnology, Korea) with 40 cycles. The cycle threshold (CT) was observed in extension step and used for calculation of relative gene expression. Analysis of melting curve was carried out in order to convict specific amplification.

**2.8. Statistical Analyses.** The values in the figures are expressed as the mean  $\pm$  SD. The figures in this study represent the results of experiments performed more than three times. Statistical analyses of the data obtained from the control and the treated groups were performed by using Student's t-test. Values of  $P < 0.05$  indicate statistical significance.

### 3. Results

**3.1. Screening of the Most Effective Anticancer Candidate from the KIST Natural Product Library.** Initially, natural product extract libraries were selected to obtain components with anti-inflammatory effects. Since recent studies have shown that cancer and inflammation are closely related [26], in this study we investigated the anticancer effects of natural product extracts from the KIST Natural Product Library. To select extracts with anticancer properties from among approximately 420 natural products, HeLa cells were treated with 50  $\mu\text{g/ml}$  of each natural product extract for 24 hours and natural product extracts that markedly reduced cell viability to below 50% were identified. Through this process, four extracts, #BE0478A1, #BE0622A1, #BE1114A1, and #BE1197A1, were selected. In order to compare the anticancer effects of the four extracts with EC50 value, HeLa cells were treated with various concentrations of each extract for 24 hours and EC50 value of the four natural product extracts was calculated (Table 1 and Figure 1(a)). The results showed that the #BE0622A1 extract was the most efficient in reducing HeLa cell viability, depending on the concentration (Figure 1(a)), and the EC<sub>50</sub> value was the lowest compared to that of the other extracts (Table 1). Apoptosis has been recognized as an important mechanism for cancer therapy, and many anticancer drugs are known to induce apoptosis in cancer cells [27]. The activation of caspase-7 (cCas-7) and the cleavage of PARP are representative markers of apoptosis. Thus, we compared the apoptosis induced by the extracts by observing cCas-7 activation and PARP cleavage (Figure 1(b)). Similarly to the cell viability, cCas-7 activation and PARP cleavage were enhanced more after treatment with the #BE0622A1 extract than with extracts #BE1114A1 and #BE1197A1.

The apoptosis mediated by the extract #BE0622A1 was also confirmed by annexin V staining (Figure 1(c)). Among the natural products evaluated, #BE0622A1 proved to be the most effective anticancer extract in HeLa cells. The extract #BE0622A1 was prepared from root of *Angelica gigas* Nakai (AGN).

**3.2. Activation of ISR by Treatment with the Angelica gigas Nakai Extract.** ISR has been known to cope with diverse stresses, resulting in cell death or adaptation [21]. Four kinases sensing various stress stimuli phosphorylate eIF2 $\alpha$  to initiate ISR. As the AGN extract is a crude mixture, we speculated that the AGN extract can offer numerous kinds of



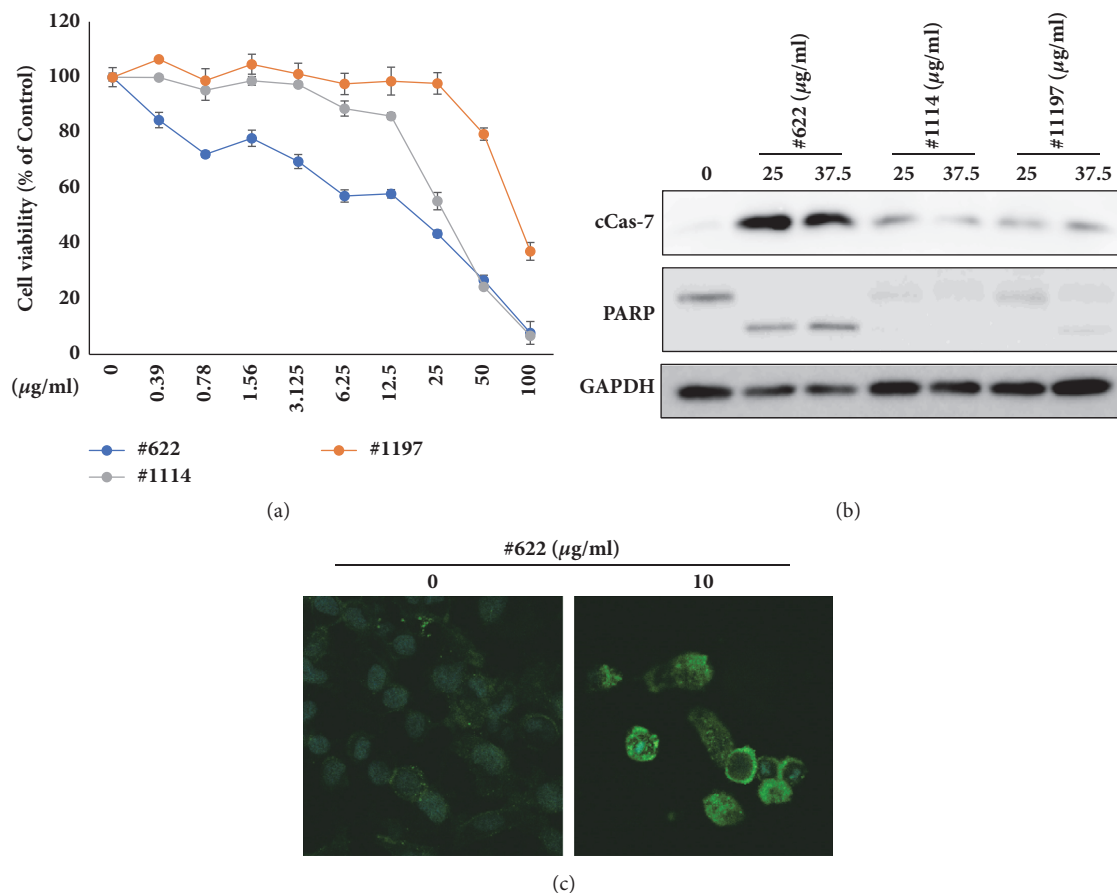


FIGURE 1: *Angelica gigas* Nakai (#BE0622A1), one of the 420 natural products, showed the most effective anticancer effect. (a) The HeLa cells were treated with various concentrations of the indicated natural products for 24 h, and the MTT assay was subsequently performed. (b) The HeLa cells were treated with various concentrations of #BE0622A1, #BE1114A1, and #BE1197A1 for 24 h, and cell lysates were subjected to immunoblot analyses using specific antibodies for cleaved form of caspase-7, PARP, and GAPDH. (c) The HeLa cells were treated with various concentrations of #BE0622A1 for 24 h and apoptosis was analyzed by annexin V staining with FITC conjugation.

stimuli to HeLa cells. Accordingly, we investigated whether the AGN extract could increase phosphorylation of eIF2 $\alpha$ . The EC<sub>50</sub> value of the AGN extract was approximately 10  $\mu$ g/ml (Figure 1(a)). Based on these results, the level of eIF2 $\alpha$  phosphorylation was measured after treatment with the AGN extract for 16 h (Figure 2(a)). The level of eIF2 $\alpha$  phosphorylation was not affected by concentration of the AGN extract. However, the expression of ATF4 and CHOP, downstream factors of eIF2 $\alpha$ , was enhanced by treatment with the AGN extract. Phosphorylation of eIF2 $\alpha$  was increased in a time-dependent manner (Figure 2(b)). The phosphorylation of eIF2 $\alpha$  was increased after 2 h treatment with the AGN extract. At the same time, the expression of PKR, one of the eIF2 $\alpha$  kinases, was also increased. The transcription of ATF4 and CHOP was increased in a time-dependent manner, and expression of ATF4 and CHOP was also increased sequentially after 4 h and 8 h, respectively (Figures 2(b)–2(d)). We therefore concluded that the AGN extract-mediated apoptosis was associated with ISR via the eIF2 $\alpha$ -ATF4-CHOP pathway. Treatment of the AGN extract also increased the splicing of XBP1 mRNA, suggesting activation of the IRE1 $\alpha$  pathway (data not shown).

**3.3. The AGN Extract Showed a Synergetic Effect on the Doxorubicin-Induced Apoptosis.** Previous studies have demonstrated that phosphorylation of eIF2 $\alpha$  improved doxorubicin-mediated cell death in cancer cells [28, 29]. In addition, combination therapy has been widely used as a method for overcoming the limitations of chemotherapy in the treatment of cancer [30]. Therefore, we hypothesized that doxorubicin and the AGN extract could exhibit a synergetic effect based on eIF2 $\alpha$  phosphorylation. To investigate whether AGN affects doxorubicin-induced cell death, doxorubicin was coadministered with the AGN extract for 24 h (Figure 3(a)). Although cotreatment with 0.5  $\mu$ g/ml AGN extract and various concentration of doxorubicin hardly affected doxorubicin-induced cell viability, cotreatment with 1  $\mu$ g/ml AGN extract and 1  $\mu$ M doxorubicin significantly reduced the cell viability. We then examined the effect of the AGN extract on doxorubicin-induced apoptosis through cCas-7 and PARP. Cotreatment with 1  $\mu$ M doxorubicin with 1  $\mu$ g/ml or 2  $\mu$ g/ml AGN extract markedly increased the activation of caspase-7 and the cleaved form of PARP (Figure 3(b)), which means that the doxorubicin-mediated apoptosis was greatly enhanced by the administration of the AGN extract. Furthermore, the

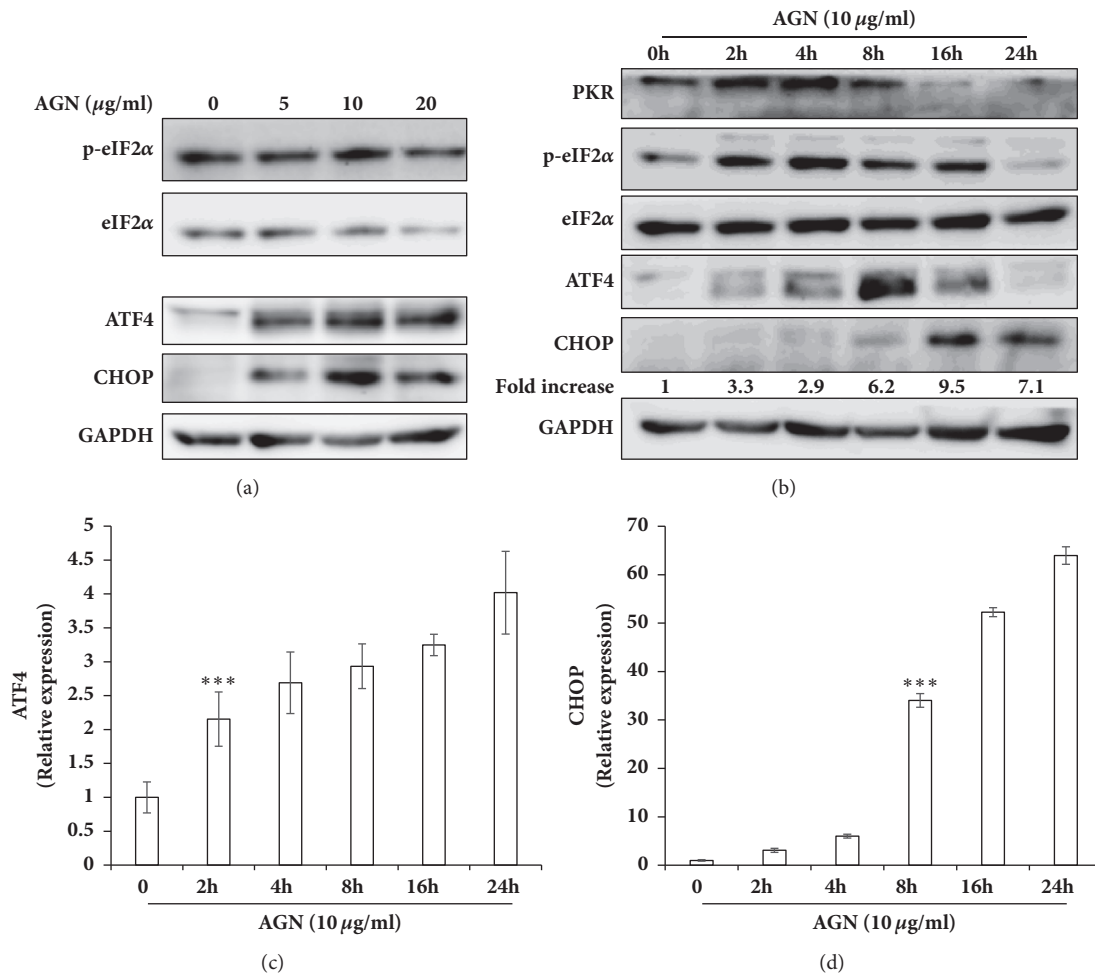


FIGURE 2: The AGN extract activated the integrated stress response (ISR) in HeLa cells. The HeLa cells were treated with the indicated concentrations of the AGN extract for 16 h (a) or with 10 μg/ml of the AGN extract for the indicated time periods (b). Cell lysates were subjected to immunoblot analyses using the indicated antibodies. The indicated fold increase in CHOP expression is the ratio of the CHOP to GAPDH. (c, d) The mRNA levels of ATF4 and CHOP were determined by real-time quantitative PCR. Statistical significance of the difference as calculated by Student's *t*-test is with \*\*\**p*<0.001.

administration of the AGN extract along with doxorubicin considerably increased the cleaved form of caspase-8 in contrast to the administration of doxorubicin alone (Figure 3(b)). The upregulation of the cleaved form of caspase-8 indicates that the receptor-mediated/extrinsic apoptotic pathway is activated [31]. The fluorescence intensity of the apoptotic marker as indicated by annexin V staining in the Hoechst-stained cells was also stronger when the cells were cotreated with doxorubicin and the AGN extract than with doxorubicin alone (Figure 3(c)). These results suggest that doxorubicin-induced apoptosis was enhanced via the extrinsic apoptotic pathway by the administration of the AGN extract.

**3.4. Upregulation of Apoptosis via the ATF4-CHOP Pathway.** The abovementioned results demonstrate that the AGN extract has a synergetic effect on doxorubicin-induced apoptosis. We further speculated whether ISR is correlated to the AGN extract-mediated synergy. To confirm the correlation, HeLa cells were cotreated with doxorubicin and the AGN

extract (Figure 4). Figures 4(a)–4(c) represent the time-dependent changes in transcriptional and translational level expression of ATF4 and CHOP at the indicated concentrations, and Figure 4(d) depicts the changes at various concentrations of doxorubicin and the AGN extract over 24 hours. Although the treatment with doxorubicin alone hardly enhanced the expression of ATF4 and CHOP, cotreatment with the AGN extract and doxorubicin increased the expression of ATF4 and CHOP. However, in comparison to the administration of the AGN extract alone, the expression level of ATF4 and CHOP was low by cotreatment (Figures 4(a) and 4(d)). The expression of death receptor 5 (DR5), which is a downstream factor of CHOP and related to caspase-8 activation, was not changed in correspondence with the expression of CHOP (Figure 4). The expression of DR5, therefore, was not related to the ATF4-CHOP pathway. Nevertheless, these results suggest that the synergetic effect of the AGN extract is related to the upregulation of ATF4 and CHOP expression.

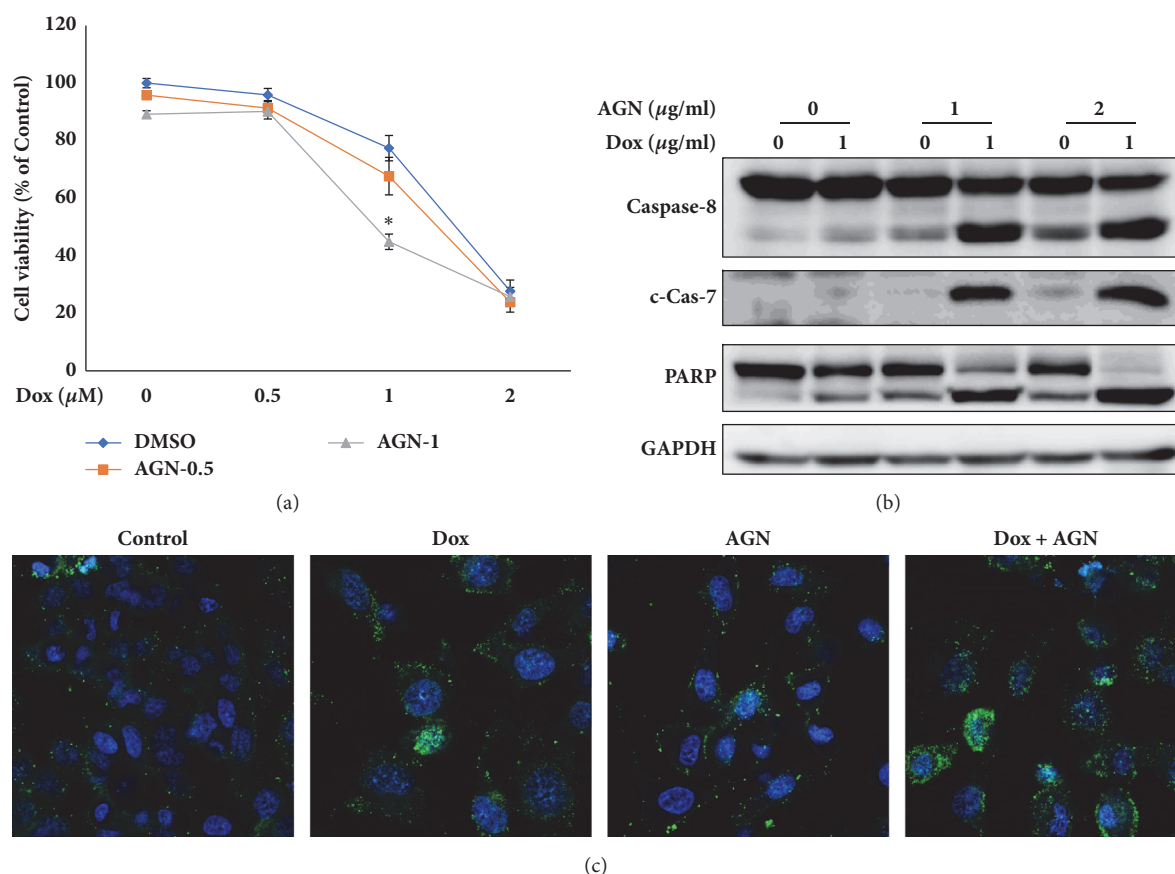


FIGURE 3: Coadministration of the AGN extract with doxorubicin enhanced doxorubicin-induced apoptosis in HeLa cells. (a) The cells were cotreated with the indicated concentrations of doxorubicin and the AGN extract for 24 h, and cell viability was measured using the MTT assay. The statistical significance of the differences, as calculated by Student's t-test, was determined with \* $p < 0.01$ . (b) The cells were cotreated with the indicated concentrations of doxorubicin and the AGN extract for 24 h and subjected to immunoblot analyses using specific antibodies as indicated. (c) The cells were cotreated with 1  $\mu$ M doxorubicin and 1  $\mu$ g/ml AGN extract for 16 h and apoptosis was analyzed by costaining with annexin V-FITC and Hoechst probes.

**3.5. Chemical Composition of the AGN Extract.** Sowndhararajan et al. reported that there are differences in major components depending on the plant part, yield, and extraction method in essential oil of various species of *Angelica* [32]. Therefore, to clarify the major components and biologically active components of the AGN extract, the AGN extract was divided into eight fractions. When HeLa cells were treated with various concentrations of each fraction for 24 hours, fraction #3 reduced HeLa cell viability most effectively (Supplementary Materials, Figure S1a). Also, fraction #3 not only activated caspase 7 but also increased expression of CHOP in HeLa cells (Supplementary Materials, Figure S1b). We then checked the HPLC-MS chromatogram and the  $^1\text{H}$  NMR spectrum of each fraction to find major components of each fraction. Figure 5(b) revealed that fraction #3 of the AGN extract contained three coumarins, 7-demethylsuberosin ( $m/z$  231), decursin ( $m/z$  329), and decursinol angelate ( $m/z$  329). Among these substances, decursin and decursinol angelate were the main constituents (Figure 5(b)). These compounds are known as the principal constituents of *A. gigas*, which have significant anticancer effects in various

cancer models [8, 9]. Therefore, the results proposed that these compounds play an important role in induction of apoptosis in HeLa cells.

## 4. Discussion

Although doxorubicin is an efficient anticancer drug, various side effects such as drug resistance and cytotoxicity have limited the use of doxorubicin. Many attempts have been made to overcome the limitations of doxorubicin usage and enhance its efficiency, and combination therapy has frequently been used as a strategy for the efficient use of doxorubicin. In the present study, the combination of doxorubicin and the AGN extract markedly enhanced doxorubicin-induced apoptosis in HeLa cells (Figure 3). This event was associated with the AGN extract-mediated expression of ATF4 and CHOP (Figures 2 and 4). Particularly, unlike in HeLa cells, cotreatment of doxorubicin and the AGN extract did not significantly increase doxorubicin-induced apoptosis in wild type WI-38 cells (Supplementary Materials, Figure S2). These results demonstrate that administration of the AGN extract

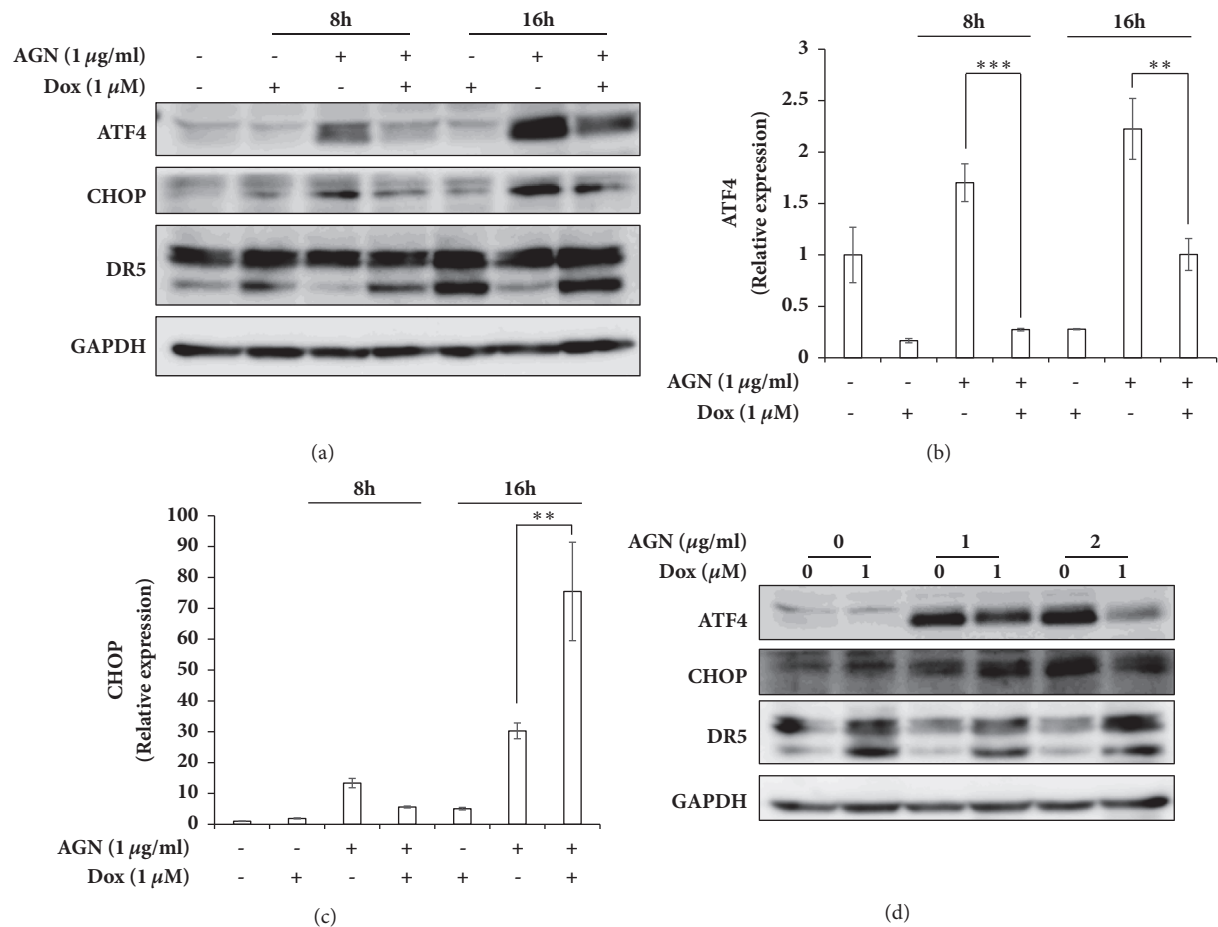


FIGURE 4: Administration of the AGN extract activated the ATF4-CHOP pathway in doxorubicin-treated HeLa cells. (a) The cells were cotreated with 1  $\mu$ M doxorubicin and 1  $\mu$ g/ml AGN extract for the indicated time periods and immunoblot analyses were performed using the indicated antibodies. (b, c) The mRNA level of ATF4 and CHOP were determined by real-time quantitative PCR. Statistical significance of the difference as calculated by Student's *t*-test is with \*\**p*<0.01 or \*\*\**p*<0.001. (d) The cells were cotreated with 1  $\mu$ M doxorubicin and 1-2  $\mu$ g/ml AGN extract for 24 h as indicated and immunoblot analyses were performed using the indicated antibodies.

increased the efficiency of doxorubicin in HeLa cells through the activation of ISR, suggesting that the AGN extract works synergistically with doxorubicin.

The AGN extract was the most effective among the natural products screened in inducing apoptosis in HeLa cells (Figure 1). AGN-mediated apoptosis was associated with the eIF2 $\alpha$ -ATF4-CHOP pathway (Figure 2). Accordingly, we investigated the activity of eIF2 $\alpha$  kinases PERK and PKR under conditions that the cells were treated with the AGN extract alone. PERK, which is known to be activated by ER stress [21], was not activated by treatment with 10  $\mu$ g/ml AGN extract (data not shown). On the other hand, the AGN extract increased the expression of PKR, which corresponded to the time when eIF2 $\alpha$  phosphorylation is increased (Figure 2(b)). Treatment with the PKR inhibitor C16 significantly inhibited the activation of cCas-7 and restored cell viability that had been reduced by treatment with the AGN extract (Supplementary Materials, Figures S3a and S3b). These data show that the AGN extract seems to induce apoptosis by activating PKR in HeLa cells. Treatment with C16, however, neither inhibited nor increased the expression

of ATF4 and CHOP (Supplementary Materials, Figure S3c). Previous studies reported that the inhibition of PKR using C16 decreased caspase-3 activation by inhibiting NF- $\kappa$ B-induced inflammation and FADD phosphorylation [33, 34]. p53 is another PKR-mediated apoptotic signal transducer [29, 35]. Therefore, it seems that there is no correlation between the activity of PKR and expression of ATF4-CHOP in AGN extract-treated HeLa cells; upregulation of the eIF2 $\alpha$ -ATF4-CHOP pathway by treatment with C16 shows the possibility of correlation to another eIF2 $\alpha$  kinase.

Expression of ATF4 and CHOP was not induced by treatment of doxorubicin alone in HeLa cells, but coadministration with the AGN extract markedly increased the expression of both genes. Indeed, the expression level of ATF4 and CHOP was higher when the cells were treated with the AGN extract alone than with cotreatment (Figure 4). Treatment of breast cancer cells with doxorubicin effectively increases the phosphorylation of eIF2 $\alpha$  but suppresses the expression of ATF4 at the transcription level [28, 36]. Nevertheless, administration of the AGN extract increased the expression of ATF4 and CHOP in doxorubicin-treated HeLa



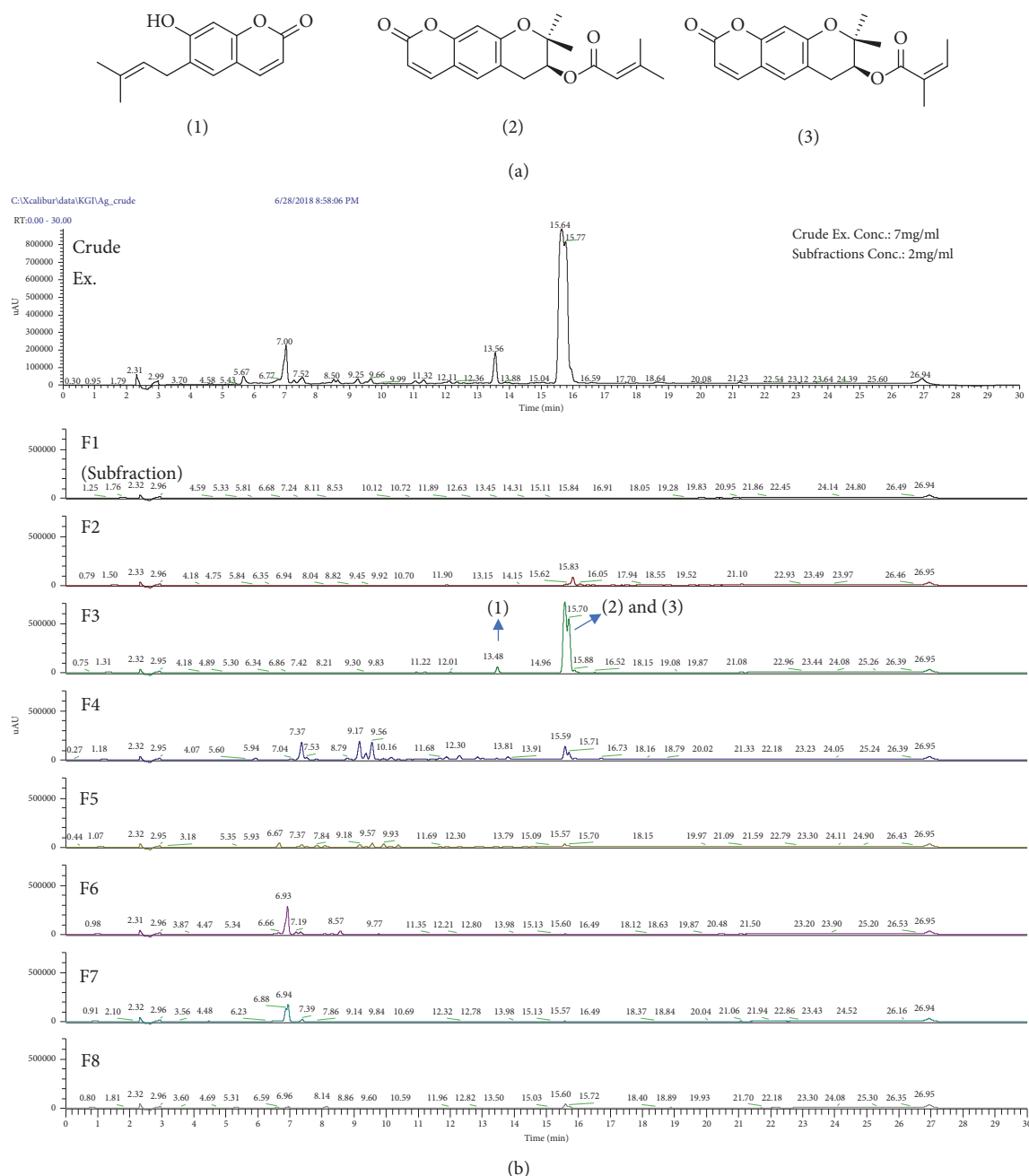


FIGURE 5: Chemical composition of the AGN extract. (a) Chemical structures of the three components: (1) 7-demethylsuberosin, (2) decursin, and (3) decursinol acetate. (b) HPLC-MS chromatograms of the AGN extract and the fractions.

cells, indicating that ATF4 and CHOP play a role in the synergetic effect of doxorubicin and the AGN extract. Both ATF4 and CHOP are recognized as key transcription factors functioning downstream of eIF2 $\alpha$ , which regulate the expression of genes associated with cellular homeostasis and cell death [24, 37]. Although many studies indicate that ATF4 plays a role in cellular protection in association with the expression of redox enzymes, autophagy, translation, and multidrug-resistant gene expression [24], ATF4 promotes proapoptotic factors such as Puma and Noxa [38, 39]. Therefore, it is likely that increased expression of ATF4 by

the AGN extract enhanced doxorubicin-induced apoptosis in HeLa cells. Indeed, an increase in protein synthesis by ATF4 expression induced ROS-mediated apoptosis [25]. However, treatment with N-acetyl-cystein (NAC), which is a precursor of glutathione, did not affect the cell viability in HeLa cells cotreatment with doxorubicin and the AGN extract (data not shown).

CHOP is a transcription factor functioning downstream of ATF4 and is a well-known death factor in ISR. CHOP-mediated apoptosis is associated with several apoptotic factors including the anti- and proapoptotic Bcl-2 families,

microRNAs, TRB3, DR5, and GADD34 [40, 41]. DR5 is known to induce apoptosis by activating caspase-8 [42]. In fact, cotreatment with doxorubicin and the AGN extract significantly increased the activation of caspase-8 (Figure 3). However, administration of the AGN extract did not enhance doxorubicin-mediated DR5 expression (Figure 4). Although the increase in caspase-8 activation by the AGN extract was not related to the expression of CHOP-DR5, the AGN extract is known to activate caspase-8 by enhancing the expression of the DR5 ligand TRAIL [43]. Accordingly, it is possible that upregulation of caspase-8 activation was caused by the expression of TRAIL in AGN extract-treated cells. Inhibition of the anti-apoptotic protein Bcl-2 and activation of the proapoptotic protein Bax/Bak are known as CHOP-mediated apoptotic mechanisms [44, 45]. Treatment with the ANG extract resulted in downregulation of Bcl-2 and upregulation of Bax expression [46]. Also, decursin and decursinol angelate, which are major components of the AGN extract, effectively decreased Bcl-2 expression [43]. Therefore, there is a possibility that CHOP functions as an apoptotic factor in AGN extract-treated cells. However, knockdown of CHOP using specific shRNA did not affect the apoptosis in AGN extract-treated HeLa cells even in cotreated conditions with doxorubicin (Supplementary Materials, Figure S4). Therefore, as mentioned above, CHOP plays an important role in ISR-mediated apoptosis but does not seem to affect AGN extract-mediated apoptosis.

Many studies have shown that decursin and decursinol angelate are major compounds of *Angelica gigas* Nakai, and they are known to have primary responsibility for the anticancer effect of *Angelica gigas* Nakai [13, 14, 46]. Therefore, we also analyzed the composition of the AGN extract and found that decursin and decursinol angelate are major components of the AGN extract (Figure 5). Previous studies have shown that decursin has synergetic effects with doxorubicin [47, 48]. Decursin enhanced caspase-9-mediated apoptosis in doxorubicin-treated multiple myeloma cells, via the mTOR and STAT3 pathways [47] and other reports showed that decursin increased caspase-8-mediated apoptosis by increasing TRAIL sensitivity [49]. Thus, the apoptotic pathway induced by decursin might activate different pathways, depending on the cell's characteristics and conditions. Further studies to characterize the relationship between decursin and doxorubicin are needed. Decursin inhibits the expression of P-glycoprotein, which is an efflux pump that reduces the efficiency of doxorubicin by lowering its cellular concentration [48]. Decursin is also known to inhibit cancer cell metastasis and angiogenesis [50, 51]. Therefore, it could be used as an efficient component in combination therapies along with several other anticancer drugs, including doxorubicin.

## 5. Conclusions

Collectively, our results showed that the AGN extract induced expression of PKR, ATF4, and CHOP as well as phosphorylation of eIF2 $\alpha$ . It significantly increased apoptosis and enhanced doxorubicin susceptibility in HeLa cells. We also analyzed the composition of the AGN extract and found that decursin and decursinol angelate were the main components

of the extract. Consequently, the AGN extract comprising decursin and decursinol angelate could be an effective material for coadministration in combination therapies along with doxorubicin.

## Data Availability

All other data arising from this study are contained within the article and supplementary information files.

## Conflicts of Interest

The authors declare no conflicts of interest.

## Authors' Contributions

Yong-Joon Jeon and Jong-Il Shin contributed equally to this work.

## Acknowledgments

The natural product samples were provided by the KIST Natural Product Library, supported by the KIST Institutional Program (2Z05320). This study was supported by a grant from the Korea Health Technology R&D Project provided to the Korea Health Industry Development Institute (KHIDI), funded by the Ministry of Health & Welfare, Republic of Korea (Grant no. HI15C1540), along with the National Research Foundation of Korea (NRF) grant, funded by the Korean government (MSIP) (no. NRF-2015R1C1A2A01053623).

## Supplementary Materials

**Figure S1:** fraction #3 of AGN extract markedly induced apoptosis and increased expression of CHOP in HeLa cells. (a) The MTT assay was performed for measurement of cell viability. (b) The cells were treated with 20  $\mu$ g/ml fraction of the AGN extract for 16 h. Immunoblot analyses were performed using specific antibodies as indicated. **Figure S2:** AGN extract did not enhance doxorubicin-induced apoptosis in wild type WI-38 cells. (a and b) WI-38 cells were treated with the indicated concentrations of the AGN extract for 24 h. (a) The MTT assay was performed for measurement of cell viability. (b) Immunoblot analyses were performed using specific antibodies as indicated. (c) The cells were cotreated with the indicated concentrations of doxorubicin and the AGN extract for 24 h and cell viability was measured using the MTT assay. (d) The cells were cotreated with 1  $\mu$ M doxorubicin and 1  $\mu$ g/ml AGN extract for the indicated time periods and subjected to immunoblot analyses using specific antibodies as indicated. **Figure S3:** C16 restored the AGN-mediated apoptosis regardless of the eIF2 $\alpha$ -ATF4-CHOP pathway. (a and b) The cells were cotreated with the indicated AGN extract and C16 for 24 h. (a) The MTT assay was performed for measurement of cell viability. Statistical significance of the difference was calculated by Student's t-test with \* $p < 0.01$ . (b) Immunoblot analyses were performed for measurement of apoptosis using specific antibodies. (c)

The cells were cotreated with 10  $\mu\text{g/ml}$  AGN extract and 500 nM C16 for 4 h (top) or 24 h (bottom) and immunoblot analyses were performed using specific antibodies. **Figure S4:** Knockdown of CHOP did not affect the apoptosis in AGN extract-treated HeLa cells. HeLa cells were transfected with EGFP- or CHOP-specific shRNA. (a) The cells were treated with the indicated concentrations of the AGN extract for 24 h, and an MTT assay was performed to determine cell viability. (b) The cells were treated with 10  $\mu\text{g/ml}$  AGN extract for 16 h and subjected to immunoblot analyses using specific antibodies as indicated. (c) The cells were cotreated with the indicated concentrations of doxorubicin and the AGN extract for 24 h and cell viability was measured using the MTT assay. (d) The cells were cotreated with 1  $\mu\text{M}$  doxorubicin and 1  $\mu\text{g/ml}$  AGN extract for the indicated time periods and subjected to immunoblot analyses using specific antibodies as indicated. (*Supplementary Materials*)

## References

- [1] F. Arcamone, G. Cassinelli, G. Fantini et al., "Adriamycin, 14-hydroxydaimomycin, a new antitumor antibiotic from *S. peucetius* var. *caesius*," *Biotechnology and Bioengineering*, vol. 11, no. 6, pp. 1101–1110, 1969.
- [2] J. V. McGowan, R. Chung, A. Maulik, I. Piotrowska, J. M. Walker, and D. M. Yellon, "Anthracycline Chemotherapy and Cardiotoxicity," *Cardiovascular Drugs and Therapy*, vol. 31, no. 1, pp. 63–75, 2017.
- [3] S. Rivankar, "An overview of doxorubicin formulations in cancer therapy," *Journal of Cancer Research and Therapeutics*, vol. 10, no. 4, pp. 853–858, 2014.
- [4] S. M. Swain, F. S. Whaley, and M. S. Ewer, "Congestive heart failure in patients treated with doxorubicin: a retrospective analysis of three trials," *Cancer*, vol. 97, no. 11, pp. 2869–2879, 2003.
- [5] L. Bao, A. Haque, K. Jackson et al., "Increased Expression of P-Glycoprotein Is Associated with Doxorubicin Chemoresistance in the Metastatic 4T1 Breast Cancer Model," *The American Journal of Pathology*, vol. 178, no. 2, pp. 838–852, 2011.
- [6] K. R. Hess et al., "Pharmacogenomic Predictor of Sensitivity to Preoperative Chemotherapy With Paclitaxel and Fluorouracil, Doxorubicin, and Cyclophosphamide in Breast Cancer," *Journal of Clinical Oncology*, vol. 24, no. 26, pp. 4236–4244, 2007.
- [7] W. Hiddemann, M. Kneba, M. Dreyling et al., "Frontline therapy with rituximab added to the combination of cyclophosphamide, doxorubicin, vincristine, and prednisone (CHOP) significantly improves the outcome for patients with advanced-stage follicular lymphoma compared with therapy with CHOP alone: results of a prospective randomized study of the German Low-Grade Lymphoma Study Group," *Blood*, vol. 106, no. 12, pp. 3725–3732, 2005.
- [8] M. S. Butler, "The role of natural product chemistry in drug discovery," *Journal of Natural Products*, vol. 67, no. 12, pp. 2141–2153, 2004.
- [9] M. Kartal, "Intellectual property protection in the natural product drug discovery, traditional herbal medicine and herbal medicinal products," *Phytotherapy Research*, vol. 21, no. 2, pp. 113–119, 2007.
- [10] A. Ganesan, "The impact of natural products upon modern drug discovery," *Current Opinion in Chemical Biology*, vol. 12, no. 3, pp. 306–317, 2008.
- [11] J. W. Li and J. C. Vederas, "Drug discovery and natural products: end of an era or an endless frontier?" *Science*, vol. 325, no. 5937, pp. 161–165, 2009.
- [12] S. D. Sarker and L. Nahar, "Natural medicine: the genus *Angelica*," *Current Medicinal Chemistry*, vol. 11, no. 11, pp. 1479–1500, 2004.
- [13] J. Zhang, L. Li, C. Jiang, C. Xing, S.-H. Kim, and J. Lü, "Anti-cancer and other bioactivities of Korean *Angelica gigas* Nakai (AGN) and its major pyranocoumarin compounds," *Anti-Cancer Agents in Medicinal Chemistry*, vol. 12, no. 10, pp. 1239–1254, 2012.
- [14] C. Reddy, S. Kim, M. Hur et al., "Natural Korean Medicine Dang-Gui: Biosynthesis, Effective Extraction and Formulations of Major Active Pyranocoumarins, Their Molecular Action Mechanism in Cancer, and Other Biological Activities," *Molecules*, vol. 22, no. 12, p. 2170, 2017.
- [15] J. H. Park, Y. J. Lee, and S. J. Keon, "Pharmacognostical studies on the Dang Gui from Korea," *Korean Journal of Pharmacognosy*, vol. 36, no. 2, pp. 141–144, 2005.
- [16] S.-K. Cho, A. M. A. El-Aty, J.-H. Choi, M. R. Kim, and J. H. Shim, "Optimized conditions for the extraction of secondary volatile metabolites in *Angelica* roots by accelerated solvent extraction," *Journal of Pharmaceutical and Biomedical Analysis*, vol. 44, no. 5, pp. 1154–1158, 2007.
- [17] M. A. Yoo, Y. K. Song, H. Jang, D. M. Kim, and S. Y. Byun, "Profiling of skin anti-aging related proteins in human dermal fibroblasts by decursin in *Angelica gigas* Nakai," *Korean Journal of Chemical Engineering*, vol. 28, no. 3, pp. 880–885, 2011.
- [18] J. H. Kim, S.-J. Jeong, H.-Y. Kwon et al., "Decursin prevents cisplatin-induced apoptosis via the enhancement of antioxidant enzymes in human renal epithelial cells," *Biological & Pharmaceutical Bulletin*, vol. 33, no. 8, pp. 1279–1284, 2010.
- [19] L. Li, W. Li, S. Jung, Y. Lee, and Y. Kim, "Protective Effects of Decursin and Decursinol Angelate against Amyloid  $\beta$ -Protein-Induced Oxidative Stress in the PC12 Cell Line: The Role of Nrf2 and Antioxidant Enzymes," *Bioscience, Biotechnology, and Biochemistry*, vol. 75, no. 3, pp. 434–442, 2014.
- [20] C. Carvalho, R. X. Santos, S. Cardoso et al., "Doxorubicin: the good, the bad and the ugly effect," *Current Medicinal Chemistry*, vol. 16, no. 25, pp. 3267–3285, 2009.
- [21] K. Pakos-Zebrucka, I. Koryga, K. Mnich, M. Ljubic, A. Samali, and A. M. Gorman, "The integrated stress response," *EMBO Reports*, vol. 17, no. 10, pp. 1374–1395, 2016.
- [22] N. Donnelly et al., "The eIF2 $\alpha$  kinases: their structures and functions," *Cellular and Molecular Life Sciences*, vol. 70, no. 19, pp. 3493–3511, 2013.
- [23] P. D. Lu, H. P. Harding, and D. Ron, "Translation reinitiation at alternative open reading frames regulates gene expression in an integrated stress response," *The Journal of Cell Biology*, vol. 167, no. 1, pp. 27–33, 2004.
- [24] J. Han and R. J. Kaufman, "Physiological/pathological ramifications of transcription factors in the unfolded protein response," *Genes & Development*, vol. 31, no. 14, pp. 1417–1438, 2017.
- [25] J. Han, S. H. Back, J. Hur et al., "ER-stress-induced transcriptional regulation increases protein synthesis leading to cell death," *Nature Cell Biology*, vol. 15, no. 5, pp. 481–490, 2013.
- [26] D. Hanahan and R. A. Weinberg, "Hallmarks of cancer: the next generation," *Cell*, vol. 144, no. 5, pp. 646–674, 2011.
- [27] R. S. Y. Wong, "Apoptosis in cancer: from pathogenesis to treatment," *Journal of Experimental & Clinical Cancer Research*, vol. 30, no. 1, article 87, 2011.

- [28] Y. J. Jeon et al., "Salubrin-Mediated Upregulation of eIF2 $\alpha$  Phosphorylation Increases Doxorubicin Sensitivity in MCF-7/ADR Cells," *Molecules and Cells*, vol. 39, no. 2, pp. 129–135, 2016.
- [29] R. L. Bennett, A. L. Carruthers, T. Hui, K. R. Kerney, X. Liu, and W. S. May, "Increased Expression of the dsRNA-Activated Protein Kinase PKR in Breast Cancer Promotes Sensitivity to Doxorubicin," *PLoS ONE*, vol. 7, no. 9, Article ID e46040, 2012.
- [30] A. C. Palmer and P. K. Sorger, "Combination Cancer Therapy Can Confer Benefit via Patient-to-Patient Variability without Drug Additivity or Synergy," *Cell*, vol. 171, no. 7, pp. 1678–1682.e13, 2017.
- [31] S. Elmore, "Apoptosis: a review of programmed cell death," *Toxicologic Pathology*, vol. 35, no. 4, pp. 495–516, 2007.
- [32] K. Sowndhararajan, P. Deepa, M. Kim, S. J. Park, and S. Kim, "A Review of the Composition of the Essential Oils and Biological Activities of Angelica Species," *Scientia Pharmaceutica*, vol. 85, no. 3, p. 33, 2017.
- [33] J. Couturier, M. Morel, R. Pontcharraud et al., "Interaction of Double-stranded RNA-dependent Protein Kinase (PKR) with the Death Receptor Signaling Pathway in Amyloid  $\beta$  (A $\beta$ )-treated Cells and in APP," *The Journal of Biological Chemistry*, vol. 285, no. 2, pp. 1272–1282, 2010.
- [34] J. Couturier, M. Paccalin, M. Morel et al., "Prevention of the  $\beta$ -amyloid peptide-induced inflammatory process by inhibition of double-stranded RNA-dependent protein kinase in primary murine mixed co-cultures," *Journal of Neuroinflammation*, vol. 8, no. 1, p. 72, 2011.
- [35] C.-H. Yoon, E.-S. Lee, D.-S. Lim, and Y.-S. Bae, "PKR, a p53 target gene, plays a crucial role in the tumor-suppressor function of p53," *Proceedings of the National Academy of Sciences of the United States of America*, vol. 106, no. 19, pp. 7852–7857, 2009.
- [36] S. J. Kim, K. M. Park, N. Kim, and Y. I. Yeom, "Doxorubicin prevents endoplasmic reticulum stress-induced apoptosis," *Biochemical and Biophysical Research Communications*, vol. 339, no. 2, pp. 463–468, 2006.
- [37] C. Hetz, "The unfolded protein response: controlling cell fate decisions under ER stress and beyond," *Nature Reviews Molecular Cell Biology*, vol. 13, no. 2, pp. 89–102, 2012.
- [38] G. Qing, B. Li, A. Vu et al., "ATF4 Regulates MYC-Mediated Neuroblastoma Cell Death upon Glutamine Deprivation," *Cancer Cell*, vol. 22, no. 5, pp. 631–644, 2012.
- [39] J. L. Armstrong, R. Flockhart, G. J. Veal, P. E. Lovat, and C. P. F. Redfern, "Regulation of endoplasmic reticulum stress-induced cell death by ATF4 in neuroectodermal tumor cells," *The Journal of Biological Chemistry*, vol. 285, no. 9, pp. 6091–6100, 2010.
- [40] Y. Li, Y. Guo, J. Tang, J. Jiang, and Z. Chen, "New insights into the roles of CHOP-induced apoptosis in ER stress," *Acta Biochimica et Biophysica Sinica*, vol. 46, no. 8, pp. 629–640, 2014.
- [41] Z. Xu, Y. Bu, N. Chitnis, C. Koumenis, S. Y. Fuchs, and J. A. Diehl, "miR-216b regulation of c-Jun mediates GADD153/CHOP-dependent apoptosis," *Nature Communications*, vol. 7, p. 11422, 2016.
- [42] A. R. Safa and K. E. Pollok, "Targeting the anti-apoptotic protein c-FLIP for cancer therapy," *Cancers*, vol. 3, no. 2, pp. 1639–1671, 2011.
- [43] N.-H. Yim, J. H. Lee, W.-K. Cho, M. C. Yang, D. H. Kwak, and J. Y. Ma, "Decursin and decursinol angelate from Angelica gigas Nakai induce apoptosis via induction of TRAIL expression on cervical cancer cells," *European Journal of Integrative Medicine*, vol. 3, no. 4, pp. e293–e301, 2011.
- [44] K. D. McCullough, J. L. Martindale, L. O. Klotz, T. Y. Aw, and N. J. Holbrook, "Gadd153 sensitizes cells to endoplasmic reticulum stress by down-regulating Bcl2 and perturbing the cellular redox state," *Molecular and Cellular Biology*, vol. 21, no. 4, pp. 1249–1259, 2001.
- [45] T. Gotoh, K. Terada, S. Oyadomari, and M. Mori, "hsp70-DnaJ chaperone pair prevents nitric oxide- and CHOP-induced apoptosis by inhibiting translocation of Bax to mitochondria," *Cell Death & Differentiation*, vol. 11, no. 4, pp. 390–402, 2004.
- [46] Y. Jiang, J. Piao, H.-J. Cho, W.-S. Kang, and H.-Y. Kim, "Improvement in antiproliferative activity of Angelica gigas Nakai by solid dispersion formation via hot-melt extrusion and induction of cell cycle arrest and apoptosis in HeLa cells," *Bioscience, Biotechnology, and Biochemistry*, vol. 79, no. 10, pp. 1635–1643, 2015.
- [47] J. Jang, S.-J. Jeong, H.-Y. Kwon et al., "Decursin and Doxorubicin Are in Synergy for the Induction of Apoptosis via STAT3 and/or mTOR Pathways in Human Multiple Myeloma Cells," *Evidence-Based Complementary and Alternative Medicine*, vol. 2013, Article ID 506324, 13 pages, 2013.
- [48] H. S. Choi, S.-G. Cho, M. K. Kim et al., "Decursin in Angelica gigas Nakai (AGN) Enhances Doxorubicin Chemosensitivity in NCI/ADR-RES Ovarian Cancer Cells via Inhibition of P-glycoprotein Expression," *Phytotherapy Research*, vol. 30, no. 12, pp. 2020–2026, 2016.
- [49] J. Kim, M. Yun, E.-O. Kim et al., "Decursin enhances TRAIL-induced apoptosis through oxidative stress mediated- endoplasmic reticulum stress signalling in non-small cell lung cancers," *British Journal of Pharmacology*, vol. 173, no. 6, pp. 1033–1044, 2016.
- [50] S. H. Son, M.-J. Kim, W.-Y. Chung et al., "Decursin and decursinol inhibit VEGF-induced angiogenesis by blocking the activation of extracellular signal-regulated kinase and c-Jun N-terminal kinase," *Cancer Letters*, vol. 280, no. 1, pp. 86–92, 2009.
- [51] S. H. Son, K.-K. Park, S. K. Park et al., "Decursin and decursinol from Angelica gigas inhibit the lung metastasis of murine colon carcinoma," *Phytotherapy Research*, vol. 25, no. 7, pp. 959–964, 2011.



## Research Article

# Volatile Oil of *Amomum villosum* Inhibits Nonalcoholic Fatty Liver Disease via the Gut-Liver Axis

Shanhong Lu, Ting Zhang, Wen Gu , Xingxin Yang, Jianmei Lu, Ronghua Zhao , and Jie Yu 

College of Pharmaceutical Science, Yunnan University of Traditional Chinese Medicine, Kunming 650500, China

Correspondence should be addressed to Ronghua Zhao; kmzhaoronghua@hotmail.com and Jie Yu; cz.yujie@gmail.com

Received 12 March 2018; Revised 18 May 2018; Accepted 5 June 2018; Published 19 July 2018

Academic Editor: Ravirajsinh N. Jadeja

Copyright © 2018 Shanhong Lu et al. This is an open access article distributed under the Creative Commons Attribution License, which permits unrestricted use, distribution, and reproduction in any medium, provided the original work is properly cited.

**Background.** The dried mature fruit of *Amomum villosum* has been historically used in China as food and in the auxiliary treatment of digestive system disorders. Numerous studies have shown that gastrointestinal function is closely related to the development of nonalcoholic fatty liver disease via the “gut-liver” axis. **Objective.** The present study aimed to explore whether the mechanism underlying the regulation of lipid accumulation in nonalcoholic fatty liver disease (NAFLD) may affect related disorders using the active ingredients in *A. villosum*. **Design.** Male Sprague-Dawley rats on a high-fat diet (HFD) to induce NAFLD were administered water extract of *A. villosum* (WEAV), volatile oil of *A. villosum* (VOAV), or bornyl acetate. After treatment, serum and liver total cholesterol (TC), triglyceride (TG), free fatty acid (FFA), aspartate aminotransferase (AST), alanine aminotransferase (ALT), high-density lipoprotein cholesterol (HDL-C), and low-density lipoprotein cholesterol (LDL-C) levels were measured. The regulatory role of *A. villosum* in the microecology of the intestines was assessed using the V4 region of the 16S rDNA sequencing. The expression of the intestinal tight junction proteins occludin and ZO-1 was also measured. The influence of *A. villosum* on TLR4-mediated chronic low-grade inflammation was evaluated based on the concentrations of key proteins of the TLR4/NF-κB signaling pathway. **Results.** *A. villosum* effectively inhibited endogenous lipid synthesis, reduced TG, TC, and FFA accumulation, regulated the expression of LDL-C, and decreased lipid accumulation in liver tissues. VOAV effectively regulated the intestinal microflora, improved chronic low-grade inflammation by promoting ZO-1 and occludin protein expressions, and inhibited the TLR4/NF-κB signaling pathway. **Conclusion.** The present study provides scientific basis for the potential application of *A. villosum* in NAFLD prevention and treatment. Additional chemical constituents other than bornyl acetate also contributed to the preventive effects of *A. villosum* on NAFLD.

## 1. Introduction

Nonalcoholic fatty liver disease (NAFLD) is a common disorder that is characterized by accumulation of excess fats in the liver of individuals who drink little or no alcohol. Epidemiological studies have shown that NAFLD may affect individuals of any age and race. The prevalence of NAFLD in Western countries is about 18%–35%, and up to 80% of obese individuals develop NAFLD [1]. NAFLD is a progressive disease that results in irreversible liver injury and may also be a risk factor for liver fibrosis and cancer [2]. Recent studies have focused on elucidating the role of the intestinal microbial environment and its feedback effects on the liver in the pathogenesis of NAFLD [3, 4]. Excess uptake of free fatty acids (FFA) from food may lead to disorders of the

intestinal microbial system. The intestinal microbial environment affects fat deposits in liver cells, which may be involved in the early pathogenesis of NAFLD. The relative balance of intestinal microflora significantly affects the absorption of fatty acids and other nutrients, and thus changes in the intestinal microbial environment and feedback may influence the pathogenesis of liver diseases [4, 5]. The gut microbiota of obese humans and HFD-fed mice was characterized by higher Firmicutes-to-Bacteroidetes ratios, an increase in the number of endotoxin-producing Proteobacteria, and a reduction in the number of immuno-homeostatic bacterial species [6, 7]. Intestinal microbial balance disorders [8], small intestinal bacterial overgrowth (SIBO) [9], changes in intestinal permeability [10], serum lipopolysaccharide (LPS) overload (endotoxemia) [11], and subsequent events are closely related

to each other and are considered indicators of NAFLD onset [12, 13] and collectively called the gut-liver axis. The efficacy and mechanism of action of treatment regimens for NAFLD are largely associated with the intestinal hepatic axis. However, no effective pharmacotherapeutic regimen for NAFLD has been established to date. Despite advances in establishing its natural history, the underlying mechanism and pathogenesis of NAFLD remain elusive [14]. Exercise and diet are the most basic therapeutic interventions for NAFLD; however, this has been determined to be insufficient [15]. Hence, a highly specific and effective drug treatment is warranted.

Amomi Fructus is the dry, mature fruit of *Amomum villosum* Lour., *A. longiligulare* T.L. Wu, and *A. villosum* Lour. var. *xanthioides* T.L. Wu et Senjen of Zingiberaceae [16]. Previous studies have indicated that Amomi Fructus has the capacity to regulate gastrointestinal flora [17]. Volatile oil of *A. villosum* significantly inhibited the growth of *Trichophyton rubrum*, *T. mentagrophytes*, *Microsporum gypseum*, *Staphylococcus aureus*, and *Enterococcus faecalis* [18]. Furthermore, research studies have shown that Amomi Fructus extracts can prevent alcohol-induced lipid oxidation in liver cells and activate alcohol dehydrogenase, aldehyde dehydrogenase, and CYP2E1 gene expression [19, 20]. However, the mechanism of action of *A. villosum* in the treatment of NAFLD remains unclear.

Recent studies have focused on elucidating the relationship between intestinal flora and NAFLD. The present study is the first to focus on the role of different *A. villosum* extracts in the regulation of intestinal microflora, adjustment of intestinal microflora equilibrium, control of low-grade chronic inflammation, reduction of fat accumulation, and consequent alleviation of NAFLD, hyperlipidemia, and related lipid metabolism disorders. Our findings indicate that *A. villosum* could effectively inhibit endogenous lipid synthesis, reduction of TG, TC, and FFA accumulation, regulation expression of LDL-C, and reduction of lipid accumulation in liver tissue. VOAV could effectively regulate the intestinal microflora, relieve chronic low-grade inflammation by promoting ZO-1 and occludin protein expressions, and inhibit the TLR4/NF- $\kappa$ B signaling pathway. VOAV showed great potential in NAFLD prevention and treatment. Possible major active constituents and dose-effect relationships of *A. villosum* were also evaluated in this study to provide evidence for its efficacy in clinic applications.

## 2. Materials and Methods

**2.1. Plant Materials and Chemicals.** The fruits of *A. villosum* Lour. were collected in June 2014 from Jinping County, Honghe Prefecture, Yunnan Province, China, and identified by Professor Ronghua Zhao, Yunnan University of Traditional Chinese Medicine. Voucher specimens (Specimen number: LSH 20140605) were deposited in the Herbarium of the Traditional Chinese Medicine Pharmacognosy Department of Yunnan University. Bornyl acetate (BA, purity: > 98%), the main constituent in volatile oil of *A. villosum* Lour. [4], was purchased from Nanjing Jingzhu Biotechnology Co., Ltd., China. Ezetimibe tablets (Hangzhou MSD Pharmaceutical Co., Ltd., Hangzhou, China) were used as positive control.

**2.2. Preparation of Water Extract of *A. villosum* (WEAV) and Volatile Oil of *A. villosum* (VOAV).** Powder (100 g, 20 mesh) of *A. villosum* fruit was weighed and immersed in water for 30 min (4°C). It was then refluxed thrice with 500 mL of water for 30 min each time. These water extracts were pooled, concentrated, and lyophilized. The final extraction rate of WEAV was 23.56% of the crude drug.

VOAV was extracted from the powdered crude drug by steam distillation according to the procedure recorded in the Chinese Pharmacopoeia (2015 edition) [5]. The powdered (100 g, 20 mesh) fruit of *A. villosum* was weighed and soaked in water for 12 h (4°C), and then steam distillation was performed with 800 mL of water for 6 h. The final extraction rate of VOAV was 3.90% of crude drug.

**2.3. Quality Control of WEAV as Indicated by High-Performance Liquid Chromatography with Diode-Array Detection (HPLC-DAD).** Flavonoids and organic acids are considered major nonvolatile constituents of *A. villosum* [21, 22]. Thus, HPLC determinations for quercitrin, isoquercitrin, and vanillic acid (4-hydroxy-3-methoxybenzoic acid) in WEAV were performed in this study.

All experiments were conducted using a Dionex Ultimate 3000 HPLC system (Dionex Technologies, Sunnyvale, California, USA). Data were analyzed with Chromeleon 6.8. These compounds were separated by a Nucleodur C18 Gravity column (4.6 mm  $\times$  250 mm, I.D., 5  $\mu$ m, Agilent Technologies, USA). The gradient elution used a mobile phase consisting of (A) 0.4% H<sub>3</sub>PO<sub>4</sub> and (B) methanol. The following gradient program was used: 20% B (0 min), 30% B (25 min), 40% B (30 min), 50% B (40 min), and 50% B (50 min). The detection wavelength was 260 nm. The sample injection volume, oven temperature, and flow rate were set at 5  $\mu$ L, 30°C, and 1.0 mL $\cdot$ min<sup>-1</sup>, respectively. Reference standards of quercitrin, isoquercitrin, and vanillic acid were weighed and dissolved in methanol.

**2.4. Quality Control of VOAV by Gas Chromatography-Mass Spectrometer (GC-MS).** Chromatographic analysis was performed for the quality control of VOAV using GC-MS (Agilent Technologies, Santa Clara, CA, USA) with a capillary column (HP-5MS Capillary; 30.0 mm  $\times$  0.25 mm  $\times$  0.25  $\mu$ m). The oven temperature was programmed as follows: an initial temperature of 80°C, which was increased to 280°C at a rate of 3°C min<sup>-1</sup> and then at 20°C min<sup>-1</sup> to a final temperature of 250°C and held for 20 min. Injection was conducted in split mode (20:1) at 250°C. The carrier gas helium was at a flow rate of 1.0 mL/min, and the injected sample volume was 1  $\mu$ L. The runtime was 35 min. The MS scan range was (m/z) 35–500 atomic mass units (AMU) under electron impact (EI) ionization (70 eV). EI source and quadrupole temperatures were set at 230°C and 150°C, respectively. The transfer line between the GC and the MS was maintained at 250°C.

**2.5. Animals, Diets, and Groups.** Eight-week-old male Sprague-Dawley rats were purchased from Chengdu, China (Certificate of Quality No. 0016254). The rats were acclimated in a controlled environment (temperature 21  $\pm$  2°C, 60  $\pm$  10% humidity, and a 12-h/12-h light/dark cycle) with free access to

TABLE 1: Animal grouping and treatment in this research.

Group	Diet	Treatment	Dose (mg/kg)
CON	Normal Diet	—	—
MOD	High fat Diet	—	—
EZE	High fat Diet	Ezetimibe	1
WEAV.L	High fat Diet	low dose of WEAV	48
WEAV.M	High fat Diet	middle dose of WEAV	96
WEAV.H	High fat Diet	high dose of WEAV	192
VOAV.L	High fat Diet	low dose of VOAV	8
VOAV.M	High fat Diet	middle dose of VOAV	16
VOAV.H	High fat Diet	high dose of VOAV	32
BA.L	High fat Diet	low dose of bornyl acetate	2
BA.M	High fat Diet	middle dose of bornyl acetate	4

water. The whole research design was reviewed and approved by the Institutional Ethical Committee on Animal Care and Experimentation of Yunnan University Traditional Chinese Medicine (R-0620150014). All reasonable efforts were made to minimize animal suffering.

Rats were randomized into 12 groups with 10 animals per group (Table 1). These were housed 10 in a stainless steel cage containing sterile wood cuttings and sawdust as bedding in ventilated animal rooms. All rats except those in the control group were fed a high-fat diet (HFD) until the end of the experiment (16 weeks). HFD contained 1% cholesterol, 10% lard, 10% egg yolk, and 79% basic feed (moisture  $\leq 10\%$ ; protein  $\geq 20\%$ ; fat mix  $\geq 4\%$ ; calcium: 1.0%–1.8%; phosphorus: 0.6–1.2; fiber  $\leq 5\%$ ; essential amino acids  $\geq 2\%$ ) (Research Diets, Suzhou, China).

These 12 groups of rats received different drug regimens. The normal control group (CON group, fed with normal diet) and MOD Group (fed with HFD) received only physiological saline. WEAV groups (WEAV.L, WEAV.M, and WEAV.H group) received 48 mg/kg, 96 mg/kg, and 192 mg/kg of WEAV orally, respectively. VOAV groups (VOAV.L, VOAV.M, and VOAV.H group) received 8 mg/kg, 16 mg/kg, and 32 mg/kg of VOAV, respectively. BA groups (BA.L, BA.M, and BA.H group) received 2 mg/kg, 4 mg/kg, and 8 mg/kg of BA, respectively. The ezetimibe (EZE group, 1 mg/kg) was used as positive control. Ezetimibe was used as a control positive drug because it was frequently used in the treatment of NAFLD. Ezetimibe could selectively inhibit the small intestine cholesterol transporter and effectively reduce intestinal cholesterol absorption; therefore it decreased cholesterol levels both in the plasma and in the liver. All rats were treated by gavage once per day for 16 consecutive weeks according to the dosages listed in Table 1.

**2.6. Assessment of Blood Lipid, Lipoprotein, and Amino-transferase Levels.** Blood samples (about 1.5–2.0 mL) were

collected from the retroorbital venous plexus of rats every 2 weeks and then centrifuged at 10,000 rpm for 15 min. The serum was stored at  $-80^{\circ}\text{C}$  until use. Serum levels of total cholesterol (TC), triglyceride (TG), free fatty acid (FFA), low-density lipoprotein cholesterol (LDL-C), high-density lipoprotein cholesterol (HDL-C), aspartate aminotransferase (AST), and alanine aminotransferase (ALT) were determined using the enzymatic colorimetric method. Serum assay detection kits were purchased from Nanjing Jiancheng Bioengineering Co., Ltd. (Nanjing, China).

After the rats were dissected, the liver was taken and weighed. The liver index was calculated by liver mass/body mass.

**2.7. Assessment of LPS Levels in the Hepatic Portal Vein.** At the end of the experiment, the rats were sacrificed using an intraperitoneal injection of 10% chloral hydrate (3.0 mL/100 g body weight). Hepatic portal vein blood was collected using a disposable vacuum blood collector. After being left to stand for 30 min, plasma was isolated by centrifugation at 3,000 rpm for 2 min. Lipopolysaccharide (LPS) contents in all groups were evaluated using tachypleus amoebocyte lysate kits (Chinese Horseshoe Crab Reagent Manufactory, Co., Ltd., Xiamen, China).

**2.8. Flow Cytometric Analysis of Occludin and ZO-1 Protein Levels.** At the end of the 16th week, the rats were executed upon anesthesia using 10% chloral hydrate solution. The jejunums of all rats were collected, cleaned, placed in PRMI-1640 culture medium solution, and cut into pieces. Cell debris in the homogenate was removed by passing this through a 70- $\mu\text{m}$  filter membrane. Cells were then diluted with staining buffer to a density of  $1 \times 10^6$  cells/mL after blocking with 3% FBS. Shortly thereafter, the cells were incubated with anti-occludin antibody (Proteintech, Chicago, Illinois, USA) and anti-ZO-1 antibody (Proteintech, USA) for 2 h and then incubated with second antibody (fluorescein isothiocyanate) in the dark for 1 h. Finally, the expression levels of occludin and ZO-1 protein were determined using flow cytometry (FACSCalibur, Becton, Dickinson and Company, San Diego, CA, USA).

**2.9. Assessment of Protein and Cytokine Levels in the TLR4/NF- $\kappa$ B Pathway in the Liver.** At the end of the 16th week, the rats were anesthetized with 10% chloral hydrate and sacrificed. Liver tissue samples were then immediately collected for biochemical analysis and morphologic observation. The liver samples were weighed, washed with 0.9% saline, and cut into pieces. Liver tissue samples (1 g) were homogenized in 9 mL normal saline and then centrifuged at 4,000 rpm for 10 min at  $4^{\circ}\text{C}$ . The supernatant was then collected for further analysis. AST, ALT, TG, TC, FFA, LDL-C, and HDL-C concentrations were determined in all supernatants. TLR4, TNF- $\alpha$ , IL-10, IL-1 $\alpha$ , and IL-6 concentrations were tested using ELISA assay kits (Cusabio Biotech Co., Ltd., China). Protein expression levels of NF- $\kappa$ B, IKK, and I $\kappa$ B were determined by western blotting. Antibodies against NF- $\kappa$ B (1:1,000), IKK (1:1,000), I $\kappa$ B $\alpha$  (1:1,000), anti-rabbit IgG



TABLE 2: The main chemical composition and content of volatile oil.

Compound	Chemical formula	Retention time (min)	Relative content (%)
Bornyl acetate	C <sub>12</sub> H <sub>12</sub> O <sub>2</sub>	13.27	54.54
Camphor	C <sub>10</sub> H <sub>16</sub> O	8.42	17.92
Camphene	C <sub>10</sub> H <sub>16</sub>	3.91	6.757
Limonene	C <sub>10</sub> H <sub>16</sub>	5.30	5.249
Borneol	C <sub>10</sub> H <sub>18</sub> O	8.97	4.068
Myrcene	C <sub>10</sub> H <sub>16</sub>	4.46	1.969
$\alpha$ -Pinene	C <sub>10</sub> H <sub>16</sub>	3.67	1.503
$\beta$ -Caryophyllene	C <sub>15</sub> H <sub>24</sub>	18.11	0.8530
$\beta$ -Pinene	C <sub>10</sub> H <sub>16</sub>	4.34	0.7950
$\alpha$ -Copaene	C <sub>15</sub> H <sub>24</sub>	16.43	0.5430

(1:10,000), and  $\beta$ -actin (1:1000) dilution were used in this study.

**2.10. Overall Structural Changes in Gut Microbiota.** The composition of the bacterial communities in each fecal sample was assessed as previously described [5, 23]. Sequencing of the variable region V4 in 16S rDNA was used in the analysis of gut microbiota species diversity in rat fecal samples.

At the end of the experiment, rat feces of the CON, MOD, EZE, WEAV.M, VOAV.M, and BA.M groups were collected in sterilized plastic tubes and stored at  $-80^{\circ}\text{C}$  until testing. All fecal samples in the same group (0.5 mg for each rat) were carefully blended, and genomic DNA was extracted from 0.5-mg portions of pooled samples using SDS. The DNA extracted from fecal samples was subjected to pyrosequencing of the V4 region of 16S rDNA. PCR amplification of the primers was performed using 515f/806r. Sequencing was conducted on an Illumina MiSeq platform [24]. The regulatory role of *A. villosum* on the intestinal microecological system was indicated by the  $\beta$  diversity and OTU analysis of the fecal samples.

### 3. Statistical Analysis

The data (mean  $\pm$  SD) were evaluated using one-way ANOVA at significance levels of  $P < 0.05$ ,  $< 0.01$ , and  $< 0.001$ . Analysis of principal coordinates (PCoA) was conducted to explore and visualize similarities among different groups. The unweighted pair-group method with arithmetic mean (UPGMA) method was used for cluster analysis to assess similarities among samples.

### 4. Results

**4.1. Chemical Profiles of WEAV and VOAV.** Here, 58 volatile components were identified in VOAV by GC-MS (Figure 1(a)). The 10 most abundant components are listed in Table 2, which included bornyl acetate, camphor, camphene, limonene, borneol, myrcene,  $\alpha$ -pinene,  $\beta$ -caryophyllene,  $\beta$ -pinene, and  $\alpha$ -copaene. These accounted for 94.2% of the total volatile compound content in *A. villosum*. BA accounted

for up to 54.54% and thus could be considered as the representative component of VOVA.

The HPLC profile of WEAV is shown in Figure 1(b). The linear ranges for quercitrin, isoquercitrin, and vanillic acid were 0.1172–0.1440  $\mu\text{g/mL}$  ( $r = 0.9999$ ,  $n = 6$ ), 0.1072–1.141  $\mu\text{g/mL}$  ( $r = 0.9999$ ,  $n = 6$ ), and 0.1040–1.120  $\mu\text{g/mL}$  ( $r = 0.9999$ ,  $n = 6$ ), respectively. Average recovery rates were 99.07% (RSD = 0.39%), 98.23% (RSD = 1.63%), and 99.31% (RSD = 0.70%), respectively. The concentrations of quercitrin, isoquercitrin, and vanillic acid in WEAV were 0.0604 mg/g, 0.0276 mg/g, and 0.1709 mg/g, respectively.

**4.2. *A. villosum* Prevents HFD-Induced NAFLD in Rats.** HFD feeding for 16 weeks led to a significant increase in body weight, liver index, accumulation of epididymal fat, and subcutaneous adipose tissue. HFD resulted in more enhancement in lipid deposition in adipocytes and hepatocytes than chow feeding. Simultaneously, the HFD group still had less brown fat. The treatment groups showed distinct differences from the MOD group in terms of increase in body weight, food intake, and white and brown fat weight (Figures 2(a)–2(d)). The application of WOVA, VOVA, and BA decreased the liver index raised by HFD (Figure 2(e)).

Fat degeneration, swelling of the liver cells, uneven lipid droplets, and large numbers of inflammatory cells were observed in the liver tissue of the HFD group. VOAV and BA were found to relieve fat degeneration and edema of liver cells (Figure 2(f)).

The levels of TG, TC, LDL-C, HDL-C, AST, ALT, and FFA were tested at the end of the study (Table 3). HFD feeding was associated with higher TC and TG levels in the liver than control cow feeding by 71.4% and 45.1%, respectively. These results indicated that the NAFLD model had been successfully established in the current study. The application of *A. villosum* resulted in a reduction in the levels of FFA, TG, and TC in the liver. The elevations of AST and ALT induced by HFD were also alleviated by *A. villosum* (Table 3). WEAV, VOAV, and BA effectively inhibited the FFA supply, thus maintaining hepatic TG content at normal levels. WEAV, VOAV, and BA reduced the expression of LDL-C and increased the expression of HDL-C, thereby reducing the accumulation of hepatic TC to some extent.

**4.3. *A. villosum* Regulates the Intestinal Microbial Balance.** Disturbances in the balance of intestinal flora here refer to changes in the number of intestinal flora, including strains and their relative proportions.

At the end of the study, the effects of *A. villosum* on the composition of gut microbiota were assessed through a sequencing-based analysis of bacterial 16S rRNA (V4 region) in the feces. UniFrac-based PCoA revealed a distinct clustering of microbiota composition for each treatment group (Figure 3(a)). The community structure of the VOAV.M group displayed considerable similarity to the control group, thus indicating that VOAV imparts considerable regulatory effects on the intestinal flora of NAFLD rats. This result was also confirmed using the UPGMA clustering tree (Figure 3(b)).

The 10 most abundant genera were compared across groups (Figure 3(c)). The composition of intestinal bacterial



TABLE 3: Lipid contents in the liver samples. (mean ± SD, n = 8).

	TC (mmol/L)	TG (mmol/L)	FFA (μmol/L)	LDL-C (mmol/L)	HDL-C (mmol/L)	AST (U/L)	ALT (U/L)
CON	0.75 ± 0.13* **	1.13 ± 0.17* **	230.99 ± 22.83**	1.39 ± 0.11* **	1.47 ± 0.16**	2199.29 ± 114.52* **	1550.52 ± 157.42* **
MOD	1.59 ± 0.04	1.64 ± 0.11	440.22 ± 31.54	2.46 ± 0.32	1.07 ± 0.27	2856.18 ± 145.88	22242.08 ± 154.16
EZE	1.05 ± 0.14* **	1.31 ± 0.19* **	263.32 ± 21.83**	1.49 ± 0.22* **	1.37 ± 0.28*	2401.43 ± 99.03**	1723.72 ± 182.66* **
WEAVL	1.18 ± 0.19**	1.45 ± 0.2	302.29 ± 33.41*	1.69 ± 0.52**	1.01 ± 0.2	2607.46 ± 58.35	2040.9 ± 145.07*
WEAVM	1.28 ± 0.20**	1.44 ± 0.2	297.78 ± 33.45**	1.70 ± 0.52 **	1.06 ± 0.22	2590.23 ± 163.64*	2042.8 ± 120.54**
WEAVH	1.15 ± 0.23**	1.39 ± 0.14**	276.34 ± 35.22**	1.90 ± 0.34 **	1.19 ± 0.35	2520.18 ± 140.79*	1756.52 ± 118.37* **
VOAVL	1.15 ± 0.14**	1.46 ± 0.15**	283.87 ± 21.89**	1.57 ± 0.48* **	1.41 ± 0.35*	2458.48 ± 110.67**	1849.07 ± 131.94* **
VOAVM	1.14 ± 0.21**	1.35 ± 0.17* **	289.06 ± 26.28**	1.46 ± 0.17* **	1.33 ± 0.31*	2457.13 ± 182.37**	1762.82 ± 116.12* **
VOAVH	1.15 ± 0.18**	1.421 ± 0.14* **	222.63 ± 22.24**	1.38 ± 0.21* **	1.39 ± 0.27*	2255.16 ± 78.83* **	1868.12 ± 200.21* **
BA.L	1.25 ± 0.18**	1.37 ± 0.22**	277.99 ± 22.44**	1.83 ± 0.41**	1.48 ± 0.42*	2616.1 ± 153.52*	1858.3 ± 131.9* **
BA.M	1.15 ± 0.23**	1.46 ± 0.09**	270.67 ± 26.81**	1.69 ± 0.51**	1.31 ± 0.36	2455.19 ± 91.44**	1848.72 ± 156.98* **
BA.H	1.17 ± 0.14**	1.32 ± 0.14* **	268.17 ± 33.29**	1.67 ± 0.34* **	1.32 ± 0.17*	2331.97 ± 167.89* **	1803.57 ± 129.19* **

\* indicates a significant difference compared with model group: \*P < 0.05, \*\*P < 0.01, \*\*\*P < 0.001.

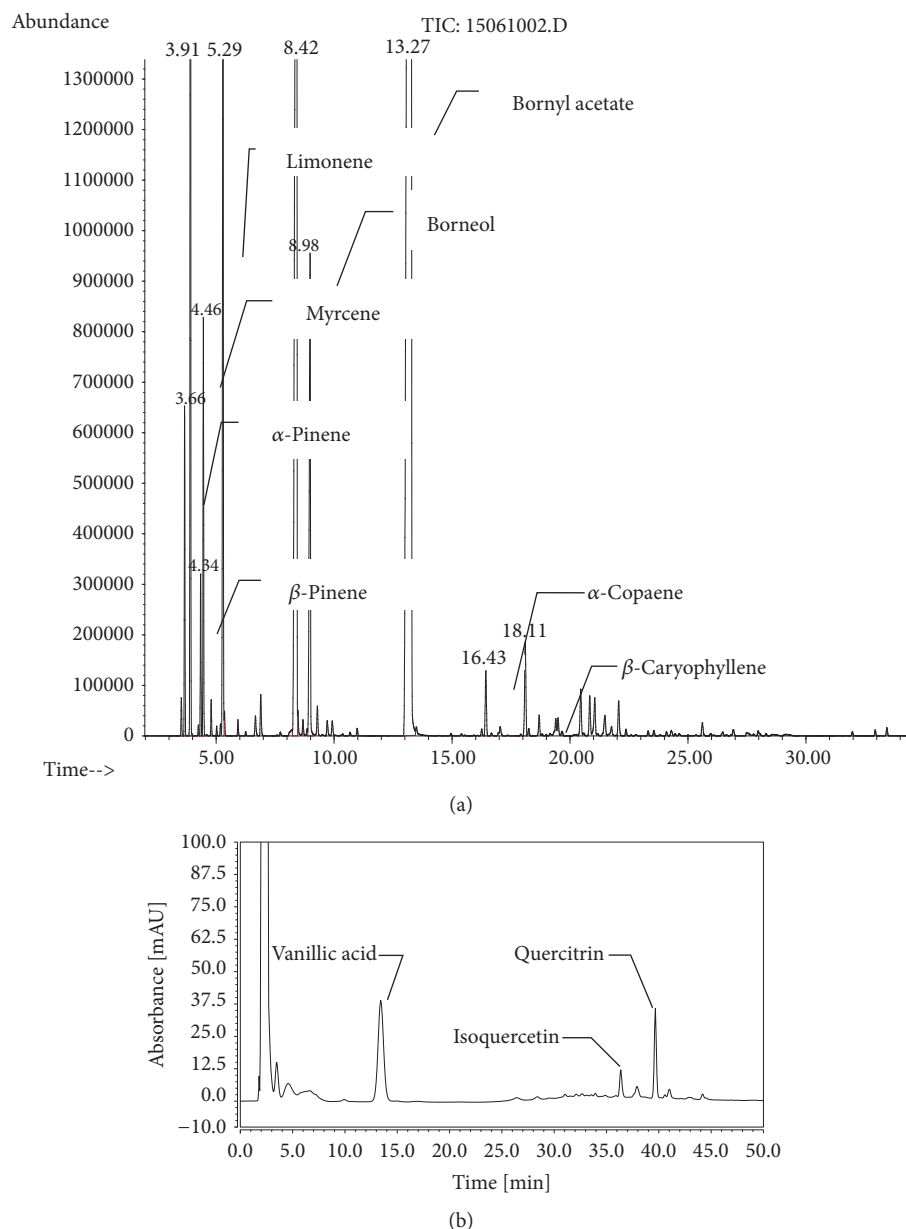


FIGURE 1: **Chemical constituents of *Amomum villosum*.** (a) GC-MS profile of the volatile oil of *A. villosum*; (b) HPLC profile of water extract of *A. villosum*.

species dramatically changed after the mice were fed HFD for 16 weeks. Abundances of *Lactobacillus* and *Prevotella* were reincreased in the treatment groups. The application of VOAV induced the greatest increase in the relative abundance of *Lactobacillus*. Relative abundances of key genera in the Bacteroidetes and Firmicutes phyla (Figure 3(d)) showed that *A. villosum* induced an increase in the densities of *Prevotella* and CF231 and reduced that of *Bacteroides* and *Parabacteroides*. These genera belong to the Bacteroidetes phylum. *A. villosum* reduced the relative abundance of some genera within the Firmicutes phylum such as *Clostridium*, *Faecalibacterium*, *Clostridium-2*, *Allobaculum*, and *Oscillospira* (Figure 3(d)). Therefore, *A. villosum* effectively ameliorates

the increase in the Firmicutes-to-Bacteroidetes ratio in HFD-fed rats (Figure 3(e)).

Heatmap and cluster analysis of the 35 most abundant orders of intestinal flora were conducted based on the abundance of species annotation information (order). These treatment groups were divided into two categories: VOAV and CN were located in one cluster unit; WEAV, BA, MOD, and EZE were located in another cluster unit (Figure 3(f)). These results suggested that the microbial abundances of high-fat-intake rats dramatically differed from that of rats fed on a normal diet. VOAV restored the disturbed balance of intestinal flora to normal levels. However, BA showed different effects on intestinal flora compared with VOAV.

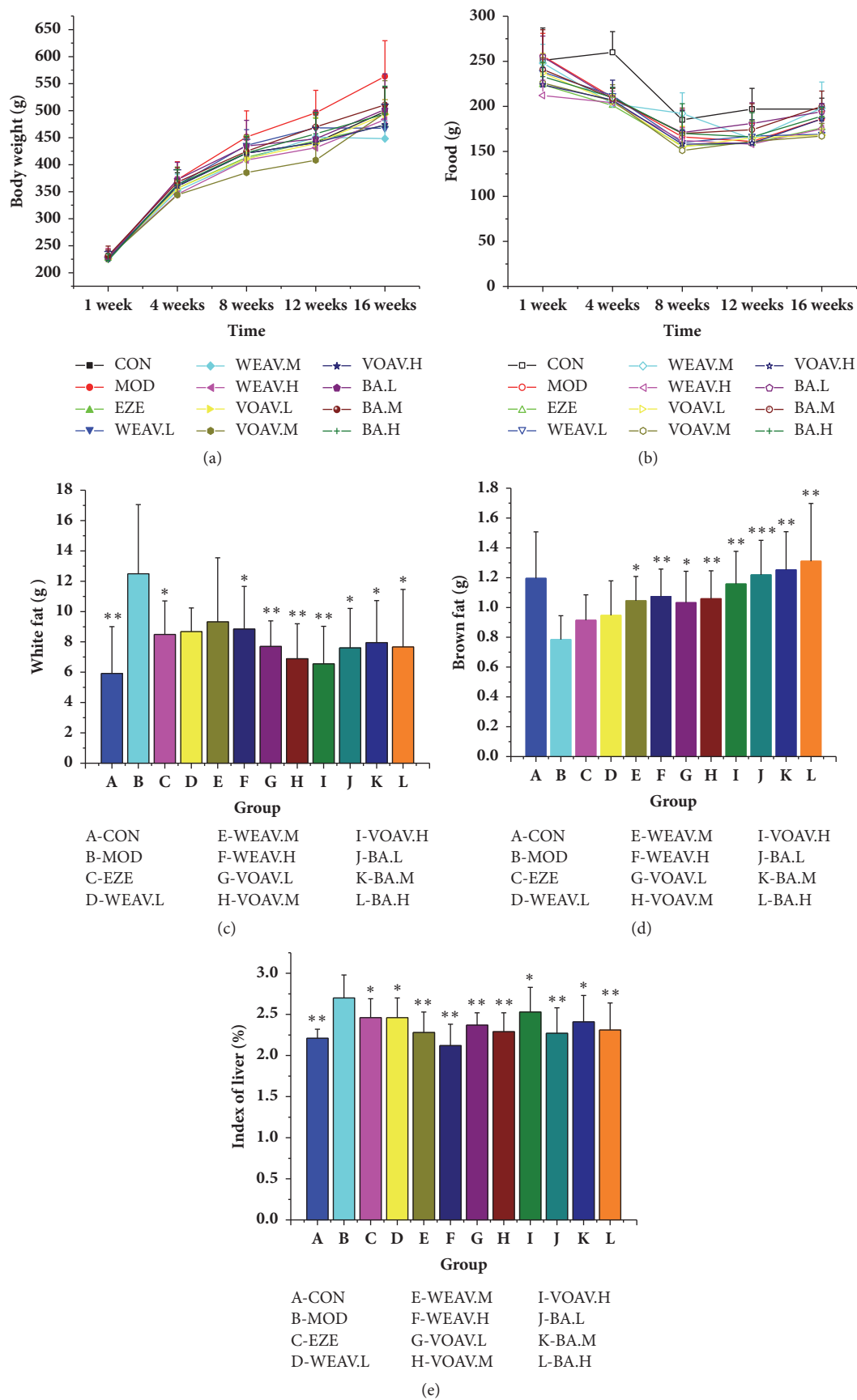
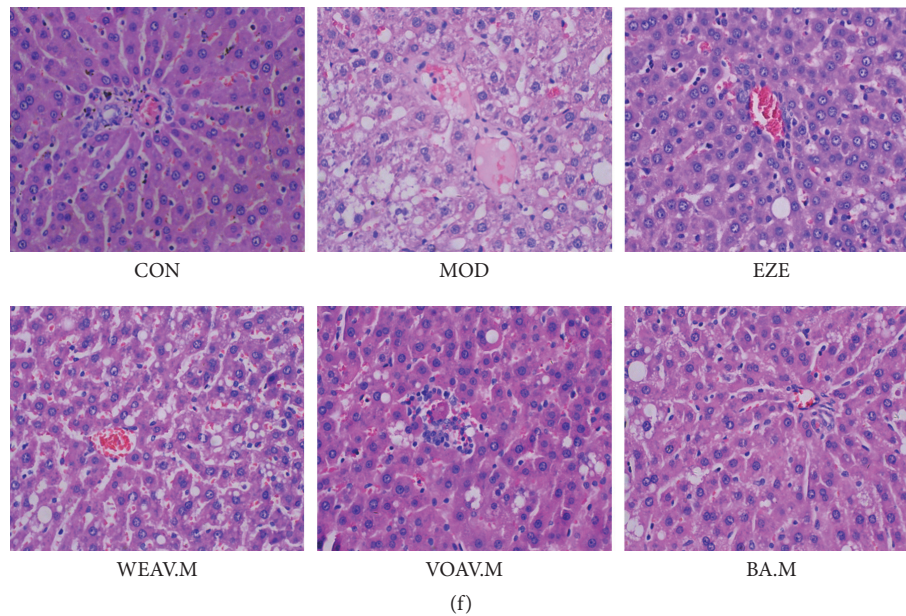


FIGURE 2: Continued.



**FIGURE 2: *Amomum villosum* reduced body weight and fat accumulation in HFD-fed rats.** Effects of *A. villosum* treatment on (a) body weight, (b) food intake, (c) white fat, (d) brown fat, (e) liver index, and (f) liver biopsy. (a–e) The difference between groups was evaluated using one-way analysis of variance (ANOVA,  $n = 10$ ). Asterisks (\*) indicate a significant difference from the model group, \* $P < 0.05$ , \*\* $P < 0.01$ , \*\*\* $P < 0.001$ . (f) Representative images (200 $\times$  magnification, hematoxylin and eosin stain) of hepatic histology in CON, MOD, EZE, WEAV.M, VOAV.M, and BA.M groups. No obvious fatty degeneration was observed in hepatocytes in the CON group. Obvious edema and steatosis were observed in hepatocytes after being fed a high-fat diet for 16 weeks. They were markedly relieved in VOVA.M and BA.M groups.

This suggests that volatile constituents other than BA may also contribute to the activity of VOAV. After comprehensive consideration of the UniFrac-based PCoA (Figure 3(a)), the UPGMA clustering tree (Figure 3(b)), the relative abundances of genera (Figures 3(c) and 3(d)), the Firmicutes-to-Bacteroidetes ratio (Figure 3(e)), and cluster analysis of the 35 most common orders (Figure 3(f)), we concluded that VOAV has a profound regulatory effect on the HFD-induced NAFLD intestinal microecological damage.

**4.3.1. *A. villosum* Protects the Intestinal Mucosal Barrier and Relieves Endotoxin.** In the present study, degeneration and necrosis in the epithelial tissue of the intestinal mucosa in NAFLD rats were observed (Figure 4(a)). Treatment of VOAV minimized the damage and maintained the structural integrity of these tissues, whereas WEAV did not.

The protein expression levels of ZO-1 and occludin were significantly lower in the model group than in the normal group (Figure 3(b)). Additionally, VOAV increased occludin protein expression to normal levels, as well as significantly increasing the protein expression of ZO-1.

The production of endotoxin by intestinal microbes can cause chronic low-grade inflammation in patients with NAFLD. After the rats were fed on an HFD for 16 weeks, significantly higher endotoxin levels were observed in the NAFLD group relative to that in the control group (Figure 4(c)). *A. villosum* inhibited the increase in LPS levels, particularly in the VOAV group ( $P < 0.001$ ). This inhibitory effect might be related to its beneficial effects on gut microbiota equilibrium.

In general, VOAV could protect the function of intestinal mucosal barrier, increase the expression of the occludin and ZO-1 proteins, and ameliorate endotoxin translocation induced endotoxemia.

**4.3.2. *A. villosum* Inhibits the TLR4/NF- $\kappa$ B Inherent Immune Response System of HFD Rats.** The TLR4 levels in the liver tissue of HFD-fed NAFLD rats showed a twofold increase compared to the CON group (Figure 5(a)). However, intervention using *A. villosum* effectively inhibited the expression of TLR4. The VOAV.M group showed superior performance with respect to reducing TLR4 levels in the liver, wherein expression dropped by about 50% reduced.

Figures 5(b)–5(d) show that WEAV, VOAV, and BA inhibited NF- $\kappa$ B and IKK production in hepatic tissues of HFD-fed rats. Moreover, the production of I $\kappa$ B, whose interaction with NF- $\kappa$ B was found to prevent NF- $\kappa$ B translocation and activation, was also enhanced after *A. villosum* treatment.

**4.3.3. *A. villosum* Suppresses the Cytokine Levels Downstream of the TLR4/NF- $\kappa$ B Pathway.** Hepatic TNF- $\alpha$ , IL-6, and IL-1 $\alpha$  expression levels were higher in HFD-fed rats than in the chow-fed rats of the control group, whereas IL-10 expression was lower (Figures 6(a)–6(d)). Chronic low-grade inflammation, which is characterized by the overproduction of inflammatory cytokines such as TNF- $\alpha$ , IL-6, and IL-1 $\alpha$ , was also controlled by *A. villosum* (Figures 6(a)–6(d)). In the meantime, VOAV showed a pronounced increase in hepatic IL-10 levels, which are typical anti-inflammatory cytokines. These results suggest that *A. villosum* suppresses the cytokine



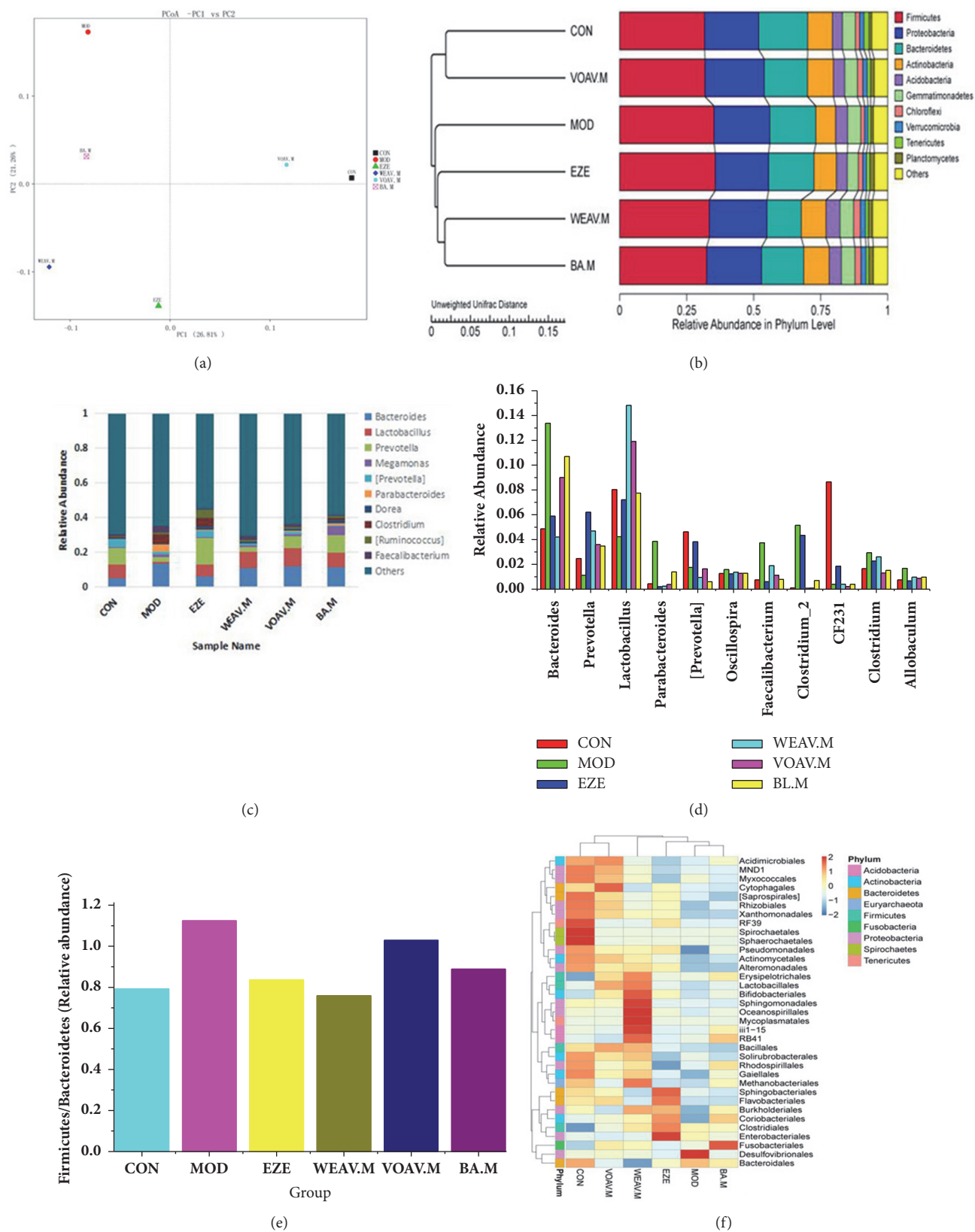


FIGURE 3: *Amomum villosum* altered the microbiota composition in HFD-fed mice. Microbiota composition in the feces of chow-fed mice; HFD mice treated with or without *A. villosum* were analyzed using 16s rDNA pyrosequencing (n = 10 for each group). (a) UniFrac-based PCoA analysis. (b) UPGMA clustering tree. (c) Relative abundance at the genus level. (d) Relative abundances of key genera in Bacteroidetes and Firmicutes phyla. (e) Firmicutes-to-Bacteroidetes ratio. (f) Species richness on the level of dendrogram order. The horizontal axis represents the sample information, the vertical axis represents species annotation information, the left side of the cluster tree represents the species cluster tree, and the top of the cluster tree represents the sample tree.

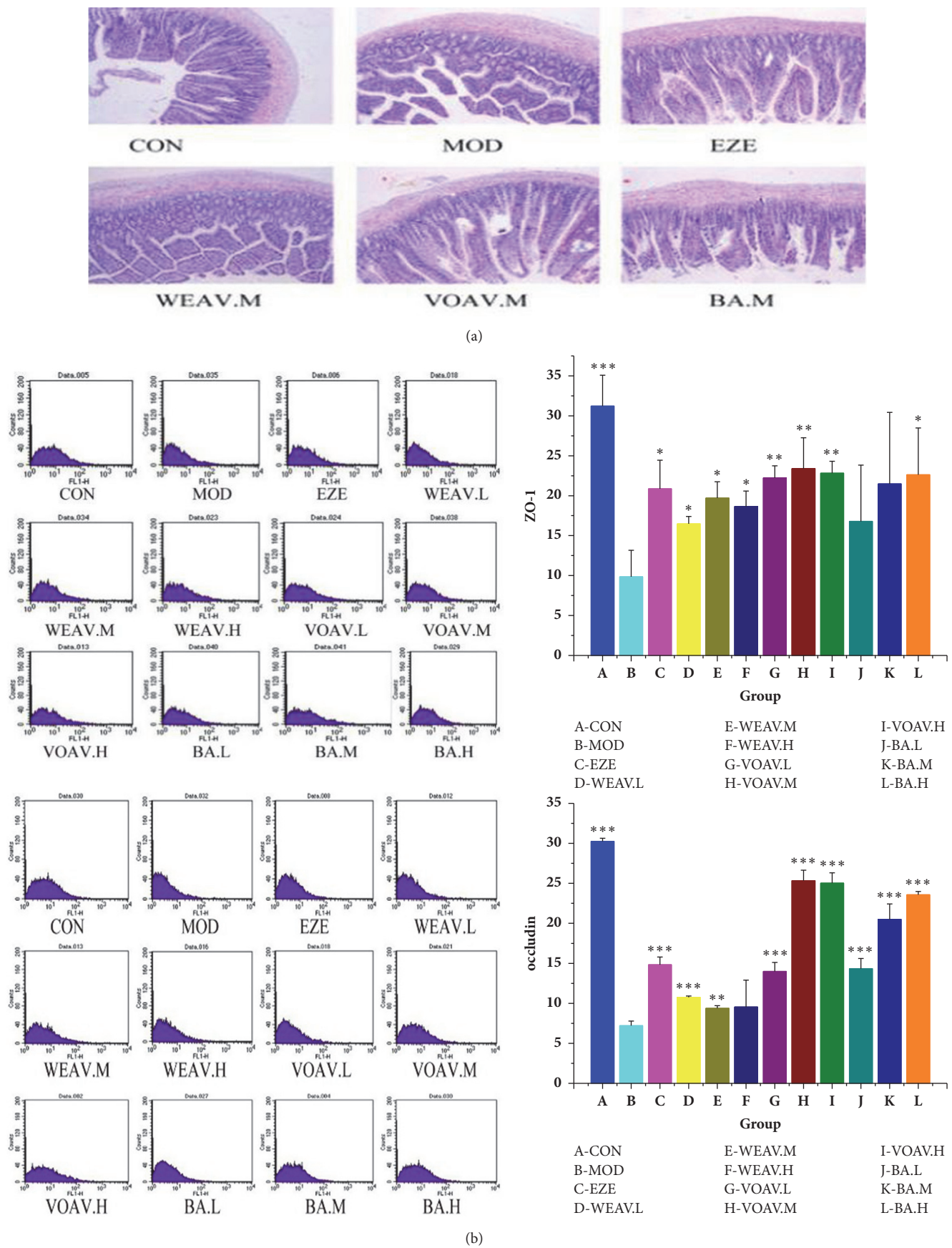


FIGURE 4: Continued.

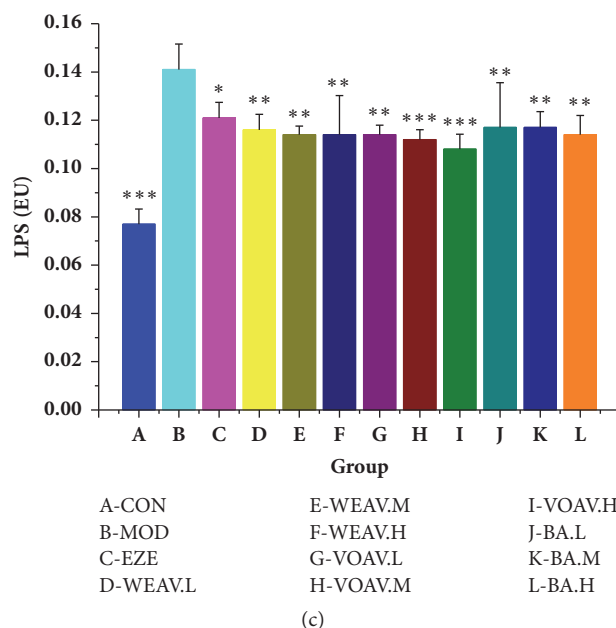


FIGURE 4: *A. villosum* protected the intestinal mucosal barrier and reduced the effects of endotoxins. (a) Comparison of microscopic morphology in ileum tissue among CON, MOD, EZE, WEAV.M, VOAV.M, and BA.M groups. Sectional representations (100× magnification, hematoxylin and eosin stain) of ileum tissues are shown. Degeneration and necrosis of ileum were relieved after VOVA and BA treatment. (b) Concentrations of ZO-1 and occludin. (c) Concentrations of LPS in hepatic portal vein. LPS levels in hepatic portal vein blood samples were measured using a tachypleus amebocyte lysate test (mean ± SD, n = 10). Statistical significance: \* $P < 0.05$  versus model; \*\* $P < 0.01$  versus model; \*\*\* $P < 0.001$  versus model.

levels downstream of the TLR4/NF- $\kappa$ B pathway, which was also beneficial by delaying the onset of NAFLD and limiting its development.

## 5. Discussion

Intestinal microbiota plays important roles in health and disease. Alterations in its healthy homeostasis might lead to the development of numerous liver disorders, including the complications of liver cirrhosis [25]. In recent years, numerous studies have shown that the intestinal microbiota is closely related to the development of NAFLD via the gut-liver axis. TLR4 occupies a decisive position between the signal produced in the gut and its biological effects in the liver. TLR4 is the main receptor that mediates LPS responses. LPS endotoxemia results in the upregulation of TLR4, promotes NF- $\kappa$ B transcription, and induces the overproduction of inflammatory cytokines that induce chronic low-grade inflammation, ultimately leading to NAFLD [26].

This study was designed to explore effect of the regulatory mechanism associated with different active ingredients of *A. villosum* on lipid accumulation in NAFLD. To elucidate the mechanism by which *A. villosum* prevents lipid metabolic disorders, all rats except those in the normal group were fed HFD until the end of the experiment (16 weeks). This HFD treatment was a typical formula for high-energy intake associated with the induction of NAFLD and hyperlipidemia in rodents [27, 28].

The present study observed the following: First, In the HPLC experiment, quercitrin, isoquercitrin, and vanilla acid

were used as reference products. Quercitrin and isoquercitrin were reported to have significant antioxidant activity [29]. Both quercitrin and isoquercitrin were reported to significantly reduce the levels of TG, TC, and MDA [30]. Furthermore, it was concluded that the anti-NAFLD activity of WEAV may be partly related to quercitrin and isoquercitrin.

In the meantime, a large number of literature sources reported that bornyl acetate, limonene,  $\alpha$ -pinene, and  $\alpha$ -copaene had obvious effects on the regulation of microbial activity [31–33], and it is speculated that regulation of intestinal microflora by VOAV was partly related to bornyl acetate, limonene,  $\alpha$ -pinene, and  $\alpha$ -copaene.

Second, *A. villosum* effectively inhibited the high-fat diet-induced accumulation of FFA in the liver, cutting off the supply of raw materials for endogenous TG synthesis. Simultaneously, *A. villosum* decreased TG accumulation in the liver by lowering the expression of LDL-C and increasing HDL-C content. VOAV showed the best lipid-lowering effect, which was highly similar to that in the positive control.

Third, *A. villosum* significantly regulated the balance of gut microbiota balance and the repair of intestinal mucous membrane barrier in NAFLD rats. *A. villosum* inhibited the increase in the ratio of Firmicutes and Bacteroidetes. *A. villosum* was found to reduce the relative abundance of some genera within Firmicutes such as *Clostridium*, *Faecalibacterium*, *Clostridium-2*, *Allobaculum*, and *Oscillospira*. *A. villosum* was also determined to adjust the relative abundance of some genera within the Bacteroides phylum effectively such as *Prevotella*, [*Prevotella*], *Parabacteroides*, *CF231*, and *Bacteroides* to normal levels. LPS is a major constituent of the

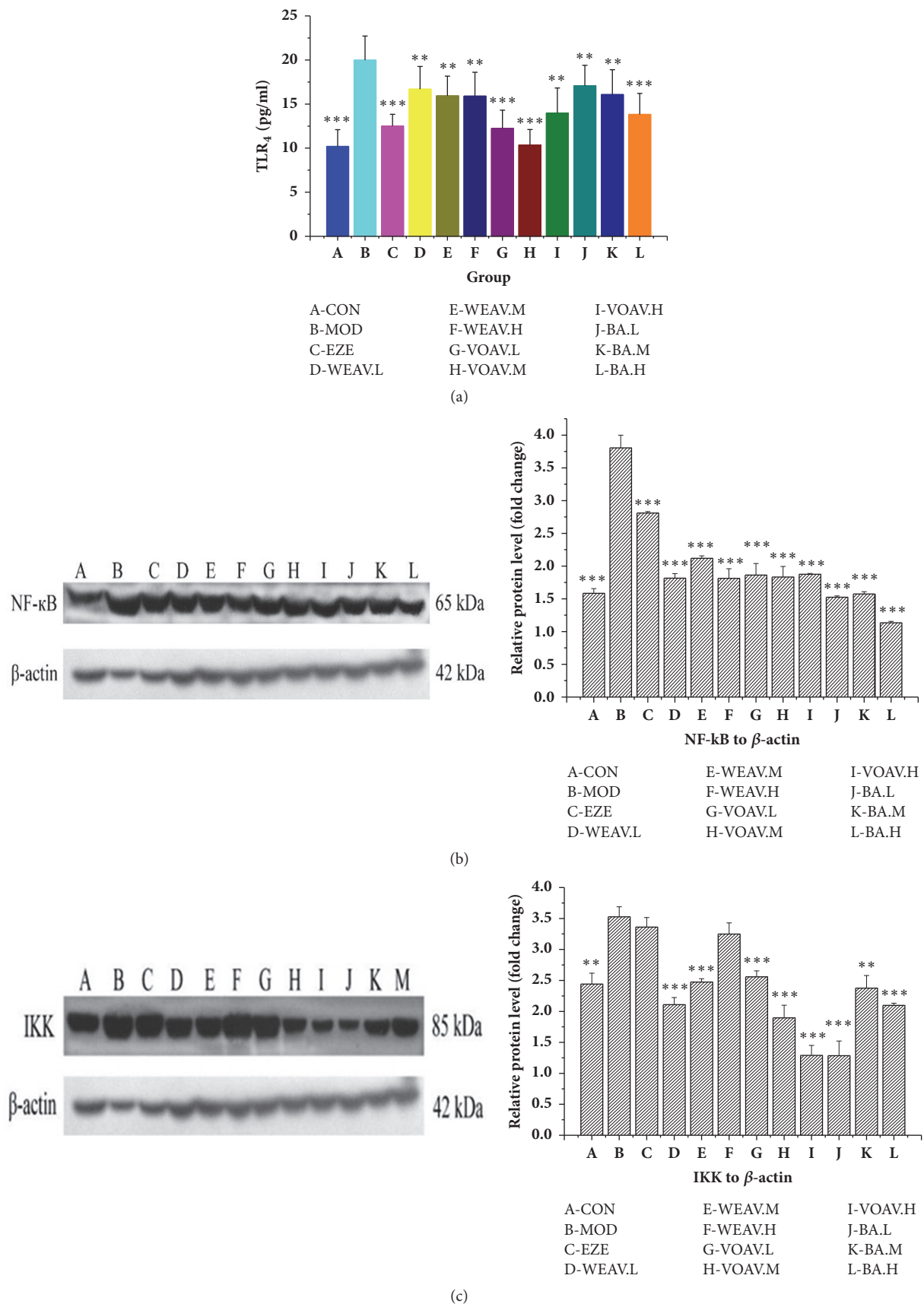


FIGURE 5: Continued.



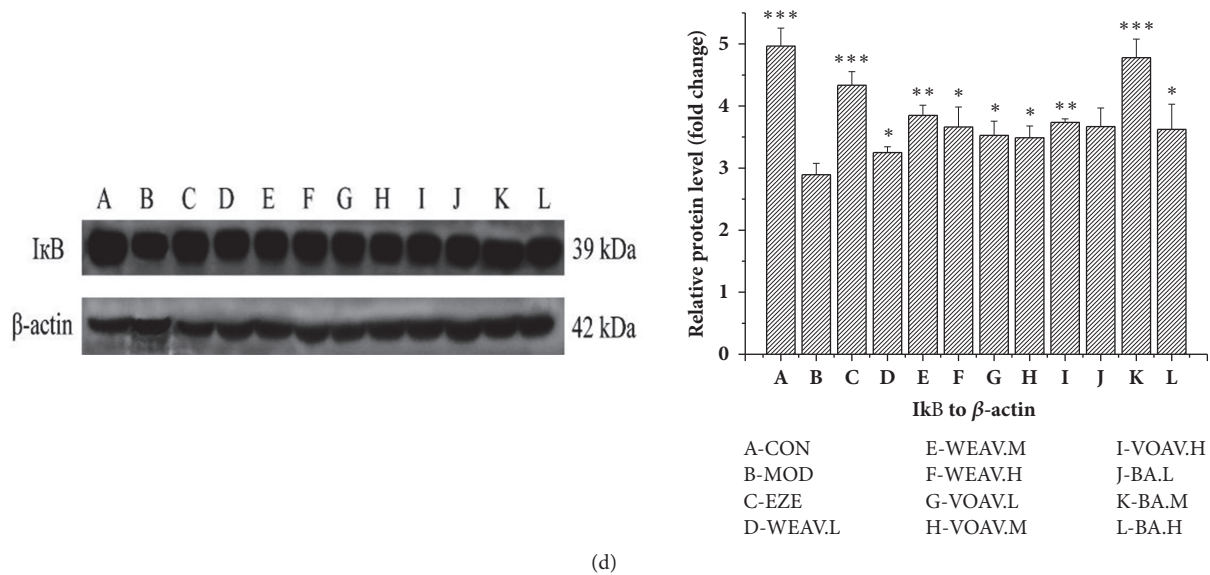


FIGURE 5: *A. villosum* reduced the TLR4/NF- $\kappa$ B inherent immune response system in HFD rat. Effects of *A. villosum* treatment on (a) TLR4 protein production, (b) NF- $\kappa$ B protein production, (c) IKK protein production, and (d) I $\kappa$ B production were examined in liver tissue. Representative immunoblots for target proteins are shown in (b), (c), and (d). Molecular weight markers are here given in kilodaltons (kDa). Protein levels were normalized to internal controls (beta-actin). Data are shown as mean  $\pm$  SD (n = 10). Statistical significance: \* $P$  < 0.05 versus model; \*\* $P$  < 0.01 versus model; \*\*\* $P$  < 0.001 versus model.

outer membranes of gram-negative bacteria. LPS recognition and signal transmission are key events in the host defense reaction towards gram-negative bacteria and are associated with various disorders [34, 35]. VOAV was shown to prevent the translocation of endotoxin and decrease the LPS content by nearly 22%. Intestinal epithelial cells play an important role in the maintenance of intestinal epithelial cells. The integrity of the small intestinal mucosa has been observed in a variety of acute or chronic intestinal diseases [7]. Tight junction proteins of small intestinal mucosa such as zonula occludens (ZO) and occludin play critical roles in the maintenance of the intestinal epithelial barrier [36]. The protein expression levels of ZO-1 and occludin were significantly lower in the model group than in the normal group, which was consistent with previous studies [37]. The regulation of the balance of gut microbiota and the strong intestinal mucosal barrier mediated by *A. villosum* might be responsible for this.

Endotoxemia and TLR4 signaling control the production of proinflammatory cytokines in target tissues, which lead to chronic inflammation and insulin resistance in HFD-fed rats [38]. TLR4 is the main receptor mediating the LPS response. Nuclear factor- $\kappa$ B (NF- $\kappa$ B), which belongs to a family of transcription factors, is the principal player in the regulation of inflammatory gene expression. Inhibitors of NF- $\kappa$ B (I- $\kappa$ B) kinase (IKKs) are a central component of the signaling cascade that controls NF- $\kappa$ B-dependent inflammatory gene transcription. IKKs activate the NF- $\kappa$ B pathway by phosphorylating I- $\kappa$ B and NF- $\kappa$ B P65, making it an attractive target for therapeutic intervention [39]. TLR4 and NF- $\kappa$ B protein expression was inhibited by VOAV and WEAV. *A. villosum* was found to downregulate IKK protein expression in the TLR4/NF- $\kappa$ B signaling pathway. The production of I $\kappa$ B, whose interactions with NF- $\kappa$ B prevented

NF- $\kappa$ B translocation and activation, was enhanced by *A. villosum* treatment. The release of downstream inflammatory cytokines in the LPS/TLR4/NF- $\kappa$ B signaling pathway was found to be mitigated by *A. villosum*. Studies showed that a high-fat diet could increase NF- $\kappa$ B activation in mice, which led to a sustained elevation in the level of I $\kappa$ B kinase epsilon (IKK epsilon) in the liver, adipocytes, and adipose tissue macrophages. IKK epsilon knockout mice were protected from high-fat diet-induced obesity, chronic inflammation of the liver and fat, hepatic steatosis, and whole-body insulin resistance [40–42].

Both ezetimibe and VOAV could inhibit the increasing of TC, TG, and FFA in liver homogenates. Among them, ezetimibe displayed better inhibitory effect on the content of TC, TG, and FFA in liver homogenate ( $P$  < 0.001), followed by the middle-dose group of volatile oil from *Amomum villosum*. However, VOAV showed better effect on the increasing of liver AST and ALT. In the meantime, *A. villosum* could effectively inhibit lipids accumulation in circulation system.

Sequencing results of 16S rDNA suggested that both ezetimibe and VOAV inhibited the increasing ratio of Firmicutes and Bacteroidetes. Ezetimibe and VOAV could effectively regulate the intestinal microflora, relieve the chronic low-grade inflammation by promoting ZO-1 and occludin protein expressions, and inhibit TLR4/NF- $\kappa$ B signaling pathway. The ezetimibe was more active in regulating the accumulation of lipids in the hepatic lipids of the high-fat diet (first strike), while *A. villosum* was more effective in intervening TLR4/NF- $\kappa$ B upstream signaling pathway and inhibiting the expression of proinflammatory cytokines.

In sum, *A. villosum* was found to effectively inhibit lipid accumulation in liver tissue, regulate the intestinal

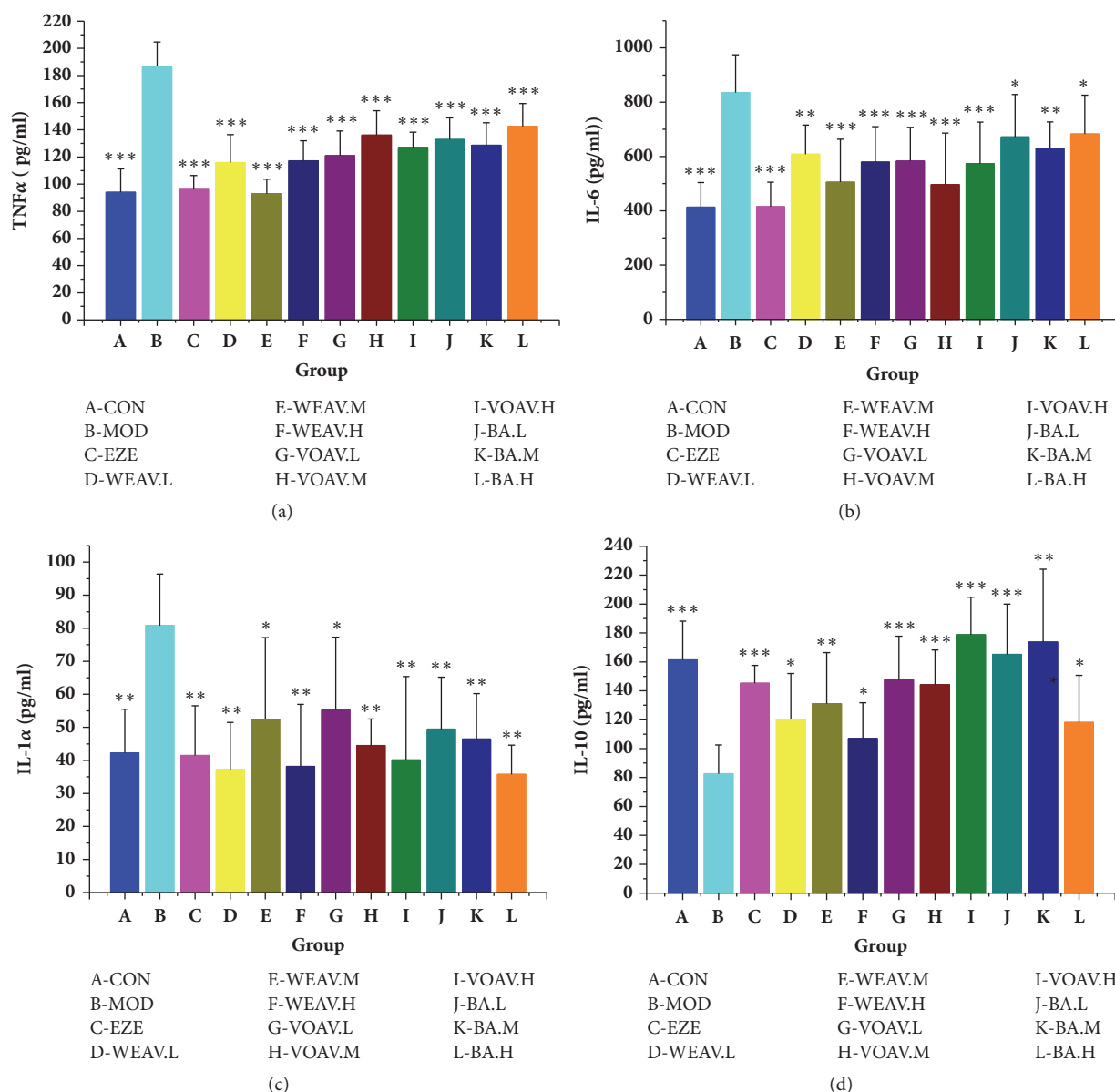


FIGURE 6: *A. villosum* suppressed the cytokine levels in the downstream of TLR4/NF- $\kappa$ B pathway. Relative expressions of (a) TNF- $\alpha$ , (b) IL-6, (c) IL-1 $\alpha$ , and (d) IL-10 in liver tissues were assessed using ELISA and are shown relative to the MOD group. Data are shown as mean  $\pm$  SD (n = 10). Statistical significance: \*  $P < 0.05$  versus model; \*\*  $P < 0.01$  versus model; \*\*\*  $P < 0.001$  versus model.

microflora, strengthen intestinal mucous membrane barrier, inhibit the TLR4/NF- $\kappa$ B signaling pathway, and relieve chronic low-grade inflammation. VOAV showed great potential in NAFLD prevention and treatment. This work could provide a scientific basis for further application and development of *A. villosum*.

The present study has investigated the role of *A. villosum* in the treatment of NAFLD. Results showed that *A. villosum* could improve the permeability of intestinal epithelial cells and regulate the balance of intestinal flora. In China, *A. villosum* is used in both medicine and cuisine food [43]. This made it possible to produce a new type of intestinal microecological preparation with better lipid-lowering effects. This research also confirmed that volatile oil is more effective

than *A. villosum* water extract, which could be considered scientific evidence that is in agreement with the traditional findings that *A. villosum* should be extracted promptly to prevent the oil from undergoing volatilization.

## Abbreviations

ALT:	Alanine aminotransferase
AST:	Aspartate aminotransferase
BA:	Bornyl acetate
FFA:	Free fatty acid
GC-MS:	Gas chromatography-mass spectrometer
HDL-C:	High-density lipoprotein cholesterol
HPLC:	High-performance liquid chromatography

HFD:	High-fat diet
IL-10:	Interleukin-10
IL-1 $\alpha$ :	Interleukin-1 alpha
IL-6:	Interleukin-6
IKK:	Inhibitor of nuclear factor-kappa-B kinase
I $\kappa$ B:	Inhibitors kappa-B
LDL-C:	Low-density lipoprotein cholesterol
LPL:	Lipoprotein lipase
LPS:	Lipopolysaccharide
NAFLD:	Nonalcoholic fatty liver disease
NF- $\kappa$ B:	Nuclear factor-kappa-B
OTUs:	Operational taxonomic units
PBS:	Phosphate buffer saline
PCoA:	Principal coordinates analysis
SIBO:	Small intestinal bacterial overgrowth
TC:	Total cholesterol
TG:	Triglyceride
TLR4:	Toll-like receptor 4
TNF- $\alpha$ :	Tumor necrosis factor alpha
UPGMA:	Unweighted pair-group method with arithmetic mean
VLDL:	Very-low-density lipoprotein
VOAV:	Volatile oil of <i>A. villosum</i>
WEAV:	Water extract of <i>A. villosum</i>
ZO-1:	Zonula occludens-1.

## Data Availability

All data are contained and described within the manuscript. The datasets used and/or analyzed during the current study are available from the corresponding author on reasonable request.

## Ethical Approval

The whole research design was reviewed and approved by the Institutional Ethical Committee on Animal Care and Experimentation of Yunnan University Traditional Chinese Medicine (R-0620150014). All reasonable efforts were made to minimize animal suffering.

## Conflicts of Interest

The authors declare that they have no conflicts of interest.

## Authors' Contributions

Shanhong Lu and Ting Zhang conducted the study, analyzed the data, and prepared the manuscript. Wen Gu, Xingxin Yang, and Jianmei Lu collected and interpreted the data. Ronghua Zhao and Jie Yu designed the study, provided the drugs and research facilities, and revised the manuscript. All authors read and approved the final manuscript.

## Acknowledgments

This study was supported by the National Natural Science Foundation of China (81460623, 81660596, 81660684, and 81760733), Kunming Key Laboratory for Metabolic

Diseases Prevention and Treatment by Chinese Medicine, Academician Workstation in Yunnan Province, the Natural Science Foundation of the Yunnan Province (2016FD050), the Southern Medicine Collaborative and Innovation Center (30270100500), and the Young and Middle-Aged Academic and Technological Leaders of Yunnan (2015HB053).

## References

- [1] C. P. Day, G. Haydon, and C. P. Day, "Non-alcoholic fatty liver disease: current concepts and management strategies," *Clinical Medicine*, vol. 6, no. 1, pp. 19–25, 2006.
- [2] R. Kumar, "Hard clinical outcomes in patients with NAFLD," *Hepatology International*, vol. 7, no. S2, pp. 790–799, 2013.
- [3] J. Boursier and A. M. Diehl, "Nonalcoholic Fatty Liver Disease and the Gut Microbiome," *Clinics in Liver Disease*, vol. 20, no. 2, pp. 263–275, 2016.
- [4] A. J. Wigg, I. C. Roberts-Thomson, R. B. Dymock, P. J. McCarthy, R. H. Grose, and A. G. Cummins, "The role of small intestinal bacterial overgrowth, intestinal permeability, endotoxaemia, and tumour necrosis factor  $\alpha$  in the pathogenesis of non-alcoholic steatohepatitis," *Gut*, vol. 48, no. 2, pp. 206–211, 2001.
- [5] J. G. Caporaso, C. L. Lauber, W. A. Walters et al., "Global patterns of 16S rRNA diversity at a depth of millions of sequences per sample," *Proceedings of the National Academy of Sciences of the United States of America*, vol. 108, no. 1, pp. 4516–4522, 2011.
- [6] R. E. Ley, P. J. Turnbaugh, S. Klein, and J. I. Gordon, "Microbial ecology: human gut microbes associated with obesity," *Nature*, vol. 444, no. 7122, pp. 1022–1023, 2006.
- [7] P. Brun, I. Castagliuolo, V. Di Leo et al., "Increased intestinal permeability in obese mice: new evidence in the pathogenesis of nonalcoholic steatohepatitis," *American Journal of Physiology-Gastrointestinal and Liver Physiology*, vol. 292, no. 2, pp. G518–G525, 2007.
- [8] P. Lin, J.-M. Lu, Y.-F. Wang, W. Gu, R.-H. Zhao, and J. Yu, "Prevention mechanism of 2,3,5,4'-Tetrahydroxy-stilbene-2-O- $\beta$ -D-glucoside on lipid accumulation in steatosis hepatic L-02 cell," *Pharmacognosy Magazine*, vol. 13, no. 50, pp. 245–253, 2017.
- [9] W. Z. Mehal, "The Gordian Knot of dysbiosis, obesity and NAFLD," *Nature Reviews Gastroenterology & Hepatology*, vol. 10, no. 11, pp. 637–644, 2013.
- [10] L. Miele, V. Valenza, G. La Torre et al., "Increased intestinal permeability and tight junction alterations in nonalcoholic fatty liver disease," *Hepatology*, vol. 49, no. 6, pp. 1877–1887, 2009.
- [11] B. Chassaing, L. Etienne-Mesmin, and A. T. Gewirtz, "Microbiota-liver axis in hepatic disease," *Hepatology*, vol. 59, no. 1, pp. 328–339, 2014.
- [12] M. V. Machado and H. Cortez-Pinto, "Gut microbiota and nonalcoholic fatty liver disease," *Annals of Hepatology*, vol. 11, no. 4, pp. 440–449, 2012.
- [13] K. Miura, E. Seki, H. Ohnishi, and D. A. Brenner, "Role of toll-like receptors and their downstream molecules in the development of nonalcoholic fatty liver disease," *Gastroenterology Research and Practice*, vol. 2010, Article ID 362847, 9 pages, 2010.
- [14] O. Cheung and A. J. Sanyal, "Recent advances in nonalcoholic fatty liver disease," *Current Opinion in Gastroenterology*, vol. 26, no. 3, pp. 202–208, 2010.
- [15] I. R. Wanless and K. Shiota, "The pathogenesis of nonalcoholic steatohepatitis and other fatty liver diseases: a four-step model

- including the role of lipid release and hepatic venular obstruction in the progression to cirrhosis," *Seminars in Liver Disease*, vol. 24, no. 1, pp. 99–106, 2004.
- [16] Commission of Chinese Pharmacopoeia, *Pharmacopoeia of the People's Republic of China*, China Medico-Pharmaceutical Science & Technology Publishing House, 2015.
- [17] YL. Huang and ZH. Zhou, "Effect of water extracts from Amomi Fructus and Millettia Reticulata on the improving the intestinal health and function," *Acad Period Farm Prod Process*, vol. 8, pp. 95–96, 2006.
- [18] S. T. Zhang, Z. Y. Wang, and T. S. Wang, "Composition and antimicrobial activities of essential oil of Amomi Fructus," in *Natural Product Research and Development*, vol. 23, pp. 464–472, 23, vol. 2011.
- [19] C.-G. Son, W.-J. Choi, J.-W. Shin et al., "Effects of Gamichung-tang on hyperlipidemia," *Acta Pharmacologica Sinica*, vol. 24, no. 2, pp. 133–139, 2003.
- [20] C. H. Halsted, J. A. Villanueva, and A. M. Devlin, "Folate deficiency, methionine metabolism, and alcoholic liver disease," *Alcohol*, vol. 27, no. 3, pp. 169–172, 2002.
- [21] ZZ. Li, RL. Pan, and Li. Zhan, "Determination of the Contents of total flavonoids, isoquercitroside and quercitroside in Amomum villosum," *Science & Technology Review*, vol. 27, pp. 30–33, 2009.
- [22] L. Sun, JG. Yu, and LD. Zhou, "Two Flavone Glycosides from Chinese Traditional Medicine Amomum villosum," *China Journal of Chinese Materia Medica*, vol. 27, pp. 36–38, 2002.
- [23] M. Ashburner, C. A. Ball, J. A. Blake et al., "Gene ontology: tool for the unification of biology," *Nature Genetics*, vol. 25, no. 1, pp. 25–29, 2000.
- [24] T. Magoč and S. L. Salzberg, "FLASH: fast length adjustment of short reads to improve genome assemblies," *Bioinformatics*, vol. 27, no. 21, pp. 2957–2963, 2011.
- [25] R. S. Lo, A. S. Austin, and J. G. Freeman, "Is there a role for probiotics in liver disease?" *The Scientific World Journal*, vol. 2014, Article ID 874768, 2014.
- [26] P. Lin, J. Lu, Y. Wang et al., "Naturally occurring stilbenoid TSG reverses non-alcoholic fatty liver diseases via gut-liver axis," *PLoS ONE*, vol. 10, no. 10, Article ID e0140346, 2015.
- [27] Y. Takahashi, Y. Soejima, and T. Fukusato, "Animal models of nonalcoholic fatty liver disease/ nonalcoholic steatohepatitis," *World Journal of Gastroenterology*, vol. 18, no. 19, pp. 2300–2308, 2012.
- [28] J.-G. Fan, L. Zhong, Z.-J. Xu et al., "Effects of low-calorie diet on steatohepatitis in rats with obesity and hyperlipidemia," *World Journal of Gastroenterology*, vol. 9, no. 9, pp. 2045–2049, 2003.
- [29] H.-C. Ni, J. Li, Y. Jin et al., "The protective and therapeutic effects of total flavonoids of litsea coreana level on nonalcoholic steatohepatitis in rats," *Chinese Pharmacological Bulletin*, vol. 22, no. 5, pp. 591–594, 2006.
- [30] J. R. Zhang, "Effect of Kaempferol and Quercetin on Blood Sugar and Fat Contents of Diabetic Model Mice," *Modern Food Science and Technology*, vol. 29, pp. 459–462, 2013.
- [31] S. Vitalini, M. Madeo, A. Tava et al., "Chemical profile, antioxidant and antibacterial activities of achillea moschata wulfen, an endemic species from the alps," *Molecules*, vol. 21, no. 7, article no. 830, 2016.
- [32] S. E. Hashim, H. M. Sirat, and K. H. Yen, "Chemical compositions and antimicrobial activity of the essential oils of hornstedtia havilandii (Zingiberaceae)," *Natural Product Communications (NPC)*, vol. 9, no. 1, pp. 119–120, 2014.
- [33] L. Yang, J. Liu, Y. Li, and G. Qi, "Bornyl acetate suppresses ox-LDL-induced attachment of THP-1 monocytes to endothelial cells," *Biomedicine & Pharmacotherapy*, vol. 103, pp. 234–239, 2018.
- [34] S. H. Diks, D. J. Richel, and M. P. Peppelenbosch, "LPS signal transduction: the picture is becoming more complex," *Current Topics in Medicinal Chemistry*, vol. 4, no. 11, pp. 1115–1126, 2004.
- [35] E. M. Pålsson-McDermott and L. A. J. O'Neill, "Signal transduction by the lipopolysaccharide receptor, Toll-like receptor-4," *The Journal of Immunology*, vol. 113, no. 2, pp. 153–162, 2004.
- [36] J. R. Turner, "Intestinal mucosal barrier function in health and disease," *Nature Reviews Immunology*, vol. 9, no. 11, pp. 799–809, 2009.
- [37] T. Suzuki, "Regulation of intestinal epithelial permeability by tight junctions," *Cellular and Molecular Life Sciences*, vol. 70, no. 4, pp. 631–659, 2013.
- [38] P. D. Cani, R. Bibiloni, C. Knauf et al., "Changes in gut microbiota control metabolic endotoxemia-induced inflammation in high-fat diet-induced obesity and diabetes in mice," *Diabetes*, vol. 57, no. 6, pp. 1470–1481, 2008.
- [39] NM. Paul, "The NF- $\kappa$ B pathway," *Journal of Cell Science*, vol. 118, pp. 389–392, 2005.
- [40] X. Zhang, G. Zhang, H. Zhang, M. Karin, H. Bai, and D. Cai, "Hypothalamic IKK $\beta$ /NF- $\kappa$ B and ER stress link overnutrition to energy imbalance and obesity," *Cell*, vol. 135, no. 1, pp. 61–73, 2008.
- [41] N. Beraza, Y. Malato, S. Vander Borghet et al., "Pharmacological IKK2 inhibition blocks liver steatosis and initiation of non-alcoholic steatohepatitis," *Gut*, vol. 57, no. 5, pp. 655–663, 2008.
- [42] S. Chiang, M. Bazuine, C. N. Lumeng et al., "The Protein Kinase IKK $\epsilon$  Regulates Energy Balance in Obese Mice," *Cell*, vol. 138, no. 5, pp. 961–975, 2009.
- [43] Department of Health Supervision and Ministry of Health of the People's Republic of China, *Compendium of Health Food Management Regulations*, Jilin Science and Technology Press, Second edition, 1998.



## Research Article

# Effects of *Juniperus phoenicea* Hydroalcoholic Extract on Inflammatory Mediators and Oxidative Stress Markers in Carrageenan-Induced Paw Oedema in Mice

Karama Zouari Bouassida <sup>1</sup>, Samar Makni,<sup>1</sup> Amina Tounsi,<sup>1</sup> Lobna Jlaiel,<sup>2</sup> Mohamed Trigui <sup>1</sup> and Slim Tounsi <sup>1</sup>

<sup>1</sup>Biopesticides Laboratory (LPIP), Center of Biotechnology of Sfax, University of Sfax, P.O. Box 1177, 3018 Sfax, Tunisia

<sup>2</sup>Analysis Department, Center of Biotechnology of Sfax, University of Sfax, P.O. Box 1177, 3018 Sfax, Tunisia

Correspondence should be addressed to Karama Zouari Bouassida; k.bouassidazouari@yahoo.fr

Received 16 April 2018; Accepted 24 June 2018; Published 9 July 2018

Academic Editor: Ravirajsinh N. Jadeja

Copyright © 2018 Karama Zouari Bouassida et al. This is an open access article distributed under the Creative Commons Attribution License, which permits unrestricted use, distribution, and reproduction in any medium, provided the original work is properly cited.

*Juniperus phoenicea* (*J. phoenicea*) is a wild tree belonging to the Cupressaceae family, commonly used for the treatment of several disorders. This study aimed to evaluate the potential protective effects of *J. phoenicea* hydroethanolic extract (EtOH-H<sub>2</sub>O<sub>2</sub>OE) against oxidation, acute inflammation, and pain in mice models. For the purpose, chemical compounds of *J. phoenicea* EtOH-H<sub>2</sub>O<sub>2</sub>OE were also analyzed by GC-MS. The *J. phoenicea* EtOH-H<sub>2</sub>O<sub>2</sub>OE showed a potent antioxidant activity *in vitro*, thanks to its richness in phenolic and flavonoid compounds. Mice treated with EtOH-H<sub>2</sub>O<sub>2</sub>OE (100 mg/kg BW) showed reduced paw oedema formation and decreased malondialdehyde (MDA) content. The evaluation of antioxidant enzyme activities in paw oedema tissue after five hours of carrageenan induction showed a significant increase ( $P < 0.05$ ). Inflammatory biomarkers explorations of *J. phoenicea* EtOH-H<sub>2</sub>O<sub>2</sub>OE-treated mice showed a restoration of the studied parameters to near-normal values. Furthermore, EtOH-H<sub>2</sub>O<sub>2</sub>OE of *J. phoenicea* produced a significant reduction of the number of abdominal writhes ( $P < 0.05$ ) in a dose-dependent way. Phytochemical analysis of the *J. phoenicea* EtOH-H<sub>2</sub>O<sub>2</sub>OE by GC-MS showed the presence of hexadecanoic and stearic acids known as anti-inflammatory and analgesic compounds. Our investigation provided evidence that *J. phoenicea* EtOH-H<sub>2</sub>O<sub>2</sub>OE can effectively reduce the inflammation and pain in mice models.

## 1. Introduction

Medicinal plants have been used in traditional health care systems since prehistoric civilizations. World Health Organization (WHO) estimates that about 85% of the worldwide traditional knowledge involves the use of plant extracts [1]. Therefore, treatment of various diseases has been carried out with medicinal plants for many years. These plants are an endless source of pharmaceutical and therapeutic products, thanks to their richness in bioactive molecules that have medicinal properties. The antioxidant compounds derived from plant extracts could be a solution to overcome diseases, caused by oxidative stress, such as inflammation [2].

Oxidative stress is the result of an imbalance between the reactive oxygen species (ROS) levels production during

metabolism and their removal by the antioxidant defense systems [3]. Excessive production of ROS in tissues may contribute to cell damage by altering cellular molecules, namely, proteins, lipids, and DNA/RNA [4, 5]. Furthermore, it was indicated that ROS excess initiates the inflammation process by stimulating the induction of proinflammatory cytokines, chemokines, and pro-inflammatory transcription factors causing tissue injury [6]. Inflammation represents a rapid yet coordinated set of events that enable tissues to respond to injuries or infections [7]. It is a natural defense mechanism that involves the recruitment of immune cells and the overproduction of inflammatory cytokines into the tissues in response to the ROS release [8]. To avoid the ROS harmful effects, human cells have developed a sophisticated antioxidant defense system that consists of an enzymes system involved in

the conversion of ROS to less reactive molecules such as  $O_2$  and water [9]. Superoxide dismutase (SOD), catalase (CAT), and glutathione peroxidase (GPx) are the main endogenous enzymes involved in protecting aerobic cells from the noxious effects of ROS. They give protection by directly scavenging superoxide radicals and hydrogen peroxide, converting them into stable species [10]. Cell damage induced by an excessive production of ROS depends on the potential of the cellular antioxidant enzymes to neutralize them [11]. Studies documented that, in addition to the enzymatic/nonenzymatic cellular antioxidant defense system's protective effects, natural products having antioxidant activities may lead to delaying the oxidative stress and inflammatory tissue damage by enhancing the cell/tissues defenses [12].

The search for natural products with antioxidant activities has increased enormously over the last decades. Plants would be a promising alternative to reduce oxidative damage, thanks to their secondary metabolites richness such as polyphenols, flavonoids, tannins, terpenoids, and anthraquinones [13]. It was reported that plant natural compounds are able to interact with ROS and thus terminate the chain reaction before the cell vital molecules were seriously damaged [14].

*Juniperus phoenicea* is a wild tree belonging to the Cupressaceae family and is popularly known as "Arâar" in Tunisia. *Juniperus* species have been widely used in the traditional medicines against various infectious and inflammatory diseases such as cold, diarrhea, fungal infections, hemorrhoids, leucorrhea, diabetes, and wounds [15]. In Tunisian folk medicine, the *J. phoenicea* leaf decoction was frequently employed to regulate menstruation and relieve the pain of menstrual cramps [16]. The mixture of berries and leaves of this plant was used traditionally as antidiabetic remedies [17]. Previous studies on the biological activities of *J. phoenicea* have mainly focused on the essential oils. Although the plant is claimed to be used for its anti-inflammatory and analgesic effects by Tunisian traditional healers, no published work so far investigates the use of *J. phoenicea* for this purpose. *J. phoenicea* has a long use record in the treatment of oedema in the Mediterranean subdivision [15].

This study aimed mainly to (1) explore the properties of *J. phoenicea* EtOH- $H_2O$ E in the management of inflammation and oxidation using carrageenan-induced paw oedema model, (2) evaluate the analgesic potential of *J. phoenicea* EtOH- $H_2O$ E using acetic acid-induced abdominal contraction, (3) identify the phytochemicals present in the extract by GC-MS, and (4) assess the relationship between the extract agents and the bioactivities.

## 2. Materials and Methods

**2.1. Drugs and Reagents.** 2,2-Diphenyl-1-picrylhydrazyl (DPPH), butylated hydroxytoluene (BHT), linoleic acid,  $\beta$ -carotene, ascorbic acid, gallic acid, quercetin, Folin-Ciocalteu reagent, Lambda carrageenan, dexamethasone, and acetic acid were purchased from Sigma-Aldrich Company (Sigma Chemical Company, USA).

**2.2. Plant Material.** *J. phoenicea* fresh leaves were collected in January from Boulifa (El Kef, northwestern part of Tunisia:

36°07'25.7"N, 8°43'07.6"E). The plant sample was identified morphologically by Professor Mohamed Chaieb, the Department of Botany and Plant Ecology of the Faculty of Sciences (University of Sfax, Tunisia). A voucher specimen was kept at the Laboratory of Biopesticides of the Centre of Biotechnology of Sfax under the reference number LBPes J.P. 01.16.

**2.3. Plant Extraction.** The *J. phoenicea* air-dried leaves (105 g) were crushed into small parts with a blender and were sequentially extracted by hydroalcoholic maceration in ethanol-water (8:2, v/v) for 48 h under continuous shaking. The resulting extract (EtOH- $H_2O$ E) was filtered through a Whatman paper (pore size: 0.45  $\mu$ m, diameter: 47 mm) and then concentrated to afford 22.69 g which made the crude extract. EtOH- $H_2O$ E was kept at +4°C in the dark until further use.

**2.4. Qualitative Analysis.** The qualitative phytochemical tests were carried out according to Sofowora [18] and Harborne [19]. They were based on the visual observation of color change of EtOH- $H_2O$ E of *J. phoenicea*. The tested phytochemicals are phenolics, flavonoids, anthraquinones, glycosides, terpenoids, tannins, saponins, and alkaloids. The results are expressed as "+" for the presence and "-" for the absence of phytochemicals.

**2.5. Gas Chromatography-Mass Spectrometry (GC-MS) Analysis.** GC-MS analysis of EtOH- $H_2O$ E of *J. phoenicea* was performed with an Agilent 6890N Network GC System (Agilent Technologies). The system was equipped with an HP-5 MS column having 30 m  $\times$  0.25 mm i.d.  $\times$  0.25  $\mu$ m film as dimensions. The used system was coupled to a mass selective detector and the carrier gas was helium. The GC oven temperature started at 40°C and was held at 60°C for 2 min and was then programmed to rise from 60 to 325°C at a rate of 5°C/min. The injected extract temperature was set at 280°C.

The components identification was achieved by careful examination of fragmentation patterns and spectral data obtained from the Wiley and NIST libraries. This determination was carried out in duplicates.

## 2.6. Phenolic Contents and Antioxidant Activity

**2.6.1. Determination of Total Phenols.** The total phenolic content was assayed using the Folin-Ciocalteu reagent and gallic acid as a standard [20]. The absorbance was measured at 760 nm and the results were expressed as mg of gallic acid equivalent per g (mg GAE/g). The assays were performed in triplicates.

**2.6.2. Determination of Total Flavonoids.** The total flavonoid content in EtOH- $H_2O$ E was estimated by the aluminum chloride spectrophotometric method [21]. The mixture absorbance was read at 430 nm and the result was expressed as mg of quercetin equivalent per g dry weight (mg QE/g). Tests were performed in triplicates.

**2.7. Determination of DPPH Radical Scavenging and  $\beta$ -Carotene Bleaching Capacity.** The free radical scavenging

capacity and the ability of the EtOH-H<sub>2</sub>O<sub>2</sub> to avoid  $\beta$ -carotene bleaching were determined using the methods described by Kirby and Schmidt [22] and Pratt [23], respectively. The ascorbic acid and the butylated hydroxytoluene (BHT) were taken as references.

## 2.8. Biological Activity Assays

**2.8.1. Animals.** Mice (30–50 g) were obtained from the Central Pharmacy of Tunisia (SIPHAT, Tunisia). They were placed in cages at a controlled temperature of 22±2°C with free access to standard laboratory diet and drinking water. Experiments and protocols were carried out in accordance with the European Community guidelines (EEC directive of 1986; 86/609/EEC) for the care and use of laboratory animals in scientific research and approved by the Institutional Animal Ethics Committee (directive 2001-2133) issued by the University of Sfax, Tunisia.

**2.8.2. Acute Toxicity Study.** The acute toxicity study was performed according to the World Health Organization recommendations (2000) with some modifications. Healthy mice (40 g) were randomly divided into four groups ( $n = 6$ ). The control group (group I) received only a water solution, while groups II, III, and IV were treated with EtOH-H<sub>2</sub>O<sub>2</sub> of *J. phoenicea* at doses of 100, 200, and 400 mg/kg body weight, respectively. Following the fasting period, the graded doses of EtOH-H<sub>2</sub>O<sub>2</sub> of *J. Phoenicea* were administered orally by gavage. The animals were maintained on standard animal diet and water. All animals were daily observed for behavioral pattern, body weight, and physical appearance changes and checked for mortality during the 2-week observation period.

**2.8.3. Anti-Inflammatory Test: Carrageenan-Induced Paw Oedema.** Anti-inflammatory activity of EtOH-H<sub>2</sub>O<sub>2</sub> of *J. phoenicea* was assessed according to the method described by Ravi et al. [24] with some modifications. Mice with a mean weight of 35 g were split into four groups ( $n = 6$ ):

(i) Group I: mice were pretreated with 1 ml/kg of sterile saline solution by subplantar injection and had no inflammation (control group)

(ii) Group II: mice were inflamed by carrageenan injection 1% and did not receive any treatment (Carr)

(iii) Group III: mice received dexamethasone (100 mg/Kg BW) by intraperitoneal injection and were considered as standard (Carr + DEX)

(iiii) Group IV: mice were given 100 mg/kg BW of EtOH-H<sub>2</sub>O<sub>2</sub> of *J. phoenicea* (Carr + EtOH-H<sub>2</sub>O<sub>2</sub> of *J. phoenicea*) by intraperitoneal injection

Paw oedema was induced [25] by administration of 50  $\mu$ L of 1% w/v carrageenan solution (type IV, Sigma Chemical Company, USA) into subplantar tissues of the right hind paw of each animal after one hour of intraperitoneal administration of plant extract and drug.

The swelling of carrageenan injected paw was measured before and 1, 2, 3, 4, and 5 hours after the induction using a Digital Vernier Caliper [26]. The anti-inflammatory activity was calculated as percentage inhibition of oedema in the

extract-treated animals under test in comparison to the carrageenan control group.

$$\text{Percent inhibition} = \left(1 - \frac{PT}{P0}\right) \times 100, \quad (1)$$

where PT represents the oedema volume of the drug-treated group and P0 is paw oedema of the carrageenan-treated group.

**2.8.4. Blood Sampling.** Five hours after the carrageenan administration, the animals were anesthetized and the blood samples were collected in heparin tubes. Plasma samples were obtained after centrifugation (15 min at 4000 rpm) and they were kept in –20°C until further analysis. The pellet obtained after centrifugation on heparin will be used for the assays of the oxidative status markers.

## 2.8.5. Exploration of Inflammatory Biomarkers

(1) **Hemogram Test.** The measurement of white blood cells and platelets is carried out with a hematology analyzer (KX21 hemogram).

(2) **Determination of C-Reactive Protein.** The serum C reactive protein levels were analyzed by an automatic analyzer “COBAS INTGRA 400.” The CRP is expressed in mg/L.

(3) **The Fibrinogen Assay.** The plasma fibrinogen assay was performed according to Clauss method [27] on the STA line analyzers using the STA fibrinogen reagent. The plasma samples were appropriately diluted with Owren-Koller buffer (pH 7.35). The fibrinogen concentrations are expressed in g/L.

(4) **Exploration of Oxidative Stress Parameters In Vivo.** The oxidative stress parameters were determined in skin tissues paw oedema. Homogenates were diluted (10%, w/v) in a Tris-buffered saline (pH 7.4) and centrifuged for 25 min (9000 rpm). The obtained supernatants were used for the determination of MDA as reported by Draper and Hadley [28].

The superoxide dismutase (SOD) content was colorimetrically assessed as reported by Beyer and Fridovich [29] using the inhibition of nitro blue tetrazolium (NBT). The catalase (CAT) activity was evaluated according to the method of Aebi [30] using H<sub>2</sub>O<sub>2</sub> as substrate. The glutathione peroxidase (GPx) content was analyzed according to the method of Flohe and Günzler [31] and expressed as  $\mu$ mol GSH/min/mg protein.

(5) **Histopathological Assessment of Skin Tissue.** Tissue specimen samples from subplantar muscles of all the studied groups were dissected five hours after carrageenan injection for histological examination. They were fixed in formalin solution (10%) and stained with hematoxylin-eosin. The sections were finally observed under a light microscope and photographed with an Olympus U-TU1X-2 camera.

**2.9. Acetic Acid Writhing Test.** The acetic acid-induced writhing test was performed as previously reported by Reza et al. [32] with some modifications. The experimental study

designed six groups of 6 mice. Group I served as control and received distilled water. Groups II and III were treated with diclofenac sodium (standard analgesic drug) at 50 and 100 mg/kg, respectively. Groups IV, V, and VI were administered 50, 100, and 150 mg/kg of the EtOH-H<sub>2</sub>O of *J. phoenicea*, respectively. After 30 minutes, acetic acid (1 mL of 1% w/v)

was administered with intraperitoneal injection for writhing induction. The total number of abdominal constrictions was counted for each group of mice after 15 minutes of acetic acid injection for the period of 5 minutes.

The protection percentage against acetic acid was calculated using the following formula:

$$\% \text{ inhibition} = \frac{\text{number of writhes (control)} - \text{number of writhes (test group)}}{\text{number of writhes (control)}} \times 100 \quad (2)$$

**2.10. Statistical Analysis.** Data were expressed as mean values  $\pm$  standard deviation (SD). A statistical significance comparison between groups was accomplished using the SPSS version 20.

The mean differences between the different groups were assessed by Duncan and Tukey's post hoc tests and compared using one-way analysis of variance (ANOVA). Differences were considered significant at  $P < 0.05$ .

### 3. Results

**3.1. Phytochemical Analysis of Organic Extract.** The phytochemical screening of hydroethanolic extract of *J. phoenicea* leaves revealed the presence of various secondary metabolites such as terpenoids, tannins, saponins, alkaloids, and anthraquinones, while glycosides were not detected in the tested extract (Table 1). Furthermore, the quantitative estimation of the total phenolic contents showed that the EtOH-H<sub>2</sub>O of *J. phoenicea* contains the highest amount of phenolics (70.30 mg GAE/g) and total flavonoid contents (11.33 mg QE/g) (Table 2).

**3.2. *J. phoenicea* EtOH-H<sub>2</sub>O GC-MS Analysis.** The identities of *J. phoenicea* constituents, their contents (%), and their retention times are listed in Table 3. The analysis of EtOH-H<sub>2</sub>O of *J. phoenicea* leaves revealed the presence of 25 compounds belonging to different chemical classes. The compounds, hexadecanoic acid (7.41%), stearic acid (5.69%), eseroline (3.15%), and azelaic acid (2.45%), were the most abundant. This extract also contains some sugars including  $\beta$ -D-Glucopyranose (1.22%), L-Fructose (0.23%), and  $\alpha$ -D-Galactopyranoside (0.17%). Besides, EtOH-H<sub>2</sub>O harbors some phenolic components including gallic, caffeic, and *p*-coumaric acids. EtOH-H<sub>2</sub>O of *J. phoenicea* leaves revealed the presence of a considerable amount of saturated fatty acids (18.42 % of the total FAs).

**3.3. Antioxidant Activity.** As shown in Table 2, the DPPH radical scavenging activity was appreciated by the determination of the IC<sub>50</sub> values. EtOH-H<sub>2</sub>O of *J. phoenicea* exhibited a remarkable free radical scavenging activity with an IC<sub>50</sub> value of 12.22  $\mu$ g/ml when compared to vitamin C (IC<sub>50</sub> = 3.5  $\mu$ g/l). In the  $\beta$ -carotene bleaching assay, the extract showed a potent activity (IC<sub>50</sub> = 15  $\mu$ g/l) less than that of the BHT (5.1  $\mu$ g/l) taken as reference (Table 2).

A positive correlation between total phenolics content and antioxidant property ( $R^2 = 0.972$ ) was noted.

**3.4. Acute Toxicity Study.** EtOH-H<sub>2</sub>O of *J. phoenicea* up to the dose of 400 mg/kg BW did not produce any signs of adverse reactions and no changes in the behavior of the treated animals up to 14 days following the extract administration. The treated animals did not display any abnormal signs such as food and water intake, convulsions, salivation, or diarrhea. No deaths or weight losses were recorded during the study. Therefore, EtOH-H<sub>2</sub>O of *J. phoenicea* at 100 mg/Kg BW was used in the *in vivo* investigation of the anti-inflammatory activity.

#### 3.5. Effects of *J. phoenicea* Leaf Extract on Carrageenan-Induced Paw Oedema

**3.5.1. Inhibitory Effect of the Extract on Paw Oedema *In Vivo*.** The comparative inhibitory effects following treatment with EtOH-H<sub>2</sub>O of *J. phoenicea* and dexamethasone on carrageenan-induced paw oedema are presented in Table 4 and Figure 1. The subcutaneous administration of carrageenan generated an increase in the paw size in mice due to oedema. This paw oedema peaked after 3 hours of experiment, especially for the untreated group, thus indicating an acute paw inflammation. The experimental data of the treated group by EtOH-H<sub>2</sub>O of *J. phoenicea* showed a significant decrease in the paw oedema size ( $P < 0.05$ ), which was time-dependent and more important than the standard drug dexamethasone. Our findings revealed an inhibition of 77.5% of the paw oedema using the EtOH-H<sub>2</sub>O compared to an inhibition of 57.89% using the standard drug after five hours. EtOH-H<sub>2</sub>O of *J. phoenicea* (100 mg/kg BW) displayed a significantly ( $P < 0.05$ ) higher anti-inflammatory capacity when compared to dexamethasone after 5 hours.

**3.5.2. Hematological, Biochemical, and Histopathological Examination.** The macroscopic results were confirmed through hematological, biochemical, and histopathological explorations. The hematological parameters were assessed by monitoring the white blood cells and blood platelet levels. A significant increase in white blood cell count and blood platelets was shown in carrageenan inflamed group compared to the negative control group (Table 5). However, the inflamed animals, treated with the EtOH-H<sub>2</sub>O of *J. phoenicea*, showed a significant decrease in the white blood cells and blood platelet counts and were close to those of control and dexamethasone-treated mice.



TABLE 1: Phytochemical analysis of *J. phoenicea* EtOH-H<sub>2</sub>O.

	Terpenoids	Tannins	Alkaloids	Anthraquinones	Saponins	Glycosides
EtOH-H <sub>2</sub> O	++	++	+	+	++	-

The sign ++ indicates being abundant; the sign + indicates being present; the sign - indicates being absent.

TABLE 2: Amounts of total phenolic compounds and total flavonoids and determined IC<sub>50</sub> values of the DPPH free radical scavenging assay and  $\beta$ -carotene bleaching test of *J. phoenicea* EtOH-H<sub>2</sub>O. Ascorbic acid and BHT were used as standards.

Extracts	Phenolic content <sup>a</sup> (mg GAE/g) <sup>b</sup>	Flavonoid content <sup>a</sup> (mg EQ/g) <sup>c</sup>	DPPH <sup>a</sup> (IC <sub>50</sub> $\mu$ g/ml)	$\beta$ -carotene (IC <sub>50</sub> $\mu$ g/ml)
EtOH-H <sub>2</sub> O	70.3 $\pm$ 0.20	11.33 $\pm$ 0.05	12.22 $\pm$ 0.02	15 $\pm$ 0.01
Ascorbic acid	-	-	3.5 $\pm$ 0.20	-
BHT	-	-	-	5.1 $\pm$ 0.10

<sup>a</sup>Each value represents the mean  $\pm$  SD of three experiments.

<sup>b</sup>(mg GAE/g): mg of gallic acid equivalent per g of dry plant extract.

<sup>c</sup>(mg EQ/g): mg of quercetin equivalent per g of dry plant extract.

-: not tested.

TABLE 3: GC/MS analysis of *J. phoenicea* EtOH-H<sub>2</sub>O.

Compounds	t <sub>R</sub> (min)	Content (%)	Characteristic mass fragments
<b>Phenolic compounds</b>			
Gallic acid	31.801	0.71	458, 281, 443, 355, 399, 179, 147, 73
Caffeic acid	28.571	1.65	219, 381, 396, 73
<i>p</i> -coumaric acid	30.937	0.55	219, 249, 293, 308, 73
<b>Alcohols</b>			
Resorcinol	12.690	0.68	257, 239, 209, 147, 112, 91, 73
Threitol	14.726	0.16	307, 217, 189, 147, 103, 73
Erythritol	14.909	0.89	307, 217, 189, 147, 103, 73
Xylitol	23.410	1.42	307, 217, 191, 147, 103, 73
Inositol	27.978	0.66	147, 191, 205, 217, 265, 306, 318, 73
<b>Sugars</b>			
L-Fructose	18.636	0.23	204, 147, 73
$\alpha$ -D-Galactopyranoside	29.048	0.17	204, 175, 147, 103, 73
$\beta$ -D-Glucopyranose	33.148	1.22	117, 147, 204, 246, 73
Galactopyranose	39.972	0.15	103, 147, 204, 249, 307, 331, 73
<b>Fatty acids</b>			
Lauric acid	5.771	0.42	95, 117, 145, 210, 229, 257
Suberic acid	6.218	0.43	95, 129, 149, 187, 217, 259, 303, 73
Hexadecanoic acid	12.310	7.41	117, 145, 129, 132, 313, 73
Azelaic acid	7.323	2.45	97, 117, 147, 171, 201, 243, 273, 317, 73
Stearic acid	20.884	5.69	117, 147, 201, 297, 341, 423, 73
Oxiraneoctanoic acid	22.875	2.02	87, 128, 177, 199
<b>Others</b>			
Ethylamine	6.518	0.46	174, 100, 86, 73
Propylene glycol	7.206	3.11	147, 117, 73
2-Ethylhexanol	8.568	0.61	187, 103, 75
Eseroline, 7-bromo-methylcarbamate	10.479	3.15	99, 130, 160, 188, 217, 240, 266, 298, 353
Xylonic acid, 1, 4 lactone	18.475	0.14	364, 321, 246, 217, 189, 147, 189, 147, 117, 73
Mannonic acid 1, 4 lactone	29.831	0.7	451, 361, 319, 220, 189, 147, 103, 73
D-Gluconic acid	33.477	0.6	219, 381, 396, 73

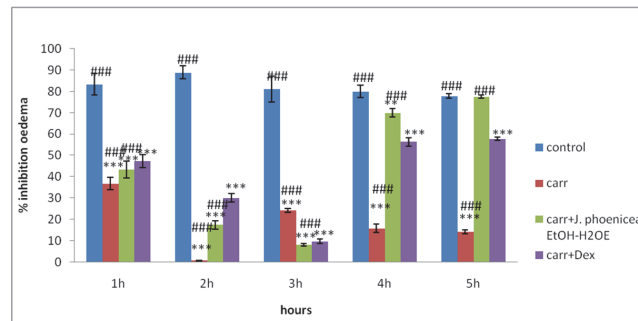


FIGURE 1: Percentage (%) of oedema inhibition data in all groups. Values represent mean  $\pm$  SD ( $n = 6$ ) in each group. \* represents  $P < 0.05$ , \*\* represents  $P < 0.01$ , and \*\*\* represents  $P < 0.001$ ; # represents  $P < 0.05$ , ## represents  $P < 0.01$ , and ### represents  $P < 0.001$ ; \* compared to control group and # compared to Carr + DEX. Control: physiological water, Carr: carrageenan, Carr + J: carrageenan + *J. phoenicea*, EtOH-H<sub>2</sub>OE, Carr + DEX: carrageenan + dexamethasone.

TABLE 4: Effects of *J. phoenicea* EtOH-H<sub>2</sub>OE and dexamethasone on paw oedema tissue after carrageenan administration. Values represent mean  $\pm$  SD ( $n = 6$ ) in each group. Each value represents the mean  $\pm$  SEM of results from six animals.

	1 h	2 h	3 h	4 h	5 h
<b>Control</b>	0.15 $\pm$ 0.03 <sup>a</sup>	0.1 $\pm$ 0.01 <sup>a</sup>	0.17 $\pm$ 0.05 <sup>a</sup>	0.18 $\pm$ 0.04 <sup>a</sup>	0.2 $\pm$ 0.06 <sup>a</sup>
<b>Carr</b>	0.75 $\pm$ 0.104 <sup>b</sup>	1.2 $\pm$ 0.12 <sup>c</sup>	1.42 $\pm$ 0.104 <sup>c</sup>	1.38 $\pm$ 0.089 <sup>d</sup>	1.36 $\pm$ 0.089 <sup>d</sup>
<b>Carr + DEX</b>	0.7 $\pm$ 0.2 <sup>b</sup>	0.93 $\pm$ 0.18 <sup>b</sup>	1.2 $\pm$ 0.14 <sup>bc</sup>	0.58 $\pm$ 0.1 <sup>c</sup>	0.56 $\pm$ 0.09 <sup>c</sup>
<b>Carr + <i>J. phoenicea</i> EtOH-H<sub>2</sub>OE</b>	0.68 $\pm$ 0.103 <sup>b</sup>	0.99 $\pm$ 0.136 <sup>bc</sup>	1.1 $\pm$ 0.08 <sup>b</sup>	0.36 $\pm$ 0.25 <sup>b</sup>	0.27 $\pm$ 0.26 <sup>b</sup>

<sup>a,b,c,d</sup> Different letters in the same column indicate significant differences ( $a > b > c > d$ ;  $P < 0.05$ ).

TABLE 5: White blood cells and platelets count and levels of fibrinogen and C-reactive protein (CRP). Values represent mean  $\pm$  SD ( $n = 6$ ) in each group.

	WBC	PLT	Fibrinogen (g/l)	CRP (mg/ml)
<b>Control</b>	3.68 $\pm$ 0.4 <sup>a</sup>	292 $\pm$ 4.2 <sup>a</sup>	3.35 $\pm$ 0.05 <sup>a</sup>	8 $\pm$ 0.83 <sup>a</sup>
<b>Carr</b>	12.13 $\pm$ 0.95 <sup>c</sup>	1207 $\pm$ 11.3 <sup>b</sup>	5.64 $\pm$ 0.07 <sup>b</sup>	24 $\pm$ 0.94 <sup>b</sup>
<b>Carr + DEX</b>	8.03 $\pm$ 0.62 <sup>b</sup>	965 $\pm$ 7.9 <sup>b</sup>	3.53 $\pm$ 0.01 <sup>b</sup>	12 $\pm$ 0.09 <sup>a</sup>
<b>Carr + <i>J. phoenicea</i> EtOH-H<sub>2</sub>OE</b>	4.4 $\pm$ 0.31 <sup>a</sup>	779.47 $\pm$ 6.04 <sup>c</sup>	3.48 $\pm$ 0.03 <sup>c</sup>	9 $\pm$ 0.36 <sup>a</sup>

<sup>a,b,c</sup> Different letters in the same column indicate significant differences ( $a > b > c$ ;  $P < 0.05$ ).

As shown in Table 4, the administration of carrageenan led to a significant enhancement in CRP level for the carrageenan group compared to the control animals. However, the CRP level significantly decreased ( $P < 0.05$ ) in the groups treated with *J. phoenicea* (62.5%) and dexamethasone (50%) when compared to the carrageenan untreated group.

The fibrinogen rate decreased significantly ( $P < 0.05$ ) in the groups of mice treated with the EtOH-H<sub>2</sub>OE of *J. phoenicea* (38.3%) and dexamethasone (37.42%) compared to the carrageenan untreated group (Table 5).

Biopsies from plantar muscles of the untreated group showed normal histological sections (Figure 2). However, biopsies from carrageenan-treated mice (Figure 2(a)) showed numerous inflammatory cells and tissue structure disruption. Biopsies from the *J. phoenicea*-treated mice (Figure 2(d)) showed absence of inflammatory cells.

**3.6. In Vivo Effects on the Malondialdehyde (MDA) Levels.** The malondialdehyde levels in oedema paw induced by carrageenan are shown in Table 6. For the carrageenan-treated

mice, the dermal MDA levels increased significantly ( $P < 0.001$ ) compared to the normal control group. Nevertheless, the treatment with 100 mg/kg BW of EtOH-H<sub>2</sub>OE showed a significant decrease ( $P < 0.001$ ) compared to the carrageenan group and even the dexamethasone group (10 mg/kg). The treatment with *J. phoenicea* reinstated the MDA formation by 95.37% against only 90.74% recorded in dexamethasone. The malondialdehyde concentrations in the *J. phoenicea* EtOH-H<sub>2</sub>O-treated group were comparable to those of the normal control group.

**3.7. Effects on Enzymatic Antioxidant Status.** The obtained results of SOD, CAT, and GSH levels in the paw oedema tissue of the different tested groups are summarized in Table 6. The carrageenan-induced inflammation mice led to a significant decrease of the dermal SOD, CAT, and GSH levels compared to the normal control mice ( $P < 0.001$ ). However, our results proved that the animals pretreated with *J. phoenicea* EtOH-H<sub>2</sub>OE did not produce any significant differences in enzymatic antioxidant levels compared to the control group.

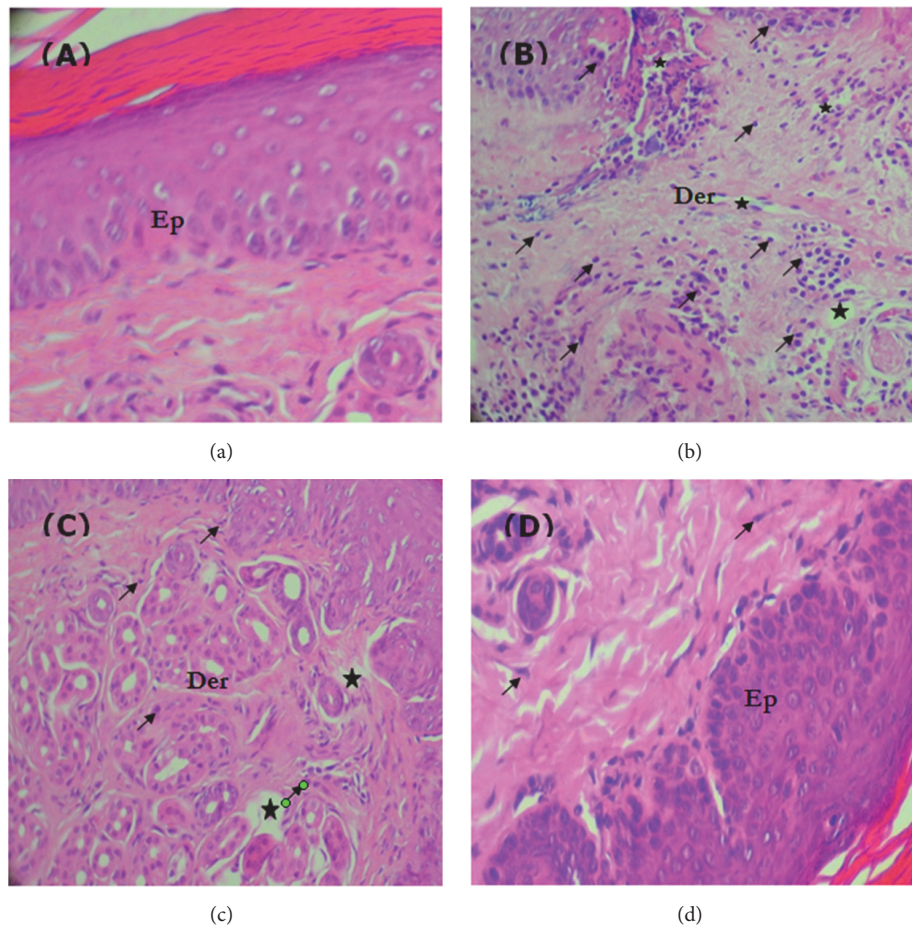


FIGURE 2: The representative photomicrographs of the skin showing the protective effects of *J. phoenicea* EtOH-H<sub>2</sub>OE against carrageenan-induced inflammation in mice. Controls (a), mice treated with carrageenan (b), the combination of carrageenan and dexamethasone (c), and mice treated with the combination of carrageenan and *J. phoenicea* EtOH-H<sub>2</sub>OE (d). Ep: epidermis, Der: dermis. ★: oedema. ↗: inflammatory cell.

TABLE 6: Effects of *J. phoenicea* EtOH-H<sub>2</sub>OE and dexamethasone on CAT, SOD, GPx, and MDA activities in carrageenan-induced paw oedema.

Treatment	MDA (nmol /mg protein)	SOD (units/mg protein)	CAT ( $\mu\text{mol H}_2\text{O}_2/\text{min/mg protein}$ )	GPx ( $\mu\text{mol GSH/mg protein}$ )
Control	1.08 $\pm$ 0.07 ###	8.44 $\pm$ 0.31###	186.04 $\pm$ 6.13###	5.6 $\pm$ 1.07 ###
Carr	1.94 $\pm$ 0.01* * *	2.26 $\pm$ 0.12* * *	77.12 $\pm$ 1.6* * *	1.23 $\pm$ 0.07* * *
Carr + DEX	0.98 $\pm$ 0.04* ###	6.65 $\pm$ 0.57* * * ###	114.13 $\pm$ 3.9	4.36 $\pm$ 0.19* * ###
Carr + <i>J. phoenicea</i> EtOH-H <sub>2</sub> OE	1.03 $\pm$ 0.009 ###	7.11 $\pm$ 0.13* * * ###	169.62 $\pm$ 4.3##	4.44 $\pm$ 0.31* ###

Values are mean  $\pm$  SE for six rats in each group. \* \* \* represents  $P < 0.001$ ; \*\* represents  $P < 0.01$ ; \* represents  $P < 0.05$ . SOD: superoxide dismutase, CAT: catalase, GSH: glutathione peroxidase, MDA: malondialdehyde.  
\* \* \* ( $P < 0.001$ ) represents highly significant difference in comparison with control mice.  
\*\* ( $P < 0.01$ ) represents moderately significant difference in comparison with control mice.  
\* ( $P < 0.05$ ) represents significant difference in comparison with control mice.  
### ( $P < 0.001$ ) represents highly significant difference in comparison with Carr group.  
## ( $P < 0.01$ ) represents moderately significant difference in comparison with Carr group.

TABLE 7: Effects of EtOH-H<sub>2</sub>O of *J. phoenicea* on acetic acid-induced writhing in mice.

Group	Dose (mg/kg)	Percentage of inhibition (%)
Acetic acid	(10ml/kg)	0 <sup>f</sup>
Diclofenac sodium	50	79.88 <sup>b</sup>
Diclofenac sodium	100	100 <sup>a</sup>
<i>J. phoenicea</i> EtOH-H <sub>2</sub> O	50	20.15 <sup>e</sup>
<i>J. phoenicea</i> EtOH-H <sub>2</sub> O	100	42.79 <sup>d</sup>
<i>J. phoenicea</i> EtOH-H <sub>2</sub> O	150	77.33 <sup>c</sup>

Values are expressed as mean  $\pm$  SD ( $n = 6$ ).

a,b,c,d,e,f Different letters in the same column indicate significant differences ( $a > b > c > d > e > f$ ;  $P < 0.05$ ).

The treatment of inflamed mice with the EtOH-H<sub>2</sub>O of *J. phoenicea* (100 mg/kg BW) restored the SOD activity by 84.24%, the CAT activity by 91.17%, and the GPx activity by 79.28%, compared to the control group. The results showed that the *J. phoenicea* leaves hydroethanolic extract displayed a protection of 84.24%, 91.17%, and 79.28% for SOD, CAT, and GSH activities, respectively, compared to 78.79%, 61.34%, and 77.85% using dexamethasone as reference drug towards inflammation induced by carrageenan.

**3.8. Acetic Acid-Induced Writhing Response.** Our results showed that the tested extract at different doses and diclofenac sodium used as a standard significantly reduced the writhing number as compared to the control untreated mice ( $P < 0.05$ ). As shown in Table 7, the pain relief was reached in a dose-dependent way with all the tested doses (50, 100, and 150 mg/kg i.p.). The writhing maximum inhibition was 77.33% recorded at 150 mg/kg dose of *J. phoenicea* EtOH-H<sub>2</sub>O.

The inhibitory effect of *J. phoenicea* EtOH-H<sub>2</sub>O (77.33%) at the dose of 150 mg/kg was just like that obtained by diclofenac sodium (79.88%) at the dose of 50 mg/kg.

## 4. Discussion

Plants have been commonly used for centuries as potential sources of new anti-inflammatory compounds. Inflammation is a physiological protective response to body tissue injury or bacterial invasion, which involves several intricate factors. During the inflammatory response, the injured tissues release mediators leading to the generation of ROS, which are well known for their deleterious effects [33]. The anti-inflammatory effects of numerous plant extracts may be attributed to the antioxidant property of their phytoconstituents. In the current study, the *J. phoenicea* EtOH-H<sub>2</sub>O was found to have potent antioxidant activity *in vitro*. The richness of EtOH-H<sub>2</sub>O of *J. phoenicea* in phenolics known for their powerful antioxidant property and also involved in the modulation of pain and reduction of inflammation

[34–36] motivated us to evaluate the analgesic and anti-inflammatory effects of *J. phoenicea* in mice models.

The paw oedema induced by carrageenan is a model often used to assess the anti-inflammatory effects of novel compounds. This inflammation type has two major phases. The first is caused by histamine, leukotriene, kinin, and cyclooxygenase release during the first hour after the carrageenan administration. The second or delayed phase is linked to the generation of prostaglandins, bradykinin, and neutrophil infiltration [37]. In the present investigation, the significant inhibitory activity ( $P < 0.001$ ) shown by EtOH-H<sub>2</sub>O of *J. phoenicea* over a period of 5 h in carrageenan-induced inflammation was higher than that elicited by dexamethasone. Dexamethasone is a prostaglandin synthesis inhibitor [38]. Our results suggest that the anti-inflammatory effect of EtOH-H<sub>2</sub>O of *J. phoenicea* may be due to the inhibition of prostaglandin biosynthesis, which is similar to that produced by steroidal anti-inflammatory drugs such as dexamethasone. However, exact mechanism of inhibition of prostaglandin synthesis could be a potential future perspective.

Carrageenan-induced local inflammation was reported to be associated with the generation of reactive oxygen species (ROS) and to play a key role in the genesis of oxidative stress [39]. Previous research has reported that ROS overproduction may lead to increasing lipid peroxidation [40]. A reduction of the MDA level, a biomarker involved in lipid peroxidation, was observed in EtOH-H<sub>2</sub>O of *J. phoenicea* treated group compared to the untreated group after 5 hours. According to the enzymatic antioxidant analysis, *J. phoenicea* may promote the activities of SOD, CAT, and GSH by boosting a cellular antioxidant protection mechanism. This implies a protective effect of *J. phoenicea* extract by stimulating the expression and the activity of antioxidant enzymes during the inflammatory process.

These results suggest that the extract contains some phytochemical compounds with antioxidant activities which could contribute to the anti-inflammatory process [41, 42]. Boughton-Smith et al. [43] showed that the carrageenan-induced rat paw oedema tissue is sensitive to antioxidants. Therefore, antioxidant components in EtOH-H<sub>2</sub>O of *J. phoenicea* may also contribute to its anti-inflammatory capacity.

It is well known that following the carrageenan-induced rat paw oedema there are changes in blood parameters that are suggestive of an acute phase reaction leading to a hemostatic imbalance [44]. Carrageenan-induced increase in total white blood cells count and platelets occurs at the site of inflammation due to the release of inflammatory cytokines, which increases the recruitment of neutrophil counts [45]. The reduced count of total white blood cells could be the result of an inhibition of carrageenan-induced total leukocytes, which occurs at the site of inflammation by the phytoconstituents of the hydroethanolic extract of *J. phoenicea*.

It is well established that dexamethasone and other anti-inflammatory drugs inhibit migration of inflammatory cells by inhibiting the release of various chemical mediators [46]. In the present study, the significant decrease in the WBC count caused by the EtOH-H<sub>2</sub>O of *J. phoenicea* and dexamethasone suggests that these agents are able to reduce inflammation by decreasing the leukocyte migration



to the tissue injury sites and possible inhibition of cellular infiltration such as neutrophils and granulocytes.

Platelets have been recognized not only to play a major role in hemostasis but also to participate in inflammation and innate and adaptive immunity responses [47]. It was reported that in the inflamed paw tissue there is platelet aggregation and fibrin deposition [48]. It has been proven that the platelets form aggregates with leukocytes and interact with neutrophils, monocytes, and lymphocytes and therefore play a critical role in the inflammatory process [49]. The decrease in platelet count, observed in EtOH-H<sub>2</sub>O<sub>2</sub> treated group, suggests a possible inhibitory effect of *J. phoenicea* components on platelet aggregation, which could contribute to the anti-inflammatory process [50].

Most inflammatory biomarkers such as fibrinogen and CRP increased significantly following the inflammation response. However, EtOH-H<sub>2</sub>O<sub>2</sub> of *J. phoenicea* significantly decreases the mean of fibrinogen and CRP levels. All these findings were also confirmed by histological examination. Indeed, the extract considerably decreases the number of cellular infiltrates and reduces oedema tissue as did reference drug dexamethasone, whereas the paw tissue of untreated mice displayed a subcutaneous oedema with invasive cell infiltration associated with an epidermal ulcer and vascular congestion compared to the treated ones.

The acetic acid-induced writhing protocol was achieved to assess the peripheral analgesic efficiency of test drugs. According to the test, the extract has significantly ( $P < 0.001$ ) decreased the total number of abdominal constrictions by boosting pain inhibitory mediators. The pain sensation is elicited by producing localized inflammatory response due to the release of endogenous substances as well as some other pain mediators such as arachidonic acid via prostaglandin biosynthesis [51]. Prostaglandin products, at damaged tissue sites, contribute to the inflammatory process and pain by increasing the capillary permeability [52]. Our results suggest that *J. phoenicea* contains some phytochemical compounds that can exert anti-inflammatory and antinociceptive effects probably by blocking the release of inflammatory mediators like serotonin, histamine, and prostaglandin and reducing blood flow.

Thus, the anti-inflammatory and analgesic activities are due to the individual or synergistic effect of the *J. phoenicea* components. The richness of *J. phoenicea* extract in terpenoids, polyphenols, and flavonoids may also synergistically promote inhibition of the enzymes involved in the prostaglandin synthesis as previously reported [53, 54].

The GC-MS analysis of *J. phoenicea* EtOH-H<sub>2</sub>O<sub>2</sub> revealed the presence of hexadecanoic acid in this extract. Earlier reports have evaluated the efficiency of hexadecanoic acid in the anti-inflammatory process and reported that hexadecanoic acid, in studies with isolated Kupffer cells, improved the inhibition of various chemical mediators such as nitric oxide, interleukin-10, tumor necrosis factor- $\alpha$ , and prostaglandin E<sub>2</sub> [55]. Moreover, recent observations highlighted the anti-inflammatory effects of azelaic acid achieved by reducing reactive oxygen species [56]. On the other hand, the tested extract contained a significant amount of stearic acid. It was reported that these fatty acids fairly produce

potent anti-inflammatory and analgesic effects [57]. Our results also suggest that *J. phoenicea* contains promisingly potent phytochemical compounds with anti-inflammatory and antinociceptive properties, which may inhibit the release of inflammatory mediators. EtOH-H<sub>2</sub>O<sub>2</sub> of *J. phoenicea* may have a potential benefit for the management of pain and inflammatory disorders. These results can justify the traditional use of this plant as a decoction to relieve the pain in Tunisia [16].

## 5. Conclusion

The current study revealed that the hydroethanolic extract obtained from *J. phoenicea* has anti-inflammatory and analgesic activities that were coupled with potent antioxidant capacity attributed to the total extract richness in various chemical compounds. Further studies are required to confirm our results for the use of this extract as a source for new pro-inflammatory drugs in human beings.

## Data Availability

No data were used to support this study.

## Conflicts of Interest

The authors declare that there are no conflicts of interest.

## Acknowledgments

This work was supported by grants from the Tunisian Ministry of Higher Education and Scientific Research.

## References

- [1] WHO, "Guidelines on safety monitoring of herbal medicines," in *Pharmacovigilance Systems*, World Health Organization, Geneva, Switzerland, 2004.
- [2] P. Arulselvan, M. T. Fard, W. S. Tan et al., "Role of antioxidants and natural products in inflammation," *Oxidative Medicine and Cellular Longevity*, vol. 2016, Article ID 5276130, pp. 1–15, 2016.
- [3] Z. Sahnoun, K. Jamoussi, and K. M. Zeghal, "Free radicals and antioxidants: human physiology, pathology and therapeutic aspects," *Thérapie*, vol. 52, no. 4, pp. 251–270, 1997.
- [4] M. S. Cooke, M. D. Evans, M. Dizdaroglu, and J. Lunec, "Oxidative DNA damage: mechanisms, mutation, and disease," *The FASEB Journal*, vol. 17, no. 10, pp. 1195–1214, 2003.
- [5] C. Borza, C. Serban, C. Dehelean et al., *Oxidative Stress and Lipid Peroxidation-a Lipid Metabolism Dysfunction*, INTECH Open Access Publisher, 2013.
- [6] S. Reuter, S. C. Gupta, M. M. Chaturvedi, and B. B. Aggarwal, "Oxidative stress, inflammation, and cancer: how are they linked?" *Free Radical Biology & Medicine*, vol. 49, no. 11, pp. 1603–1616, 2010.
- [7] S. Saha, E. V. S. Subrahmanyam, C. Kodangala, S. C. Mandal, and S. C. Shastri, "Evaluation of antinociceptive and anti-inflammatory activities of extract and fractions of *Eugenia jambolana* root bark and isolation of phytoconstituents," *Revista Brasileira de Farmacognosia*, vol. 23, no. 4, pp. 651–661, 2013.

- [8] H. Mangge, K. Becker, D. Fuchs, and J. M. Gostner, "Antioxidants, inflammation and cardiovascular disease," *World Journal of Cardiology*, vol. 6, no. 6, pp. 462–477, 2014.
- [9] B. Uttara, A. V. Singh, P. Zamboni, and R. T. Mahajan, "Oxidative stress and neurodegenerative diseases: a review of upstream and downstream antioxidant therapeutic options," *Current Neuropharmacology*, vol. 7, no. 1, pp. 65–74, 2009.
- [10] M. B. Salem, H. Affes, K. Ksouda et al., "Pharmacological studies of artichoke leaf extract and their health benefits," *Plant Foods for Human Nutrition*, vol. 70, no. 4, pp. 441–453, 2015.
- [11] M. Valko, D. Leibfritz, J. Moncol, M. T. D. Cronin, M. Mazur, and J. Telser, "Free radicals and antioxidants in normal physiological functions and human disease," *The International Journal of Biochemistry & Cell Biology*, vol. 39, no. 1, pp. 44–84, 2007.
- [12] A. Crozier, I. B. Jaganath, and M. N. Clifford, "Dietary phenolics: chemistry, bioavailability and effects on health," *Natural Product Reports*, vol. 26, no. 8, pp. 1001–1043, 2009.
- [13] C. Sacchet, R. Mocelin, A. Sachett et al., "Antidepressant-like and antioxidant effects of *Plinia trunciflora* in mice," *Evidence-Based Complementary and Alternative Medicine*, vol. 2015, Article ID 601503, 9 pages, 2015.
- [14] B. Halliwell, "How to characterize an antioxidant: an update," *Biochemical Society Symposium*, vol. 61, pp. 73–101, 1995.
- [15] E. Yeşilada, G. Honda, E. Sezik, M. Tabata, K. Goto, and Y. Ikeshiro, "Traditional medicine in Turkey IV. Folk medicine in the Mediterranean subdivision," *Journal of Ethnopharmacology*, vol. 39, no. 1, pp. 31–38, 1993.
- [16] Z. Yaniv and N. Dudai, *Medicinal and Aromatic Plants of the Middle-east*, vol. 2, Springer, Dordrecht Heidelberg New York London, 2014.
- [17] H. Keskes, K. Mnafigui, K. Hamden, M. Damak, A. El Feki, and N. Allouche, "In vitro anti-diabetic, anti-obesity and antioxidant properties of *Juniperus phoenicea* L. leaves from Tunisia," *Asian Pacific Journal of Tropical Biomedicine*, vol. 4, pp. S649–S655, 2014.
- [18] A. Sofowora, *Medicinal Plants and Traditional Medicine in Africa*, 1993.
- [19] J. B. Harborne, "Methods of plant analysis," in *Phytochemical Methods*, Springer Netherlands, 1984.
- [20] P. G. Waterman and S. Mole, *Analysis of Phenolic Plant Metabolites*, Blackwell Scientific Publications, Oxford, 2000.
- [21] C. Quettier-Deleu, B. Gressier, J. Vasseur et al., "Phenolic compounds and antioxidant activities of buckwheat (*Fagopyrum esculentum* Moench) hulls and flour," *Journal of Ethnopharmacology*, vol. 72, no. 1–2, pp. 35–42, 2000.
- [22] A. J. Kirby and R. J. Schmidt, "The antioxidant activity of Chinese herbs for eczema and of placebo herbs—I," *Journal of Ethnopharmacology*, vol. 56, no. 2, pp. 103–108, 1997.
- [23] D. E. Pratt, "Natural antioxidants of soybean and other oilseeds," in *Autoxidation in Food and Biological Systems*, M. G. Simic and M. Karel, Eds., pp. 283–292, New York, NY, USA, 1980.
- [24] V. Ravi, T. S. M. Saleem, S. S. Patel, J. Raamamurthy, and K. Gauthaman, "Anti-inflammatory effect of methanolic extract of *Solanum nigrum* Linn Berries," *International Journal of Applied Research in Natural Products*, vol. 2, no. 2, pp. 33–36, 2009.
- [25] E. A. Winter, E. A. Risley, and G. W. Nuss, "Carrageenan induced paw edema in hind paw as an assay for anti-inflammatory drugs," *Journal of Pharmacology and Experimental Therapeutics*, vol. 141, pp. 369–373, 1963.
- [26] J.-C. Liao, J.-S. Deng, C.-S. Chiu et al., "Anti-inflammatory activities of *Cinnamomum cassia* constituents in vitro and in vivo," *Evidence-Based Complementary and Alternative Medicine*, vol. 2012, Article ID 429320, 12 pages, 2012.
- [27] A. Claus, "Gerinnungsphysiologische Schnellmethode zur Bestimmung des Fibrinogens," *Acta Haematologica*, vol. 17, no. 4, pp. 237–246, 1957.
- [28] H. H. Draper and M. Hadley, "Malondialdehyde determination as index of lipid peroxidation," *Methods in Enzymology*, vol. 186, pp. 421–431, 1990.
- [29] W. F. Beyer Jr. and I. Fridovich, "Assaying for superoxide dismutase activity: some large consequences of minor changes in conditions," *Analytical Biochemistry*, vol. 161, no. 2, pp. 559–566, 1987.
- [30] H. Aebi, "Catalase," in *Method of Enzymatic Analysis*, H. U. Bergmeyer, Ed., vol. 2, Academic Press, New York, NY, USA, 1974.
- [31] L. Flohe and W. A. Gunzler, "Assays of glutathione peroxidase," *Methods in Enzymology*, vol. 105, pp. 114–121, 1984.
- [32] M. S. H. Reza, C. Mandal, K. A. Alam et al., "Phytochemical, antibacterial and antinociceptive studies of *Hoya parasitica*," *Journal of Pharmacology and Toxicology*, vol. 2, no. 8, pp. 753–756, 2007.
- [33] E. R. Stadtman and B. S. Berlett, "Reactive oxygen-mediated protein oxidation in aging and disease," *Drug Metabolism Reviews*, vol. 30, no. 2, pp. 225–243, 1998.
- [34] A. Di Sotto, F. Maffei, P. Hrelia, F. Castelli, M. G. Sarpietro, and G. Mazzanti, "Genotoxicity assessment of  $\beta$ -caryophyllene oxide," *Regulatory Toxicology and Pharmacology*, vol. 66, no. 3, pp. 264–268, 2013.
- [35] O. A. Fawole, S. O. Amoo, A. R. Ndhlala, M. E. Light, J. F. Finnie, and J. Van Staden, "Anti-inflammatory, anticholinesterase, antioxidant and phytochemical properties of medicinal plants used for pain-related ailments in South Africa," *Journal of Ethnopharmacology*, vol. 127, no. 2, pp. 235–241, 2010.
- [36] S. J. Uddin, D. Grice, and E. Tiralongo, "Evaluation of cytotoxic activity of patriscabratine, tetracosane and various flavonoids isolated from the Bangladeshi medicinal plant *Acrostichum aureum*," *Pharmaceutical Biology*, vol. 50, no. 10, pp. 1276–1280, 2012.
- [37] R. Vinegar, J. F. Truax, P. R. Selph, P. R. Johnston, A. L. Venable, and K. K. McKenzie, "Pathway to carrageenan-induced inflammation in the hind limb of the rat," *Federation Proceedings*, vol. 46, no. 1, pp. 118–126, 1987.
- [38] J. Weidenfeld, J. Lysy, and E. Shohami, "Effect of dexamethasone on prostaglandin synthesis in various areas of the rat brain," *Journal of Neurochemistry*, vol. 48, no. 5, pp. 1351–1354, 1987.
- [39] S. B. Khedir, M. Mzid, S. Bardaa, D. Moalla, Z. Sahnoun, and T. Rebai, "In vivo evaluation of the anti-inflammatory effect of *Pistacia lentiscus* fruit oil and its effects on oxidative stress," *Evidence-Based Complementary and Alternative Medicine*, vol. 2016, Article ID 6108203, 12 pages, 2016.
- [40] A. Goel, V. Dani, and D. K. Dhawan, "Protective effects of zinc on lipid peroxidation, antioxidant enzymes and hepatic histology in chlorpyrifos-induced toxicity," *Chemico-Biological Interactions*, vol. 156, no. 2–3, pp. 131–140, 2005.
- [41] S. S. Sakat, A. R. Juvekar, and M. N. Gambhire, "In-vitro antioxidant and anti-inflammatory activity of methanol extract of *Oxalis corniculata* Linn," *International Journal of Pharmacy and Pharmaceutical Sciences*, vol. 2, no. 1, pp. 146–155, 2010.
- [42] V. K. R. Garg, M. Jain, P. K. R. Sharma, and G. Garg, "Anti-inflammatory activity of *Spinacia oleracea*," *International Journal of Pharma Professional's Research*, vol. 1, pp. 1–4.

- [43] N. K. Boughton-Smith, A. M. Deakin, R. L. Follenfant, B. J. R. Whittle, and L. G. Garland, "Role of oxygen radicals and arachidonic acid metabolites in the reverse passive Arthus reaction and carrageenin paw oedema in the rat," *British Journal of Pharmacology*, vol. 110, no. 2, pp. 896–902, 1993.
- [44] C. Cicala, S. Morello, A. Alfieri, V. Vellecco, S. Marzocco, and G. Autore, "Haemostatic imbalance following carrageenan-induced rat paw oedema," *European Journal of Pharmacology*, vol. 577, no. 1-3, pp. 156–161, 2007.
- [45] E. Umapathy, E. J. Ndebia, A. Meeme et al., "An experimental evaluation of *Albuca setosa* aqueous extract on membrane stabilization, protein denaturation and white blood cell migration during acute inflammation," *Journal of Medicinal Plants Research*, vol. 4, no. 9, pp. 789–795, 2010.
- [46] S. Cuzzocrea, G. Costantino, E. Mazzon, B. Zingarelli, A. De Sarro, and A. P. Caputi, "Protective effects of Mn(III)tetrakis (4-benzoic acid) porphyrin (MnTBAP), a superoxide dismutase mimetic, in paw oedema induced by carrageenan in the rat," *Biochemical Pharmacology*, vol. 58, no. 1, pp. 171–176, 1999.
- [47] J. W. Semple, J. E. Italiano Jr., and J. Freedman, "Platelets and the immune continuum," *Nature Reviews Immunology*, vol. 11, no. 4, pp. 264–274, 2011.
- [48] N. Busso, V. Chobaz-Péclat, J. Hamilton, P. Spee, N. Wagtmann, and A. So, "Essential role of platelet activation via protease activated receptor 4 in tissue factor-initiated inflammation," *Arthritis Research & Therapy*, vol. 10, no. 2, article no. R42, 2008.
- [49] D. Duerschmied, G. L. Suidan, M. Demers et al., "Platelet serotonin promotes the recruitment of neutrophils to sites of acute inflammation in mice," *Blood*, vol. 121, no. 6, pp. 1008–1015, 2013.
- [50] C. N. Morrell, A. A. Aggrey, L. M. Chapman, and K. L. Modjeski, "Emerging roles for platelets as immune and inflammatory cells," *Blood*, vol. 123, no. 18, pp. 2759–2767, 2014.
- [51] H. Khan, M. Saeed, A.-U. Gilani, M. A. Khan, A. Dar, and I. Khan, "The antinociceptive activity of *Polygonatum verticillatum* rhizomes in pain models," *Journal of Ethnopharmacology*, vol. 127, no. 2, pp. 521–527, 2010.
- [52] I. D. G. Duarte, M. Nakamura, and S. H. Ferreira, "Participation of the sympathetic system in acetic acid-induced writhing in mice," *Brazilian Journal of Medical and Biological Research*, vol. 21, no. 2, pp. 341–343, 1988.
- [53] J. S. Deng, C. S. Chi, S. S. Huang, P. H. Shie, T. H. Lin, and G. J. Huang, "Antioxidant, analgesic and anti-inflammatory activities of the ethanolic extracts of *Taxillus liquidambaricola*," *Journal of Ethnopharmacology*, vol. 137, pp. 1161–1171, 2011.
- [54] O. E. Obaseki, O. I. Adesegun, G. N. Anyasor, and O. O. Abebawo, "Evaluation of the anti-inflammatory properties of the hexane extract of *Hydrocotyle bonariensis* Comm. Ex Lam. leaves," *African Journal of Biotechnology*, vol. 15, no. 49, pp. 2759–2771, 2016.
- [55] V. Aparna, K. V. Dileep, P. K. Mandal, P. Karthe, C. Sadasivan, and M. Haridas, "Anti-inflammatory property of n-hexadecanoic acid: structural evidence and kinetic assessment," *Chemical Biology & Drug Design*, vol. 80, no. 3, pp. 434–439, 2012.
- [56] A. Mastrofrancesco, M. Ottaviani, N. Aspite et al., "Azelaic acid modulates the inflammatory response in normal human keratinocytes through PPAR $\gamma$  activation," *Experimental Dermatology*, vol. 19, no. 9, pp. 813–820, 2010.
- [57] A. S. Shah and K. R. Alagawadi, "Anti-inflammatory, analgesic and antipyretic properties of *Thespesia populnea* Soland ex. Correa seed extracts and its fractions in animal models," *Journal of Ethnopharmacology*, vol. 137, no. 3, pp. 1504–1509, 2011.